

Mechanisms responsible for the transgenerational inheritance of intrauterine growth restriction phenotypes

This thesis submitted to The University of Adelaide in the fulfilment of the
requirements for the degree of Doctor of Philosophy

Ngoc Anh Thu Doan

Bachelor (Honours) of Applied Biology



THE UNIVERSITY
of ADELAIDE

Faculty of Sciences

School of Agriculture, Food and Wine

November 2023

TABLE OF CONTENTS

DECLARATION	vi
ACKNOWLEDGEMENTS.....	vii
LIST OF PUBLICATIONS AND EXPECTED PUBLICATIONS.....	ix
CHAPTER 1 – THESIS INTRODUCTION.....	1
CHAPTER 2 – Epigenetic mechanisms responsible for the transgenerational inheritance of intrauterine growth restriction phenotypes	5
Statement of Authorship.....	6
Abstract.....	9
Introduction	9
Intrauterine growth restriction and chronic disease risk	10
Intrauterine growth restriction and the associated altered epigenetic mechanisms	19
Discussion.....	31
References	32
Article	48
CHAPTER 3 - Imprinted gene alterations in the kidneys of growth restricted offspring may be mediated by a long non-coding RNA.....	59
Statement of Authorship	60

Abstract.....	64
Introduction	65
Materials and Methods	66
Results	69
Discussion.....	76
References	82
Supplementary tables	92
Supplementary figures.....	96
Article	98
CHAPTERS 4 & 5 INTRODUCTION & MATERIALS AND METHODS	110
Introduction	111
Materials and Methods	112
References	119
CHAPTER 4 – Uteroplacental insufficiency results in an increased risk of developing metabolic disease across generations in the paternal line of growth restricted rats	125
Statement of Authorship.....	126
Abstract.....	129

Results	130
Discussions	172
References	177
Supplementary tables	182
Supplementary figures.....	187
CHAPTER 5 – Uteroplacental insufficiency results in an increased risk of developing renal dysfunction across generations in the paternal line of growth restricted rats	201
Statement of Authorship	202
Abstract.....	205
Results	206
Discussion.....	225
References	229
Supplementary table	232
Supplementary figure	234
CHAPTER 6 - FINAL DISCUSSION	235
Final Discussion	236
References	240

APPENDIX A – Review article: The role of Angiotensin II and relaxin in vascular adaptation to pregnancy	241
Statement of Authorship	242
Abstract.....	245
Introduction	246
Materials and Methods	247
Results and Discussion.....	248
Future perspective	268
Conclusion.....	269
References	270
Article	289
APPENDIX B – Supplementary data of chapter 4 – time point effect for repeated measurements, including body weight, blood pressure, glucose tolerance test and insulin challenge.....	302
Supplementary data	303

DECLARATION

I certify that this work contains no material which has been accepted for the award of any other degree or diploma in my name, in any university or other tertiary institution and, to the best of my knowledge and belief, contains no material previously published or written by another person, except where due reference has been made in the text. In addition, I certify that no part of this work will, in the future, be used in a submission in my name, for any other degree or diploma in any university or other tertiary institution without the prior approval of the University of Adelaide and where applicable, any partner institution responsible for the joint award of this degree.

The author acknowledges that copyright of published works contained within the thesis resides with the copyright holder(s) of those works.

I give permission for the digital version of my thesis to be made available on the web, via the University's digital research repository, the Library Search and also through web search engines, unless permission has been granted by the University to restrict access for a period of time.

Ngoc Anh Thu Doan

14.11.2023

ACKNOWLEDGEMENTS

I acknowledge and pay my respect to the Kaurna people, the traditional custodians whose ancestral lands I study and live on. I also acknowledge the financial support from the Adelaide Graduate Research Scholarship, Adelaide Graduate Research School, The University of Adelaide.

“Feeling grateful” is not enough to describe my emotions, looking back at my PhD journey. I was surrounded and supported by the most wonderful people in the world! First of all, I would like to thank Dr Tina Bianco – my primary supervisor for both Honours and PhD degrees. You inspired me to do Science, to think of challenges as opportunities, and to have a self-trust mindset. Thank you for being patient with me even when you had explained something three times to me, and I still did not get it.

I sincerely thank my co-supervisor, Dr Lisa Akison. Thank you for always immediately responding to my very-long, full-of-questions emails with the most detailed answers and guidance. Your help has truly made a difference and I appreciate your support. I also want to express my deepest gratitude to Professor Mary Wlodek, who has generously provided samples and physiological data of the animal model used in my PhD project. I appreciate your unwavering support, and your in-depth knowledge truly is an inspiration to me.

I would like to thank Professor Laura Parry, Dr Marnie Winter, Dr Karen Moritz, Dr Helle Bielefeldt-Ohmann, Dr Aaron Phillips, Dr James Cowley, Dr Jessica Briffa, and Dr Tania

Romano, whom I have been lucky enough to collaborate with. Thank you for taking your time to share your knowledge with me.

To my RABLAB “family”, studying abroad as a PhD candidate has been made an enjoyable experience, thanks to you. I would like to thank the past and present members of RABLAB for their unconditional support, for creating a friendly and inclusive environment. And the amazing sweet-treats! Thank you, Professor Rachel Burton, “Lab Mum” Sandy Khor, Dr Renee Phillips, Dr Carolyn Schultz, Dr Ali Hassan, Dr Matthias Salomon, Dr Lisa O'Donovan, Dr Juanita Lauer, Dr Nahal Habibi, Dr James Cowley, Dr Aaron Phillips, Belinda Akomeah, Alison Gill, Lucija Strkalj, Alex Clare, Chelsea Matthews, Saber Sohrabi, Sara Jalali. Jacqui and Zane! I would say the “PhD students Coffee Club” catch-ups were one of best things about doing a PhD. Thank you for being my companions over the years. I wish you all the best, and good luck with your PhD journeys! (P/S, Tina is now yours).

To Lucid Dream Music Club, you were the sunshine on my cloudy days. I made (lots of) friends who are not only willing to teach me how to sing in mixed voice, but also willing to do grocery shopping for me and put them in front of my door when I tested positive for Covid. To Trang, Duc, Tung, thank you for cooking for me when I got back home at 9pm from the lab!

Finally, to my family, my mum, my dad, my brother and sister-in-law, and my future nephew, this Thesis is dedicated to you. Thank you for all the love and support you have always given me so that I can pursue my dreams.

LIST OF PUBLICATIONS AND EXPECTED PUBLICATIONS

- 1. Doan, T. N. A.,** Akison, L. K., & Bianco-Miotto, T. (2022). Epigenetic mechanisms responsible for the transgenerational inheritance of intrauterine growth restriction phenotypes. *Frontiers in Endocrinology*, 13, 838737. <https://doi.org/10.3389/fendo.2022.838737>.
- 2. Doan, T.N.A.,** Cowley, M. J., Phillips, L. A., Briffa, F. J., Leemaqz, Y. S., Burton, A. R., Romano, T., Wlodek, E. M., & Bianco-Miotto, T. (2024). Imprinted gene alterations in the kidneys of growth restricted offspring may be mediated by a long non-coding RNA. *Epigenetics*, 19(1), 2294516. <https://doi.org/10.1080/15592294.2023.2294516>.
- 3. Doan, T. N. A.,** Bianco-Miotto, T., Parry, L., & Winter, M. (2022). The role of angiotensin II and relaxin in vascular adaptation to pregnancy. *Reproduction*, 164(4), R87-R99. <https://doi.org/10.1530/REP-21-0428>.
- 4. Doan, T.N.A.,** Cowley, M. J., Phillips, L. A., Briffa, F. J., Burton, A. R., Romano, T., Wlodek, E. M., & Bianco-Miotto, T. (2023). Uteroplacental insufficiency results in an increased risk of developing metabolic disease across generations in the paternal line of growth restricted rats. Target journal: *The Journal of Physiology*.
- 5. Doan, T.N.A.,** Cowley, M. J., Phillips, L. A., Briffa, F. J., Burton, A. R., Romano, T., Wlodek, E. M., & Bianco-Miotto, T. (2023). Uteroplacental insufficiency results in an increased risk of developing renal dysfunction across generations in the paternal line of growth restricted rats. Target journal: *The Journal of Physiology*.

CHAPTER 1

THESIS INTRODUCTION

Introduction

The *in utero* developmental environment is known to play an important role in shaping future health and susceptibility to chronic diseases. Exposure to environmental factors during pregnancy, including but not limited to uteroplacental insufficiency (UPI), suboptimal diets, drugs, caffeine, or pathogen-induced immune activation results in the intrauterine growth restriction (IUGR) of the developing fetus, otherwise known as “small for gestational age” (SGA). Most IUGR babies are born with low birth weight and signs of aberrant cardiorenal or metabolic function, predisposing them to late-onset health problems. Due to the difficulties in obtaining the appropriate tissues for sampling, as well as carrying out both longitudinal and generational studies in humans, rodent studies are more advantageous for investigating the effects of IUGR on offspring phenotypes, as well as the mechanisms behind the increased disease risk.

This Thesis is comprised of 5 chapters. **Chapter 1** is the Introduction, which provides the general rationale for this PhD project and the layout of the Thesis. **Chapter 2** is a published review (2022) on health outcomes of the growth restricted offspring in both human and rodent studies. The associations between IUGR and each specific chronic disease risk, including hypertension, kidney disease, and diabetes were discussed in detail. Using tissues extracted from offspring across different generations, epigenetic mechanisms such as DNA methylation, histone modifications and long non-coding RNAs were investigated and suggested to play a role in the sex-specific and multigenerational transmission of IUGR phenotypes in these studies. One of the IUGR models mentioned in this chapter was a UPI-induced IUGR model in rats, established by Professor Mary Wlodek (The University of Melbourne). This model has been shown to reflect metabolic characteristics in humans. We

previously reported* changes to expression of a DNA methyltransferase and two imprinted genes (*Cdkn1c* and *Kcnq1*) known to be important in both human and rodent kidney development in kidneys of offspring from this model. The mentioned review and this article provide the rationale for the remainder of the thesis, highlighting that the mechanisms involved in the sex-specific differences and transgenerational transmission of IUGR phenotypes requires further studies.

**Doan TNA, et al. Epigenetic mechanisms involved in intrauterine growth restriction and aberrant kidney development and function. Journal of Developmental Origins of Health and Disease. 2021;12(6):952-962. doi:10.1017/S2040174420001257.*

In **Chapter 3** (research article, recently published, 2024), we examined the epigenetic alterations that may explain the changes to imprinted gene expression we had previously reported in this IUGR rat model. DNA methylation of an imprinting control region (KvDMR1) known to regulate expression of *Cdkn1c* and *Kcnq1* was studied using region-specific DNA methylation analysis. Additionally, expression of the antisense long non-coding *Kcnq1ot1* was investigated as well as additional neighbouring imprinted and non-imprinted genes in this cluster.

Besides investigating the molecular mechanisms that may be involved in the IUGR induced phenotypes, another focus of this Thesis was whether there was transmission of IUGR phenotypes across generations down the paternal line of the UPI model, similar to the published maternal line. In **Chapters 4 and 5** (research manuscripts, unsubmitted), data of growth profiles, cardiovascular function, metabolic function (**Chapter 4**) and renal function (**Chapter 5**) of growth restricted offspring in the first (F1), second (F2), and third (F3) generations from the paternal line were analysed. Results from Chapters 4 and 5 suggest that there are changes to the metabolic and renal function of offspring in the paternal line, even in

the F2 and F3 generations which are not directly affected by the *in utero* insult. These offspring are potentially at a higher risk of developing chronic diseases later in life, especially if exposed to another environmental stress postnatally. For instance, the extensive vasculature and haemodynamic changes occurring during a normal pregnancy (discussed in **Appendix A** (review, published 2020)) might act as a “second hit” in the growth restricted females, magnifying the early symptoms into clinical conditions. The final chapter, **Chapter 6**, presents a general discussion of findings from this research, the significance of these findings, and future directions.

CHAPTER 2

EPIGENETIC MECHANISMS

RESPONSIBLE FOR THE

TRANSGENERATIONAL

INHERITANCE OF

INTRAUTERINE

GROWTH RESTRICTION

PHENOTYPES

Statement of Authorship

Statement of Authorship

Title of Paper	Epigenetic mechanisms responsible for the transgenerational inheritance of intrauterine growth restriction phenotypes		
Publication Status	<input checked="" type="checkbox"/> Published	<input type="checkbox"/> Accepted for Publication	
	<input type="checkbox"/> Submitted for Publication	<input type="checkbox"/> Unpublished and Unsubmitted work written in manuscript style	
Publication Details	Doan, T. N. A. , Akison, L. K., & Bianco-Miotto, T. (2022). Epigenetic mechanisms responsible for the transgenerational inheritance of intrauterine growth restriction phenotypes. <i>Frontiers in endocrinology</i> , 13, 838737. https://doi.org/10.3389/fendo.2022.838737		

Principal Author

Name of Principal Author (Candidate)	Ngoc Anh Thu Doan		
Contribution to the Paper	Performed the literature search, interpreted the data and wrote the manuscript		
Overall percentage (%)	90		
Certification:	This paper reports on original research I conducted during the period of my Higher Degree by Research candidature and is not subject to any obligations or contractual agreements with a third party that would constrain its inclusion in this thesis. I am the primary author of this paper.		
Signature		Date	6.11.2023

Co-Author Contributions

By signing the Statement of Authorship, each author certifies that:

- i. the candidate's stated contribution to the publication is accurate (as detailed above);
- ii. permission is granted for the candidate to include the publication in the thesis; and
- iii. the sum of all co-author contributions is equal to 100% less the candidate's stated contribution.

Name of Co-Author	Lisa K. Akison		
Contribution to the Paper	Critically revised the manuscript		
Signature		Date	6.11.2023

Name of Co-Author	Tina Bianco-Miotto		
Contribution to the Paper	Critically revised the manuscript and supervised the project		
Signature		Date	6.11.2023

Epigenetic mechanisms responsible for the transgenerational inheritance of intrauterine growth restriction phenotypes

Thu Ngoc Anh Doan^{1,2}, Lisa K. Akison³, Tina Bianco-Miotto^{1,2*}

¹School of Agriculture, Food and Wine, & Waite Research Institute, University of Adelaide, Adelaide, South Australia, Australia

²Robinson Research Institute, University of Adelaide, Adelaide, South Australia, Australia

³School of Biomedical Sciences, University of Queensland, Brisbane, Queensland, Australia

*** Correspondence:**

Tina Bianco-Miotto

tina.bianco@adelaide.edu.au

Keywords: intrauterine growth restriction, uteroplacental insufficiency, small for gestational age, transgenerational transmission, epigenetic mechanisms, cardiometabolic disease, kidney dysfunction

Article type: narrative review

Abstract

A poorly functioning placenta results in impaired exchanges of oxygen, nutrition, wastes and hormones between the mother and her fetus. This can lead to restriction of fetal growth.

These growth restricted babies are at increased risk of developing chronic diseases, such as type-2 diabetes, hypertension, and kidney disease, later in life. Animal studies have shown that growth restricted phenotypes are sex-dependent and can be transmitted to subsequent generations through both the paternal and maternal lineages. Altered epigenetic mechanisms, specifically changes in DNA methylation, histone modifications, and non-coding RNAs that regulate expression of genes that are important for fetal development have been shown to be associated with the transmission pattern of growth restricted phenotypes. This review will discuss the subsequent health outcomes in the offspring after growth restriction and the transmission patterns of these diseases. Evidence of altered epigenetic mechanisms in association with fetal growth restriction will also be reviewed.

Introduction

Intrauterine growth restriction (IUGR) refers to poor growth during pregnancy, which results in babies being born small for gestational age (SGA), and with low birth weight (LBW) (1).

One of the common causes of IUGR is uteroplacental insufficiency (UPI), in which the placenta functions poorly, causing an insufficient supply of oxygen and nutrients to the developing fetus (2).

There is a high prevalence of IUGR worldwide, especially in developing countries (approximately 27% of all live births (3)), which is a significant concern, as epidemiological studies have shown that being growth restricted is associated with an increased risk of

developing chronic diseases later in life (1, 4-9). In addition, various animal models have shown that IUGR offspring develop kidney dysfunction and cardiometabolic disease later in life (2, 10-15). Interestingly, these IUGR phenotypes are sex-specific and their transmission is multigenerational through both the maternal and paternal lines (11-14, 16-18).

The underlying mechanisms of how IUGR predispose offspring to chronic disease later in life remains to be determined. However, epigenetic mechanisms may be involved as they have been shown in several animal studies to be potential mechanisms for the multigenerational transmission of disease (17).

Intrauterine growth restriction and chronic disease risk

Hypertension and kidney disease

Epidemiological studies in humans have reported that growth restricted infants have an increased risk of developing chronic diseases later in life (Figure 1, (5-8, 19-24)). For instance, IUGR children at 6 years of age have been shown to have a 1.8 times higher risk of developing hypertension compared to non-IUGR children (6). Additionally, individuals born SGA had increased systolic and diastolic blood pressure by 4.5 and 3.4 mmHg, respectively, at the age of 50 (5). When these results were adjusted for confounding factors such as sex, age, and body-mass index, IUGR was still significantly associated with hypertension (5, 6). In other studies, when sex is taken into consideration, the development of hypertension in association with LBW can produce conflicting results. For example, there was one study that found an association in IUGR males only (24), while a different one found an association only with IUGR females (23). However, differences in the size of the study (15600 vs 976 children), method of measuring blood pressure (one-time systolic and diastolic blood pressure

measurement vs 24h systolic blood pressure measurement), and the age of examined children (3-6 years old (24) vs 6-16 years old (23)) may be factors that contributed to the observed sex-specific differences. In line with this finding, an inverse relationship was found between birthweight and blood pressure of IUGR infants in a study that examined 1310 junior high school students (20). However, this relationship was then lost as the children reached adolescence (12-14 years of age), even when adjusted for confounding factors. This suggests that there might be a possible adaptation mechanism in the adolescents to overcome IUGR-related hypertension.

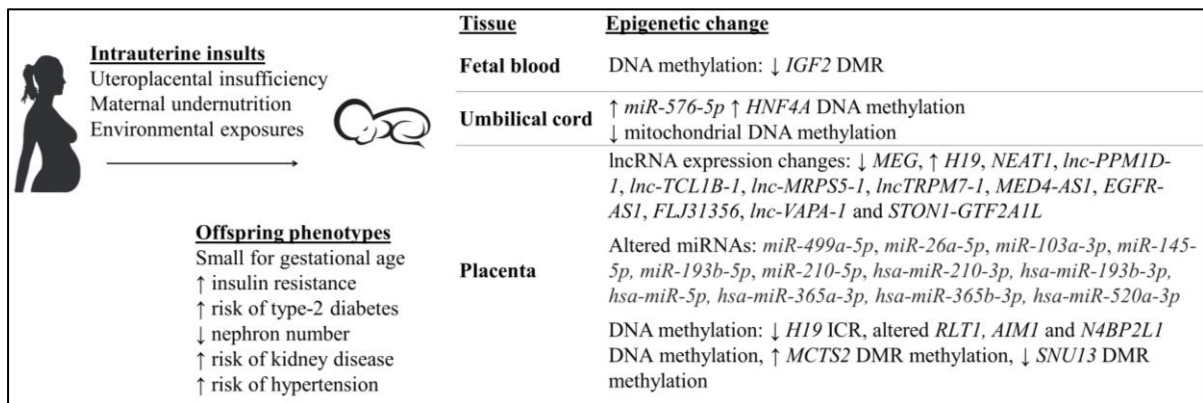


Figure 1. Small for gestational age (SGA) babies who were exposed to intrauterine insults have altered epigenetic mechanisms and aberrant physiological changes, predisposing them to an increased risk of developing various chronic diseases later in life (5-8, 19-24, 63-76, 91, 94).

Unlike the examination of hypertension by measuring blood pressure, the precise determination of kidney disease mostly requires more invasive measurement methods, such as counting of glomerular number after organ collection and sample sectioning (7, 8).

Therefore, few studies are carried out in humans, especially in growth restricted infants, to

evaluate the association between IUGR and kidney disease. However, papers published by Wang *et al.* in 2014 (9) and 2016 (25), respectively, were two of the rare studies that investigated the effect of human aberrant fetal growth environment on kidneys of fetuses. In both studies, fetuses and their kidney samples were collected from mothers who terminate their pregnancy due to preeclampsia (9), placental abruption, deformities of fetuses, and other intrauterine insults (25). Both papers reported negative effects that IUGR had on the fetuses, including significantly low birth weight (< 2 kg), approximately 0.4 times less nephron number, increased expression of pre-apoptosis proteins within kidney tissues (9), and reduced renal renin-angiotensinogen RNA levels by half the non-growth restricted fetuses (25). This is significant, as the renin-angiotensinogen system is known to play a crucial role in maintaining the sodium homeostasis within the kidney, as well as regulating blood pressure, especially during pregnancy (25). These papers are consistent with studies that have shown a decline in glomerular number (more than 20%) in low birth weight individuals who died from cardiovascular disease as adults, in comparison to normotensive people (7, 8). Together, these studies suggest an important contribution of the kidney to hypertension development in IUGR individuals.

Using different animal models, the association between IUGR and the development of chronic diseases can also be evaluated (Figure 2, (2, 10-15, 18, 26-41)). In the early 2000s, the association between IUGR induced by UPI and blood pressure level was studied using a model in which placental insufficiency was established by placing silver clips around the abdominal aorta and on the branches of uterine arteries of pregnant rats at day 14 of gestation, which severely reduced blood flow between mother and the fetus (27). UPI-induced rats produced LBW offspring, 12% lighter in weight compared to control, with an increased risk of developing hypertension in both IUGR males and females, as their mean

arterial pressure at 8 weeks of age was 12 mmHg higher than the control (27). However, at 12 weeks of age, only the increased mean arterial pressure in F1 male offspring was still significant, suggesting a sex-specific hypertension maintenance mechanism. There was no statistically significant association between the observed increased arterial pressure and renal function of the offspring found in this study. Glomerular filtration rate, effective renal plasma flow and 24-hour sodium excretion were not different in IUGR rats compared to the control, even when they were adjusted for kidney weight (27). Meanwhile, the bilateral uterine vessel ligation model produced restricted F1 male offspring that had higher blood pressure and an enlargement of the heart's left ventricle at 22 weeks of age, compared to the control, as a consequence of persisting high blood pressure (10). Lower body weight and glomerular number (clusters of capillaries in the kidney, reduced by 27% of the control) were also reported at 6 months of age (10). These results were reproducible in other studies, with lower kidney weight (measured at postnatal day 1 and 7) and nephron deficit (at 18 months of age) occurring in both sexes and hypertension (at 18 months of age) being present only in male rats (2, 11, 37). Glomerular hypertrophy, an outcome to compensate for the IUGR-related glomerulus reduction, was found to be higher in the F1 growth restricted male rats compared to females at day 120 after birth, suggesting a sex-specific response of the growth restricted offspring towards kidney injury (15). Similarly, 18-month-old growth restricted female rats had preserved mesenteric and renal arterial smooth muscle and endothelial function, which may in part explain why they did not develop hypertension (32). However, the mechanisms behind this remains to be identified. Interestingly, the transmission of hypertension and kidney diseases is multigenerational, as reduced nephron number, left ventricular hypertrophy and hypertension were reported in the non-restricted F2 generation (13, 14).

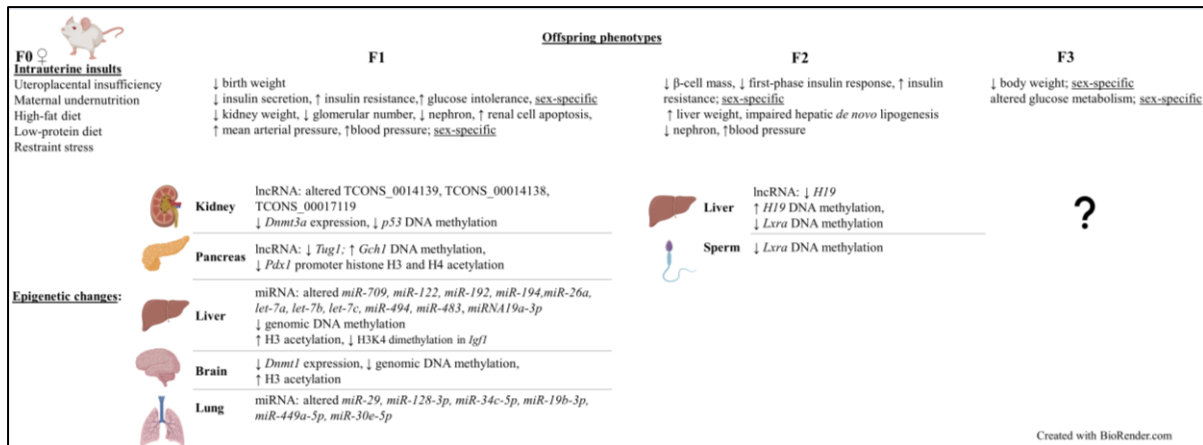


Figure 2. Intrauterine growth restriction (IUGR) phenotypes are sex-specific and can be transmitted to subsequent generations, including the restricted F1 and non-restricted F2 and F3 offspring (intergenerational). Similar to human studies, altered epigenetic mechanisms such as non-coding RNA modifications, DNA methylation, and histone modifications were also found in these offspring. Results obtained from different rat and mouse IUGR models (2, 10-15, 18, 26-41, 47, 48, 78, 80-87, 89, 93).

Apart from rats, studies of UPI-induced IUGR in other animal models (e.g. rabbit (42) and guinea pig (43)) also support the association between IUGR and reduced glomerular number and/or hypertension in the growth restricted offspring. IUGR induced by other intrauterine causes was also shown to be associated with hypertension or aberrant renal function and development (34, 36, 40). For example, F0 pregnant rats were fed a 50% deficit food intake diet throughout pregnancy to produce growth restricted F1 offspring (40). F1 males were mated with control healthy females to produce the F2 generation (paternal line). In a normoxia environment (where the oxygen concentration is normal), mean pulmonary arterial pressure, right ventricular hypertrophy index, and media wall area thickness were not significantly different between IUGR and the control males, in both generations. However, F1 and F2 male rats that were placed in an oxygen-deficient chamber for 2 weeks showed an

increase in all three mentioned parameters, indicating an increased risk of developing pulmonary arterial hypertension later in life (40). In line with this finding, the expression of endothelin-1 (ET-1), a vasoconstrictor that is important for cell proliferation, cell migration, and blood vessel development, was significantly increased in pulmonary vascular endothelial cells (PVECs) extracted from F1 and F2 IUGR males. This led to aberrant PVEC proliferation, migration, and angiogenesis, all of which are signs of pulmonary vascular endothelial dysfunction (40). On the other hand, in 6-month-old LBW restricted rats whose mothers received only 50% the calories during pregnancy, there was a significant reduction in kidney weight (maximal value only reached 91% of the control) and glomerular number (by 27% the control) (36). Meanwhile, a low-protein diet (reduced by 11% of the control) in pregnant rats resulted in a significant decrease in glomerular number (by 22.6% the control; at 3 months of age) and increased renal cell apoptosis of LBW F1 offspring (34).

Diabetes

Besides hypertension and kidney dysfunction, diabetes is another disease that has been shown to be associated with IUGR. Women whose birth weights were less than 2.5 kg (typically the clinical definition for LBW (44)) have a 1.83 times higher risk of developing type 2 diabetes as they age compared to women with birthweights above this threshold (19, 21). Decreased insulin-stimulated glucose uptake, or insulin resistance, one of the common hallmarks of type 2 diabetes, was also reported in IUGR young adults whose birth weights were below the 10th percentile for their gestational age (22).

Different animal models can be used to study the association between IUGR and the development of type-2 diabetes, such as UPI model that has metabolic characteristics

comparable to that of humans (18, 26, 29), IUGR rats induced by maternal calorie restriction (41, 45), or IUGR fetal sheep induced by exposing pregnant ewes to an environment with highly increased humidity and temperature (46). When both uterine arteries of pregnant rats are ligated at day 19 of gestation to imitate UPI occurring in pregnancy, F1 growth restricted rat offspring had significantly lower birth weight (5.96 g) compared to the sham control offspring (7.00 g) (26). Rat offspring in both restricted and control group then reached relatively similar body weights at approximately 7 weeks of age. However, as the IUGR F1 rats aged, they had significantly reduced insulin secretion of β -cells (by half the control at 1 week of age and completely absent at 26 weeks of age), insulin-resistance and glucose-intolerance hence hyperglycemia (26). Similar findings were also reported in other studies that applied the same UPI-inducing method of uterine arteries ligation (18, 29). Three months old growth restricted F1 rats developed hepatic insulin resistance, which was represented by its impaired insulin function in controlling the hepatic glucose production (HGP) important for maintaining blood glucose equilibrium (1.6 times higher HGP in IUGR rats compared to the control) (29). A decrease by 50% of pancreatic insulin content was also reported in the LBW growth restricted rats compared to control at the same time point of age (18). Moreover, there was a sex-specific reduction of β -cells mass in these restricted offspring compared to the control, with 40% and 50% reduction in IUGR males and females, respectively (18).

Similar to the observations for hypertension and kidney disease risks in IUGR animal studies, both of the F1 and F2 generations are at a higher risk of developing diabetes, suggesting that there is a multigenerational transmission of IUGR phenotypes (12). When growth restricted F1 female rats were mated with healthy males, 6-month-old F2 offspring also had altered pancreatic β -cell mass (reduced by 29% in males and increased by two-fold the control in females) and first-phase insulin response (reduced by 35% in males and 38% in females)

(12). The sex-specific differences in pancreatic β -cell mass between 3 months old F1 rats (18) and 6 months old F2 rats might be due to the difference in time point in which they were examined. For instance, at 6 months of age, female rats may have developed compensatory mechanisms for the disease. Additionally, as these defects were resolved when the rats aged (determined at 12 months of age (12)), male rats may have also developed similar mechanisms at a later age. However, this remains to be shown. In a different IUGR model where F0 pregnant rats were injected with the corticosteroid dexamethasone, from day 15 to 21 of gestation, F2 offspring had reduced birth weight and F2 5-week-old males developed glucose tolerance, represented by a significant increase in the activity of hepatic phosphoenolpyruvate carboxykinase (PEPCK), an enzyme that is involved in glucose metabolism (47). Additionally, these F2 growth restricted males were reported to have higher plasma glucose level at 4 months of age, and higher basal insulin level at 6 months of age, compared to the control (47). Similarly, when F0 pregnant rats received a restricted diet (food intake reduced by 50% the control) from day 11 to 21 of pregnancy, the effect of IUGR on insulin resistance was also seen in a multigenerational pattern (41). Specifically, F1 restricted females were also given a restricted diet from day 1 to day 21 postnatal. At 2 months of age, F1 females were mated with control males, and F2 1-day-old embryos were transferred to control recipient females. F2 female offspring from the IUGR group had significantly higher liver weight, baseline fasting plasma glucose, and insulin concentrations, despite a similar weight from birth to 15 months postnatal, compared to the control (41). The F2 IUGR group also developed insulin resistance at 15 months of age, represented by reduced plasma glucose/insulin ratio during glucose tolerant test, and lower concentration of plasma membrane-associated GLUT4, a protein that plays an important role in insulin-dependent glucose transport into skeletal muscles. Reduced function of PKC ζ , an enzyme involved in insulin-signalling pathway, was also found in skeletal muscle of 15 months old F2 females in

the IUGR group (41). Likewise, in a model of *in utero* low-protein consumption in rats, there was an adverse effect of IUGR on the glucose metabolism of F3 offspring at approximately 2 months of age (30). To be specific, there was a significantly higher fasting plasma glucose level in F3 females compared to sham. Meanwhile, there was a significant increase in insulin level of F3 males compared to sham at both fasting stage and 30 minutes after the glucose injection (30), suggesting that IUGR phenotypes are sex-specific and their transmission can be intergenerational. In line with this finding, reduced body weight at days 1 and 7 after birth by 0.5g, compared to the control offspring, was also reported in the F3 rats whose grandmothers were exposed to restraint stress during pregnancy (39). Additionally, these animals were reported to have sensorimotor dysfunction at postnatal day 7, as their response time during the inclined plane test was significantly slower compared to the control (39). On the other hand, altered glucose tolerance and insulin secretion could be improved (determined in F1 male rats at 6 months of age) by cross-fostering the UPI-induced growth restricted offspring to a sham control mother for lactation, a period important for offspring development (31). This proposed that there could be reversal strategies for IUGR-related diseases and/or solution to modify their effects on the growth restricted offspring. However, intervention studies are beyond the scope of this review. Additionally, it should be noted that when IUGR was caused by a severe maternal protein-restriction diet (e.g. 5 g of protein/100 g of diet) during pregnancy, postnatal catch-up could be impaired (48). Male and female rats at 6 months of age had significantly increased fasting serum glucose level (20% and 25% the control values in F1 and F2 generation, respectively), despite being fed a control diet during lactation (48). F1 and F2 male offspring also developed insulin resistance at 6 months of age (48).

In summary, the above observations of IUGR infants having an increased risk of developing various diseases later in life are in line with the Developmental Origins of Health and Disease hypothesis, proposing that adverse events that occur during the maturation of gametes, at conception and early embryonic development can program long-term risks of chronic diseases in the LBW offspring (49). As the world-wide prevalence of type 2 diabetes, chronic kidney disease and hypertension is significantly high (6.28 % for diabetes, 9.1% for kidney disease, and approximately 30% for hypertension (in adults) (50-52)), there is an urgency for researchers to investigate IUGR and its mechanisms in programming chronic diseases in humans. Nevertheless, due to the complexity and ethical rules in human research, most in-depth experiments that study IUGR are carried out in rodents. Additionally, animal models provide a mechanism for investigating the impact of IUGR across multiple generations and to determine the possible molecular mechanisms involved.

Intrauterine growth restriction and the associated altered epigenetic mechanisms

Epigenetic mechanisms

Epigenetics can be described as heritable modifications to the chromatin that regulate gene expression without altering the DNA nucleotide sequence (53). An example of a modification that creates such changes is DNA methylation. DNA methylation involves the DNA methyltransferase-catalysed addition of a methyl group to a DNA cytosine base (54). In mammals, DNA methylation happens primarily at CpG sites, that is, a cytosine adjacent to a guanine base in the 5'-3' direction. DNA methylation at gene regulatory regions such as promoters is associated with gene silencing (55). Additionally, DNA methylation has an important role in other processes such as X-chromosome inactivation and imprinting (56).

Another epigenetic modification is histone modifications. These include histone acetylation, which is the addition of an acetyl group to the lysine residue of the nucleosomal core histones' N-terminal tail (54). Histone deacetylation, specifically at histones H3 and H4 is associated with gene repression (57). In addition to this, regulatory non-coding RNAs are known to be involved in transcriptional, post-transcriptional, and translational regulation hence are also involved in gene silencing (58, 59). Two large subsets of non-coding RNAs are long non-coding RNAs which are > 200 nucleotide-long, and short non-coding RNAs like microRNAs (miRNAs), short interfering RNAs (siRNAs), and piwi-interacting RNAs (piRNAs) which are all less than 200 nucleotide-long (60). Altered expression of both miRNAs and lncRNAs have been shown to be associated with altered histone modifications and DNA methylation status of genes (61, 62).

Studies of blood samples

IUGR has been shown to be associated with altered epigenetic mechanisms (Figure 1, (63-76)).

Blood samples from the Dutch Hunger Winter famine were used to investigate DNA methylation from individuals exposed to reduced calorie intake in very early (60 people) or late (62 people) gestation (77). Although there was no significant difference in birth weight among the individuals (64), there was a decrease by 5.2 % in DNA methylation of the *IGF2* imprinted gene differentially methylated region (DMR) in people exposed to famine in early gestation, compared to the same-sex siblings who were not exposed to famine during pregnancy. Whilst, people exposed to famine in late gestation had no altered DNA methylation (77). This observation suggests the importance of the timing of exposure to intrauterine insults, specifically during the early developmental stage, in which epigenetic

mechanisms within the fetus is programmed and may be permanently maintained into adulthood. In a different study, blood samples from 24 IUGR infants were investigated using Illumina Human Methylation 450 k array to analyse differences in genome-wide DNA methylation and gene expression, compared to data from 12 control healthy infants (78). Within the IUGR group, 5460 differentially methylated CpG loci from 2254 genes were identified. Using Kyoto Encyclopedia of Genes and Genomes database, more than 50 pathways affected by changes in the methylation status of these gene were determined, such as metabolic pathways, antigen processing and presentation, apoptosis, insulin signalling pathway, and neurological disorder pathways (78). In addition to this, increased DNA methylation, by 6.1% the control, of the type 2 diabetes-related *HNF4A* gene promoter was found in CD34+ stem cells from umbilical cord blood samples of IUGR newborns (65). More than 800 genome differentially methylated positions (DMPs) was found in leucocytes from umbilical cord blood samples of IUGR neonates, compared to the control (79). These DMPs were located within genes that are critical for key cellular processes that impact the fetal growth and development, such as organogenesis, metabolism, and immunity. *D-loop* hypomethylation of mitochondrial DNA found in fetal cord blood samples was also reported in IUGR neonates who were exposed to placental insufficiency (70). The hypomethylation was in association with higher mitochondrial biogenesis (i.e., increased mitochondrial DNA levels), which is a possible mechanism to compensate for reduced oxygen by UPI. Results in these studies were all adjusted for other complications that may have occurred during pregnancy such as gestational hypertension, gestational diabetes and preeclampsia (65, 70, 79).

Besides DNA methylation, altered expression of miRNAs have been recently reported in human umbilical cord tissues collected from IUGR pregnancies (73). To be specific, the study

included samples from IUGR children with or without growth catch-up at 1 and 6 years of age, and control children who were born appropriate for gestational age (73). At 1 year of age, the expression of a miRNA *miR-576-5p*, which is known to be involved in kidney and liver diseases, was significantly enhanced in IUGR with catch-up children compared to both IUGR without catch-up and control children (73). Moreover, within the IUGR with catch-up group, *miR-576-5p* expression was shown to have a significant association with weight, height, catch-up weight, and catch-up height of the children, after being adjusted for confounding factors such as sex, gestational age, maternal smoking status, etc. Besides the mentioned parameters, at 6 years of age, *miR-576-5p* expression was also shown to be associated with renal fat, suggesting an important role of *miR-576-5p* in cardiometabolic diseases, and that alterations of this miRNA due to IUGR may increase the risk of developing these diseases later in life (73).

Studies of kidney tissues

Animal studies that specifically focused on altered epigenetic mechanisms in the UPI-induced IUGR offspring have also been carried out in different organs and tissues (Figure 2, (28, 33, 35, 37, 38, 80-87)). Decreased expression, by 19% the control, of *Dnmt3a*, a gene that is responsible for *de novo* DNA methylation was found in kidney tissues of F1 IUGR rats at embryonic day 20 (37). Meanwhile, decreased apoptosis-suppressing *Bcl-2* gene expression and increased pro-apoptotic protein-encoding *Bax* and *p53* expression were identified in kidneys of F1 IUGR rats at term, which was associated with reduced glomerular number (by 23% the control) of rat pups (28). Correlatively, there was reduced DNA methylation of CpG islands at the promoter region (by 56.3% the control) of *p53* (28).

Whilst, significantly altered expression of three long non-coding RNAs (lncRNAs) (TCONS_0014139, TCONS_00014138, and TCONS_00017119) at day 1 and day 10 postpartum (pn1 and pn10), confirmed by both microarray and qPCR, were found in kidneys of LBW male rats whose mothers were also fed a low-protein diet during pregnancy (35). The altered expression of these lncRNAs were associated with altered mRNA expression at pn1 and pn10 of *MAPK4*, which encodes for a protein that involves in renal ureteric bud morphogenesis. Additionally, the aberrant expression of these lncRNAs is also correlated with a decrease in nephron number of LBW rats at pn1, suggesting an important role of them in nephron endowment (35). Furthermore, altered expression of *Cdkn1c* and *Kcnq1*, two imprinted genes that are regulated by the *Kcnq1ot1* lncRNA, was found in kidney tissues of UPI-induced IUGR rats at day 1 after birth (37). However, further research is required to investigate whether changes to *Kcnq1ot1* was the epigenetic mechanism that affected the imprinted gene expression in this study.

Studies of liver tissues and pancreas tissues

Similar to results obtained from blood samples and kidney tissues, abnormal DNA methylation have also been found in hepatic tissues from IUGR studies (33, 84, 85). Importantly, in hepatic tissues, the multigenerational transmission and reversibility of the altered epigenetics was detected in F2 non-restricted offspring (85). Growth restricted F1 rats that underwent intrauterine UPI were fed with either a control diet or essential nutrient supplemented (ENS) diet (i.e. rich in methyl donors) and bred spontaneously to produce the F2 offspring (85). Within the F2 generation, 21-day-old rats whose F1 mothers received a control diet had statistically reduced DNA methylation of the *H19* gene promoter (7% less than the sham lineage), in association with reduced *H19* expression (0.4-fold the sham

lineage) (85). Meanwhile, 21-day-old F2 rats whose F1 mothers received ENS diet had increased *H19* promoter methylation (34% more than the sham lineage), with a 6.6-fold increase in *H19* expression (85). In line with this finding, F2 offspring of pregnant mice that were fed with only 50% the control group's food intake had significantly lowered expression of the *Lxra* gene ($p < 0.01$) in their liver tissues, which plays a key role in *de novo* lipogenesis (33). Hepatic *de novo* lipogenesis was also impaired in the F2 adult mice (33). Furthermore, this was associated with statistically reduced methylation within the 5'UTR region of *Lxra*, both in the sperm samples of IUGR F1 males and liver samples of non-restricted F2 fetuses and adult mice. Therefore, it is suggested that there was a multigenerational transmission of altered *Lxra* methylation within both F1 and F2 generations (33). Meanwhile, one of the first studies to investigate whole-genome DNA methylation from pancreatic islet samples in the UPI-induced IUGR 7-week-old male rats discovered 1912 differentially methylated loci compared to the control, most of which occurred within the non-coding intergenic sequences between genes rather than promoter regions (84). Interestingly, the differential methylation was 45kb upstream of genes known to be important for homeostasis-maintaining processes (e.g. *Fgrfl*, *Gchl*, and *Vgf*) and were correlated with altered expression of these genes (84).

UPI-induced IUGR in several animal studies has also been shown to be associated with altered histone modifications (80-82, 88, 89). Histone H3 hyperacetylation, increased to 233% the control value, was detected in the liver of UPI-induced IUGR newborn rats, in association with hepatic genomic DNA hypomethylation (reduced methylation by 13.7% the control at day 21 after birth) (80). On the other hand, significantly reduced dimethylation at H3K4 in the *Igfl* region was reported in livers of IUGR rats whose mothers had a food restriction during pregnancy (89). Meanwhile, locus-specific assessment of the *Pdx1* gene, a

gene important for β -cell development and function, showed loss of *Pdx1* promoter H3 and H4 acetylation at 6 months of age and significant DNA hypermethylation (increased by 51.3% the control) in the pancreatic islets of F1 IUGR adult rats, and was associated with silencing of *Pdx1* (mRNA level reduced by 50.4%) (82). This may contribute to the later onset of type-2 diabetes in the growth restricted offspring.

In regards to non-coding RNAs, not many IUGR studies have been carried out to investigate their changes in the growth restricted offspring. Nonetheless, in agreement with results obtained from the placentas in human studies, reduced expression of the lncRNA *H19* and reduced DNA methylation status of its promoter region were reported in hepatic tissues of F2 growth restricted rats whose grandmothers (F0) underwent UPI (85). In hepatic tissues of F1 growth restricted mice whose mothers were fed with a high-fat diet pre-, during and post-pregnancy, there was also a significant reduction in expression of the miRNAs, including *miR-709*, *miR-122*, *miR-192*, *miR-194*, *miR-26a*, *let-7a*, *let-7b*, *let-7c*, *miR-494* and *miR-483* (83). Interestingly, a major of the altered miRNAs are predicted to have a common target, which is methyl-CpG binding protein 2 (83). In a different study where F0 pregnant mice were fed a low-protein/calorie-deficit (-40%) diet from week 3 of gestation, and growth restricted pups were cross-fostered to 3 different groups right after birth, either normal milk feeding (6 pups/dam), overfed (3 pups/dam), or nutrition restriction (10 pups/dam), significantly reduced H3K4me3 (trimethylated histone H3 on lysine 4) region at the *Akt1* gene, a gene that is known to play an important role in insulin resistance, was found in livers of 3-month-old IUGR males that either received normal milk feeding or were overfed, in association with reduced expression of *Akt1* (90). Interestingly, higher protein level of PTEN, one of the *Akt* activation inhibitors, was also found in livers of overfed 3-month-old males. In addition to this, significantly decreased levels of circulating *miRNA19a-3p*, a miRNA that

acts to regulate PTEN, were found in both normally fed and overfed IUGR males (90). These finding hence suggests an association between altered epigenetic mechanisms and the risk of developing insulin resistance later in life of IUGR offspring. Indeed, compared to F1 healthy control males, males that were either under nutrition restriction or overfed both had an increase in sensitivity to insulin at 3 months of age (90). At 12 months of age, the sensitivity to insulin increased for the nutrition restriction group but attenuated for the overfed group. Meanwhile, IUGR males that received normal milk feeding showed no difference in insulin sensitivity compared to healthy control males at 3 months of age. However, at 12 months of age, they developed insulin resistance (90). On the other hand, in pancreatic islets of growth restricted mice whose mothers were fed a low-protein diet, the expression of *Tug1*, a lncRNA that involves in diabetes and tumour development, were significantly lower at 1 day, 8 weeks, and 12 weeks post-partum, compared to the control (38). The aberrant glucose tolerance observed at 10 weeks old IUGR mice could be partially rescued by injection of 150 µg of *Tug1* overexpression sequence, suggesting that *Tug1* may play an important role in the mouse pancreatic development and function (38).

Studies of placental tissues

Altered DNA methylation of genes that are important for fetal growth and development has been reported in placentas from both human and animal IUGR pregnancies (72, 91-93). For example, placenta samples from healthy and complicated human pregnancies were investigated using the Illumina Infinium Human Methylation450 BeadChip arrays (HM450k) array platform (67 samples) and quantitative pyrosequencing (127 samples) (91). Specifically, 35 DMRs that are expressed across tissues (ubiquitous) were identified. In general, DNA methylation status of all DMRs was not significantly different between

complicated pregnancies and the control group. However, DNA hypermethylation was found at the *MCTS2* DMR, while hypomethylation was found at the *SNUI3* and *H19* ICR in IUGR placentas (91). Additionally, RT-PCR and Sanger sequencing confirmed that *H19* hypomethylation results in the biallelic expression of *H19* in the IUGR group. Similarly, a loss of methylation in *SNUI3* is associated with increased expression of this gene in the IUGR placentas. Interestingly, despite a similar DNA methylation status compared to that of the control, there was an increase in expression of *ZNF331* and a decrease in expression of *PEG10* and *ZDBF2* in the IUGR placentas (91). For DMRs that are placenta-specific, the same HM450k array data was used, and results were also confirmed using pyrosequencing. Out of 32 placenta-specific DMRs, methylation status of *AIM1* and *N4BP2L1* was significantly different in the IUGR group compared to the control. However, using microfluidic-based quantitative RT-PCR analysis, only four placenta-specific genes that had altered expression in IUGR samples compared to the control were identified, all of which were reduced in IUGR, including *ADAM23*, *GPR1-AS1*, *LIN28B*, and *ZHX3* (91). In line with this, altered DNA methylation of CpG island 1 of *RLTI*, a gene known to be important in placental development, was found in placenta samples from SGA and severe SGA fetuses, compared to healthy controls (72). Whilst, genome-wide DNA methylation patterns were investigated in placentas of IUGR identical twins who shared the same placenta (monozygotic twins) and had significant growth difference, represented by birthweight variations in the range of 21-59% (92). In placental tissues of IUGR twins, altered DNA methylation status (with differences larger than 10% compared to healthy control twins) were identified in DMRs that overlapped the promoters of 8 genes that are known to be important for lipid metabolism and neural development, including *DECRI*, *ZNF300*, *DNAJA4*, *CCL28*, *LEPR*, *HSPA1A/L*, *GSTO1*, and *GNE* (92). These results were still significant after being adjusted for twins' sex, gestational age, and maternal age. Interestingly, *DECRI* and *GSTO1*,

the two genes play a role in fetal growth, have also been altered in other IUGR studies in animal and human singleton pregnancies, suggesting potential shared molecular mechanisms in comparison to the IUGR growth-discordant monozygotic twins (92). Meanwhile, at embryonic day 10.5, altered DNA methylation was found within 20 different DMRs of imprinted loci from the placentas of F2 mice, whose grandmothers had a hypomorphic mutation in methionine synthase reductase (*Mtrr*), a gene that is important for methyl group utilisation and maternal folate metabolism (93). Changes in DNA methylation status of these DMRs were associated with changes in expression of imprinted genes such as *Zdbf2*, *Igf2*, and *Dlk1*, all of which play a key role in fetal development (93). As expected, growth restriction, delayed development, and defects of different organs including brain, heart and placenta were also found in these offspring (93), suggesting a multigenerational transmission of IUGR phenotypes and altered epigenetic mechanisms.

Altered expression of long non-coding RNAs that are important for angiogenesis, inflammation fetal growth has also been reported in placentas collected from pregnancies that are affected by IUGR (63, 66, 69, 76, 94). The investigation of 30 IUGR and 46 gestational age-matched non-IUGR placentas revealed decreased expression of *MEG3*, a lncRNA that is involved in placental and fetal growth, by more than 50% in the IUGR samples compared to the non-IUGR control (63). In line with this, the expression of *H19*, another lncRNA that is important for fetal development, was also reduced by half the non-IUGR control in IUGR placentas (69). This reduction in *H19* expression was shown to be strongly correlated with a 50% decrease of expression of the type III TGF- β receptor (T β R3), one of the downstream signalling molecules that control trophoblast cell migration and invasion (69). However, in a different study, the expression of *H19* was shown to be similar between IUGR and non-IUGR placental tissues (66). Nonetheless, in IUGR placentas, there was a significantly lower DNA

methylation status in the imprinting control region 1 (ICR1), which regulates the expression of *H19*, in comparison to the control (66). Increased expression of another lncRNA *NEAT1*, a gene expression regulator which expression is usually up-regulated in human cancers, was also seen in placentas from IUGR pregnancies with a 4.14-fold increase in IUGR placentas compared to the control (67). In contrast, in a different study, *NEAT1* expression in the placentas was not statistically different between IUGR and the non-IUGR group (95). Differences in sample size, ethnicity, or maternal age might be an explanation for the differences in *H19* and *NEAT1* expression in IUGR placentas in the above studies. In a recent study, altered expression of 133 lncRNAs (36 increased in expression and 98 decreased in expression, in comparison to non-IUGR control) was reported in placentas from 12 pregnant women whose pregnancies were complicated with IUGR (76). Interestingly, the overexpression of several lncRNAs such as *lnc-PPM1D-1*, *lnc-TCL1B-1*, *lnc-MRPS5-1*, *lncTRPM7-1*, *MED4-AS1*, *EGFR-AS1*, *FLJ31356*, *lnc-VAPA-1* and *STON1-GTF2A1L* in the IUGR group was also found in placentas from the pregnancy group affected by preeclampsia (76). Most of these lncRNAs have been shown to play a role in pathways that lead to placental ischemia, which results in reduced blood supply to the placenta (76). This suggests that these pregnancy complications might act via some shared mechanisms and/or there are similar signalling pathways can be activated by them.

Similar to the observations for lncRNAs, there are miRNAs that have been shown to be altered in placentas from both IUGR and preeclampsia pregnancies, such as *miR-499a-5p*, *miR-26a-5p*, *miR-103a-3p*, *miR-145-5p* (68), *miR-193b-5p* (74), *miR-210-5p* (75), *hsa-miR-210-3p*, *hsa-miR-193b-3p*, *hsa-miR-5p*, *hsa-miR-365a-3p*, *hsa-miR-365b-3p*, and *hsa-miR-520a-3p* (71), most of which play a role in cellular functions, including cellular

differentiation, migration and invasion, suggesting shared signalling pathways and mechanisms between these pregnancy complications.

Studies of other tissues

The focus of this review is on the risk of developing renal and cardiometabolic diseases, such as hypertension and diabetes, in association with IUGR induced by UPI. Therefore, most of the studies reported are on either blood samples, kidneys, livers, pancreas, or placentas.

However, it should be noticed that there are other tissues that can also be affected by IUGR, such as lungs or brains. For example, when F0 pregnant rats were fed a 50% deficit food intake diet throughout pregnancy, in PVECs extracted from the F1 and F2 IUGR rats, there was a significant enrichment of H3K4me3 regions in F1 IUGR males, and a significant reduction in DNA methylation at ET-1 CpG sites in both F1 and F2 IUGR males, compared to the control (40). Interestingly, ET-1 CpG methylation was also significantly reduced in F1 IUGR rat sperm, suggesting epigenetic modifications as a potential mechanism for the multigenerational transmission of these IUGR phenotypes, via the paternal line (40). In line with this finding, altered expression of various miRNAs were found in lung tissues at day 10, day 21, and 5 months after birth of IUGR rat offspring whose mothers were either undernutrition (87) or fed with a low-protein diet (86) during pregnancy. Most of these miRNAs (*miR-29*, *miR-128-3p*, *miR-34c-5p*, *miR-19b-3p*, *miR-449a-5p*, and *miR-30e-5p*) are involved in lung development and injury-repair (86, 87). Microarray analysis and homologous analysis of brain tissues containing hippocampus from growth restricted F1 rats whose mothers received a 50% reduction in food intake throughout pregnancy also revealed 49 rat genes that are homologous in humans, and had a negative correlation between gene expression and DNA methylation status (78). Most of these genes are involved in metabolism

pathways, nervous system dysfunction, cancer, and immune response regulation (78). Increased cerebral total H3 acetylation (to 157% of control values), decreased genome-wide DNA methylation (to 52.8% the control), and decreased CpG island methylation (to 65.0% the control) were also found in brains of IUGR rat offspring (81). Simultaneously, the expression of cerebral chromatin-affecting enzymes DNA methyltransferase 1 and methyl-CpG binding protein 2 were decreased in neonatal IUGR rats, with the mRNA abundances of 50% and 38% the control values, respectively (81).

4. Discussion

From the above evidence it is clear that the effects of intrauterine growth restriction may have on the long-term health and well-being of infants are extensive. Diabetes, hypertension, and kidney dysfunction in growth restricted offspring are the most common diseases that were shown to be related to IUGR. Moreover, as the frequency of this pregnancy complication and its associated diseases is high, especially in developing countries, there is a need to determine the mechanisms of how aberrant phenotypes are programmed and the diseases are transferred to subsequent generations. In comparison to humans, the examination of tissues and organs in animals is more accessible for scientists, ethically. Therefore, the proposed potential mechanisms for the diseases' multigenerational transmission will come from in-depth studies of animal experimental models. Additionally, sex-specific expression of the diseases' phenotypic outcomes was also observed in animal offspring. Therefore, further assessments are required to determine whether epigenetic mechanisms are responsible for the sex-specific differences of IUGR related diseases. Subsequently, future studies may focus on investigating similar mechanisms and markers in humans, which will help identify people who are at risk and/or identify potential prevention strategies for these diseases.

Conflict of Interest

The authors declare that the research was conducted in the absence of any commercial or financial relationships that could be construed as a potential conflict of interest.

Author Contributions

TNAD performed the literature search, interpreted the data and wrote the manuscript

TBM critically revised the manuscript and supervised the project

LKA critically revised the manuscript

Data availability statement

Data availability is not applicable to this article as no new data were created or analysed in this study

References

1. Luyckx VA, Brenner BM. Low birth weight, nephron number, and kidney disease. *Kidney Int* (2005) 68:S68-S77. doi: 10.1111/j.1523-1755.2005.09712.x.
2. Moritz KM, Mazzuca MQ, Siebel AL, Mibus A, Arena D, Tare M, et al. Uteroplacental insufficiency causes a nephron deficit, modest renal insufficiency but no hypertension with ageing in female rats. *The Journal of physiology* (2009) 587(Pt 11):2635-46. doi: 10.1113/jphysiol.2009.170407.

3. Black RE. Global prevalence of small for gestational age births. *Nestle Nutr Inst Workshop Ser* (2015) 81:1-7. doi: 10.1159/000365790.
4. Luyckx VA, Bertram JF, Brenner BM, Fall C, Hoy WE, Ozanne SE, et al. Effect of fetal and child health on kidney development and long-term risk of hypertension and kidney disease. *The Lancet* (2013) 382(9888):273-83. doi: 10.1016/S0140-6736(13)60311-6.
5. Spence D, Stewart MC, Alderdice FA, Patterson CC, Halliday HL. Intra-uterine growth restriction and increased risk of hypertension in adult life: a follow-up study of 50-year-olds. *Public Health* (2012) 126(7):561-5. doi: 10.1016/j.puhe.2012.03.010.
6. Shankaran S, Das A, Bauer CR, Bada H, Lester B, Wright L, et al. Fetal origin of childhood disease: intrauterine growth restriction in term infants and risk for hypertension at 6 years of age. *Arch Pediatr Adolesc Med* (2006) 160(9):977-81. doi: 10.1001/archpedi.160.9.977.
7. Keller G, Zimmer G, Mall G, Ritz E, Amann K. Nephron number in patients with primary hypertension. *N Engl J Med* (2003) 348(2):101-8. doi: 10.1056/NEJMoa020549.
8. Hughson MD, Douglas DR, Bertram JF, Hoy WE. Hypertension, glomerular number, and birth weight in African Americans and white subjects in the southeastern United States. *Kidney Int* (2006) 69(4):671-8. doi: 10.1038/sj.ki.5000041.
9. Wang YP, Chen X, Zhang ZK, Cui HY, Wang P, Wang Y. Effects of a restricted fetal growth environment on human kidney morphology, cell apoptosis and gene expression. *J Renin Angiotensin Aldosterone Syst* (2014) 16(4):1028-35. doi: 10.1177/1470320314543808.

10. Wlodek ME, Westcott K, Siebel AL, Owens JA, Moritz KM. Growth restriction before or after birth reduces nephron number and increases blood pressure in male rats. *Kidney Int* (2008) 74(2):187-95. doi: 10.1038/ki.2008.153.
11. Cuffe JSM, Briffa JF, Rosser S, Siebel AL, Romano T, Hryciw DH, et al. Uteroplacental insufficiency in rats induces renal apoptosis and delays nephrogenesis completion. *Acta Physiologica* (2018) 222(3):e12982. doi: 10.1111/apha.12982.
12. Melanie T, Linda AG, Andrew JJ, Karen MM, Mary EW. Transgenerational metabolic outcomes associated with uteroplacental insufficiency. *J Endocrinol* (2013) 217(1):105-18. doi: 10.1530/JOE-12-0560.
13. Gallo LA, Tran M, Cullen-McEwen LA, Denton KM, Jefferies AJ, Moritz KM, et al. Transgenerational programming of fetal nephron deficits and sex-specific adult hypertension in rats. *Reproduction, Fertility and Development* (2014) 26(7):1032-43. doi: 10.1071/RD13133.
14. Master JS, Zimanyi MA, Yin KV, Moritz KM, Gallo LA, Tran M, et al. Transgenerational left ventricular hypertrophy and hypertension in offspring after uteroplacental insufficiency in male rats. *Clin Exp Pharmacol Physiol* (2014) 41(11):884-90. doi: 10.1111/1440-1681.12303.
15. Baserga M, Bares AL, Hale MA, Callaway CW, McKnight RA, Lane PH, et al. Uteroplacental insufficiency affects kidney VEGF expression in a model of IUGR with compensatory glomerular hypertrophy and hypertension. *Early Hum Dev* (2009) 85(6):361-7. doi: 10.1016/j.earlhumdev.2008.12.015.

16. Jefferies AJ, Cheong JN, Wlodek ME, Anevskaja K, Moritz KM, Cuffe JSM. Sex-specific metabolic outcomes in offspring of female rats born small or exposed to stress during pregnancy. *Endocrinology* (2016) 157(11):4104-20. doi: 10.1210/en.2016-1335.
17. Briffa JF, Wlodek ME, Moritz KM. Transgenerational programming of nephron deficits and hypertension. *Semin Cell Dev Biol* (2018) S1084-9521(17):30447-0. doi: 10.1016/j.semcdb.2018.05.025.
18. Styruud J, Eriksson UJ, Grill V, Swenne I. Experimental intrauterine growth retardation in the rat causes a reduction of pancreatic B-cell mass, which persists into adulthood. *Neonatology* (2005) 88(2):122-8. doi: 10.1159/000086136.
19. Barker DJP, Hales CN, Fall CHD, Osmond C, Phipps K, Clark PMS. Type 2 (non-insulin-dependent) diabetes mellitus, hypertension and hyperlipidaemia (syndrome X): relation to reduced fetal growth. *Diabetologia* (1993) 36(1):62-7. doi: 10.1007/BF00399095.
20. Rabbia F, Veglio F, Grosso T, Nacca R, Martini G, Riva P, et al. Relationship between birth weight and blood pressure in adolescence. *Prev Med* (1999) 29(6):455-9. doi: 10.1006/pmed.1999.0577.
21. Rich-Edwards JW, Colditz GA, Stampfer MJ, Willett WC, Gillman MW, Hennekens CH, et al. Birthweight and the risk for type 2 diabetes mellitus in adult women. *Ann Intern Med* (1999) 130(4):278-84. doi: 10.7326/0003-4819-130-4_part_1-199902160-00005.
22. Gaboriau A, Levy-Marchal C, Czernichow P, Jaquet D. Insulin resistance early in adulthood in subjects born with intrauterine growth retardation. *The Journal of Clinical Endocrinology & Metabolism* (2000) 85(4):1401-6. doi: 10.1210/jcem.85.4.6544.

23. O'Sullivan J, Wright C, Pearce MS, Parker L. The influence of age and gender on the relationship between birth weight and blood pressure in childhood: a study using 24-hour and casual blood pressure. *Eur J Pediatr* (2002) 161(8):423-7. doi: 10.1007/s00431-002-0985-x.
24. Bowers K, Liu G, Wang P, Ye T, Tian Z, Liu E, et al. Birth weight, postnatal weight change, and risk for high blood pressure among Chinese children. *Pediatrics* (2011) 127(5):e1272-e9. doi: 10.1542/peds.2010-2213.
25. Wang YP, Chen X, Zhang ZK, Cui HY, Wang P, Wang Y. Increased renal apoptosis and reduced renin–angiotensin system in fetal growth restriction. *J Renin Angiotensin Aldosterone Syst* (2016) 17(3):1470320316654810. doi: 10.1177/1470320316654810.
26. Simmons RA, Templeton LJ, Gertz SJ. Intrauterine growth retardation leads to the development of type 2 diabetes in the rat. *Diabetes* (2001) 50(10):2279-86. doi: 10.2337/diabetes.50.10.2279.
27. Alexander BT. Placental insufficiency leads to development of hypertension in growth-restricted offspring. *Hypertension* (2003) 41(3):457. doi: 10.1161/01.HYP.0000053448.95913.3D.
28. Pham TD, MacLennan NK, Chiu CT, Laksana GS, Hsu JL, Lane RH. Uteroplacental insufficiency increases apoptosis and alters *p53* gene methylation in the full-term IUGR rat kidney. *American Journal of Physiology-Regulatory, Integrative and Comparative Physiology* (2003) 285(5):R962-R70. doi: 10.1152/ajpregu.00201.2003.
29. Vuguin P, Raab E, Liu B, Barzilai N, Simmons R. Hepatic insulin resistance precedes the development of diabetes in a model of intrauterine growth retardation. *Diabetes* (2004) 53(10):2617-22. doi: 10.2337/diabetes.53.10.2617.

30. Benyshek DC, Johnston CS, Martin JF. Glucose metabolism is altered in the adequately-nourished grand-offspring (F3 generation) of rats malnourished during gestation and perinatal life. *Diabetologia* (2006) 49(5):1117-9. doi: 10.1007/s00125-006-0196-5.
31. Mibus A, Westcott KT, Wlodek ME, Siebel AL, Prior L, Owens JA, et al. Improved lactational nutrition and postnatal growth ameliorates impairment of glucose tolerance by uteroplacental insufficiency in male rat offspring. *Endocrinology* (2008) 149(6):3067-76. doi: 10.1210/en.2008-0128.
32. Mazzuca MQ, Wlodek ME, Dragomir NM, Parkington HC, Tare M. Uteroplacental insufficiency programs regional vascular dysfunction and alters arterial stiffness in female offspring. *The Journal of Physiology* (2010) 588(11):1997-2010. doi: 10.1113/jphysiol.2010.187849.
33. Martínez D, Pentinat T, Ribó S, Daviaud C, Bloks Vincent W, Cebrià J, et al. *In utero* undernutrition in male mice programs liver lipid metabolism in the second-generation offspring involving altered *Lxra* DNA methylation. *Cell Metab* (2014) 19(6):941-51. doi: 10.1016/j.cmet.2014.03.026.
34. He X, Xie Z, Dong Q, Chen P, Hu J, Wang T. Apoptosis in the kidneys of rats that experienced intrauterine growth restriction. *Nephrology* (2015) 20(1):34-9. doi: 10.1111/nep.12340.
35. Li Y, Wang X, Li M, Pan J, Jin M, Wang J, et al. Long non-coding RNA expression profile in the kidneys of male, low birth weight rats exposed to maternal protein restriction at postnatal day 1 and day 10. *PLoS One* (2015) 10(3):e0121587. doi: 10.1371/journal.pone.0121587.

36. Alwasel SH. Glomerular filtration barrier in rat offspring exposed to maternal undernutrition. *Journal of King Saud University - Science* (2017) 29(2):206-13. doi: 10.1016/j.jksus.2016.03.004.
37. Doan TNA, Briffa JF, Phillips AL, Leemaqz SY, Burton RA, Romano T, et al. Epigenetic mechanisms involved in intrauterine growth restriction and aberrant kidney development and function. *J Dev Orig Health Dis* (2020):1-11. doi: 10.1017/S2040174420001257.
38. Li Y, Dai C, Yuan Y, You L, Yuan Q. The mechanisms of lncRNA Tug1 in islet dysfunction in a mouse model of intrauterine growth retardation. *Cell Biochem Funct* (2020) 38(8):1129-38. doi: 10.1002/cbf.3575.
39. Yao Y, Robinson AM, Zucchi FCR, Robbins JC, Babenko O, Kovalchuk O, et al. Ancestral exposure to stress epigenetically programs preterm birth risk and adverse maternal and newborn outcomes. *BMC Med* (2014) 12(1):121. doi: 10.1186/s12916-014-0121-6.
40. Zhang Z, Luo X, Lv Y, Yan L, Xu S, Wang Y, et al. Intrauterine growth restriction programs intergenerational transmission of pulmonary arterial hypertension and endothelial dysfunction via sperm epigenetic modifications. *Hypertension* (2019) 74(5):1160-71. doi: 10.1161/HYPERTENSIONAHA.119.13634.
41. Thamocharan M, Garg M, Oak S, Rogers LM, Pan G, Sangiorgi F, et al. Transgenerational inheritance of the insulin-resistant phenotype in embryo-transferred intrauterine growth-restricted adult female rat offspring. *American Journal of Physiology-Endocrinology and Metabolism* (2007) 292(5):E1270-E9. doi: 10.1152/ajpendo.00462.2006.
42. Bassan H, Leider TL, Kariv N, Bassan M, Berger E, Fattal A, et al. Experimental intrauterine growth retardation alters renal development. *Pediatr Nephrol* (2000) 15(3):192-5. doi: 10.1007/s004670000457.

43. Briscoe TA, Rehn AE, Dieni S, Duncan JR, Wlodek ME, Owens JA, et al. Cardiovascular and renal disease in the adolescent guinea pig after chronic placental insufficiency. *Am J Obstet Gynecol* (2004) 191(3):847-55. doi: 10.1016/j.ajog.2004.01.050.
44. Abitbol CL, Rodriguez MM. The long-term renal and cardiovascular consequences of prematurity. *Nature Reviews Nephrology* (2012) 8:265-74. doi: 10.1038/nrneph.2012.38.
45. Duan C, Xu H, Liu J, Hou L, Tang W, Li L, et al. Decreased expression of GLUT4 in male CG-IUGR rats may play a vital role in their increased susceptibility to diabetes mellitus in adulthood. *Acta Biochimica et Biophysica Sinica* (2016) 48(10):872-82. doi: 10.1093/abbs/gmw088.
46. Thorn SR, Brown LD, Rozance PJ, Hay WW, Friedman JE. Increased hepatic glucose production in fetal sheep with intrauterine growth restriction is not suppressed by insulin. *Diabetes* (2013) 62(1):65-73. doi: 10.2337/db11-1727.
47. Drake AJ, Walker BR, Seckl JR. Intergenerational consequences of fetal programming by in utero exposure to glucocorticoids in rats. *American Journal of Physiology-Regulatory, Integrative and Comparative Physiology* (2005) 288(1):R34-R8. doi: 10.1152/ajpregu.00106.2004.
48. Pinheiro AR, Salvucci ID, Aguila MB, Mandarim-de-Lacerda CA. Protein restriction during gestation and/or lactation causes adverse transgenerational effects on biometry and glucose metabolism in F1 and F2 progenies of rats. *Clin Sci (Lond)* (2008) 114(5):381-92. doi: 10.1042/cs20070302.
49. Barker DJP. The developmental origins of adult disease. *J Am Coll Nutr* (2004) 23(sup6):588S-95S. doi: 10.1111/j.1365-2796.2007.01809.x.

50. Khan MAB, Hashim MJ, King JK, Govender RD, Mustafa H, Al Kaabi J. Epidemiology of type 2 diabetes - global burden of disease and forecasted trends. *J Epidemiol Glob Health* (2020) 10(1):107-11. doi: 10.2991/jegh.k.191028.001.
51. Cockwell P, Fisher L-A. The global burden of chronic kidney disease. *The Lancet* (2020) 395(10225):662-4. doi: 10.1016/S0140-6736(19)32977-0.
52. Zhou B, Carrillo-Larco RM, Danaei G, Riley LM, Paciorek CJ, Stevens GA, et al. Worldwide trends in hypertension prevalence and progress in treatment and control from 1990 to 2019: a pooled analysis of 1201 population-representative studies with 104 million participants. *The Lancet* (2021) 398(10304):957-80. doi: 10.1016/S0140-6736(21)01330-1.
53. Dwi Putra SE, Neuber C, Reichetzeder C, Hocher B, Kleuser B. Analysis of genomic DNA methylation levels in human placenta using liquid chromatography-electrospray ionization tandem mass spectrometry. *Cell Physiol Biochem* (2014) 33(4):945-52. doi: 10.1159/000358666.
54. Nelissen ECM, van Montfoort APA, Dumoulin JCM, Evers JLH. Epigenetics and the placenta. *Hum Reprod Update* (2010) 17(3):397-417. doi: 10.1093/humupd/dmq052.
55. Curradi M, Izzo A, Badaracco G, Landsberger N. Molecular mechanisms of gene silencing mediated by DNA methylation. *Mol Cell Biol* (2002) 22(9):3157-73. doi: 10.1128/MCB.22.9.3157-3173.2002.
56. Handy DE, Castro R, Loscalzo J. Epigenetic modifications: basic mechanisms and role in cardiovascular disease. *Circulation* (2011) 123(19):2145-56. doi: 10.1161/circulationaha.110.956839.

57. Dobosy JR, Selker EU. Emerging connections between DNA methylation and histone acetylation. *Cellular and Molecular Life Sciences CMLS* (2001) 58(5):721-7. doi: 10.1007/pl00000895.
58. Saxena A, Carninci P. Long non-coding RNA modifies chromatin. *Bioessays* (2011) 33(11):830-9. doi: 10.1002/bies.201100084.
59. Neve B, Jonckheere N, Vincent A, Van Seuning I. Epigenetic regulation by lncRNAs: an overview focused on UCA1 in colorectal cancer. *Cancers (Basel)* (2018) 10(11):440. doi: 10.3390/cancers10110440.
60. Wei J-W, Huang K, Yang C, Kang C-S. Non-coding RNAs as regulators in epigenetics (Review). *Oncol Rep* (2017) 37(1):3-9. doi: 10.3892/or.2016.5236.
61. Jiang W, Agrawal DK, Boosani CS. Non-coding RNAs as Epigenetic Gene Regulators in Cardiovascular Diseases. In: Xiao J, editor. *Non-coding RNAs in Cardiovascular Diseases*. Singapore: Springer Singapore (2020). p. 133-48.
62. Zhou JX, Li X. Non-Coding RNAs in hereditary kidney disorders. *Int J Mol Sci* (2021) 22(6):3014. doi: 10.3390/ijms22063014.
63. McMinn J, Wei M, Schupf N, Cusmai J, Johnson EB, Smith AC, et al. Unbalanced placental expression of imprinted genes in human intrauterine growth restriction. *Placenta* (2006) 27(6):540-9. doi: 10.1016/j.placenta.2005.07.004.
64. Lumey L, Susser ES, Stein AD, Kahn HS, van der Pal-de Bruin KM, Blauw G, et al. Cohort profile: the Dutch Hunger Winter families study. *Int J Epidemiol* (2007) 36(6):1196-204. doi: 10.1093/ije/dym126.

65. Einstein F, Thompson RF, Bhagat TD, Fazzari MJ, Verma A, Barzilai N, et al. Cytosine methylation dysregulation in neonates following intrauterine growth restriction. *PLoS One* (2010) 5(1):e8887. doi: 10.1371/journal.pone.0008887.
66. Cordeiro A, Neto AP, Carvalho F, Ramalho C, Dória S. Relevance of genomic imprinting in intrauterine human growth expression of *CDKN1C*, *H19*, *IGF2*, *KCNQ1* and *PHLDA2* imprinted genes. *J Assist Reprod Genet* (2014) 31(10):1361-8. doi: 10.1007/s10815-014-0278-0.
67. Gremlich S, Damnon F, Reymondin D, Braissant O, Schittny JC, Baud D, et al. The long non-coding RNA NEAT1 is increased in IUGR placentas, leading to potential new hypotheses of IUGR origin/development. *Placenta* (2014) 35(1):44-9. doi: 10.1016/j.placenta.2013.11.003.
68. Hromadnikova I, Kotlabova K, Hympanova L, Krofta L. Cardiovascular and cerebrovascular disease associated microRNAs are dysregulated in placental tissues affected with gestational hypertension, preeclampsia and intrauterine growth restriction. *PLoS One* (2015) 10(9):e0138383-e. doi: 10.1371/journal.pone.0138383.
69. Zuckerwise L, Li J, Lu L, Men Y, Geng T, Buhimschi CS, et al. H19 long noncoding RNA alters trophoblast cell migration and invasion by regulating T β R3 in placentae with fetal growth restriction. *Oncotarget* (2016) 7(25):38398-407. doi: 10.18632/oncotarget.9534.
70. Novielli C, Mandò C, Tabano S, Anelli GM, Fontana L, Antonazzo P, et al. Mitochondrial DNA content and methylation in fetal cord blood of pregnancies with placental insufficiency. *Placenta* (2017) 55:63-70. doi: 10.1016/j.placenta.2017.05.008.

71. Awamleh Z, Gloor GB, Han VKM. Placental microRNAs in pregnancies with early onset intrauterine growth restriction and preeclampsia: potential impact on gene expression and pathophysiology. *BMC Med Genomics* (2019) 12(1):91-. doi: 10.1186/s12920-019-0548-x.
72. Fujioka K, Nishida K, Ashina M, Abe S, Fukushima S, Ikuta T, et al. DNA methylation of the *Rtl1* promoter in the placentas with fetal growth restriction. *Pediatr Neonatol* (2019) 60(5):512-6. doi: 10.1016/j.pedneo.2019.01.001.
73. Mas-Parés B, Xargay-Torrent S, Bonmatí A, Lizarraga-Mollinedo E, Martínez-Calcerrada JM, Carreras-Badosa G, et al. Umbilical cord miRNAs in small-for-gestational-age children and association with catch-up growth: a pilot study. *The Journal of Clinical Endocrinology & Metabolism* (2019) 104(11):5285-98. doi: 10.1210/jc.2018-02346.
74. Awamleh Z, Han VKM. Potential pathophysiological role of microRNA 193b-5p in human placentae from pregnancies complicated by preeclampsia and intrauterine growth restriction. *Mol Biol Rep* (2020) 47(9):6531-44. doi: 10.1007/s11033-020-05705-y.
75. Awamleh Z, Han VKM. Identification of miR-210-5p in human placentae from pregnancies complicated by preeclampsia and intrauterine growth restriction, and its potential role in the pregnancy complications. *Pregnancy Hypertens* (2020) 19:159-68. doi: 10.1016/j.preghy.2020.01.002.
76. Medina-Bastidas D, Guzmán-Huerta M, Borboa-Olivares H, Ruiz-Cruz C, Parra-Hernández S, Flores-Pliego A, et al. Placental microarray profiling reveals common mRNA and lncRNA expression patterns in preeclampsia and intrauterine growth restriction. *Int J Mol Sci* (2020) 21(10):3597. doi: 10.3390/ijms21103597.

77. Heijmans BT, Tobi EW, Stein AD, Putter H, Blauw GJ, Susser ES, et al. Persistent epigenetic differences associated with prenatal exposure to famine in humans. *Proceedings of the National Academy of Sciences* (2008) 105(44):17046-9. doi: 10.1073/pnas.0806560105.
78. Ding Y-x, Cui H. Integrated analysis of genome-wide DNA methylation and gene expression data provide a regulatory network in intrauterine growth restriction. *Life Sci* (2017) 179:60-5. doi: 10.1016/j.lfs.2017.04.020.
79. Hillman SL, Finer S, Smart MC, Mathews C, Lowe R, Rakyan VK, et al. Novel DNA methylation profiles associated with key gene regulation and transcription pathways in blood and placenta of growth-restricted neonates. *Epigenetics* (2015) 10(1):1-12. doi: 10.4161/15592294.2014.989741.
80. MacLennan NK, James SJ, Melnyk S, Piroozzi A, Jernigan S, Hsu JL, et al. Uteroplacental insufficiency alters DNA methylation, one-carbon metabolism, and histone acetylation in IUGR rats. *Physiol Genomics* (2004) 18(1):43-50. doi: 10.1152/physiolgenomics.00042.2004.
81. Ke X, Lei Q, James SJ, Kelleher SL, Melnyk S, Jernigan S, et al. Uteroplacental insufficiency affects epigenetic determinants of chromatin structure in brains of neonatal and juvenile IUGR rats. *Physiol Genomics* (2006) 25(1):16-28. doi: 10.1152/physiolgenomics.00093.2005.
82. Park JH, Stoffers DA, Nicholls RD, Simmons RA. Development of type 2 diabetes following intrauterine growth retardation in rats is associated with progressive epigenetic silencing of *Pdx1*. *The Journal of clinical investigation* (2008) 118(6):2316-24. doi: 10.1172/JCI33655.

83. Zhang J, Zhang F, Didelot X, Bruce KD, Cagampang FR, Vatish M, et al. Maternal high fat diet during pregnancy and lactation alters hepatic expression of insulin like growth factor-2 and key microRNAs in the adult offspring. *BMC Genomics* (2009) 10:478-. doi: 10.1186/1471-2164-10-478.
84. Thompson RF, Fazzari MJ, Niu H, Barzilai N, Simmons R, Greally JM. Experimental intrauterine growth restriction induces alterations in DNA methylation and gene expression in pancreatic islets of rats. *The Journal of Biological Chemistry* (2010) 285:15111-8. doi: 10.1074/jbc.M109.095133.
85. Gonzalez-Rodriguez P, Cantu J, O'Neil D, Seferovic MD, Goodspeed DM, Suter MA, et al. Alterations in expression of imprinted genes from the *H19/Igf2* loci in a multigenerational model of intrauterine growth restriction (IUGR). *Am J Obstet Gynecol* (2016) 214(5):625.e1-.e11. doi: 10.1016/j.ajog.2016.01.194.
86. Dravet-Gounot P, Morin C, Jacques S, Dumont F, Ely-Marius F, Vaiman D, et al. Lung microRNA deregulation associated with impaired alveolarization in rats after intrauterine growth restriction. *PLoS One* (2017) 12(12):e0190445-e. doi: 10.1371/journal.pone.0190445.
87. Chuang T-D, Sakurai R, Gong M, Khorram O, Rehan VK. Role of miR-29 in mediating offspring lung phenotype in a rodent model of intrauterine growth restriction. *American Journal of Physiology-Regulatory, Integrative and Comparative Physiology* (2018) 315(5):R1017-R26. doi: 10.1152/ajpregu.00155.2018.
88. Fu Q, Yu X, Callaway CW, Lane RH, McKnight RA. Epigenetics: intrauterine growth retardation (IUGR) modifies the histone code along the rat hepatic *IGF-1* gene. *FASEB journal : official publication of the Federation of American Societies for Experimental Biology* (2009) 23(8):2438-49. doi: 10.1096/fj.08-124768.

89. Tosh DN, Fu Q, Callaway CW, McKnight RA, McMillen IC, Ross MG, et al. Epigenetics of programmed obesity: alteration in IUGR rat hepatic IGF1 mRNA expression and histone structure in rapid vs. delayed postnatal catch-up growth. *American journal of physiology Gastrointestinal and liver physiology* (2010) 299(5):G1023-G9. doi: 10.1152/ajpgi.00052.2010.
90. Saget S, Cong R, Decourtye L, Endale M-L, Martinerie L, Girardet C, et al. Changes in circulating miRNA19a-3p precede insulin resistance programmed by intra-uterine growth retardation in mice. *Mol Metab* (2020) 42:101083-. doi: 10.1016/j.molmet.2020.101083.
91. Monteagudo-Sánchez A, Sánchez-Delgado M, Mora JRH, Santamaría NT, Gratacós E, Esteller M, et al. Differences in expression rather than methylation at placenta-specific imprinted loci is associated with intrauterine growth restriction. *Clin Epigenetics* (2019) 11(1):35-. doi: 10.1186/s13148-019-0630-4.
92. Roifman M, Choufani S, Turinsky AL, Drewlo S, Keating S, Brudno M, et al. Genome-wide placental DNA methylation analysis of severely growth-discordant monochorionic twins reveals novel epigenetic targets for intrauterine growth restriction. *Clin Epigenetics* (2016) 8:70-. doi: 10.1186/s13148-016-0238-x.
93. Padmanabhan N, Jia D, Geary-Joo C, Wu X, Ferguson-Smith Anne C, Fung E, et al. Mutation in folate metabolism causes epigenetic instability and transgenerational effects on development. *Cell* (2013) 155(1):81-93. doi: 10.1016/j.cell.2013.09.002.
94. Majewska M, Lipka A, Paukzsto L, Jastrzebski JP, Szeszko K, Gowkielewicz M, et al. Placenta transcriptome profiling in intrauterine growth restriction (IUGR). *Int J Mol Sci* (2019) 20(6):1510. doi: 10.3390/ijms20061510.

95. Azari I, Ghafouri-Fard S, Omrani MD, Arsang-Jang S, Kordi Tamandani DM, Saroone Rigi M, et al. Expression of long non-coding RNAs in placentas of intrauterine growth restriction (IUGR) pregnancies. *Rep Biochem Mol Biol* (2019) 8(1):25-31.



Epigenetic Mechanisms Responsible for the Transgenerational Inheritance of Intrauterine Growth Restriction Phenotypes

Thu Ngoc Anh Doan^{1,2}, Lisa K. Akison³ and Tina Bianco-Miotto^{1,2*}

¹ School of Agriculture, Food and Wine, Waite Research Institute, University of Adelaide, Adelaide, SA, Australia,

² Robinson Research Institute, University of Adelaide, Adelaide, SA, Australia, ³ School of Biomedical Sciences, University of Queensland, Brisbane, QLD, Australia

OPEN ACCESS

Edited by:

Anurag Sharma,
NITTE University Center for Science
Education and Research (NUCSEER),
India

Reviewed by:

Satyajeet Pramod Khare,
Symbiosis International University,
India
Renjie Jiao,
Guangzhou Medical University, China

*Correspondence:

Tina Bianco-Miotto
tina.bianco@adelaide.edu.au

Specialty section:

This article was submitted to
Pediatric Endocrinology,
a section of the journal
Frontiers in Endocrinology

Received: 18 December 2021

Accepted: 02 March 2022

Published: 31 March 2022

Citation:

Doan TNA, Akison LK and
Bianco-Miotto T (2022) Epigenetic
Mechanisms Responsible
for the Transgenerational
Inheritance of Intrauterine
Growth Restriction Phenotypes.
Front. Endocrinol. 13:838737.
doi: 10.3389/fendo.2022.838737

A poorly functioning placenta results in impaired exchanges of oxygen, nutrition, wastes and hormones between the mother and her fetus. This can lead to restriction of fetal growth. These growth restricted babies are at increased risk of developing chronic diseases, such as type-2 diabetes, hypertension, and kidney disease, later in life. Animal studies have shown that growth restricted phenotypes are sex-dependent and can be transmitted to subsequent generations through both the paternal and maternal lineages. Altered epigenetic mechanisms, specifically changes in DNA methylation, histone modifications, and non-coding RNAs that regulate expression of genes that are important for fetal development have been shown to be associated with the transmission pattern of growth restricted phenotypes. This review will discuss the subsequent health outcomes in the offspring after growth restriction and the transmission patterns of these diseases. Evidence of altered epigenetic mechanisms in association with fetal growth restriction will also be reviewed.

Keywords: intrauterine growth restriction, uteroplacental insufficiency, small for gestational age, transgenerational transmission, epigenetic mechanisms, cardiometabolic disease, kidney dysfunction

INTRODUCTION

Intrauterine growth restriction (IUGR) refers to poor growth during pregnancy, which results in babies being born small for gestational age (SGA), and with low birth weight (LBW) (1). One of the common causes of IUGR is uteroplacental insufficiency (UPI), in which the placenta functions poorly, causing an insufficient supply of oxygen and nutrients to the developing fetus (2).

There is a high prevalence of IUGR worldwide, especially in developing countries [approximately 27% of all live births (3)], which is a significant concern, as epidemiological studies have shown that being growth restricted is associated with an increased risk of developing chronic diseases later in life (1, 4–9). In addition, various animal models have shown that IUGR offspring develop kidney dysfunction and cardiometabolic disease later in life (2, 10–15).

Interestingly, these IUGR phenotypes are sex-specific and their transmission is multigenerational through both the maternal and paternal lines (11–14, 16–18).

The underlying mechanisms of how IUGR predispose offspring to chronic disease later in life remains to be determined. However, epigenetic mechanisms may be involved as they have been shown in several animal studies to be potential mechanisms for the multigenerational transmission of disease (17).

INTRAUTERINE GROWTH RESTRICTION AND CHRONIC DISEASE RISK

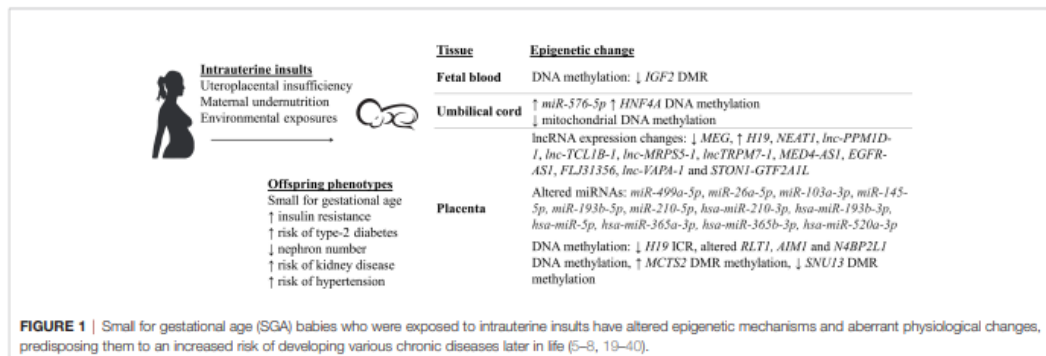
Hypertension and Kidney Disease

Epidemiological studies in humans have reported that growth restricted infants have an increased risk of developing chronic diseases later in life [Figure 1 (5–8, 19–24)]. For instance, IUGR children at 6 years of age have been shown to have a 1.8 times higher risk of developing hypertension compared to non-IUGR children (6). Additionally, individuals born SGA had increased systolic and diastolic blood pressure by 4.5 and 3.4 mmHg, respectively, at the age of 50 (5). When these results were adjusted for confounding factors such as sex, age, and body-mass index, IUGR was still significantly associated with hypertension (5, 6). In other studies, when sex is taken into consideration, the development of hypertension in association with LBW can produce conflicting results. For example, there was one study that found an association in IUGR males only (24), while a different one found an association only with IUGR females (23). However, differences in the size of the study (15600 vs 976 children), method of measuring blood pressure (one-time systolic and diastolic blood pressure measurement vs 24h systolic blood pressure measurement), and the age of examined children [3–6 years old (24) vs 6–16 years old (23)] may be factors that contributed to the observed sex-specific differences. In line with this finding, an inverse relationship was found between birthweight and blood pressure of IUGR infants in

a study that examined 1310 junior high school students (20). However, this relationship was then lost as the children reached adolescence (12–14 years of age), even when adjusted for confounding factors. This suggests that there might be a possible adaptation mechanism in the adolescents to overcome IUGR-related hypertension.

Unlike the examination of hypertension by measuring blood pressure, the precise determination of kidney disease mostly requires more invasive measurement methods, such as counting of glomerular number after organ collection and sample sectioning (7, 8). Therefore, few studies are carried out in humans, especially in growth restricted infants, to evaluate the association between IUGR and kidney disease. However, papers published by Wang et al. in 2014 (9) and 2016 (41), respectively, were two of the rare studies that investigated the effect of human aberrant fetal growth environment on kidneys of fetuses. In both studies, fetuses and their kidney samples were collected from mothers who terminate their pregnancy due to preeclampsia (9), placental abruption, deformities of fetuses, and other intrauterine insults (41). Both papers reported negative effects that IUGR had on the fetuses, including significantly low birth weight (< 2 kg), approximately 0.4 times less nephron number, increased expression of pre-apoptosis proteins within kidney tissues (9), and reduced renal renin-angiotensinogen RNA levels by half the non-growth restricted fetuses (41). This is significant, as the renin-angiotensinogen system is known to play a crucial role in maintaining the sodium homeostasis within the kidney, as well as regulating blood pressure, especially during pregnancy (41). These papers are consistent with studies that have shown a decline in glomerular number (more than 20%) in low birth weight individuals who died from cardiovascular disease as adults, in comparison to normotensive people (7, 8). Together, these studies suggest an important contribution of the kidney to hypertension development in IUGR individuals.

Using different animal models, the association between IUGR and the development of chronic diseases can also be evaluated [Figure 2 (2, 10–15, 18, 42–57)]. In the early 2000s, the association between IUGR induced by UPI and blood pressure level was studied using a model in which placental insufficiency



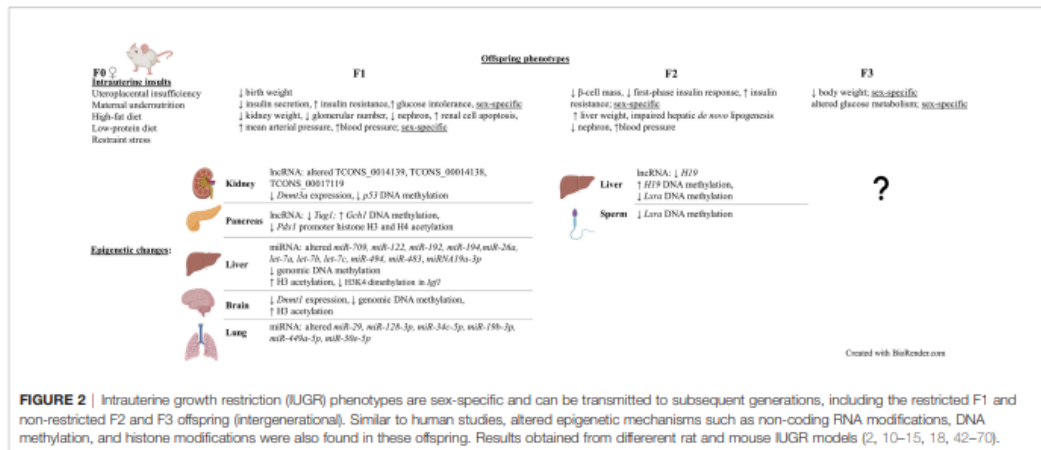


FIGURE 2 | Intrauterine growth restriction (IUGR) phenotypes are sex-specific and can be transmitted to subsequent generations, including the restricted F1 and non-restricted F2 and F3 offspring (intergenerational). Similar to human studies, altered epigenetic mechanisms such as non-coding RNA modifications, DNA methylation, and histone modifications were also found in these offspring. Results obtained from different rat and mouse IUGR models (2, 10–15, 18, 42–70).

was established by placing silver clips around the abdominal aorta and on the branches of uterine arteries of pregnant rats at day 14 of gestation, which severely reduced blood flow between mother and the fetus (43). UPI-induced rats produced LBW offspring, 12% lighter in weight compared to control, with an increased risk of developing hypertension in both IUGR males and females, as their mean arterial pressure at 8 weeks of age was 12 mmHg higher than the control (43). However, at 12 weeks of age, only the increased mean arterial pressure in F1 male offspring was still significant, suggesting a sex-specific hypertension maintenance mechanism. There was no statistically significant association between the observed increased arterial pressure and renal function of the offspring found in this study. Glomerular filtration rate, effective renal plasma flow and 24-hour sodium excretion were not different in IUGR rats compared to the control, even when they were adjusted for kidney weight (43). Meanwhile, the bilateral uterine vessel ligation model produced restricted F1 male offspring that had higher blood pressure and an enlargement of the heart's left ventricle at 22 weeks of age, compared to the control, as a consequence of persisting high blood pressure (10). Lower body weight and glomerular number (clusters of capillaries in the kidney, reduced by 27% of the control) were also reported at 6 months of age (10). These results were reproducible in other studies, with lower kidney weight (measured at postnatal day 1 and 7) and nephron deficit (at 18 months of age) occurring in both sexes and hypertension (at 18 months of age) being present only in male rats (2, 11, 53). Glomerular hypertrophy, an outcome to compensate for the IUGR-related glomerulus reduction, was found to be higher in the F1 growth restricted male rats compared to females at day 120 after birth, suggesting a sex-specific response of the growth restricted offspring towards kidney injury (15). Similarly, 18 month old growth restricted female rats had preserved mesenteric and renal arterial smooth muscle and endothelial function, which may in part explain why they did not develop

hypertension (48). However, the mechanisms behind this remains to be identified. Interestingly, the transmission of hypertension and kidney diseases is multigenerational, as reduced nephron number, left ventricular hypertrophy and hypertension were reported in the non-restricted F2 generation (13, 14).

Apart from rats, studies of UPI-induced IUGR in other animal models [e.g. rabbit (71) and guinea pig (72)] also support the association between IUGR and reduced glomerular number and/or hypertension in the growth restricted offspring. IUGR induced by other intrauterine causes was also shown to be associated with hypertension or aberrant renal function and development (50, 52, 56). For example, F0 pregnant rats were fed a 50% deficit food intake diet throughout pregnancy to produce growth restricted F1 offspring (56). F1 males were mated with control healthy females to produce the F2 generation (paternal line). In a normoxia environment (where the oxygen concentration is normal), mean pulmonary arterial pressure, right ventricular hypertrophy index, and media wall area thickness were not significantly different between IUGR and the control males, in both generations. However, F1 and F2 male rats that were placed in an oxygen-deficient chamber for 2 weeks showed an increase in all three mentioned parameters, indicating an increased risk of developing pulmonary arterial hypertension later in life (56). In line with this finding, the expression of endothelin-1 (ET-1), a vasoconstrictor that is important for cell proliferation, cell migration, and blood vessel development, was significantly increased in pulmonary vascular endothelial cells (PVECs) extracted from F1 and F2 IUGR males. This led to aberrant PVEC proliferation, migration, and angiogenesis, all of which are signs of pulmonary vascular endothelial dysfunction (56). On the other hand, in 6-month-old LBW restricted rats whose mothers received only 50% the calories during pregnancy, there was a significant reduction in kidney weight (maximal value only reached 91% of the control) and glomerular number (by 27% the control) (52). Meanwhile, a low-protein diet

(reduced by 11% of the control) in pregnant rats resulted in a significant decrease in glomerular number (by 22.6% the control; at 3 months of age) and increased renal cell apoptosis of LBW F1 offspring (50).

Diabetes

Besides hypertension and kidney dysfunction, diabetes is another disease that has been shown to be associated with IUGR. Women whose birth weights were less than 2.5 kg [typically the clinical definition for LBW (73)] have a 1.83 times higher risk of developing type 2 diabetes as they age compared to women with birthweights above this threshold (19, 21). Decreased insulin-stimulated glucose uptake, or insulin resistance, one of the common hallmarks of type 2 diabetes, was also reported in IUGR young adults whose birth weights were below the 10th percentile for their gestational age (22).

Different animal models can be used to study the association between IUGR and the development of type-2 diabetes, such as UPI model that has metabolic characteristics comparable to that of humans (18, 42, 45), IUGR rats induced by maternal calorie restriction (57, 74), or IUGR fetal sheep induced by exposing pregnant ewes to an environment with highly increased humidity and temperature (75). When both uterine arteries of pregnant rats are ligated at day 19 of gestation to imitate UPI occurring in pregnancy, F1 growth restricted rat offspring had significantly lower birth weight (5.96 g) compared to the sham control offspring (7.00 g) (42). Rat offspring in both restricted and control group then reached relatively similar body weights at approximately 7 weeks of age. However, as the IUGR F1 rats aged, they had significantly reduced insulin secretion of β -cells (by half the control at 1 week of age and completely absent at 26 weeks of age), insulin-resistance and glucose-intolerance hence hyperglycemia (42). Similar findings were also reported in other studies that applied the same UPI-inducing method of uterine arteries ligation (18, 45). Three months old growth restricted F1 rats developed hepatic insulin resistance, which was represented by its impaired insulin function in controlling the hepatic glucose production (HGP) important for maintaining blood glucose equilibrium (1.6 times higher HGP in IUGR rats compared to the control) (45). A decrease by 50% of pancreatic insulin content was also reported in the LBW growth restricted rats compared to control at the same time point of age (18). Moreover, there was a sex-specific reduction of β -cell mass in these restricted offspring compared to the control, with 40% and 50% reduction in IUGR males and females, respectively (18).

Similar to the observations for hypertension and kidney disease risks in IUGR animal studies, both the F1 and F2 generations are at a higher risk of developing diabetes, suggesting that there is a multigenerational transmission of IUGR phenotypes (12). When growth restricted F1 female rats were mated with healthy males, 6-month-old F2 offspring also had altered pancreatic β -cell mass (reduced by 29% in males and increased by two-fold the control in females) and first-phase insulin response (reduced by 35% in males and 38% in females) (12). The sex-specific differences in pancreatic β -cell mass between 3 months old F1 rats (18) and 6 months old F2 rats

might be due to the difference in time point in which they were examined. For instance, at 6 months of age, female rats may have developed compensatory mechanisms for the disease. Additionally, as these defects were resolved when the rats aged [determined at 12 months of age (12)], male rats may have also developed similar mechanisms at a later age. However, this remains to be shown. In a different IUGR model where F0 pregnant rats were injected with the corticosteroid dexamethasone, from day 15 to 21 of gestation, F2 offspring had reduced birth weight and F2 5-week-old males developed glucose tolerance, represented by a significant increase in the activity of hepatic phosphoenolpyruvate carboxykinase (PEPCK), an enzyme that is involved in glucose metabolism (58). Additionally, these F2 growth restricted males were reported to have higher plasma glucose level at 4 months of age, and higher basal insulin level at 6 months of age, compared to the control (58). Similarly, when F0 pregnant rats received a restricted diet (food intake reduced by 50% the control) from day 11 to 21 of pregnancy, the effect of IUGR on insulin resistance was also seen in a multigenerational pattern (57). Specifically, F1 restricted females were also given a restricted diet from day 1 to day 21 postnatal. At 2 months of age, F1 females were mated with control males, and F2 1-day-old embryos were transferred to control recipient females. F2 female offspring from the IUGR group had significantly higher liver weight, baseline fasting plasma glucose, and insulin concentrations, despite a similar weight from birth to 15 months postnatal, compared to the control (57). The F2 IUGR group also developed insulin resistance at 15 months of age, represented by reduced plasma glucose/insulin ratio during glucose tolerant test, and lower concentration of plasma membrane-associated GLUT4, a protein that plays an important role in insulin-dependent glucose transport into skeletal muscles. Reduced function of PKC ζ , an enzyme involved in insulin-signalling pathway, was also found in skeletal muscle of 15 month old F2 females in the IUGR group (57). Likewise, in a model of *in utero* low-protein consumption in rats, there was an adverse effect of IUGR on the glucose metabolism of F3 offspring at approximately 2 months of age (46). To be specific, there was a significantly higher fasting plasma glucose level in F3 females compared to sham. Meanwhile, there was a significant increase in insulin level of F3 males compared to sham at both fasting stage and 30 minutes after the glucose injection (46), suggesting that IUGR phenotypes are sex-specific and their transmission can be intergenerational. In line with this finding, reduced body weight at days 1 and 7 after birth by 0.5 g, compared to the control offspring, was also reported in the F3 rats whose grandmothers were exposed to restraint stress during pregnancy (55). Additionally, these animals were reported to have sensorimotor dysfunction at postnatal day 7, as their response time during the inclined plane test was significantly slower compared to the control (55). On the other hand, altered glucose tolerance and insulin secretion could be improved (determined in F1 male rats at 6 months of age) by cross-fostering the UPI-induced growth restricted offspring to a sham control mother for lactation, a period important for offspring development (47). This proposed that there could be reversal

strategies for IUGR-related diseases and/or solution to modify their effects on the growth restricted offspring. However, intervention studies are beyond the scope of this review. Additionally, it should be noted that when IUGR was caused by a severe maternal protein-restriction diet (e.g. 5 g of protein/100 g of diet) during pregnancy, postnatal catch-up could be impaired (59). Male and female rats at 6 months of age had significantly increased fasting serum glucose level (20% and 25% the control values in F1 and F2 generation, respectively), despite being fed a control diet during lactation (59). F1 and F2 male offspring also developed insulin resistance at 6 months of age (59).

In summary, the above observations of IUGR infants having an increased risk of developing various diseases later in life are in line with the Developmental Origins of Health and Disease hypothesis, proposing that adverse events that occur during the maturation of gametes, at conception and early embryonic development can program long-term risks of chronic diseases in the LBW offspring (76). As the world-wide prevalence of type 2 diabetes, chronic kidney disease and hypertension is significantly high [6.28% for diabetes, 9.1% for kidney disease, and approximately 30% for hypertension (in adults) (77–79)], there is an urgency for researchers to investigate IUGR and its mechanisms in programming chronic diseases in humans. Nevertheless, due to the complexity and ethical rules in human research, most in-depth experiments that study IUGR are carried out in rodents. Additionally, animal models provide a mechanism for investigating the impact of IUGR across multiple generations and to determine the possible molecular mechanisms involved.

INTRAUTERINE GROWTH RESTRICTION AND THE ASSOCIATED ALTERED EPIGENETIC MECHANISMS

Epigenetic Mechanisms

Epigenetics can be described as heritable modifications to the chromatin that regulate gene expression without altering the DNA nucleotide sequence (80). An example of a modification that creates such changes is DNA methylation. DNA methylation involves the DNA methyltransferase-catalysed addition of a methyl group to a DNA cytosine base (81). In mammals, DNA methylation happens primarily at CpG sites, that is, a cytosine adjacent to a guanine base in the 5'-3' direction. DNA methylation at gene regulatory regions such as promoters is associated with gene silencing (82). Additionally, DNA methylation has an important role in other processes such as X-chromosome inactivation and imprinting (83).

Another epigenetic modification is histone modifications. These include histone acetylation, which is the addition of an acetyl group to the lysine residue of the nucleosomal core histones' N-terminal tail (81). Histone deacetylation, specifically at histones H3 and H4 is associated with gene repression (84). In addition to this, regulatory non-coding RNAs are known to be involved in transcriptional, post-transcriptional, and translational regulation hence are also involved in gene regulation (85, 86). Two large subsets of non-

coding RNAs are long non-coding RNAs which are > 200 nucleotide-long, and short non-coding RNAs like microRNAs (miRNAs), short interfering RNAs (siRNAs), and piwi-interacting RNAs (piRNAs) which are all less than 200 nucleotide-long (87). Altered expression of both miRNAs and lncRNAs have been shown to be associated with altered histone modifications and DNA methylation status of genes (88, 89).

Studies of Blood Samples

IUGR has been shown to be associated with altered epigenetic mechanisms [Figure 1 (25–38)].

Blood samples from the Dutch Hunger Winter famine were used to investigate DNA methylation from individuals exposed to reduced calorie intake in very early (60 people) or late (62 people) gestation (90). Although there was no significant difference in birth weight among the individuals (26), there was a decrease by 5.2% in DNA methylation of the *IGF2* imprinted gene differentially methylated region (DMR) in people exposed to famine in early gestation, compared to the same-sex siblings who were not exposed to famine during pregnancy. Whilst, people exposed to famine in late gestation had no altered DNA methylation (90). This observation suggests the importance of the timing of exposure to intrauterine insults, specifically during the early developmental stage, in which epigenetic mechanisms within the fetus is programmed and may be permanently maintained into adulthood. In a different study, blood samples from 24 IUGR infants were investigated using Illumina Human Methylation 450 k array to analyse differences in genome-wide DNA methylation and gene expression, compared to data from 12 control healthy infants (60). Within the IUGR group, 5460 differentially methylated CpG loci from 2254 genes were identified. Using Kyoto Encyclopedia of Genes and Genomes database, more than 50 pathways affected by changes in the methylation status of these gene were determined, such as metabolic pathways, antigen processing and presentation, insulin signalling pathway, and neurological disorder pathways (60). In addition to this, increased DNA methylation, by 6.1% the control, of the type 2 diabetes-related *HNF4A* gene promoter was found in CD34+ stem cells from umbilical cord blood samples of IUGR newborns (27). More than 800 genome differentially methylated positions (DMPs) was found in leucocytes from umbilical cord blood samples of IUGR neonates, compared to the control (91). These DMPs were located within genes that are critical for key cellular processes that impact the fetal growth and development, such as organogenesis, metabolism, and immunity. *D-loop* hypomethylation of mitochondrial DNA found in fetal cord blood samples was also reported in IUGR neonates who were exposed to placental insufficiency (32). The hypomethylation was in association with higher mitochondrial biogenesis (i.e. increased mitochondrial DNA levels), which is a possible mechanism to compensate for reduced oxygen by UPI. Results in these studies were all adjusted for other complications that may have occurred during pregnancy such as gestational hypertension, gestational diabetes and preeclampsia (27, 32, 91).

Besides DNA methylation, altered expression of miRNAs have been recently reported in human umbilical cord tissues

collected from IUGR pregnancies (35). To be specific, the study included samples from IUGR children with or without growth catch-up at 1 and 6 years of age, and control children who were born appropriate for gestational age (35). At 1 year of age, the expression of a miRNA *miR-576-5p*, which is known to be involved in kidney and liver diseases, was significantly enhanced in IUGR with catch-up children compared to both IUGR without catch-up and control children (35). Moreover, within the IUGR with catch-up group, *miR-576-5p* expression was shown to have a significant association with weight, height, catch-up weight, and catch-up height of the children, after being adjusted for confounding factors such as sex, gestational age, maternal smoking status, etc. Besides the mentioned parameters, at 6 years of age, *miR-576-5p* expression was also shown to be associated with renal fat, suggesting an important role of *miR-576-5p* in cardiometabolic diseases, and that alterations of this miRNA due to IUGR may increase the risk of developing these diseases later in life (35).

Studies of Kidney Tissues

Animal studies that specifically focused on altered epigenetic mechanisms in the UPI-induced IUGR offspring have also been carried out in different organs and tissues [Figure 2 (44, 49, 51, 53, 54, 61–68)]. Decreased expression, by 19% the control, of *Dnmt3a*, a gene that is responsible for *de novo* DNA methylation was found in kidney tissues of F1 IUGR rats at embryonic day 20 (53). Meanwhile, decreased apoptosis-suppressing *Bcl-2* gene expression and increased pro-apoptotic protein-encoding *Bax* and *p53* expression were identified in kidneys of F1 IUGR rats at term, which was associated with reduced glomerular number (by 23% the control) of rat pups (44). Correlatively, there was reduced DNA methylation of CpG islands at the promoter region (by 56.3% the control) of *p53* (44).

Whilst, significantly altered expression of three long non-coding RNAs (lncRNAs) (TCONS_0014139, TCONS_00014138, and TCONS_00017119) at day 1 and day 10 postpartum (pn1 and pn10), confirmed by both microarray and qPCR, were found in kidneys of LBW male rats whose mothers were also fed a low-protein diet during pregnancy (51). The altered expression of these lncRNAs were associated with altered mRNA expression at pn1 and pn10 of *MAPK4*, which encodes for a protein that involves in renal ureteric bud morphogenesis. Additionally, the aberrant expression of these lncRNAs is also correlated with a decrease in nephron number of LBW rats at pn1, suggesting an important role of them in nephron endowment (51). Furthermore, altered expression of *Cdkn1c* and *Kcnq1*, two imprinted genes that are regulated by the *Kcnq1ot1* lncRNA, was found in kidney tissues of UPI-induced IUGR rats at day 1 after birth (53). However, further research is required to investigate whether changes to *Kcnq1ot1* was the epigenetic mechanism that affected the imprinted gene expression in this study.

Studies of Liver Tissues and Pancreas Tissues

Similar to results obtained from blood samples and kidney tissues, abnormal DNA methylation have also been found in hepatic tissues from IUGR studies (49, 65, 66). Importantly, in hepatic

tissues, the multigenerational transmission and reversibility of the altered epigenetics was detected in F2 non-restricted offspring (66). Growth restricted F1 rats that underwent intrauterine UPI were fed with either a control diet or essential nutrient supplemented (ENS) diet (i.e. rich in methyl donors) and bred spontaneously to produce the F2 offspring (66). Within the F2 generation, 21-day-old rats whose F1 mothers received a control diet had statistically reduced DNA methylation of the *H19* gene promoter (7% less than the sham lineage), in association with reduced *H19* expression (0.4-fold the sham lineage) (66). Meanwhile, 21-day-old F2 rats whose F1 mothers received ENS diet had increased *H19* promoter methylation (34% more than the sham lineage), with a 6.6-fold increase in *H19* expression (66). In line with this finding, F2 offspring of pregnant mice that were fed with only 50% the control group's food intake had significantly lowered expression of the *Lxra* gene ($p < 0.01$) in their liver tissues, which plays a key role in *de novo* lipogenesis (49). Hepatic *de novo* lipogenesis was also impaired in the F2 adult mice (49). Furthermore, this was associated with statistically reduced methylation within the 5'UTR region of *Lxra*, both in the sperm samples of IUGR F1 males and liver samples of non-restricted F2 fetuses and adult mice. Therefore, it is suggested that there was a multigenerational transmission of altered *Lxra* methylation within both F1 and F2 generations (49). Meanwhile, one of the first studies to investigate whole-genome DNA methylation from pancreatic islet samples in the UPI-induced IUGR 7-week-old male rats discovered 1912 differentially methylated loci compared to the control, most of which occurred within the non-coding intergenic sequences between genes rather than promoter regions (65). Interestingly, the differential methylation was 45kb upstream of genes known to be important for homeostasis-maintaining processes (e.g. *Fgf1*, *Gch1*, and *Vgf*) and were correlated with altered expression of these genes (65).

UPI-induced IUGR in several animal studies has also been shown to be associated with altered histone modifications (61–63, 69, 92). Histone H3 hyperacetylation, increased to 233% the control value, was detected in the liver of UPI-induced IUGR newborn rats, in association with hepatic genomic DNA hypomethylation (reduced methylation by 13.7% the control at day 21 after birth) (61). On the other hand, significantly reduced dimethylation at H3K4 in the *Igf1* region was reported in livers of IUGR rats whose mothers had a food restriction during pregnancy (69). Meanwhile, locus-specific assessment of the *Pdx1* gene, a gene important for β -cell development and function, showed loss of *Pdx1* promoter H3 and H4 acetylation at 6 months of age and significant DNA hypermethylation (increased by 51.3% the control) in the pancreatic islets of F1 IUGR adult rats, and was associated with silencing of *Pdx1* (mRNA level reduced by 50.4%) (63). This may contribute to the later onset of type-2 diabetes in the growth restricted offspring.

In regards to non-coding RNAs, not many IUGR studies have been carried out to investigate their changes in the growth restricted offspring. Nonetheless, in agreement with results obtained from the placentas in human studies, reduced expression of the lncRNA *H19* and reduced DNA methylation status of its promoter region were reported in hepatic tissues of F2 growth restricted rats whose grandmothers (F0) underwent

UPI (66). In hepatic tissues of F1 growth restricted mice whose mothers were fed with a high-fat diet pre-, during and post-pregnancy, there was also a significant reduction in expression of the miRNAs, including *miR-709*, *miR-122*, *miR-192*, *miR-194*, *miR-26a*, *let-7a*, *let-7b*, *let-7c*, *miR-494* and *miR-483* (64). Interestingly, a major of the altered miRNAs are predicted to have a common target, which is methyl-CpG binding protein 2 (64). In a different study where F0 pregnant mice were fed a low-protein/calorie-deficit (-40%) diet from week 3 of gestation, and growth restricted pups were cross-fostered to 3 different groups right after birth, either normal milk feeding (6 pups/dam), overfed (3 pups/dam), or nutrition restriction (10 pups/dam), significantly reduced H3K4me3 (trimethylated histone H3 on lysine 4) region at the *Akt1* gene, a gene that is known to play an important role in insulin resistance, was found in livers of 3-month-old IUGR males that either received normal milk feeding or were overfed, in association with reduced expression of *Akt1* (93). Interestingly, higher protein level of PTEN, one of the *Akt* activation inhibitors, was also found in livers of overfed 3-month-old males. In addition to this, significantly decreased levels of circulating *miRNA19a-3p*, a miRNA that acts to regulate PTEN, were found in both normally fed and overfed IUGR males (93). These finding hence suggests an association between altered epigenetic mechanisms and the risk of developing insulin resistance later in life of IUGR offspring. Indeed, compared to F1 healthy control males, males that were either under nutrition restriction or overfed both had an increase in sensitivity to insulin at 3 months of age (93). At 12 months of age, the sensitivity to insulin increased for the nutrition restriction group but attenuated for the overfed group. Meanwhile, IUGR males that received normal milk feeding showed no difference in insulin sensitivity compared to healthy control males at 3 months of age. However, at 12 months of age, they developed insulin resistance (93). On the other hand, in pancreatic islets of growth restricted mice whose mothers were fed a low-protein diet, the expression of *Tug1*, a lncRNA that involves in diabetes and tumour development, were significantly lower at 1 day, 8 weeks, and 12 weeks post-partum, compared to the control (54). The aberrant glucose tolerance observed at 10 weeks old IUGR mice could be partially rescued by injection of 150 μ g of *Tug1* overexpression sequence, suggesting that *Tug1* may play an important role in the mouse pancreatic development and function (54).

Studies of Placental Tissues

Altered DNA methylation of genes that are important for fetal growth and development has been reported in placentas from both human and animal IUGR pregnancies (34, 39, 70, 94). For example, placenta samples from healthy and complicated human pregnancies were investigated using the Illumina Infinium Human Methylation450 BeadChip arrays (HM450k) array platform (67 samples) and quantitative pyrosequencing (127 samples) (39). Specifically, 35 DMRs that are expressed across tissues (ubiquitous) were identified. In general, DNA methylation status of all DMRs was not significantly different between complicated pregnancies and the control group.

However, DNA hypermethylation was found at the *MCTS2* DMR, while hypomethylation was found at the *SNU13* and *H19* ICR in IUGR placentas (39). Additionally, RT-PCR and Sanger sequencing confirmed that *H19* hypomethylation results in the biallelic expression of *H19* in the IUGR group. Similarly, a loss of methylation in *SNU13* is associated with increased expression of this gene in the IUGR placentas. Interestingly, despite a similar DNA methylation status compared to that of the control, there was an increase in expression of *ZNF331* and a decrease in expression of *PEG10* and *ZDBF2* in the IUGR placentas (39). For DMRs that are placenta-specific, the same HM450k array data was used, and results were also confirmed using pyrosequencing. Out of 32 placenta-specific DMRs, methylation status of *AIM1* and *N4BP2L1* was significantly different in the IUGR group compared to the control. However, using microfluidic-based quantitative RT-PCR analysis, only four placenta-specific genes that had altered expression in IUGR samples compared to the control were identified, all of which were reduced in IUGR, including *ADAM23*, *GPRI-AS1*, *LIN28B*, and *ZHX3* (39). In line with this, altered DNA methylation of CpG island 1 of *RLT1*, a gene known to be important in placental development, was found in placenta samples from SGA and severe SGA fetuses, compared to healthy controls (34). Whilst, genome-wide DNA methylation patterns were investigated in placentas of IUGR identical twins who shared the same placenta (monochorionic twines) and had significant growth difference, represented by birthweight variations in the range of 21-59% (94). In placental tissues of IUGR twins, altered DNA methylation status (with differences larger than 10% compared to healthy control twins) were identified in DMRs that overlapped the promoters of 8 genes that are known to be important for lipid metabolism and neural development, including *DECRI*, *ZNF300*, *DNAJA4*, *CCL28*, *LEPR*, *HSPA1A/L*, *GSTO1*, and *GNE* (94). These results were still significant after being adjusted for twins' sex, gestational age, and maternal age. Interestingly, *DECRI* and *GSTO1*, the two genes play a role in fetal growth, have also been altered in other IUGR studies in animal and human singleton pregnancies, suggesting potential shared molecular mechanisms in comparison to the IUGR growth-discordant monochorionic twins (94). Meanwhile, at embryonic day 10.5, altered DNA methylation was found within 20 different DMRs of imprinted loci from the placentas of F2 mice, whose grandmothers had a hypomorphic mutation in methionine synthase reductase (*Mtrr*), a gene that is important for methyl group utilisation and maternal folate metabolism (70). Changes in DNA methylation status of these DMRs were associated with changes in expression of imprinted genes such as *Zdbf2*, *Igf2*, and *Dlk1*, all of which play a key role in fetal development (70). As expected, growth restriction, delayed development, and defects of different organs including brain, heart and placenta were also found in these offspring (70), suggesting a multigenerational transmission of IUGR phenotypes and altered epigenetic mechanisms.

Altered expression of long non-coding RNAs that are important for angiogenesis, inflammation fetal growth has also

been reported in placentas collected from pregnancies that are affected by IUGR (25, 28, 31, 38, 40). The investigation of 30 IUGR and 46 gestational age-matched non-IUGR placentas revealed decreased expression of *MEG3*, a lncRNA that is involved in placental and fetal growth, by more than 50% in the IUGR samples compared to the non-IUGR control (25). In line with this, the expression of *H19*, another lncRNA that is important for fetal development, was also reduced by half the non-IUGR control in IUGR placentas (31). This reduction in *H19* expression was shown to be strongly correlated with a 50% decrease of expression of the type III TGF- β receptor (TBR3), one of the downstream signalling molecules that control trophoblast cell migration and invasion (31). However, in a different study, the expression of *H19* was shown to be similar between IUGR and non-IUGR placental tissues (28). Nonetheless, in IUGR placentas, there was a significantly lower DNA methylation status in the imprinting control region 1 (ICR1), which regulates the expression of *H19*, in comparison to the control (28). Increased expression of another lncRNA *NEAT1*, a gene expression regulator which expression is usually up-regulated in human cancers, was also seen in placentas from IUGR pregnancies with a 4.14-fold increase in IUGR placentas compared to the control (29). In contrast, in a different study, *NEAT1* expression in the placentas was not statistically different between IUGR and the non-IUGR group (95). Differences in sample size, ethnicity, or maternal age might be an explanation for the differences in *H19* and *NEAT1* expression in IUGR placentas in the above studies. In a recent study, altered expression of 133 lncRNAs (36 increased in expression and 98 decreased in expression, in comparison to non-IUGR control) was reported in placentas from 12 pregnant women whose pregnancies were complicated with IUGR (38). Interestingly, the overexpression of several lncRNAs such as *lnc-PPM1D-1*, *lnc-TCL1B-1*, *lnc-MRPS5-1*, *lncTRPM7-1*, *MED4-AS1*, *EGFR-AS1*, *FLJ31356*, *lnc-VAPA-1* and *STON1-GTF2A1L* in the IUGR group was also found in placentas from the pregnancy group affected by preeclampsia (38). Most of these lncRNAs have been shown to play a role in pathways that lead to placental ischemia, which results in reduced blood supply to the placenta (38). This suggests that these pregnancy complications might act via some shared mechanisms and/or there are similar signalling pathways can be activated by them.

Similar to the observations for lncRNAs, there are miRNAs that have been shown to be altered in placentas from both IUGR and preeclampsia pregnancies, such as *miR-499a-5p*, *miR-26a-5p*, *miR-103a-3p*, *miR-145-5p* (30), *miR-193b-5p* (36), *miR-210-5p* (37), *hsa-miR-210-3p*, *hsa-miR-193b-3p*, *hsa-miR-5p*, *hsa-miR-365a-3p*, *hsa-miR-365b-3p*, and *hsa-miR-520a-3p* (33), most of which play a role in cellular functions, including cellular differentiation, migration and invasion, suggesting shared signalling pathways and mechanisms between these pregnancy complications.

Studies of Other Tissues

The focus of this review is on the risk of developing renal and cardiometabolic diseases, such as hypertension and diabetes, in

association with IUGR induced by UPI. Therefore, most of the studies reported are on either blood samples, kidneys, livers, pancreas, or placentas. However, it should be noted that there are other tissues that can also be affected by IUGR, such as lungs or brains. For example, when F0 pregnant rats were fed a 50% deficit food intake diet throughout pregnancy, in PVECs extracted from the F1 and F2 IUGR rats, there was a significant enrichment of H3K4me3 regions in F1 IUGR males, and a significant reduction in DNA methylation at ET-1 CpG sites in both F1 and F2 IUGR males, compared to the control (56). Interestingly, ET-1 CpG methylation was also significantly reduced in F1 IUGR rat sperm, suggesting epigenetic modifications as a potential mechanism for the multigenerational transmission of these IUGR phenotypes, via the paternal line (56). In line with this finding, altered expression of various miRNAs were found in lung tissues at day 10, day 21, and 5 months after birth of IUGR rat offspring whose mothers were either undernourished (68) or fed with a low-protein diet (67) during pregnancy. Most of these miRNAs (*miR-29*, *miR-128-3p*, *miR-34c-5p*, *miR-19b-3p*, *miR-449a-5p*, and *miR-30e-5p*) are involved in lung development and injury-repair (67, 68). Microarray analysis and homologous analysis of brain tissues containing hippocampus from growth restricted F1 rats whose mothers received a 50% reduction in food intake throughout pregnancy also revealed 49 rat genes that are homologous in humans, and had a negative correlation between gene expression and DNA methylation status (60). Most of these genes are involved in metabolism pathways, nervous system dysfunction, cancer, and immune response regulation (60). Increased cerebral total H3 acetylation (to 157% of control values), decreased genome-wide DNA methylation (to 52.8% the control), and decreased CpG island methylation (to 65.0% the control) were also found in brains of IUGR rat offspring (62). Simultaneously, the expression of cerebral chromatin-affecting enzymes DNA methyltransferase 1 and methyl-CpG binding protein 2 were decreased in neonatal IUGR rats, with the mRNA abundances of 50% and 38% the control values, respectively (62).

DISCUSSION

From the above evidence it is clear that the effects of intrauterine growth restriction may have on the long-term health and well-being of infants are extensive. Diabetes, hypertension, and kidney dysfunction in growth restricted offspring are the most common diseases that were shown to be related to IUGR. Moreover, as the frequency of this pregnancy complication and its associated diseases is high, especially in developing countries, there is a need to determine the mechanisms of how aberrant phenotypes are programmed and transferred to subsequent generations. In comparison to humans, the examination of tissues and organs in animals is more accessible for scientists, ethically. Therefore, the proposed potential mechanisms for the diseases' multigenerational transmission will come from in-depth studies of animal experimental models. Additionally, sex-specific expression of the diseases' phenotypic outcomes

was also observed in animal offspring. Therefore, further assessments are required to determine whether epigenetic mechanisms are responsible for the sex-specific differences of IUGR related diseases. Subsequently, future studies may focus on investigating similar mechanisms and markers in humans, which will help identify people who are at risk and/or identify potential prevention strategies for these diseases.

REFERENCES

- Luyckx VA, Brenner BM. Low Birth Weight, Nephron Number, and Kidney Disease. *Kidney Int* (2005) 68:568–77. doi: 10.1111/j.1523-1755.2005.09712.x
- Moritz KM, Mazzaqa MQ, Siebel AL, Mibus A, Arena D, Tare M, et al. Uteroplacental Insufficiency Causes a Nephron Deficit, Modest Renal Insufficiency But No Hypertension With Ageing in Female Rats. *J Physiol* (2009) 587(Pt 11):2635–46. doi: 10.1113/jphysiol.2009.170407
- Black RE. Global Prevalence of Small for Gestational Age Births. *Nestle Nutr Inst Workshop Ser* (2015) 81:1–7. doi: 10.1159/000365790
- Luyckx VA, Bertram JF, Brenner BM, Fall C, Hoy WE, Ozanne SE, et al. Effect of Fetal and Child Health on Kidney Development and Long-Term Risk of Hypertension and Kidney Disease. *Lancet* (2013) 382(9888):273–83. doi: 10.1016/S0140-6736(13)60311-6
- Spence D, Stewart MC, Alderdice FA, Patterson CC, Halliday HL. Intra-Uterine Growth Restriction and Increased Risk of Hypertension in Adult Life: A Follow-Up Study of 50-Year-Olds. *Public Health* (2012) 126(7):561–5. doi: 10.1016/j.puhe.2012.03.010
- Shankaran S, Das A, Bauer CR, Bada H, Lester B, Wright L, et al. Fetal Origin of Childhood Disease: Intrauterine Growth Restriction in Term Infants and Risk for Hypertension at 6 Years of Age. *Arch Pediatr Adolesc Med* (2006) 160(9):977–81. doi: 10.1001/archpedi.160.9.977
- Keller G, Zimmer G, Mall G, Ritz E, Amann K. Nephron Number in Patients With Primary Hypertension. *N Engl J Med* (2003) 348(2):101–8. doi: 10.1056/NEJMoa020549
- Hughson MD, Douglas DR, Bertram JF, Hoy WE. Hypertension, Glomerular Number, and Birth Weight in African Americans and White Subjects in the Southeastern United States. *Kidney Int* (2006) 69(4):671–8. doi: 10.1038/sj.ki.5000041
- Wang YP, Chen X, Zhang ZK, Cui HY, Wang P, Wang Y. Effects of a Restricted Fetal Growth Environment on Human Kidney Morphology, Cell Apoptosis and Gene Expression. *J Renin Angiotensin Aldosterone Syst* (2014) 16(4):1028–35. doi: 10.1177/1470320314543808
- Wlodek ME, Westcott K, Siebel AL, Owens JA, Moritz KM. Growth Restriction Before or After Birth Reduces Nephron Number and Increases Blood Pressure in Male Rats. *Kidney Int* (2008) 74(2):187–95. doi: 10.1038/ki.2008.153
- Cuffe JSM, Briffa JF, Rosser S, Siebel AL, Romano T, Hryciw DH, et al. Uteroplacental Insufficiency in Rats Induces Renal Apoptosis and Delays Nephrogenesis Completion. *Acta Physiol* (2018) 222(3):e12982. doi: 10.1111/apha.12982
- Melanie T, Linda AG, Andrew JJ, Karen MM, Mary EW. Transgenerational Metabolic Outcomes Associated With Uteroplacental Insufficiency. *J Endocrinol* (2013) 217(1):105–18. doi: 10.1530/JOE-12-0560
- Gallo LA, Tran M, Cullen-McEwen LA, Denton KM, Jefferies AJ, Moritz KM, et al. Transgenerational Programming of Fetal Nephron Deficits and Sex-Specific Adult Hypertension in Rats. *Reprod Fertil Dev* (2014) 26(7):1032–43. doi: 10.1071/RD13133
- Master JS, Zimanyi MA, Yin KV, Moritz KM, Gallo LA, Tran M, et al. Transgenerational Left Ventricular Hypertrophy and Hypertension in Offspring After Uteroplacental Insufficiency in Male Rats. *Clin Exp Pharmacol Physiol* (2014) 41(11):884–90. doi: 10.1111/1440-1681.12303
- Baserga M, Bares AL, Hale MA, Callaway CW, McKnight RA, Lane PH, et al. Uteroplacental Insufficiency Affects Kidney VEGF Expression in a Model of IUGR With Compensatory Glomerular Hypertrophy and Hypertension. *Early Hum Dev* (2009) 85(6):361–7. doi: 10.1016/j.earlhumdev.2008.12.015
- Jefferies AJ, Cheong JN, Wlodek ME, Anevska K, Moritz KM, Cuffe JSM. Sex-Specific Metabolic Outcomes in Offspring of Female Rats Born Small or Exposed to Stress During Pregnancy. *Endocrinology* (2016) 157(11):4104–20. doi: 10.1210/en.2016-1335
- Briffa JF, Wlodek ME, Moritz KM. Transgenerational Programming of Nephron Deficits and Hypertension. *Semin Cell Dev Biol* (2018) S1084–9521(17):30447–0. doi: 10.1016/j.semcdb.2018.05.025
- Styrod J, Eriksson UJ, Grill V, Swenne I. Experimental Intrauterine Growth Retardation in the Rat Causes a Reduction of Pancreatic B-Cell Mass, Which Persists Into Adulthood. *Neonatology* (2005) 88(2):122–8. doi: 10.1159/000086136
- Barker DJP, Hales CN, Fall CHD, Osmond C, Phipps K, Clark PMS. Type 2 (non-Insulin-Dependent) Diabetes Mellitus, Hypertension and Hyperlipidaemia (Syndrome X): Relation to Reduced Fetal Growth. *Diabetologia* (1993) 36(1):62–7. doi: 10.1007/BF00399095
- Rabbia F, Veglio F, Grosso T, Nacca R, Martini G, Riva P, et al. Relationship Between Birth Weight and Blood Pressure in Adolescence. *Prev Med* (1999) 29(6):455–9. doi: 10.1006/pmed.1999.0577
- Rich-Edwards JW, Colditz GA, Stampfer MJ, Willett WC, Gillman MW, Hennekens CH, et al. Birthweight and the Risk for Type 2 Diabetes Mellitus in Adult Women. *Ann Intern Med* (1999) 130(4):278–84. doi: 10.7326/0003-4819-130-4_part_1-199902160-00005
- Gaboriau A, Levy-Marchal C, Czernichow P, Jaquet D. Insulin Resistance Early in Adulthood in Subjects Born With Intrauterine Growth Retardation. *J Clin Endocrinol Metab* (2000) 85(4):1401–6. doi: 10.1210/jcem.85.4.6544
- O'Sullivan J, Wright C, Pearce MS, Parker L. The Influence of Age and Gender on the Relationship Between Birth Weight and Blood Pressure in Childhood: A Study Using 24-Hour and Casual Blood Pressure. *Eur J Pediatr* (2002) 161(8):423–7. doi: 10.1007/s00431-002-0985-x
- Bowers K, Liu G, Wang P, Ye T, Tian X, Liu E, et al. Birth Weight, Postnatal Weight Change, and Risk for High Blood Pressure Among Chinese Children. *Pediatrics* (2011) 127(5):e1272–e9. doi: 10.1542/peds.2010-2213
- McMinn J, Wei M, Schupf N, Cusmai J, Johnson EB, Smith AC, et al. Unbalanced Placental Expression of Imprinted Genes in Human Intrauterine Growth Restriction. *Placenta* (2006) 27(6):540–9. doi: 10.1016/j.placenta.2005.07.004
- Lumey L, Susser ES, Stein AD, Kahn HS, van der Pal-de Bruin KM, Blauw G, et al. Cohort Profile: The Dutch Hunger Winter Families Study. *Int J Epidemiol* (2007) 36(6):1196–204. doi: 10.1093/ije/dym126
- Einstein F, Thompson RF, Bhagat TD, Fazzari MJ, Verma A, Barzilai N, et al. Cytosine Methylation Dysregulation in Neonates Following Intrauterine Growth Restriction. *PLoS One* (2010) 5(1):e8887. doi: 10.1371/journal.pone.008887
- Cordeiro A, Neto AP, Carvalho F, Ramalho C, Dória S. Relevance of Genomic Imprinting in Intrauterine Human Growth Expression of *CDKN1C*, *H19*, *IGF2*, *KCNQ1* and *PHLDA2* Imprinted Genes. *J Assist Reprod Genet* (2014) 31(10):1361–8. doi: 10.1007/s10815-014-0278-0
- Gremlich S, Dammon F, Reymondin D, Braissant O, Schittny JC, Baud D, et al. The Long non-Coding RNA NEAT1 is Increased in IUGR Placentas, Leading to Potential New Hypotheses of IUGR Origin/Development. *Placenta* (2014) 35(1):44–9. doi: 10.1016/j.placenta.2013.11.003
- Hromadnikova I, Kotlabova K, Hympanova L, Krofta L. Cardiovascular and Cerebrovascular Disease Associated microRNAs are Dysregulated in Placental Tissues Affected With Gestational Hypertension, Preeclampsia and Intrauterine Growth Restriction. *PLoS One* (2015) 10(9):e0138383–e. doi: 10.1371/journal.pone.0138383
- Zuckerman L, Li J, Lu L, Men Y, Geng T, Buhimchi CS, et al. H19 Long Noncoding RNA Alters Trophoblast Cell Migration and Invasion by Regulating Tβr3 in Placentae With Fetal Growth Restriction. *Oncotarget* (2016) 7(25):38398–407. doi: 10.18632/oncotarget.9534

32. Novielli C, Mandò C, Tabano S, Anelli GM, Fontana L, Antonazzo P, et al. Mitochondrial DNA Content and Methylation in Fetal Cord Blood of Pregnancies With Placental Insufficiency. *Placenta* (2017) 55:63–70. doi: 10.1016/j.placenta.2017.05.008
33. Awamleh Z, Gloor GB, Han VKM. Placental microRNAs in Pregnancies With Early Onset Intrauterine Growth Restriction and Preeclampsia: Potential Impact on Gene Expression and Pathophysiology. *BMC Med Genomics* (2019) 12(1):91–. doi: 10.1186/s12920-019-0548-x
34. Fujioka K, Nishida K, Ashina M, Abe S, Fukushima S, Ikuta T, et al. DNA Methylation of the *Rtl1* Promoter in the Placentas With Fetal Growth Restriction. *Pediatr Neonatol* (2019) 60(5):512–6. doi: 10.1016/j.jpeds.2019.01.001
35. Mas-Parés B, Xargay-Torrent S, Bonmatí A, Lizarraga-Mollinedo E, Martínez-Calcerada JM, Carreras-Badosa G, et al. Umbilical Cord miRNAs in Small-for-Gestational-Age Children and Association With Catch-Up Growth: A Pilot Study. *J Clin Endocrinol Metab* (2019) 104(11):5285–98. doi: 10.1210/clinem.2018-02346
36. Awamleh Z, Han VKM. Potential Pathophysiological Role of microRNA 193b-5p in Human Placentae From Pregnancies Complicated by Preeclampsia and Intrauterine Growth Restriction. *Mol Biol Rep* (2020) 47(9):6531–44. doi: 10.1007/s11033-020-05705-y
37. Awamleh Z, Han VKM. Identification of miR-210-5p in Human Placentae From Pregnancies Complicated by Preeclampsia and Intrauterine Growth Restriction, and its Potential Role in the Pregnancy Complications. *Pregnancy Hypertens* (2020) 19:159–68. doi: 10.1016/j.preghy.2020.01.002
38. Medina-Bastidas D, Guzmán-Huerta M, Borboa-Olivares H, Ruiz-Cruz C, Parra-Hernández S, Flores-Pliego A, et al. Placental Microarray Profiling Reveals Common mRNA and lncRNA Expression Patterns in Preeclampsia and Intrauterine Growth Restriction. *Int J Mol Sci* (2020) 21(10):3597. doi: 10.3390/ijms21103597
39. Monteagudo-Sánchez A, Sánchez-Delgado M, Mora JRH, Santamaria NT, Gratacós E, Esteller M, et al. Differences in Expression Rather Than Methylation at Placenta-Specific Imprinted Loci is Associated With Intrauterine Growth Restriction. *Clin Epigenet* (2019) 11(1):35. doi: 10.1186/s13148-019-0630-4
40. Majewska M, Lipka A, Pauksztó L, Jastrzebski JP, Szeszko K, Gowkielewicz M, et al. Placenta Transcriptome Profiling in Intrauterine Growth Restriction (IUGR). *Int J Mol Sci* (2019) 20(6):1510. doi: 10.3390/ijms20061510
41. Wang YP, Chen X, Zhang ZK, Cui HY, Wang P, Wang Y. Increased Renal Apoptosis and Reduced Renin-Angiotensin System in Fetal Growth Restriction. *J Renin Angiotensin Aldosterone Syst* (2016) 17(3):1470320316654810. doi: 10.1177/1470320316654810
42. Simmons RA, Templeton LJ, Gertz SJ. Intrauterine Growth Retardation Leads to the Development of Type 2 Diabetes in the Rat. *Diabetes* (2001) 50(10):2279–86. doi: 10.2337/diabetes.50.10.2279
43. Alexander BT. Placental Insufficiency Leads to Development of Hypertension in Growth-Restricted Offspring. *Hypertension* (2003) 41(3):457. doi: 10.1161/01.HYP.0000053448.95913.3D
44. Pham TD, MacLennan NK, Chiu CT, Laksana GS, Hsu JL, Lane RH. Uteroplacental Insufficiency Increases Apoptosis and Alters *P53* Gene Methylation in the Full-Term IUGR Rat Kidney. *Am J Physiology-Regul Integr Comp Physiol* (2003) 285(5):R962–R70. doi: 10.1152/ajpregu.00201.2003
45. Vuguin P, Raab E, Liu B, Barzilai N, Simmons R. Hepatic Insulin Resistance Precedes the Development of Diabetes in a Model of Intrauterine Growth Retardation. *Diabetes* (2004) 53(10):2617–22. doi: 10.2337/diabetes.53.10.2617
46. Benyshek DC, Johnston CS, Martin JF. Glucose Metabolism is Altered in the Adequately-Nourished Grand-Offspring (F3 Generation) of Rats Malnourished During Gestation and Perinatal Life. *Diabetologia* (2006) 49(5):1117–9. doi: 10.1007/s00125-006-0196-5
47. Mibus A, Westcott KT, Wlodek ME, Siebel AL, Prior L, Owens JA, et al. Improved Lactational Nutrition and Postnatal Growth Ameliorates Impairment of Glucose Tolerance by Uteroplacental Insufficiency in Male Rat Offspring. *Endocrinology* (2008) 149(6):3067–76. doi: 10.1210/en.2008-0128
48. Mazzuca MQ, Wlodek ME, Dragomir NM, Parkington HC, Tare M. Uteroplacental Insufficiency Programs Regional Vascular Dysfunction and Alters Arterial Stiffness in Female Offspring. *J Physiol* (2010) 588(11):1997–2010. doi: 10.1113/jphysiol.2010.187849
49. Martínez D, Pentinat T, Ribó S, Daviaud C, Bloks Vincent W, Cebría J, et al. *In Utero* Undernutrition in Male Mice Programs Liver Lipid Metabolism in the Second-Generation Offspring Involving Altered *Lxra* DNA Methylation. *Cell Metab* (2014) 19(6):941–51. doi: 10.1016/j.cmet.2014.03.026
50. He X, Xie Z, Dong Q, Chen P, Hu J, Wang T. Apoptosis in the Kidneys of Rats That Experienced Intrauterine Growth Restriction. *Nephrology* (2015) 20(1):34–9. doi: 10.1111/nep.12340
51. Li Y, Wang X, Li M, Pan J, Jin M, Wang J, et al. Long non-Coding RNA Expression Profile in the Kidneys of Male, Low Birth Weight Rats Exposed to Maternal Protein Restriction at Postnatal Day 1 and Day 10. *PLoS One* (2015) 10(3):e0121587. doi: 10.1371/journal.pone.0121587
52. Alwaseel SH. Glomerular Filtration Barrier in Rat Offspring Exposed to Maternal Undernutrition. *J King Saud Univ - Sci* (2017) 29(2):206–13. doi: 10.1016/j.jksus.2016.03.004
53. Doan TNA, Briffa JF, Phillips AL, Leemaqz SY, Burton RA, Romano T, et al. Epigenetic Mechanisms Involved in Intrauterine Growth Retardation and Aberrant Kidney Development and Function. *J Dev Orig Health Dis* (2020) 12(6):952–62. doi: 10.1017/S2040174420001257
54. Li Y, Dai C, Yuan Y, You L, Yuan Q. The Mechanisms of lncRNA Tug1 in Islet Dysfunction in a Mouse Model of Intrauterine Growth Retardation. *Cell Biochem Funct* (2020) 38(8):1129–38. doi: 10.1002/cbf.3575
55. Yao Y, Robinson AM, Zucchi FCR, Robbins JC, Babenko O, Kovalchuk O, et al. Ancestral Exposure to Stress Epigenetically Programs Preterm Birth Risk and Adverse Maternal and Newborn Outcomes. *BMC Med* (2014) 12(1):121. doi: 10.1186/s12916-014-0121-6
56. Zhang Z, Luo X, Lv Y, Yan L, Xu S, Wang Y, et al. Intrauterine Growth Restriction Programs Intergenerational Transmission of Pulmonary Arterial Hypertension and Endothelial Dysfunction via Sperm Epigenetic Modifications. *Hypertension* (2019) 74(5):1160–71. doi: 10.1161/HYPERTENSIONAHA.119.13634
57. Thamocharan M, Garg M, Oak S, Rogers LM, Pan G, Sangiorgi F, et al. Transgenerational Inheritance of the Insulin-Resistant Phenotype in Embryo-Transferred Intrauterine Growth-Restricted Adult Female Rat Offspring. *Am J Physiology-Endocrinol Metab* (2007) 292(5):E1270–E9. doi: 10.1152/ajpendo.00462.2006
58. Drake AJ, Walker BR, Seckl JR. Intergenerational Consequences of Fetal Programming by *In Utero* Exposure to Glucocorticoids in Rats. *Am J Physiology-Regul Integr Comp Physiol* (2005) 288(1):R34–R8. doi: 10.1152/ajpregu.00106.2004
59. Pinheiro AR, Salvucci ID, Aguilá MB, Mandarim-de-Lacerda CA. Protein Restriction During Gestation and/or Lactation Causes Adverse Transgenerational Effects on Biometry and Glucose Metabolism in F1 and F2 Progenies of Rats. *Clin Sci (Lond)* (2008) 114(5):381–92. doi: 10.1042/cs20070302
60. Ding Y-x, Cui H. Integrated Analysis of Genome-Wide DNA Methylation and Gene Expression Data Provide a Regulatory Network in Intrauterine Growth Restriction. *Life Sci* (2017) 179:60–5. doi: 10.1016/j.lfs.2017.04.020
61. MacLennan NK, James SJ, Melnyk S, Piroozzi A, Jernigan S, Hsu JL, et al. Uteroplacental Insufficiency Alters DNA Methylation, One-Carbon Metabolism, and Histone Acetylation in IUGR Rats. *Physiol Genomics* (2004) 18(1):43–50. doi: 10.1152/physiolgenomics.00042.2004
62. Ke X, Lei Q, James SJ, Kelleher SL, Melnyk S, Jernigan S, et al. Uteroplacental Insufficiency Affects Epigenetic Determinants of Chromatin Structure in Brains of Neonatal and Juvenile IUGR Rats. *Physiol Genomics* (2006) 25(1):16–28. doi: 10.1152/physiolgenomics.00093.2005
63. Park JH, Stoffers DA, Nicholls RD, Simmons RA. Development of Type 2 Diabetes Following Intrauterine Growth Retardation in Rats Is Associated With Progressive Epigenetic Silencing of *Pdx1*. *J Clin Invest* (2008) 118(6):2316–24. doi: 10.1172/JCI33655
64. Zhang J, Zhang F, Didelot X, Bruce KD, Cagampang FR, Vatish M, et al. Maternal High Fat Diet During Pregnancy and Lactation Alters Hepatic Expression of Insulin Like Growth Factor-2 and Key microRNAs in the Adult Offspring. *BMC Genomics* (2009) 10:478–. doi: 10.1186/1471-2164-10-478
65. Thompson RF, Fazzari MJ, Niu H, Barzilai N, Simmons R, Grealley JM. Experimental Intrauterine Growth Restriction Induces Alterations in DNA Methylation and Gene Expression in Pancreatic Islets of Rats. *J Biol Chem* (2010) 285:15111–8. doi: 10.1074/jbc.M109.095133
66. Gonzalez-Rodriguez P, Cantu J, O'Neil D, Seferovic MD, Goodspeed DM, Suter MA, et al. Alterations in Expression of Imprinted Genes From the *H19*/

- Igf2* Loci in a Multigenerational Model of Intrauterine Growth Restriction (IUGR). *Am J Obstet Gynecol* (2016) 214(5):625.e1–e11. doi: 10.1016/j.ajog.2016.01.194
67. Dravet-Gounot P, Morin C, Jacques S, Dumont F, Ely-Marius F, Vaiman D, et al. Lung microRNA Deregulation Associated With Impaired Alveolarization in Rats After Intrauterine Growth Restriction. *PLoS One* (2017) 12(12):e0190445–e. doi: 10.1371/journal.pone.0190445
 68. Chuang T-D, Sakurai R, Gong M, Khorram O, Rehan VK. Role of miR-29 in Mediating Offspring Lung Phenotype in a Rodent Model of Intrauterine Growth Restriction. *Am J Physiology-Regul Integr Comp Physiol* (2018) 315(5):R1017–R26. doi: 10.1152/ajpregu.00155.2018
 69. Tosh DN, Fu Q, Callaway CW, McKnight RA, McMillen IC, Ross MG, et al. Epigenetics of Programmed Obesity: Alteration in IUGR Rat Hepatic IGF1 mRNA Expression and Histone Structure in Rapid vs. Delayed Postnatal Catch-Up Growth. *Am J Physiol Gastrointest Liver Physiol* (2010) 299(5):G1023–G9. doi: 10.1152/ajpgi.00052.2010
 70. Padmanabhan N, Jia D, Geary-Joo C, Wu X, Ferguson-Smith Anne C, Fung E, et al. Mutation in Folate Metabolism Causes Epigenetic Instability and Transgenerational Effects on Development. *Cell* (2013) 155(1):81–93. doi: 10.1016/j.cell.2013.09.002
 71. Bassan H, Leider TL, Kariv N, Bassan M, Berger E, Fattal A, et al. Experimental Intrauterine Growth Retardation Alters Renal Development. *Pediatr Nephrol* (2000) 15(3):192–5. doi: 10.1007/s004670000457
 72. Briscoe TA, Rehn AE, Dieni S, Duncan JR, Wlodek ME, Owens JA, et al. Cardiovascular and Renal Disease in the Adolescent Guinea Pig After Chronic Placental Insufficiency. *Am J Obstet Gynecol* (2004) 191(3):847–55. doi: 10.1016/j.ajog.2004.01.050
 73. Abitbol CL, Rodriguez MM. The Long-Term Renal and Cardiovascular Consequences of Prematurity. *Nat Rev Nephrol* (2012) 8:265–74. doi: 10.1038/nrneph.2012.38
 74. Duan C, Xu H, Liu J, Hou L, Tang W, Li L, et al. Decreased Expression of GLUT4 in Male CG-IUGR Rats may Play a Vital Role in Their Increased Susceptibility to Diabetes Mellitus in Adulthood. *Acta Biochim Biophys Sin* (2016) 48(10):872–82. doi: 10.1093/abbs/gmw088
 75. Thorn SR, Brown LD, Rozance PJ, Hay WW, Friedman JE. Increased Hepatic Glucose Production in Fetal Sheep With Intrauterine Growth Restriction is Not Suppressed by Insulin. *Diabetes* (2013) 62(1):65–73. doi: 10.2337/db11-1727
 76. Barker DJP. The Developmental Origins of Adult Disease. *J Am Coll Nutr* (2004) 23(sup6):588S–95S. doi: 10.1111/j.1365-2796.2007.01809.x
 77. Khan MAB, Hashim MJ, King JK, Govender RD, Mustafa H, Al Kaabi J. Epidemiology of Type 2 Diabetes - Global Burden of Disease and Forecasted Trends. *J Epidemiol Glob Health* (2020) 10(1):107–11. doi: 10.2991/jegh.k.191028.001
 78. Cockwell P, Fisher L-A. The Global Burden of Chronic Kidney Disease. *Lancet* (2020) 395(10225):662–4. doi: 10.1016/S0140-6736(19)32977-0
 79. Zhou B, Carrillo-Larco RM, Danaei G, Riley LM, Paciorek CJ, Stevens GA, et al. Worldwide Trends in Hypertension Prevalence and Progress in Treatment and Control From 1990 to 2019: A Pooled Analysis of 1201 Population-Representative Studies With 104 Million Participants. *Lancet* (2021) 398(10304):957–80. doi: 10.1016/S0140-6736(21)01330-1
 80. Dwi Putra SE, Neuber C, Reichetzedler C, Hocher B, Kleuser B. Analysis of Genomic DNA Methylation Levels in Human Placenta Using Liquid Chromatography-Electrospray Ionization Tandem Mass Spectrometry. *Cell Physiol Biochem* (2014) 33(4):945–52. doi: 10.1159/000358666
 81. Nelissen ECM, van Montfoort APA, Dumoulin JCM, Evers JH. Epigenetics and the Placenta. *Hum Reprod Update* (2010) 17(3):397–417. doi: 10.1093/humupd/dmq052
 82. Curradi M, Izzo A, Badaracco G, Landsberger N. Molecular Mechanisms of Gene Silencing Mediated by DNA Methylation. *Mol Cell Biol* (2002) 22(9):3157–73. doi: 10.1128/MCB.22.9.3157-3173.2002
 83. Handy DE, Castro R, Loscalzo J. Epigenetic Modifications: Basic Mechanisms and Role in Cardiovascular Disease. *Circulation* (2011) 123(19):2145–56. doi: 10.1161/circulationaha.110.956839
 84. Dobosy JR, Selker EU. Emerging Connections Between DNA Methylation and Histone Acetylation. *Cell Mol Life Sci CMLS* (2001) 58(5):721–7. doi: 10.1007/pl00000895
 85. Saxena A, Carninci P. Long non-Coding RNA Modifies Chromatin. *Bioessays* (2011) 33(11):830–9. doi: 10.1002/bies.201100084
 86. Neve B, Jonckheere N, Vincent A, Van Seuningen I. Epigenetic Regulation by lncRNAs: An Overview Focused on UCA1 in Colorectal Cancer. *Cancers (Basel)* (2018) 10(11):440. doi: 10.3390/cancers10110440
 87. Wei J-W, Huang K, Yang C, Kang C-S. Non-Coding RNAs as Regulators in Epigenetics (Review). *Oncol Rep* (2017) 37(1):3–9. doi: 10.3892/or.2016.5236
 88. Jiang W, Agrawal DK, Boosani CS. Non-Coding RNAs as Epigenetic Gene Regulators in Cardiovascular Diseases. In: J Xiao, editor. *Non-Coding RNAs in Cardiovascular Diseases*. Singapore: Springer Singapore (2020). p. 133–48.
 89. Zhou JX, Li X. Non-Coding RNAs in Hereditary Kidney Disorders. *Int J Mol Sci* (2021) 22(6):3014. doi: 10.3390/ijms22063014
 90. Heijmans BT, Tobi EW, Stein AD, Putter H, Blauw GJ, Susser ES, et al. Persistent Epigenetic Differences Associated With Prenatal Exposure to Famine in Humans. *Proc Natl Acad Sci* (2008) 105(44):17046–9. doi: 10.1073/pnas.0806560105
 91. Hillman SL, Finer S, Smart MC, Mathews C, Lowe R, Rakyan VK, et al. Novel DNA Methylation Profiles Associated With Key Gene Regulation and Transcription Pathways in Blood and Placenta of Growth-Restricted Neonates. *Epigenetics* (2015) 10(1):1–12. doi: 10.4161/15592294.2014.989741
 92. Fu Q, Yu X, Callaway CW, Lane RH, McKnight RA. Epigenetics: Intrauterine Growth Retardation (IUGR) Modifies the Histone Code Along the Rat Hepatic *IGF-1* Gene. *FASEB J* (2009) 23(8):2438–49. doi: 10.1096/fj.08-124768
 93. Saget S, Cong R, Decourtye L, Endale M-L, Martinierie L, Girardet C, et al. Changes in Circulating Mirna19a-3p Precede Insulin Resistance Programmed by Intra-Uterine Growth Retardation in Mice. *Mol Metab* (2020) 42:101083–. doi: 10.1016/j.molmet.2020.101083
 94. Roifman M, Choufani S, Turinsky AL, Drewlo S, Keating S, Budno M, et al. Genome-Wide Placental DNA Methylation Analysis of Severely Growth-Discordant Monozygotic Twins Reveals Novel Epigenetic Targets for Intrauterine Growth Restriction. *Clin Epigenet* (2016) 8:70–. doi: 10.1186/s13148-016-0238-x
 95. Azari I, Ghafouri-Fard S, Omrani MD, Arsang-Jang S, Kordi Tamandani DM, Saroone Rigi M, et al. Expression of Long Non-Coding RNAs in Placentas of Intrauterine Growth Restriction (IUGR) Pregnancies. *Rep Biochem Mol Biol* (2019) 8(1):25–31.

Conflict of Interest: The authors declare that the research was conducted in the absence of any commercial or financial relationships that could be construed as a potential conflict of interest.

Publisher's Note: All claims expressed in this article are solely those of the authors and do not necessarily represent those of their affiliated organizations, or those of the publisher, the editors and the reviewers. Any product that may be evaluated in this article, or claim that may be made by its manufacturer, is not guaranteed or endorsed by the publisher.

Copyright © 2022 Doan, Akison and Bianco-Miotto. This is an open-access article distributed under the terms of the Creative Commons Attribution License (CC BY). The use, distribution or reproduction in other forums is permitted, provided the original author(s) and the copyright owner(s) are credited and that the original publication in this journal is cited, in accordance with accepted academic practice. No use, distribution or reproduction is permitted which does not comply with these terms.

CHAPTER 3

IMPRINTED GENE

ALTERATIONS IN THE KIDNEYS

OF GROWTH RESTRICTED

OFFSPRING MAY BE MEDIATED

BY A LONG NON-CODING RNA

Statement of Authorship

Statement of Authorship

Title of Paper	Imprinted gene alterations in the kidneys of growth restricted offspring may be mediated by a long non-coding RNA		
Publication Status	<input checked="" type="checkbox"/> Published	<input type="checkbox"/> Accepted for Publication	
	<input type="checkbox"/> Submitted for Publication	<input type="checkbox"/> Unpublished and Unsubmitted work written in manuscript style	
Publication Details	Doan, T.N.A., Cowley, M. J., Phillips, L. A., Briffa, F. J., Leemaqz, Y. S., Burton, A. R., Romano, T., Wlodek, E. M., & Bianco-Miotto, T. (2024). Imprinted gene alterations in the kidneys of growth restricted offspring may be mediated by a long non-coding RNA. <i>Epigenetics</i> , 19(1), 2294516. https://doi.org/10.1080/15592294.2023.2294516 .		

Principal Author

Name of Principal Author (Candidate)	Ngoc Anh Thu Doan		
Contribution to the Paper	Conducted all the experiments, analysed the data and wrote the manuscript		
Overall percentage (%)	70		
Certification:	This paper reports on original research I conducted during the period of my Higher Degree by Research candidature and is not subject to any obligations or contractual agreements with a third party that would constrain its inclusion in this thesis. I am the primary author of this paper.		
Signature		Date	6.11.2023

Co-Author Contributions

By signing the Statement of Authorship, each author certifies that:

- i. the candidate's stated contribution to the publication is accurate (as detailed above);
- ii. permission is granted for the candidate to include the publication in the thesis; and
- iii. the sum of all co-author contributions is equal to 100% less the candidate's stated contribution.

CI - Internal use

Name of Co-Author	James M. Cowley		
Contribution to the Paper	Contributed to statistical analyses and critical review and revision of the manuscript		
Signature		Date	10.11.2023

Name of Co-Author	Aaron L. Phillips		
Contribution to the Paper	Contributed to statistical analyses and critical review and revision of the manuscript		
Signature		Date	8.11.2023

Name of Co-Author	Jessica F. Briffa		
Contribution to the Paper	Generated the animal model tissues, acquired animal tissues and phenotypic data, provided tissue and phenotypic data, critical review of the manuscript		
Signature		Date	7.11.2023

Name of Co-Author	Shalem Y. Leemaqz		
Contribution to the Paper	Contributed to statistical analyses and critical review of the manuscript		
Signature		Date	11.11.2023

Name of Co-Author	Rachel A. Burton		
Contribution to the Paper	Provided intellectual input and resources, critical review of the manuscript		
Signature		Date	6/11/23

Name of Co-Author	Tania Romano		
Contribution to the Paper	Contributed to generation of animal tissues, and critical review of the manuscript		
Signature		Date	8.11.2023

Name of Co-Author	Mary E. Wlodek		
Contribution to the Paper	Generated the animal model, acquired animal tissues and phenotypic data, provided tissue and phenotypic data, contributed to study design, critical review of the manuscript		
Signature		Date	12.11.2023

Name of Co-Author	Tina Bianco-Miotto		
Contribution to the Paper	Designed and supervised the project, critical review and revision of the manuscript		
Signature		Date	6.11.2023

TITLE PAGE:

Article title

Imprinted gene alterations in the kidneys of growth restricted offspring may be mediated by a long non-coding RNA.

Author information

Thu N.A. Doan^{1,2}, James M. Cowley¹, Aaron L. Phillips¹, Jessica F. Briffa³, Shalem Y. Leemaqz^{2,4,5}, Rachel A. Burton¹, Tania Romano⁶, Mary E. Wlodek^{3,7} and Tina Bianco-Miotto^{1,2a}

¹School of Agriculture, Food and Wine, & Waite Research Institute, University of Adelaide, Adelaide, South Australia, Australia

²Robinson Research Institute, University of Adelaide, South Australia, Australia

³Department of Anatomy and Physiology, The University of Melbourne, Parkville, Victoria, Australia

⁴South Australian Health & Medical Research Institute, SAHMRI Women and Kids, Adelaide, Australia

⁵College of Medicine and Public Health, Flinders University, Bedford Park, SA, Australia.

⁶Department of Physiology, Anatomy and Microbiology, La Trobe University, Bundoora, Victoria, Australia

⁷Department of Obstetrics and Gynaecology, The University of Melbourne, Parkville, Victoria, Australia

^aCorrespondence: tina.bianco@adelaide.edu.au 0000-0002-8431-5338

Word count 3879

Number of figures and tables 4 figures, 2 supplementary figures, 1 table, 3 supplementary tables

ABSTRACT

Altered epigenetic mechanisms have been previously reported in growth restricted offspring whose mothers experienced environmental insults during pregnancy in both human and rodent studies. We previously reported changes in the expression of the DNA methyltransferase *Dnmt3a* and the imprinted genes *Cdkn1c* (Cyclin dependent kinase inhibitor 1C) and *Kcnq1* (Potassium voltage-gated channel subfamily Q member 1) in the kidney tissue of growth restricted rats whose mothers had uteroplacental insufficiency induced on day 18 of gestation, at both embryonic day 20 (E20) and postnatal day 1 (PN1). To determine the mechanisms responsible for changes in the expression of these imprinted genes, we investigated DNA methylation of KvDMR1, an imprinting control region (ICR) that includes the promoter of the antisense long non-coding RNA *Kcnq1ot1* (*Kcnq1* opposite strand/antisense transcript 1). *Kcnq1ot1* expression decreased by 51% in growth restricted offspring compared to sham at PN1. Interestingly, there was a negative correlation between *Kcnq1ot1* and *Kcnq1* in the E20 growth restricted group (Spearman's $\rho = 0.014$). No correlation was observed between *Kcnq1ot1* and *Cdkn1c* expression in either group at any time point. Additionally, there was a 11.25% decrease in the methylation level at one CpG site within KvDMR1 ICR. This study, together with others, support that long non-coding RNAs may mediate the changes seen in tissues obtained from growth restricted offspring.

Keywords Intrauterine growth restriction, uteroplacental insufficiency, epigenetic mechanisms, long non-coding RNA, DNA methylation

INTRODUCTION

Development is susceptible to environmental insults, such as uteroplacental insufficiency, maternal suboptimal diets, and other environmental exposures to chemicals, infections, drugs and alcohol [1, 2, 3, 4, 5, 6, 7]. Developmental environmental exposure early in life has been shown to be associated with epigenetic changes, including changes in DNA methylation, histone modifications, long non-coding RNA (lncRNA), and micro-RNA (miRNA) expression, in both human and rodent studies, which can have a significant impact on short- and long-term offspring health [1, 4, 5, 6, 8, 9, 10]. Additionally, altered epigenetic mechanisms and physiology due to environmental exposure during gametogenesis/gestation have been reported to have multigenerational or transgenerational effects that occur in a sex-specific manner [4, 5, 6, 7, 9, 10, 11, 12, 13, 14, 15, 16, 17].

We have recently shown in our rodent model of uteroplacental insufficiency (UPI) that the expression of *Dnmt3a*, a *de novo* DNA methyltransferase, but not *Dnmt1*, which primary role is maintaining the DNA methylation landscape, was decreased in the kidney of embryonic day 20 (E20) offspring, which is during the embryonic nephron formation period [12]. Concurrently, expression of imprinted genes that are known to be important in kidney development, *Cdkn1c* and *Kcnq1*, were also altered at both E20 (*Cdkn1c*; sex-specific) and postnatal day 1 (PN1; *Cdkn1c* and *Kcnq1*) [12]. Specifically, at E20, *Cdkn1c* expression was only reduced in growth restricted females. At PN1, regardless of sex, *Cdkn1c* expression was lower and *Kcnq1* expression was higher in growth restricted offspring, in association with reduced absolute and percentage left kidney weight [12]. Interestingly, *Kcnq1* and *Cdkn1c* are both known to be regulated by KvDMR1, an imprinting control region (ICR), which includes the promoter of the imprinted antisense lncRNA *Kcnq1ot1* [18, 19]. These results raised a

question of whether epigenetic mechanisms, such as DNA methylation or lncRNAs, can explain the multigenerational and sex-specific alterations in both gene expression and growth phenotypes in the kidneys of growth restricted offspring.

In the current study, we investigated the relationship between *Kcnq1* and *Cdkn1c* with *Kcnq1ot1* and KvDMR1 by examining the expression of *Kcnq1ot1* and the DNA methylation status of two CpG islands within the KvDMR1 ICR in the kidneys of F1 growth restricted offspring. The study will contribute to the understanding of the potential mechanisms controlling the gene expression of imprinted genes in the kidney that might be susceptible to adverse *in utero* environments.

MATERIALS AND METHODS

Kidney tissue collection

The intrauterine growth restricted (IUGR) Wistar Kyoto rat model was generated as previously described (The University of Melbourne AEC 04138, 1011865, and 1112130; La Trobe University AEC 12-42) [12, 20, 21]. In short, pregnant female rats (F0) underwent bilateral uterine vessel (artery and vein) ligation at day 18 of pregnancy (late gestation; term = 22 days) to induce UPI. The control group underwent sham surgery (no vessel ligation). Left kidney samples were collected at embryonic day 20 (E20) and post-natal day 1 (PN1) from the first-generation rat offspring, with one male and one female examined per litter [12]. Samples were snap frozen in liquid nitrogen and stored at -80°C.

RNA and DNA extraction

RNA was extracted from samples as described previously [12]. For DNA extraction, 30 mg of left kidney tissue was quickly cut on a plastic weight boat on ice. Only PN1 tissues were available for DNA extraction as the whole E20 kidney was used in RNA extraction [12].

Tissue homogenisation was carried out in 500 μL of TES (10 mM Tris (pH 8.0), 1mM EDTA, 0.1M NaCl; Invitrogen) with the following PowerLyser settings: time “T” = 15 s, cycles “C” = 1, dwell/pause time “D” = 0 s, and speed “S” = 3,500 rpm. DNA was then extracted using the salting out method [22] with modifications. Thirty microliters of 20 $\mu\text{g}/\mu\text{L}$ Proteinase K (Invitrogen) was added to each tube of homogenised tissue (mixed by inversion), followed by 60 μL of 20% SDS (Invitrogen) (mixed by inversion). The samples were then incubated at 37°C for 24 h. After incubation, 300 μL of 3M NaCl was added to each tube and mixed vigorously by shaking for at least 10 s. Tubes were placed on ice for 10 min, followed by centrifugation at 13,000 rpm for 15 min, and a maximum of 450 μL of the supernatant was collected. Two microliters of glycogen (Invitrogen) was added to each tube, followed by 900 μL of 100% molecular biology grade ethanol (Sigma-Aldrich) (mixed by inversion). The DNA was pelleted by centrifugation at 13,000 rpm for 2 min. The DNA pellet was washed with 900 μL 70% ethanol (mixed by inversion) and centrifuged at 13,000 rpm for 1 min. The supernatant was then removed and the DNA pellet was centrifuged at 13,000 rpm for 1 min. The DNA pellet was dried at room temperature before resuspension in TE buffer (Invitrogen) (50 μL , pH 8.0). Samples were stored at 4°C and the DNA concentration was quantitated using a NanoDrop spectrophotometer (Thermo Fisher Scientific). DNA integrity was checked using 1% agarose gel electrophoresis.

Genomic DNA (gDNA) contamination check and reverse transcription

RNA samples (20 ng, in duplicate) were checked for contamination of gDNA as previously described [12] using the SsoAdvanced™ Universal SYBR® Green Supermix (Bio-Rad) and primers that targeted an *Actb* intronic region. Contaminated RNA samples (Cq < 35) were DNase-treated using the TURBO DNA-free™ kit (Thermo Fisher Scientific) and checked again using the same qPCR method.

qPCR gene expression analysis

Tbp and *Ywhaz* were determined to be the two most stable reference genes in our previous study [12]. As the lncRNA *Kcnq1ot1* sequence is not available on the rat assembly (UCSC Genome Browser Nov. 2020 (mRatBN7/rn7)), *Kcnq1ot1* sequence from the mouse genome (UCSC Genome Browser Jun. 2020 (GRCm39/mm39)) was submitted to a UCSC BLAT search against the rat genome. Primers for *Kcnq1ot1*, *Slc22a18*, and *Cars* were then designed using NCBI Primer-BLAST (**Table S1**). Primer optimisation, master mix preparation and qPCRs were performed as previously described [12], with cycling conditions shown in **Table S1**.

DNA methylation analysis

A total of 34 rat PN1 DNA samples (1000 ng each) were sent to the Australian Genome Research Facility (AGRF) for region-specific quantitative DNA methylation analysis. Primers targeting two CpG islands (chr1:198,492,806 - 198,493,065 (CpG: 23) and chr1:198,493,269 - 198,493,580 (CpG: 20) (mRatBN7/rn7)) on the KvDMR1 imprinting control region were designed by AGRF (**Table S2**). DNA samples were bisulfite modified, followed by analyses using EpiTYPER Agena MassArray and Mass Cleave Chemistry test methods [23].

Data analysis

Data were analyzed using a linear mixed-effect model, with adjustments for litter size and relatedness between litter siblings as previously reported [12], using R version 4.1.1 [24, 25]. Power of the linear mixed-effect model was determined to be 0.998 and 0.993 for the analysis of gene expression and DNA methylation, respectively, calculated using the "pwr.f2.test" function ("pwr" package) in the R environment, with n (sample size) = 38 for our expression studies and $n = 33$ for the DNA methylation analyses, respectively. Correlation between gene expression levels were determined using Spearman's non-parametric correlation coefficient (no assumptions regarding data distribution), calculated using PAST 4.03 software [26]. Sham and IUGR data were combined to investigate whether there was a relationship between expression of different pairs of genes, regardless of treatment. The relationships within each group were then examined to determine whether a correlation present in one group was absent/altered in the other group, potentially indicating disruption due to growth restriction.

RESULTS

Expression of imprinted and non-imprinted genes in the kidney

The expression of *Kcnq1ot1* was not different between the sham and IUGR offspring at E20 (**Fig. 1a**). However, at PN1, there was a significantly lower expression of *Kcnq1ot1* in IUGR offspring than in sham offspring (reduced by approximately 50%, $p < 0.01$). The expression of another imprinted gene in the same KvDMR1 ubiquitously imprinted cluster (*Slc22a18*) and a non-imprinted gene (*Cars*) was also examined to determine whether the changes observed in *Kcnq1ot1*, *Kcnq1* and *Cdkn1c* extended to other genes in this imprinting cluster. There was no significant difference in the expression of either *Slc22a18* (**Fig. 1b**) or *Cars* (**Fig. 1c**) between the sham and IUGR offspring at any time point.

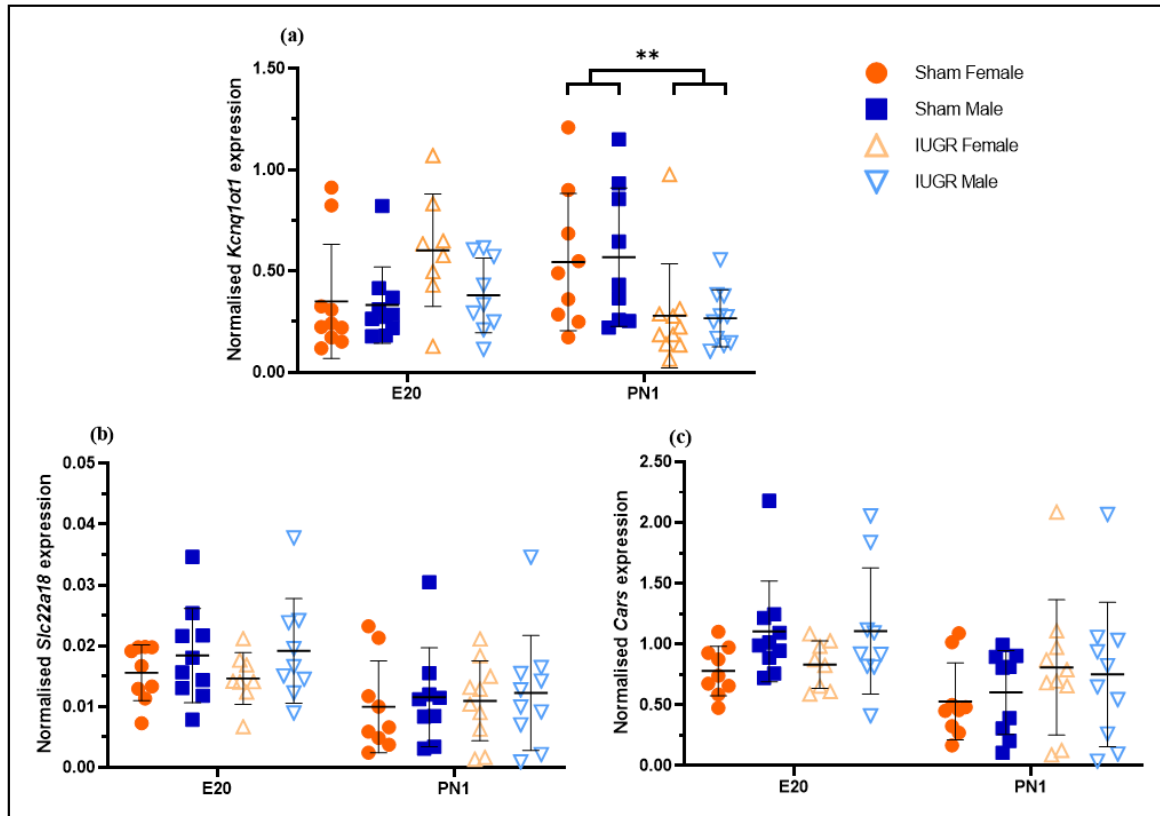


Figure 1. Normalised expression of the imprinted genes *Kcnq1ot1* (a), *Slc22a18* (b), and the non-imprinted gene *Cars* (c) in kidney tissues of sham and IUGR rat offspring at embryonic day 20 (E20) and postnatal day 1 (PN1). Significance was determined by linear mixed effect models, followed by a Tukey's *post hoc* test (** $p < 0.01$). Data is expressed as mean \pm SD; $n = 8-10$ /group.

Correlation between gene expression levels in rat kidney

Pairwise non-parametric correlation analyses were carried out to investigate the potential correlations between the expression levels of genes in sham and IUGR offspring at E20 and PN1, including between pairs of imprinted genes known to be important in kidney development and regulated by the KvDMR1 ICR (*Cdkn1c*, *Kcnq1* and *Kcnq1ot1*; **Fig. 2 and Table S3**), as well as between imprinted genes and other genes (*Dnmt1a*, *Dnmt3a*, *Peg3*,

Snrpn, *Slc22a18*, and *Cars*; **Fig. S1 and Table S3**). The expression of *Cdkn1c*, *Kcnq1*, *Dnmt1a*, *Dnmt3a*, *Peg3* and *Snrpn* has been previously reported [12].

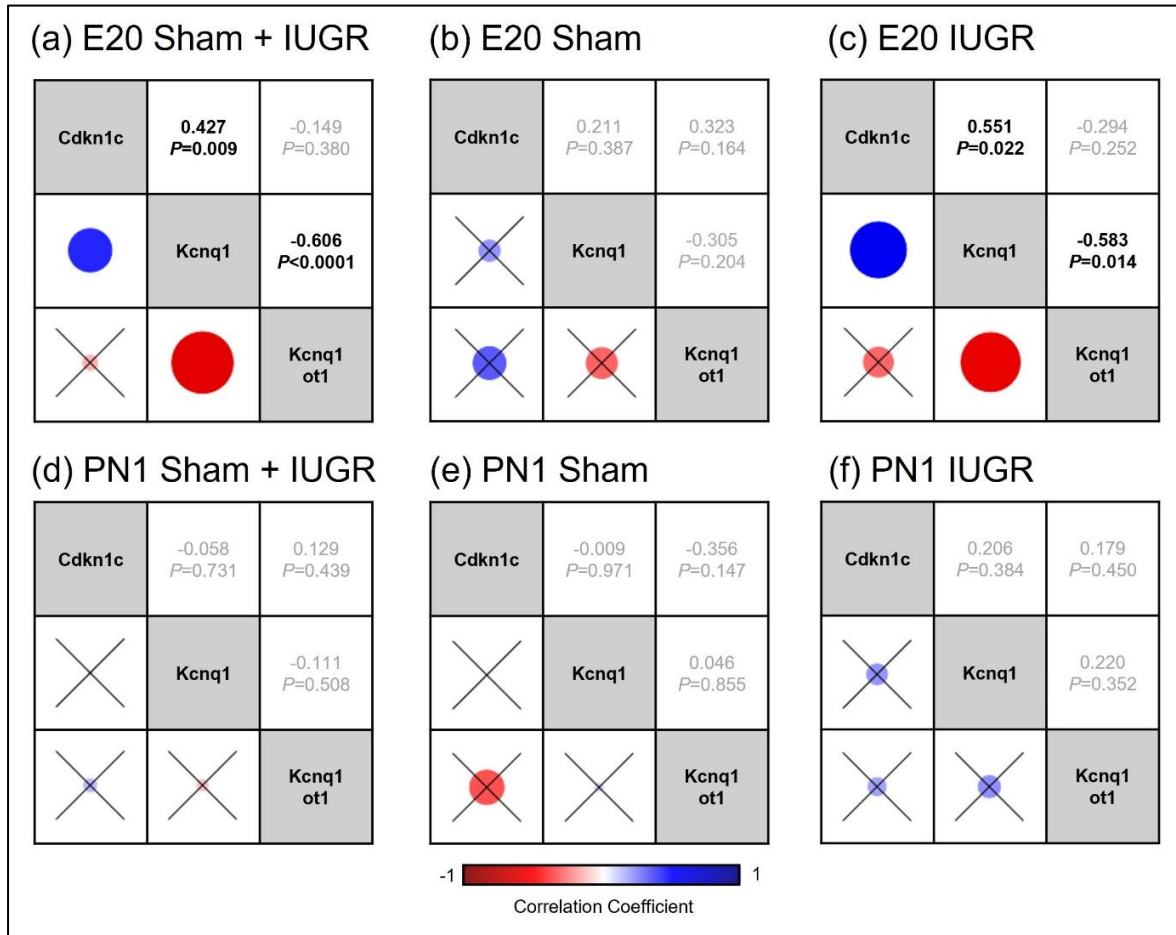


Figure 2. Spearman's non-parametric correlation matrices between 3 imprinted genes known to be important in kidney development and regulated by the KvDMR1 imprinting control region (*Kcnqlot1*, *Cdkn1c* and *Kcnq1*) in kidney tissues of sham and IUGR rat offspring at embryonic day 20 (E20) and postnatal day 1 (PN1). Sham and IUGR data were combined in (a) for E20 and (d) for PN1. Spearman correlation coefficients (top number) and *p*-values (bottom number) are displayed on the right triangles. A cross through the box indicates a non-significant *p*-value. The size of the circle indicates how strong the correlation is (corresponded to the Spearman correlation coefficients).

When sham and IUGR data were combined, there was a significant negative correlation between the expression of *Dnmt3a* and lncRNA *Kcnq1ot1* at E20 (Spearman's $\rho = -0.455$, $p = 0.006$, **Fig. S1a and Table S3**), as well as significant positive correlations between *Dnmt3a* and *Kcnq1* and *Dnmt3a* and *Cdkn1c* (Spearman's $\rho = 0.896$, $p < 0.0001$ and Spearman's $\rho = 0.349$, $p = 0.040$, respectively; **Fig. S1a and Table S3**). Additionally, at E20, there was a negative correlation between *Kcnq1ot1* and *Kcnq1* and a positive correlation between *Kcnq1* and *Cdkn1c* (Spearman's $\rho = -0.606$, $p < 0.0001$ and Spearman's $\rho = 0.427$, $p = 0.009$, respectively; **Fig. 2a and Table S3**). The relationships between these pairs of genes (except *Dnmt3a-Kcnq1*) were no longer present at PN1 (**Fig. S1b and Table S3**).

Interestingly, when sham and IUGR were investigated individually at each time point, the negative correlation between *Kcnq1ot1* and *Kcnq1* was significant only in the E20 IUGR group (Spearman's $\rho = -0.583$, $p = 0.014$, **Fig. 2c, 2e, 2f, S1c-f and Table S3**). Additionally, there was a significant positive correlation between *Kcnq1* and *Cdkn1c* in the E20 IUGR group (Spearman's $\rho = 0.551$, $p = 0.022$), but not in the E20 sham group (**Fig. 2b, 2c, S1c, S1e and Table S3**). No correlation was observed between *Kcnq1ot1* and *Cdkn1c* expression in any of the groups at any time point. On the other hand, there was an inverse relationship between *Dnmt3a* and *Kcnq1ot1* in the IUGR group, whereby at E20, there was a negative association (Spearman's $\rho = -0.421$) and at PN1, there was a positive association (Spearman's $\rho = 0.370$) (**Fig. S1e, S1f and Table S3**). However, these differences were not statistically significant.

DNA methylation status of the KvDMR1 imprinting control region

Base-specific cleavage of bisulfite-modified DNA yielded usable signals for four out of 16 (amplicon 1, **Fig. 3a**) and seven out of 20 (amplicon 13, **Fig. 3b**) CpG positions within CpG 23 and CpG 20 islands, respectively, in KvDMR1 ICR. There was hypomethylation ($p < 0.05$) at CpG site 6 of the CpG 23 island in IUGR males only ($\downarrow 11.25\%$, methylation level in IUGR males 6% vs. sham males 17.25%, amplicon 1, **Fig. 3a**). Interestingly, unlike other CpG sites within this region where the DNA methylation level was $\sim 50\%$ (as expected for imprinted genes), there was a lower than 20% methylation level at CpG site 6, even in the sham animals. There was no statistically significant difference in the methylation status between sham and IUGR offspring at any site of the CpG 20 island (amplicon 13, **Fig. 3b**).

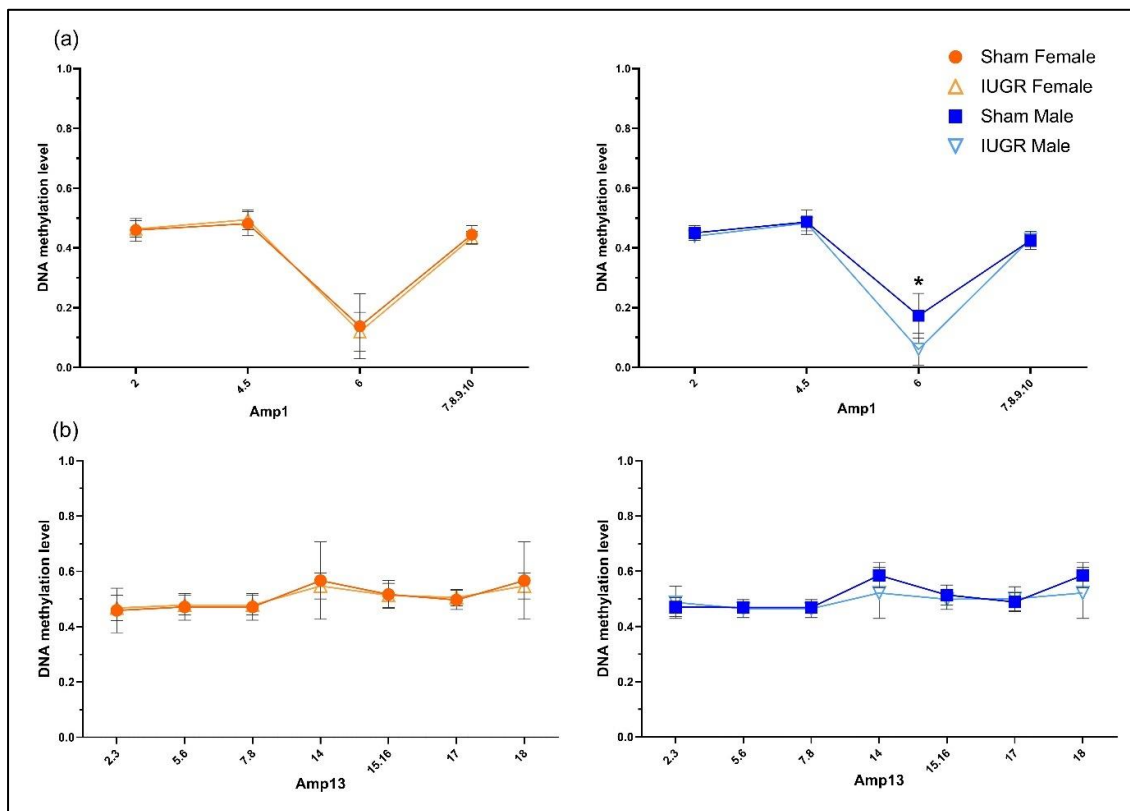


Figure 3. DNA methylation status of the KvDMR1 imprinting control region containing (a) CpG 23 (amplicon 1 (amp1), chr1:198,492,806 - 198,493,065, UCSC Genome Browser Nov.

2020 (mRatBN7/rn7)) and (b) CpG 20 (amplicon 13 (amp13), chr1:198,493,269 - 198,493,580 (mRatBN7/rn7)) in sham and IUGR rat offspring at postnatal day 1 (PN1), determined using EpiTYPER Agena MassArray and Mass Cleave Chemistry analyses. For CpG fragments that had the same mass peaks as other fragments containing same number of CpGs (Amp13, CpG_5.6 versus CpG_7.8 and CpG_14 versus CpG_18), methylation % was calculated between CpGs. Significance was determined by linear mixed effect models, followed by a Tukey's *post hoc* test ($*p < 0.05$). Data is expressed as mean \pm SD; n = 8-9/group.

KvDMR1 ICR was further analyzed to identify the location of these CpG sites. As mentioned previously, the *Kcnqlot1* sequence is not available in the mRatBN7/rn7 rat genome.

However, there was an uncharacterized lncRNA named LOC120099961 found in the rat mRatBN7.2 genome (NCBI Reference Sequence: NC_051336.1), which is located in a similar position as *Kcnqlot1* in other species genomes. Therefore, this rat sequence, together with other mouse sequences including the KvDMR1 region [27], *Kcnqlot1* transcriptional repressor CTCF binding sites [28], enhancer, promoter [29], and TSS [29, 30] were used in a BLAT search against the rat genome. The results for the (approximate) positions are shown in

Fig. 4. While amplicon 13 (CpG 20) was located within both *Kcnqlot1* TSS and CTCF binding site 2, amplicon 1 (CpG 23) was not located within any of the sequences mentioned above (**Fig. 4**). Using TFBIND software (weight matrix in transcription factor database TRANSFAC R.3.4, similarity $\geq 80\%$) [31] and TRANSFAC FACTOR TABLE (Release 2017.2), CpG site 6 (amplicon 1) was determined to correspond to different transcription factor binding sites (TFBSs) (**Table 1**). Among these, there were 4 TF that have been previously reported to play a role in kidney development and disease, as well as to be regulated by DNA methylation, including Chicken Ovalbumin Upstream Promoter

Transcription Factor 2 (COUP-TF2) [32, 33, 34, 35], GATA-binding Factor 2 (GATA-2) [36, 37], Serum Response Factor (SRF) [38, 39, 40], and Activating enhancer binding Protein 2 alpha (AP-2 α) [41, 42]. When data from all examined CpG sites within each CpG island were combined, no significant difference in DNA methylation levels was found between the sham and IUGR kidney samples (Fig. S2).

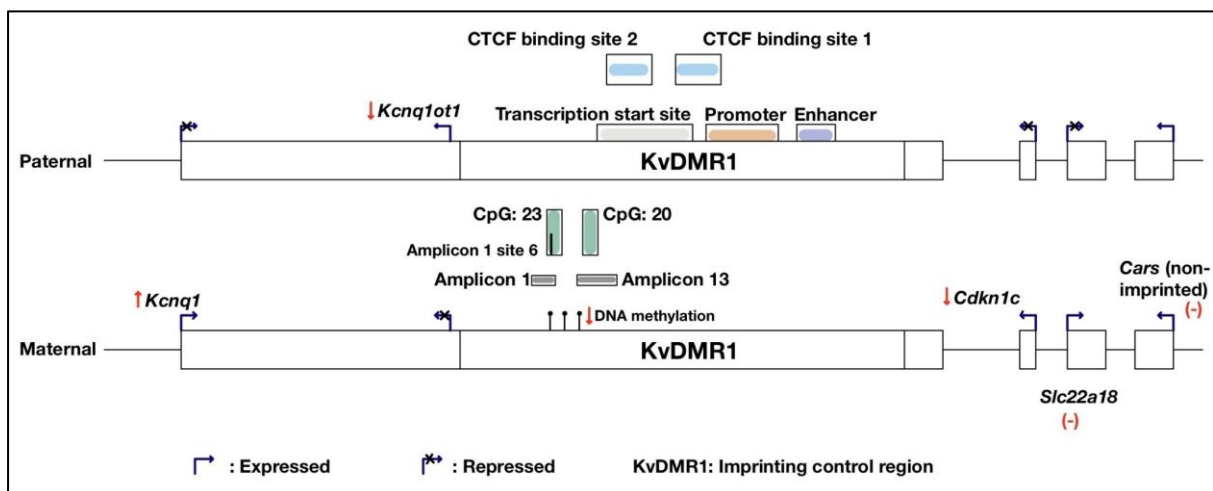


Figure 4. Approximate positions of the two amplicons (amplicon 1 and 13, targeting CpG island 23 (chr1:198,492,806 - 198,493,065) and 20 (chr1:198,493,269 - 198,493) (mRatBN7/rn7), respectively) in the rat KvDMR1 imprinting control region (modified from Doan *et al.* [12]), examined using region-specific quantitative DNA methylation analysis. DNA methylation of KvDMR1 and/or expression of the lncRNA *Kcnq1ot1* is known to play a role in controlling the monoallelic expression of imprinted genes in the KvDMR1 imprinting cluster. Primers were designed by the Australian Genome Research Facility (AGRF). There was a hypomethylation ($\downarrow 11.25\%$, $p < 0.05$) at CpG site 6 of CpG 23 island in PN1 growth restricted male kidneys. *Kcnq1ot1* sequence is not available on the mRatBN7/rn7 rat genome. Hence, sequence from the uncharacterized lncRNA named LOC120099961 found on the rat mRatBN7.2 genome (NCBI Reference Sequence: NC_051336.1, similar position) was used.

Mouse sequences, including KvDMR1 region [27], *Kcnq1ot1* transcriptional repressor CTCF binding sites [28], enhancer, promoter [29], and transcription start site [29, 30] were used in a BLAT search against the rat genome. ↓: expression decreased; ↑: expression increased; (-): no change in gene expression. Note that the annotations of gene expressions in this figure is based on the circumstance that in a healthy animal, the imprinted genes *Kcnq1* and *Cdkn1c* are expressed on the maternal allele, while *Kcnq1ot1* is preferentially expressed on the paternal allele.

Table 1. Transcription factor binding sites (TFBSs) correspond to CpG:23 island (amplicon 1, chr1:198,492,806 - 198,493,065, rat), where there was hypomethylation at CpG site 6 (coloured in red) in IUGR male kidneys. TFBSs were determined using TFBIND software (weight matrix in transcription factor database TRANSFAC R.3.4) [31] and TRANSFAC FACTOR TABLE (Release 2017.2). Left to right: TF name, matrix ID (from TRANSFAC R.3.4), label in TFBIND, similarity compared to input sequence, strand that the transcription factor binds, and sequence of the TFBS.

Factor	ID	Label	Similarity	Forward (+) or reverse (-)	Sequence
COUP-TF2	M00155	ARP1_01	0.806	(+)	CGCGGCCATGAAA CG ⁶ C
GATA-2	M00076	GATA2_01	0.806	(-)	CG ⁶ CCAACCGG
SRF	M00215	SRF_C	0.803	(+)	GCCATGAAAC CG ⁶ CCAA
AP-2 α	M00189	AP2_Q6	0.801	(+)	CG ⁶ CCAACCGGGC

DISCUSSION

The imprinted gene *Kcnq1ot1* has been previously shown to be altered in growth restricted offspring due to environment exposure during early life [43, 44]. Specifically, reduced expression of this lncRNA has been reported in placentae of E16.5 growth restricted male mice whose mothers were exposed to 50 ppm of the heavy metal cadmium throughout pre-

conception, mating, and pregnancy [43], as well as in E18.5 growth restricted mice who were conceived through *in vitro* fertilisation (IVF) [44]. In our current study, as expected, there was a significant decrease in *Kcnq1ot1* expression in kidneys of F1 growth restricted rat offspring at PN1. From studies in mice, the function of *Kcnq1ot1* is suggested to partially control the allele-specific expression of other imprinted genes in the same KvDMR1 imprinting cluster, including those investigated in this current study, in a tissue-specific manner; however, the exact mechanism is still unclear [28, 45, 46]. For instance, deletion of the whole KvDMR1 ICR (2.8 kb [45] or 3.6 kb [46], which abolished *Kcnq1ot1* expression), deletion of *Kcnq1ot1* promoter and TSS region (224 bp) [46], producing a shorter transcript by inserting a transcription stop element at 1.5 kb downstream of the lncRNA TSS [46], or truncation of *Kcnq1ot1* (2.6 kb downstream of its promoter) [28], on the paternal allele, was reported to be associated with activation of the normally paternally silenced genes in mouse embryonic tissues (E11.5-16.5). Biallelic gene expression was reported for *Slc22a18* (placenta [28, 46], liver, gut, kidney, lung, heart, brain, and fibroblast [28]), *Kcnq1* (placenta [28, 46], liver [28, 45], gut, kidney, lung, heart, brain, and fibroblast [28]), and *Cdkn1c* (whole embryo, placenta [28, 46], liver [45], heart, brain, and gut [28]). However, monoallelic expression of *Cdkn1c* has been reported in the liver, kidney, lung, and fibroblasts of mice at E15.5, despite the *Kcnq1ot1* truncation, which remains to be explained [28].

In line with the above findings, studies in mouse IUGR models also reported alterations to the imprinted genes that are known to be regulated by KvDMR1, in association with decreased *Kcnq1ot1* expression [43, 44]. Growth restricted mice conceived through IVF have decreased placental *Cdkn1c* expression compared to *in vivo* controls at E18.5, despite a similar expression at E14.5 [44]. In contrast, *Cdkn1c* overall expression was increased in the placentae of E18.5 growth restricted mice whose mothers were exposed to Cadmium [43].

Meanwhile, there was no alteration in placental *Kcnq1* expression in these mice [43]. Additionally, allele-specific expression analysis indicated no difference in *Cdkn1c* expression between growth restricted and sham animals [43]. In our study of growth restricted rat kidneys, *Cdkn1c* expression was reduced only in IUGR females at E20, while PN1 IUGR offspring had decreased *Cdkn1c* and increased *Kcnq1* expression compared to sham [12]. Together with the above-mentioned findings, the fact that our results report decreased *Kcnq1ot1* only in PN1, but not E20, IUGR rats as well as no correlation between *Kcnq1ot1* and *Cdkn1c* expression in any of the groups, at any timepoint, suggests that changes in lncRNA *Kcnq1ot1* expression alone is not sufficient to explain changes in *Cdkn1c* in IUGR rat kidneys. Allele-specific expression analysis of these imprinted genes would provide a better understanding of their potential relationships.

As *Dnmt3a* was reported in our previous study to be decreased in IUGR kidneys at E20 [12], we hypothesized that there were alterations in the DNA methylation profile, including that of the KvDMR1 ICR, which is involved in dysregulation of the expression of imprinted genes that are known to be important in fetal kidney development. In babies diagnosed with Russell-Silver syndrome, characterised by intrauterine and postnatal growth restriction, alterations in KvDMR1 DNA methylation, either hypermethylation [47, 48, 49] or hypomethylation [50], have been reported in their blood samples. In human IUGR studies, KvDMR1 DNA methylation status was mostly studied using placental tissues, with no significant difference observed between growth restricted tissues and healthy controls [51, 52, 53, 54]. In the current study of rat kidneys, hypomethylation was found at a CpG site of CpG 23 island (chr1:198,492,806 - 198,493,065) within KvDMR1 in PN1 IUGR males. This CpG site was not located within any of the *Kcnq1ot1* regulatory regions that we were able to assess. However, this position is a potential target for several TFs known to be important in

kidney development and disease, including but not limited to COUP-TF2, GATA-2, SRF, and AP-2 α . Future studies should investigate the potential interaction of these TFs within the KvDMR1 and the biological function of such events. Furthermore, as these TFs have been previously shown to be impacted by DNA methylation [32, 33, 37, 38, 41], alteration to the *Dnmt3a* expression in our study could also impact their expression. Another important point to mention here is DNA methylation level of this specific site was also lower than 50% in sham animals, which is not typical for imprinted genes where the silenced allele is often methylated. Meanwhile, investigation of the CpG 41 island in the placentae of E18.5 growth restricted female mice (conserved sequence of KvDMR1 CpG 23 island in rats) showed no change in DNA methylation of any other CpG sites within this region (chr1:198,493,086-198,493,233) [43]. In addition, our results show that the mean DNA methylation levels within this CpG 23 island as well as within the CpG 20 island (chr1:198,493,269 - 198,493,580) of the KvDMR1 ICR were also not different between sham and IUGR offspring. Nonetheless, apart from the differences in tissues examined, it should be noted that different regions within and near the KvDMR1 ICR were investigated in the above studies, which could be a potential limitation of the present study. Additionally, the kidney is a complex organ that comprises of more than 20 differentiated cell types [55]. Recent single-cell RNA sequencing databases in both adult mice [56, 57] and rats [58] suggest that the 3 imprinted genes (*Cdkn1c*, *Kcnq1*, and *Kcnq1ot1*) investigated in our study have different expression levels in different renal cell types. Specifically, *Cdkn1c* is highly expressed in stromal cells and podocytes (visceral epithelium), while *Kcnq1* is highly expressed in collecting duct intercalated cells and connecting tubule principal-like cells. *Kcnq1ot1* (mouse data) is also highly expressed in podocytes. Since we only assessed DNA methylation of one region using a region-specific quantitative DNA methylation analysis method, this did not allow for assessing or adjusting for different cell types.

Besides KvDMR1, DNA methylation of the *Cdkn1c* promoter region is also an important mechanism that needs to be explored, as it is known to be important in maintaining allele-specific gene expression during embryonic development in healthy mice [59]. However, in the mouse *Kcnq1ot1* truncation model, where *Cdkn1c* allele-specific expression was shown to be either altered or unchanged in different embryonic tissues, there was no difference in *Cdkn1c* promoter DNA methylation levels in all tissues at E15.5, suggesting a different mechanism for maintaining *Cdkn1c* monoallelic expression [28]. In contrast, in the placentae of E18.5 Cadmium-exposed growth restricted mice, where expression of *Kcnq1ot1* decreased and expression of *Cdkn1c* increased, there was a reduction in DNA methylation in one out of 23 investigated CpG sites in the *Cdkn1c* promoter region [43]. However, the mean methylation level of the whole CpG island did not change compared with that of the sham offspring [43]. Future studies should investigate epigenetic alterations in the *Cdkn1c* promoter region.

In summary, at PN1, there was a 50% decrease in the expression of an antisense lncRNA (*Kcnq1ot1*) in IUGR rats compared to that in sham animals. This is the first study to report changes in *Kcnq1ot1* in UPI-induced growth restricted rat kidneys. *H19* is another lncRNA and imprinted gene that plays an important role in development. *H19* has also been shown to be altered in rodent and human IUGR studies, with significant changes in its expression and DNA methylation in many tissues (e.g., sperm, liver, blood, and placenta [1, 60, 61, 62]). In this study, there was a negative correlation between *Kcnq1ot1* and the gene that it is located within (*Kcnq1*), only in E20 IUGR kidneys. As *Kcnq1* was also altered at PN1 [12], these results suggest that an abnormal event occurred early during fetal nephron formation, which later affected the expression of imprinted genes within the KvDMR1 ICR. In contrast, changes in *Kcnq1ot1* were not sufficient to explain the decrease in the expression of another

imprinted gene within the same KvDMR1 imprinting cluster, *Cdkn1c*, at both E20 (IUGR females) and PN1 (IUGR males and females) [12], as no correlation was found between the two genes in any group at any time point. As there was a decrease in *Dnmt3a* expression in E20 IUGR kidneys [12] and significant correlations between *Dnmt3a* and *Kcnq1/Kcnq1ot1/Cdkn1c* at E20, the DNA methylation profile of KvDMR1 was investigated. Hypomethylation was found at a CpG site only in PN1 IUGR males. However, the importance of the alteration of this specific CpG site and its effect on the IUGR kidney is yet to be determined. Future studies should investigate the allele-specific expression of these genes, the reason for DNA methylation changes at one CpG site in KvDMR1, and other epigenetic mechanisms.

DISCLAIMERS

The views expressed in this manuscript are those of the authors.

ACKNOWLEDGEMENTS

The authors would like to thank Sandy Khor and Neil Shirley (University of Adelaide) for their help in Qiagility liquid-handling robot programming and setup.

SOURCE OF SUPPORT

This research was supported by the National Health and Medical Research Council (NHMRC) of Australia (M.E.W.; 1045602), the Heart Foundation (M.E.W.; G 11M 5785), a La Trobe University Faculty of Health Sciences Research Grant Award (T.R.), and a

Robinson Research Institute (RRI) Seed Grant (T.B-M, M.E.W., and J.F.B.), and supported by the School of Agriculture, Food and Wine, University of Adelaide.

DISCLOSURE STATEMENT

The authors report no conflict of interest.

DATA AVAILABILITY STATEMENT

The data that support the findings of this study are available from the corresponding author (tina.bianco@adelaide.edu.au) upon request.

REFERENCES

1. Doan TNA, Akison LK, Bianco-Miotto T. Epigenetic mechanisms responsible for the transgenerational inheritance of intrauterine growth restriction phenotypes. *Frontiers in Endocrinology*. 2022;13:838737. doi: 10.3389/fendo.2022.838737.
2. Sharma D, Shastri S, Sharma P. Intrauterine growth restriction: antenatal and postnatal aspects. *Clinical Medicine Insights: Pediatrics*. 2016;10:67-83. doi: 10.4137/CMPed.S40070.
3. Dalle Molle R, Bischoff AR, Portella AK, Silveira PP. The fetal programming of food preferences: current clinical and experimental evidence. *Journal of Developmental Origins of Health and Disease*. 2016;7(3):222-230. doi: 10.1017/S2040174415007187.
4. Skinner MK, Manikkam M, Tracey R, Guerrero-Bosagna C, Haque M, Nilsson EE. Ancestral dichlorodiphenyltrichloroethane (DDT) exposure promotes epigenetic

- transgenerational inheritance of obesity. *BMC Medicine*. 2013;11:228. doi: 10.1186/1741-7015-11-228.
5. Skinner MK, Ben Maamar M, Sadler-Riggleman I, Beck D, Nilsson E, McBirney M, Klukovich R, Xie Y, Tang C, Yan W. Alterations in sperm DNA methylation, non-coding RNA and histone retention associate with DDT-induced epigenetic transgenerational inheritance of disease. *Epigenetics Chromatin*. 2018;11(1):8. doi: 10.1186/s13072-018-0178-0.
 6. Thorson JLM, Beck D, Ben Maamar M, Nilsson EE, Skinner MK. Ancestral plastics exposure induces transgenerational disease-specific sperm epigenome-wide association biomarkers. *Environmental Epigenetics*. 2021;7(1):dvaa023. doi: 10.1093/eep/dvaa023.
 7. Weber-Stadlbauer U, Richetto J, Zwamborn RAJ, Sliker RC, Meyer U. Transgenerational modification of dopaminergic dysfunctions induced by maternal immune activation. *Neuropsychopharmacology*. 2021;46(2):404-412. doi: 10.1038/s41386-020-00855-w.
 8. Goyal D, Limesand SW, Goyal R. Epigenetic responses and the developmental origins of health and disease. *Journal of Endocrinology*. 2019;242(1):T105-T119. doi: 10.1530/joe-19-0009.
 9. Siklenka K, Erkek S, Godmann M, Lambrot R, McGraw S, Lafleur C, Cohen T, Xia J, Suderman M, Hallett M, Trasler J, Peters AHFM, Kimmins S. Disruption of histone methylation in developing sperm impairs offspring health transgenerationally. *Science*. 2015;350(6261):aab2006. doi: 10.1126/science.aab2006.
 10. Lismer A, Siklenka K, Lafleur C, Dumeaux V, Kimmins S. Sperm histone H3 lysine 4 trimethylation is altered in a genetic mouse model of transgenerational epigenetic

- inheritance. *Nucleic Acids Research*. 2020;48(20):11380-11393. doi: 10.1093/nar/gkaa712.
11. Briffa JF, Wlodek ME, Moritz KM. Transgenerational programming of nephron deficits and hypertension. *Seminars in Cell and Developmental Biology*. 2018;S1084-9521(17):30447-0. doi: 10.1016/j.semcdb.2018.05.025.
 12. Doan TNA, Briffa JF, Phillips AL, Leemaqz SY, Burton RA, Romano T, Wlodek ME, Bianco-Miotto T. Epigenetic mechanisms involved in intrauterine growth restriction and aberrant kidney development and function. *Journal of Developmental Origins of Health and Disease*. 2021;12(6):952-962. doi: 10.1017/S2040174420001257.
 13. Gallo LA, Tran M, Cullen-McEwen LA, Denton KM, Jefferies AJ, Moritz KM, Wlodek ME. Transgenerational programming of fetal nephron deficits and sex-specific adult hypertension in rats. *Reproduction, Fertility and Development*. 2014;26(7):1032-1043. doi: 10.1071/RD13133.
 14. Gallo LA, Tran M, Moritz KM, Mazzuca MQ, Parry LJ, Westcott KT, Jefferies AJ, Cullen-McEwen LA, Wlodek ME. Cardio-renal and metabolic adaptations during pregnancy in female rats born small: implications for maternal health and second generation fetal growth. *The Journal of physiology*. 2012;590(3):617-630. doi: 10.1113/jphysiol.2011.219147.
 15. Master JS, Zimanyi MA, Yin KV, Moritz KM, Gallo LA, Tran M, Wlodek ME, Black MJ. Transgenerational left ventricular hypertrophy and hypertension in offspring after uteroplacental insufficiency in male rats. *Clinical and Experimental Pharmacology and Physiology*. 2014;41(11):884-890. doi: 10.1111/1440-1681.12303.

16. Tran M, Gallo LA, Jefferies AJ, Moritz KM, Wlodek ME. Transgenerational metabolic outcomes associated with uteroplacental insufficiency. *Journal of Endocrinology*. 2013;217(1):105-118. doi: 10.1530/JOE-12-0560.
17. Wadley GD, Siebel AL, Cooney GJ, McConell GK, Wlodek ME, Owens JA. Uteroplacental insufficiency and reducing litter size alters skeletal muscle mitochondrial biogenesis in a sex-specific manner in the adult rat. *American Journal of Physiology-Endocrinology and Metabolism*. 2008;294(5):E861-E869. doi: 10.1152/ajpendo.00037.2008.
18. Cordeiro A, Neto AP, Carvalho F, Ramalho C, Dória S. Relevance of genomic imprinting in intrauterine human growth expression of *CDKN1C*, *H19*, *IGF2*, *KCNQ1* and *PHLDA2* imprinted genes. *Journal of Assisted Reproduction and Genetics*. 2014;31(10):1361-1368. doi: 10.1007/s10815-014-0278-0.
19. Saha P, Verma S, Pathak RU, Mishra RK. Long noncoding RNAs in mammalian development and diseases. *Advances in Experimental Medicine and Biology*. 2017;1008:155-198. doi: 10.1007/978-981-10-5203-3_6.
20. Wlodek ME, Westcott K, Siebel AL, Owens JA, Moritz KM. Growth restriction before or after birth reduces nephron number and increases blood pressure in male rats. *Kidney International*. 2008;74(2):187-195. doi: 10.1038/ki.2008.153.
21. Wlodek ME, Mibus A, Tan A, Siebel AL, Owens JA, Moritz KM. Normal lactational environment restores nephron endowment and prevents hypertension after placental restriction in the rat. *Journal of the American Society of Nephrology*. 2007;18(6):1688-1696. doi: 10.1681/asn.2007010015.
22. Miller SA, Dykes DD, Polesky HF. A simple salting out procedure for extracting DNA from human nucleated cells. *Nucleic Acids Research*. 1988;16(3):1215. doi: 10.1093/nar/16.3.1215.

23. Suchiman HE, Sliker RC, Kremer D, Slagboom PE, Heijmans BT, Tobi EW. Design, measurement and processing of region-specific DNA methylation assays: the mass spectrometry-based method EpiTYPER. *Front Genet.* 2015;6:287. doi: 10.3389/fgene.2015.00287.
24. R Core Team. R: A language and environment for statistical computing. Vienna, Austria: R Foundation for Statistical Computing; 2018. Available from: <http://www.R-project.org/>
25. RStudio Team. RStudio: integrated development for R. Boston, MA: RStudio, PBC; 2020. Available from: <http://www.rstudio.com/>
26. Øyvind H, David ATH, Paul DR. PAST: Paleontological statistics software package for education and data analysis. *Palaeontologia Electronica.* 2001;4(1):1-9.
27. Fitzpatrick GV, Pugacheva EM, Shin JY, Abdullaev Z, Yang Y, Khatod K, Lobanenko VV, Higgins MJ. Allele-specific binding of CTCF to the multipartite imprinting control region KvDMR1. *Molecular and Cellular Biology.* 2007;27(7):2636-47. doi: 10.1128/mcb.02036-06.
28. Shin JY, Fitzpatrick GV, Higgins MJ. Two distinct mechanisms of silencing by the KvDMR1 imprinting control region. *The EMBO Journal.* 2008;27(1):168-78. doi: 10.1038/sj.emboj.7601960.
29. Mancini-DiNardo D, Steele SJS, Ingram RS, Tilghman SM. A differentially methylated region within the gene *Kcnql* functions as an imprinted promoter and silencer. *Human Molecular Genetics.* 2003;12(3):283-294. doi: 10.1093/hmg/ddg024.
30. Abugessaisa I, Noguchi S, Hasegawa A, Kondo A, Kawaji H, Carninci P, Kasukawa T. refTSS: a reference data set for human and mouse transcription start sites. *Journal of Molecular Biology.* 2019;431(13):2407-2422. doi: 10.1016/j.jmb.2019.04.045.

31. Tsunoda T, Takagi T. Estimating transcription factor bindability on DNA. *Bioinformatics*. 1999 Jul-Aug;15(7-8):622-30. doi: 10.1093/bioinformatics/15.7.622.
32. Baribault C, Ehrlich KC, Ponnaluri VKC, Pradhan S, Lacey M, Ehrlich M. Developmentally linked human DNA hypermethylation is associated with down-modulation, repression, and upregulation of transcription. *Epigenetics*. 2018 2018/03/04;13(3):275-289. doi: 10.1080/15592294.2018.1445900.
33. Kao C-Y, Xu M, Wang L, Lin S-C, Lee H-J, Duraine L, Bellen HJ, Goldstein DS, Tsai SY, Tsai M-J. Elevated COUP-TFII expression in dopaminergic neurons accelerates the progression of Parkinson's disease through mitochondrial dysfunction. *PLOS Genetics*. 2020;16(6):e1008868. doi: 10.1371/journal.pgen.1008868.
34. Li L, Galichon P, Xiao X, Figueroa-Ramirez AC, Tamayo D, Lee JJ, Kalocsay M, Gonzalez-Sanchez D, Chancay MS, McCracken KW, Lee NN, Ichimura T, Mori Y, Valerius MT, Wilflingseder J, Lemos DR, Edelman ER, Bonventre JV. Orphan nuclear receptor COUP-TFII enhances myofibroblast glycolysis leading to kidney fibrosis. *EMBO Rep*. 2021;22(6):e51169. doi: 10.15252/embr.202051169.
35. Ishii S, Koibuchi N. COUP-TFII in Kidneys, from Embryos to Sick Adults. *Diagnostics (Basel)*. 2022;12(5). doi: 10.3390/diagnostics12051181.
36. Estrela GR, Freitas-Lima LC, Budu A, Arruda ACd, Perilhão MS, Fock RA, Barrera-Chimal J, Araújo RC. Chronic Kidney Disease Induced by Cisplatin, Folic Acid and Renal Ischemia Reperfusion Induces Anemia and Promotes GATA-2 Activation in Mice. *Biomedicines*. 2021;9(7):769. doi: 10.3390/biomedicines9070769.
37. Yang X, Mei C, Nie H, Zhou J, Ou C, He X. Expression profile and prognostic values of GATA family members in kidney renal clear cell carcinoma. *Aging*. 2023;15(6):2170-2188. doi: 10.18632/aging.204607.

38. Liu Z, Zhang J, Gao Y, Pei L, Zhou J, Gu L, Zhang L, Zhu B, Hattori N, Ji J, Yuasa Y, Kim W, Ushijima T, Shi H, Deng D. Large-Scale Characterization of DNA Methylation Changes in Human Gastric Carcinomas with and without Metastasis. *Clinical Cancer Research*. 2014;20(17):4598-4612. doi: 10.1158/1078-0432.CCR-13-3380.
39. Zhao L, Li C, Guan C, Song N, Luan H, Luo C, Jiang W, Bu Q, Wang Y, Che L, Xu Y. Serum response factor, a novel early diagnostic biomarker of acute kidney injury. *Aging (Albany NY)*. 2021 Jan 5;13(2):2885-2894. doi: 10.18632/aging.202381.
40. Drake KA, Chaney C, Patel M, Das A, Bittencourt J, Cohn M, Carroll TJ. Transcription Factors YAP/TAZ and SRF Cooperate To Specify Renal Myofibroblasts in the Developing Mouse Kidney. *Journal of the American Society of Nephrology*. 2022;33(9):1694-1707. doi: 10.1681/asn.2021121559.
41. Makhov PB, Golovine KV, Kutikov A, Canter DJ, Rybko VA, Roshchin DA, Matveev VB, Uzzo RG, Kolenko VM. Reversal of epigenetic silencing of AP-2alpha results in increased zinc uptake in DU-145 and LNCaP prostate cancer cells. *Carcinogenesis*. 2011;32(12):1773-81. doi: 10.1093/carcin/bgr212.
42. Lamontagne JO, Zhang H, Zeid AM, Strittmatter K, Rocha AD, Williams T, Zhang S, Marneros AG. Transcription factors AP-2 α and AP-2 β regulate distinct segments of the distal nephron in the mammalian kidney. *Nature Communications*. 2022;13(1):2226. doi: 10.1038/s41467-022-29644-3.
43. Simmers MD, Hudson KM, Baptissart M, Cowley M. Epigenetic control of the imprinted growth regulator Cdkn1c in cadmium-induced placental dysfunction. *Epigenetics*. 2022:1-17. doi: 10.1080/15592294.2022.2088173.

44. Chen S, Sun FZ, Huang X, Wang X, Tang N, Zhu B, Li B. Assisted reproduction causes placental maldevelopment and dysfunction linked to reduced fetal weight in mice. *Scientific Reports*. 2015;5:10596. doi: 10.1038/srep10596.
45. Fitzpatrick GV, Soloway PD, Higgins MJ. Regional loss of imprinting and growth deficiency in mice with a targeted deletion of KvDMR1. *Nature Genetics*. 2002;32(3):426-431. doi: 10.1038/ng988.
46. Mancini-Dinardo D, Steele SJS, Levorse JM, Ingram RS, Tilghman SM. Elongation of the *Kcnqlot1* transcript is required for genomic imprinting of neighboring genes. *Genes and Development*. 2006;20(10):1268-1282. doi: 10.1101/gad.1416906.
47. Cytrynbaum C, Chong K, Hannig V, Choufani S, Shuman C, Steele L, Morgan T, Scherer SW, Stavropoulos DJ, Basran RK, Weksberg R. Genomic imbalance in the centromeric 11p15 imprinting center in three families: Further evidence of a role for IC2 as a cause of Russell–Silver syndrome. *American Journal of Medical Genetics Part A*. 2016;170(10):2731-2739. doi: 10.1002/ajmg.a.37819.
48. Bonaldi A, Mazzeu JF, Costa SS, Honjo RS, Bertola DR, Albano LMJ, Furquim IM, Kim CA, Vianna-Morgante AM. Microduplication of the ICR2 domain at chromosome 11p15 and familial Silver–Russell syndrome. *American Journal of Medical Genetics Part A*. 2011;155(10):2479-2483. doi: 10.1002/ajmg.a.34023.
49. Mio C, Allegri L, Passon N, Bregant E, Demori E, Franzoni A, Driul D, Riccio A, Damante G, Baldan F. A paternally inherited 1.4 kb deletion of the 11p15.5 imprinting center 2 is associated with a mild familial Silver–Russell syndrome phenotype. *European Journal of Human Genetics*. 2021;29(3):447-454. doi: 10.1038/s41431-020-00753-1.
50. Passaretti F, Pignata L, Vitiello G, Alesi V, D’Elia G, Cecere F, Acquaviva F, De Brasi D, Novelli A, Riccio A, Iolascon A, Cerrato F. Different mechanisms cause

- hypomethylation of both *H19* and *KCNQ1OT1* imprinted differentially methylated regions in two cases of Silver-Russell syndrome spectrum. *Genes*. 2022;13(10):1875. doi: 10.3390/genes13101875.
51. López-Abad M, Iglesias-Platas I, Monk D. Epigenetic Characterization of CDKN1C in Placenta Samples from Non-syndromic Intrauterine Growth Restriction. *Front Genet*. 2016;7:62. doi: 10.3389/fgene.2016.00062.
 52. Caniçais C, Vasconcelos S, Ramalho C, Marques CJ, Dória S. Deregulation of imprinted genes expression and epigenetic regulators in placental tissue from intrauterine growth restriction. *Journal of Assisted Reproduction and Genetics*. 2021;38(4):791-801. doi: 10.1007/s10815-020-02047-3.
 53. Guo L, Choufani S, Ferreira J, Smith A, Chitayat D, Shuman C, Uxa R, Keating S, Kingdom J, Weksberg R. Altered gene expression and methylation of the human chromosome 11 imprinted region in small for gestational age (SGA) placentae. *Developmental Biology*. 2008 2008;320(1):79-91. doi: 10.1016/j.ydbio.2008.04.025.
 54. Bourque DK, Avila L, Peñaherrera M, von Dadelszen P, Robinson WP. Decreased placental methylation at the H19/IGF2 imprinting control region is associated with normotensive intrauterine growth restriction but not preeclampsia. *Placenta*. 2010;31(3):197-202. doi: 10.1016/j.placenta.2009.12.003.
 55. Al-Awqati Q, Oliver JA. Stem cells in the kidney. *Kidney International*. 2002;61(2):387-395. doi: 10.1046/j.1523-1755.2002.00164.x.
 56. Park J, Shrestha R, Qiu C, Kondo A, Huang S, Werth M, Li M, Barasch J, Suszták K. Single-cell transcriptomics of the mouse kidney reveals potential cellular targets of kidney disease. *Science*. 2018;360(6390):758-763. doi: 10.1126/science.aar2131.
 57. Ransick A, Lindström NO, Liu J, Zhu Q, Guo JJ, Alvarado GF, Kim AD, Black HG, Kim J, McMahon AP. Single-Cell Profiling Reveals Sex, Lineage, and Regional

- Diversity in the Mouse Kidney. *Developmental Cell*. 2019;51(3):399-413.e7. doi: 10.1016/j.devcel.2019.10.005.
58. Ding F, Tian X, Mo J, Wang B, Zheng J. Determination of the dynamic cellular transcriptional profiles during kidney development from birth to maturity in rats by single-cell RNA sequencing. *Cell Death Discov*. 2021;7(1):162. doi: 10.1038/s41420-021-00542-9.
59. Bhogal B, Arnaudo A, Dymkowski A, Best A, Davis TL. Methylation at mouse *Cdkn1c* is acquired during postimplantation development and functions to maintain imprinted expression. *Genomics*. 2004;84(6):961-970. doi: 10.1016/j.ygeno.2004.08.004.
60. Guo T, Luo F, Lin Q. You are affected by what your parents eat: diet, epigenetics, transgeneration and intergeneration. *Trends in Food Science & Technology*. 2020;100:248-261. doi: 10.1016/j.tifs.2020.04.021.
61. Salmeri N, Carbone IF, Cavoretto PI, Farina A, Morano D. Epigenetics beyond fetal growth restriction: a comprehensive overview. *Molecular Diagnosis & Therapy*. 2022;26(6):607-626. doi: 10.1007/s40291-022-00611-4.
62. Basak T, Ain R. Long non-coding RNAs in placental development and disease. *Non-coding RNA Investigation*. 2019;3. doi: 10.21037/ncri.2019.03.01.

SUPPLEMENTARY TABLES

Table S1. Primer sequences for the rat reference (*Tbp* and *Ywhaz*), imprinted (*Kcnq1ot1* (long non-coding RNA), *Slc22a18*), and non-imprinted (*Cars*) genes. Primers were optimised at the following qPCR cycling conditions: 98°C for 3 minutes, (98°C for 10 seconds, 60 or 63°C for 30 seconds (*)) – repeated for 40 cycles, followed by melt curve analysis: 65°C to 90°C with 0.5°C increment per 5 seconds.

Gene	Primers	Sequence (5' to 3')	Primer length	PCR product length (bp)	Annealing temperature (*)
<i>Tbp</i>	<i>RTTbpF</i>	CTAACCACAGCACCATTG	18	152	63°C
	<i>RTTbpR</i>	TTACAGCCAAGATTCACG	18		
<i>Ywhaz</i>	<i>RTYwhazF</i>	ACCCACTCCGGACACAGAAT	20	111	63°C
	<i>RTYwhazR</i>	GACTTCATGCAGGCTGCCA	19		
<i>Kcnq1ot1</i>	<i>RTKcnq1ot1F</i>	AAAATGAAAAGGGTGAGACATGG	23	150	63°C
	<i>RTKcnq1ot1R</i>	TCACAAATTTGGTTTTTCTACCCA	24		
<i>Slc22a18</i>	<i>RTSlc22a18F</i>	CTCTTCGCCTCGCGTCTAC	19	152	60°C
	<i>RTSlc22a18R</i>	AGCAGGGAGCCGAAGATAAC	20		
<i>Cars</i>	<i>RTCarsF</i>	ATCGGGAGCAGAAACCTTCG	20	152	60°C
	<i>RTCarsR</i>	TGGTTCTGTGGCAAGCTTCA	20		

Table S2. Primer sequences for DNA methylation analysis of two CpG islands (chr1:198,492,806 - 198,493,065 (CpG: 23, Amp_1) and chr1:198,493,269 - 198,493,580 (CpG: 20, Amp_13) (mRatBN7/rn7)) on the rat KvDMR1 imprinting control region. Primers were designed by the Australian Genome Research Facility (AGRF) using EpiDesigner (Agena Bioscience). Blue texts denote CpG site positions that were investigated.

Amplicon name	Primers		Direction	Target sequence	Target length	Target CpG	CpG analysed in T	CpG analysed in C	Primer C
Amp_1	Left	GTTTAGGGGTTTAATGGATTTTAAG	F	GCTTAGGGGCTCAATGGACCTCAAGACC ACCTCG ¹ GCTTCTGTGAGCCTGGGCTGC G ² AAGATGGAGCCCTGCCTGGGGAGATG TGGCCCAAGGATGAGAACC ³ AGCCG ⁴ C G ⁵ GCCATGAAACG ⁶ CCAACCG ⁷ GGCCG ⁸ CG ⁹ GCCG ¹⁰ TAAATCG ¹¹ AATACG ¹² GAGCC CCAACCG ¹³ CCAAACG ¹⁴ AATCCCG ¹⁵ AGC CACTGTTGCAAAA ¹⁶ AAGATGGAGCC CCAGCCATGGAGGTAAGCAATGGATTCA TCTCTGCTTCTGGCCATGTGTGCTTG	260	16	11	0	6
	Right	CAAACACACATAACCAAAAACAAAA							7
Amp_13	Left	GGATTTTGGTTGGTTAAAGAATGTT	F	GGACCCTGGCTGGCTAAAGAATGCTGAG AAGCAAAGCG ¹ GAGCG ² CG ³ CCAAGGCA GCCG ⁴ ACCG ⁵ CG ⁶ CTGGAGACCG ⁷ CG ⁸ TT GGAGTGATCCG ⁹ TACTGAAATGATCCACA CTTAAGTGACC ¹⁰ ATTGCTGAGGTAGA TCAGACTGTAGCG ¹¹ AGGACCACCATGCC G ¹² AAACAAGATAAAGACCTCACCG ¹³ AG GAGGTCTATGCTCAGGAGAAACTGAGGC CG ¹⁴ ATCG ¹⁵ CG ¹⁶ TTGAGCAAAGCACACT GATGATGGCTGGT ¹⁷ GGACTGAGGCG ¹ ⁸ CACCG ¹⁹ CACTCAAGTGATCCG ²⁰ AGCAG AGGCAGATCCAAAAGAATTGTGAAC	312	20	18	0	6
	Right	ATTCACAATTCTTTAAATCTACCTCT							4

Table S3. Values of correlations matrices displayed in **Figure 2** and **Figure S1**. The lower triangle displays the Spearman correlation coefficients and the upper triangle displays the p -value. In the lower triangle, blue text denotes a positive correlation (> 0) while red text denotes a negative correlation (< 0). Significant correlations ($p < 0.05$) are bolded and, in the upper triangle, not greyed out.

E20 Sham + IUGR

<i>Cars</i>	0.134	0.154	0.816	0.827	0.745	0.295	0.000	0.002
0.255	<i>Cdkn1c</i>	0.850	0.040	0.009	0.380	0.806	0.017	0.000
-0.250	0.033	<i>Dnmt1</i>	0.000	0.000	0.071	0.177	0.061	0.497
0.041	0.349	0.795	<i>Dnmt3a</i>	0.000	0.006	0.705	0.375	0.554
-0.038	0.427	0.736	0.896	<i>Kcnq1</i>	0.000	0.119	0.854	0.173
0.056	-0.149	-0.308	-0.455	-0.606	<i>Kcnq1ot1</i>	0.051	0.326	0.713
-0.179	-0.042	0.233	0.066	0.265	-0.324	<i>Peg3</i>	0.313	0.263
0.673	0.395	-0.325	-0.157	-0.032	0.168	-0.173	<i>Slc22a18</i>	0.000
0.501	0.719	-0.119	0.105	0.232	-0.064	-0.192	0.607	<i>Snrpn</i>

E20 Sham

<i>Cars</i>	0.318	0.130	0.295	0.526	0.254	0.808	0.000	0.016
0.242	<i>Cdkn1c</i>	0.737	0.814	0.387	0.164	0.821	0.218	0.046
-0.370	-0.082	<i>Dnmt1</i>	0.000	0.000	0.201	0.538	0.381	0.960
-0.261	0.058	0.920	<i>Dnmt3a</i>	0.000	0.567	0.647	0.210	0.587
-0.160	0.211	0.865	0.922	<i>Kcnq1</i>	0.204	0.307	0.900	0.359
0.275	0.323	-0.307	-0.140	-0.305	<i>Kcnq1ot1</i>	0.083	0.096	0.156
-0.060	0.054	0.151	-0.112	0.247	-0.397	<i>Peg3</i>	0.424	0.753
0.774	0.296	-0.220	-0.311	-0.032	0.393	0.195	<i>Slc22a18</i>	0.004
0.560	0.463	0.012	0.137	0.223	0.339	-0.077	0.639	<i>Snrpn</i>

E20 IUGR

<i>Cars</i>	0.228	0.812	0.279	0.701	0.694	0.273	0.034	0.066
0.309	<i>Cdkn1c</i>	0.888	0.113	0.022	0.252	0.468	0.045	0.000
-0.065	0.038	<i>Dnmt1</i>	0.000	0.039	0.284	0.478	0.144	0.204
0.288	0.412	0.824	<i>Dnmt3a</i>	0.001	0.105	0.812	0.957	0.871
0.100	0.551	0.521	0.765	<i>Kcnq1</i>	0.014	0.660	0.830	0.411
-0.103	-0.294	-0.285	-0.421	-0.583	<i>Kcnq1ot1</i>	0.715	0.722	0.504
-0.282	-0.189	0.191	0.065	0.115	-0.096	<i>Peg3</i>	0.042	0.178
0.517	0.493	-0.382	-0.015	0.056	0.093	-0.498	<i>Slc22a18</i>	0.004
0.456	0.824	-0.335	-0.044	0.213	-0.174	-0.343	0.654	<i>Snrpn</i>

PN1 Sham + IUGR

<i>Cars</i>	0.785	0.000	0.000	0.000	0.028	0.000	0.000	0.103
-0.046	<i>Cdkn1c</i>	0.460	0.136	0.731	0.439	0.836	0.807	0.043
0.696	0.124	<i>Dnmt1</i>	0.000	0.000	0.299	0.000	0.000	0.211
0.604	0.246	0.936	<i>Dnmt3a</i>	0.000	0.489	0.000	0.000	0.204
0.751	-0.058	0.694	0.686	<i>Kcnq1</i>	0.508	0.000	0.000	0.605
0.357	0.129	0.173	0.116	-0.111	<i>Kcnq1ot1</i>	0.305	0.103	0.550
0.751	-0.035	0.744	0.663	0.616	0.171	<i>Peg3</i>	0.000	0.330
0.821	-0.041	0.633	0.587	0.710	0.269	0.616	<i>Slc22a18</i>	0.128
0.268	0.330	0.208	0.211	0.087	0.100	0.162	0.251	<i>Snrpn</i>

PN1 Sham

<i>Cars</i>	0.385	0.000	0.008	0.000	0.128	0.006	0.000	0.542
-0.218	<i>Cdkn1c</i>	0.705	0.088	0.971	0.147	0.735	0.150	0.604
0.759	0.096	<i>Dnmt1</i>	0.000	0.000	0.699	0.000	0.020	0.489
0.604	0.414	0.870	<i>Dnmt3a</i>	0.001	0.798	0.001	0.075	0.428
0.761	-0.009	0.798	0.725	<i>Kcnq1</i>	0.855	0.021	0.009	0.616
0.373	-0.356	0.098	0.065	0.046	<i>Kcnq1ot1</i>	0.779	0.191	0.906
0.624	0.086	0.740	0.703	0.540	0.071	<i>Peg3</i>	0.021	0.448
0.835	-0.354	0.544	0.430	0.595	0.323	0.540	<i>Slc22a18</i>	0.280
0.154	0.131	0.174	0.199	0.127	-0.030	0.191	0.269	<i>Snrpn</i>

PN1 IUGR

<i>Cars</i>	0.292	0.008	0.034	0.001	0.002	0.000	0.001	0.232
0.248	<i>Cdkn1c</i>	0.363	0.409	0.384	0.450	0.940	0.283	0.010
0.577	0.215	<i>Dnmt1</i>	0.000	0.003	0.084	0.003	0.002	0.298
0.477	0.195	0.943	<i>Dnmt3a</i>	0.003	0.108	0.015	0.003	0.356
0.662	0.206	0.627	0.621	<i>Kcnq1</i>	0.352	0.018	0.001	0.743
0.638	0.179	0.395	0.370	0.220	<i>Kcnq1ot1</i>	0.011	0.027	0.668
0.717	0.018	0.635	0.534	0.522	0.555	<i>Peg3</i>	0.007	0.439
0.666	0.253	0.650	0.636	0.695	0.493	0.585	<i>Slc22a18</i>	0.466
0.280	0.562	0.245	0.218	0.078	0.102	0.183	0.173	<i>Snrpn</i>

SUPPLEMENTARY FIGURES

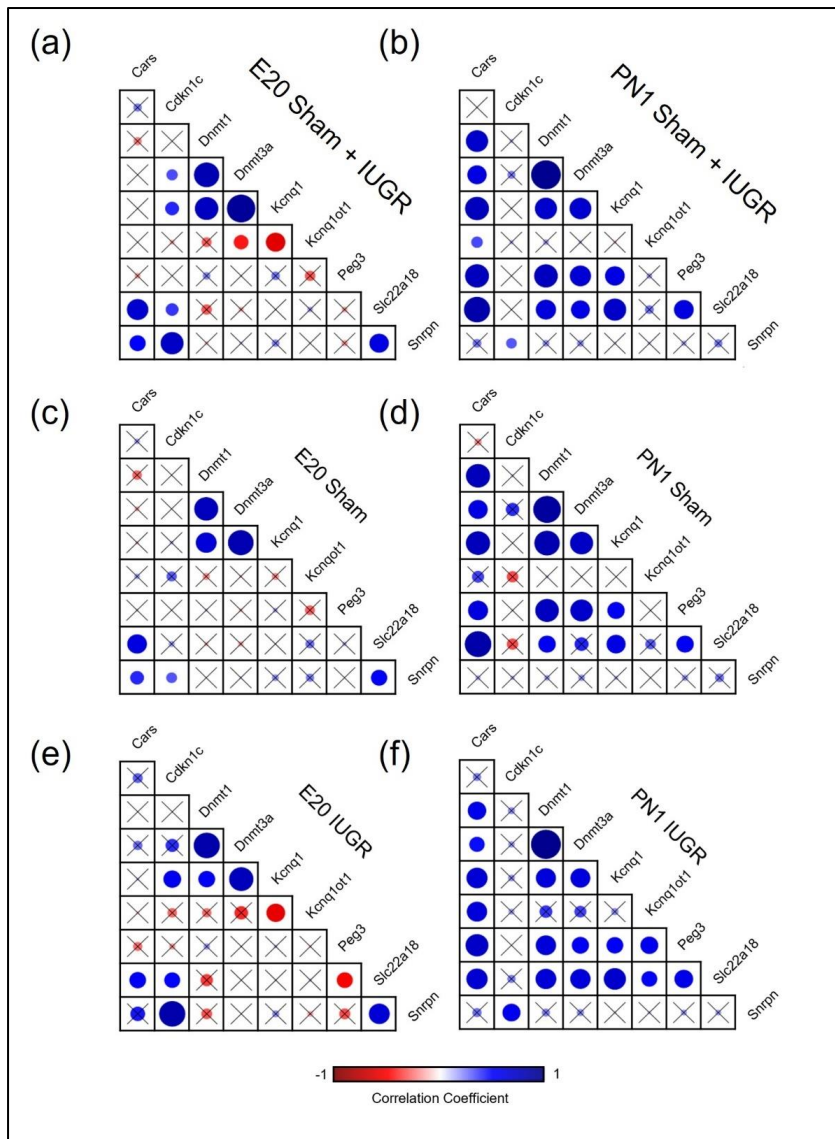


Figure S1. Spearman's non-parametric correlation matrices between expression levels of DNA methyltransferases (*Dnmt1* and *Dnmt3a*), imprinted (*Cdkn1c*, *Kcnq1*, *Kcnq1ot1*, *Peg3*, *Snrpn*, and *Slc22a18*) and non-imprinted (*Cars*) genes in kidney tissues of sham and IUGR rat offspring at embryonic day 20 (E20) and postnatal day 1 (PN1). Sham and IUGR data were combined in (a) for E20 and (b) for PN1. Spearman correlation coefficients and p -values are reported in **Table S3**. A cross through the box indicates a non-significant p -value. The size of the circle indicates how strong the correlation is (corresponded to the Spearman correlation coefficients).

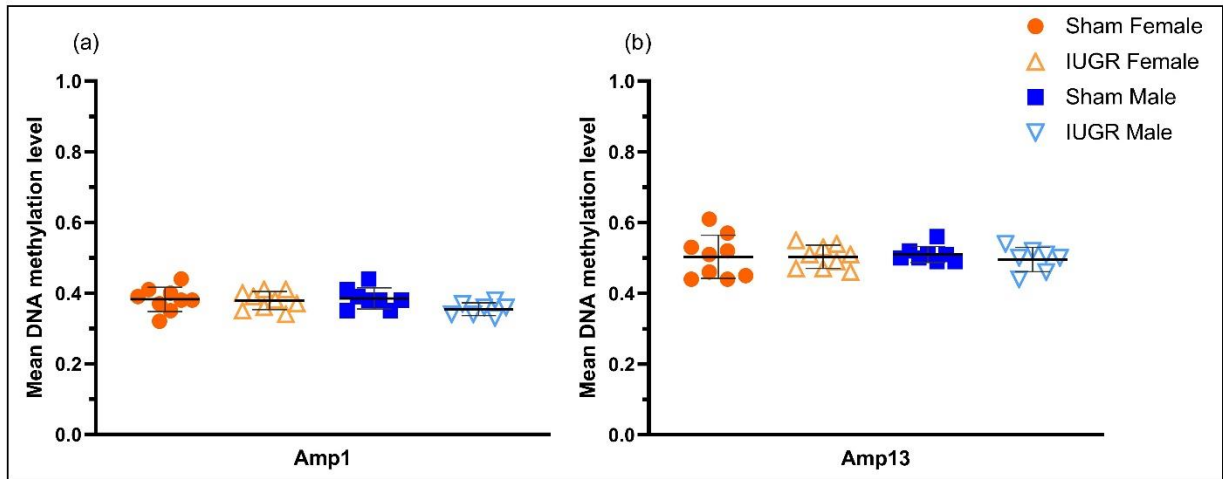




Figure S2. Mean DNA methylation level of two CpG islands within the KvDMR1 imprinting control region, including (a) CpG 23 (amplicon 1 (amp1), chr1:198,492,806 - 198,493,065, UCSC Genome Browser Nov. 2020 (mRatBN7/rn7)) and (b) CpG 20 (amplicon 13 (amp13), chr1:198,493,269 - 198,493,580 (mRatBN7/rn7)) in sham and IUGR rat offspring at postnatal day 1 (PN1), determined using EpiTYPER Agena MassArray and Mass Cleave Chemistry analyses. Data is expressed as mean \pm SD; n = 8-9/group.

BRIEF REPORT

OPEN ACCESS 

Imprinted gene alterations in the kidneys of growth restricted offspring may be mediated by a long non-coding RNA

Thu N. A. Doan^{a,b}, James M. Cowley^a, Aaron L. Phillips^a, Jessica F. Briffa^c, Shalem Y. Leemaqz^{b,d,e}, Rachel A. Burton^a, Tania Romano^f, Mary E. Wlodek^{c,g}, and Tina Bianco-Miotto ^{a,b}

^aSchool of Agriculture, Food and Wine, & Waite Research Institute, University of Adelaide, Adelaide, South Australia, Australia; ^bRobinson Research Institute, University of Adelaide, Adelaide, South Australia, Australia; ^cDepartment of Anatomy and Physiology, The University of Melbourne, Parkville, Victoria, Australia; ^dSAHMRI Women and Kids, South Australian Health & Medical Research Institute, Adelaide, South Australia, Australia; ^eCollege of Medicine and Public Health, Flinders University, Bedford Park, SA, Australia; ^fDepartment of Physiology, Anatomy and Microbiology, La Trobe University, Bundoora, Victoria, Australia; ^gDepartment of Obstetrics and Gynaecology, The University of Melbourne, Parkville, Victoria, Australia

ABSTRACT

Altered epigenetic mechanisms have been previously reported in growth restricted offspring whose mothers experienced environmental insults during pregnancy in both human and rodent studies. We previously reported changes in the expression of the DNA methyltransferase *Dnmt3a* and the imprinted genes *Cdkn1c* (Cyclin-dependent kinase inhibitor 1C) and *Kcnq1* (Potassium voltage-gated channel subfamily Q member 1) in the kidney tissue of growth restricted rats whose mothers had uteroplacental insufficiency induced on day 18 of gestation, at both embryonic day 20 (E20) and postnatal day 1 (PN1). To determine the mechanisms responsible for changes in the expression of these imprinted genes, we investigated DNA methylation of KvDMR1, an imprinting control region (ICR) that includes the promoter of the antisense long non-coding RNA *Kcnq1ot1* (*Kcnq1* opposite strand/antisense transcript 1). *Kcnq1ot1* expression decreased by 51% in growth restricted offspring compared to sham at PN1. Interestingly, there was a negative correlation between *Kcnq1ot1* and *Kcnq1* in the E20 growth restricted group (Spearman's $\rho = 0.014$). No correlation was observed between *Kcnq1ot1* and *Cdkn1c* expression in either group at any time point. Additionally, there was a 11.25% decrease in the methylation level at one CpG site within KvDMR1 ICR. This study, together with others in the literature, supports that long non-coding RNAs may mediate changes seen in tissues of growth restricted offspring.

ARTICLE HISTORY

Received 31 July 2023
Revised 6 December 2023
Accepted 6 December 2023

KEYWORDS



Intrauterine growth restriction; uteroplacental insufficiency; epigenetic mechanisms; long non-coding RNA; DNA methylation


Introduction

Development is susceptible to environmental insults, such as uteroplacental insufficiency, maternal suboptimal diets, and other environmental exposures to chemicals, infections, drugs, and alcohol [1–7]. Developmental environmental exposure early in life has been shown to be associated with epigenetic changes, including changes in DNA methylation, histone modifications, long non-coding RNA (lncRNA), and micro-RNA (miRNA) expression, in both human and rodent studies, which can have a significant impact on short- and long-term offspring health [1,4–6,8–10]. Additionally, altered epigenetic mechanisms and physiology due to environmental exposure during gametogenesis/gestation have been

reported to have multigenerational or transgenerational effects that occur in a sex-specific manner in rodent studies [4–7,9–17]. These animal models have been suggested to be more appropriate for transgenerational studies, as besides the availability of tissues for sampling, inbred strains and strictly controlled experimental environments can help reduce biases found in human studies, such as genetic, ecological, and cultural factors [18].

We have recently shown in our rodent model of uteroplacental insufficiency (UPI) that the expression of *Dnmt3a*, a *de novo* DNA methyltransferase, but not *Dnmt1*, whose primary role is maintaining the DNA methylation landscape, was decreased in the kidney of embryonic day 20 (E20) offspring, which is during the embryonic

CONTACT Tina Bianco-Miotto  tina.bianco@adelaide.edu.au  School of Agriculture, Food and Wine, & Waite Research Institute, University of Adelaide, Adelaide, South Australia, Australia

 Supplemental data for this article can be accessed online at <https://doi.org/10.1080/15592294.2023.2294516>

© 2023 The Author(s). Published by Informa UK Limited, trading as Taylor & Francis Group.

This is an Open Access article distributed under the terms of the Creative Commons Attribution License (<http://creativecommons.org/licenses/by/4.0/>), which permits unrestricted use, distribution, and reproduction in any medium, provided the original work is properly cited. The terms on which this article has been published allow the posting of the Accepted Manuscript in a repository by the author(s) or with their consent.

nephron formation period [12]. Concurrently, expression of imprinted genes that are known to be important in kidney development, *Cdkn1c* and *Kcnq1*, was also altered at both E20 (*Cdkn1c*; sex-specific) and postnatal day 1 (PN1; *Cdkn1c* and *Kcnq1*) [12]. Specifically, at E20, *Cdkn1c* expression was only reduced in growth restricted females. At PN1, regardless of sex, *Cdkn1c* expression was lower and *Kcnq1* expression was higher in growth restricted offspring, in association with reduced absolute and percentage left kidney weight [12]. Interestingly, *Kcnq1* and *Cdkn1c* are both known to be regulated by KvDMR1, an imprinting control region (ICR), which includes the promoter of the imprinted antisense lncRNA *Kcnq1ot1* [19,20]. These results raised a question of whether epigenetic mechanisms, such as DNA methylation or lncRNAs, can explain the multi-generational and sex-specific alterations in both gene expression and growth phenotypes in the kidneys of growth restricted offspring.

In the current study, we investigated the relationship between *Kcnq1* and *Cdkn1c* with *Kcnq1ot1* and KvDMR1 by examining the expression of *Kcnq1ot1* and the DNA methylation status of two CpG islands within the KvDMR1 ICR in the kidneys of F1 growth restricted offspring. The study will contribute to the understanding of the potential mechanisms controlling the gene expression of imprinted genes in the kidney that might be susceptible to adverse *in utero* environments.

Materials and methods

Kidney tissue collection

The intrauterine growth restricted (IUGR) Wistar Kyoto rat model was generated as previously described (The University of Melbourne AEC 04138, 1011865, and 1112130; La Trobe University AEC 12–42) [12,21,22]. In short, pregnant female rats (F0) underwent bilateral uterine vessel (artery and vein) ligation at day 18 of pregnancy (late gestation; term = 22 days) to induce UPI. The control group underwent sham surgery (no vessel ligation). Left kidney samples were collected at embryonic day 20 (E20) and post-natal day 1 (PN1) from the first-generation rat

offspring, with one male and one female examined per litter [12]. Samples were snap frozen in liquid nitrogen and stored at -80°C .

RNA and DNA extraction

RNA was extracted from samples as described previously [12]. For DNA extraction, 30 mg of left kidney tissue was quickly cut on a plastic weight boat on ice. Only PN1 tissues were available for DNA extraction as the whole E20 kidney was used in RNA extraction [12]. Tissue homogenization was carried out in 500 μL of TES (10 mM Tris (pH 8.0), 1 mM EDTA, 0.1 M NaCl; Invitrogen) with the following PowerLyser settings: time 'T' = 15 s, cycles 'C' = 1, dwell/pause time 'D' = 0 s, and speed 'S' = 3,500 rpm. DNA was then extracted using the salting out method [23] with modifications. Thirty microlitres of 20 $\mu\text{g}/\mu\text{L}$ Proteinase K (Invitrogen) was added to each tube of homogenized tissue (mixed by inversion), followed by 60 μL of 20% SDS (Invitrogen) (mixed by inversion). The samples were then incubated at 37°C for 24 h. After incubation, 300 μL of 3 M NaCl was added to each tube and mixed vigorously by shaking for at least 10 s. Tubes were placed on ice for 10 min, followed by centrifugation at 13,000 rpm for 15 min, and a maximum of 450 μL of the supernatant was collected. Two microlitres of glycogen (Invitrogen) was added to each tube, followed by 900 μL of 100% molecular biology grade ethanol (Sigma-Aldrich) (mixed by inversion). The DNA was pelleted by centrifugation at 13,000 rpm for 2 min. The DNA pellet was washed with 900 μL 70% ethanol (mixed by inversion) and centrifuged at 13,000 rpm for 1 min. The supernatant was then removed, and the DNA pellet was centrifuged at 13,000 rpm for 1 min. The DNA pellet was dried at room temperature before resuspension in TE buffer (Invitrogen) (50 μL , pH 8.0). Samples were stored at 4°C , and the DNA concentration was quantitated using a NanoDrop spectrophotometer (Thermo Fisher Scientific). DNA integrity was checked using 1% agarose gel electrophoresis.

Genomic DNA (gDNA) contamination check and reverse transcription

RNA samples (20 ng, in duplicate) were checked for contamination of gDNA as previously described [12] using the SsoAdvanced™ Universal

SYBR[®] Green Supermix (Bio-Rad) and primers that targeted an *Actb* intronic region. Contaminated RNA samples ($C_q < 35$) were DNase-treated using the TURBO DNA-free[™] kit (Thermo Fisher Scientific) and checked again using the same qPCR method.

qPCR gene expression analysis

Tbp and *Ywhaz* were determined to be the two most stable reference genes in our previous study [12]. As the lncRNA *Kcnq1ot1* sequence is not available on the rat assembly (UCSC Genome Browser Nov. 2020 (mRatBN7/rn7)), *Kcnq1ot1* sequence from the mouse genome (UCSC Genome Browser Jun. 2020 (GRCm39/mm39)) was submitted to a UCSC BLAT search against the rat genome. Primers for *Kcnq1ot1*, *Slc22a18*, and *Cars* were then designed using NCBI Primer-BLAST (Table S1). Primer optimization, master mix preparation and qPCRs were performed as previously described [12], with cycling conditions shown in Table S1.

DNA methylation analysis

A total of 34 rat PN1 DNA samples (1000 ng each) were sent to the Australian Genome Research Facility (AGRF) for region-specific quantitative DNA methylation analysis. Primers targeting two CpG islands (chr1:198,492,806–198,493,065 (CpG: 23) and chr1:198,493,269–198,493,580 (CpG: 20) (mRatBN7/rn7)) on the KvDMR1 imprinting control region were designed by AGRF (Table S2). DNA samples were bisulphite modified, followed by analyses using EpiTYPER Agena MassArray and Mass Cleave Chemistry test methods [24].

Data analysis

Data were analysed using a linear mixed-effect model, with adjustments for litter size and relatedness between litter siblings as previously reported [12], using R version 4.1.1 [25,26]. Power of the linear mixed-effect model was determined to be 0.998 and 0.993 for the analysis of gene expression and DNA methylation, respectively, calculated using the 'pwr.f2.test' function ('pwr' package) in the R environment, with n (sample size) = 38 for

our expression studies and $n = 33$ for the DNA methylation analyses, respectively. Correlation between gene expression levels were determined using Spearman's non-parametric correlation coefficient (no assumptions regarding data distribution), calculated using PAST 4.03 software [27]. Sham and IUGR data were combined to investigate whether there is a relationship between expression of different pairs of genes, regardless of treatment. The relationships within each group were then examined to explore whether a certain correlation is present in one group and is absent/ altered in the other group, potentially indicating disruption due to growth restriction.

Results

Expression of imprinted and non-imprinted genes in the kidney

The expression of *Kcnq1ot1* was not different between the sham and IUGR offspring at E20 (Figure 1a). However, at PN1, there was a significantly lower expression of *Kcnq1ot1* in IUGR offspring than in sham offspring (reduced by approximately 50%, $p < 0.01$). The expression of another imprinted gene in the same KvDMR1 ubiquitously imprinted cluster (*Slc22a18*) and a non-imprinted gene (*Cars*) was also examined to determine whether the changes observed in *Kcnq1ot1*, *Kcnq1* and *Cdkn1c* extended to other genes in this imprinting cluster. There was no significant difference in the expression of either *Slc22a18* (Figure 1b) or *Cars* (Figure 1c) between the sham and IUGR offspring at any time point.

Correlation between gene expression levels in rat kidney

Pairwise non-parametric correlation analyses were carried out to investigate the potential correlations between the expression levels of genes in sham and IUGR offspring at E20 and PN1, including between pairs of imprinted genes known to be important in kidney development and regulated by the KvDMR1 ICR (*Cdkn1c*, *Kcnq1*, and *Kcnq1ot1*; Figure 2 and Table S3), as well as between imprinted genes and other genes (*Dnmt1a*, *Dnmt3a*, *Peg3*, *Snrpn*, *Slc22a18*, and

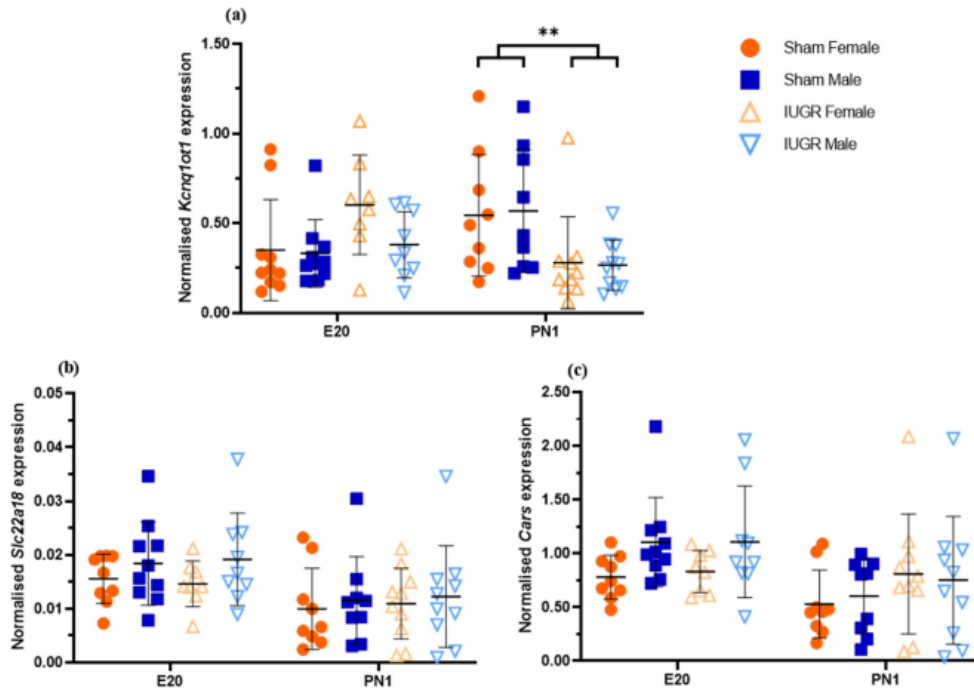


Figure 1. Normalised expression of the imprinted genes *Kcnq1ot1* (a), *Slc22a18* (b), and the non-imprinted gene *Cars* (c) in kidney tissues of sham and IUGR rat offspring at embryonic day 20 (E20) and postnatal day 1 (PN1). Significance was determined by linear mixed effect models, followed by a Tukey's *post hoc* test (** $p < 0.01$). Data is expressed as mean \pm SD; $n = 8-10$ /group.

Cars; Fig. S1 and Table S3). The expression of *Cdkn1c*, *Kcnq1*, *Dnmt1a*, *Dnmt3a*, *Peg3*, and *Snrpn* has been previously reported [12].

When sham and IUGR data were combined, there was a significant negative correlation between the expression of *Dnmt3a* and lncRNA *Kcnq1ot1* at E20 (Spearman's $\rho = -0.455$, $p = 0.006$, Fig. S1a and Table S3), as well as significant positive correlations between *Dnmt3a* and *Kcnq1* and *Dnmt3a* and *Cdkn1c* (Spearman's $\rho = 0.896$, $p < 0.0001$ and Spearman's $\rho = 0.349$, $p = 0.040$, respectively; Fig. S1a and Table S3). Additionally, at E20, there was a negative correlation between *Kcnq1ot1* and *Kcnq1* and a positive correlation between *Kcnq1* and *Cdkn1c* (Spearman's $\rho = -0.606$, $p < 0.0001$ and Spearman's $\rho = 0.427$, $p = 0.009$, respectively; Figure 2a and Table S3). The relationships between these pairs of genes (except *Dnmt3a-Kcnq1*) were no longer present at PN1 (Fig. S1b and Table S3).

Interestingly, when sham and IUGR were investigated individually at each time point, the negative correlation between *Kcnq1ot1* and *Kcnq1* was significant only in the E20 IUGR group (Spearman's $\rho = -0.583$, $p = 0.014$, Figure 2c-f, S1c-f and Table S3). Additionally, there was a significant positive correlation between *Kcnq1* and *Cdkn1c* in the E20 IUGR group (Spearman's $\rho = 0.551$, $p = 0.022$), but not in the E20 sham group (Figure 2b,c, S1c, S1e and Table S3). No correlation was observed between *Kcnq1ot1* and *Cdkn1c* expression in any of the groups at any time point. On the other hand, there was an inverse relationship between *Dnmt3a* and *Kcnq1ot1* in the IUGR group, whereby at E20, there was a negative association (Spearman's $\rho = -0.421$) and at PN1, there was a positive association (Spearman's $\rho = 0.370$) (Fig. S1e, S1f and Table S3). However, these differences were not statistically significant.

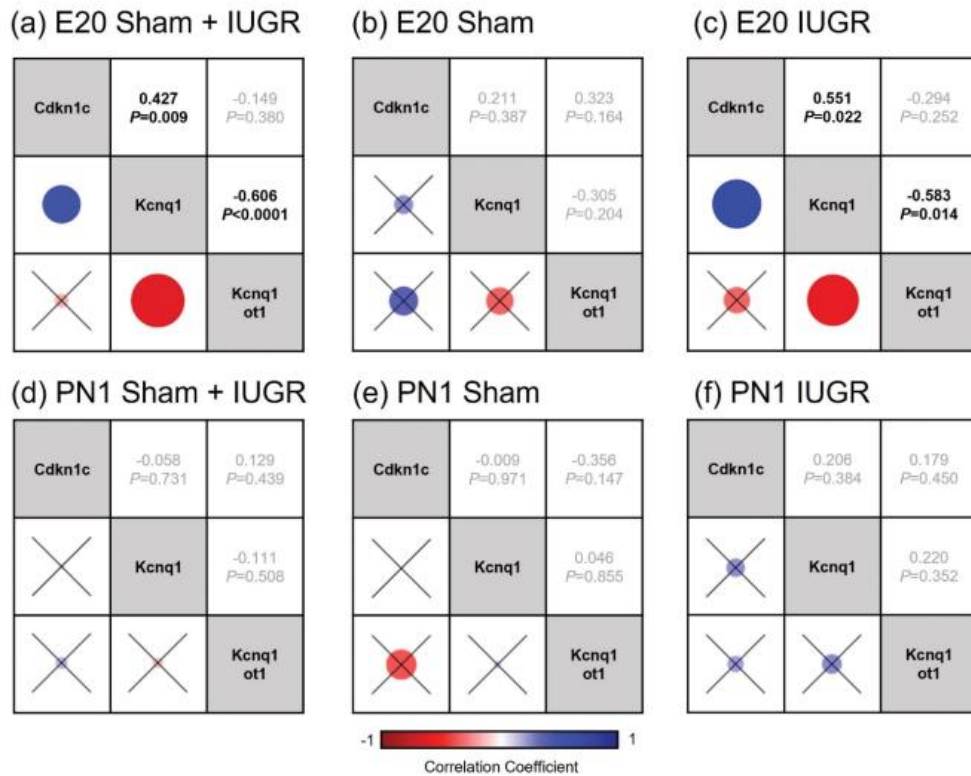


Figure 2. Spearman's non-parametric correlation matrices between three imprinted genes known to be important in kidney development and regulated by the KvDMR1 imprinting control region (*Kcnq1ot1*, *Cdkn1c* and *Kcnq1*) in kidney tissues of sham and IUGR rat offspring at embryonic day 20 (E20) and postnatal day 1 (PN1). Sham and IUGR data were combined in (a) for E20 and (d) for PN1. Spearman correlation coefficients (top number) and *p*-values (bottom number) are displayed on the right triangles. A cross through the box indicates a non-significant *p*-value. The size of the circle indicates how strong the correlation is (corresponded to the Spearman correlation coefficients).

DNA methylation status of the KvDMR1 imprinting control region

Base-specific cleavage of bisulphite-modified DNA yielded usable signals for four out of 16 (amplicon 1, Figure 3a) and seven out of 20 (amplicon 13, Figure 3b) CpG positions within CpG 23 and CpG 20 islands, respectively, in KvDMR1 ICR. There was hypomethylation ($p < 0.05$) at CpG site 6 of the CpG 23 island in IUGR males only ($\downarrow 11.25\%$, methylation level in IUGR males 6% vs. sham males 17.25%, amplicon 1, Figure 3a). Interestingly, unlike other CpG sites within this region where the DNA methylation level was $\sim 50\%$ (as expected for imprinted genes),

there was a lower than 20% methylation level at CpG site 6, even in the sham animals. There was no statistically significant difference in the methylation status between sham and IUGR offspring at any site of the CpG 20 island (amplicon 13, Figure 3b).

KvDMR1 ICR was further analysed to identify the location of these CpG sites. As mentioned previously, the *Kcnq1ot1* sequence is not available in the mRatBN7/rn7 rat genome. However, there was an uncharacterized lncRNA named LOC120099961 found in the rat mRatBN7.2 genome (NCBI Reference Sequence: NC_051336.1), which is located in a similar position as *Kcnq1ot1* in other species

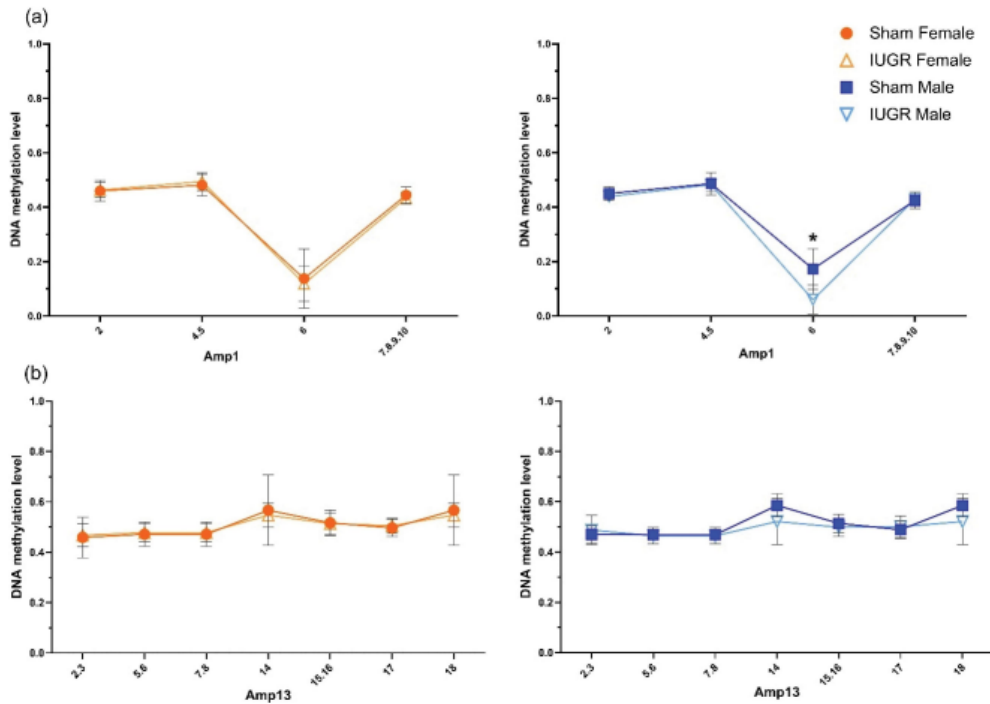


Figure 3. DNA methylation status of the KvDMR1 imprinting control region containing (a) CpG 23 (amplicon 1 (amp1), chr1:198,492–806–198,493,065, UCSC genome Browser Nov. 2020 (mRatbn7/m7)) and (b) CpG 20 (amplicon 13 (amp13), chr1:198,493,269–198,493,580 (mRatbn7/m7)) in sham and IUGR rat offspring at postnatal day 1 (PN1), determined using EpiTYPER Agena MassArray and mass cleave chemistry analyses. For CpG fragments that had the same mass peaks as other fragments containing same number of CpGs (Amp13, CpG_5.6 versus CpG_7.8 and CpG_14 versus CpG_18), methylation % was calculated between CpGs. Significance was determined by linear mixed effect models, followed by a Tukey's *post hoc* test (* $p < 0.05$). Data is expressed as mean \pm SD; $n = 8$ –9/group.

genomes. Therefore, this rat sequence, together with other mouse sequences including the KvDMR1 region [28], *Kcnq1ot1* transcriptional repressor CTCF binding sites [29], enhancer, promoter [30], and TSS [30,31] were used in a BLAT search against the rat genome. The results for the (approximate) positions are shown in Figure 4. While amplicon 13 (CpG 20) was located within both *Kcnq1ot1* TSS and CTCF binding site 2, amplicon 1 (CpG 23) was not located within any of the sequences mentioned above (Figure 4). Using TFBIND software (weight matrix in transcription factor database TRANSFAC R.3.4, similarity $\geq 80\%$) [32] and TRANSFAC FACTOR TABLE (Release 2017.2), CpG site 6 (amplicon 1) was determined to correspond to

different transcription factor binding sites (TFBSs) (Table 1). Among these, there were four TF that have been previously reported to play a role in kidney development and disease, as well as to be regulated by DNA methylation, including Chicken Ovalbumin Upstream Promoter Transcription Factor 2 (COUP-TF2) [33–36], GATA-binding Factor 2 (GATA-2) [37,38], Serum Response Factor (SRF) [39–41], and Activating enhancer binding Protein 2 alpha (AP-2 α) [42,43]. When data from all examined CpG sites within each CpG island were combined, no significant difference in DNA methylation levels was found between the sham and IUGR kidney samples (Fig. S2).

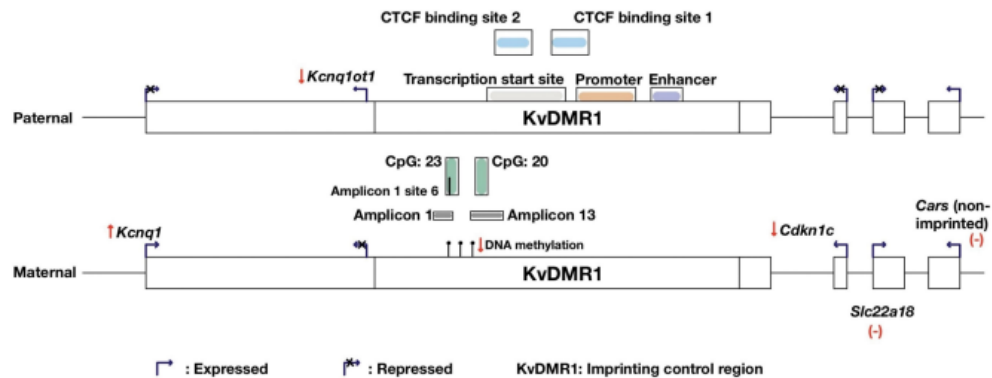


Figure 4. Approximate positions of the two amplicons (amplicon 1 and 13, targeting CpG island 23 (chr1:198,492,806–198,493,065) and 20 (chr1:198,493,269–198,493) (mRatbn7/rn7), respectively) in the rat KvDMR1 imprinting control region (modified from Doan *et al* [12]), examined using region-specific quantitative DNA methylation analysis. DNA methylation of KvDMR1 and/or expression of the lncRNA *Kcnq1ot1* is known to play a role in controlling the monoallelic expression of imprinted genes in the KvDMR1 imprinting cluster. Primers were designed by the Australian genome Research Facility (AGRF). There was a hypomethylation (\downarrow 11.25%, $p < 0.05$) at CpG site 6 of CpG 23 island in PN1 growth restricted male kidneys. *Kcnq1ot1* sequence is not available on the mRatbn7/rn7 rat genome. Hence, sequence from the uncharacterized lncRNA named LOC120099961 found on the rat mRatbn7.2 genome (NCBI reference sequence: NC_051336.1, similar position) was used. Mouse sequences, including KvDMR1 region [28], *Kcnq1ot1* transcriptional repressor CTCF binding sites [29], enhancer, promoter [30], and transcription start site [30,31] were used in a BLAT search against the rat genome. \downarrow : expression decreased; \uparrow : expression increased; (-): no change in gene expression. Note that the annotations of gene expressions in this figure is based on the circumstance that in a healthy animal, the imprinted genes *Kcnq1* and *Cdkn1c* are expressed on the maternal allele, while *Kcnq1ot1* is preferentially expressed on the paternal allele.

Table 1. Transcription factor binding sites (TFBSs) correspond to CpG:23 island (amplicon 1, chr1:198,492,806–198,493,065), where there was a hypomethylation at CpG site 6 (coloured in red) in IUGR male kidneys. TFBSs were determined using TFBIND software (weight matrix in transcription factor database TRANSFAC R.3.4) [32] and TRANSFAC FACTOR TABLE (release 2017.2). Left to right: TF name, matrix ID (from TRANSFAC R.3.4), label in TFBIND, similarity compared to input sequence, strand that the transcription factor binds, and sequence of the TFBS.

Factor	ID	Label	Similarity	Forward (+) or reverse (-)	Sequence
COUP-TF2	M00155	ARP1_01	0.806	(+)	CGCGGCCATGAAACG ^c C
GATA-2	M00076	GATA2_01	0.806	(-)	CG ^c CCAACCGG
SRF	M00215	SRF_C	0.803	(+)	GCCATGAAACG ^c CCAA
AP-2 α	M00189	AP2_Q6	0.801	(+)	CG ^c CCAACCGGC

Discussion

The imprinted gene *Kcnq1ot1* has been previously shown to be altered in growth restricted offspring due to environmental exposure during early life [44,45]. Specifically, reduced expression of this lncRNA has been reported in placentae of E16.5 growth restricted male mice whose mothers were exposed to 50 ppm of the heavy metal cadmium throughout pre-conception, mating, and pregnancy [44], as well as in E18.5 growth restricted mice who were conceived through *in vitro* fertilization (IVF) [45]. In our current study, as expected, there was a significant decrease in

Kcnq1ot1 expression in kidneys of F1 growth restricted rat offspring at PN1. From studies in mice, the function of *Kcnq1ot1* is suggested to partially control the allele-specific expression of other imprinted genes in the same KvDMR1 imprinting cluster, including those investigated in this current study, in a tissue-specific manner; however, the exact mechanism is still unclear [29,46,47]. For instance, deletion of the whole KvDMR1 ICR (2.8 kb [46] or 3.6 kb [47], which abolished *Kcnq1ot1* expression), deletion of *Kcnq1ot1* promoter and TSS region (224 bp [47], producing a shorter transcript by inserting

a transcription stop element at 1.5 kb downstream of the lncRNA TSS [47], or truncation of *Kcnq1ot1* (2.6 kb downstream of its promoter) [29], on the paternal allele, was reported to be associated with activation of the normally paternally silenced genes in mouse embryonic tissues (E11.5–16.5). Biallelic gene expression was reported for *Slc22a18* (placenta [29,47], liver, gut, kidney, lung, heart, brain, and fibroblast [29]), *Kcnq1* (placenta [29,47], liver [29,46], gut, kidney, lung, heart, brain, and fibroblast [29]), and *Cdkn1c* (whole embryo, placenta [29,47], liver [46], heart, brain, and gut [29]). However, monoallelic expression of *Cdkn1c* has been reported in the liver, kidney, lung, and fibroblasts of mice at E15.5, despite the *Kcnq1ot1* truncation, which remains to be explained [29].

In line with the above findings, studies in mouse IUGR models also reported alterations to the imprinted genes that are known to be regulated by KvDMR1, in association with decreased *Kcnq1ot1* expression [44,45]. Growth restricted mice conceived through IVF have decreased placental *Cdkn1c* expression compared to *in vivo* controls at E18.5, despite a similar expression at E14.5 [45]. In contrast, *Cdkn1c* overall expression was increased in the placentae of E18.5 growth restricted mice whose mothers were exposed to Cadmium [44]. Meanwhile, there was no alteration in placental *Kcnq1* expression in these mice [44]. Additionally, allele-specific expression analysis indicated no difference in *Cdkn1c* expression between growth restricted and sham animals [44]. In our study of growth restricted rat kidneys, *Cdkn1c* expression was reduced only in IUGR females at E20, while PN1 IUGR offspring had decreased *Cdkn1c* and increased *Kcnq1* expression compared to sham [12]. Together with the above-mentioned findings, the fact that our results report decreased *Kcnq1ot1* only in PN1, but not E20, IUGR rats as well as no correlation between *Kcnq1ot1* and *Cdkn1c* expression in any of the groups, at any timepoint, suggests that changes in lncRNA *Kcnq1ot1* expression alone is not sufficient to explain changes in *Cdkn1c* in IUGR rat kidneys. Allele-specific expression analysis of these imprinted genes would provide a better understanding of their potential relationships.

As *Dnmt3a* was reported in our previous study to be decreased in IUGR kidneys at E20 [12], we

hypothesized that there were alterations in the DNA methylation profile, including that of the KvDMR1 ICR, which is involved in dysregulation of the expression of imprinted genes that are known to be important in foetal kidney development. In babies diagnosed with Russell-Silver syndrome, characterized by intrauterine and postnatal growth restriction, alterations in KvDMR1 DNA methylation, either hypermethylation [48–50] or hypomethylation [51], have been reported in their blood samples. In human IUGR studies, KvDMR1 DNA methylation status was mostly studied using placental tissues, with no significant difference observed between growth restricted tissues and healthy controls [52–55]. In the current study of rat kidneys, hypomethylation was found at a CpG site of CpG 23 island (chr1:198,492,806–198,493,065) within KvDMR1 in PN1 IUGR males. This CpG site was not located within any of the *Kcnq1ot1* regulatory regions that we were able to assess. However, this position is a potential target for several TFs known to be important in kidney development and disease, including but not limited to COUP-TF2, GATA-2, SRF, and AP-2a. Future studies should investigate the potential interaction of these TFs with KvDMR1 and the biological function of such event. Furthermore, as these TFs have been previously shown to be impacted by DNA methylation [33,34,38,39,42], alteration to the *Dnmt3a* expression in our study could also have an effect on their expression and/or function. Another important point to mention here is that DNA methylation level of this specific site was also lower than 50% in sham animals, which is not typical for imprinted genes where the silenced allele is often methylated. Meanwhile, investigation of the CpG 41 island in the placentae of E18.5 growth restricted female mice (conserved sequence of KvDMR1 CpG 23 island in rats) showed no change in DNA methylation of any other CpG sites within this region (chr1:198,493,086–198,493,233) [44]. In addition, our results show that the mean DNA methylation levels within this CpG 23 island as well as within the CpG 20 island (chr1:198,493,269–198,493,580) of the KvDMR1 ICR were also not different between sham and IUGR offspring. Nonetheless, apart from the differences in tissues

examined, it should be noted that different regions within and near the KvDMR1 ICR were investigated in the above studies, which could be a potential limitation of the present study. Additionally, the kidney is a complex organ that comprises more than 20 differentiated cell types [56]. Recent single-cell RNA sequencing databases in both adult mice [57,58] and rats [59] suggest that the three imprinted genes (*Cdkn1c*, *Kcnq1*, and *Kcnq1ot1*) investigated in our study have different expression levels in different renal cell types. Specifically, *Cdkn1c* is highly expressed in stromal cells and podocytes (visceral epithelium), while *Kcnq1* is highly expressed in collecting duct intercalated cells and connecting tubule principal-like cells. *Kcnq1ot1* (mouse data) is also highly expressed in podocytes. Since we only assessed DNA methylation of one region using region-specific quantitative DNA methylation analysis method, this did not allow for assessing or adjusting for different cell types.

Besides KvDMR1, DNA methylation of the *Cdkn1c* promoter region is also an important mechanism that needs to be explored, as it is known to be important in maintaining allele-specific gene expression during embryonic development in healthy mice [60]. However, in the mouse *Kcnq1ot1* truncation model, where *Cdkn1c* allele-specific expression was shown to be either altered or unchanged in different embryonic tissues, there was no difference in *Cdkn1c* promoter DNA methylation levels in all tissues at E15.5, suggesting a different mechanism for maintaining *Cdkn1c* monoallelic expression [29]. In contrast, in the placentae of E18.5 Cadmium-exposed growth restricted mice, where expression of *Kcnq1ot1* decreased and expression of *Cdkn1c* increased, there was a reduction in DNA methylation in one out of 23 investigated CpG sites in the *Cdkn1c* promoter region [44]. However, the mean methylation level of the whole CpG island did not change compared with that of the sham offspring [44]. Future studies should investigate epigenetic alterations in the *Cdkn1c* promoter region.

In summary, at PN1, there was a 50% decrease in the expression of an antisense lncRNA (*Kcnq1ot1*) in IUGR rats compared to that in sham animals. This is the first study to report changes in *Kcnq1ot1*

in UPI-induced growth restricted rat kidneys. *H19* is another lncRNA and imprinted gene that plays an important role in development. *H19* has also been shown to be altered in rodent and human IUGR studies, with significant changes in its expression and DNA methylation in many tissues (e.g., sperm, liver, blood, and placenta [1,61–63]). In this study, there was a negative correlation between *Kcnq1ot1* and the gene that it is located within (*Kcnq1*), only in E20 IUGR kidneys. As *Kcnq1* was also altered at PN1 [12], these results suggest that an abnormal event occurred early during foetal nephron formation, which later affected the expression of imprinted genes within the KvDMR1 ICR. In contrast, changes in *Kcnq1ot1* were not sufficient to explain the decrease in the expression of another imprinted gene within the same KvDMR1 imprinting cluster, *Cdkn1c*, at both E20 (IUGR females) and PN1 (IUGR males and females) [12], as no correlation was found between the two genes in any group at any time point. As there was a decrease in *Dnmt3a* expression in E20 IUGR kidneys [12] and significant correlations between *Dnmt3a* and *Kcnq1/Kcnq1ot1/Cdkn1c* at E20, the DNA methylation profile of KvDMR1 was investigated. Hypomethylation was found at a CpG site only in PN1 IUGR males. However, the importance of the alteration of this specific CpG site and its effect on the IUGR kidney is yet to be determined. Future studies should investigate the allele-specific expression of these genes, the reason for DNA methylation changes at one CpG site in KvDMR1, and other epigenetic mechanisms.

Disclaimers

The views expressed in this manuscript are those of the authors.

Acknowledgments

The authors would like to thank Sandy Khor and Neil Shirley (University of Adelaide) for their help in Qiagility liquid-handling robot programming and setup.

Disclosure statement

No potential conflict of interest was reported by the authors.

Funding

The work was supported by the National Health and Medical Research Council [1045602]; National Heart Foundation of Australia [G 11 M 5785]; La Trobe University Faculty of Health Sciences Research Grant Award Robinson Research Institute [Seed Grant]; Robinson Research Institute [Seed Funding].

Source of support

This research was supported by the National Health and Medical Research Council (NHMRC) of Australia (M.E.W.; 1045602), the Heart Foundation (M.E.W.; G 11 M 5785), a La Trobe University Faculty of Health Sciences Research Grant Award (T.R.), and a Robinson Research Institute (RRI) Seed Grant (T.B.-M, M.E.W., and J.F.B.), and supported by the School of Agriculture, Food and Wine, University of Adelaide.

Data availability statement

The data that support the findings of this study are available from the corresponding author (tina.bianco@adelaide.edu.au) upon request.

ORCID

Tina Bianco-Miotto  <http://orcid.org/0000-0002-8431-5338>

References

- [1] Doan TNA, Akison LK, Bianco-Miotto T. Epigenetic mechanisms responsible for the transgenerational inheritance of intrauterine growth restriction phenotypes. *Front Endocrinol (Lausanne)*. 2022;13:838737. doi: 10.3389/fendo.2022.838737
- [2] Sharma D, Shastri S, Sharma P. Intrauterine growth restriction: antenatal and postnatal aspects. *Clin Med Insights Pediatr*. 2016;10:67–83. doi: 10.4137/CMPed.S40070
- [3] Dalle Molle R, Bischoff AR, Portella AK, et al. The fetal programming of food preferences: current clinical and experimental evidence. *J Dev Orig Health Dis*. 2016;7(3):222–230. doi: 10.1017/S2040174415007187
- [4] Skinner MK, Manikkam M, Tracey R, et al. Ancestral dichlorodiphenyltrichloroethane (DDT) exposure promotes epigenetic transgenerational inheritance of obesity. *BMC Med*. 2013;11:228. doi: 10.1186/1741-7015-11-228
- [5] Skinner MK, Ben Maamar M, Sadler-Riggleman I, et al. Alterations in sperm DNA methylation, non-coding RNA and histone retention associate with DDT-induced epigenetic transgenerational inheritance of disease. *Epigenet Chromatin*. 2018;11(1):8. doi: 10.1186/s13072-018-0178-0
- [6] Thorson JLM, Beck D, Ben Maamar M, et al. Ancestral plastics exposure induces transgenerational disease-specific sperm epigenome-wide association biomarkers. *Environ Epigenet*. 2021;7(1):dvaa023. doi: 10.1093/eep/dvaa023
- [7] Weber-Stadlbauer U, Richetto J, Zwamborn RAJ, et al. Transgenerational modification of dopaminergic dysfunctions induced by maternal immune activation. *Neuropsychopharmacology*. 2021;46(2):404–412. doi: 10.1038/s41386-020-00855-w
- [8] Goyal D, Limesand SW, Goyal R. Epigenetic responses and the developmental origins of health and disease. *J Endocrinol*. 2019;242(1):T105–T119. doi: 10.1530/joe-19-0009
- [9] Siklenka K, Erkek S, Godmann M, et al. Disruption of histone methylation in developing sperm impairs offspring health transgenerationally. *Science*. 2015;350(6261):aab2006. doi: 10.1126/science.aab2006
- [10] Lismer A, Siklenka K, Lafleur C, et al. Sperm histone H3 lysine 4 trimethylation is altered in a genetic mouse model of transgenerational epigenetic inheritance. *Nucleic Acids Res*. 2020;48(20):11380–11393. doi: 10.1093/nar/gkaa712
- [11] Briffa JF, Wlodek ME, Moritz KM. Transgenerational programming of nephron deficits and hypertension. *Semin Cell Dev Biol*. 2018;S1084-9521(17):30447–0. doi: 10.1016/j.semcdb.2018.05.025
- [12] Doan TNA, Briffa JF, Phillips AL, et al. Epigenetic mechanisms involved in intrauterine growth restriction and aberrant kidney development and function. *J Dev Orig Health Dis*. 2021;12(6):952–962. doi: 10.1017/S2040174420001257
- [13] Gallo LA, Tran M, Cullen-McEwen LA, et al. Transgenerational programming of fetal nephron deficits and sex-specific adult hypertension in rats. *Reprod Fertil Dev*. 2014;26(7):1032–1043. doi: 10.1071/RD13133
- [14] Gallo LA, Tran M, Moritz KM, et al. Cardio-renal and metabolic adaptations during pregnancy in female rats born small: implications for maternal health and second generation fetal growth. *Journal Of Physiology*. 2012;590(3):617–630. doi: 10.1113/jphysiol.2011.219147
- [15] Master JS, Zimanyi MA, Yin KV, et al. Transgenerational left ventricular hypertrophy and hypertension in offspring after uteroplacental insufficiency in male rats. *Clin Exp Pharmacol Physiol*. 2014;41(11):884–890. doi: 10.1111/1440-1681.12303
- [16] Tran M, Gallo LA, Jefferies AJ, et al. Transgenerational metabolic outcomes associated with uteroplacental insufficiency. *J Endocrinol*. 2013;217(1):105–118. doi: 10.1530/JOE-12-0560
- [17] Wadley GD, Siebel AL, Cooney GJ, et al. Uteroplacental insufficiency and reducing litter size alters skeletal muscle mitochondrial biogenesis in a

- sex-specific manner in the adult rat. *Am J Physiol Endocrinol Metab.* 2008;294(5):E861–E869. doi: 10.1152/ajpendo.00037.2008
- [18] Horsthemke B. A critical view on transgenerational epigenetic inheritance in humans. *Nat Commun.* 2018;9(1):2973. doi: 10.1038/s41467-018-05445-5
- [19] Cordeiro A, Neto AP, Carvalho F, et al. Relevance of genomic imprinting in intrauterine human growth expression of *CDKN1C*, *H19*, *IGF2*, *KCNQ1* and *PHLDA2* imprinted genes. *J Assist Reprod Genet.* 2014;31(10):1361–1368. doi: 10.1007/s10815-014-0278-0
- [20] Saha P, Verma S, Pathak RU, et al. Long noncoding RNAs in mammalian development and diseases. *Adv Exp Med Biol.* 2017;1008:155–198. doi: 10.1007/978-981-10-5203-3_6
- [21] Wlodek ME, Westcott K, Siebel AL, et al. Growth restriction before or after birth reduces nephron number and increases blood pressure in male rats. *Kidney Int.* 2008;74(2):187–195. doi: 10.1038/ki.2008.153
- [22] Wlodek ME, Mibus A, Tan A, et al. Normal lactational environment restores nephron endowment and prevents hypertension after placental restriction in the rat. *J Am Soc Nephrol.* 2007;18(6):1688–1696. doi: 10.1681/asn.2007010015
- [23] Miller SA, Dykes DD, Polesky HF. A simple salting out procedure for extracting DNA from human nucleated cells. *Nucleic Acids Res.* 1988;16(3):1215. doi: 10.1093/nar/16.3.1215
- [24] Suchiman HE, Sliker RC, Kremer D, et al. Design, measurement and processing of region-specific DNA methylation assays: the mass spectrometry-based method EpiTYPER. *Front Genet.* 2015;6:287. doi: 10.3389/fgene.2015.00287
- [25] R Core Team. R: A language and environment for statistical computing. Vienna, Austria: R Foundation for Statistical Computing; 2018. Available from: <http://www.R-project.org/>
- [26] Team R. RStudio: integrated development for R. Boston, MA: RStudio, PBC; 2020. Available from: <http://www.rstudio.com/>
- [27] Øyvind H, David ATH, Paul DR. PAST: Paleontological statistics software package for education and data analysis. *Palaeont Electr.* 2001;4(1):1–9.
- [28] Fitzpatrick GV, Pugacheva EM, Shin JY, et al. Allele-specific binding of CTCF to the multipartite imprinting control region KvDMR1. *Mol Cell Biol.* 2007;27(7):2636–2647. doi: 10.1128/mcb.02036-06
- [29] Shin JY, Fitzpatrick GV, Higgins MJ. Two distinct mechanisms of silencing by the KvDMR1 imprinting control region. *EMBO J.* 2008;27(1):168–178. doi: 10.1038/sj.emboj.7601960
- [30] Mancini-DiNardo D, Steele SJS, Ingram RS, et al. A differentially methylated region within the gene *Kcnq1* functions as an imprinted promoter and silencer. *Hum Mol Genet.* 2003;12(3):283–294. doi: 10.1093/hmg/ddg024
- [31] Abugessaisa I, Noguchi S, Hasegawa A, et al. refTSS: a reference data set for human and mouse transcription start sites. *J Mol Biol.* 2019;431(13):2407–2422. doi: 10.1016/j.jmb.2019.04.045
- [32] Tsunoda T, Takagi T. Estimating transcription factor bindability on DNA. *Bioinformatics.* 1999;15(7–8):622–30. doi: 10.1093/bioinformatics/15.7.622
- [33] Baribault C, Ehrlich KC, Ponnaluri VKC, et al. Developmentally linked human DNA hypermethylation is associated with down-modulation, repression, and upregulation of transcription. *Epigenetics.* 2018;13(3):275–289. doi: 10.1080/15592294.2018.1445900
- [34] Kao C-Y, Xu M, Wang L, et al. Elevated COUP-TFII expression in dopaminergic neurons accelerates the progression of Parkinson's disease through mitochondrial dysfunction. *PLoS Genet.* 2020;16(6):e1008868. doi: 10.1371/journal.pgen.1008868
- [35] Li L, Galichon P, Xiao X, et al. Orphan nuclear receptor COUP-TFII enhances myofibroblast glycolysis leading to kidney fibrosis. *EMBO Rep.* 2021;22(6):e51169. doi: 10.15252/embr.202051169
- [36] Ishii S, Koibuchi N. COUP-TFII in kidneys, from embryos to sick adults. *Diagnostics.* 2022;12(5). doi: 10.3390/diagnostics12051181
- [37] Estrela GR, Freitas-Lima LC, Budu A, et al. Chronic kidney disease induced by Cisplatin, folic acid and renal ischemia reperfusion induces anemia and promotes GATA-2 activation in mice. *Biomedicines.* 2021;9(7):769. doi: 10.3390/biomedicines9070769
- [38] Yang X, Mei C, Nie H, et al. Expression profile and prognostic values of GATA family members in kidney renal clear cell carcinoma. *Aging.* 2023;15(6):2170–2188. doi: 10.18632/aging.204607
- [39] Liu Z, Zhang J, Gao Y, et al. Large-scale characterization of DNA methylation changes in human gastric carcinomas with and without metastasis. *Clin Cancer Res.* 2014;20(17):4598–4612. doi: 10.1158/1078-0432.CCR-13-3380
- [40] Zhao L, Li C, Guan C, et al. Serum response factor, a novel early diagnostic biomarker of acute kidney injury. *Aging.* 2021 Jan 5;13(2):2885–2894. doi: 10.18632/aging.202381
- [41] Drake KA, Chaney C, Patel M, et al. Transcription factors YAP/TAZ and SRF cooperate to specify renal myofibroblasts in the developing mouse kidney. *J Am Soc Nephrol.* 2022;33(9):1694–1707. doi: 10.1681/asn.2021121559
- [42] Makhov PB, Golovine KV, Kutikov A, et al. Reversal of epigenetic silencing of AP-2alpha results in increased zinc uptake in DU-145 and LNCaP prostate cancer cells. *Carcinogenesis.* 2011;32(12):1773–1781. doi: 10.1093/carcin/bgr212
- [43] Lamontagne JO, Zhang H, Zeid AM, et al. Transcription factors AP-2α and AP-2β regulate distinct segments of the distal nephron in the mammalian kidney. *Nat Commun.* 2022;13(1):2226. doi: 10.1038/s41467-022-29644-3

- [44] Simmers MD, Hudson KM, Baptissart M, et al. Epigenetic control of the imprinted growth regulator *Cdkn1c* in cadmium-induced placental dysfunction. *Epigenetics*. 2022;18:1–17. doi: 10.1080/15592294.2022.2088173
- [45] Chen S, Sun FZ, Huang X, et al. Assisted reproduction causes placental maldevelopment and dysfunction linked to reduced fetal weight in mice. *Sci Rep*. 2015;5:10596. doi: 10.1038/srep10596
- [46] Fitzpatrick GV, Soloway PD, Higgins MJ. Regional loss of imprinting and growth deficiency in mice with a targeted deletion of *KvDMR1*. *Nature Genet*. 2002;32(3):426–431. doi: 10.1038/ng988
- [47] Mancini-Dinardo D, Steele SJS, Levorso JM, et al. Elongation of the *Kcnq1ot1* transcript is required for genomic imprinting of neighboring genes. *Genes Dev*. 2006;20(10):1268–1282. doi: 10.1101/gad.1416906
- [48] Cytrynbaum C, Chong K, Hannig V, et al. Genomic imbalance in the centromeric 11p15 imprinting center in three families: further evidence of a role for IC2 as a cause of Russell–Silver syndrome. *Am J Med Genet A*. 2016;170(10):2731–2739. doi: 10.1002/ajmg.a.37819
- [49] Bonaldi A, Mazzeu JF, Costa SS, et al. Microduplication of the ICR2 domain at chromosome 11p15 and familial Silver–Russell syndrome. *Am J Med Genet A*. 2011;155(10):2479–2483. doi: 10.1002/ajmg.a.34023
- [50] Mio C, Allegri L, Passon N, et al. A paternally inherited 1.4 kb deletion of the 11p15.5 imprinting center 2 is associated with a mild familial Silver–Russell syndrome phenotype. *Eur J Hum Genet*. 2021;29(3):447–454. doi: 10.1038/s41431-020-00753-1
- [51] Passaretti F, Pignata L, Vitiello G, et al. Different mechanisms cause hypomethylation of both *H19* and *KCNQ1OT1* imprinted differentially methylated regions in two cases of Silver–Russell syndrome spectrum. *Genes*. 2022;13(10):1875. doi: 10.3390/genes13101875
- [52] López-Abad M, Iglesias-Platas I, Monk D. Epigenetic characterization of *CDKN1C* in placenta samples from non-syndromic intrauterine growth restriction. *Front Genet*. 2016;7:62. doi: 10.3389/fgene.2016.00062
- [53] Caniçais C, Vasconcelos S, Ramalho C, et al. Deregulation of imprinted genes expression and epigenetic regulators in placental tissue from intrauterine growth restriction. *J Assist Reprod Genet*. 2021;38(4):791–801. doi: 10.1007/s10815-020-02047-3
- [54] Guo L, Choufani S, Ferreira J, et al. Altered gene expression and methylation of the human chromosome 11 imprinted region in small for gestational age (SGA) placentae. *Dev Biology*. 2008;320(1):79–91. doi: 10.1016/j.ydbio.2008.04.025
- [55] Bourque DK, Avila L, Peñaherrera M, et al. Decreased placental methylation at the H19/IGF2 imprinting control region is associated with normotensive intrauterine growth restriction but not preeclampsia. *Placenta*. 2010;31(3):197–202. doi: 10.1016/j.placenta.2009.12.003
- [56] Al-Awqati Q, Oliver JA. Stem cells in the kidney. *Kidney Int*. 2002;61(2):387–395. doi: 10.1046/j.1523-1755.2002.00164.x
- [57] Park J, Shrestha R, Qiu C, et al. Single-cell transcriptomics of the mouse kidney reveals potential cellular targets of kidney disease. *Science*. 2018;360(6390):758–763. doi: 10.1126/science.aar2131
- [58] Ransick A, Lindström NO, Liu J, et al. Single-cell Profiling Reveals sex, lineage, and regional diversity in the mouse kidney. *Dev Cell*. 2019;51(3):399–413.e7. doi: 10.1016/j.devcel.2019.10.005
- [59] Ding F, Tian X, Mo J, et al. Determination of the dynamic cellular transcriptional profiles during kidney development from birth to maturity in rats by single-cell RNA sequencing. *Cell Death Discov*. 2021;7(1):162. doi: 10.1038/s41420-021-00542-9
- [60] Bhogal B, Arnaudo A, Dymkowski A, et al. Methylation at mouse *Cdkn1c* is acquired during post-implantation development and functions to maintain imprinted expression. *Genomics*. 2004;84(6):961–970. doi: 10.1016/j.ygeno.2004.08.004
- [61] Guo T, Luo F, Lin Q. You are affected by what your parents eat: diet, epigenetics, transgenerational and intergenerational. *Trends Food Sci Technol*. 2020;100:248–261. doi: 10.1016/j.tifs.2020.04.021
- [62] Salmeri N, Carbone IF, Cavoretto PI, et al. Epigenetics beyond fetal growth restriction: a comprehensive overview. *Mol Diagn Ther*. 2022;26(6):607–626. doi: 10.1007/s40291-022-00611-4
- [63] Basak T, Ain R. Long non-coding RNAs in placental development and disease. *Non-Cod RNA Investgat*. 2019;3. doi: 10.21037/ncri.2019.03.01

CHAPTER 4 & 5

INTRODUCTION

&

MATERIALS AND METHODS

Introduction

As previously discussed in **Chapter 2**, the rat uteroplacental insufficiency (UPI; induced at day 18 of gestation) model of intrauterine growth restriction (IUGR) mimics metabolic characteristics in humans and provides evidence for the sex-specific and multigenerational transmission of IUGR phenotypes, such as increased blood pressure, left ventricle hypertrophy, impaired glucose tolerance, reduced β -cell response to glucose, and reduced glomerular number [1, 2, 3, 4, 5, 6, 7]. Specifically, F1 offspring had reduced birth weight compared to sham [4, 8, 9, 10, 11], while F2 offspring birth weight remained within the normal range [4, 12]. Blood pressure has been shown to be higher in both F1 and F2 IUGR males, from the juvenile period to adulthood [5, 6, 8, 11]. Meanwhile, contrasting results have been reported for the F2 offspring first-phase insulin secretion at 6 months of age, either lower [4] or similar [12] to the sham controls, in both sexes. Nephron number was reduced in F1 male and female rats at 6 months of age, as well as in F2 males and females at embryonic day 20 (E20) [1, 2, 6, 8, 11]. However, there was no alteration to the renal function of F2 rats at both 6 and 12 months of age.

It should be noted that the above results of cardio-metabolic and kidney functions came from offspring in the maternal line (F1 females, F2 males and females), or just the F1 males in the paternal line. F2 and F3 rat offspring from the paternal line of this UPI model have only been investigated for bone health at 6, 12 and 16 (males only) months of age, and there was no significant difference compared to sham being reported [10]. Other IUGR models have reported the transgenerational transmission of IUGR-related metabolic and renal dysfunction phenotypes down to the F2 generation in the paternal line [13], and F3 generation in the maternal line [14, 15, 16, 17]. Specifically, inducing UPI at day 19.5 of gestation was

reported to result in reduced body weight at postnatal day (PN) 21 in F2 male and female rats from the paternal line [13]. *In utero* exposure to caffeine ($\sim 120 \text{ mg}\cdot\text{kg}^{-1}\cdot\text{d}^{-1}$) resulted in growth restricted F1 females and inheritance of adrenal gland dysfunction in the F2 and F3 offspring [14, 15]. F1 female rats whose mother had a low-protein diet (8%) during pregnancy had reduced insulin secretion, while their grand-offspring in the F3 generation, had increased fasting plasma glucose (F3 females), increased plasma fasting insulin, and increased plasma insulin at 30 minutes post-glucose injection (F3 males) (glucose tolerance test), compared to control animals [16]. Restraint stress and forced swimming from day 12 to 18 of pregnancy in F0 rats resulted in significantly lower body weights at PN1 and 7 of F3 offspring from the maternal line [17]. Meanwhile, rodent studies of other non IUGR-inducing *in utero* insults, such as exposure of the F0 pregnant animal to a high-fat diet [18, 19] have reported the transmission of metabolic disease phenotypes down to the F3 generation in the paternal line.

To determine whether there is a sex-specific and transgenerational transmission of cardio-metabolic or renal disease phenotypes in the paternal line of the UPI-induced IUGR model, we investigated the F2 and F3 male and female offspring generated from F1 IUGR rats. Animals were examined from early postnatal life through to lactation, puberty, juvenile period, and adulthood.

Materials and Methods

Rat model of intrauterine growth restriction (IUGR)

The use of animals (rats) in this study has been approved by the University of Melbourne's Animal Experimentation Sub-Committee (AEC 04138, 1011865, and 1112130) and the La Trobe University's Animal Ethics Committee (AEC 12-42). The animal model was

established by Professor Mary E. Wlodek (The University of Melbourne). Animal surgery and physiological data collection (including body weights, postmortem organ weights, blood pressure, glucose tolerance test, insulin challenge, nephron number, renal function) were performed by Professor Wlodek's laboratory. Laboratory books and excel sheets with collected data were sent to the researcher (TNAD) for proofing and statistical analyses. Kidney samples in formalin/ 70% alcohol were also received for histological analysis.

Model: Uteroplacental insufficiency (UPI) was induced by uterine vessel (artery and vein) ligation in F0 pregnant rats at embryonic day 18 (E18; term is 22 days), as previously described [10, 11, 20]. Pregnant rats in the sham (control) group underwent a similar surgical procedure without uterine vessel ligation. F1 males were mated with normal females to produce F2 offspring (paternal line), with no additional *in utero* insult being introduced during F1 pregnancy. Similarly, F2 males were mated with normal females to produce the F3 paternal generation [10]. All pups remained with their mother until weaning (postnatal day 35 (PN35)).

Body weight measurement

Offspring body weight was measured repeatedly over time (at birth (PN1), PN7, PN14, PN35, 2 months of age (mo), 3mo (F1 males only), 4mo, 6mo, 9mo, and 12mo). PN1 weight was the average weight of same-sex litter mates. Body weight at other time points were individual values. To access growth profiles of offspring, absolute growth rate ($\text{g}\cdot\text{day}^{-1}$) and fractional growth rate ($\%\cdot\text{day}^{-1}$) were calculated using body weights over time [4]. Absolute growth rate: *(body weight at later time point (g) - body weight at earlier time point*

(g) ÷ days between two timepoints. Fractional growth rate: (absolute growth rate (g.day⁻¹) ÷ body weight at earlier time point (g)) x 100.

Tissue collection

Postmortem body weight, used in calculations of relative organ weight (% body weight), were measured before tissue collection. Heart, left ventricle, kidney (left and right) and liver tissues were collected at 12mo for F1 males, as other time points have previously been investigated for the F1 paternal line [1, 5, 8]. For F2 and F3 offspring, heart, left ventricle, kidney (left and right), adrenal gland (left and right), liver, and pancreas tissues were collected at PN35, 6mo, and 12mo. Tissue weights were reported as absolute (g) and relative (% body weight) weights.

Systolic blood pressure measurement

Offspring systolic blood pressure was measured by non-invasive tail cuff plethysmography [1, 11] in F1 males, F2, and F3 animals. Measurements were carried out repeatedly at 2mo, 3mo (F1 males only), 4mo, 6mo, 9mo, and 12mo.

Glucose tolerance test/Insulin challenge

F2 and F3 male and female offspring were subjected to a glucose tolerance test (GTT; 1g.kg⁻¹ body weight glucose injection) and insulin challenge (IC; 1U.kg⁻¹ body weight insulin injection) at 6mo and 12mo, as previously described [12, 21]. For GTT, blood samples were collected at 10 and 5 minutes prior to the glucose injection, as well as 5, 10, 20, 30, 45, 60, 90, and 120 minutes after injection. Fasting (basal) values were calculated as the average of

the two time points: 10 and 5 minutes prior to the glucose injection. GTT glucose and insulin area under curves (AUC) were calculated as the total AUC from basal to 120 minutes. First-phase and second-phase insulin secretion was calculated as the insulin AUC from basal to 5 minutes (1st) and insulin AUC from 5 to 120 minutes (2nd), respectively. The homeostasis model of assessment of insulin resistance (HOMA-IR) was calculated using the formula: $(\text{fasting insulin } (\mu\text{U.ml}^{-1}) \times \text{fasting glucose } (\text{mg.dL}^{-1})) \div 2430$ [22, 23]. During IC, blood samples were collected right before the insulin injection (basal) and 20, 40, 60, and 90 minutes after injection. Glucose AUC was calculated as the total AUC from basal to 90 minutes.

Nephron number and renal function

Nephron number of sham and IUGR offspring in both F2 and F3 generations were determined from the right kidney at PN35, using Cavalieri principle and physical dissector method as previously reported [1, 6, 11]. At 6 and 12 months of age, F2 and F3 animals were placed in metabolic cages for renal function examinations (24 hours), including measurements of food intake, water intake, urine produced, and excretion of ions and proteins [2, 6]. Plasma samples (plasma creatinine) were collected right after the renal function examination. Creatinine clearance was calculated using the formula: $(\text{urine creatinine } (\mu\text{mol.L}^{-1}) \times \text{urine flow rate } (\text{L.24h}^{-1}.\text{kg}^{-1})) \div \text{plasma creatinine } (\mu\text{mol.L}^{-1})$ [24, 25].

Kidney histopathology

Fixed right kidney from F2 and F3 offspring at 6 months of age were sent to Histology Services (The Adelaide Medical School, University of Adelaide) for processing, sectioning (5 μm) and staining for Haematoxylin and Eosin (H&E), Periodic Acid-Schiff (PAS), and

Masson's trichrome – see **Fig. 1**. Kidney histopathology analysis was carried out by an expert pathologist (Dr Helle Bielefeldt-Ohmann, The University of Queensland). Histopathological scores included: Bowman's capsule, glomerulus, epithelial cells, basement membrane, luminal casts, leukocyte infiltration, fibrosis, blood vessels, and total score. Score of 0 = within normal limits (wnl); 1 = minimal change; 2 = mild change; 3 = moderate change; 4 = severe change in < 50% of section; 5 = severe change in > 50% of section.

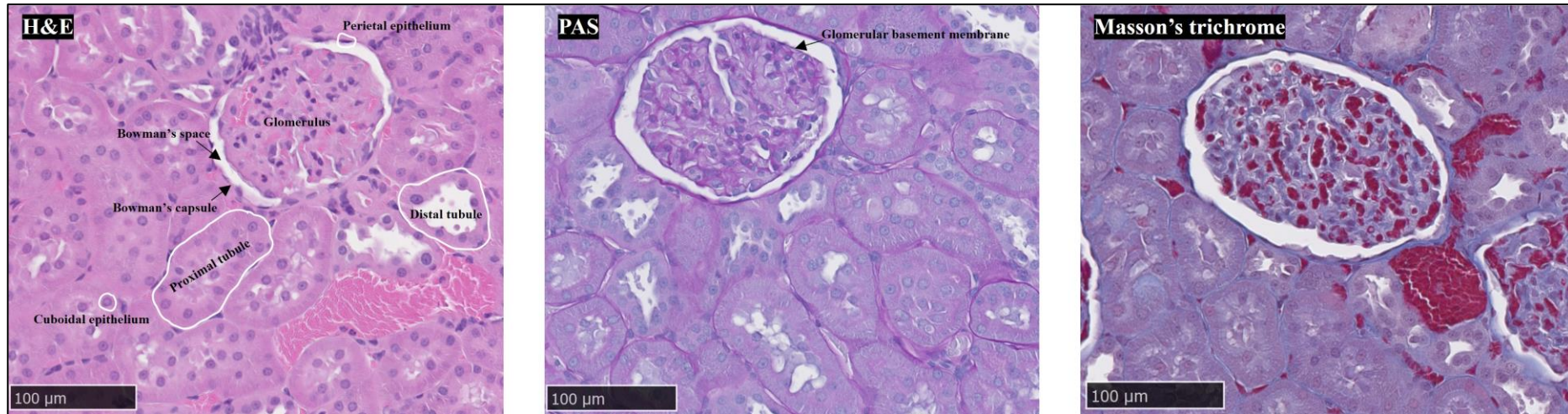


Figure 1. Representative Haematoxylin and Eosin (H&E, left), Periodic Acid-Schiff (PAS, middle), and Masson's trichrome (right) stained kidney sections from F2 sham male at 6 months of age. Kidney slides were viewed using NDP View 2 program. H&E stains cell nuclei purplish blue and extracellular matrix and cytoplasm pink. PAS stains structures containing a high proportion of carbohydrates (e.g., glycogen) purplish red/purple. Masson's trichrome stains collagen blue, cytoplasm pink, and muscle tissue/fibre red.

Statistical analysis

Data processing: Data values beyond ± 2 standard deviations (SD) from the sample's observed/descriptive means were considered as outliers and removed. Data was checked for homoscedasticity, normal distribution, and a constant variance of errors/residuals using residuals versus fits plot, qq plot, histogram, and Shapiro-Wilk normality test. Males and females were investigated separately, as the physiological data of each sex was previously reported to be different [2, 6, 8, 12, 26], similar to our preliminary statistical analyses. Only males were investigated in the F1 generation (paternal). Adjustment for random effects (litter size, relatedness between litter siblings, and repeated measurement, if present) were also included in the statistical models below.

A linear mixed-effect model, followed by Tukey's *post hoc* tests if there was an interaction between fixed effects, was used to analyse metabolic data in the R environment (v 4.1.1) [27]. Treatment (control (sham) or restricted (IUGR)) was considered as a fixed effect, except for the analyses of body weight, blood pressure, and GTT/IC responses. As body weight, blood pressure, and GTT/IC responses of each offspring were measured over time, both treatment and time point (body weight: birth to 12 months, systolic blood pressure: 2 months to 12 months, GTT: basal to 120 min, and IC: basal to 90 min) were considered as fixed effects. For comparisons between groups, estimated marginal means (emmeans) of the linear mixed-effect model were reported instead of the sample's observed/descriptive means. Degrees-of-freedom method used was Kenward-Roger. Confidence level used was 95%. As emmeans were extracted from the assumption that all groups had the same variance (balanced population), standard deviations (SD) were not reported. Instead, standard errors (SE) of emmeans were reported.

One-way ordinal regression with Cumulative Linked Model (CLM) was used to analyse histopathological scores of 6mo sham and IUGR rats kidneys in the R environment (v 4.1.1) [27]. Treatment (sham/IUGR) was identified as the independent variable, while histopathological score (ordered factor) was identified as the dependent variable. Observations between groups were not paired or repeated measures. Emmeans were not reported for ordinal data. Correlation between total kidney weight (% body weight), renal function measurements (24 hours) and kidney total histological score were determined using Spearman's non-parametric correlation coefficient (no assumptions regarding data distribution), calculated using PAST 4.03 software [28].

Exact *P* values were stated to three significant figures (e.g., $P = 0.053$), except when $P < 0.0001$ (expressed as $P < 0.0001$), or $0.0001 < P < 0.001$ (e.g., $P = 0.0002$, instead of $P = 0.000$), or when R statistical package specifically reported $P < 0.001$ instead of a number. Graphs were plotted with the sample's data points and their observed means \pm SD, using GraphPad Prism 9.0.0.

References

1. Wlodek ME, Westcott K, Siebel AL, Owens JA, Moritz KM. Growth restriction before or after birth reduces nephron number and increases blood pressure in male rats. *Kidney International*. 2008;74(2):187-195. doi: 10.1038/ki.2008.153.
2. Moritz KM, Mazzuca MQ, Siebel AL, Mibus A, Arena D, Tare M, Owens JA, Wlodek ME. Uteroplacental insufficiency causes a nephron deficit, modest renal insufficiency

- but no hypertension with ageing in female rats. *The Journal of Physiology*. 2009;587(Pt 11):2635-2646.
3. Mazzuca MQ, Wlodek ME, Dragomir NM, Parkington HC, Tare M. Uteroplacental insufficiency programs regional vascular dysfunction and alters arterial stiffness in female offspring. *Journal of Physiology*. 2010;588(Pt 11):1997-2010. doi: 10.1113/jphysiol.2010.187849.
 4. Tran M, Gallo LA, Jefferies AJ, Moritz KM, Wlodek ME. Transgenerational metabolic outcomes associated with uteroplacental insufficiency. *Journal of Endocrinology*. 2013;217(1):105-118. doi: 10.1530/JOE-12-0560.
 5. Master JS, Zimanyi MA, Yin KV, Moritz KM, Gallo LA, Tran M, Wlodek ME, Black MJ. Transgenerational left ventricular hypertrophy and hypertension in offspring after uteroplacental insufficiency in male rats. *Clinical and Experimental Pharmacology and Physiology*. 2014;41(11):884-890. doi: 10.1111/1440-1681.12303.
 6. Gallo LA, Tran M, Cullen-McEwen LA, Denton KM, Jefferies AJ, Moritz KM, Wlodek ME. Transgenerational programming of fetal nephron deficits and sex-specific adult hypertension in rats. *Reproduction, Fertility and Development*. 2014;26(7):1032-1043. doi: 10.1071/RD13133.
 7. Cuffe JSM, Briffa JF, Rosser S, Siebel AL, Romano T, Hryciw DH, Wlodek ME, Moritz KM. Uteroplacental insufficiency in rats induces renal apoptosis and delays nephrogenesis completion. *Acta Physiologica*. 2018;222(3):e12982. doi: 10.1111/apha.12982.
 8. Tran M, Young ME, Jefferies AJ, Hryciw DH, Ward MM, Fletcher EL, Wlodek ME, Wadley GD. Uteroplacental insufficiency leads to hypertension, but not glucose intolerance or impaired skeletal muscle mitochondrial biogenesis, in 12-month-old rats. *Physiol Rep*. 2015;3(9). doi: 10.14814/phy2.12556.

9. Siebel AL, Mibus A, De Blasio MJ, Westcott KT, Morris MJ, Prior L, Owens JA, Wlodek ME. Improved lactational nutrition and postnatal growth ameliorates impairment of glucose tolerance by uteroplacental insufficiency in male rat offspring. *Endocrinology*. 2008;149(6):3067-3076. doi: 10.1210/en.2008-0128.
10. Anevskaja K, Wark JD, Wlodek ME, Romano T. The transgenerational effect of maternal and paternal F1 low birth weight on bone health of second and third generation offspring. *Journal of Developmental Origins of Health and Disease*. 2019;10(2):144-153. doi: 10.1017/S204017441800020X.
11. Wlodek ME, Mibus A, Tan A, Siebel AL, Owens JA, Moritz KM. Normal lactational environment restores nephron endowment and prevents hypertension after placental restriction in the rat. *Journal of the American Society of Nephrology*. 2007;18(6):1688-1696. doi: 10.1681/asn.2007010015.
12. Cheong JN, Cuffe JS, Jefferies AJ, Anevskaja K, Moritz KM, Wlodek ME. Sex-specific metabolic outcomes in offspring of female rats born small or exposed to stress during pregnancy. *Endocrinology*. 2016;157(11):4104-4120. doi: 10.1210/en.2016-1335.
13. Gonzalez-Rodriguez P, Cantu J, O'Neil D, Seferovic MD, Goodspeed DM, Suter MA, Aagaard KM. Alterations in expression of imprinted genes from the *H19/Igf2* loci in a multigenerational model of intrauterine growth restriction (IUGR). *American Journal of Obstetrics and Gynecology*. 2016;214(5):625.e1-625.e11.
14. Chen G, Yuan C, Duan F, Liu Y, Zhang J, He Z, Huang H, He C, Wang H. IGF1/MAPK/ERK signaling pathway-mediated programming alterations of adrenal cortex cell proliferation by prenatal caffeine exposure in male offspring rats. *Toxicology and Applied Pharmacology*. 2018;341:64-76. doi: <https://doi.org/10.1016/j.taap.2018.01.008>.

15. He Z, Zhang J, Chen G, Cao J, Chen Y, Ai C, Wang H. H19/let-7 axis mediates caffeine exposure during pregnancy induced adrenal dysfunction and its multi-generation inheritance. *Science of the Total Environment*. 2021;792:148440. doi: <https://doi.org/10.1016/j.scitotenv.2021.148440>.
16. Benyshek DC, Johnston CS, Martin JF. Glucose metabolism is altered in the adequately-nourished grand-offspring (F3 generation) of rats malnourished during gestation and perinatal life. *Diabetologia*. 2006;49(5):1117-1119. doi: [10.1007/s00125-006-0196-5](https://doi.org/10.1007/s00125-006-0196-5).
17. Yao Y, Robinson AM, Zucchi FC, Robbins JC, Babenko O, Kovalchuk O, Kovalchuk I, Olson DM, Metz GA. Ancestral exposure to stress epigenetically programs preterm birth risk and adverse maternal and newborn outcomes. *BMC Medicine*. 2014;12:121. doi: [10.1186/s12916-014-0121-6](https://doi.org/10.1186/s12916-014-0121-6).
18. Wei Y, Yang CR, Wei YP, Zhao ZA, Hou Y, Schatten H, Sun QY. Paternally induced transgenerational inheritance of susceptibility to diabetes in mammals. *Proceedings of the National Academy of Sciences of the United States of America*. 2014;111(5):1873-8. doi: [10.1073/pnas.1321195111](https://doi.org/10.1073/pnas.1321195111).
19. Dunn GA, Bale TL. Maternal high-fat diet effects on third-generation female body size via the paternal lineage. *Endocrinology*. 2011;152(6):2228-36. doi: [10.1210/en.2010-1461](https://doi.org/10.1210/en.2010-1461).
20. Wlodek ME, Westcott KT, O'Dowd R, Serruto A, Wassef L, Moritz KM, Moseley JM. Uteroplacental restriction in the rat impairs fetal growth in association with alterations in placental growth factors including PTHrP. *American Journal of Physiology-Regulatory, Integrative and Comparative Physiology*. 2005;288(6):R1620-R1627. doi: [10.1152/ajpregu.00789.2004](https://doi.org/10.1152/ajpregu.00789.2004).

21. Laker RC, Gallo LA, Wlodek ME, Siebel AL, Wadley GD, McConell GK. Short-term exercise training early in life restores deficits in pancreatic β -cell mass associated with growth restriction in adult male rats. *American Journal of Physiology: Endocrinology and Metabolism*. 2011;301(5):E931-40. doi: 10.1152/ajpendo.00114.2011.
22. Cacho J, Sevillano J, de Castro J, Herrera E, Ramos MP. Validation of simple indexes to assess insulin sensitivity during pregnancy in Wistar and Sprague-Dawley rats. *American Journal of Physiology-Endocrinology and Metabolism*. 2008;295(5):E1269-E1276. doi: 10.1152/ajpendo.90207.2008.
23. Nguyen TMT, Steane SE, Moritz KM, Akison LK. Prenatal alcohol exposure programmes offspring disease: insulin resistance in adult males in a rat model of acute exposure. *The Journal of Physiology*. 2019;597(23):5619-5637. doi: <https://doi.org/10.1113/JP278531>.
24. Gallo LA, Tran M, Moritz KM, Mazzuca MQ, Parry LJ, Westcott KT, Jefferies AJ, Cullen-McEwen LA, Wlodek ME. Cardio-renal and metabolic adaptations during pregnancy in female rats born small: implications for maternal health and second generation fetal growth. *The Journal of Physiology*. 2012;590(3):617-630. doi: 10.1113/jphysiol.2011.219147.
25. Mahizir D, Briffa JF, Anevska K, Wadley GD, Moritz KM, Wlodek ME. Exercise alters cardiovascular and renal pregnancy adaptations in female rats born small on a high-fat diet. *American Journal of Physiology-Regulatory, Integrative and Comparative Physiology*. 2021;320(4):R404-R416. doi: 10.1152/ajpregu.00260.2020.
26. Wadley GD, Siebel AL, Cooney GJ, McConell GK, Wlodek ME, Owens JA. Uteroplacental insufficiency and reducing litter size alters skeletal muscle mitochondrial biogenesis in a sex-specific manner in the adult rat. *American Journal*

of Physiology-Endocrinology and Metabolism. 2008;294(5):E861-E869. doi:
10.1152/ajpendo.00037.2008.

27. RStudio Team. RStudio: integrated development for R. Boston, MA: RStudio, PBC; 2020. Available from: <http://www.rstudio.com/>
28. Øyvind H, David ATH, Paul DR. PAST: Paleontological statistics software package for education and data analysis. *Palaeontologia Electronica*. 2001;4(1):1-9.

CHAPTER 4

UTEROPLACENTAL

INSUFFICIENCY RESULTS IN AN

INCREASED RISK OF

DEVELOPING METABOLIC

DISEASE ACROSS GENERATIONS

IN THE PATERNAL LINE OF

GROWTH RESTRICTED RATS

Statement of Authorship

Statement of Authorship

Title of Paper	Uteroplacental insufficiency results in an increased risk of developing metabolic disease across generations in the paternal line of growth restricted rats	
Publication Status	<input type="checkbox"/> Published	<input type="checkbox"/> Accepted for Publication
	<input type="checkbox"/> Submitted for Publication	<input checked="" type="checkbox"/> Unpublished and Unsubmitted work written in manuscript style
Publication Details	Doan, T.N.A. , Cowley, M. J., Phillips, L. A., Briffa, F. J., Burton, A. R., Romano, T., Wlodek, E. M., & Bianco-Miotto, T. (2023). Uteroplacental insufficiency results in an increased risk of developing metabolic disease across generations in the paternal line of growth restricted rats. <u>Target journal</u> : <i>The Journal of Physiology</i>	

Principal Author

Name of Principal Author (Candidate)	Ngoc Anh Thu Doan		
Contribution to the Paper	Analysed the data and wrote the manuscript		
Overall percentage (%)	70		
Certification:	This paper reports on original research I conducted during the period of my Higher Degree by Research candidature and is not subject to any obligations or contractual agreements with a third party that would constrain its inclusion in this thesis. I am the primary author of this paper.		
Signature		Date	13.11.2023

Co-Author Contributions

By signing the Statement of Authorship, each author certifies that:

- i. the candidate's stated contribution to the publication is accurate (as detailed above);
- ii. permission is granted for the candidate to include the publication in the thesis; and

iii. the sum of all co-author contributions is equal to 100% less the candidate's stated contribution.

Name of Co-Author	James M. Cowley		
Contribution to the Paper	Contributed to statistical analyses and critical review and revision of the manuscript		
Signature		Date	13.11.2023

Name of Co-Author	Aaron L. Phillips		
Contribution to the Paper	Contributed to statistical analyses and critical review and revision of the manuscript		
Signature		Date	13.11.2023

Name of Co-Author	Jessica F. Briffa		
Contribution to the Paper	Generated the animal model tissues, acquired animal tissues and phenotypic data, provided tissue and phenotypic data, critical review of the manuscript		
Signature		Date	13.11.2023

Name of Co-Author	Rachel A. Burton		
Contribution to the Paper	Provided intellectual input and resources, critical review of the manuscript		
Signature		Date	13.11.23

Name of Co-Author	Tania Romano		
Contribution to the Paper	Contributed to generation of animal tissues, and critical review of the manuscript		
Signature		Date	13.11.2023

Name of Co-Author	Mary E. Wlodek		
Contribution to the Paper	Generated the animal model, acquired animal tissues and phenotypic data, provided tissue and phenotypic data, contributed to study design, critical review of the manuscript		
Signature		Date	13.11.2023

Name of Co-Author	Tina Bianco-Miotto		
Contribution to the Paper	Supervised the project, critical review and revision of the manuscript		
Signature		Date	13.11.2023

Abstract

Intrauterine growth restriction (IUGR) is associated with an increased risk of developing cardiovascular and metabolic diseases later in life. This increased risk of chronic disease was not only seen in the growth restricted offspring in the first (F1) generation, but also in the second (F2) generation offspring whose birth weights are comparable to that of healthy controls. While the physiopathology of offspring from the maternal line of the uteroplacental insufficiency induced IUGR rat model has extensively been studied over the last decade, the paternal line has not been as well studied. This current study investigated the growth profiles, postmortem organ weights, blood pressure and metabolic functions via responses to glucose tolerance test and insulin challenge across three generations (F1-F3) of growth restricted offspring from the paternal line. Accelerated growth was observed in male and female offspring in the F2 generation ($+0.20 \text{ \%}\cdot\text{day}^{-1}$ during juvenile period in IUGR males; $+1.55 \text{ \%}\cdot\text{day}^{-1}$ at early postnatal life, and $+0.38 \text{ \%}\cdot\text{day}^{-1}$ during puberty in IUGR females). Similarly, F3 IUGR males had an increased fractional growth rate ($+0.84 \text{ \%}\cdot\text{day}^{-1}$) during puberty, while F3 IUGR females had increased fractional growth rate at early postnatal life ($+0.70 \text{ \%}\cdot\text{day}^{-1}$) and in juvenile period ($+0.05 \text{ \%}\cdot\text{day}^{-1}$), increasing the likelihood of animals developing metabolic diseases. Postmortem organ weights were found to be altered at weaning and adulthood of both F2 and F3 offspring. Additionally, F3 males and females had impaired insulin secretions at 12 months of age, with a decrease by 40.15% in first-phase insulin secretion of IUGR males, and a decrease by 20.27% in second-phase insulin secretion of IUGR females, compared to same-sex controls. However, in contrast to the maternal line, there was no significant alteration to blood pressure in all animals, apart from F2 IUGR males at 6 months of age, which had a lower blood pressure (-7.38 mmHg or 5.36%) compared to sham controls. Taken together, these results suggest that there is transgenerational transmission of IUGR-related metabolic disease risk in offspring from the paternal line,

occurring even in the offspring that were not directly affected by the *in utero* developmental insult.

Results

Offspring body weights over time

As expected, body weights of all animals, regardless of treatment, increased with age (**Supplementary data (Appendix B)**). There was no difference F1 male body weights when comparing sham and IUGR at birth ($P=1$), PN7 ($P=1$), PN14 ($P=0.970$), and PN35 ($P=0.240$) (**Table S1** and **Fig. 1a**). From 2 months of age (2mo), F1 IUGR males were significantly smaller ($P < 0.001$) for all time points from 2mo to 12mo (**Table S1** and **Fig. 1a**). Absolute growth rate ($\text{g}\cdot\text{day}^{-1}$), which is the increment in body weight (g) between two time points (days), of F1 IUGR males was significantly lower compared to sham when calculated between PN1-2mo and 4mo-6mo (**Table 1** and **Fig. 2a**). However, fractional growth rates ($\%\cdot\text{day}^{-1}$) of IUGR males were significantly higher at PN7-PN14 ($20.39 \pm 0.69 \%\cdot\text{day}^{-1}$ vs. sham $16.25 \pm 0.78 \%\cdot\text{day}^{-1}$, $P < 0.0001$), PN14-PN35 ($13.62 \pm 0.30 \%\cdot\text{day}^{-1}$ vs. sham $12.56 \pm 0.31 \%\cdot\text{day}^{-1}$, $P = 0.008$), and 2mo-3mo ($1.47 \pm 0.11 \%\cdot\text{day}^{-1}$ vs. sham $1.01 \pm 0.10 \%\cdot\text{day}^{-1}$, $P = 0.0002$) (**Table 1** and **Fig. 3a**), which were signs of catch-up growth during early postnatal life, throughout lactation, and during the juvenile period, respectively.

In contrast, F2 IUGR males had a higher body weight compared to sham males at 4mo and 6mo (increased by 3.36%, $P = 0.004$ and 3.43%, $P = 0.0002$, respectively; **Table S1** and **Fig. 1c**). This result was as expected, as accelerated growth in F2 IUGR males was observed at 2mo-4mo, with increased fractional growth rate compared to sham ($1.12 \pm 0.07 \%\cdot\text{day}^{-1}$ vs. $0.92 \pm 0.07 \%\cdot\text{day}^{-1}$, respectively, $P = 0.0006$, **Table 1** and **Fig. 3c**). Accelerated growth in

IUGR females, represented by an increase in both absolute and fractional growth rates, was evident at early postnatal life (PN7-14) and during puberty (PN35-2mo) (**Table 2** and **Fig. 2b, 3b**).

In the F3 generation, there were little differences in body weight in IUGR males or IUGR females when compared to their sham control (**Table 1** and **Fig. 1d, 1e**). F3 IUGR males had increased absolute ($5.94 \pm 0.19 \text{ g}\cdot\text{day}^{-1}$ vs. $5.27 \pm 0.20 \text{ g}\cdot\text{day}^{-1}$, $P < 0.0001$) and fractional ($6.82 \pm 0.19 \text{ }\%\cdot\text{day}^{-1}$ vs. $5.98 \pm 0.19 \text{ }\%\cdot\text{day}^{-1}$, $P < 0.0001$) growth rates compared to sham males at PN35-2mo (**Table 1** and **Fig. 2e, 3e**). Meanwhile, in the F3 IUGR females, despite the similarity in body weights compared to sham at all time points, increased absolute and fractional growth rates were also found at PN7-PN14 ($1.85 \pm 0.05 \text{ g}\cdot\text{day}^{-1}$ vs. $1.75 \pm 0.05 \text{ g}\cdot\text{day}^{-1}$, $P = 0.002$ and $17.31 \pm 0.50 \text{ }\%\cdot\text{day}^{-1}$ vs. $16.61 \pm 0.51 \text{ }\%\cdot\text{day}^{-1}$, $P = 0.022$) and 4mo-6mo ($0.29 \pm 0.03 \text{ g}\cdot\text{day}^{-1}$ vs. $0.19 \pm 0.04 \text{ g}\cdot\text{day}^{-1}$, $P = 0.023$ and $0.13 \pm 0.01 \text{ }\%\cdot\text{day}^{-1}$ vs. $0.08 \pm 0.02 \text{ }\%\cdot\text{day}^{-1}$, $P = 0.027$) (**Table 2** and **Fig. 2d, 3d**).

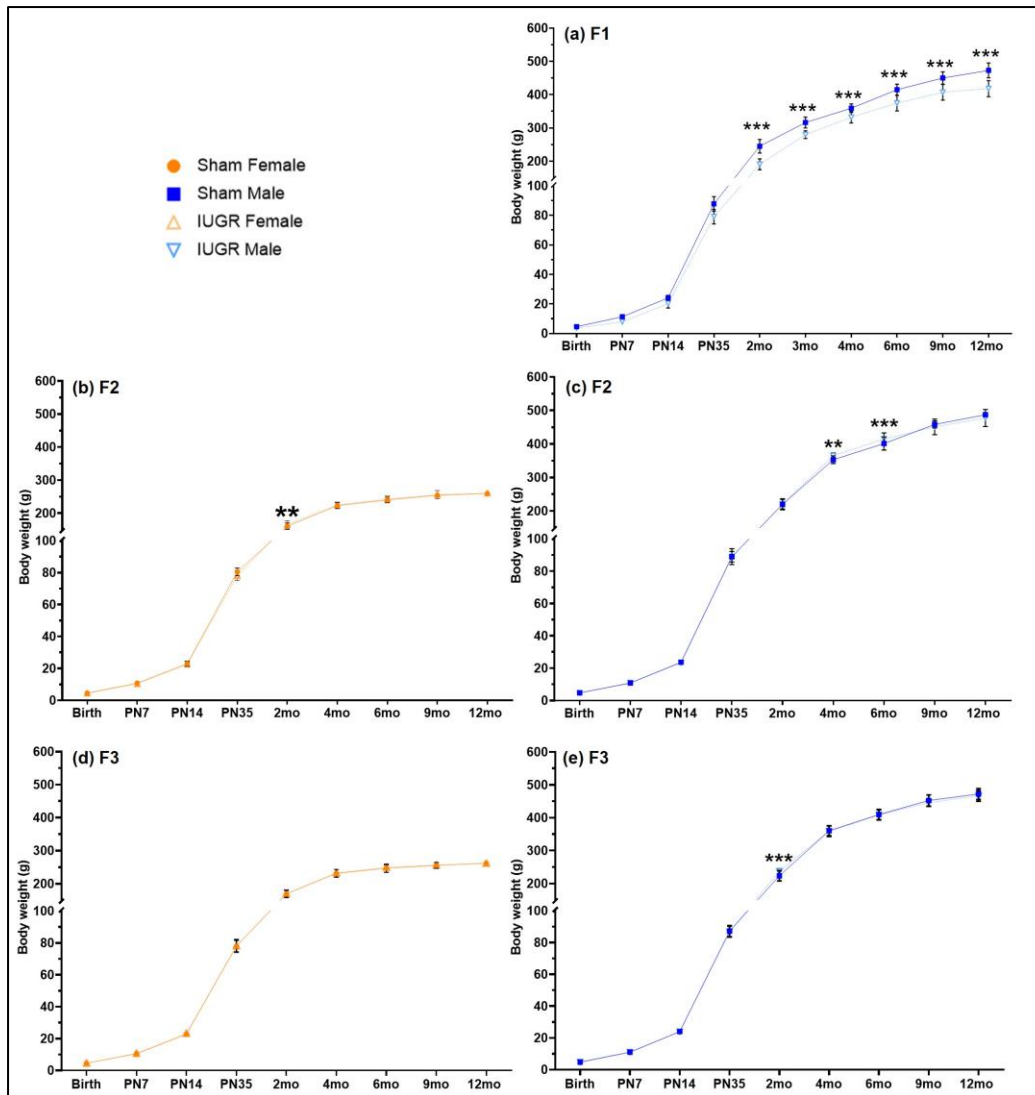


Figure 1. Body weight at birth (postnatal day (PN) 1), PN7-35, and 2-12 months of age (2mo-12mo) of sham and IUGR rat offspring (paternal line) in the first (F1, a), second (F2, b, c) and third (F3, d, e) generations. Significance was determined by a linear mixed-effect model with adjustment for litter size, relatedness of litter siblings (if present), and repeated measurement, followed by a Tukey's post hoc test (***) $P < 0.001$, ** $P < 0.01$). See **Table S1** for exact P -values. Time point effect: **Supplementary data (Appendix B)**. Data is expressed as observed mean \pm SD; $n_{F1} = 14-28$, $n_{F2} = 13-50$, $n_{F3} = 10-51$ samples per group. Birth weight was the average PN1 weight of same-sex litter mates. Body weight at other time points were individual values.

Table 1. Estimated marginal means (emmeans) of sham and IUGR male rat offspring absolute ($\text{g}\cdot\text{day}^{-1}$) and fractional ($\%\cdot\text{day}^{-1}$) growth rates over time in the first (F1), second (F2) and third (F3) generations (paternal line). Absolute growth rate was calculated using the formula: $(\text{body weight at later time point (g)} - \text{body weight at earlier time point (g)}) \div \text{days between two timepoints}$. Fractional growth rate equals $(\text{absolute growth rate (g}\cdot\text{day}^{-1}) \div \text{body weight at earlier time point (g)}) \times 100$. SE: standard error. Degrees-of-freedom method: Kenward-Roger. Confidence level used: 95%. PN: postnatal day, mo: months of age. Significance was determined by a linear mixed-effect model with adjustment for litter size and relatedness of litter siblings (if present). *** $P < 0.001$, ** $P < 0.01$, * $P < 0.05$.

Generation	Absolute growth rate ($\text{g}\cdot\text{day}^{-1}$)	Males				Treatment effect (Sham males vs. IUGR males)	Fractional growth rate ($\%\cdot\text{day}^{-1}$)	Males				Treatment effect (Sham males vs. IUGR males)
		Sham		IUGR				Sham		IUGR		
		Emmean	SE	Emmean	SE			Emmean	SE	Emmean	SE	
F1	PN1 - PN7	1.45	0.10	0.98	0.09	$6.992 \times 10^{-05***}$	PN1 - PN7	24.84	1.38	19.57	1.26	0.002***
	PN7 - PN14	1.83	0.07	1.60	0.06	0.003**	PN7 - PN14	16.25	0.78	20.39	0.69	$1.814 \times 10^{-06***}$
	PN14 - PN35	3.03	0.05	2.78	0.04	$1.318 \times 10^{-05***}$	PN14 - PN35	12.56	0.31	13.62	0.30	0.008***
	PN35 - 2mo	6.38	0.21	4.73	0.22	$0.522 \times 10^{-09***}$	PN35 - 2mo	7.30	0.27	6.18	0.28	0.002**
	2mo - 3mo	2.36	0.18	2.81	0.20	0.050	2mo - 3mo	1.01	0.10	1.47	0.11	0.0002***
	3mo - 4mo	1.54	0.11	1.58	0.10	0.744	3mo - 4mo	0.49	0.03	0.57	0.03	0.051
	4mo - 6mo	0.88	0.05	0.72	0.04	0.007**	4mo - 6mo	0.25	0.01	0.22	0.01	0.110
	6mo - 9mo	0.41	0.04	0.33	0.04	0.139	6mo - 9mo	0.10	0.01	0.09	0.01	0.222
	9mo - 12mo	0.27	0.05	0.21	0.05	0.277	9mo - 12mo	0.06	0.01	0.05	0.01	0.573
F2	PN1 - PN7	1.02	0.08	0.99	0.07	0.653	PN1 - PN7	20.85	1.28	20.92	1.13	0.959
	PN7 - PN14	1.80	0.04	1.81	0.03	0.844	PN7 - PN14	16.67	0.44	16.99	0.39	0.496
	PN14 - PN35	3.18	0.07	3.07	0.06	0.178	PN14 - PN35	13.22	0.20	13.13	0.18	0.618

	PN35 - 2mo	5.39	0.19	5.31	0.21	0.739	PN35 - 2mo	6.03	0.17	5.97	0.16	0.755
	2mo - 4mo	2.17	0.10	2.41	0.11	0.069	2mo - 4mo	0.92	0.07	1.12	0.07	0.0006***
	4mo - 6mo	0.87	0.05	0.85	0.05	0.656	4mo - 6mo	0.25	0.01	0.23	0.01	0.346
	6mo - 9mo	0.50	0.04	0.42	0.04	0.101	6mo - 9mo	0.12	0.01	0.10	0.01	0.104
	9mo - 12mo	0.30	0.05	0.29	0.04	0.861	9mo - 12mo	0.07	0.01	0.07	0.01	0.973
	12mo - 16mo	0.23	0.05	0.22	0.04	0.938	12mo - 16mo	0.05	0.01	0.05	0.01	0.959
F3	PN1 - PN7	1.08	0.04	1.06	0.06	0.746	PN1 - PN7	22.91	1.19	22.46	1.86	0.811
	PN7 - PN14	1.84	0.04	1.85	0.03	0.971	PN7 - PN14	16.66	0.41	16.74	0.38	0.791
	PN14 - PN35	3.02	0.03	2.99	0.03	0.472	PN14 - PN35	12.63	0.22	12.53	0.19	0.598
	PN35 - 2mo	5.27	0.20	5.94	0.19	$5.773 \times 10^{-10}***$	PN35 - 2mo	5.98	0.19	6.82	0.19	$5.27 \times 10^{-08}***$
	2mo - 4mo	2.30	0.10	2.04	0.10	$2.229 \times 10^{-06}***$	2mo - 4mo	1.04	0.07	0.86	0.07	$7.875 \times 10^{-10}***$
	4mo - 6mo	0.85	0.05	0.86	0.05	0.791	4mo - 6mo	0.24	0.02	0.25	0.02	0.689
	6mo - 9mo	0.45	0.05	0.40	0.04	0.174	6mo - 9mo	0.11	0.01	0.10	0.01	0.201
	9mo - 12mo	0.23	0.04	0.25	0.04	0.550	9mo - 12mo	0.05	0.01	0.06	0.01	0.529
	12mo - 16mo	0.13	0.04	0.15	0.04	0.748	12mo - 16mo	0.03	0.01	0.03	0.01	0.648

Table 2. Estimated marginal means (emmeans) of sham and IUGR female rat offspring absolute ($\text{g}\cdot\text{day}^{-1}$) and fractional ($\%\cdot\text{day}^{-1}$) growth rates over time in the second (F2) and third (F3) generations (paternal line) (only male offspring was investigated in the F1 generation). Absolute growth rate was calculated using the formula: $(\text{body weight at later time point (g)} - \text{body weight at earlier time point (g)}) \div \text{days between two timepoints}$. Fractional growth rate equals $(\text{absolute growth rate (g}\cdot\text{day}^{-1}) \div \text{body weight at earlier time point (g)}) \times 100$. SE: standard error. Degrees-of-freedom method: Kenward-Roger. Confidence level used: 95%. PN: postnatal day, mo: months of age. Significance was determined by a linear mixed-effect model with adjustment for litter size and relatedness of litter siblings (if present). *** $P < 0.001$, ** $P < 0.01$, * $P < 0.05$.

Generation	Absolute growth rate ($\text{g}\cdot\text{day}^{-1}$)	Females				Treatment effect (Sham females vs. IUGR females)	Fractional growth rate ($\%\cdot\text{day}^{-1}$)	Females				Treatment effect (Sham females vs. IUGR females)
		Sham		IUGR				Sham		IUGR		
		Emmean	SE	Emmean	SE			Emmean	SE	Emmean	SE	
F2	PN1 - PN7	1.04	0.05	0.95	0.04	0.095	PN1 - PN7	23.11	1.03	21.47	0.95	0.186
	PN7 - PN14	1.72	0.06	1.80	0.05	0.027*	PN7 - PN14	16.10	0.54	17.65	0.50	0.001**
	PN14 - PN35	2.73	0.02	2.64	0.02	0.0003***	PN14 - PN35	11.98	0.30	11.53	0.28	0.031*
	PN35 - 2mo	3.28	0.09	3.51	0.08	0.016*	PN35 - 2mo	4.10	0.12	4.48	0.11	0.002**
	2mo - 4mo	0.99	0.04	0.99	0.04	0.901	2mo - 4mo	0.63	0.03	0.61	0.03	0.641
	4mo - 6mo	0.29	0.02	0.30	0.02	0.669	4mo - 6mo	0.13	0.01	0.13	0.01	0.806
	6mo - 9mo	0.16	0.02	0.14	0.02	0.301	6mo - 9mo	0.07	0.01	0.06	0.01	0.207
	9mo - 12mo	0.07	0.01	0.10	0.02	0.100	9mo - 12mo	0.03	0.01	0.04	0.01	0.086
F3	PN1 - PN7	1.02	0.05	1.05	0.05	0.599	PN1 - PN7	23.02	1.30	23.23	1.48	0.894
	PN7 - PN14	1.75	0.05	1.85	0.05	0.002**	PN7 - PN14	16.61	0.51	17.31	0.50	0.022*
	PN14 - PN35	2.64	0.03	2.62	0.03	0.663	PN14 - PN35	11.70	0.21	11.21	0.20	0.006**
	PN35 - 2mo	3.63	0.12	3.58	0.11	0.598	PN35 - 2mo	4.63	0.17	4.59	0.15	0.807

2mo - 4mo	1.06	0.06	1.06	0.04	0.963	2mo - 4mo	0.64	0.05	0.64	0.04	0.903
4mo - 6mo	0.19	0.04	0.29	0.03	0.023*	4mo - 6mo	0.08	0.02	0.13	0.01	0.027*
6mo - 9mo	0.08	0.01	0.09	0.01	0.194	6mo - 9mo	0.03	0.004	0.04	0.005	0.222
9mo - 12mo	0.08	0.03	0.09	0.03	0.807	9mo - 12mo	0.03	0.01	0.04	0.01	0.842

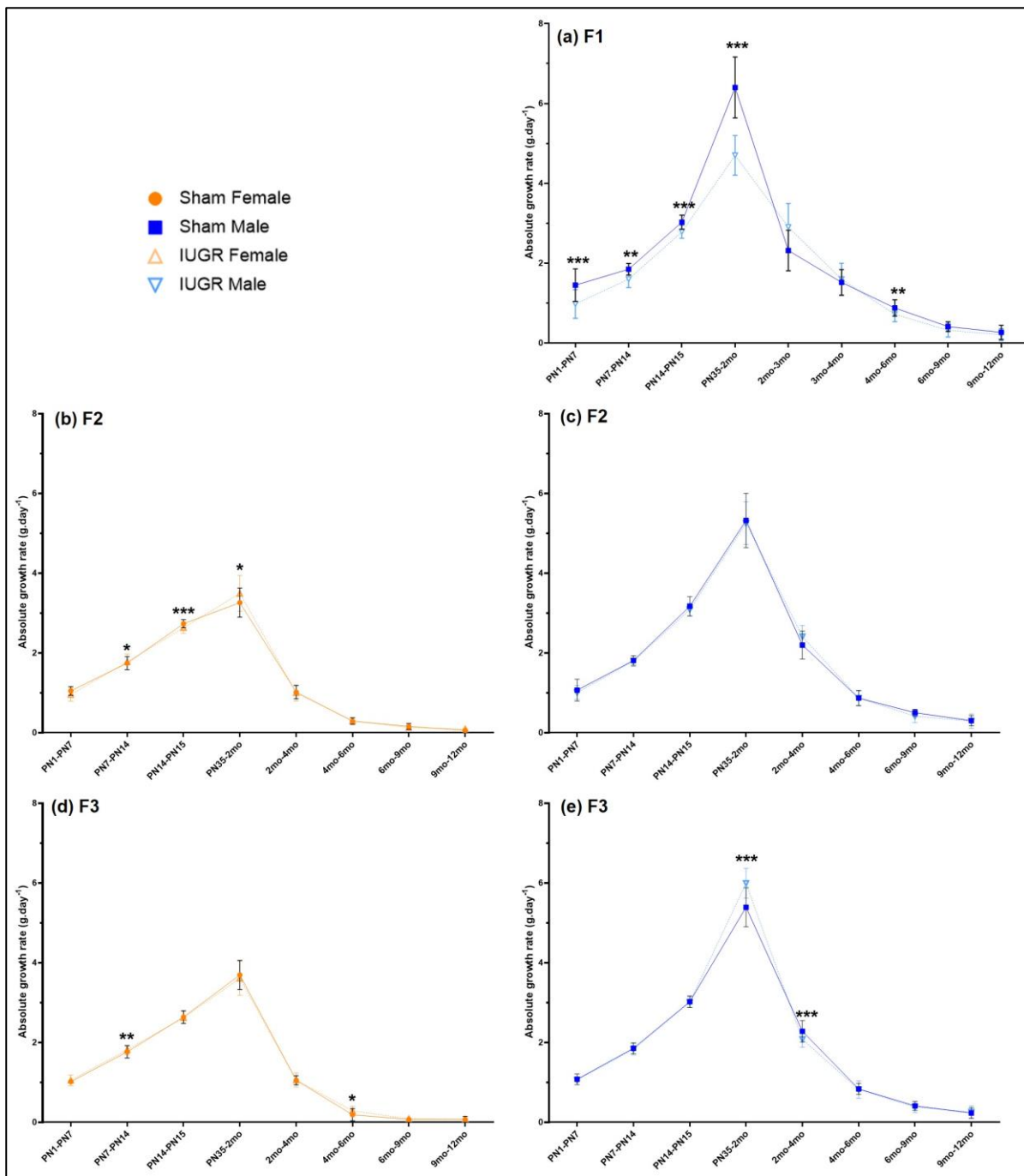


Figure 2. Absolute growth rate from birth (postnatal day (PN) 1) to 12 months of age (12mo) of sham and IUGR rat offspring (paternal line) in the first (F1, a), second (F2, b, c) and third (F3, d, e) generations. Absolute growth rate was calculated using the formula: $(\text{body weight at later time point (g)} - \text{body weight at earlier time point (g)}) \div \text{days between two timepoints}$. Significance was determined by a linear mixed-effect model with adjustment for litter size and relatedness of litter siblings (if present), *** $P < 0.001$, ** $P < 0.01$, * $P < 0.05$. See **Tables 1 and 2** for exact P -values. Data is expressed as observed mean \pm SD; $n = 5-49$ samples per group.

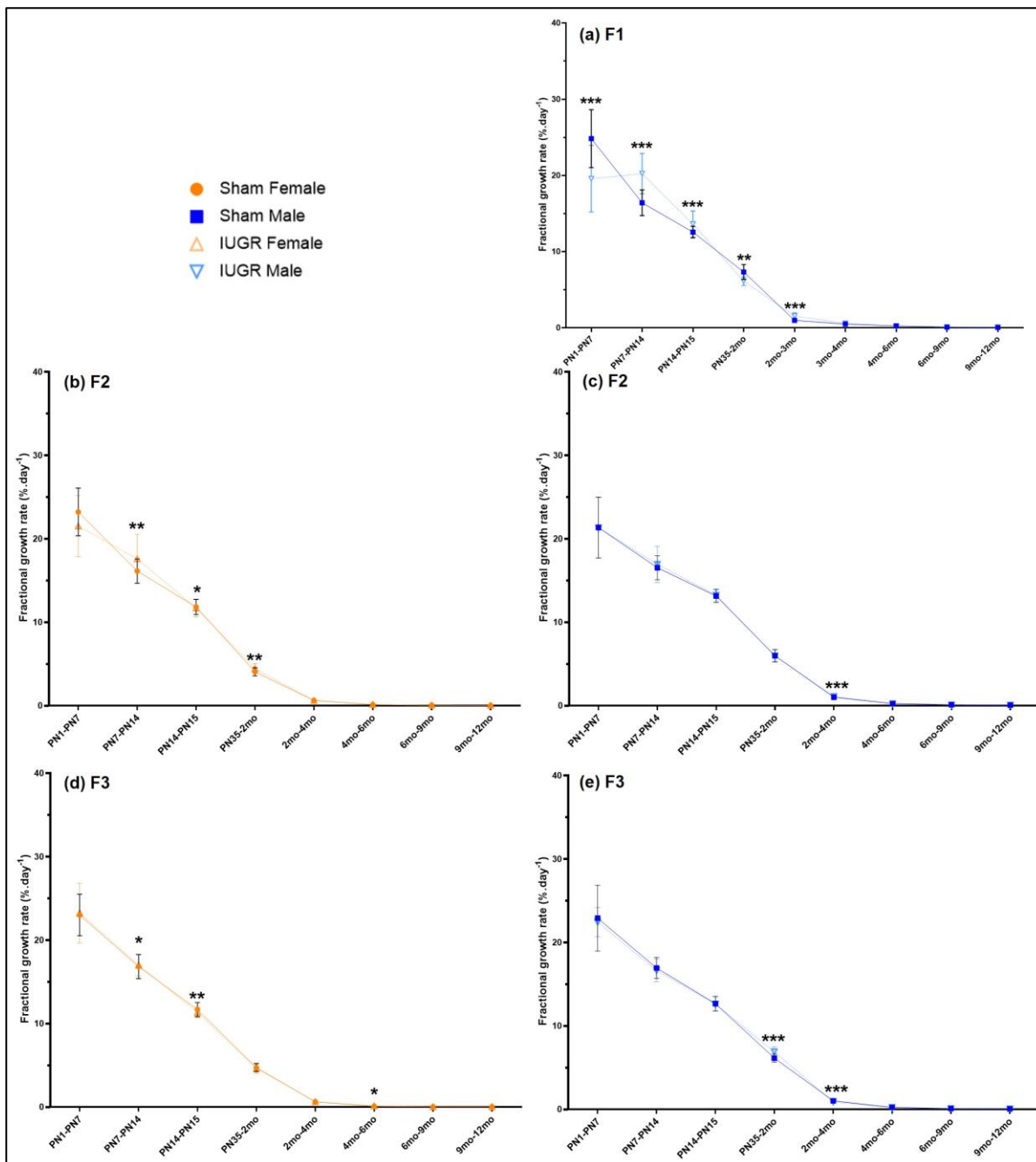


Figure 3. Fractional growth rate from birth (postnatal day (PN) 1) to 12 months of age (12mo) of sham and IUGR rat offspring (paternal line) in the first (F1, a), second (F2, b, c) and third (F3, d, e) generations. Fractional growth rate equals (*absolute growth rate (g·day⁻¹) ÷ body weight at earlier time point (g) × 100*). Significance was determined by a linear mixed-effect model with adjustment for litter size and relatedness of litter siblings (if present), *** $P < 0.001$, ** $P < 0.01$, * $P < 0.05$. See **Tables 1 and 2** for exact P -values. Data is expressed as observed mean \pm SD; $n = 5$ -49 samples per group.

Postmortem organ weights

F1 male offspring at 12mo

Relative weights of some of the F1 IUGR male organs have been previously reported at PN35, 6mo, and 12mo [1, 2, 3]. In this current study, postmortem body weight of F1 IUGR males (435.18 ± 7.38 g) was significantly lower than that of sham males (483.46 ± 8.24 g) ($P < 0.0001$, **Table 3** and **Fig. S1**). These IUGR males also had decreased absolute heart weight (1.37 ± 0.03 g vs. sham 1.51 ± 0.03 g, $P < 0.0001$), left ventricle weight (0.99 ± 0.02 vs. sham 1.14 ± 0.02 , $P < 0.0001$), total kidney weight (2.36 ± 0.06 vs. sham 2.73 ± 0.06 , $P < 0.0001$), and liver weight (10.26 ± 0.26 vs. sham 12.27 ± 0.29 , $P < 0.0001$) (**Table 3** and **Fig. 4a, 4c, 5a, and 5c**, respectively). After adjusting for body weight, only left ventricle weight (-0.02% , $P < 0.0001$) and total kidney weight (-0.04% , $P < 0.0001$) were statistically different between IUGR and sham males at 12 months of age (**Table 3** and **Fig. 4d, 5b**, respectively).

Table 3. Estimated marginal means (emmeans) of sham and IUGR male rat offspring postmortem body weight, absolute organ weights, and organ weights (% body weight) in the first (F1) generation (paternal line), at 12 months of age (12mo). SE: standard error. Degrees-of-freedom method: Kenward-Roger. Confidence level used: 95%. Significance was determined by a linear mixed-effect model with adjustment for litter size and relatedness of litter siblings (if present). *** $P < 0.001$.

Generation	Time point	Weight	Males				Treatment effect (Sham males vs. IUGR males)
			Sham		IUGR		
			Emmean	SE	Emmean	SE	
F1	12mo	Body weight (g)	483.46	8.24	435.18	7.38	< 0.0001***
		Heart (g)	1.51	0.03	1.37	0.03	6.62×10^{-05} ***
		Heart (%)	0.32	0.01	0.31	0.005	0.512
		Left ventricle (g)	1.14	0.02	0.99	0.02	8.14×10^{-10} ***
		Left ventricle (%)	0.24	0.004	0.22	0.004	1.30×10^{-05} ***
		Total kidney (g)	2.73	0.06	2.36	0.06	2.93×10^{-08} ***
		Total kidney (%)	0.57	0.01	0.53	0.01	0.0003***
		Liver (g)	12.27	0.29	10.26	0.26	3.37×10^{-09} ***
		Liver (%)	2.52	0.06	2.40	0.06	0.065

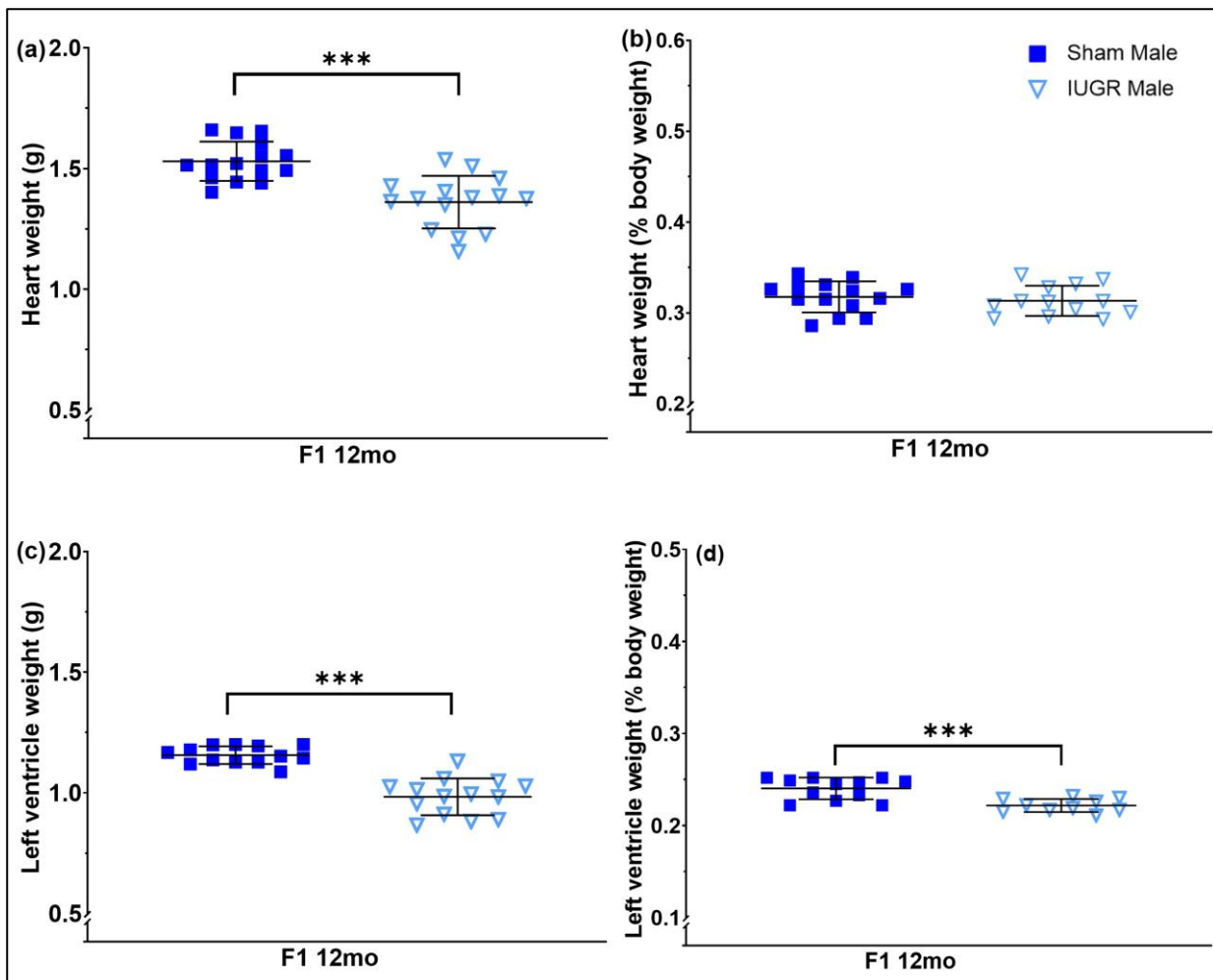


Figure 4. Postmortem heart (a, b) and left ventricle (c, d) weights (absolute vs. % body weight) of sham and IUGR male rat offspring (paternal line) in the first generation (F1), at 12 months of age (12mo). Significance was determined by a linear mixed-effect model with adjustment for litter size and relatedness of litter siblings (if present). *** $P < 0.001$. See **Table 3** for exact P -values. Data is expressed as mean \pm SD; $n = 10-15$ samples per group.

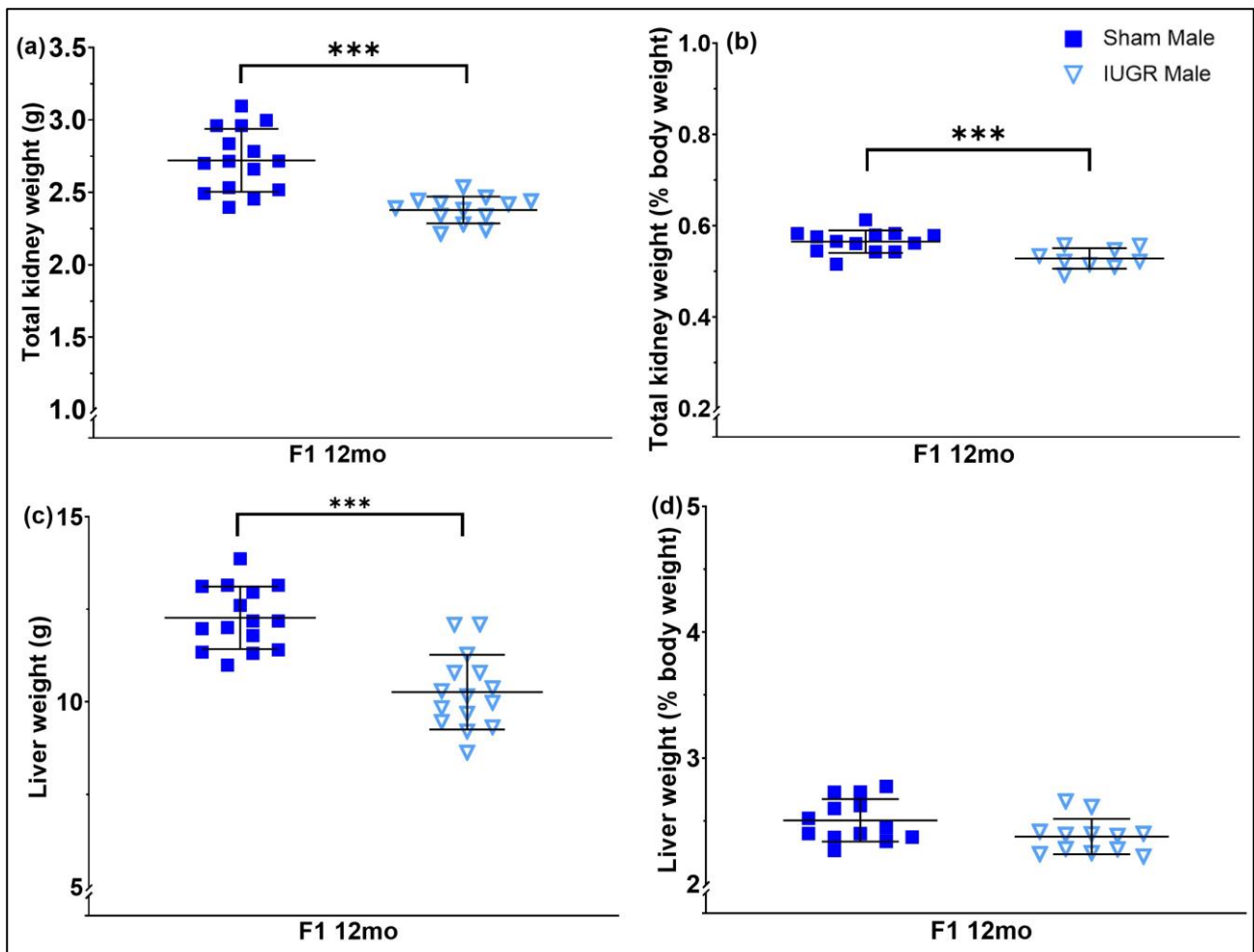


Figure 5. Postmortem total kidney and weights (absolute (a, c) vs. % body weight (b, d)) of sham and IUGR male rat offspring (paternal line) in the first generation (F1), at 12 months of age (12mo). Significance was determined by a linear mixed-effect model with adjustment for litter size and relatedness of litter siblings (if present). *** $P < 0.001$. See **Table 3** for exact P -values. Data is expressed as mean \pm SD; $n = 9$ -15 samples per group.

F2 offspring at PN35, 6mo, and 12mo

F2 postmortem body weight was 6.13% higher in 6mo IUGR males (422.63 ± 8.46 g vs. sham 398.23 ± 8.11 g, $P = 0.021$), but not females ($P = 0.891$) (**Table 4** and **Fig. S2b**). There was no difference in postmortem body weight between sham and IUGR group at PN35 and 12mo, in either sex (**Table 4** and **Fig. S2a, S2c**). Absolute and relative (% body weight) weights of heart and left ventricle was similar between sham and IUGR at all time points, in both males and females (**Table 4** and **Fig. 6a-f, Fig. 7a-f**). Meanwhile, at 6mo, IUGR males had significantly higher absolute total kidney weight (2.43 ± 0.07 g vs. sham 2.18 ± 0.08 g) and total adrenal gland weight (0.05 ± 0.002 vs. sham 0.04 ± 0.002) ($P = 0.002$, **Table 4, Fig. 8c**, and $P = 0.005$, **Table 4, Fig. 9c**, respectively). Only relative total kidney weight (% body weight) was significant at 6mo ($+0.02\%$, $P = 0.030$, **Table 4** and **Fig. 8d**). Regarding liver weights, F2 IUGR females showed a decrease in liver weight (% body weight) compared to sham at PN35 (-0.18% , $P = 0.004$, **Table 4** and **Fig. 10b**), while F2 IUGR males had a decrease at 12mo (-0.10% , $P = 0.014$, **Table 4** and **Fig. 10f**). In addition to this, F2 PN35 IUGR females also had lower absolute (0.25 ± 0.01 g vs. sham 0.28 ± 0.01 g, $P = 0.002$, **Table 4** and **Fig. 11a**) and relative (-0.05% , $P = 0.0008$, **Table 4** and **Fig. 11b**) pancreas weight.

Table 4. Estimated marginal means (emmeans) of sham and IUGR rat offspring postmortem body weight, absolute organ weights, and organ weights (% body weight) in the second (F2) generation (paternal line), at postnatal day 35 (PN35), 6 (6mo) and 12 (12mo) months of age. SE: standard error. Degrees-of-freedom method: Kenward-Roger. Confidence level used: 95%. Significance was determined by a linear mixed-effect model with adjustment for litter size and relatedness of litter siblings (if present). *** $P < 0.001$, ** $P < 0.01$, * $P < 0.05$.

Generation	Time point	Weight	Males				Treatment effect (Sham males vs. IUGR males)	Females				Treatment effect (Sham females vs. IUGR females)
			Sham		IUGR			Sham		IUGR		
			Emmean	SE	Emmean	SE		Emmean	SE	Emmean	SE	
F2	PN35	Body weight (g)	85.22	3.02	87.62	2.49	0.420	78.31	1.91	77.46	1.58	0.656
		Heart (g)	0.37	0.02	0.38	0.02	0.355	0.34	0.01	0.33	0.01	0.430
		Heart (%)	0.43	0.01	0.43	0.01	0.815	0.43	0.01	0.43	0.01	0.505
		Left ventricle (g)	0.25	0.01	0.26	0.01	0.369	0.23	0.01	0.23	0.01	0.759
		Left ventricle (%)	0.29	0.004	0.29	0.003	0.323	0.29	0.01	0.29	0.01	0.816
		Total kidney (g)	0.67	0.03	0.72	0.02	0.054	0.64	0.02	0.62	0.02	0.353
		Total kidney (%)	0.80	0.01	0.83	0.01	0.120	0.82	0.01	0.80	0.01	0.333
		Adrenal gland (g)	0.02	0.001	0.02	0.001	1	0.02	0.001	0.02	0.001	0.414
		Adrenal gland (%)	0.02	0.001	0.02	0.001	0.800	0.02	0.001	0.02	0.001	0.220
		Liver (g)	3.07	0.13	3.20	0.10	0.337	3.05	0.10	2.87	0.09	0.117
		Liver (%)	3.61	0.10	3.68	0.08	0.556	3.81	0.06	3.63	0.05	0.004**
		Pancreas (g)	0.26	0.02	0.25	0.01	0.551	0.28	0.01	0.25	0.01	0.002**
	Pancreas (%)	0.31	0.02	0.28	0.01	0.140	0.36	0.01	0.31	0.01	0.0008***	
	6mo	Body weight (g)	398.23	8.11	422.63	8.46	0.021*	254.44	2.54	254.01	2.38	0.891
Heart (g)		1.37	0.03	1.39	0.03	0.606	0.99	0.01	0.97	0.01	0.168	

		Heart (%)	0.34	0.01	0.33	0.01	0.334	0.39	0.01	0.38	0.01	0.052
		Left ventricle (g)	1.02	0.03	1.03	0.03	0.895	0.73	0.02	0.70	0.02	0.085
		Left ventricle (%)	0.26	0.01	0.24	0.01	0.077	0.28	0.01	0.28	0.01	0.286
		Total kidney (g)	2.18	0.08	2.43	0.07	0.0002***	1.65	0.04	1.59	0.04	0.214
		Total kidney (%)	0.57	0.01	0.59	0.01	0.030*	0.65	0.01	0.63	0.01	0.112
		Adrenal gland (g)	0.04	0.002	0.05	0.002	0.005**	0.07	0.002	0.07	0.003	0.169
		Adrenal gland (%)	0.01	0.0004	0.01	0.0004	0.661	0.03	0.001	0.03	0.001	0.143
		Liver (g)	11.01	0.34	11.31	0.33	0.479	7.75	0.18	8.07	0.18	0.174
		Liver (%)	2.76	0.05	2.73	0.06	0.635	3.06	0.06	3.07	0.06	0.980
		Pancreas (g)	1.11	0.07	1.15	0.07	0.709	1.03	0.04	1.03	0.04	0.906
		Pancreas (%)	0.28	0.02	0.28	0.02	0.921	0.40	0.01	0.42	0.01	0.168
	12mo	Body weight (g)	475.85	5.44	466.07	5.49	0.088	266.51	3.75	264.81	3.44	0.690
		Heart (g)	1.55	0.03	1.54	0.03	0.826	1.04	0.02	1.03	0.02	0.762
		Heart (%)	0.33	0.01	0.33	0.01	0.497	0.40	0.01	0.38	0.01	0.100
		Left ventricle (g)	1.20	0.02	1.20	0.03	0.968	0.81	0.02	0.83	0.02	0.535
		Left ventricle (%)	0.26	0.01	0.26	0.01	0.923	0.31	0.01	0.31	0.01	0.365
		Total kidney (g)	2.70	0.08	2.60	0.09	0.319	1.63	0.03	1.67	0.03	0.243
		Total kidney (%)	0.57	0.02	0.55	0.02	0.507	0.63	0.01	0.61	0.01	0.179
		Adrenal gland (g)	0.04	0.002	0.04	0.002	0.171	0.06	0.003	0.07	0.004	0.489
		Adrenal gland (%)	0.01	0.0003	0.01	0.0003	0.356	0.03	0.001	0.02	0.001	0.785
		Liver (g)	12.48	0.33	11.98	0.37	0.140	7.94	0.16	8.03	0.19	0.697
		Liver (%)	2.70	0.03	2.60	0.04	0.014*	2.98	0.05	2.96	0.04	0.704
		Pancreas (g)	1.32	0.07	1.23	0.08	0.315	1.01	0.03	1.04	0.03	0.359
		Pancreas (%)	0.28	0.01	0.26	0.01	0.128	0.39	0.01	0.38	0.01	0.598

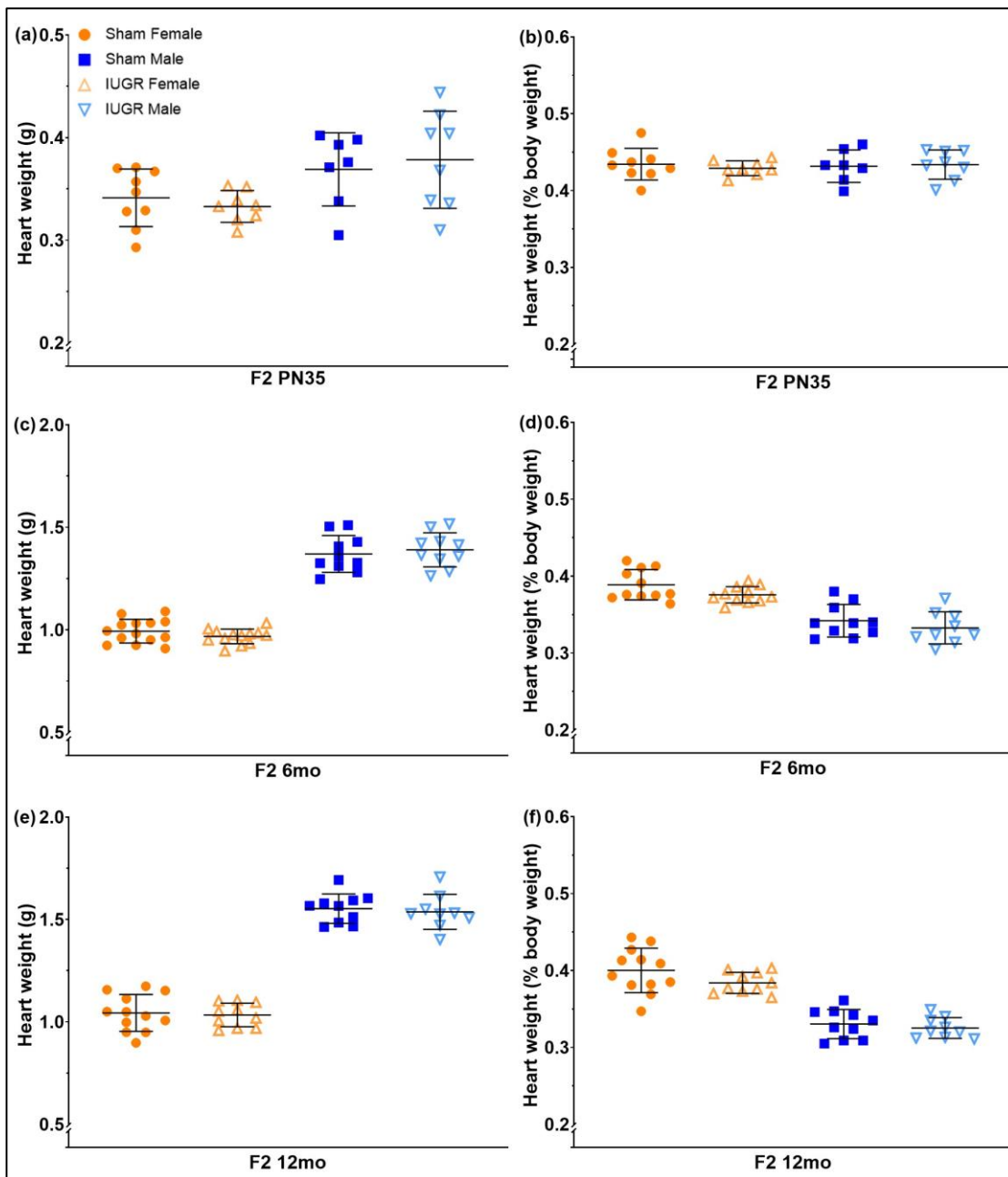


Figure 6. Postmortem heart weights (absolute vs. % body weight) of sham and IUGR rat offspring (paternal line) in the second generation (F2), at postnatal day 35 (PN35; a, b), 6 (6mo; c,d) and 12 (12mo; e, f) months of age. Significance was determined by a linear mixed-effect model with adjustment for litter size and relatedness of litter siblings (if present). See **Table 4** for exact *P*-values. Data is expressed as mean \pm SD; $n = 7$ -14 samples per group.

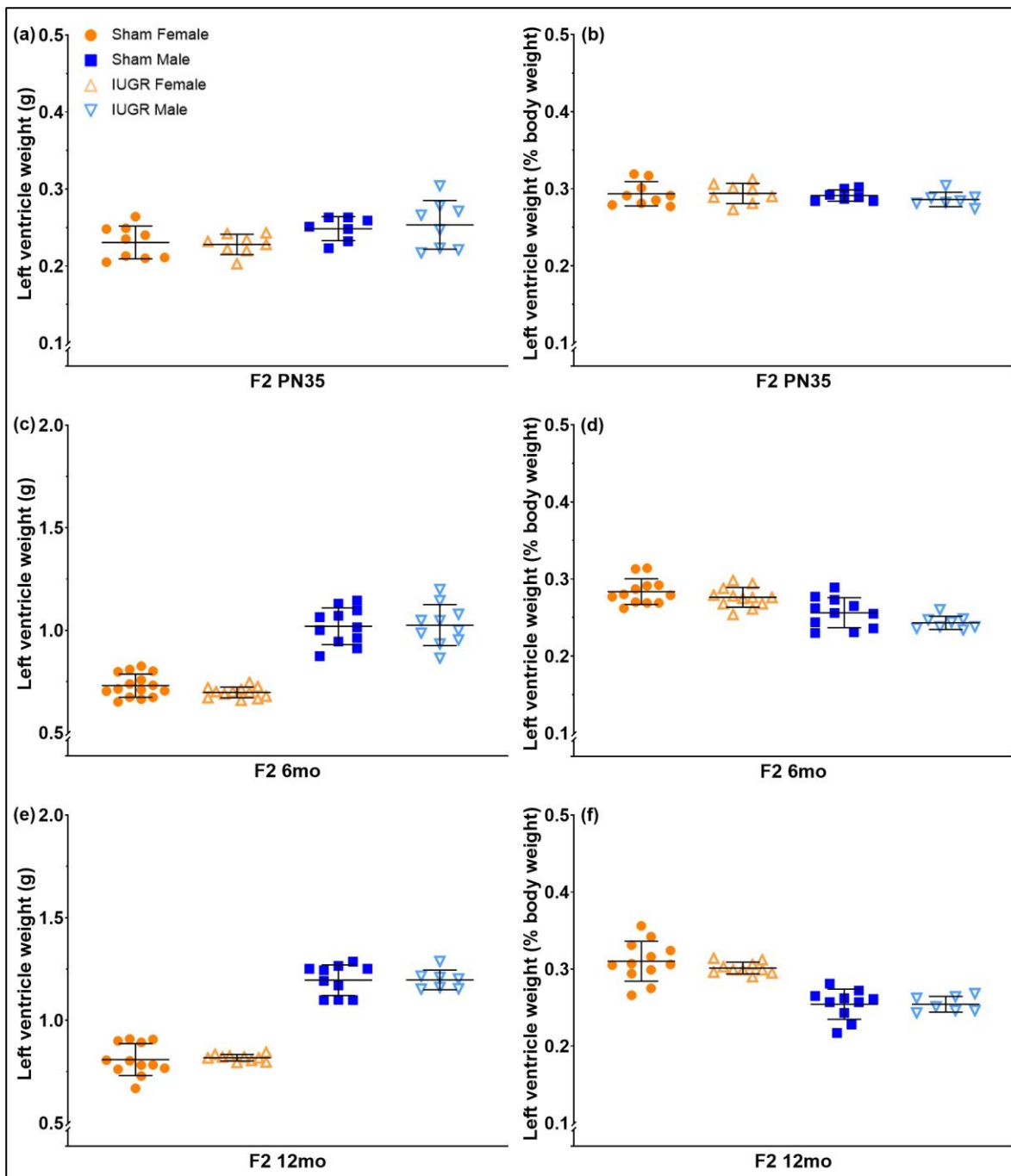


Figure 7. Postmortem left ventricle weights (absolute vs. % body weight) of sham and IUGR rat offspring (paternal line) in the second generation (F2), at postnatal day 35 (PN35; a, b), 6 (6mo; c,d) and 12 (12mo; e, f) months of age. Significance was determined by a linear mixed-effect model with adjustment for litter size and relatedness of litter siblings (if present). See **Table 4** for exact *P*-values. Data is expressed as mean \pm SD; $n = 7$ -15 samples per group.

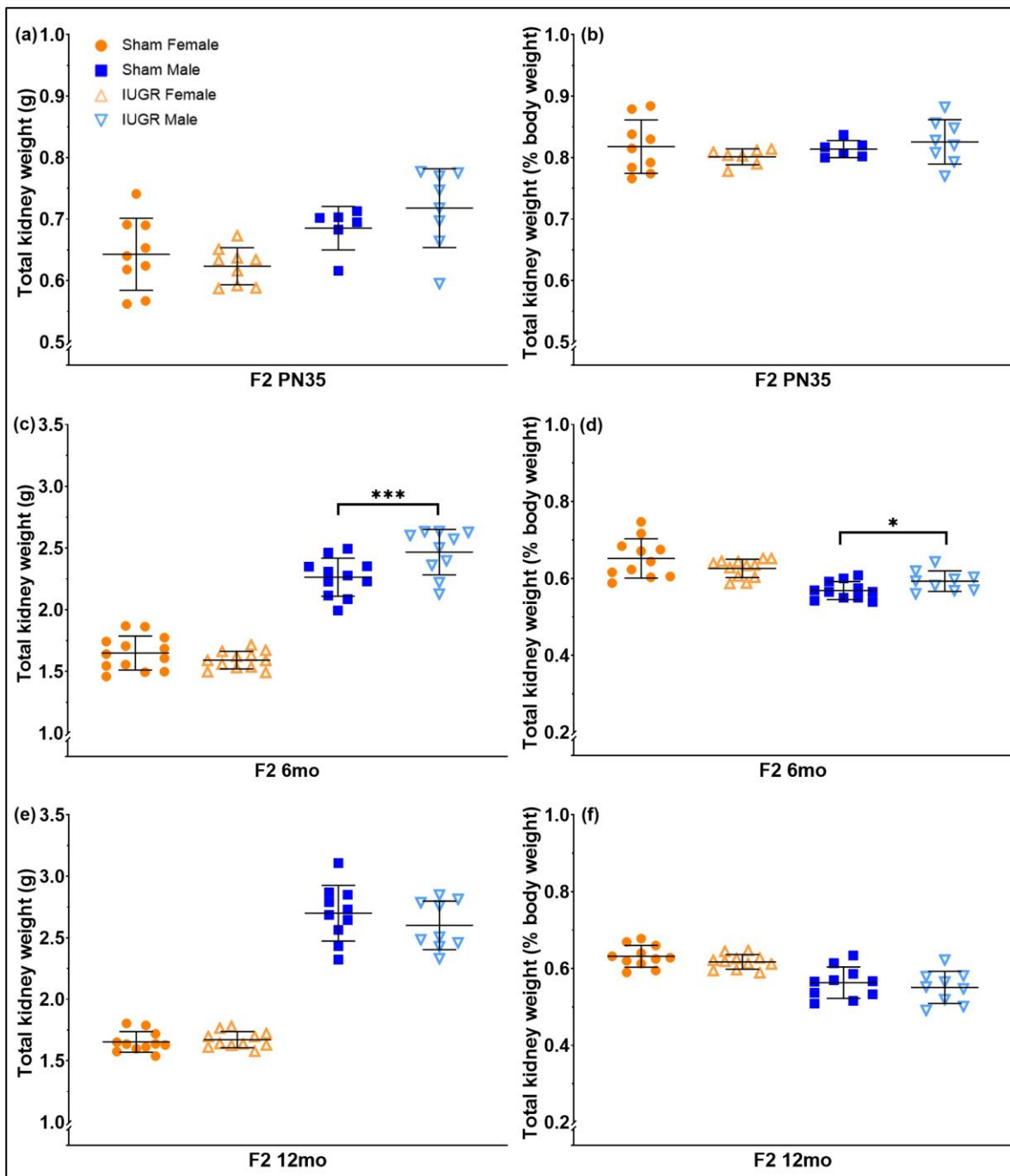


Figure 8. Postmortem total kidney weights (absolute vs. % body weight) of sham and IUGR rat offspring (paternal line) in the second generation (F2), at postnatal day 35 (PN35; a, b), 6 (6mo; c,d) and 12 (12mo; e, f) months of age. Significance was determined by a linear mixed-effect model with adjustment for litter size and relatedness of litter siblings (if present). *** $P < 0.001$, * $P < 0.05$. See **Table 4** for exact P -values. Data is expressed as mean \pm SD; $n = 6$ -13 samples per group.

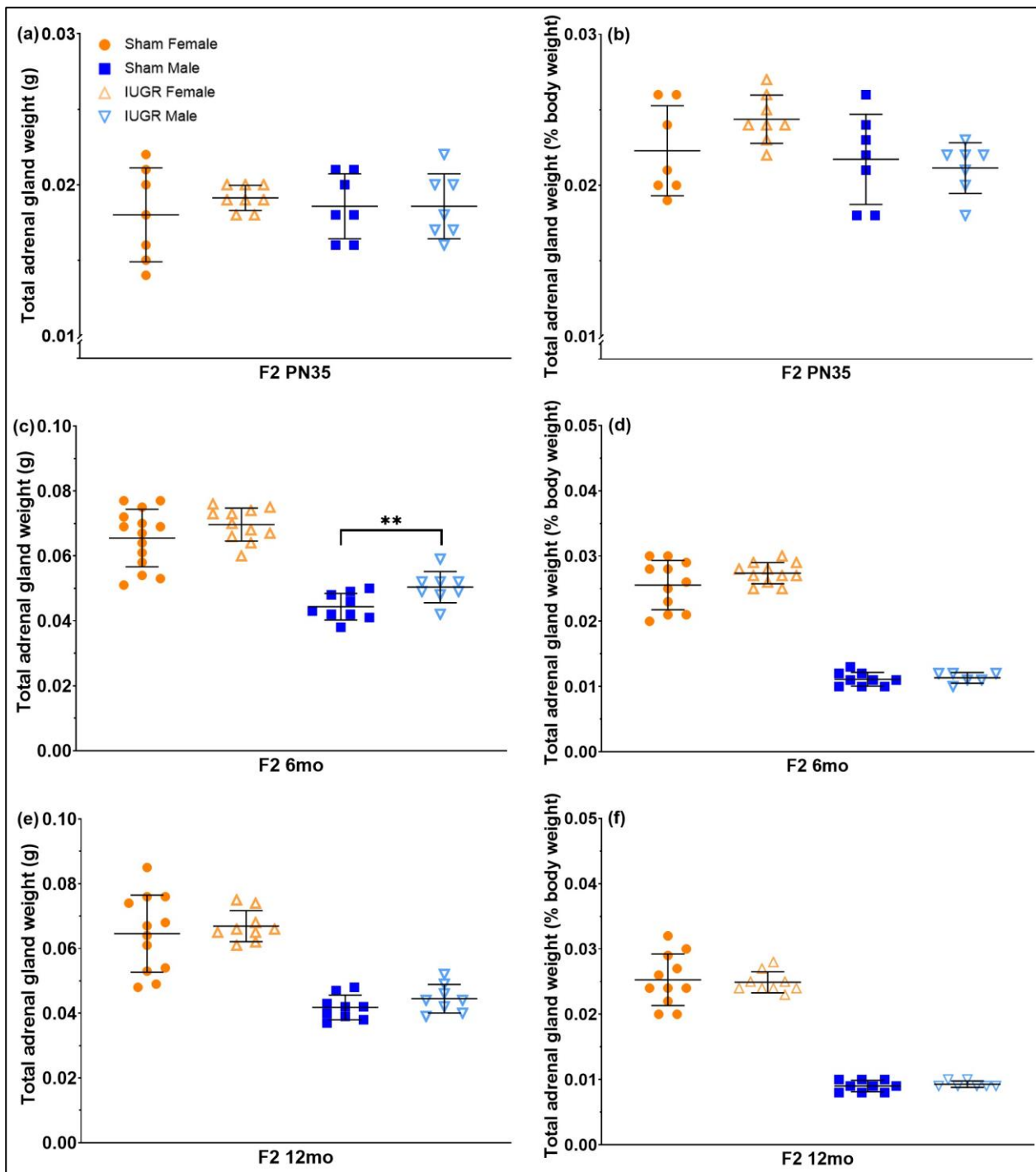


Figure 9. Postmortem total adrenal gland weights (absolute vs. % body weight) of sham and IUGR rat offspring (paternal line) in the second generation (F2), at postnatal day 35 (PN35; a, b), 6 (6mo; c, d) and 12 (12mo; e, f) months of age. Significance was determined by a linear mixed-effect model with adjustment for litter size and relatedness of litter siblings (if present). ** $P < 0.01$. See **Table 4** for exact P -values. Data is expressed as mean \pm SD; $n = 6$ -14 samples per group.

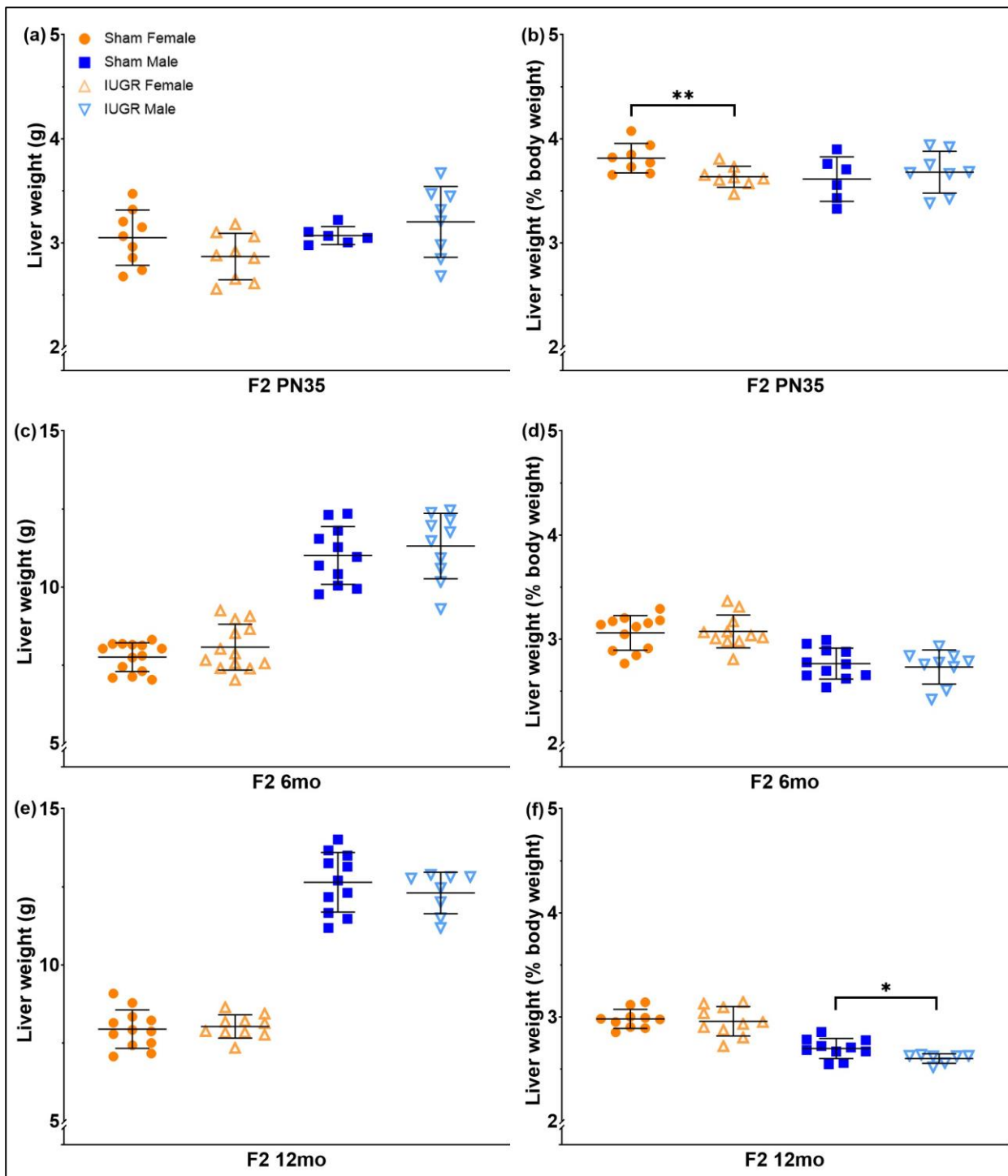


Figure 10. Postmortem liver weights (absolute vs. % body weight) of sham and IUGR rat offspring (paternal line) in the second generation (F2), at postnatal day 35 (PN35; a, b), 6 (6mo; c,d) and 12 (12mo; e, f) months of age. Significance was determined by a linear mixed-effect model with adjustment for litter size and relatedness of litter siblings (if present). ** $P < 0.01$, * $P < 0.05$. See **Table 4** for exact P -values. Data is expressed as mean \pm SD; $n = 6$ -14 samples per group.

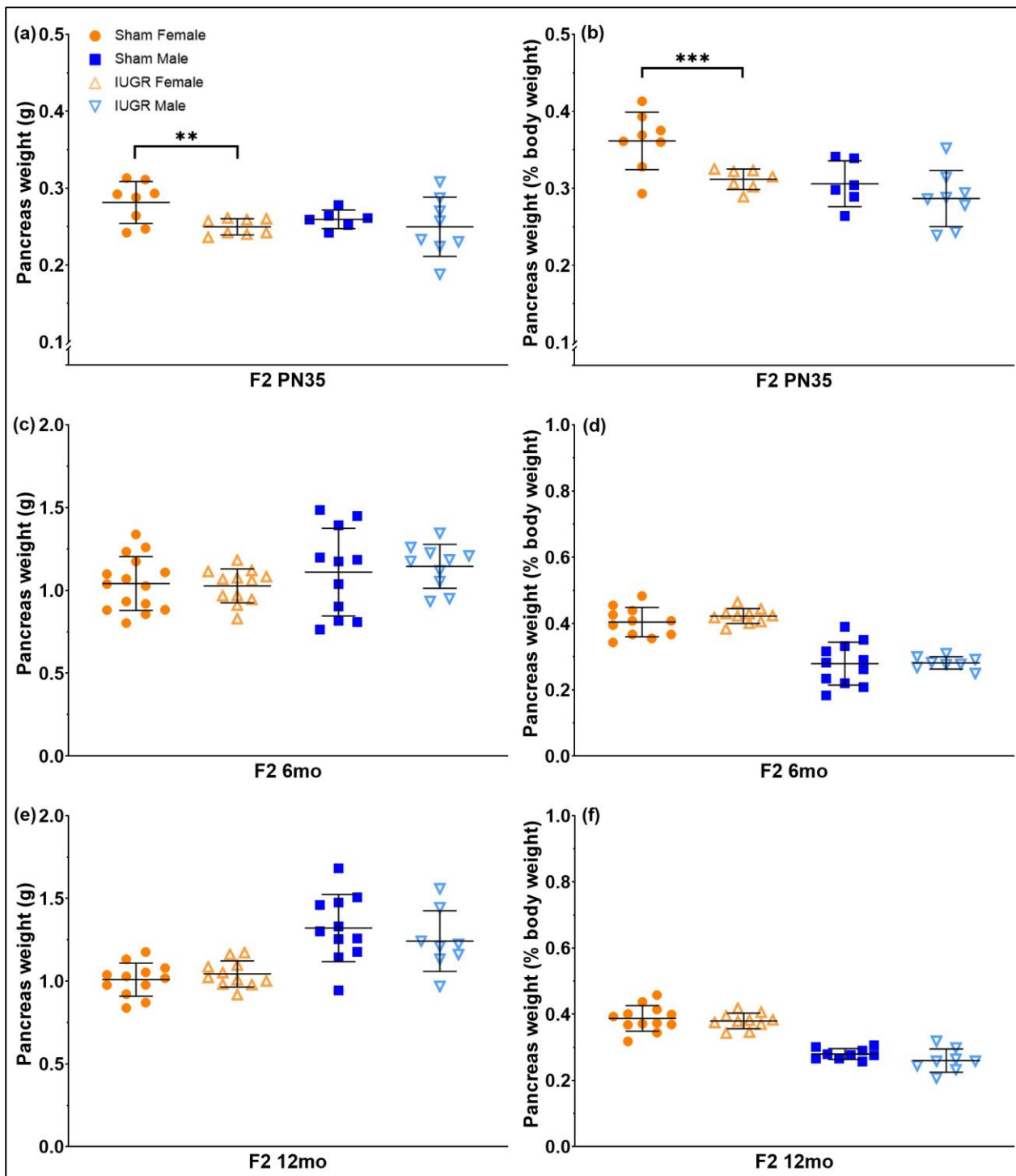


Figure 11. Postmortem pancreas weights (absolute vs. % body weight) of sham and IUGR rat offspring (paternal line) in the second generation (F2), at postnatal day 35 (PN35; a, b), 6 (6mo; c,d) and 12 (12mo; e, f) months of age. Significance was determined by a linear mixed-effect model with adjustment for litter size and relatedness of litter siblings (if present). *** $P < 0.001$, ** $P < 0.01$. See **Table 4** for exact P -values. Data is expressed as mean \pm SD; n = 6-15 samples per group.

F3 offspring at PN35, 6mo, and 12mo

F3 offspring postmortem body weight was significantly higher in IUGR males, only at PN35 (+6.87%, IUGR 87.34 ± 1.95 g vs. sham 81.72 ± 1.96 g, $P = 0.013$, **Table 5** and **Fig. S2d**). Heart weight (% body weight) was not significantly different between F3 PN35 sham and IUGR offspring (males $P = 0.811$, females $P = 0.492$, **Table 5** and **Fig. S3a, S3b**). On the other hand, PN35 IUGR females had reduced relative left ventricle weight (-0.02%, $P = 0.035$, **Fig. 12b**), and increased relative total kidney weight (+0.03%, $P = 0.007$, **Fig. 13b**) compared to sham animals (**Table 5**). A change to the relative weight of these two tissues was also observed in F3 6mo IUGR females (+0.06% in relative left ventricle weight ($P < 0.0001$, **Table 5** and **Fig. 12d**), and -0.02% in relative total kidney weight ($P = 0.027$, **Table 5** and **Fig. 13d**)). However, total adrenal gland weight was not altered at any time point in the F3 generation (**Table 5** and **Fig. S4a-f**). At 12mo, increased heart and left ventricle weight (% body weight) was found only in the IUGR male offspring (+0.01%, $P = 0.012$, **Table 5** and **Fig. S3f**, and +0.03%, $P = 0.0003$, **Table 5** and **Fig. 12f**, respectively). Meanwhile, 12mo IUGR females had increased relative liver weight compared to sham females (+0.26%, $P < 0.0001$, **Table 5** and **Fig. 14f**). Regarding pancreas weight (% body weight), F3 IUGR males had a 0.06% increase compared to the sham group ($P = 0.006$, **Table 5**), only at PN35 time point (**Fig. 15b**).

Table 5. Estimated marginal means (emmeans) of sham and IUGR rat offspring postmortem body weight, absolute organ weights, and organ weights (% body weight) in the third (F3) generation (paternal line), at postnatal day 35 (PN35), 6 (6mo) and 12 (12mo) months of age. SE: standard error. Degrees-of-freedom method: Kenward-Roger. Confidence level used: 95%. Significance was determined by a linear mixed-effect model with adjustment for litter size and relatedness of litter siblings (if present). *** $P < 0.001$, ** $P < 0.01$, * $P < 0.05$.

Generation	Time point	Weight	Males				Treatment effect (Sham males vs. IUGR males)	Females				Treatment effect (Sham females vs. IUGR females)
			Sham		IUGR			Sham		IUGR		
			Emmean	SE	Emmean	SE		Emmean	SE	Emmean	SE	
F3	PN35	Body weight (g)	81.72	1.96	87.34	1.95	0.013*	75.81	1.76	77.87	1.93	0.368
		Heart (g)	0.37	0.01	0.39	0.01	0.083	0.35	0.01	0.35	0.01	0.656
		Heart (%)	0.45	0.01	0.45	0.01	0.811	0.46	0.01	0.45	0.01	0.492
		Left ventricle (g)	0.25	0.01	0.27	0.01	0.227	0.24	0.01	0.24	0.01	0.506
		Left ventricle (%)	0.31	0.01	0.31	0.01	0.717	0.32	0.01	0.30	0.01	0.035*
		Total kidney (g)	0.72	0.03	0.72	0.02	0.853	0.62	0.02	0.66	0.02	0.037*
		Total kidney (%)	0.87	0.01	0.84	0.01	0.111	0.81	0.01	0.84	0.01	0.007**
		Adrenal gland (g)	0.02	0.001	0.02	0.001	0.913	0.02	0.001	0.02	0.001	0.124
		Adrenal gland (%)	0.02	0.001	0.02	0.001	0.985	0.02	0.001	0.02	0.001	0.272
		Liver (g)	3.13	0.13	3.25	0.13	0.422	2.87	0.11	3.13	0.12	0.064
		Liver (%)	3.79	0.09	3.80	0.11	0.878	3.83	0.14	4.03	0.13	0.110
		Pancreas (g)	0.26	0.02	0.29	0.02	0.110	0.27	0.01	0.25	0.01	0.256
	Pancreas (%)	0.29	0.03	0.35	0.02	0.006**	0.36	0.01	0.32	0.02	0.067	
	6mo	Body weight (g)	423.53	4.72	423.83	5.32	0.960	256.38	5.00	261.02	4.36	0.416
Heart (g)		1.41	0.02	1.40	0.02	0.851	0.91	0.03	0.97	0.03	0.126	

		Heart (%)	0.33	0.01	0.33	0.01	0.848	0.36	0.01	0.36	0.01	0.945
		Left ventricle (g)	1.03	0.02	1.06	0.02	0.247	0.71	0.02	0.73	0.02	0.605
		Left ventricle (%)	0.24	0.005	0.25	0.01	0.245	0.28	0.01	0.34	0.01	< 0.0001***
		Total kidney (g)	2.38	0.02	2.40	0.02	0.293	1.57	0.03	1.54	0.02	0.256
		Total kidney (%)	0.56	0.01	0.56	0.01	0.705	0.61	0.01	0.59	0.01	0.027*
		Adrenal gland (g)	0.04	0.001	0.04	0.001	0.518	0.07	0.002	0.07	0.002	0.757
		Adrenal gland (%)	0.01	0.0004	0.01	0.0005	0.738	0.03	0.001	0.03	0.0005	0.291
		Liver (g)	12.17	0.25	12.05	0.30	0.699	8.11	0.20	8.29	0.17	0.401
		Liver (%)	2.86	0.05	2.84	0.06	0.753	3.18	0.09	3.15	0.08	0.756
		Pancreas (g)	1.23	0.08	1.17	0.09	0.545	1.10	0.07	1.03	0.06	0.238
		Pancreas (%)	0.29	0.02	0.29	0.02	0.887	0.43	0.02	0.39	0.02	0.113
	12mo	Body weight (g)	475.85	5.44	466.07	5.49	0.088	266.51	3.75	264.81	3.44	0.690
		Heart (g)	1.45	0.03	1.52	0.03	0.060	0.98	0.02	0.98	0.02	0.889
		Heart (%)	0.31	0.01	0.32	0.01	0.012*	0.37	0.01	0.37	0.01	0.784
		Left ventricle (g)	1.06	0.04	1.20	0.04	0.003**	0.75	0.02	0.75	0.02	0.934
		Left ventricle (%)	0.23	0.01	0.26	0.01	0.0003***	0.28	0.01	0.28	0.01	0.516
		Total kidney (g)	2.55	0.06	2.63	0.05	0.197	1.64	0.03	1.65	0.03	0.865
		Total kidney (%)	0.54	0.01	0.55	0.01	0.124	0.62	0.01	0.62	0.01	0.875
		Adrenal gland (g)	0.04	0.002	0.04	0.001	0.300	0.06	0.003	0.06	0.003	0.416
		Adrenal gland (%)	0.01	0.0001	0.01	0.0001	0.358	0.02	0.001	0.02	0.001	0.479
		Liver (g)	12.44	0.36	12.67	0.37	0.588	7.61	0.17	8.18	0.15	0.002**
		Liver (%)	2.61	0.04	2.64	0.04	0.618	2.85	0.04	3.11	0.04	< 0.0001***
		Pancreas (g)	1.25	0.06	1.20	0.06	0.472	0.97	0.06	0.98	0.05	0.845
	Pancreas (%)	0.26	0.01	0.25	0.01	0.232	0.37	0.02	0.37	0.02	0.782	

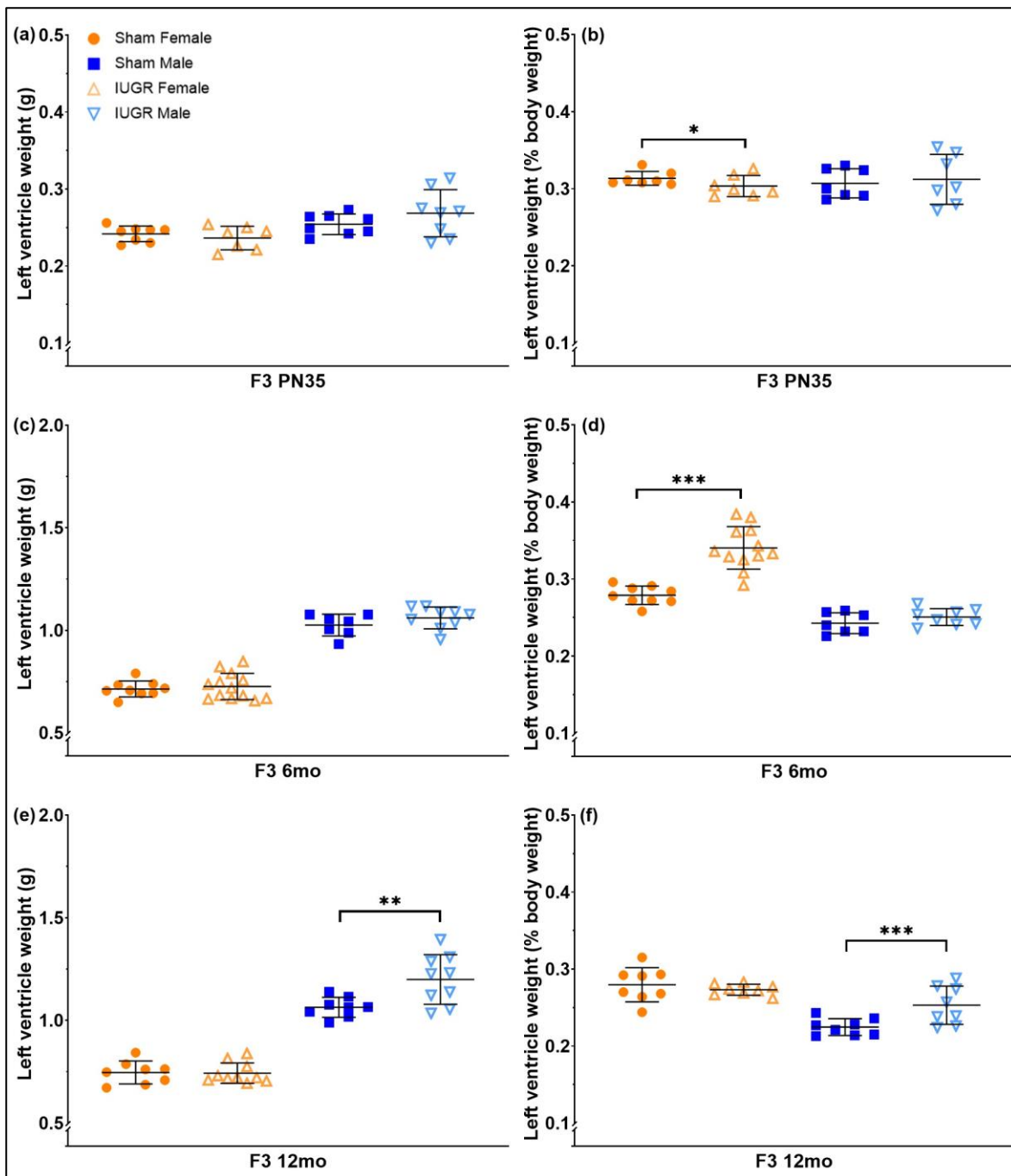


Figure 12. Postmortem left ventricle weights (absolute vs. % body weight) of sham and IUGR rat offspring (paternal line) in the third generation (F3), at postnatal day 35 (PN35; a, b), 6 (6mo; c,d) and 12 (12mo; e, f) months of age. Significance was determined by a linear mixed-effect model with adjustment for litter size and relatedness of litter siblings (if present). *** $P < 0.001$, ** $P < 0.01$, * $P < 0.05$. See **Table 5** for exact P -values. Data is expressed as mean \pm SD; $n = 7$ -13 samples per group.

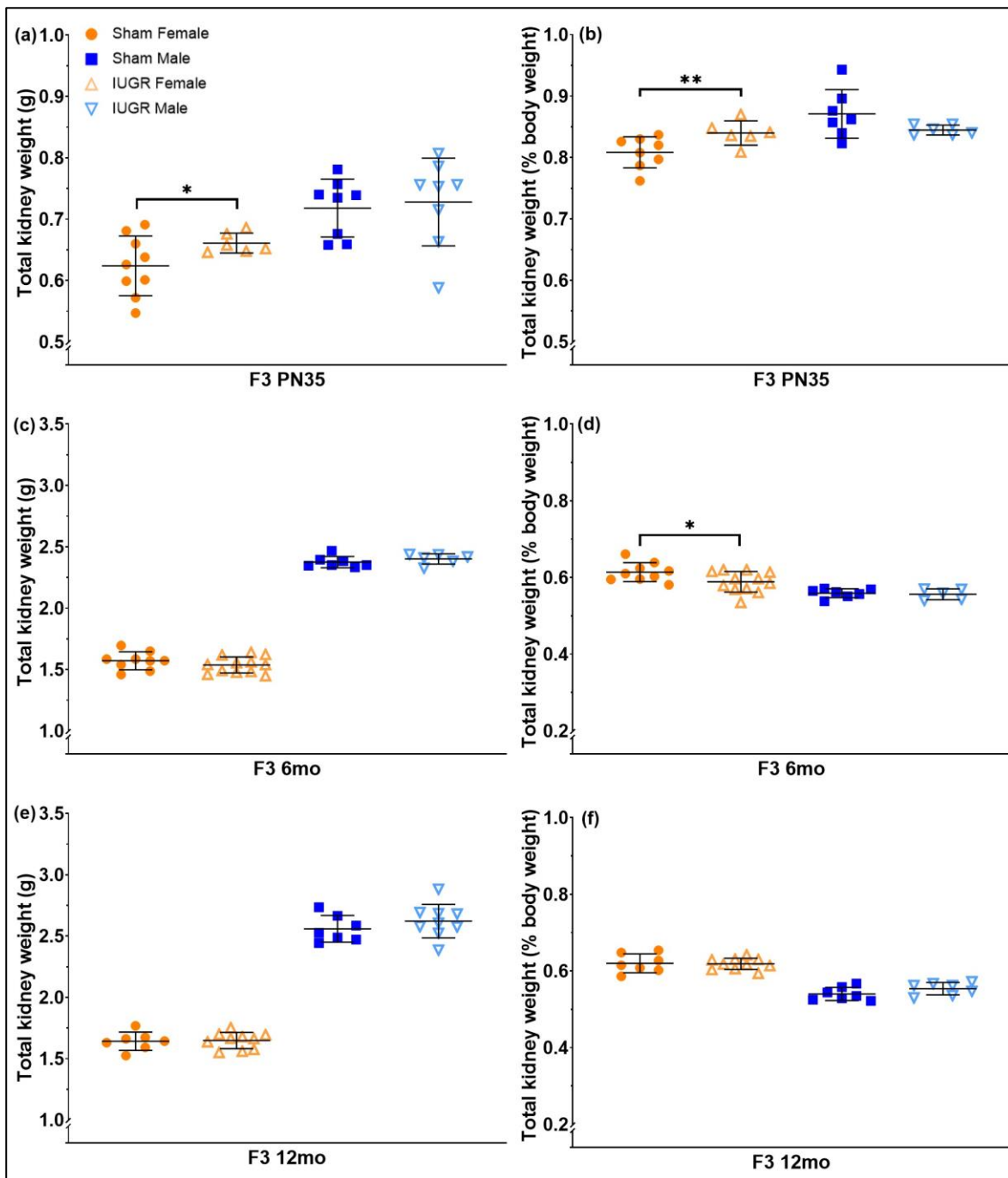


Figure 13. Postmortem total kidney weights (absolute vs. % body weight) of sham and IUGR rat offspring (paternal line) in the third generation (F3), at postnatal day 35 (PN35; a, b), 6 (6mo; c,d) and 12 (12mo; e, f) months of age. Significance was determined by a linear mixed-effect model with adjustment for litter size and relatedness of litter siblings (if present). ** $P < 0.01$, * $P < 0.05$. See **Table 5** for exact P -values. Data is expressed as mean \pm SD; $n = 6$ -12 samples per group.

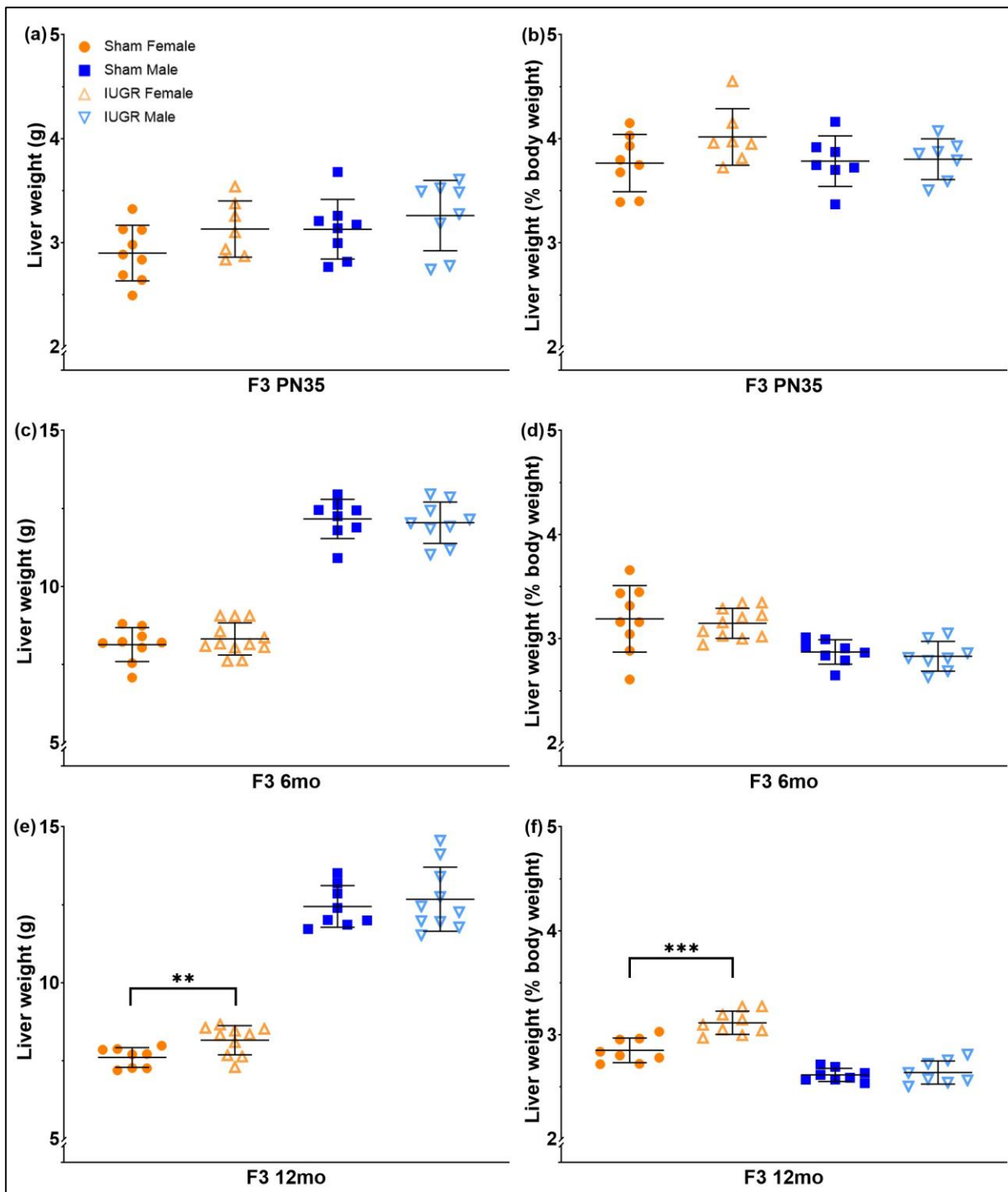


Figure 14. Postmortem liver weights (absolute vs. % body weight) of sham and IUGR rat offspring (paternal line) in the third generation (F3), at postnatal day 35 (PN35; a, b), 6 (6mo; c,d) and 12 (12mo; e, f) months of age. Significance was determined by a linear mixed-effect model with adjustment for litter size and relatedness of litter siblings (if present). *** $P < 0.001$, ** $P < 0.01$. See **Table 5** for exact P -values. Data is expressed as mean \pm SD; $n = 7$ -12 samples per group.

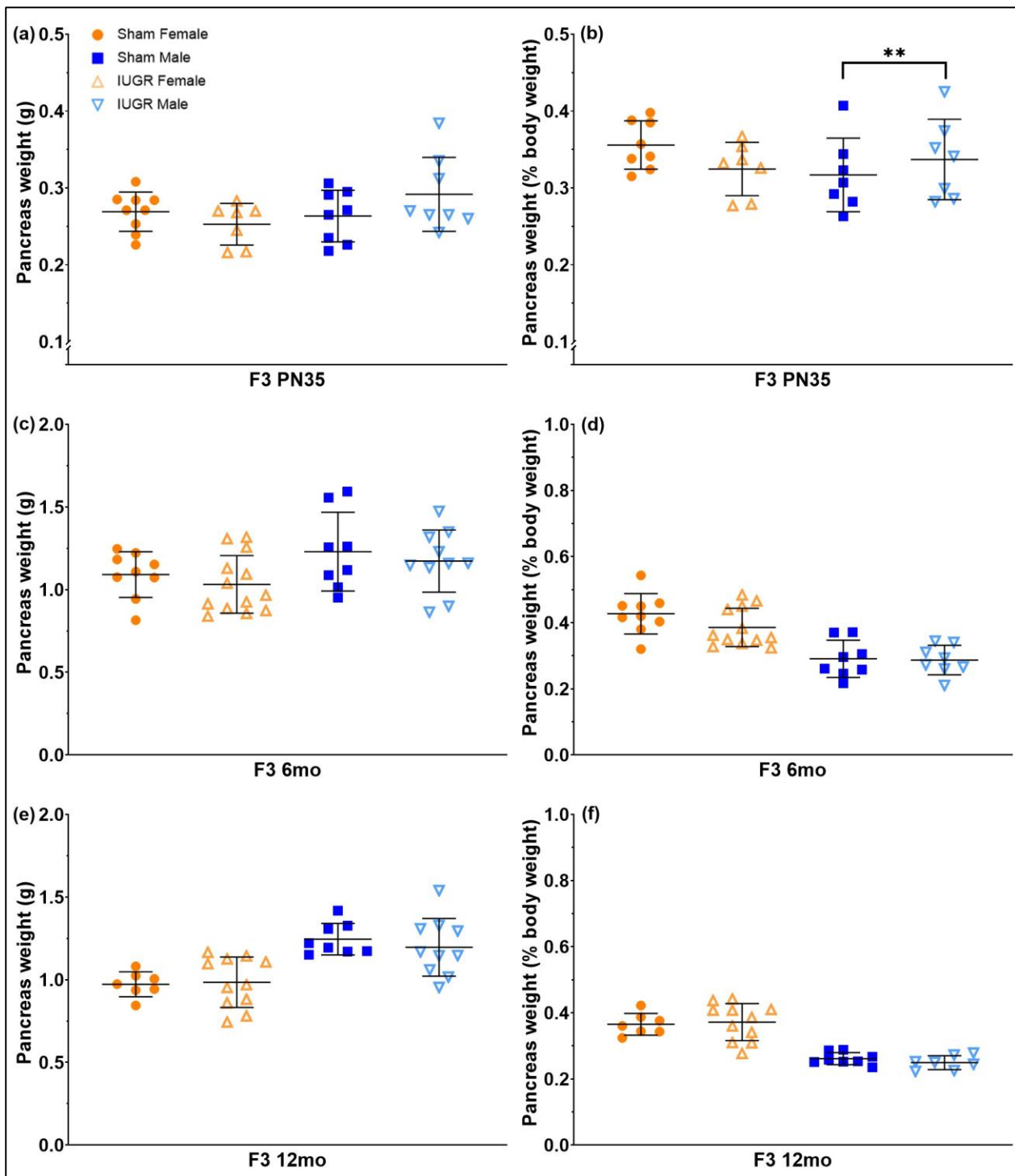


Figure 15. Postmortem pancreas weights (absolute vs. % body weight) of sham and IUGR rat offspring (paternal line) in the third generation (F3), at postnatal day 35 (PN35; a, b), 6 (6mo; c,d) and 12 (12mo; e, f) months of age. Significance was determined by a linear mixed-effect model with adjustment for litter size and relatedness of litter siblings (if present). ** $P < 0.01$. See **Table 5** for exact P -values. Data is expressed as mean \pm SD; $n = 7$ -13 samples per group.

Offspring tail-cuff systolic blood pressure

Regardless of treatment, there was a general increase in blood pressure with age, specifically from 2mo to 4mo, in all generations (**Supplementary data (Appendix B)**). Interestingly, the increase in blood pressure at 2mo-4mo was always higher in male offspring. There was a further increase in blood pressure in F3 males at 4mo-6mo and 6mo-9mo (**Supplementary data (Appendix B)**). Additionally, in general, males had higher blood pressure than females at the same age (**Table 6**). However, besides a decrease by 5.36% ($P = 0.008$) in F2 IUGR males at 6mo (IUGR 130.35 ± 1.74 mmHg vs. sham 137.73 ± 1.82 mmHg), there was no significant difference between sham and IUGR blood pressure at any time point, in neither sex, within any generation (**Table 6** and **Fig. 16**).

Table 6. Estimated marginal means (emmeans) of sham and IUGR rat offspring tail-cuff systolic blood pressure (mmHg) over time in the first (F1), second (F2) and third (F3) generations (paternal line). SE: standard error. Degrees-of-freedom method: Kenward-Roger. Confidence level used: 95%. mo: months of age. Significance was determined by a linear mixed-effect model with adjustment for litter size, relatedness of litter siblings (if present), and repeated measurement. A Tukey's *post hoc* test would be used in the subsequent analysis if there was an interaction between treatment and time point effects. ** $P < 0.01$, * $P < 0.05$. Time point effect: **Supplementary data (Appendix B)**. Only male offspring (paternal) was investigated in the F1 generation. N/A: test not applicable.

Generation	Time point	Blood pressure (males)				Treatment_Timepoint interaction (Type II Wald chisquare tests)	Tukey's <i>post hoc</i> test (Sham males vs. IUGR males)	Blood pressure (females)				Treatment_Timepoint interaction (Type II Wald chisquare tests)	Tukey's <i>post hoc</i> test (Sham females vs. IUGR females)
		Sham		IUGR				Sham		IUGR			
		Emmean	SE	Emmean	SE			Emmean	SE	Emmean	SE		
F1	2mo	126.91	2.92	127.77	2.44	0.116	N/A	N/A				N/A	N/A
	3mo	135.10	2.52	137.14	2.46								
	4mo	135.86	2.85	144.64	2.38								
	6mo	136.99	2.54	142.44	2.45								
	9mo	134.30	2.54	135.82	2.46								

	12mo	138.30	2.58	134.66	2.39								
F2	2mo	120.86	1.78	122.66	1.67	0.004**	0.958	123.93	1.60	118.90	1.67	0.031*	0.120
	4mo	131.21	2.00	135.54	1.67		0.346	131.51	1.57	133.10	1.70		0.960
	6mo	137.73	1.82	130.35	1.74		0.008**	129.29	1.64	133.56	1.62		0.250
	9mo	135.47	2.06	133.00	1.88		0.913	131.43	2.02	129.66	2.11		0.980
	12mo	132.81	2.01	130.31	1.80		0.894	130.52	2.29	128.20	2.34		0.960
	16mo	132.11	2.79	133.53	2.64		0.999	N/A					N/A
F3	2mo	126.05	2.45	121.19	2.10	0.142	N/A	125.43	1.68	123.21	1.66	0.757	N/A
	4mo	137.20	2.34	138.92	2.13			131.91	1.72	131.38	1.62		
	6mo	144.76	2.34	146.11	2.04			128.50	1.89	129.30	1.80		
	9mo	153.23	2.72	151.25	2.54			134.71	2.12	131.72	1.95		
	12mo	150.56	2.67	152.72	2.42			137.15	2.80	133.62	2.44		
	16mo	155.32	3.90	145.48	3.35			N/A					

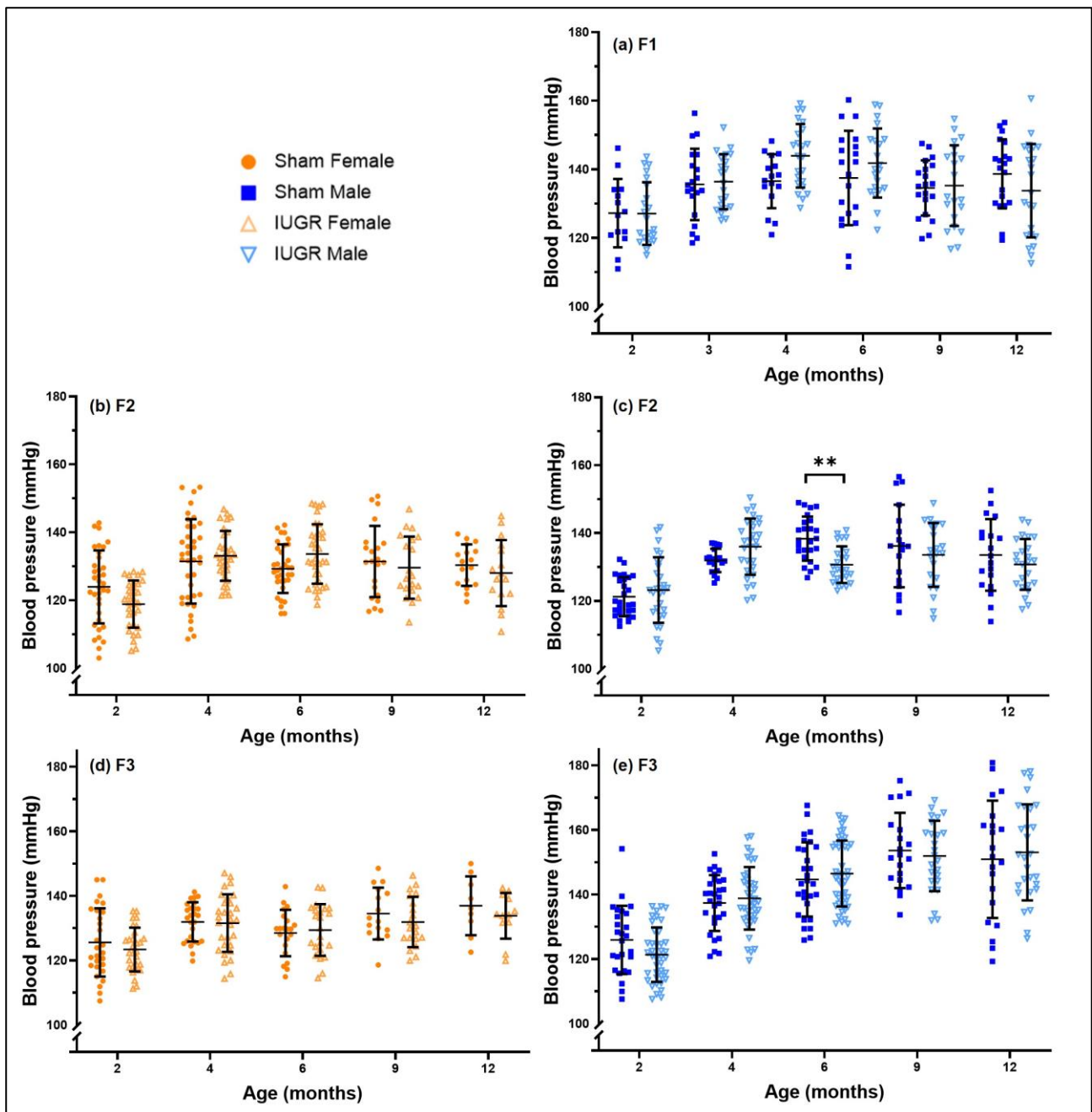


Figure 16. Tail cuff systolic blood pressure at 2-12 months of age (2mo-12mo) of sham and IUGR rat offspring (paternal line) in the first (F1, a), second (F2, b, c) and third (F3, d, e) generations. Significance was determined by a linear mixed-effect model with adjustment for litter size, relatedness of litter siblings (if present), and repeated measurement, followed by a Tukey's post hoc test (** $P < 0.01$). See **Table 6** for exact P -values. Time point effect: **Supplementary data (Appendix B)**. Data is expressed as observed mean \pm SD; $n = 9-44$ samples per group.

Glucose tolerance test (GTT)

Previously, it was shown in this model that for the F1 males, increased plasma glucose area under curve (AUC) in GTT was observed at 6mo [4]. Reduced first-phase insulin secretion was also reported in these males [4]. However, these alterations were not observed at 12mo [3]. In the F2 generation in this study, plasma glucose responses prior to glucose injection, as well as post-glucose injection, were not different between sham and IUGR offspring, at 6mo and 12mo (**Table 7** and **Fig. S5a, S5b, S6a, S6b**). Additionally, there was no difference in plasma glucose AUC in either sex, at any time point (**Table 8** and **Fig. S5c, S6c**). Examination of insulin profiles during GTT also showed no abnormal change in plasma insulin concentrations (**Fig. S7a, S7b, S8a, and S8b**), plasma insulin total AUC (**Fig. S7c and S8c**), plasma insulin first-phase secretion (**Fig. S7d and S8d**), plasma insulin second-phase secretion (**Fig. S7e and S8e**), or homeostasis model of assessment of insulin resistance (HOMA-IR, **Fig. S7f and S8f**) in the F2 6mo and 12mo IUGR offspring, compared to sham (**Tables 7 and 8**).

Table 7. Estimated marginal means (emmeans) of sham and IUGR rat offspring responses to Glucose Tolerance Test (GTT) in the second (F2) and third (F3) generations (paternal line), at 6 (6mo) and 12 (12mo) months of age. Plasma glucose concentration: mmol.L^{-1} , plasma insulin concentration: ng.mL^{-1} . Fasting (basal) value was calculated as the average of the two time points: 10 and 5 minutes prior to the glucose injection. SE: standard error. Degrees-of-freedom method: Kenward-Roger. Confidence level used: 95%. Significance was determined by a linear mixed-effect model with adjustment for litter size, relatedness of litter siblings (if present), and repeated measurement. A Tukey's *post hoc* test would be used in the subsequent

analysis if there was an interaction between treatment and time point effects. ** $P < 0.01$, * $P < 0.05$. Time point effect: **Supplementary data**

(Appendix B). N/A: test not applicable.

Generation	Age	Response	Males				Treatment_Timepoint interaction (Type II Wald chisquare tests)	Tukey's <i>post hoc</i> test (Sham males vs. IUGR males)	Females				Treatment_Timepoint interaction (Type II Wald chisquare tests)	Tukey's <i>post hoc</i> test (Sham females vs. IUGR females)
			Sham		IUGR				Sham		IUGR			
			Emmean	SE	Emmean	SE			Emmean	SE	Emmean	SE		
F2	6mo	GTT plasma glucose basal	6.80	1.00	6.99	0.92	0.846	N/A	7.98	1.05	7.02	0.91	0.051	N/A
		GTT plasma glucose 5min	14.76	1.00	15.88	0.92			18.09	1.05	15.62	0.87		
		GTT plasma glucose 10min	15.08	1.00	17.15	0.92			17.90	1.05	16.03	0.95		
		GTT plasma glucose 20min	15.75	1.00	17.00	0.92			17.02	1.05	15.74	0.87		
		GTT plasma glucose 30min	15.44	1.00	16.37	0.92			13.94	1.05	15.82	0.91		
		GTT plasma glucose 45min	12.62	1.00	15.10	0.92			12.89	1.05	14.26	0.87		
		GTT plasma glucose 60min	11.32	1.00	13.71	0.92			11.67	1.05	10.90	0.90		
		GTT plasma glucose 90min	9.89	1.00	11.72	0.92			10.78	1.05	8.53	0.87		
		GTT plasma glucose 120min	7.95	1.00	8.89	0.92			9.96	1.05	8.95	0.87		
	GTT plasma insulin basal	0.72	0.26	0.45	0.24	0.092	N/A	0.29	0.11	0.21	0.09	0.080	N/A	
	GTT plasma insulin 5min	1.32	0.26	0.85	0.24			0.35	0.11	0.61	0.09			
	GTT plasma insulin 10min	1.62	0.26	0.80	0.25			0.47	0.11	0.73	0.09			
	GTT plasma insulin 20min	1.83	0.26	1.41	0.24			0.87	0.10	1.06	0.09			
	GTT plasma insulin 30min	1.66	0.26	1.37	0.24			1.01	0.10	1.09	0.09			
	GTT plasma insulin 45min	1.29	0.26	1.33	0.24			0.72	0.10	0.77	0.10			
	GTT plasma insulin 60min	0.92	0.26	1.02	0.24			0.67	0.10	0.87	0.09			
	GTT plasma insulin 90min	0.98	0.26	0.87	0.24			0.65	0.10	0.57	0.09			

		GTT plasma insulin 120min	1.00	0.26	0.87	0.24			0.48	0.10	0.48	0.09		
	12mo	GTT plasma glucose basal	7.68	1.97	6.28	2.16	0.003**	0.980	6.80	1.01	6.19	1.08	0.826	N/A
		GTT plasma glucose 5min	16.75	1.97	13.02	2.16		0.379	15.00	1.01	15.00	1.08		
		GTT plasma glucose 10min	20.79	1.97	15.40	2.16		0.106	17.54	1.01	16.04	1.08		
		GTT plasma glucose 20min	22.63	1.97	16.99	2.16		0.084	20.21	1.01	19.18	1.08		
		GTT plasma glucose 30min	21.62	1.97	15.51	2.16		0.053	18.75	1.01	18.60	1.08		
		GTT plasma glucose 45min	19.07	1.97	15.18	2.16		0.342	16.28	1.01	16.22	1.08		
		GTT plasma glucose 60min	18.30	1.97	13.69	2.16		0.203	14.43	1.01	14.63	1.14		
		GTT plasma glucose 90min	15.96	1.97	10.59	2.19		0.112	12.73	1.01	10.67	1.08		
		GTT plasma glucose 120min	11.49	2.03	11.60	2.18		1	9.59	1.07	10.55	1.08		
			GTT plasma insulin basal	0.87	0.21	0.62		0.22	0.363	N/A	0.16	0.08		
	GTT plasma insulin 5min	0.55	0.21	0.65	0.22	0.43	0.08	0.34			0.08			
	GTT plasma insulin 10min	0.52	0.21	0.76	0.22	0.49	0.08	0.36			0.09			
	GTT plasma insulin 20min	1.42	0.21	1.36	0.22	0.79	0.08	0.71			0.08			
	GTT plasma insulin 30min	1.20	0.21	1.27	0.22	0.81	0.08	0.65			0.09			
	GTT plasma insulin 45min	1.30	0.21	1.22	0.22	0.61	0.08	0.63			0.08			
	GTT plasma insulin 60min	1.19	0.21	1.05	0.22	0.46	0.08	0.67			0.08			
	GTT plasma insulin 90min	1.11	0.21	0.76	0.22	0.45	0.08	0.44			0.09			
	GTT plasma insulin 120min	1.26	0.21	0.94	0.23	0.47	0.08	0.47			0.09			
F3	6mo	GTT plasma glucose basal	5.73	1.12	5.76	0.98	0.795	N/A			5.06	1.13	5.88	1.13
		GTT plasma glucose 5min	13.34	1.12	13.59	0.98			12.38	1.13	14.85	1.13		
		GTT plasma glucose 10min	15.45	1.12	16.71	0.98			15.24	1.13	16.12	1.13		
		GTT plasma glucose 20min	17.00	1.12	16.26	0.98			17.41	1.13	17.19	1.13		
		GTT plasma glucose 30min	14.99	1.12	14.59	1.03			14.60	1.13	15.84	1.13		
		GTT plasma glucose 45min	14.80	1.12	13.39	0.98			12.95	1.13	13.44	1.13		

		GTT plasma glucose 60min	11.75	1.12	11.43	0.98	0.507	N/A	11.14	1.13	11.15	1.13	0.447	N/A			
		GTT plasma glucose 90min	10.34	1.12	8.49	0.98			10.59	1.13	9.96	1.13					
		GTT plasma glucose 120min	7.99	1.12	7.23	0.98			8.65	1.13	7.74	1.13					
		GTT plasma insulin basal	0.33	0.25	0.47	0.22			0.30	0.17	0.29	0.20					
		GTT plasma insulin 5min	0.37	0.25	0.79	0.22			0.51	0.17	0.54	0.20					
		GTT plasma insulin 10min	0.40	0.25	0.91	0.22			0.83	0.17	0.65	0.20					
		GTT plasma insulin 20min	0.91	0.25	1.33	0.22			1.33	0.17	0.97	0.20					
		GTT plasma insulin 30min	1.28	0.25	1.32	0.22			1.07	0.17	1.21	0.20					
		GTT plasma insulin 45min	1.21	0.25	1.21	0.22			1.19	0.17	0.91	0.20					
		GTT plasma insulin 60min	0.98	0.25	1.13	0.22			0.69	0.17	0.90	0.20					
		GTT plasma insulin 90min	0.82	0.25	0.88	0.22			0.81	0.17	0.77	0.20					
		GTT plasma insulin 120min	0.71	0.25	1.03	0.22			0.68	0.17	0.75	0.20					
	12mo	GTT plasma glucose basal	6.78	0.92	6.74	0.92	0.013**	1	6.01	0.97	5.92	1.02	0.671	N/A			
		GTT plasma glucose 5min	14.55	0.92	14.75	0.92		1	15.69	0.97	15.44	1.02					
		GTT plasma glucose 10min	15.78	0.96	17.58	0.92		0.554	17.51	0.97	17.99	1.02					
		GTT plasma glucose 20min	16.66	0.92	20.11	0.92		0.025*	18.08	0.97	18.38	1.02					
		GTT plasma glucose 30min	16.60	0.92	19.19	0.92		0.159	15.77	0.97	17.45	1.02					
		GTT plasma glucose 45min	15.24	0.96	16.71	0.92		0.758	13.37	0.97	14.91	1.02					
		GTT plasma glucose 60min	13.68	0.92	14.14	0.92		1	11.75	0.97	11.61	1.02					
		GTT plasma glucose 90min	10.70	0.92	11.12	0.92		1	10.10	0.97	8.73	1.02					
		GTT plasma glucose 120min	8.68	0.92	8.96	0.92		1	8.36	0.97	8.91	1.02					
		GTT plasma insulin basal	0.62	0.18	0.38	0.18		0.337	N/A	0.35	0.16	0.53			0.18	0.652	N/A
		GTT plasma insulin 5min	0.74	0.18	0.44	0.18				0.58	0.16	0.74			0.18		
		GTT plasma insulin 10min	0.74	0.18	0.58	0.18				1.18	0.16	1.00			0.18		
GTT plasma insulin 20min	1.45	0.18	1.16	0.18	1.46	0.16	1.51			0.18							

	GTT plasma insulin 30min	1.41	0.18	1.56	0.18		1.32	0.16	1.11	0.18	
	GTT plasma insulin 45min	1.28	0.18	1.14	0.18		1.33	0.16	1.04	0.18	
	GTT plasma insulin 60min	1.55	0.18	1.18	0.18		1.04	0.16	0.76	0.18	
	GTT plasma insulin 90min	1.09	0.18	1.24	0.18		0.95	0.16	0.71	0.18	
	GTT plasma insulin 120min	1.51	0.18	1.11	0.18		0.69	0.16	0.73	0.18	

Table 8. Estimated marginal means (emmeans) of sham and IUGR rat offspring Glucose Tolerance Test (GTT) assessments in the second (F2) and third (F3) generations (paternal line), at 6 (6mo) and 12 (12mo) months of age. Glucose area under curve (AUC) was calculated as the total AUC from basal (pre-glucose injection) to 120 minutes post-glucose injection. Total insulin AUC was calculated as the total AUC from basal to 120 minutes. Insulin AUC from basal to 5 minutes represents first-phase insulin response to GTT, while insulin AUC from 5 to 120 minutes represents second-phase insulin response to GTT. Rat offspring homeostasis model of assessment of insulin resistance (HOMA-IR) was calculated using the formula: $(fasting\ insulin\ (\mu U.ml^{-1}) \times fasting\ glucose\ (mg.dL^{-1})) \div 2430$. SE: standard error. Degrees-of-freedom method: Kenward-Roger. Confidence level used: 95%. Significance was determined by a linear mixed-effect model with adjustment for litter size and relatedness of litter siblings (if present). *** $P < 0.001$, * $P < 0.05$. Time point effect: **Supplementary data (Appendix B)**. N/A: test not applicable.

Generation	Age	Calculation	Males				Treatment effect (Sham males vs. IUGR males)	Females				Treatment effect (Sham females vs. IUGR females)
			Sham		IUGR			Sham		IUGR		
			Emmean	SE	Emmean	SE		Emmean	SE	Emmean	SE	
F2	6mo	GTT plasma glucose AUC	1490.17	106.63	1699.53	98.08	0.100	1608.63	99.86	1492.90	71.55	0.259
		GTT plasma insulin AUC	151.33	25.77	129.89	24.10	0.493	79.98	10.54	92.13	7.99	0.275
		GTT plasma insulin (1 st phase)	12.29	2.39	7.78	2.23	0.119	3.69	0.57	4.58	0.46	0.172
		GTT plasma insulin (2 nd phase)	139.00	24.14	122.11	22.46	0.562	76.74	9.68	86.72	7.34	0.330
		GTT HOMA - IR	1.11	0.25	0.72	0.21	0.133	0.54	0.14	0.26	0.11	0.066
	12mo	GTT plasma glucose AUC	2049.88	233.25	1630.61	259.34	0.133	1791.75	80.49	1756.75	85.72	0.743
		GTT plasma insulin AUC	141.30	19.79	118.03	22.00	0.326	67.68	6.27	61.90	6.19	0.460
		GTT plasma insulin (1 st phase)	7.57	2.45	7.73	2.82	0.960	3.59	0.61	3.21	0.63	0.602
GTT plasma insulin (2 nd phase)		132.83	18.60	110.40	20.68	0.314	64.07	6.01	58.55	5.94	0.462	

		GTT HOMA - IR	0.89	0.37	0.66	0.42	0.617	0.30	0.06	0.29	0.06	0.894
F3	6mo	GTT plasma glucose AUC	1538.83	113.94	1434.58	104.85	0.393	1510.94	126.65	1541.46	127.08	0.799
		GTT plasma insulin AUC	108.67	24.24	131.66	21.05	0.378	106.87	15.59	104.33	19.84	0.875
		GTT plasma insulin (1 st phase)	4.27	2.27	8.00	2.06	0.136	4.89	0.87	4.96	1.10	0.938
		GTT plasma insulin (2 nd phase)	104.50	22.44	124.08	19.49	0.417	101.99	15.18	99.35	19.32	0.867
		GTT HOMA - IR	0.54	0.17	0.70	0.15	0.365	0.36	0.13	0.37	0.13	0.981
	12mo	GTT plasma glucose AUC	1642.17	103.20	1775.17	103.20	0.293	1569.12	105.90	1530.41	118.05	0.743
		GTT plasma insulin AUC	156.82	18.30	138.73	18.30	0.420	129.61	7.85	106.57	8.52	0.0002***
		GTT plasma insulin (1 st phase)	8.17	1.11	4.89	1.11	0.016*	5.65	1.79	7.58	2.08	0.400
		GTT plasma insulin (2 nd phase)	148.63	17.76	133.87	17.76	0.497	124.49	7.69	99.26	8.61	0.0006***
		GTT HOMA - IR	0.77	0.21	0.62	0.21	0.570	0.37	0.13	0.46	0.14	0.622

Similar to the F2 6mo offspring, there was no difference in GTT plasma glucose (**Tables 7 and 8, Fig. S9**) or plasma insulin (**Tables 7 and 8, Fig. S10**) profiles between F3 6mo sham and IUGR animals. However, at 12mo, F3 IUGR males had an increase by 20.71% in GTT plasma glucose concentration at 20 minutes post-glucose injection ($20.11 \pm 0.92 \text{ mmol.L}^{-1}$), compared to sham ($16.66 \pm 0.92 \text{ mmol.L}^{-1}$) ($P = 0.025$, **Table 7** and **Fig. 17b**). In regard to the plasma insulin profile at 12mo, despite no statistical difference found in plasma insulin concentrations between sham and IUGR animals throughout the test (**Table 7** and **Fig. 18a, 18b**), F3 IUGR males developed impaired first-phase insulin secretion, with a decrease by 40.15% in insulin AUC from basal to 5 minutes post-glucose injection (IUGR males 4.89 ± 1.11 vs. sham males 8.17 ± 1.11 , $P = 0.016$) (1st phase, **Table 8** and **Fig. 18d**), whereas IUGR females had reduced second-phase insulin secretion, represented by a decrease of 20.27% in insulin AUC from 5 to 120 minutes post-glucose injection (IUGR females 99.26 ± 8.61 vs. sham females 124.49 ± 7.69) (2nd phase, **Table 8** and **Fig. 18e**). Additionally, total plasma insulin AUC was reduced only in F3 12mo IUGR females (106.57 ± 8.52 , compared to sham, 129.61 ± 7.85) (-17.78%, $P = 0.0002$, **Table 8** and **Fig. 18c**).

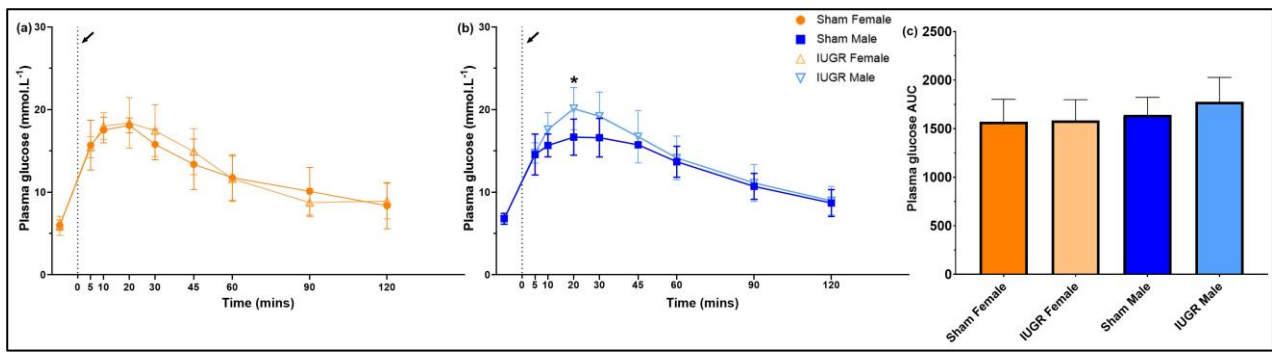


Figure 17. Plasma glucose profile during the Glucose Tolerance Test (GTT) of sham and IUGR rat offspring (paternal line) in the third generation (F3), at 12 months of age. The black arrow indicates when glucose injection occurred. Fasting (basal) value was calculated as the average of the two time points: 10 and 5 minutes prior to the glucose injection. Comparisons were made between sham and IUGR offspring, within each sex (females, a, and males, b). Glucose area under curve (AUC, c) was calculated as the total AUC from basal to 120 minutes. Significance was determined by a linear mixed-effect model with adjustment for litter size, relatedness of litter siblings (if present), and repeated measurement (for plasma glucose responses (a, b) only). * $P < 0.05$. See **Tables 7 and 8** for exact P -values. Time point effect: **Supplementary data (Appendix B)**. Data is expressed as mean \pm SD; $n = 6$ samples per group.

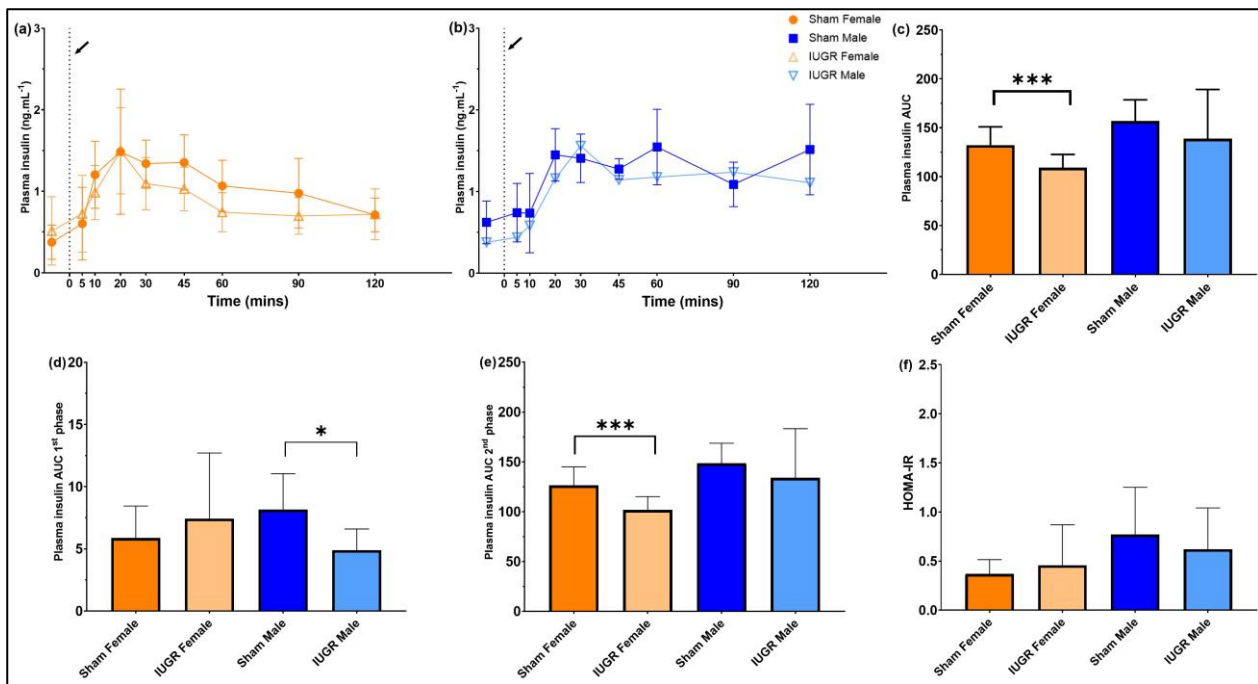


Figure 18. Plasma insulin profile during the Glucose Tolerant Test (GTT) of sham and IUGR rat offspring (paternal line) in the third generation (F3), at 12 months of age. The black arrow indicates when glucose injection occurred. Fasting (basal) value was calculated as the average of the two time points: 10 and 5 minutes prior to the glucose injection. Comparisons were made between sham and IUGR offspring, within each sex (females, a, and males, b). Insulin area under curve (AUC) was calculated as the total AUC from basal to 120 minutes (c), AUC from basal to 5 minutes (1st phase, d), and AUC from 5 to 120 minutes (2nd phase, e). Rat offspring homeostasis model of assessment of insulin resistance (HOMA-IR, f) was calculated using the formula: $(fasting\ insulin\ (\mu U.mL^{-1}) \times fasting\ glucose\ (mg.dL^{-1})) \div 2430$. Significance was determined by a linear mixed-effect model with adjustment for litter size, relatedness of litter siblings (if present), and repeated measurement (for plasma insulin responses (a, b) only). *** $P < 0.001$, * $P < 0.05$. See **Tables 7 and 8** for exact P -values. Time point effect: **Supplementary data (Appendix B)**. Data is expressed as mean \pm SD; $n = 5-6$ samples per group.

Insulin challenge (IC)

It has been reported that in the F1 males, whole-body insulin sensitivity, represented by plasma glucose AUC in IC, was not different between sham and IUGR group, at both 6mo [4] and 12mo [3]. In the F2 and F3 generations, there was no difference in plasma glucose concentrations between sham and IUGR animals, in response to the insulin injection (**Table S2** and **Fig. S11a-b, S12a-b, S13a-b, S14a-b**). Furthermore, plasma glucose AUCs in the IUGR group also remained unchanged compared to sham in F2 at 6mo (males $P = 0.695$, females $P = 0.599$), F2 at 12mo (males $P = 0.879$, females $P = 0.453$), F3 at 6mo (males $P = 0.431$, females $P = 0.631$), and F3 at 12mo (males $P = 0.837$, females $P = 0.621$) (**Table S3** and **Fig. S11c, S12c, S13c, S14c**).

Discussion

This study is the first to investigate the physiology, specifically growth, vascular and metabolic functions of the paternal line of rat UPI-induced IUGR model from F1 males, whose mothers (F0) had uterine artery and vein ligation during pregnancy. Our collaborators have previously investigated the effect of UPI/IUGR on bone health of the F2 and F3 offspring from both parental lines, and reported no transgenerational transmission of IUGR phenotypes [5]. In contrast, data from other recent rodent studies have suggested that there is a transgenerational transmission of adverse environmental pregnancy effects in both maternal and paternal lines [6, 7, 8, 9, 10].

Animals in this current study were examined over different developmental stages, from birth (PN1) to weaning (PN35) to adulthood (up to 12mo) in F2 and F3 male and female offspring from the F1 paternal line.

Inducing UPI at day 18 of gestation in rats has been reported to result in reduced F1 fetal weight *in utero* at E20 [11, 12], as well as reduced [3, 4, 5, 13, 14, 15, 16, 17] birth weight. In this current

study, F1 IUGR male birth weight was not statistically different compared to sham males. This result is not surprising as birth weight is only one of the surrogates of fetal growth, and offspring who were exposed to environmental insults *in utero*, for example – maternal protein restriction, despite having a normal birth weight, can still have an aberrant postnatal growth rate and/or have a higher risk of developing late-onset diseases, such as high blood pressure and renal disease [18, 19, 20]. Indeed, F1 IUGR male body weight in this current study was found to be significantly lower compared to sham males post-weaning (after PN35), up to 12mo. Previous studies have also reported this decrease in F1 IUGR male body weights at postnatal periods, as well as decreased absolute growth rate from PN14 to 2mo [3, 4, 13, 15].

Similar to the F1 generation, IUGR offspring birth weights in the paternal F2 and F3 were also unaffected, regardless of sex, which is in line with previously published data in both maternal and paternal lines [2, 5, 21, 22]. In this current study, the effect of accelerated growth at postnatal stages in F2 and F3 generations was more substantial compared to that in the F1, as it resulted in higher body weights in IUGR males and females, at 2mo (F2 IUGR females and F3 IUGR males), 4mo, and 6mo (F2 IUGR males), which has the potential to predispose offspring to an increased risk of developing metabolic disease later in life [23]. In the maternal line of this UPI model, F2 IUGR males who were heavier than sham males at 2mo were shown to have reduced pancreatic β -cell mass at 6mo, as well as reduced adrenal androgenic gene expression [22]. Meanwhile, F2 IUGR females who were heavier than sham females at 4mo remained unaffected at 6mo, indicating a sex-specific effect [22]. In an IUGR model of *in utero* betamethasone exposure at E17-18, catch-up growth was also observed in the paternal growth restricted F2 offspring at PN21 and PN70 (~2.3mo), in association with reduced organ weights, including brain, liver, kidney, lung, and pancreas [24].

F1 IUGR males have previously been reported to have increased relative heart and left ventricle weights at PN35 [2], similar relative left ventricle and total kidney weights compared to sham at 6mo [1, 2] and 12mo [3]. One study reported increased relative left ventricle weight in 6mo F1 IUGR males [1]. In this current study, F1 IUGR males had decreased relative left ventricle weight and total kidney weight at 12mo. On the other hand, no change to the F1 IUGR offspring relative heart and liver weights was previously reported, at both 6mo and 12mo [1, 2, 3], which is in line with our results. Regarding the paternal F2 generation, we reported a decrease in relative liver and pancreas weights in IUGR females at PN35, increased relative total kidney weight in IUGR males at 6mo, and decreased relative liver weight in IUGR males at 12mo, compared to sham. Surprisingly, these exact measurements were reported to be comparable between sham and IUGR offspring, including both males and females, in the F2 maternal line at PN35 (pancreas weight [21]), 6mo (kidney weight [25]), and 12mo (liver weight [21, 25]). Our recent study of this UPI model also reported no alteration to the F2 IUGR offspring left kidney weight (% body weight) at 6mo, in both maternal and paternal lines [12]. Regarding the paternal F3 generation, altered relative organ weights were also observed at PN35, 6mo and 12 for IUGR females, and at PN35 and 12mo for IUGR males. Taken together, these changes in organ weights suggests a sex-specific and transgenerational effect of IUGR on the morphology of offspring in the paternal line, especially in the presence of catch-up growth.

Based on findings in previous IUGR studies, F1 IUGR males were expected to have elevated systolic blood pressure compared to sham at around 2mo-9mo age [1, 2, 3, 13, 15, 26, 27]. However, we observed no alteration in blood pressure between F1 IUGR and sham males, at any time point, which remains to be explained. On the contrary, F2 IUGR males had a lower blood pressure measured at 6mo. This result was surprising, as F2 IUGR males in the maternal line of UPI model had increased blood pressure measured at 6mo, and persisted to 9mo [2, 25]. In an IUGR model where maternal inflammation was induced at E8.5-E12.5, offspring in the paternal F2-F4

generations, including both males and females, had elevated blood pressure compared to healthy controls at 2mo, 3mo, 4mo, 5mo, 6mo, and 7mo [26].

As mentioned previously, increased plasma glucose AUC (impaired glucose tolerance) and reduced first-phase insulin secretion (reduced β -cell response to glucose) were evident in F1 IUGR male offspring at 6mo, but not 12mo [3, 4]. Similarly, reduced first-phase insulin secretion was previously reported in the F2 6mo, but not 12mo, male and female IUGR offspring from the maternal line of UPI model [21]. Meanwhile, a different study on the same model/maternal line reported no difference in all GTT measurement assessments, including first-phase insulin secretion, in F2 male and female IUGR offspring, at both 6mo and 12mo [22], which was in line with our results in the paternal line. Interestingly, we showed for the first time that in the paternal line, there was an impaired glucose-stimulated first-phase insulin secretion in F3 12mo IUGR males, and an impaired second-phase insulin secretion in the females, both of which are an indication for a higher risk of developing type-2 diabetes [28]. Future studies need to investigate the pancreas and β -cells of IUGR offspring to see if this can explain the above observations.

Previous studies investigating this same model used different statistical approaches to analyse offspring physiological measurements, such as investigating only male offspring (using one-way ANOVA [13], two-way ANOVA (treatment x exercise) with adjustment for repeated measurements [14], two-way ANOVA (treatment x age) [2], Student's *t* test [2], or Mann-Whitney U test [15]), investigating males separately from females (using two-way ANOVA (time x treatment) with adjustment for repeated measurements within each sex [4], or one-way ANOVA within each sex [4]), or combining both sexes in the statistical analysis (using 2-way ANOVA (treatment x sex) [11, 12, 16, 17]). In this current study, we examined each sex separately using a linear mixed effect model (treatment x time point effects for body weight, blood pressure, and GTT/IC, and treatment

effect only for other measurements) with adjustment for litter size, relatedness between litter siblings, and repeated measurement. Additionally, we report emmeans of the statistical model instead of the sample's descriptive means. Taken together, these might contribute to the differences between our results and previous studies.

In conclusion, results from our study indicated that similar to the maternal line, *in utero* exposure to UPI of the F1 offspring resulted in altered growth profile, specifically accelerated growth in the paternal F2 males and females. However, as discussed above, while changes to the offspring morphology (altered F2 postmortem tissue weights) were apparent in the paternal line, abnormal vascular (increased blood pressure in F2 males) and metabolic (reduced first-phase insulin secretion in F2 males and females) functions were greater in the maternal line. This may be due to the main difference between maternal and paternal lines, which is the growth restricted F1 females, despite having the ability to adapt better to the *in utero* insults, became pregnant (i.e., experienced 'second hit') and the physiological changes during pregnancy exacerbated the concealed metabolic dysfunctions. This resulted in a poor *in utero* environment for the developing F2 fetuses from the maternal line [29, 30, 31]. On the other hand, as germ cells that produced the F2 paternal offspring were not present in the F1 growth restricted males at the time of *in utero* insult exposure [31], our observations of altered organ weights in the paternal F2 and F3 generations, and impaired first- and second-phase insulin secretion in the paternal F3 offspring might be an indication of a true transgenerational transmission of IUGR effect. The mechanism for this transmission, as well as the sex-specific phenotypic differences is to be determined, while emerging evidence suggests a role of altered epigenetic mechanisms, such as DNA methylation, histone modifications, and non-coding RNAs [32, 33].

References

1. Wlodek ME, Westcott K, Siebel AL, Owens JA, Moritz KM. Growth restriction before or after birth reduces nephron number and increases blood pressure in male rats. *Kidney International*. 2008;74(2):187-195. doi: 10.1038/ki.2008.153.
2. Master JS, Zimanyi MA, Yin KV, Moritz KM, Gallo LA, Tran M, Wlodek ME, Black MJ. Transgenerational left ventricular hypertrophy and hypertension in offspring after uteroplacental insufficiency in male rats. *Clinical and Experimental Pharmacology and Physiology*. 2014;41(11):884-890. doi: 10.1111/1440-1681.12303.
3. Tran M, Young ME, Jefferies AJ, Hryciw DH, Ward MM, Fletcher EL, Wlodek ME, Wadley GD. Uteroplacental insufficiency leads to hypertension, but not glucose intolerance or impaired skeletal muscle mitochondrial biogenesis, in 12-month-old rats. *Physiol Rep*. 2015;3(9). doi: 10.14814/phy2.12556.
4. Siebel AL, Mibus A, De Blasio MJ, Westcott KT, Morris MJ, Prior L, Owens JA, Wlodek ME. Improved lactational nutrition and postnatal growth ameliorates impairment of glucose tolerance by uteroplacental insufficiency in male rat offspring. *Endocrinology*. 2008;149(6):3067-3076. doi: 10.1210/en.2008-0128.
5. Anevskaa K, Wark JD, Wlodek ME, Romano T. The transgenerational effect of maternal and paternal F1 low birth weight on bone health of second and third generation offspring. *Journal of Developmental Origins of Health and Disease*. 2019;10(2):144-153. doi: 10.1017/S204017441800020X.
6. Zhang Z, Luo X, Lv Y, Yan L, Xu S, Wang Y, Zhong Y, Hang C, Jyotsnav J, Lai D, Shen Z, Xu X, Ma X, Chen Z, Pan Y, Du L. Intrauterine growth restriction programs intergenerational transmission of pulmonary arterial hypertension and endothelial dysfunction via sperm epigenetic modifications. *Hypertension*. 2019;74(5):1160-1171. doi: 10.1161/HYPERTENSIONAHA.119.13634.

7. Skinner MK, Ben Maamar M, Sadler-Riggleman I, Beck D, Nilsson E, McBirney M, Klukovich R, Xie Y, Tang C, Yan W. Alterations in sperm DNA methylation, non-coding RNA and histone retention associate with DDT-induced epigenetic transgenerational inheritance of disease. *Epigenetics Chromatin*. 2018;11(1):8. doi: 10.1186/s13072-018-0178-0.
8. Lismer A, Siklenka K, Lafleur C, Dumeaux V, Kimmins S. Sperm histone H3 lysine 4 trimethylation is altered in a genetic mouse model of transgenerational epigenetic inheritance. *Nucleic Acids Research*. 2020;48(20):11380-11393. doi: 10.1093/nar/gkaa712.
9. Thorson JLM, Beck D, Ben Maamar M, Nilsson EE, Skinner MK. Ancestral plastics exposure induces transgenerational disease-specific sperm epigenome-wide association biomarkers. *Environmental Epigenetics*. 2021;7(1):dvaa023. doi: 10.1093/eep/dvaa023.
10. Weber-Stadlbauer U, Richetto J, Zwamborn RAJ, Sliker RC, Meyer U. Transgenerational modification of dopaminergic dysfunctions induced by maternal immune activation. *Neuropsychopharmacology*. 2021;46(2):404-412. doi: 10.1038/s41386-020-00855-w.
11. Briffa JF, O'Dowd R, Moritz KM, Romano T, Jedwab LR, McAinch AJ, Hryciw DH, Wlodek ME. Uteroplacental insufficiency reduces rat plasma leptin concentrations and alters placental leptin transporters: ameliorated with enhanced milk intake and nutrition. *The Journal of Physiology*. 2017;595(11):3389-3407. doi: 10.1113/JP273825.
12. Doan TNA, Briffa JF, Phillips AL, Leemaqz SY, Burton RA, Romano T, Wlodek ME, Bianco-Miotto T. Epigenetic mechanisms involved in intrauterine growth restriction and aberrant kidney development and function. *Journal of Developmental Origins of Health and Disease*. 2021;12(6):952-962. doi: 10.1017/S2040174420001257.
13. Wlodek ME, Mibus A, Tan A, Siebel AL, Owens JA, Moritz KM. Normal lactational environment restores nephron endowment and prevents hypertension after placental restriction in the rat. *Journal of the American Society of Nephrology*. 2007;18(6):1688-1696. doi: 10.1681/asn.2007010015.

14. Laker RC, Gallo LA, Wlodek ME, Siebel AL, Wadley GD, McConell GK. Short-term exercise training early in life restores deficits in pancreatic β -cell mass associated with growth restriction in adult male rats. *American Journal of Physiology: Endocrinology and Metabolism*. 2011;301(5):E931-40. doi: 10.1152/ajpendo.00114.2011.
15. Master JS, Thouas GA, Harvey AJ, Sheedy JR, Hannan NJ, Gardner DK, Wlodek ME. Fathers that are born small program alterations in the next-generation preimplantation rat embryos. *Journal of Nutrition*. 2015;145(5):876-83. doi: 10.3945/jn.114.205724.
16. Cuffe JSM, Briffa JF, Rosser S, Siebel AL, Romano T, Hryciw DH, Wlodek ME, Moritz KM. Uteroplacental insufficiency in rats induces renal apoptosis and delays nephrogenesis completion. *Acta Physiologica*. 2018;222(3):e12982. doi: 10.1111/apha.12982.
17. Sutherland MR, Ng KW, Drenckhahn JD, Wlodek ME, Black MJ. Impact of intrauterine growth restriction on the capillarization of the early postnatal rat heart. *The Anatomical Record*. 2019;302(9):1580-1586. doi: <https://doi.org/10.1002/ar.24037>.
18. Harrison M, Langley-Evans SC. Intergenerational programming of impaired nephrogenesis and hypertension in rats following maternal protein restriction during pregnancy. *British Journal of Nutrition*. 2009;101(7):1020-30. doi: 10.1017/s0007114508057607.
19. Moritz KM, Singh RR, Probyn ME, Denton KM. Developmental programming of a reduced nephron endowment: more than just a baby's birth weight. *American Journal of Physiology-Renal Physiology*. 2009;296(1):F1-F9. doi: 10.1152/ajprenal.00049.2008.
20. Wood-Bradley RJ, Henry SL, Evans RG, Bertram JF, Cullen-McEwen LA, Armitage JA. Cardiovascular and renal profiles in rat offspring that do not undergo catch-up growth after exposure to maternal protein restriction. *Journal of Developmental Origins of Health and Disease*. 2023;14(3):426-436. doi: 10.1017/S2040174422000666.
21. Tran M, Gallo LA, Jefferies AJ, Moritz KM, Wlodek ME. Transgenerational metabolic outcomes associated with uteroplacental insufficiency. *Journal of Endocrinology*. 2013;217(1):105-118. doi: 10.1530/JOE-12-0560.

22. Cheong JN, Cuffe JS, Jefferies AJ, Anevskaja K, Moritz KM, Wlodek ME. Sex-specific metabolic outcomes in offspring of female rats born small or exposed to stress during pregnancy. *Endocrinology*. 2016;157(11):4104-4120. doi: 10.1210/en.2016-1335.
23. Singhal A, Lucas A. Early origins of cardiovascular disease: is there a unifying hypothesis? *The Lancet*. 2004;363(9421):1642-1645. doi: [https://doi.org/10.1016/S0140-6736\(04\)16210-7](https://doi.org/10.1016/S0140-6736(04)16210-7).
24. Abrantes MA, Valencia AM, Bany-Mohammed F, Aranda JV, Beharry KD. Intergenerational influence of antenatal betamethasone on growth, growth factors, and neurological outcomes in rats. *Reproductive Sciences*. 2020;27(1):418-431. doi: 10.1007/s43032-019-00073-w.
25. Gallo LA, Tran M, Cullen-McEwen LA, Denton KM, Jefferies AJ, Moritz KM, Wlodek ME. Transgenerational programming of fetal nephron deficits and sex-specific adult hypertension in rats. *Reproduction, Fertility and Development*. 2014;26(7):1032-1043. doi: 10.1071/RD13133.
26. Guan X, Dan G-r, Yang Y, Ji Y, Lai W-j, Wang F-j, Meng M, Mo B-h, Huang P, You T-t, Deng Y-f, Song L, Guo W, Yi P, Yu J-h, Gao Y, Shou W-n, Chen B-b, Deng Y-c, Li X-h. Prenatal inflammation exposure-programmed hypertension exhibits multi-generational inheritance via disrupting DNA methylome. *Acta Pharmacologica Sinica*. 2022;43(6):1419-1429. doi: 10.1038/s41401-021-00772-8.
27. Yu C, Chen S, Wang X, Wu G, Zhang Y, Fu C, Hu C, Liu Z, Luo X, Wang J, Chen L. Exposure to maternal diabetes induces endothelial dysfunction and hypertension in adult male rat offspring. *Microvascular Research*. 2021;133:104076. doi: <https://doi.org/10.1016/j.mvr.2020.104076>.
28. Seino S, Shibasaki T, Minami K. Dynamics of insulin secretion and the clinical implications for obesity and diabetes. *The Journal of Clinical Investigation*. 2011;121(6):2118-2125. doi: 10.1172/JCI45680.

29. Gallo LA, Tran M, Moritz KM, Mazzuca MQ, Parry LJ, Westcott KT, Jefferies AJ, Cullen-McEwen LA, Wlodek ME. Cardio-renal and metabolic adaptations during pregnancy in female rats born small: implications for maternal health and second generation fetal growth. *The Journal of Physiology*. 2012;590(3):617-630. doi: 10.1113/jphysiol.2011.219147.
30. Ushida T, Cotechini T, Protopapas N, Atallah A, Collyer C, Toews AJ, Macdonald-Goodfellow SK, Tse MY, Winn LM, Pang SC, Adams MA, Othman M, Kotani T, Kajiyama H, Graham CH. Aberrant inflammation in rat pregnancy leads to cardiometabolic alterations in the offspring and intrauterine growth restriction in the F2 generation. *Journal of Developmental Origins of Health and Disease*. 2022;13(6):706-718. doi: 10.1017/S2040174422000265.
31. Cheong JN, Wlodek ME, Moritz KM, Cuffe JSM. Programming of maternal and offspring disease: impact of growth restriction, fetal sex and transmission across generations. *The Journal of Physiology*. 2016;594(17):4727-4740. doi: <https://doi.org/10.1113/JP271745>.
32. Doan TNA, Akison LK, Bianco-Miotto T. Epigenetic mechanisms responsible for the transgenerational inheritance of intrauterine growth restriction phenotypes. *Frontiers in Endocrinology*. 2022;13:838737. doi: 10.3389/fendo.2022.838737.
33. Argyraki M, Damdimopoulou P, Chatzimeletiou K, Grimbizis GF, Tarlatzis BC, Syrrou M, Lambropoulos A. In-utero stress and mode of conception: impact on regulation of imprinted genes, fetal development and future health. *Human Reproduction Update*. 2019;25(6):777-801. doi: 10.1093/humupd/dmz025.

SUPPLEMENTARY TABLES

Table S1. Estimated marginal means (emmeans) of sham and IUGR rat offspring body weights (g) over time in the first (F1), second (F2) and third (F3) generations (paternal line). SE: standard error. Degrees-of-freedom method: Kenward-Roger. Confidence level used: 95%. PN: postnatal day, mo: months of age. Significance was determined by a linear mixed-effect model with adjustment for litter size, relatedness of litter siblings (if present), and repeated measurement. A Tukey's *post hoc* test would be used in the subsequent analysis if there was an interaction between treatment and time point effects. *** $P < 0.001$, ** $P < 0.01$. Time point effect: **Supplementary data (Appendix B)**. Only male offspring (paternal) was investigated in the F1 generation. N/A: test not applicable.

Generation	Time point	Weight (males)				Treatment_Timepoint interaction (Type II Wald chisquare tests)	Tukey's <i>post hoc</i> test (Sham males vs. IUGR males)	Weight (females)				Treatment_Timepoint interaction (Type II Wald chisquare tests)	Tukey's <i>post hoc</i> test (Sham females vs. IUGR females)
		Sham		IUGR				Sham		IUGR			
		Emmean	SE	Emmean	SE			Emmean	SE	Emmean	SE		
F1	Birth (PN1)	3.19	4.19	3.06	3.66	< 2.20 x 10 ⁻¹⁶ ***	1	N/A				N/A	N/A
	PN7	10.05	3.83	10.39	3.42		1						
	PN14	23.25	3.69	19.02	3.39		0.970						
	PN35	86.86	3.69	76.84	3.38		0.240						
	2mo	245.86	3.82	193.99	3.62		< 0.001***						
	3mo	316.38	3.60	280.97	3.42		< 0.001***						
	4mo	360.44	3.78	331.65	3.31		< 0.001***						
	6mo	414.41	3.57	373.88	3.23		< 0.001***						
	9mo	449.62	3.60	405.46	3.34		< 0.001***						
12mo	473.02	3.61	419.14	3.42	< 0.001***								
F2	Birth (PN1)	4.20	3.93	4.37	3.49	1.02 x 10 ⁻⁵ ***	1	2.98	1.81	4.94	1.82	0.004***	0.985
	PN7	9.10	2.78	10.62	2.63		1	9.72	1.32	10.11	1.24		1
	PN14	21.53	2.91	23.57	2.67		0.999	21.85	1.31	22.62	1.24		0.999
	PN35	86.65	2.88	88.31	2.63		1	79.03	1.34	77.88	1.25		0.989
	2mo	218.38	2.85	219.55	2.92		1	159.72	1.34	165.45	1.33		0.001**
	4mo	350.90	2.97	362.68	2.96		0.004**	221.53	1.37	225.16	1.32		0.126
	6mo	400.11	2.98	413.84	2.79		0.0002***	239.07	1.39	243.13	1.32		0.065
	9mo	454.84	3.37	450.65	2.98		0.939	253.17	1.63	255.90	1.56		0.746
	12mo	484.14	3.65	477.20	2.98		0.542	258.54	1.71	261.31	1.88		0.867
16mo	513.852	4.2	507.86	3.77919	0.920	N/A				N/A	N/A		
F3	Birth (PN1)	4.66	3.41	4.12	3.45	9.05 x 10 ⁻⁷ ***	1	4.27	2.27	3.64	2.12	0.859	N/A
	PN7	10.79	2.12	10.88	2.11		1	10.41	1.54	10.38	1.52		
	PN14	23.53	2.17	23.92	2.05		1	22.88	1.48	23.16	1.50		
	PN35	86.94	2.20	86.77	2.03		1	77.81	1.44	78.33	1.48		

2mo	222.81	2.35	235.67	2.23	<0.001***	169.05	1.52	169.41	1.53		
4mo	359.72	2.27	359.03	2.10	1	231.96	2.10	232.62	1.55		
6mo	409.32	2.27	408.70	2.11	1	246.74	1.50	250.05	1.57		
9mo	451.92	2.59	445.21	2.52	0.340	255.47	1.80	257.37	1.84		
12mo	472.04	2.63	466.64	2.44	0.600	262.65	2.27	263.15	2.20		
16mo	493.34	3.55	483.41	3.09	0.220	N/A			N/A	N/A	N/A

Table S2. Estimated marginal means (emmeans) of sham and IUGR rat offspring responses to Insulin Challenge (IC) in the second (F2) and third (F3) generations (paternal line), at 6 (6mo) and 12 (12mo) months of age. Basal value was determined to be at 0 minute (prior to the insulin injection). SE: standard error. Degrees-of-freedom method: Kenward-Roger. Confidence level used: 95%. Significance was determined by a linear mixed-effect model with adjustment for litter size, relatedness of litter siblings (if present), and repeated measurement. A Tukey's *post hoc* test would be used in the subsequent analysis if there was an interaction between treatment and time point effects. *** $P < 0.001$, * $P < 0.05$. Time point effect: **Supplementary data (Appendix B)**. N/A: test not applicable.

Generation	Age	Response	Males				Treatment_Timepoint interaction (Type II Wald chisquare tests)	Tukey's <i>post hoc</i> test (Sham males vs. IUGR males)	Females				Treatment_Timepoint interaction (Type II Wald chisquare tests)	Tukey's <i>post hoc</i> test (Sham females vs. IUGR females)
			Sham		IUGR				Sham		IUGR			
			Emmean	SE	Emmean	SE			Emmean	SE	Emmean	SE		
F2	6mo	IC plasma glucose basal	5.56	0.31	6.24	0.28	0.470	N/A	5.90	0.29	5.85	0.26	0.170	N/A
		IC plasma glucose 20min	2.92	0.31	3.85	0.28			2.92	0.29	2.32	0.26		
		IC plasma glucose 40min	2.66	0.31	2.96	0.28			2.43	0.29	2.56	0.26		
		IC plasma glucose 60min	3.09	0.31	3.44	0.28			2.76	0.29	3.09	0.26		
		IC plasma glucose 90min	3.47	0.31	3.92	0.29			3.52	0.29	2.96	0.26		
	12mo	IC plasma glucose basal	7.93	0.43	8.56	0.47	0.42	N/A	7.63	0.33	7.23	0.34	0.804	N/A
		IC plasma glucose 20min	4.44	0.44	4.84	0.47			3.28	0.33	3.28	0.37		
		IC plasma glucose 40min	3.52	0.43	3.58	0.47			2.62	0.33	2.92	0.34		
		IC plasma glucose 60min	3.95	0.43	3.49	0.47			2.87	0.33	3.09	0.34		
		IC plasma glucose 90min	3.81	0.44	3.84	0.48			3.67	0.33	3.94	0.34		

F3	6mo	IC plasma glucose basal	7.75	0.32	6.54	0.30	0.0003***	0.0173*	6.82	0.40	6.41	0.56	0.525	N/A
		IC plasma glucose 20min	3.49	0.32	4.09	0.30		0.499	2.61	0.40	3.24	0.56		
		IC plasma glucose 40min	2.80	0.32	3.09	0.30		0.945	2.60	0.40	2.81	0.56		
		IC plasma glucose 60min	3.39	0.32	3.59	0.30		0.988	3.20	0.40	3.12	0.56		
		IC plasma glucose 90min	3.63	0.32	4.22	0.30		0.522	3.45	0.40	3.69	0.56		
	12mo	IC plasma glucose basal	8.11	0.48	8.47	0.44	0.303	N/A	6.82	0.40	6.97	0.37	0.738	N/A
		IC plasma glucose 20min	4.72	0.48	5.62	0.44			3.13	0.40	3.38	0.37		
		IC plasma glucose 40min	3.61	0.48	3.32	0.44			2.80	0.40	2.46	0.37		
		IC plasma glucose 60min	3.69	0.48	3.21	0.44			2.76	0.40	2.54	0.37		
		IC plasma glucose 90min	3.78	0.48	3.83	0.44			3.63	0.40	3.04	0.37		

Table S3. Estimated marginal means (emmeans) of sham and IUGR rat offspring Insulin Challenge (IC) assessments in the second (F2) and third (F3) generations (paternal line), at 6 (6mo) and 12 (12mo) months of age. Glucose area under curve (AUC) was calculated as the total AUC from basal (prior to insulin injection) to 90 minutes (post-insulin injection). SE: standard error. Degrees-of-freedom method: Kenward-Roger. Confidence level used: 95%. Significance was determined by a linear mixed-effect model with adjustment for litter size and relatedness of litter siblings (if present). Time point effect: **Supplementary data (Appendix B)**. N/A: test not applicable.

Generation	Age	Calculation	Males				Treatment effect (Sham males vs. IUGR males)	Females				Treatment effect (Sham females vs. IUGR females)
			Sham		IUGR			Sham		IUGR		
			Emmean	SE	Emmean	SE		Emmean	SE	Emmean	SE	
F2	6mo	IC plasma glucose AUC	321.67	20.39	329.92	16.79	0.695	288.32	18.68	277.74	14.86	0.599
	12mo	IC plasma glucose AUC	385.21	31.54	391.07	35.40	0.879	322.20	15.38	337.00	16.40	0.453
F3	6mo	IC plasma glucose AUC	342.52	20.30	362.23	18.25	0.431	304.20	25.25	318.44	41.88	0.631
	12mo	IC plasma glucose AUC	393.96	33.56	401.23	28.11	0.837	310.36	24.20	295.62	22.24	0.621

SUPPLEMENTARY FIGURES

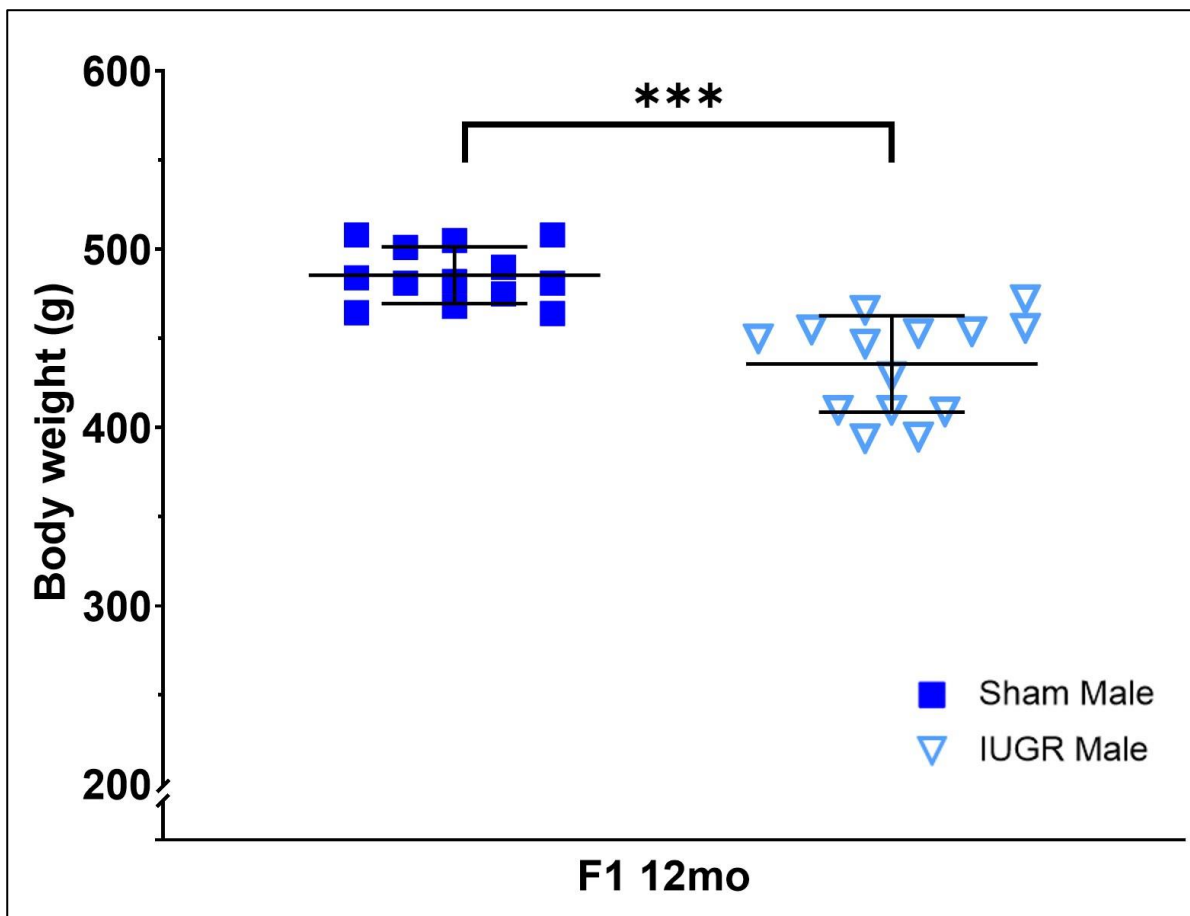


Figure S1. Postmortem body weight of sham and IUGR male rat offspring (paternal line) in the first generation (F1), at 12 months of age (12mo). Significance was determined by a linear mixed-effect model with adjustment for litter size and relatedness of litter siblings (if present). *** $P < 0.001$.

See **Table 3** for exact P -value. Data is expressed as mean \pm SD; $n = 13$ -14 samples per group.

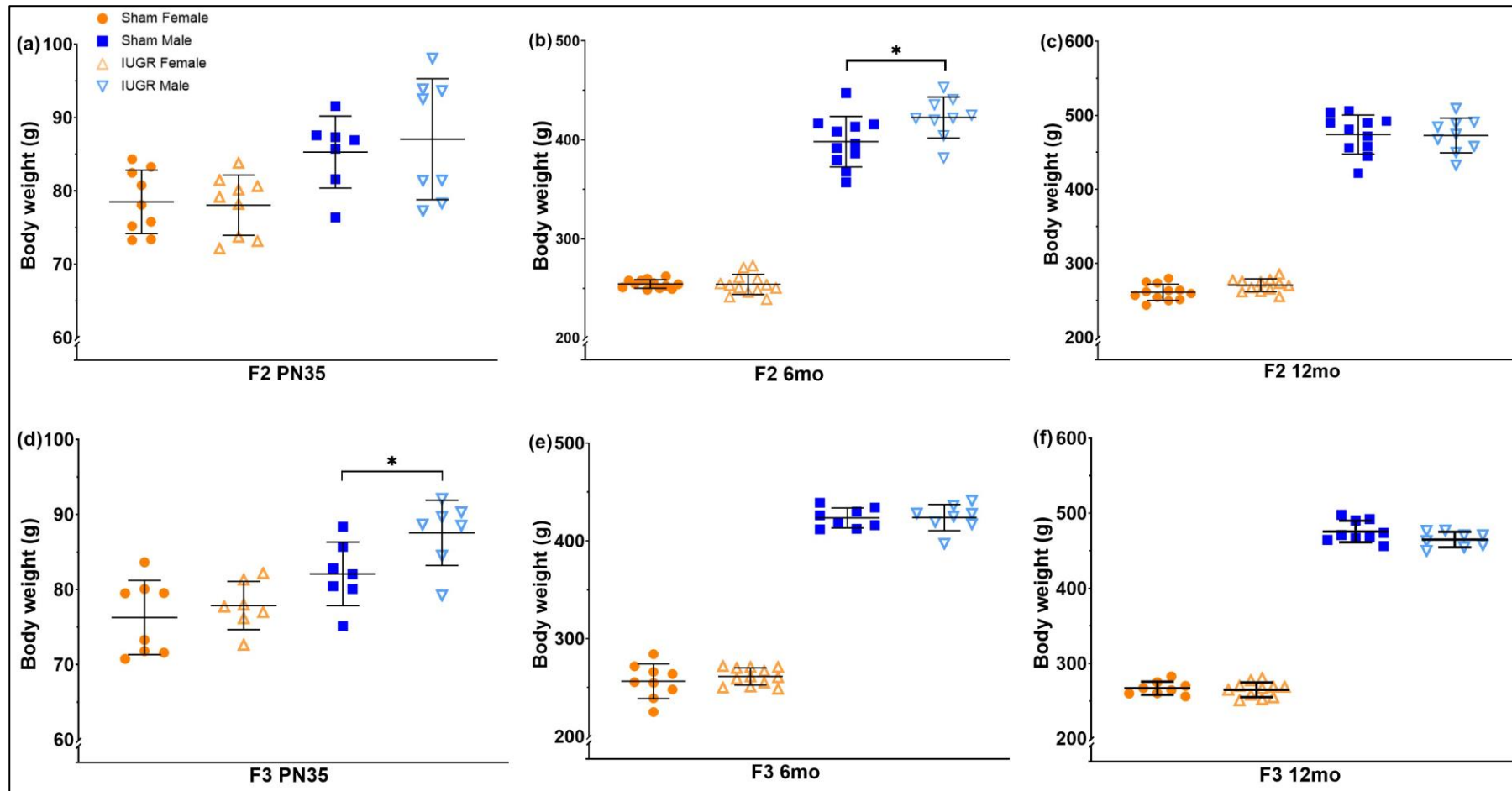


Figure S2. Postmortem body weight of sham and IUGR rat offspring (paternal line) in the second (F2) and third (F3) generations, at postnatal day 35 (PN35), 6 (6mo) and 12 (12mo) months of age. Significance was determined by a linear mixed-effect model with adjustment for litter size and relatedness of litter siblings (if present). * $P < 0.05$. See **Tables 4 and 5** for exact P -values. Data is expressed as mean \pm SD; $n = 7$ -13 samples per group.

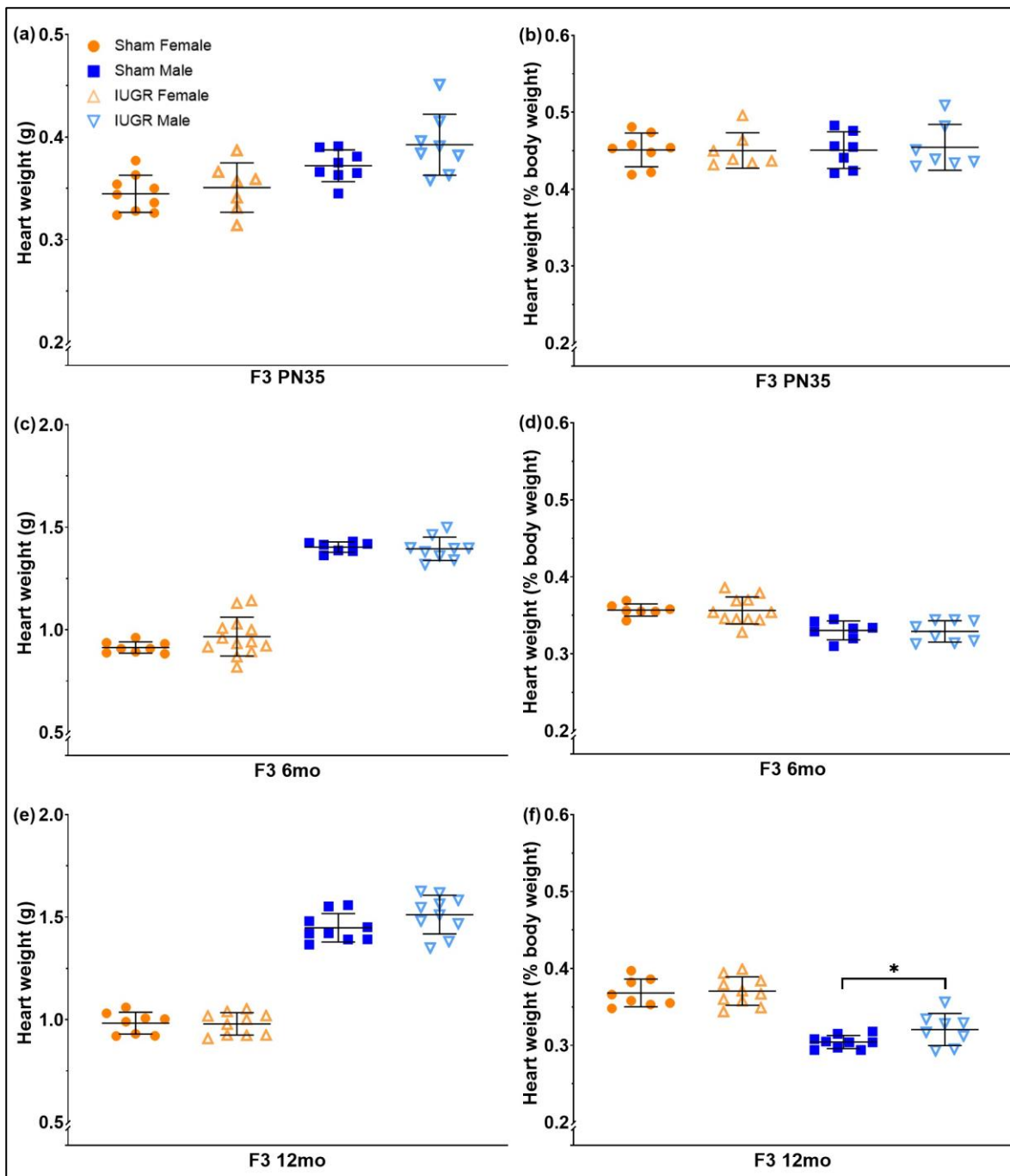


Figure S3. Postmortem heart weights (absolute vs. % body weight) of sham and IUGR rat offspring (paternal line) in the third generation (F3), at postnatal day 35 (PN35; a, b), 6 (6mo; c,d) and 12 (12mo; e, f) months of age. Significance was determined by a linear mixed-effect model with adjustment for litter size and relatedness of litter siblings (if present). * $P < 0.05$. See **Table 5** for exact P -values. Data is expressed as mean \pm SD; $n = 7$ -13 samples per group.

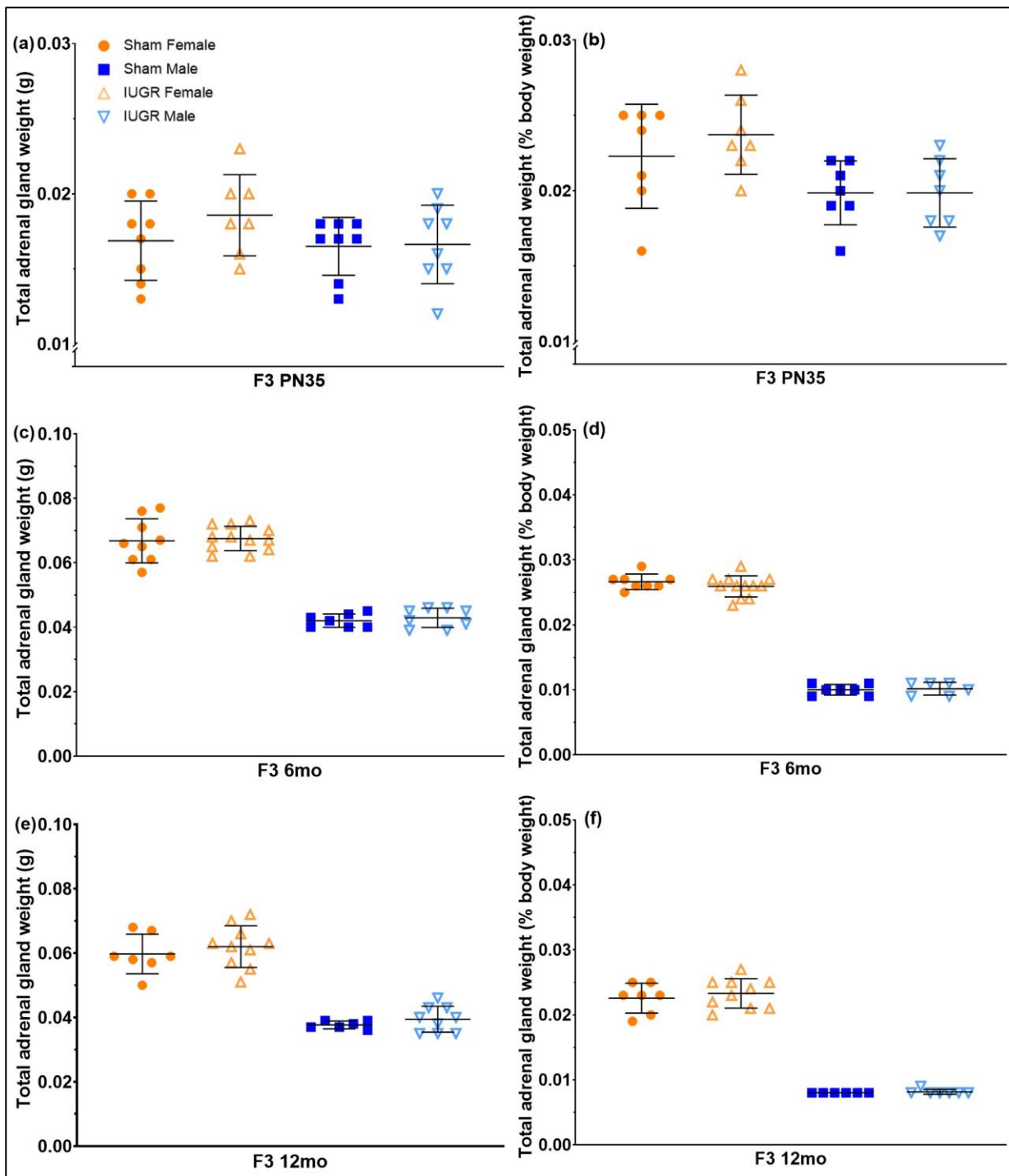


Figure S4. Postmortem total adrenal gland weights (absolute vs. % body weight) of sham and IUGR rat offspring (paternal line) in the third generation (F3), at postnatal day 35 (PN35; a, b), 6 (6mo; c,d) and 12 (12mo; e, f) months of age. Significance was determined by a linear mixed-effect model with adjustment for litter size and relatedness of litter siblings (if present). See **Table 5** for exact *P*-values. Data is expressed as mean \pm SD; *n* = 6-12 samples per group.

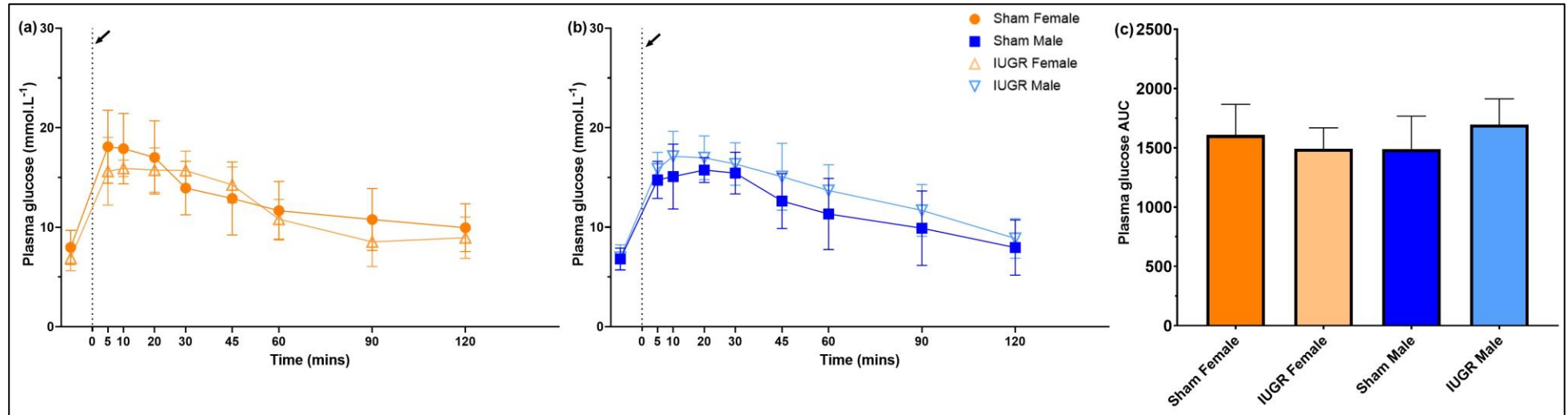


Figure S5. Plasma glucose profile during the Glucose Tolerance Test (GTT) of sham and IUGR rat offspring (paternal line) in the second generation (F2), at 6 months of age. The black arrow indicates when glucose injection occurred. Fasting (basal) value was calculated as the average of the two time points: 10 and 5 minutes prior to the glucose injection. Comparisons were made between sham and IUGR offspring, within each sex (females, a, and males, b). Glucose area under curve (AUC, c) was calculated as the total AUC from basal to 120 minutes. Significance was determined by a linear mixed-effect model with adjustment for litter size, relatedness of litter siblings (if present), and repeated measurement (for plasma glucose responses (a, b) only). See **Tables 7 and 8** for exact *P*-values. Time point effect: **Supplementary data (Appendix B)**. Data is expressed as mean \pm SD; $n = 7$ -10 samples per group.

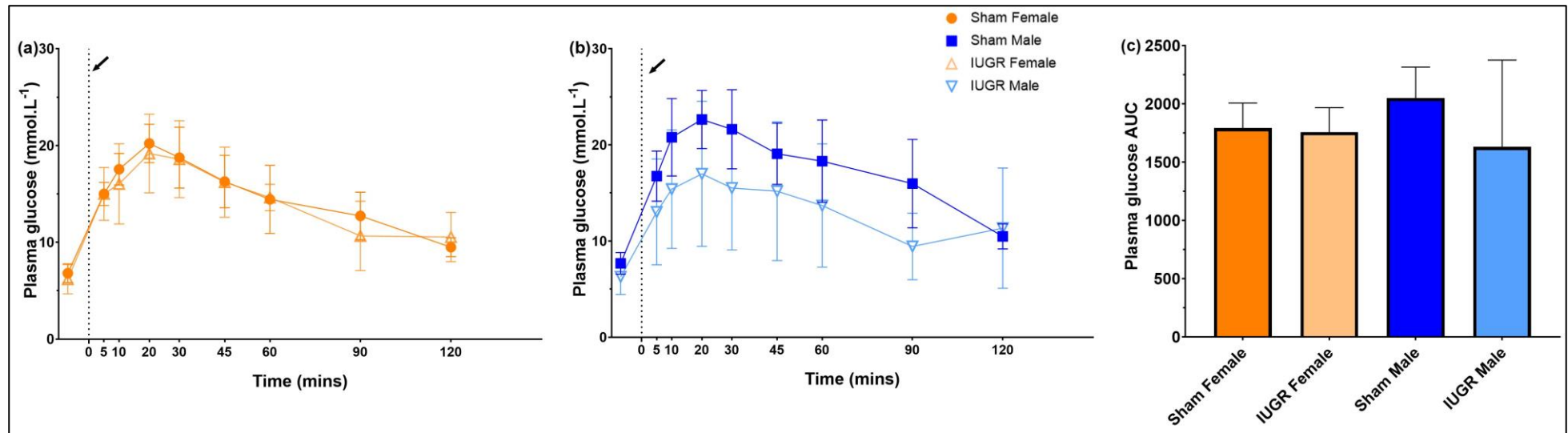


Figure S6. Plasma glucose profile during the Glucose Tolerance Test (GTT) of sham and IUGR rat offspring (paternal line) in the second generation (F2), at 12 months of age. The black arrow indicates when glucose injection occurred. Fasting (basal) value was calculated as the average of the two time points: 10 and 5 minutes prior to the glucose injection. Comparisons were made between sham and IUGR offspring, within each sex (females, a, and males, b). Glucose area under curve (AUC, c) was calculated as the total AUC from basal to 120 minutes. Significance was determined by a linear mixed-effect model with adjustment for litter size, relatedness of litter siblings (if present), and repeated measurement (for plasma glucose responses (a, b) only). See **Tables 7 and 8** for exact *P*-values. Time point effect: **Supplementary data (Appendix B)**. Data is expressed as mean \pm SD; $n = 8$ samples per group.

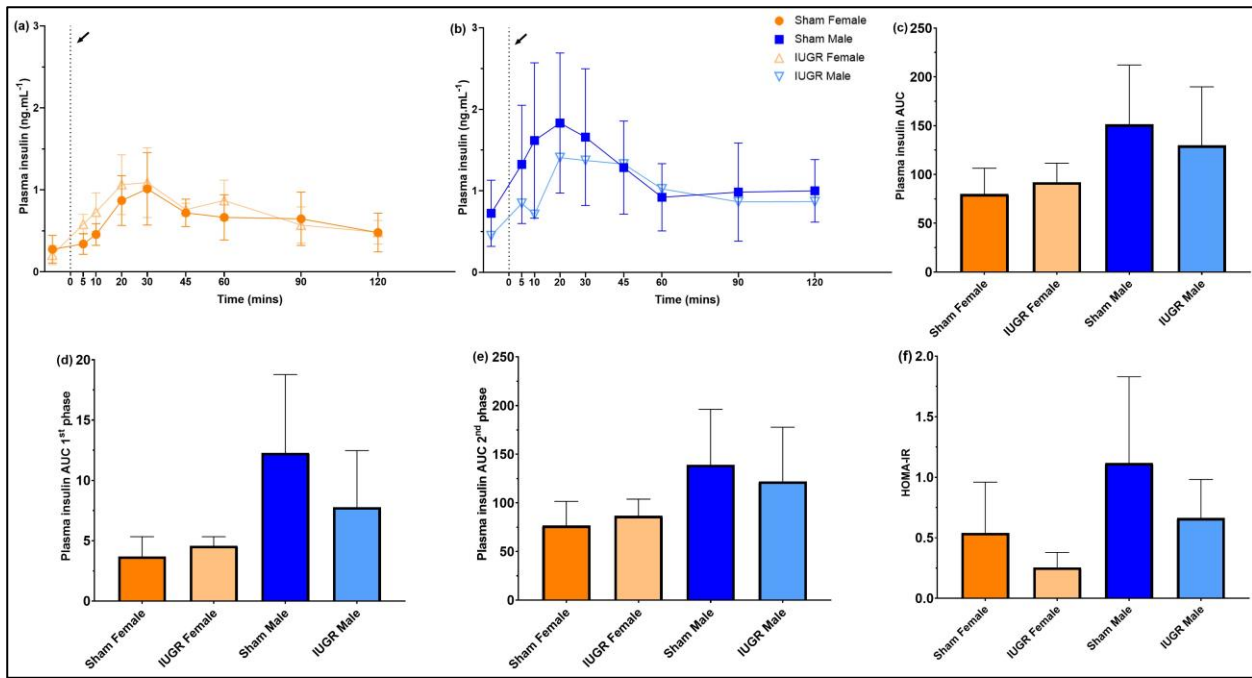


Figure S7. Plasma insulin profile during the Glucose Tolerant Test (GTT) of sham and IUGR rat offspring (paternal line) in the second generation (F2), at 6 months of age. The black arrow indicates when glucose injection occurred. Fasting (basal) value was calculated as the average of the two time points: 10 and 5 minutes prior to the glucose injection. Comparisons were made between sham and IUGR offspring, within each sex (females, a, and males, b). Insulin area under curve (AUC) was calculated as the total AUC from basal to 120 minutes (c), AUC from basal to 5 minutes (1st phase, d), and AUC from 5 to 120 minutes (2nd phase, e). Rat offspring homeostasis model of assessment of insulin resistance (HOMA-IR, f) was calculated using the formula: $(fasting\ insulin\ (\mu U.mL^{-1}) \times fasting\ glucose\ (mg.dL^{-1})) \div 2430$. Significance was determined by a linear mixed-effect model with adjustment for litter size, relatedness of litter siblings (if present), and repeated measurement (for plasma insulin responses (a, b) only). See **Tables 7 and 8** for exact *P*-values. Time point effect: **Supplementary data (Appendix B)**. Data is expressed as mean \pm SD; n = 7-9 samples per group.

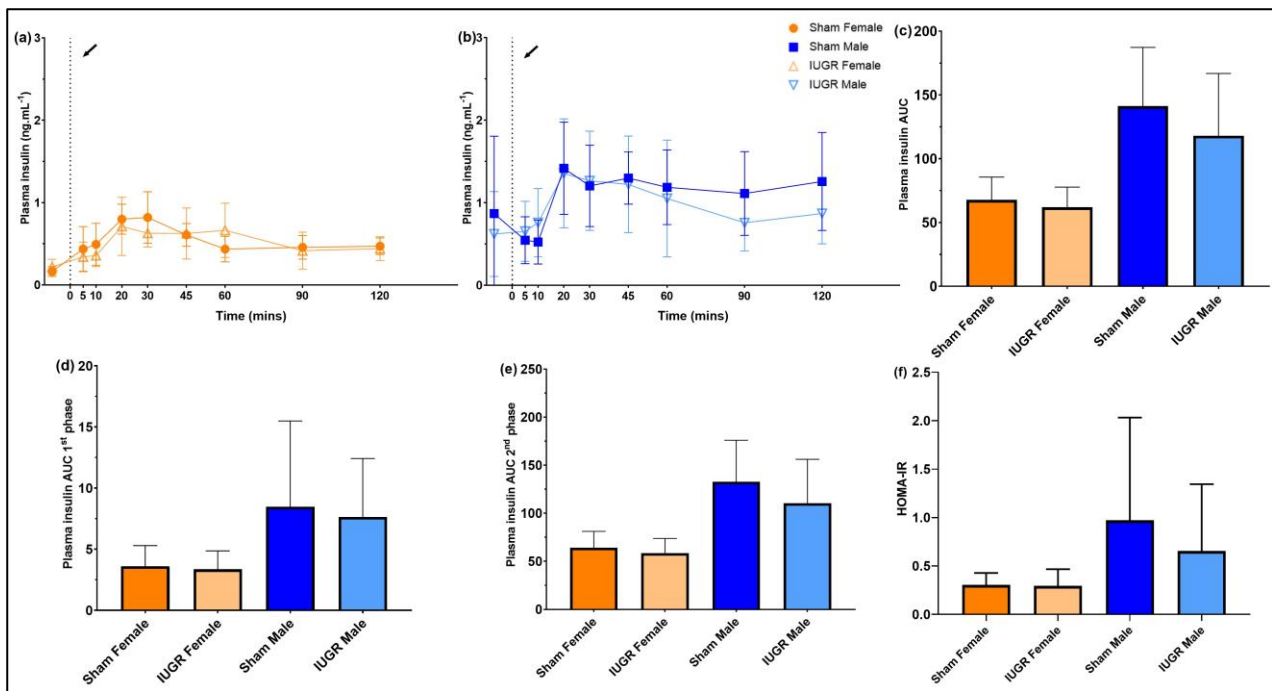


Figure S8. Plasma insulin profile during the Glucose Tolerant Test (GTT) of sham and IUGR rat offspring (paternal line) in the second generation (F2), at 12 months of age. The black arrow indicates when glucose injection occurred. Fasting (basal) value was calculated as the average of the two time points: 10 and 5 minutes prior to the glucose injection. Comparisons were made between sham and IUGR offspring, within each sex (females, a, and males, b). Insulin area under curve (AUC) was calculated as the total AUC from basal to 120 minutes (c), AUC from basal to 5 minutes (1st phase, d), and AUC from 5 to 120 minutes (2nd phase, e). Rat offspring homeostasis model of assessment of insulin resistance (HOMA-IR, f) was calculated using the formula: $(fasting\ insulin\ (\mu U.mL^{-1}) \times fasting\ glucose\ (mg.dL^{-1})) \div 2430$. Significance was determined by a linear mixed-effect model with adjustment for litter size, relatedness of litter siblings (if present), and repeated measurement (for plasma insulin responses (a, b) only). See **Tables 7 and 8** for exact *P*-values. Time point effect: **Supplementary data (Appendix B)**. Data is expressed as mean \pm SD; *n* = 8-10 samples per group.

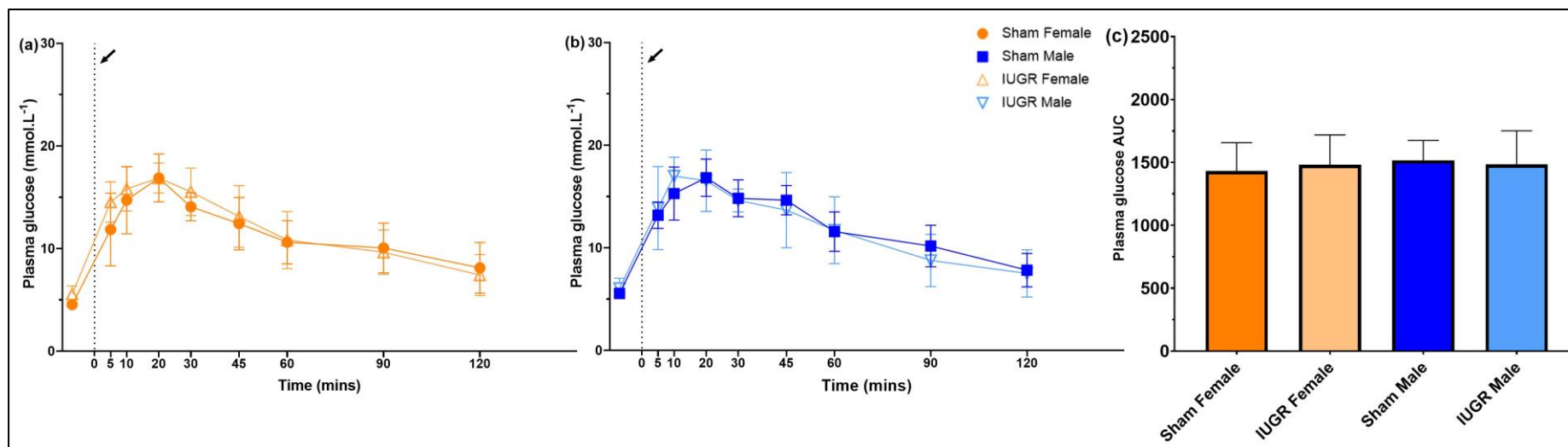


Figure S9. Plasma glucose profile during the Glucose Tolerance Test (GTT) of sham and IUGR rat offspring (paternal line) in the third generation (F3), at 6 months of age. The black arrow indicates when glucose injection occurred. Fasting (basal) value was calculated as the average of the two time points: 10 and 5 minutes prior to the glucose injection. Comparisons were made between sham and IUGR offspring, within each sex (females, a, and males, b). Glucose area under curve (AUC, c) was calculated as the total AUC from basal to 120 minutes. Significance was determined by a linear mixed-effect model with adjustment for litter size, relatedness of litter siblings (if present), and repeated measurement (for plasma glucose responses (a, b) only). See **Tables 7 and 8** for exact *P*-values. Time point effect: **Supplementary data (Appendix B)**. Data is expressed as mean \pm SD; *n* = 5-7 samples per group.

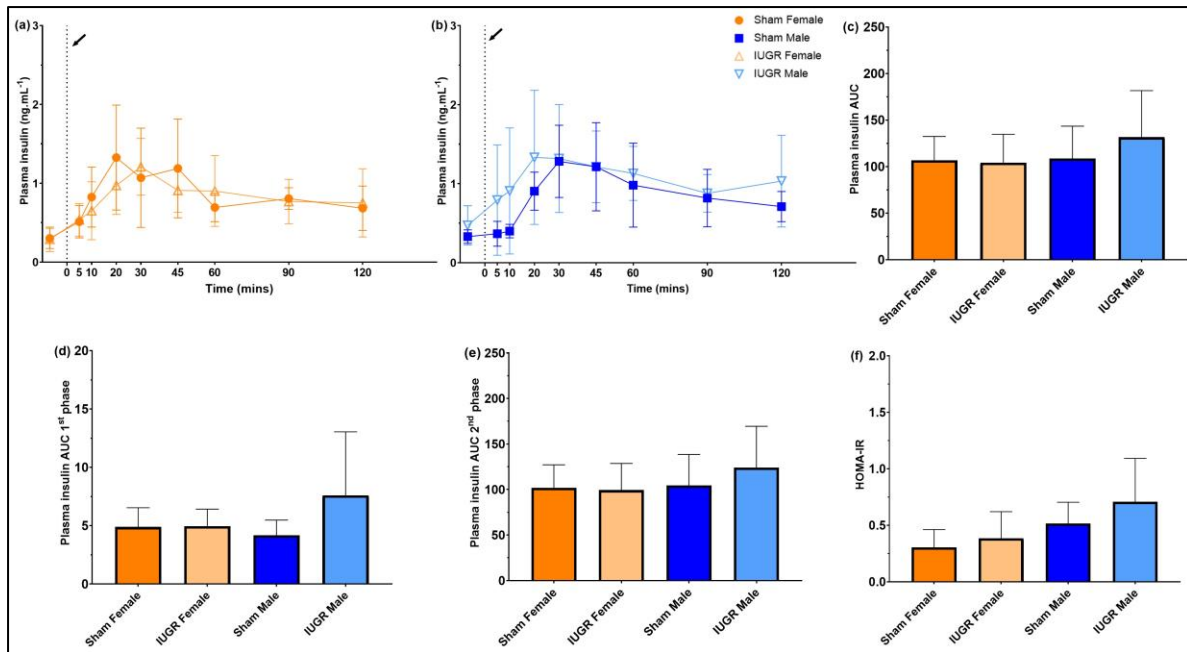


Figure S10. Plasma insulin profile during the Glucose Tolerant Test (GTT) of sham and IUGR rat offspring (paternal line) in the third generation (F3), at 6 months of age. The black arrow indicates when glucose injection occurred. Fasting (basal) value was calculated as the average of the two time points: 10 and 5 minutes prior to the glucose injection. Comparisons were made between sham and IUGR offspring, within each sex (females, a, and males, b). Insulin area under curve (AUC) was calculated as the total AUC from basal to 120 minutes (c), AUC from basal to 5 minutes (1st phase, d), and AUC from 5 to 120 minutes (2nd phase, e). Rat offspring homeostasis model of assessment of insulin resistance (HOMA-IR, f) was calculated using the formula: $(fasting\ insulin\ (\mu U.mL^{-1}) \times fasting\ glucose\ (mg.dL^{-1})) \div 2430$. Significance was determined by a linear mixed-effect model with adjustment for litter size, relatedness of litter siblings (if present), and repeated measurement (for plasma insulin responses (a, b) only). See **Tables 7 and 8** for exact *P*-values. Time point effect: **Supplementary data (Appendix B)**. Data is expressed as mean \pm SD; n = 5-7 samples per group.

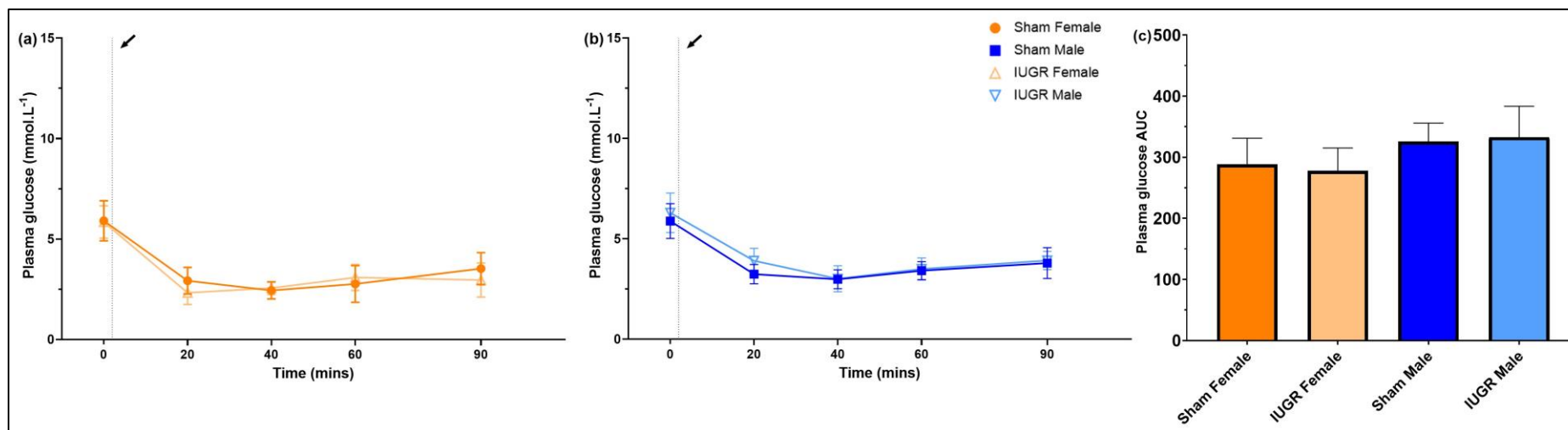


Figure S11. Plasma glucose profile during the Insulin Challenge (IC) of sham and IUGR rat offspring (paternal line) in the second generation (F2), at 6 months of age. The black arrow indicates when insulin injection occurred. Basal value was determined to be at 0 minute (prior to the insulin injection). Comparisons were made between sham and IUGR offspring, within each sex (females, a, and males, b). Glucose area under curve (AUC, c) was calculated as the total AUC from basal to 90 minutes. Significance was determined by a linear mixed-effect model with adjustment for litter size, relatedness of litter siblings (if present), and repeated measurement (for plasma glucose responses (a, b) only). See **Tables S2 and S3** for exact *P*-values. Time point effect: **Supplementary data (Appendix B)**. Data is expressed as mean \pm SD; $n = 7-8$ samples per group.

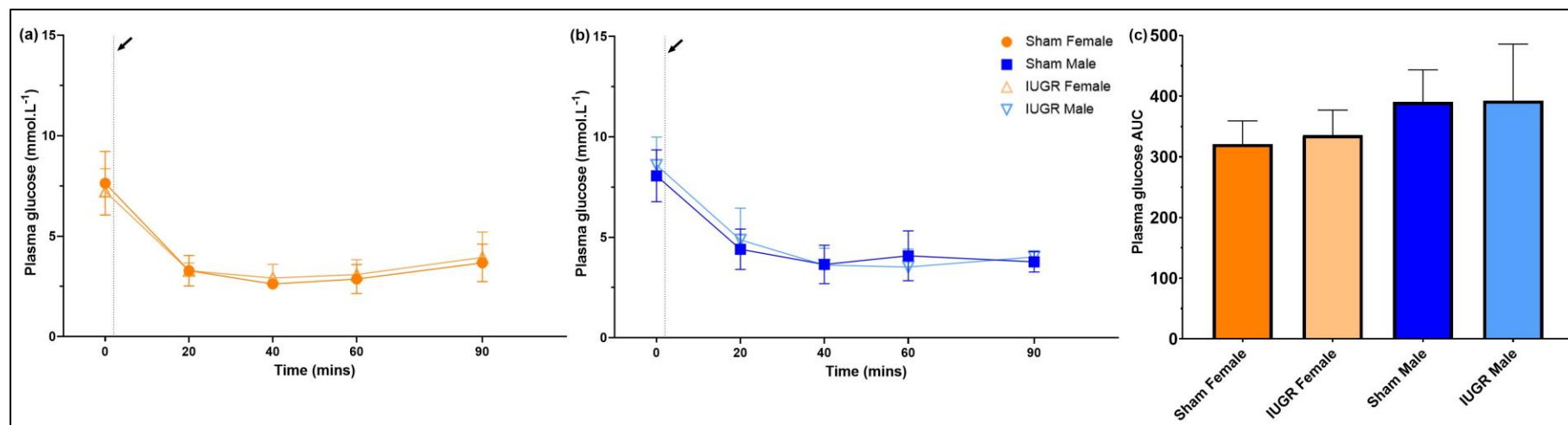


Figure S12. Plasma glucose profile during the Insulin Challenge (IC) of sham and IUGR rat offspring (paternal line) in the second generation (F2), at 12 months of age. The black arrow indicates when insulin injection occurred. Basal value was determined to be at 0 minute (prior to the insulin injection). Comparisons were made between sham and IUGR offspring, within each sex (females, a, and males, b). Glucose area under curve (AUC, c) was calculated as the total AUC from basal to 90 minutes. Significance was determined by a linear mixed-effect model with adjustment for litter size, relatedness of litter siblings (if present), and repeated measurement (for plasma glucose responses (a, b) only). See **Tables S2 and S3** for exact *P*-values. Time point effect: **Supplementary data (Appendix B)**. Data is expressed as mean \pm SD; *n* = 7-8 samples per group.

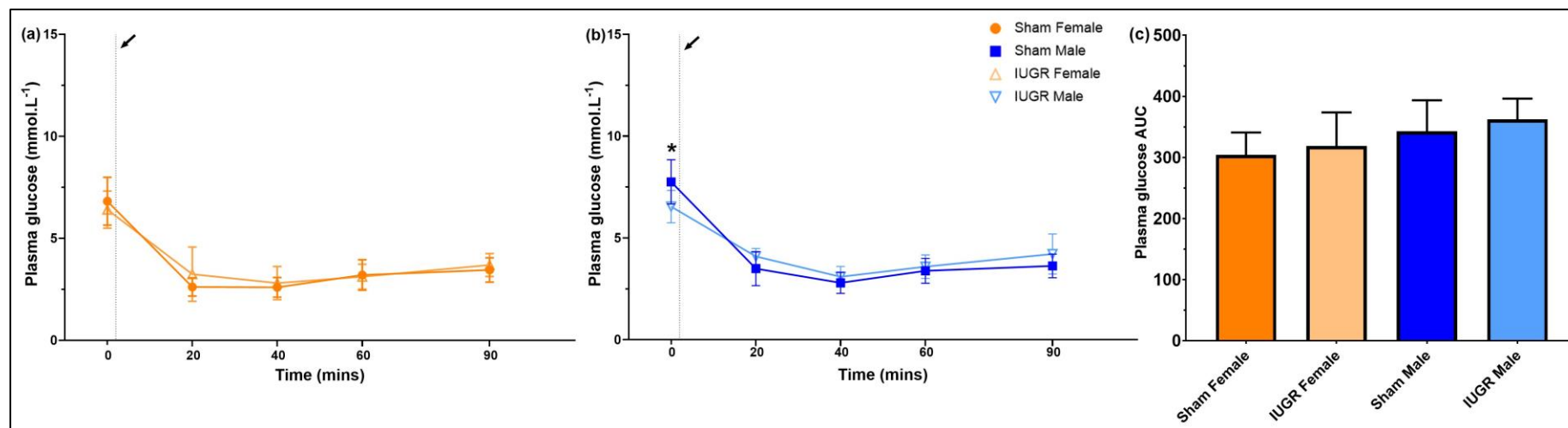


Figure S13. Plasma glucose profile during the Insulin Challenge (IC) of sham and IUGR rat offspring (paternal line) in the third generation (F3), at 6 months of age. The black arrow indicates when insulin injection occurred. Basal value was determined to be at 0 minute (prior to the insulin injection). Comparisons were made between sham and IUGR offspring, within each sex (females, a, and males, b). Glucose area under curve (AUC, c) was calculated as the total AUC from basal to 90 minutes. Significance was determined by a linear mixed-effect model with adjustment for litter size, relatedness of litter siblings (if present), and repeated measurement (for plasma glucose responses (a, b) only). * $P < 0.05$. See **Tables S2 and S3** for exact P -values. Time point effect: **Supplementary data (Appendix B)**. Data is expressed as mean \pm SD; $n = 5$ -6 samples per group.

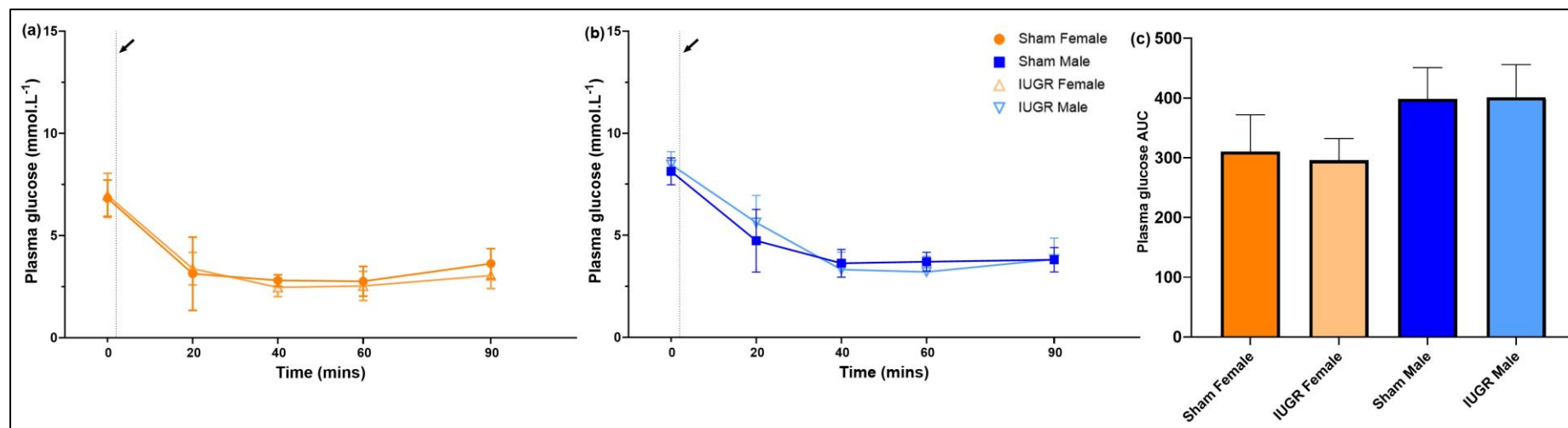


Figure S14. Plasma glucose profile during the Insulin Challenge (IC) of sham and IUGR rat offspring (paternal line) in the third generation (F3), at 12 months of age. The black arrow indicates when insulin injection occurred. Basal value was determined to be at 0 minute (prior to the insulin injection). Comparisons were made between sham and IUGR offspring, within each sex (females, a, and males, b). Glucose area under curve (AUC, c) was calculated as the total AUC from basal to 90 minutes. Significance was determined by a linear mixed-effect model with adjustment for litter size, relatedness of litter siblings (if present), and repeated measurement (for plasma glucose responses (a, b) only). See **Tables S2 and S3** for exact *P*-values. Time point effect: **Supplementary data (Appendix B)**. Data is expressed as mean \pm SD; n = 5-6 samples per group.

CHAPTER 5

UTEROPLACENTAL

INSUFFICIENCY RESULTS IN AN

INCREASED RISK OF

DEVELOPING RENAL

DYSFUNCTION ACROSS

GENERATIONS IN THE

PATERNAL LINE OF GROWTH

RESTRICTED RATS

Statement of Authorship

Statement of Authorship

Title of Paper	Uteroplacental insufficiency results in an increased risk of developing renal dysfunction across generations in the paternal line of growth restricted rats	
Publication Status	<input type="checkbox"/> Published	<input type="checkbox"/> Accepted for Publication
	<input type="checkbox"/> Submitted for Publication	<input checked="" type="checkbox"/> Unpublished and Unsubmitted work written in manuscript style
Publication Details	Doan, T.N.A. , Cowley, M. J., Phillips, L. A., Briffa, F. J., Burton, A. R., Romano, T., Wlodek, E. M., & Bianco-Miotto, T. (2023). Uteroplacental insufficiency results in an increased risk of developing renal dysfunction across generations in the paternal line of growth restricted rats. <u>Target journal</u> : <i>The Journal of Physiology</i>	

Principal Author

Name of Principal Author (Candidate)	Ngoc Anh Thu Doan		
Contribution to the Paper	Analysed the data and wrote the manuscript		
Overall percentage (%)	70		
Certification:	This paper reports on original research I conducted during the period of my Higher Degree by Research candidature and is not subject to any obligations or contractual agreements with a third party that would constrain its inclusion in this thesis. I am the primary author of this paper.		
Signature		Date	13.11.2023

Co-Author Contributions

By signing the Statement of Authorship, each author certifies that:

- i. the candidate's stated contribution to the publication is accurate (as detailed above);
- ii. permission is granted for the candidate to include the publication in the thesis; and

C1 - Internal use

iii. the sum of all co-author contributions is equal to 100% less the candidate's stated contribution.

Name of Co-Author	James M. Cowley		
Contribution to the Paper	Contributed to statistical analyses and critical review and revision of the manuscript		
Signature		Date	13.11.2023

Name of Co-Author	Aaron L. Phillips		
Contribution to the Paper	Contributed to statistical analyses and critical review and revision of the manuscript		
Signature		Date	13.11.2023

Name of Co-Author	Jessica F. Briffa		
Contribution to the Paper	Generated the animal model tissues, acquired animal tissues and phenotypic data, provided tissue and phenotypic data, critical review of the manuscript		
Signature		Date	13.11.2023

Name of Co-Author	Rachel A. Burton		
Contribution to the Paper	Provided intellectual input and resources, critical review of the manuscript		
Signature		Date	13.11.23

C1 - Internal use

Name of Co-Author	Tania Romano		
Contribution to the Paper	Contributed to generation of animal tissues, and critical review of the manuscript		
Signature		Date	13.11.2023

Name of Co-Author	Mary E. Wlodek		
Contribution to the Paper	Generated the animal model, acquired animal tissues and phenotypic data, provided tissue and phenotypic data, contributed to study design, critical review of the manuscript		
Signature		Date	13.11.2023

Name of Co-Author	Tina Bianco-Miotto		
Contribution to the Paper	Supervised the project, critical review and revision of the manuscript		
Signature		Date	13.11.2023

C1 - Internal use

Abstract

We have previously reported that there were morphological signs of cardio-renal dysfunction in the paternal line of intrauterine growth restricted (IUGR) rats, including altered blood pressure and relative total kidney weight of males in the second (F2) generation, left ventricle hypertrophy and altered total kidney weight in F3 females, as well as left ventricle hypertrophy in F3 males. To investigate further into the kidney health of offspring, nephron number at postnatal day (PN) 35 and urinary electrolyte and protein excretions (24 hours) at 6 months of age (mo) and 12mo were examined. Nephron number was only reduced in F2 PN35 females (-3.48% compared to same-sex sham control). However, symptoms of reduced renal function at 6mo were mostly observed in F2 males (reduced urine Na⁺ (-9.53%) and total protein (-35.94%) excretions, reduced albumin/creatinine ratio (-43.51%), reduced creatinine clearance (-44.03%), and increased plasma creatinine (+11.62%)). Similar symptoms were also seen in the F3 females, suggesting the sex-specific and transgenerational developmental programming of chronic kidney disease risk. Some of the renal function alterations were also significant at 12mo time point. There was no significant difference between the kidney histology of IUGR and sham offspring, which remains to be explained. Nonetheless, these findings imply that the non-exposed offspring generations of IUGR in the paternal line might still inherit the renal disease risk and develop renal dysfunction later in life, independent of their nephron number. As the aberrant cardiovascular function is often linked to an abnormal functioning kidney (and vice versa), these animals also have a higher long-term risk of developing cardiovascular disease.

Results

Nephron number

Nephron number was previously shown to be reduced by 26-27% in F1 growth restricted males compared to sham males, at 6 months of age [1, 2]. There was no difference in 6mo relative kidney weight between the two groups [1]. In this current study, nephron number of F1 male offspring was significantly decreased in PN35 kidneys of F2 IUGR females (**Fig. 1**), but changes in nephron number were not seen in the F3 generation (**Fig. 2**). Despite having a similar kidney weight (% body weight) compared to the sham females ($P = 0.368$, **Table 1** and **Fig. 1c**), F2 IUGR females had a 3.48% decrease in nephron number (21188 ± 880 vs. 21951 ± 890 in sham, $P = 0.0007$, **Table 1** and **Fig. 1d**). Meanwhile, F3 IUGR females had significantly higher kidney weight (% body weight) compared to sham (0.42 ± 0.01 vs. 0.39 ± 0.01 , respectively, $P = 0.0005$, **Table 1** and **Fig. 2c**), but nephron numbers were similar ($P = 0.244$, **Table 1** and **Fig. 2d**). There was no difference in nephron number between IUGR and sham males at PN35, in either the F2 ($P = 0.768$) or F3 ($P = 0.611$) generation.

Table 1. Estimated marginal means (emmeans) of sham and IUGR rat offspring nephron number (obtained from the right kidney) in the second (F2) and third (F3) generations (paternal line), at postnatal day 35 (PN35). Right kidney weight (%) was calculated as a percentage of PN35 body weight. SE: standard error. Degrees-of-freedom method: Kenward-Roger. Confidence level used: 95%. Significance was determined by a linear mixed-effect model with adjustment for litter size and relatedness of litter siblings (if present). *** $P < 0.001$.

Generation	Time point	Measurement	Males				Treatment effect (Sham males vs. IUGR males)	Females				Treatment effect (Sham females vs. IUGR females)
			Sham		IUGR			Sham		IUGR		
			Emmean	SE	Emmean	SE		Emmean	SE	Emmean	SE	
F2	PN35	Body weight (g)	87.45	2.87	87.12	2.36	0.907	81.58	1.93	81.12	1.48	0.822
		Right kidney weight (g)	0.37	0.02	0.36	0.02	0.512	0.32	0.02	0.33	0.02	0.447
		Right kidney weight (%)	0.43	0.02	0.42	0.014	0.799	0.39	0.03	0.41	0.019	0.368
		Nephron number	19474	1157	19808	859	0.768	21951	890	21188	880	0.0007***
F3	PN35	Body weight (g)	84.62	2.46	85.93	2.22	0.611	77.94	1.69	78.74	1.62	0.704
		Right kidney weight (g)	0.34	0.01	0.36	0.01	0.159	0.31	0.004	0.33	0.004	0.0001***
		Right kidney weight (%)	0.40	0.01	0.42	0.01	0.054	0.39	0.01	0.42	0.01	0.0005***
		Nephron number	17526	1349	18288	1293	0.611	18626	771	19746	738	0.244

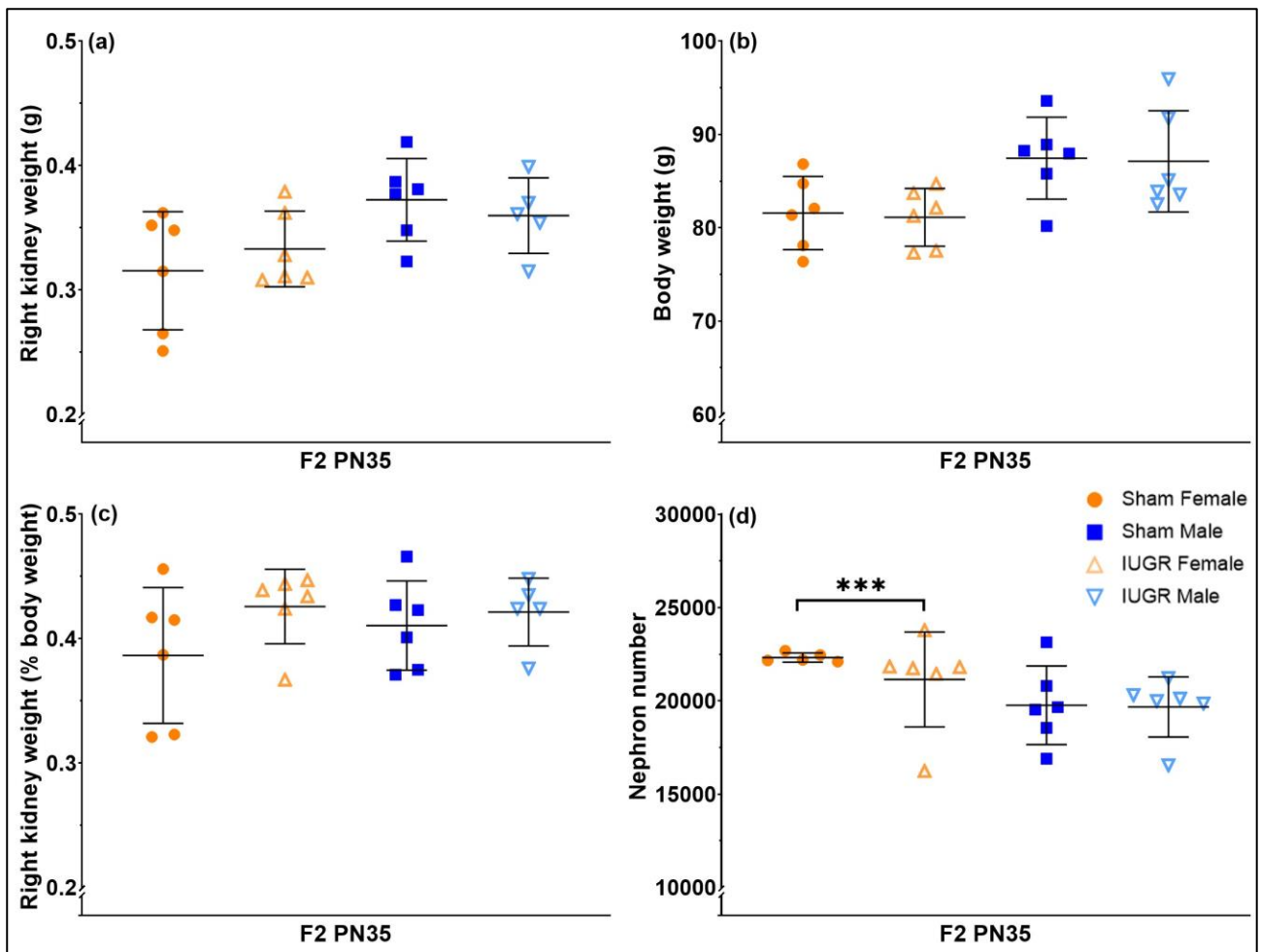


Figure 1. Nephron number obtained from the right kidney (postmortem; kidney absolute weight: a, offspring body weight: b, kidney weight (% body weight): c) of sham and IUGR rat offspring (paternal line) in the second generation (F2), at postnatal day 35 (PN35). Nephron number (d) was calculated using unbiased stereology (Gold Standard). *** $P < 0.001$. See **Table 1** for exact P -values. Data is expressed as mean \pm SD; n = 5-6 samples per group.

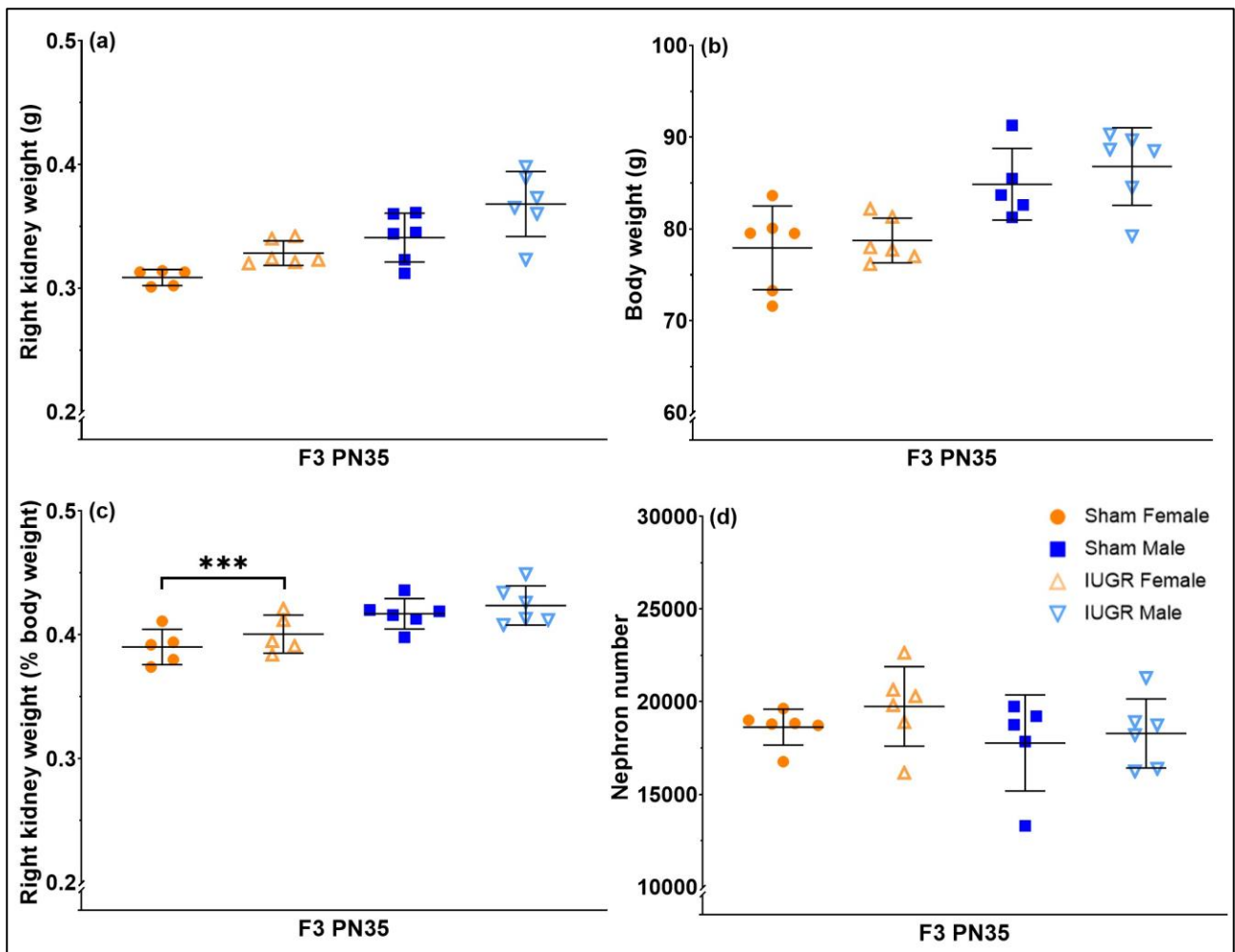


Figure 2. Nephron number obtained from the right kidney (postmortem; kidney absolute weight: a, offspring body weight: b, kidney weight (% body weight): c) of sham and IUGR rat offspring (paternal line) in the third generation (F3), at postnatal day 35 (PN35). Nephron number (d) was calculated using unbiased stereology (Gold Standard). *** $P < 0.001$. See **Table 1** for exact P -values. Data is expressed as mean \pm SD; n = 5-6 samples per group.

Renal function

Food intake, water intake and urine production during renal function examination (24 hours)

F2 IUGR male offspring had a 15.60% decrease in food intake at 6mo ($P = 0.026$, **Table 2** and **Fig. 3a**). At 12mo, female IUGR offspring had an increase in water intake (+19.69%, $P = 0.035$, **Table 2** and **Fig. 4b**). No change in volume of urine produced (**Fig. 3c and 4c**) and urine flow rate (**Fig. 3d and 4d**) between sham and IUGR was observed in the F2 generation, at 6mo or 12mo (**Table 2**).

In the F3 6mo animals, there was no significant difference in food intake (males $P = 0.200$, females $P = 0.882$), water intake (males $P = 0.108$, females $P = 0.987$), urine produced (males $P = 0.052$, females $P = 0.190$), or urine flow rate measured (males $P = 0.053$, females $P = 0.187$) (**Table 3** and **Fig. 5a-d**). However, at 12mo, there was a significant reduction in water intake (-24.29%, $P < 0.0001$), urine produced (-34.04%, $P = 0.0003$) and urine flow rate (-34.06%, $P = 0.0003$) in the F3 IUGR females (**Table 3** and **Fig. 6b-d**).

Table 2. Estimated marginal means (emmeans) of sham and IUGR rat offspring renal function measurements (24 hours) in the second (F2) generation (paternal line), at 6 (6mo) and 12 (12mo) months of age. Creatinine clearance was calculated using the formula: $(\text{urine creatinine } (\mu\text{mol.L}^{-1}) \times \text{urine flow rate } (\text{L.24h}^{-1}.\text{kg}^{-1})) \div \text{plasma creatinine } (\mu\text{mol.L}^{-1})$. SE: standard error. Degrees-of-freedom method: Kenward-Roger. Confidence level used: 95%. Significance was determined by a linear mixed-effect model with adjustment for litter size and relatedness of litter siblings (if present). *** $P < 0.001$, ** $P < 0.01$, * $P < 0.05$.

Generation	Age	Renal function	Males				Treatment effect (Sham males vs. IUGR males)	Females				Treatment effect (Sham females vs. IUGR females)
			Sham		IUGR			Sham		IUGR		
			Emmean	SE	Emmean	SE		Emmean	SE	Emmean	SE	
F2	6mo	Food intake (g.24h ⁻¹ .kg ⁻¹)	55.18	3.11	46.57	3.05	0.028*	64.14	2.35	66.64	2.47	0.337
		Water intake (mL.24h ⁻¹ .g ⁻¹)	0.08	0.01	0.08	0.005	0.454	0.14	0.01	0.14	0.01	1.000
		Urine produced (mL.24h ⁻¹ .kg ⁻¹)	38.42	2.44	35.83	2.03	0.354	67.90	3.97	73.96	4.21	0.240
		Urine flow rate (L.24h ⁻¹ .kg ⁻¹)	0.04	0.002	0.04	0.002	0.374	0.07	0.004	0.07	0.004	0.246
		Urine Na ⁺ (mmol.L ⁻¹ .24h ⁻¹ .kg ⁻¹)	2.13	0.16	1.72	0.13	0.020*	2.83	0.27	2.94	0.29	0.754
		Urine K ⁺ (mmol.L ⁻¹ .24h ⁻¹ .kg ⁻¹)	4.02	0.52	3.77	0.41	0.668	6.81	0.45	7.36	0.45	0.316
		Urine total protein (mg.L ⁻¹ .24h ⁻¹ .kg ⁻¹)	41.22	6.07	26.41	4.18	0.011*	9.02	2.03	9.45	2.01	0.866
		Urine albumin (mg.L ⁻¹ .24h ⁻¹ .kg ⁻¹)	0.87	0.13	0.41	0.11	0.002**	0.21	0.03	0.25	0.02	0.157

		Urine creatinine (mmol.L ⁻¹ .24h ⁻¹ .kg ⁻¹)	0.21	0.03	0.15	0.02	0.029*	0.16	0.02	0.19	0.02	0.457
		Plasma creatinine (μmol.L ⁻¹)	36.22	1.20	40.43	1.47	0.010**	36.33	1.65	44.88	1.91	0.0002***
		Creatinine clearance (mL.min ⁻¹ .kg ⁻¹)	3.30	0.41	1.85	0.49	0.006**	3.16	0.40	2.87	0.44	0.581
		Urine albumin/creatinine ratio (mg.mmol ⁻¹)	4.98	0.81	2.81	0.60	0.007**	1.14	0.16	1.32	0.15	0.346
	12mo	Food intake (g.24h ⁻¹ .kg ⁻¹)	42.86	1.82	42.85	2.22	0.997	59.12	2.60	62.95	2.65	0.277
		Water intake (mL.24h ⁻¹ .g ⁻¹)	0.07	0.004	0.06	0.01	0.258	0.12	0.01	0.14	0.01	0.035*
		Urine produced (mL.24h ⁻¹ .kg ⁻¹)	31.85	3.17	30.88	3.64	0.808	67.70	7.84	69.12	7.28	0.886
		Urine flow rate (L.24h ⁻¹ .kg ⁻¹)	0.03	0.003	0.03	0.004	0.638	0.07	0.01	0.07	0.01	0.986
		Urine Na ⁺ (mmol.L ⁻¹ .24h ⁻¹ .kg ⁻¹)	1.09	0.11	1.19	0.12	0.499	2.64	0.31	2.20	0.28	0.186
		Urine K ⁺ (mmol.L ⁻¹ .24h ⁻¹ .kg ⁻¹)	3.47	0.26	3.54	0.30	0.838	7.06	0.72	7.11	0.68	0.956
		Urine total protein (mg.L ⁻¹ .24h ⁻¹ .kg ⁻¹)	58.42	20.72	58.78	19.12	0.988	6.65	1.11	8.09	1.07	0.305
		Urine albumin (mg.L ⁻¹ .24h ⁻¹ .kg ⁻¹)	0.57	0.21	0.25	0.27	0.271	0.26	0.05	0.21	0.05	0.480
		Urine creatinine (mmol.L ⁻¹ .24h ⁻¹ .kg ⁻¹)	0.18	0.02	0.20	0.02	0.527	0.17	0.01	0.23	0.01	0.004**
		Plasma creatinine (μmol.L ⁻¹)	34.32	1.57	32.85	1.81	0.443	34.75	2.44	38.30	2.07	0.227
		Creatinine clearance (mL.min ⁻¹ .kg ⁻¹)	3.43	0.51	4.25	0.62	0.236	3.38	0.57	3.94	0.49	0.405
		Urine albumin/creatinine ratio (mg.mmol ⁻¹)	3.28	1.04	1.16	1.26	0.124	1.53	0.27	0.95	0.26	0.090

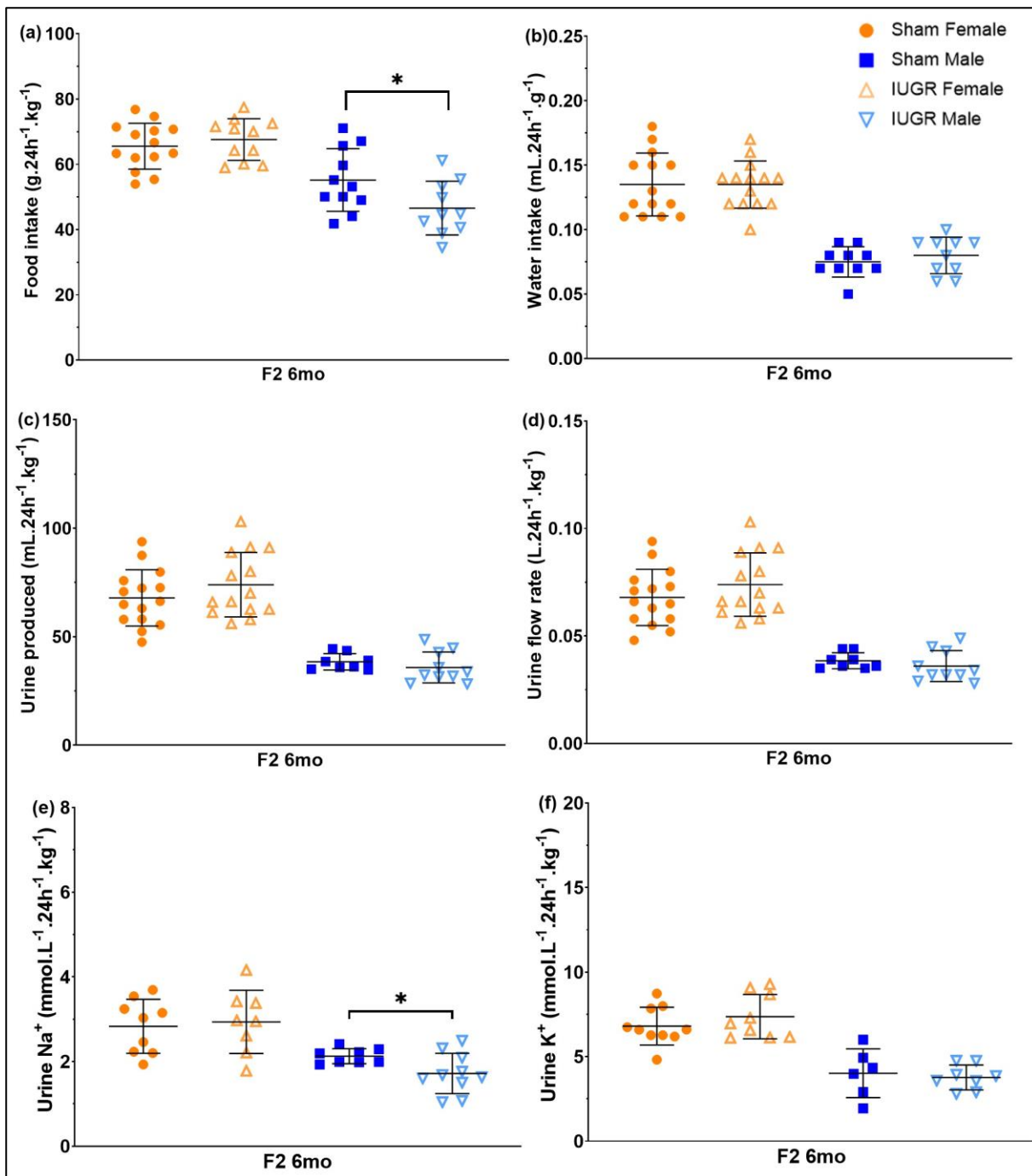


Figure 3. Food intake (a), water intake (b), volume (c) and flow rate (d) produced, sodium excretion (e) and potassium excretion (f) during renal function examination (24h) of sham and IUGR rat offspring (paternal line) in the second generation (F2), at 6 months of age (6mo). Significance was determined by a linear mixed-effect model with adjustment for litter size and relatedness of litter siblings (if present). * $P < 0.05$. See **Table 2** for exact P -values. Data is expressed as mean \pm SD; $n = 6$ -15 samples per group.

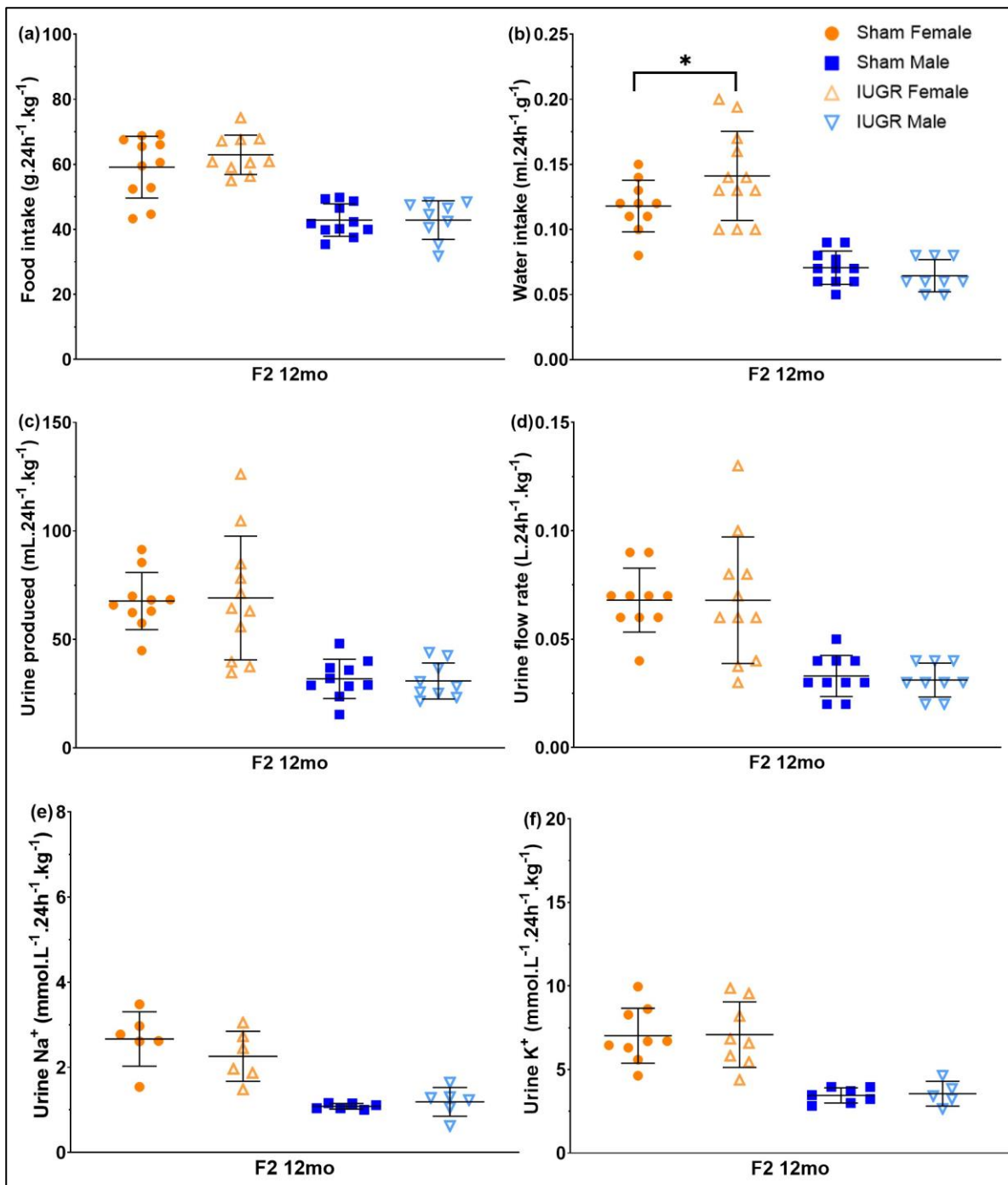


Figure 4. Food intake (a), water intake (b), volume (c) and flow rate (d) produced, sodium excretion (e) and potassium excretion (f) during renal function examination (24h) of sham and IUGR rat offspring (paternal line) in the second generation (F2), at 12 months of age (12mo). Significance was determined by a linear mixed-effect model with adjustment for litter size and relatedness of litter siblings (if present). * $P < 0.05$. See **Table 2** for exact P -values. Data is expressed as mean \pm SD; $n = 5$ -12 samples per group.

Table 3. Estimated marginal means (emmeans) of sham and IUGR rat offspring renal function measurements (24 hours) in the third (F3) generation (paternal line), at 6 (6mo) and 12 (12mo) months of age. Creatinine clearance was calculated using the formula: $(\text{urine creatinine } (\mu\text{mol.L}^{-1}) \times \text{urine flow rate } (\text{L.24h}^{-1}.\text{kg}^{-1})) \div \text{plasma creatinine } (\mu\text{mol.L}^{-1})$. SE: standard error. Degrees-of-freedom method: Kenward-Roger. Confidence level used: 95%. Significance was determined by a linear mixed-effect model with adjustment for litter size and relatedness of litter siblings (if present). *** $P < 0.001$, ** $P < 0.01$, * $P < 0.05$.

Generation	Age	Renal function	Males				Treatment effect (Sham males vs. IUGR males)	Females				Treatment effect (Sham females vs. IUGR females)
			Sham		IUGR			Sham		IUGR		
			Emmean	SE	Emmean	SE		Emmean	SE	Emmean	SE	
F3	6mo	Food intake (g.24h ⁻¹ .kg ⁻¹)	45.86	3.06	50.71	3.19	0.200	59.13	4.71	58.29	5.03	0.882
		Water intake (mL.24h ⁻¹ .g ⁻¹)	0.08	0.005	0.09	0.005	0.108	0.13	0.01	0.13	0.01	0.987
		Urine produced (mL.24h ⁻¹ .kg ⁻¹)	46.38	4.21	36.87	4.03	0.052	90.96	10.82	74.16	11.21	0.190
		Urine flow rate (L.24h ⁻¹ .kg ⁻¹)	0.05	0.004	0.04	0.005	0.053	0.09	0.01	0.07	0.01	0.187
		Urine Na ⁺ (mmol.L ⁻¹ .24h ⁻¹ .kg ⁻¹)	2.68	0.33	1.50	0.37	0.003**	4.06	0.55	2.59	0.58	0.025*
		Urine K ⁺ (mmol.L ⁻¹ .24h ⁻¹ .kg ⁻¹)	6.20	0.43	5.75	0.45	0.369	9.98	1.21	6.49	1.19	0.0096**
		Urine total protein (mg.L ⁻¹ .24h ⁻¹ .kg ⁻¹)	67.40	7.68	43.45	8.43	0.007**	17.68	2.55	10.38	2.45	0.011*
		Urine albumin (mg.L ⁻¹ .24h ⁻¹ .kg ⁻¹)	1.44	0.35	1.05	0.36	0.328	0.72	0.13	0.40	0.13	0.039*
		Urine creatinine (mmol.L ⁻¹ .24h ⁻¹ .kg ⁻¹)	0.27	0.02	0.24	0.02	0.060	0.33	0.04	0.22	0.03	0.003**
		Plasma creatinine (μmol.L ⁻¹)	30.83	3.09	34.00	3.72	0.349	29.86	4.00	40.44	4.34	0.018*
		Creatinine clearance (mL.min ⁻¹ .kg ⁻¹)	5.76	0.70	4.58	0.78	0.107	9.04	1.19	4.24	1.35	0.0005***
	Urine albumin/creatinine ratio (mg.mmol ⁻¹)	4.95	1.15	4.58	1.15	0.733	2.51	0.56	1.57	0.64	0.171	
	12mo	Food intake (g.24h ⁻¹ .kg ⁻¹)	43.70	1.48	43.42	1.56	0.875	57.47	3.97	63.77	4.51	0.210
Water intake (mL.24h ⁻¹ .g ⁻¹)	0.09	0.01	0.09	0.01	0.334	0.18	0.01	0.13	0.01	2.07 x 10 ⁻⁰⁵ ***		

Urine produced (mL.24h ⁻¹ .kg ⁻¹)	27.68	3.41	34.14	3.66	0.112	85.44	6.44	56.36	7.58	0.0003***
Urine flow rate (L.24h ⁻¹ .kg ⁻¹)	0.03	0.003	0.03	0.004	0.128	0.09	0.01	0.06	0.01	0.0003***
Urine Na ⁺ (mmol.L ⁻¹ .24h ⁻¹ .kg ⁻¹)	1.04	0.18	1.78	0.15	9.48 x 10 ⁻⁰⁹ ***	3.47	0.76	2.71	0.68	0.338
Urine K ⁺ (mmol.L ⁻¹ .24h ⁻¹ .kg ⁻¹)	3.74	1.08	4.53	0.71	0.456	8.42	1.20	7.88	0.90	0.634
Urine total protein (mg.L ⁻¹ .24h ⁻¹ .kg ⁻¹)	50.68	32.61	57.48	25.78	0.824	16.94	2.09	13.88	2.08	0.301
Urine albumin (mg.L ⁻¹ .24h ⁻¹ .kg ⁻¹)	0.14	0.10	0.32	0.07	0.053	0.96	0.23	0.44	0.23	0.058
Urine creatinine (mmol.L ⁻¹ .24h ⁻¹ .kg ⁻¹)	0.13	0.03	0.22	0.02	0.006**	0.25	0.02	0.26	0.02	0.568
Plasma creatinine (μmol.L ⁻¹)	42.33	39.05	43.33	15.03	2.20 x 10 ⁻¹⁶ ***	28.00	2.65	31.80	1.99	0.128
Creatinine clearance (mL.min ⁻¹ .kg ⁻¹)	3.92	1.85	3.42	0.83	0.692	6.35	0.25	5.27	0.18	8.95 x 10 ⁻⁰⁷ ***
Urine albumin/creatinine ratio (mg.mmol ⁻¹)	1.68	0.62	1.37	0.47	0.548	3.74	1.00	1.87	1.00	0.114

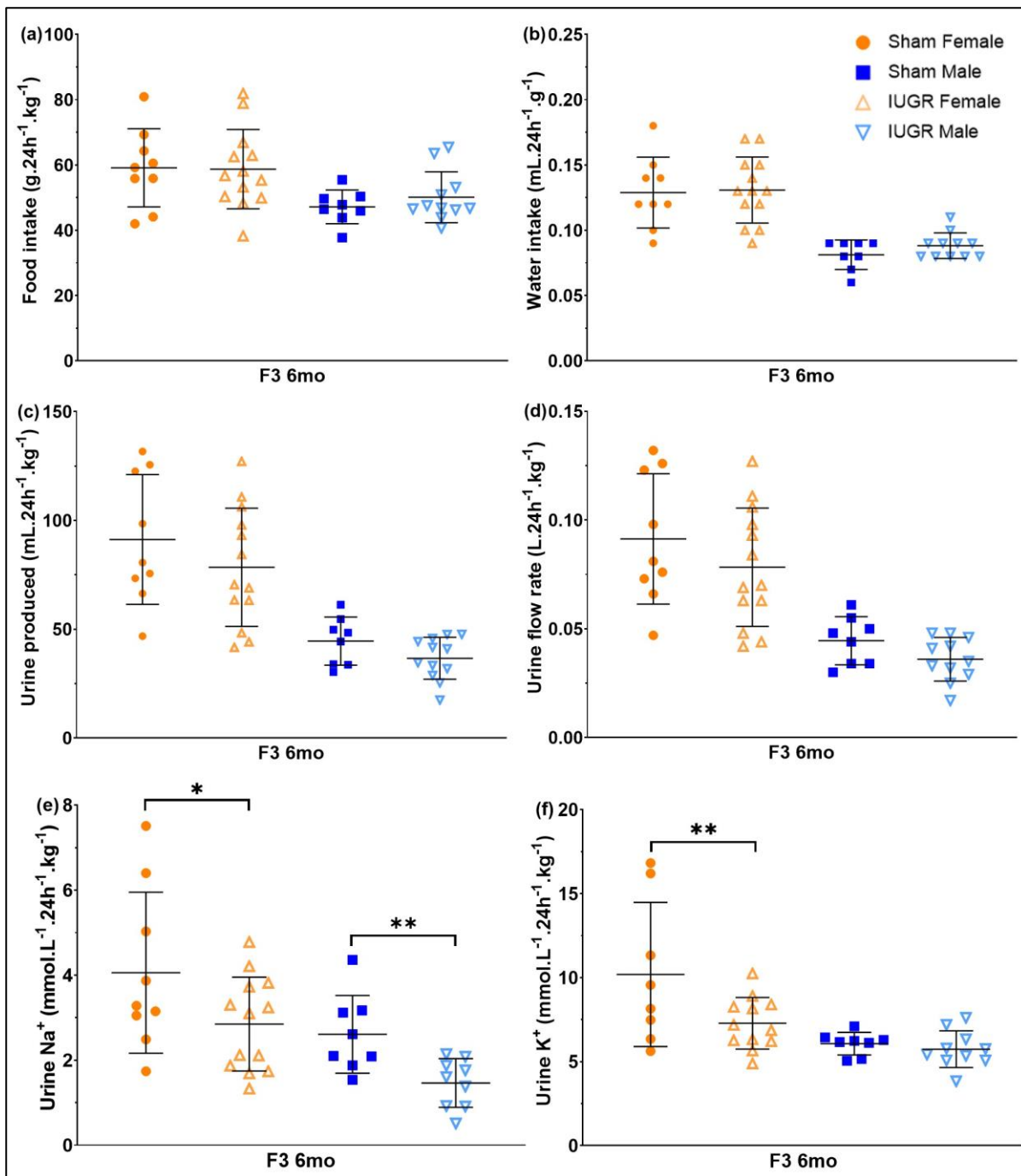


Figure 5. Food intake (a), water intake (b), volume (c) and flow rate (d) produced, sodium excretion (e) and potassium excretion (f) during renal function examination (24h) of sham and IUGR rat offspring (paternal line) in the third generation (F3), at 6 months of age (6mo). Significance was determined by a linear mixed-effect model with adjustment for litter size and relatedness of litter siblings (if present). ** $P < 0.01$, * $P < 0.05$. See **Table 3** for exact P -values. Data is expressed as mean \pm SD; n = 9-13 samples per group.

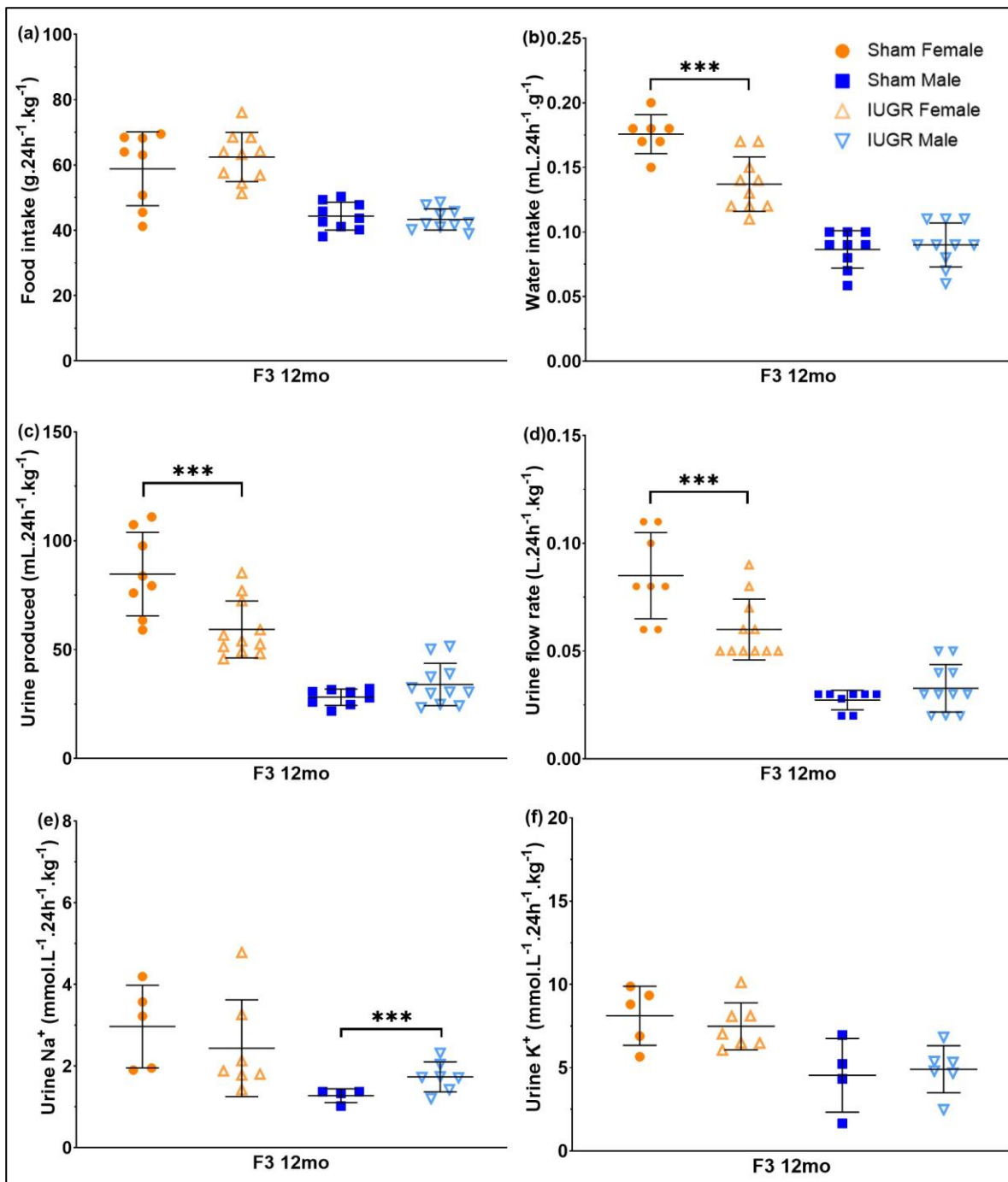


Figure 6. Food intake (a), water intake (b), volume (c) and flow rate (d) produced, sodium excretion (e) and potassium excretion (f) during renal function examination (24h) of sham and IUGR rat offspring (paternal line) in the third generation (F3), at 12 months of age (12mo). Significance was determined by a linear mixed-effect model with adjustment for litter size and relatedness of litter siblings (if present). *** $P < 0.001$. See **Table 3** for exact P -values. Data is expressed as mean \pm SD; $n = 4$ -11 samples per group.

Sodium (Na^+) and potassium (K^+) excretion during renal function examination (24 hours)

Urine sodium excretion was reduced in F2 IUGR males (-19.53%, $P = 0.020$) (**Table 2** and **Fig. 3e**) and F3 IUGR males at 6 mo (-43.98%, $P = 0.003$). In females, there was also a decrease in urine sodium excretion in the F3 generation at 6mo (-36.08%, $P = 0.025$) (**Table 3** and **Fig. 5e**). However, at 12mo, F3 IUGR males had an increase in sodium excretion compared to sham animals (IUGR $1.04 \pm 0.18 \text{ mmol.L}^{-1} \cdot 24\text{h}^{-1} \cdot \text{kg}^{-1}$ vs. sham $1.78 \pm 0.15 \text{ mmol.L}^{-1} \cdot 24\text{h}^{-1} \cdot \text{kg}^{-1}$, $P < 0.0001$) (**Table 3** and **Fig. 6e**). Regarding urine potassium secretion, there was a significant decrease observed only in F3 6mo IUGR females (-34.94%, $P = 0.0096$, **Table 3** and **Fig. 5f**).

Urine total protein, creatinine clearance and urine albumin/creatinine ratio during renal function examination (24 hours)

In the F2 generation, in comparison to sham offspring, IUGR males had a significant reduction in urine total protein excretion (-35.94%, $P = 0.011$, **Fig. 7a**), creatinine clearance (-44.03%, $P = 0.006$, **Fig. 7e**), as well as urine albumin/creatinine ratio (-43.51%, $P = 0.007$, **Fig. 7f**) (**Table 2**). Plasma creatinine was increased in IUGR males and females at 6mo, compared to sham (+11.62%, $P = 0.010$ and +23.53%, $P = 0.0002$, respectively, **Table 2** and **Fig. 7d**). These measurements were not significant at 12mo ($P = 0.988$, $P = 0.236$, $P = 0.124$, $P = 0.443$, and $P = 0.227$, respectively, **Fig. S1**). Meanwhile, both F3 6mo IUGR males and females had decreased urine total protein excretion compared to sham animals (-35.54%, $P = 0.007$ and -41.29%, $P = 0.011$, respectively, **Table 3** and **Fig. 8a**). Plasma creatinine increased in F3 6mo IUGR females (+35.43%, $P = 0.018$, **Table 3** and **Fig. 8d**) and 12mo IUGR males (+2.36%, $P < 0.0001$, **Table 3** and **Fig. 9d**). A statistically significant difference was only detected for creatinine clearance in F3 6mo IUGR females (-53.11%, $P = 0.0005$, **Table 3** and **Fig. 8e**), which persisted until 12mo (-17.05%, $P < 0.0001$, **Table 3** and **Fig. 9e**).

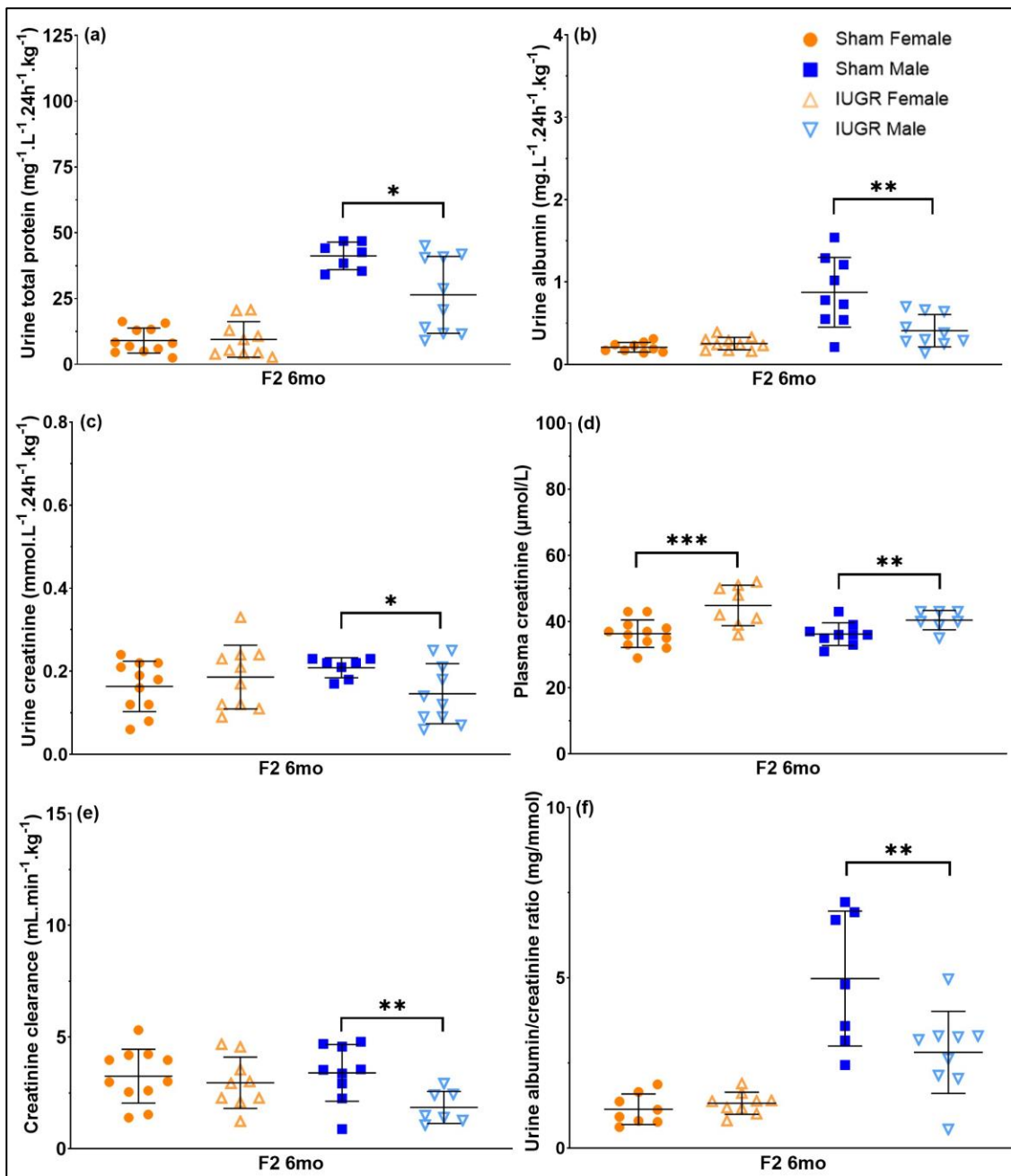


Figure 7. Biochemical analysis including urine total protein (a), albumin (b) and creatinine (c) excretion, plasma creatinine (d) and urine albumin/creatinine ratio (f) during renal function examination (24h) of sham and IUGR rat offspring (paternal line) in the second generation (F2), at 6 months of age (6mo). Creatinine clearance (e) was calculated using the formula: $(\text{urine creatinine } (\mu\text{mol.L}^{-1}) \times \text{urine flow rate } (\text{L.24h}^{-1}.\text{kg}^{-1})) \div \text{plasma creatinine } (\mu\text{mol.L}^{-1})$. Significance was determined by a linear mixed-effect model with adjustment for litter size and relatedness of litter siblings (if present). ** $P < 0.01$, * $P < 0.05$. See **Table 2** for exact P -values. Data is expressed as mean \pm SD; $n = 7$ -12 samples per group.

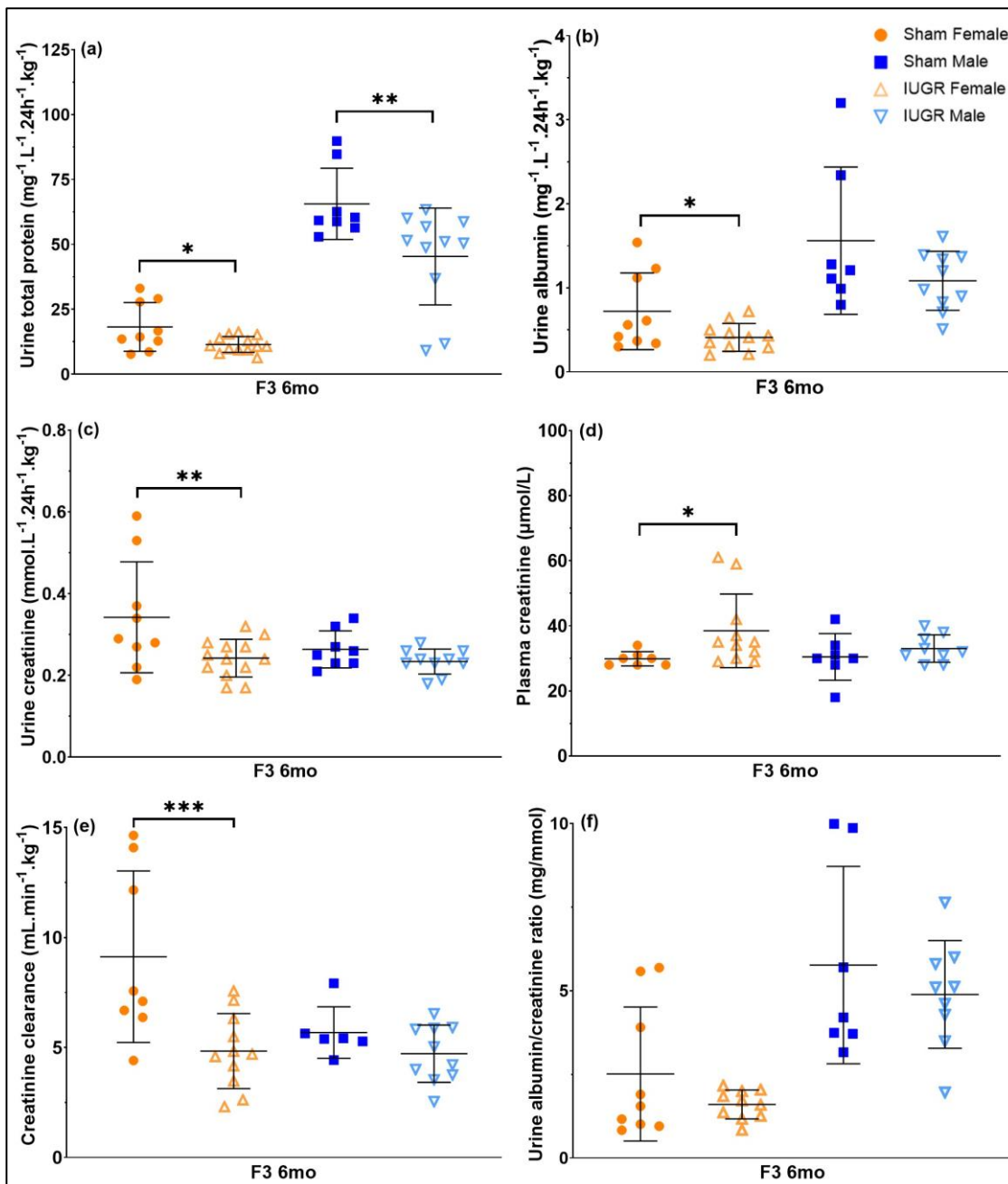


Figure 8. Biochemical analysis including urine total protein (a), albumin (b) and creatinine (c) excretion, plasma creatinine (d) and urine albumin/creatinine ratio (f) during renal function examination (24h) of sham and IUGR rat offspring (paternal line) in the third generation (F3), at 6 months of age (6mo). Creatinine clearance (e) was calculated using the formula: $(\text{urine creatinine } (\mu\text{mol.L}^{-1}) \times \text{urine flow rate } (\text{L.24h}^{-1}.\text{kg}^{-1})) \div \text{plasma creatinine } (\mu\text{mol.L}^{-1})$. Significance was determined by a linear mixed-effect model with adjustment for litter size and relatedness of litter siblings (if present). *** $P < 0.001$, ** $P < 0.01$, * $P < 0.05$. See **Table 3** for exact P -values. Data is expressed as mean \pm SD; n = 6-13 samples per group.

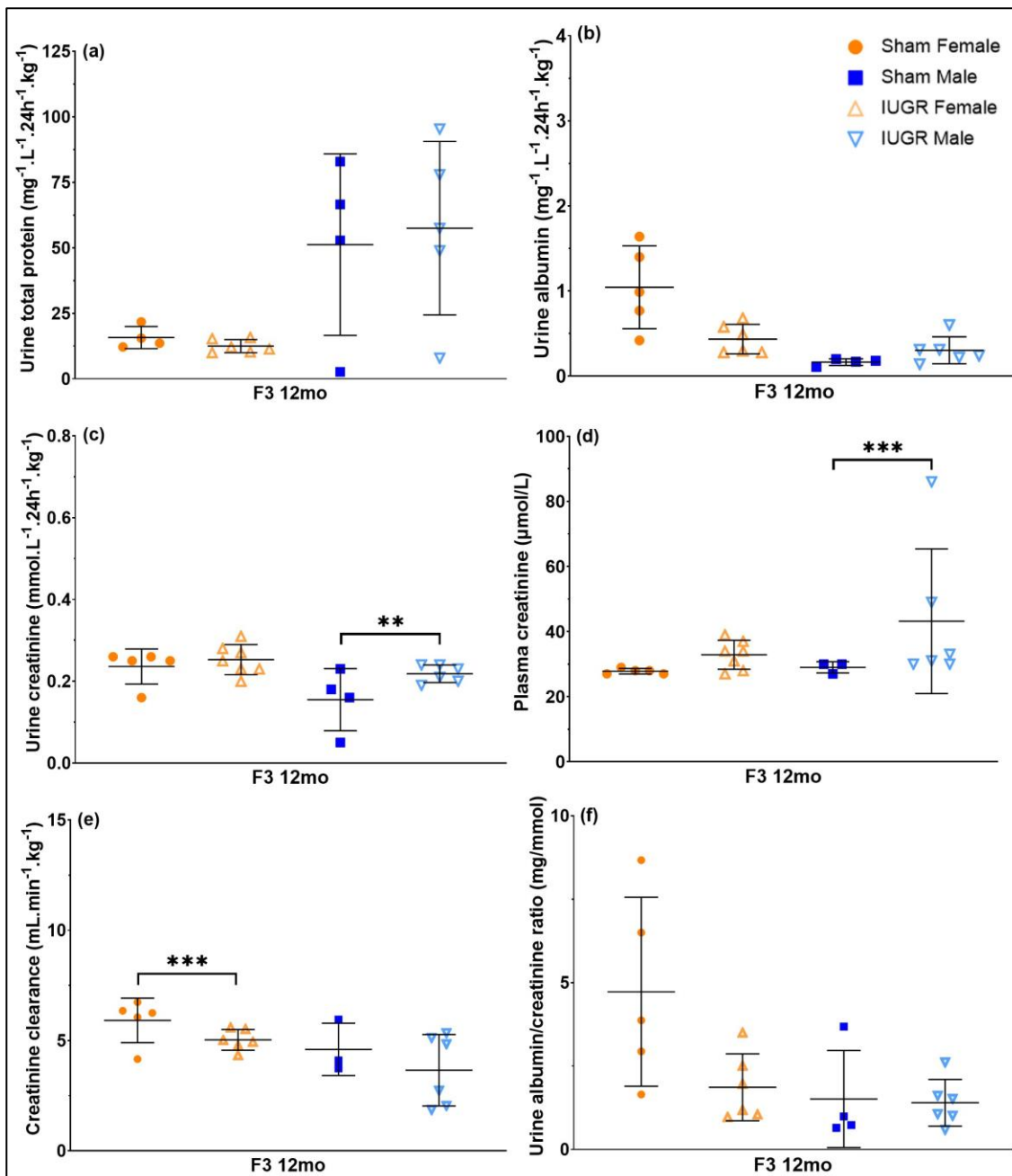


Figure 9. Biochemical analysis including urine total protein (a), albumin (b) and creatinine (c) excretion, plasma creatinine (d) and urine albumin/creatinine ratio (f) during renal function examination (24h) of sham and IUGR rat offspring (paternal line) in the third generation (F3), at 12 months of age (12mo). Creatinine clearance (e) was calculated using the formula: $(\text{urine creatinine } (\mu\text{mol} \cdot \text{L}^{-1}) \times \text{urine flow rate } (\text{L} \cdot 24\text{h}^{-1} \cdot \text{kg}^{-1})) \div \text{plasma creatinine } (\mu\text{mol} \cdot \text{L}^{-1})$. Significance was determined by a linear mixed-effect model with adjustment for litter size and relatedness of litter siblings (if present). *** $P < 0.001$, ** $P < 0.01$. See **Table 3** for exact P -values. Data is expressed as mean \pm SD; $n = 3$ -7 samples per group.

Histology

Three different stains, Haematoxylin and Eosin (H&E), Periodic Acid-Schiff (PAS), and Masson's trichrome were used to assess the presence of abnormal histopathology in kidney tissues of F2 and F3 6mo offspring [3, 4, 5]. A semiquantitative scale was used to score the histopathology of renal corpuscles (Bowman's capsule and glomerulus), tubules (epithelial cells, basement membrane and luminal casts), interstitial (leukocyte infiltration and fibrosis), and blood vessels (see Chapter 4 & 5 Materials and Methods for details).

There was no significant difference found between 6mo sham and IUGR offspring histopathological scores, in either sex within F2 and F3 generations (**Table S1**). Spearman's pairwise non-parametric correlation analyses were performed to investigate the relationship between 6mo total kidney weight (% body weight) renal function and kidney histopathology of F2 and F3 offspring, regardless of sex and treatment (**Fig. 10**). There was a negative correlation between kidney total histopathological score and total kidney weight (% body weight), only in the F3 generation ($\rho = -0.698, P < 0.001$). Negative correlations were also found between kidney total histopathological score and urine Na⁺ excretion, in both F2 ($\rho = -0.477, P = 0.029$) and F3 ($\rho = -0.516, P = 0.007$) 6mo offspring. Similar observations for the relationship between histopathological score and K⁺ excretion: F2 $\rho = -0.706, P = 0.001$; F3 $\rho = -0.632, P = 0.001$ (**Fig. 10**). Meanwhile, there were positive correlations between urine total protein excretion, urine albumin excretion, and urine albumin to creatinine (excretion) ratio and total histopathological score in both F2 ($\rho = 0.566, P = 0.006$; $\rho = 0.489, P = 0.018$; and $\rho = 0.543, P = 0.011$; respectively) and F3 generations ($\rho = 0.607, P = 0.001$; $\rho = 0.583, P = 0.001$; and $\rho = 0.536, P = 0.005$; respectively).

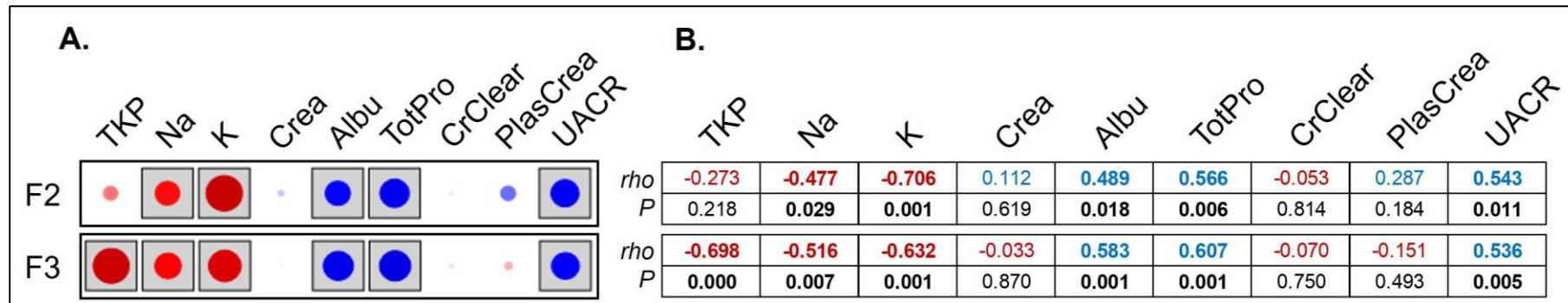


Figure 10. Non-parametric Spearman's ρ correlations between kidney parameters (including total kidney weight (% body weight) and renal function measurements (24 hours)) and total kidney histological score of rat offspring at 6 months of age, in the paternal F2 and F3 generations. **A.** Blue and red circles visually represent the strength of positive and negative correlations, respectively, and the size of the circle represents the strength of the correlation where larger circles are nearer to -1 or 1 and an invisible circle would be 0. **B.** calculated Spearman's ρ values and P -values of the correlation. Significant correlations ($P < 0.05$) are backed by a grey square in **A.** or bolded in **B.**

Abbreviations: TKP = total kidney weight percentage; Na = urine sodium excretion; K = urine potassium excretion; Crea = urine creatinine excretion; Albu = urine albumin excretion; TotPro = urine total protein excretion; CrClear = creatinine clearance rate; PlasCrea = plasma creatinine concentration; UACR = urine albumin to creatinine ratio.

Discussion

Table 4 summarises the changes in nephron number and renal function in F1, F2 and F3 offspring of UPI-induced IUGR model, from both maternal and paternal lines.

Table 4. Alterations to nephron number (from embryonic day 20 (E20) to 18 months of ages (18mo)) and renal function (examined at 6 and 12 months of age (6mo and 12mo)) in IUGR offspring compared to sham animals. Changes were investigated across generations (first (F1), second (F2) and third (F3) generations), from both paternal (this current study) and maternal [1, 2, 6, 7, 8] lines. ↓: reduced, ↑: increased, (-): no change, blank: has not been investigated.

	Paternal line					Maternal line				
	F1 male	F2 female	F2 male	F3 female	F3 male	F1 female	F2 female	F2 male	F3 female	F3 male
E20 nephron number							↓	↓		
PN35 nephron number		↓	(-)	(-)	(-)		(-)	(-)		
6mo nephron number	↓					↓				
18mo nephron number						↓				
6mo urine Na ⁺		(-)	↓	↓	↓		(-)	(-)		
6mo urine K ⁺	(-)	(-)	(-)	↓	(-)					
6mo urine total protein		(-)	↓	↓	↓		(-)	(-)		
6mo urine albumin		(-)	↓	↓	(-)					
6mo urine creatinine		(-)	↓	↓	(-)					
6mo plasma creatinine		↑	↑	↑	(-)					
6mo creatinine clearance		(-)	↓	↓	(-)		(-)	(-)		
6mo urine albumin/creatinine ratio		(-)	↓	(-)	(-)					
12mo urine Na ⁺	(-)	(-)	(-)	(-)	↑		(-)	(-)		
12mo urine K ⁺	(-)	(-)	(-)	(-)	(-)					
12mo urine total protein	(-)	(-)	(-)	(-)	(-)		(-)	(-)		

12mo urine albumin	(-)	(-)	(-)	(-)	(-)				
12mo urine creatinine	(-)	↑	(-)	(-)	↑				
12mo plasma creatinine		(-)	(-)	(-)	↑				
12mo creatinine clearance		(-)	(-)	↓	(-)		(-)	(-)	
12mo urine albumin/creatinine ratio		(-)	(-)	(-)	(-)				

In studies on the maternal line of this UPI-induced IUGR model, nephron number was reported to be reduced by approximately 20% in both F2 IUGR males and females at E20 (i.e., during nephron formation process), but was not different compared to sham at PN35 when kidney development is complete [7]. These animals also had no change in relative total kidney weight (% body weight) at PN35, 6 and 12mo [7]. However, F2 IUGR males and females from F1 females had increased absolute growth rate at PN14-2mo and 2mo-3mo periods [7], a sign of catch-up growth (see **Chapter 4**), which might potentially explain the increase of nephron number to sham level in IUGR offspring at PN35. In this current study of the paternal line, F2 and F3 IUGR males did not have changes in nephron number or right kidney weight (% body weight) at PN35. However, F2 PN35 IUGR females had reduced nephron number, and F3 PN35 IUGR females had increased right kidney weight, indicating a sex-specific effect. Future studies should investigate the individual glomerular volume of these females in adulthood, as a reduction in glomerular/nephron number in IUGR females was previously reported to be associated with increased individual glomerular volume (i.e., glomerular hypertrophy) at 18 months of age, predisposing them to renal dysfunction [6].

Food intake, water intake and renal function (including urine produced, urine creatinine/total protein/albumin/Na⁺/K⁺ excretion) of UPI-induced growth restricted F1 males at 12mo was previously reported to be similar compared to sham offspring [8]. Similarly, F2 males and females from the maternal line had no change in urine flow rate, urine Na⁺/total protein excretion, and

creatinine clearance examined at 6mo and 12mo [7]. In this current study, F2 IUGR females who had decreased nephron number at PN35 also had an increase in plasma creatinine concentration at 6mo, an early sign of kidney dysfunction [6, 9]. Interestingly, F3 IUGR females whose right kidney weights were higher than sham at PN35 also exhibited symptoms of renal function failure at 6mo, including reduced Na^+ and K^+ excretion, reduced total protein excretion, reduced creatinine clearance, and increased plasma creatinine. This suggests transgenerational transmission of kidney dysfunction phenotypes in IUGR offspring through the paternal line. In agreement with this, F2 and F3 IUGR males in the paternal line, despite having no alteration to nephron number or kidney weight at PN35, developed renal function abnormalities. Increased plasma creatinine, reduced creatinine clearance and urine albumin/creatinine ratio were observed in F2 IUGR males at 6mo. Meanwhile, decreased urine Na^+ excretion and total protein excretion were found in both F2 and F3 IUGR 6mo males. Some of these functional aberrations persisted in 12mo rats in the F3 generation. Upon postnatal exposure to other environmental factors, such as a high-fat diet [10, 11], these animals may be more likely to develop chronic kidney disease later in life. We further investigated the histopathology of IUGR kidneys at 6mo in both F2 and F3 offspring. However, there was no significant histopathological change found between sham and IUGR, although histological scores were correlated with renal function.

One of the limitations of the current study is that the renal function examinations of rats in metabolic cages are one-off measures (e.g., single measure of creatinine in a 24-hour urine sample, with a single plasma sample taken at the end of the urine collection), which could only provide proximal estimation of glomerular filtration rate [12, 13]. A recent study in rats suggested the use of an equation that includes plasma creatinine and plasma urea measures [14]. Meanwhile, the use of radiolabelled isotopes [15] or inulin [16] to examine glomerular filtration rate are suggested to be more accurate. In addition to this, although urine Na^+ excretion was shown to be significantly altered in 6mo and 12mo IUGR offspring in both F2 and F3 generations, calculation of the

fractional excretion of Na^+ would provide a clearer indication of renal dysfunction, as it also takes into account the glomerular filtration rate and plasma Na^+ concentration [17]. However, plasma Na^+ concentration was not measured in this study. Lastly, other staining methods could be used to examine kidney sections, such as terminal dideoxyuridine transferase-mediated nick end labeling (TUNEL) assay and activated Caspase-3 immunostaining to detect kidney cell apoptosis [18, 19].

In conclusion, we have shown that F2 and F3 male and female offspring from the F1 IUGR male are at an increased risk of developing renal disease compared to sham offspring. Despite the reduction in nephron number being apparent only in F2 females, animals in both generations had renal dysfunction at 6 months of age, with some of the disease phenotypes still present at 12 months of age. This suggests that reduced nephron number is only one of the many markers of kidney disease, and the restoration of nephron number in IUGR offspring during postnatal growth might not rescue the disease phenotypes. In addition, there seemed to be a sex-specific effect of IUGR within each generation, as renal dysfunction in F2 males was more severe than females, while F3 females showed more signs of renal function failure compared to males. As renal function data from the maternal line of this UPI model is not fully completed, it might not be reasonable to draw a conclusion of whether IUGR offspring from the maternal or paternal line are more susceptible to kidney disease. However, it should be noted that changes to urine Na^+ excretion, urine total protein excretion, and creatinine clearance observed in F2 6mo IUGR males in the paternal line were not significant in the maternal line.

References

1. Wlodek ME, Westcott K, Siebel AL, Owens JA, Moritz KM. Growth restriction before or after birth reduces nephron number and increases blood pressure in male rats. *Kidney International*. 2008;74(2):187-195. doi: 10.1038/ki.2008.153.
2. Wlodek ME, Mibus A, Tan A, Siebel AL, Owens JA, Moritz KM. Normal lactational environment restores nephron endowment and prevents hypertension after placental restriction in the rat. *Journal of the American Society of Nephrology*. 2007;18(6):1688-1696. doi: 10.1681/asn.2007010015.
3. Gallo LA, Walton SL, Mazzuca MQ, Tare M, Parkington HC, Wlodek ME, Moritz KM. Uteroplacental insufficiency temporally exacerbates salt-induced hypertension associated with a reduced natriuretic response in male rat offspring. *The Journal of Physiology*. 2018;596(23):5859-5872. doi: <https://doi.org/10.1113/JP275655>.
4. Gallo LA, Ward MS, Fotheringham AK, Zhuang A, Borg DJ, Flemming NB, Harvie BM, Kinneally TL, Yeh S-M, McCarthy DA, Koepsell H, Vallon V, Pollock C, Panchapakesan U, Forbes JM. Once daily administration of the SGLT2 inhibitor, empagliflozin, attenuates markers of renal fibrosis without improving albuminuria in diabetic db/db mice. *Scientific Reports*. 2016;6(1):26428. doi: 10.1038/srep26428.
5. Garcia-Gomez I, Pancholi N, Patel J, Gudehithlu KP, Sethupathi P, Hart P, Dunea G, Arruda JA, Singh AK. Activated omentum slows progression of CKD. *Journal of the American Society of Nephrology*. 2014;25(6):1270-81. doi: 10.1681/asn.2013040387.
6. Moritz KM, Mazzuca MQ, Siebel AL, Mibus A, Arena D, Tare M, Owens JA, Wlodek ME. Uteroplacental insufficiency causes a nephron deficit, modest renal insufficiency but no hypertension with ageing in female rats. *The Journal of Physiology*. 2009;587(Pt 11):2635-2646.
7. Gallo LA, Tran M, Cullen-McEwen LA, Denton KM, Jefferies AJ, Moritz KM, Wlodek ME. Transgenerational programming of fetal nephron deficits and sex-specific adult

- hypertension in rats. *Reproduction, Fertility and Development*. 2014;26(7):1032-1043. doi: 10.1071/RD13133.
8. Tran M, Young ME, Jefferies AJ, Hryciw DH, Ward MM, Fletcher EL, Wlodek ME, Wadley GD. Uteroplacental insufficiency leads to hypertension, but not glucose intolerance or impaired skeletal muscle mitochondrial biogenesis, in 12-month-old rats. *Physiol Rep*. 2015;3(9). doi: 10.14814/phy2.12556.
 9. Renczés E, Marônek M, Gaál Kovalčíková A, Vavrincová-Yaghi D, Tóthová Lu, Hodosy J. Behavioral changes during development of chronic kidney disease in rats. *Frontiers in Medicine*. 2020;6. doi: 10.3389/fmed.2019.00311.
 10. Intapad S, Dasinger JH, Johnson JM, Brown AD, Ojeda NB, Alexander BT. Male and female intrauterine growth-restricted offspring differ in blood pressure, renal function, and glucose homeostasis responses to a postnatal diet high in fat and sugar. *Hypertension*. 2019;73(3):620-629. doi: doi:10.1161/HYPERTENSIONAHA.118.12134.
 11. Aliou Y, Liao M-C, Zhao X-P, Chang S-Y, Chenier I, Ingelfinger JR, Zhang S-L. Post-weaning high-fat diet accelerates kidney injury, but not hypertension programmed by maternal diabetes. *Pediatric Research*. 2016;79(3):416-424. doi: 10.1038/pr.2015.236.
 12. Rácz O, Lepej J, Fodor B, Lepejová K, Jarčuška P, Kováčová A. Pitfalls in the measurements and assesment of glomerular filtration rate and how to escape them. *Ejifcc*. 2012;23(2):33-40.
 13. Luis-Lima S, Porrini E. An overview of errors and flaws of estimated gfr versus true gfr in patients with diabetes mellitus. *Nephron*. 2016;136(4):287-291. doi: 10.1159/000453531.
 14. Besseling PJ, Pieters TT, Nguyen ITN, Bree PMd, Willekes N, Dijk AH, Bovée DM, Hoorn EJ, Rookmaaker MB, Gerritsen KG, Verhaar MC, Gremmels H, Joles JA. A plasma creatinine- and urea-based equation to estimate glomerular filtration rate in rats. *American Journal of Physiology-Renal Physiology*. 2021;320(3):F518-F524. doi: 10.1152/ajprenal.00656.2020.

15. Holweger K, Bokemeyer C, Lipp H-P. Accurate measurement of individual glomerular filtration rate in cancer patients: an ongoing challenge. *Journal of Cancer Research and Clinical Oncology*. 2005;131(9):559-567. doi: 10.1007/s00432-005-0679-7.
16. Gallo LA, Denton KM, Moritz KM, Tare M, Parkington HC, Davies M, Tran M, Jefferies AJ, Wlodek ME. Long-term alteration in maternal blood pressure and renal function after pregnancy in normal and growth-restricted rats. *Hypertension*. 2012;60(1):206-213. doi: doi:10.1161/HYPERTENSIONAHA.112.195578.
17. Lankadeva YR, Singh RR, Hilliard LM, Moritz KM, Denton KM. Blunted sodium excretion in response to a saline load in 5 year old female sheep following fetal uninephrectomy. *PloS One*. 2012;7(10):e47528. doi: 10.1371/journal.pone.0047528.
18. Ramamoorthy H, Abraham P, Isaac B, Selvakumar D. Mitochondrial pathway of apoptosis and necrosis contribute to tenofovir disoproxil fumarate–induced renal damage in rats. *Human and Experimental Toxicology*. 2019;38(3):288-302. doi: 10.1177/0960327118802619.
19. Akison LK, Probyn ME, Gray SP, Cullen-McEwen LA, Tep K, Steane SE, Gobe GC, Wlodek ME, Bertram JF, Moritz KM. Moderate prenatal ethanol exposure in the rat promotes kidney cell apoptosis, nephron deficits, and sex-specific kidney dysfunction in adult offspring. *The Anatomical Record*. 2020;303(10):2632-2645. doi: <https://doi.org/10.1002/ar.24370>.

SUPPLEMENTARY TABLE

Table S1. One-way ordinal regression with Cumulative Linked Model (CLM) for histopathological scores of sham and IUGR rats kidneys in the second (F2) and third (F3) generations (paternal line), at 6 months of age (6mo). Treatment (sham/IUGR) was identified as the independent variable, while histopathological score (ordered factor) was identified as the dependent variable. Observations between groups were not paired or repeated measures. As only one pup was examined per litter, and sex were analysed separately, no adjustment for litter siblings was needed. Litter size was checked and confirmed not a random effect. N/A: statistical analyses could not be done due to missing data/nature of data did not meet the required criteria.

Generation	Time point	Histology	Type II Analysis of Deviance Table with Wald chi-square tests	
			Males	Females
F2	6mo	Bowman's capsule	0.695	0.288
		Glomerulus	0.383	0.896
		Epithelial cells	0.323	0.467
		Basement membranes	0.449	0.893
		Luminal casts	0.137	0.077
		Leukocyte infiltration	0.624	0.641
		Fibrosis	0.376	N/A
		Total scores	0.428	0.321
F3	6mo	Bowman's capsule	0.909	0.872
		Glomerulus	0.910	0.579
		Epithelial cells	0.326	N/A
		Basement membranes	0.225	N/A
		Luminal casts	0.204	N/A
		Leukocyte infiltration	0.914	0.281

		Fibrosis	0.598	0.447
		Total scores	1	0.306

SUPPLEMENTARY FIGURE

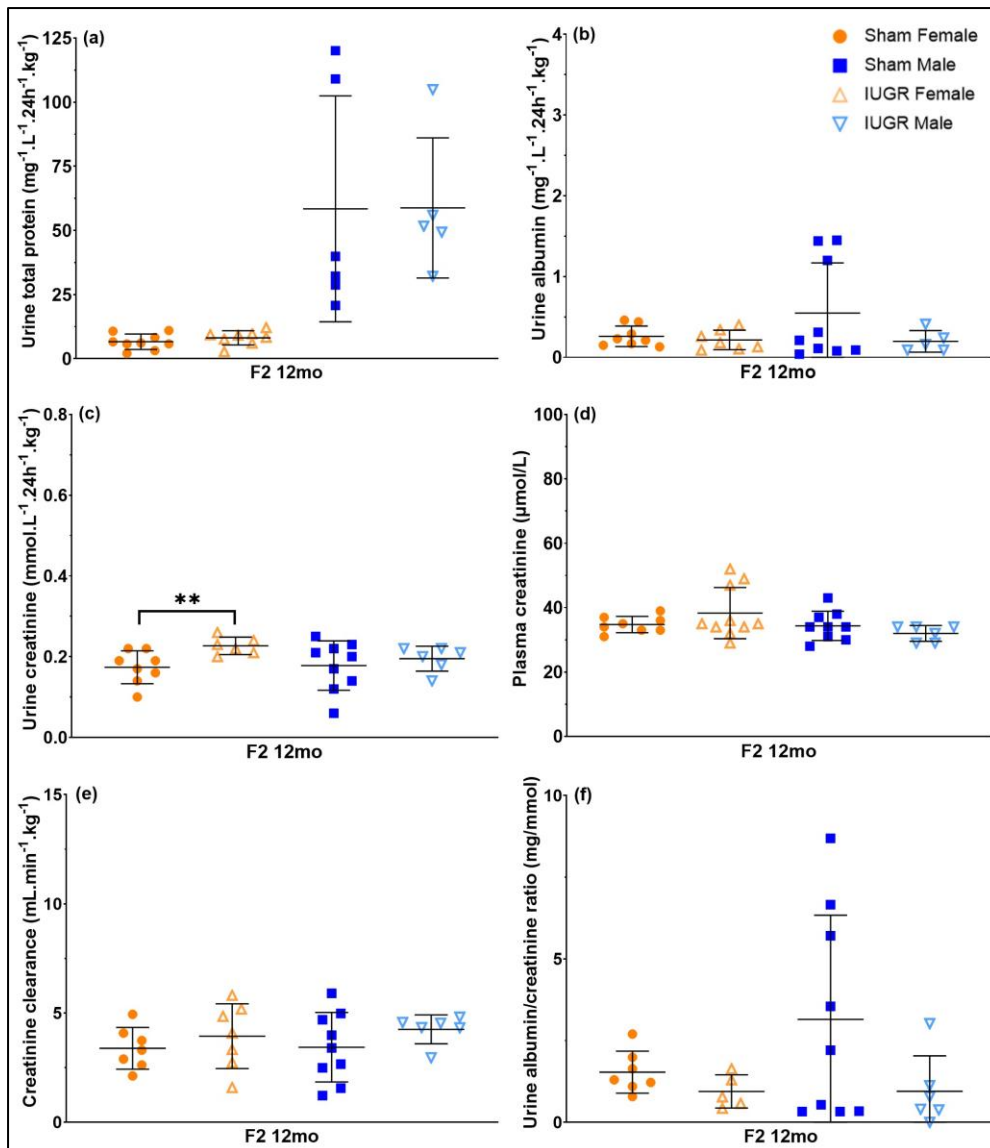


Figure S1. Biochemical analysis including urine total protein (a), albumin (b) and creatinine (c) excretion, plasma creatinine (d) and urine albumin/creatinine ratio (f) during renal function examination (24h) of sham and IUGR rat offspring (paternal line) in the second generation (F2), at 12 months of age (12mo). Creatinine clearance (e) was calculated using the formula: $(\text{urine creatinine } (\mu\text{mol} \cdot \text{L}^{-1}) \times \text{urine flow rate } (\text{L} \cdot 24\text{h}^{-1} \cdot \text{kg}^{-1})) \div \text{plasma creatinine } (\mu\text{mol} \cdot \text{L}^{-1})$. Significance was determined by a linear mixed-effect model with adjustment for litter size and relatedness of litter siblings (if present). ** $P < 0.01$. See **Table 1** for exact P -values. Data is expressed as mean \pm SD; $n = 5$ -10 samples per group.

CHAPTER 6

FINAL DISCUSSION

Final Discussion

Findings presented in **Chapter 2** affirm that there is a close relationship between babies being small for gestational age due to intrauterine growth restriction (IUGR) and having an increased risk of developing chronic diseases later in life. Interestingly, there is evidence of sex differences in the susceptibility to future chronic diseases after IUGR in humans, such as cardiovascular and renal dysfunction [1, 2]. As the incidence of IUGR is relatively high, especially in developing countries (~ 1 in 4 of all live births), this might contribute to the high prevalence of hypertension, kidney disease, and metabolic diseases worldwide. Due to the challenges in conducting human research, most data from human IUGR studies have come from studying the placenta, umbilical cord, or fetal blood samples. Collectively, these studies provide early insight into the potential mechanisms behind IUGR, as they reported changes in epigenetic mechanisms of genes important for fetal development and growth in the growth restricted babies. However, it should be acknowledged that results from human IUGR studies might be biased by confounding factors such as genetics and ecological factors as well as the tissue type that is available for assessment. On the other hand, animal models of IUGR, with strictly controlled experimental environments and the availability of tissues for sampling throughout developmental stages and across generations, can help explore the pattern of disease risk transmission, as well as the potential mechanisms in a more robust fashion.

Different rodent models of IUGR have been developed using different adverse exposures during pregnancy like restricted calorie intake, low-protein diet, exposure to high levels of glucocorticoids, or placental insufficiency. IUGR phenotypes are reproducible in these models, however the severity of phenotypes depends on the severity, timing, and duration of *in utero* insults, which is expected. For instance, as discussed in **Chapter 2**, a 5% protein

maternal diet or placing silver clips around the abdominal aorta and on the branches of uterine arteries of pregnant rats results in a more extreme IUGR phenotype than a 8% protein diet or ligating just the uterine vessels of rats, respectively. Additionally, changes in the offspring phenotypes are known to be sensitive to the timing of *in utero* insults. As shown from the classical human example, the Dutch Hunger Winter famine, reducing maternal calorie intake during early gestation resulted in more disease phenotypes than at late gestation [3]. The focus of our research group was inducing IUGR via uteroplacental insufficiency (UPI) from day 18 of gestation in rats, which reflects several disease characteristics seen in humans. IUGR phenotypes in this model are similar compared to other UPI models that induce insults during the late gestational period (e.g., at day 19 or 19.5 of gestation). However, future studies should investigate the effect of inducing UPI at earlier developmental time points to better explain results found in human studies. Additionally, it should be mentioned that while the development of organs is fully completed before birth in humans, most organs in rats are structurally established during gestation and functionally completed after birth. Moreover, different organs have different developmental timelines, therefore, inducing UPI at a specific time point may impact the disease phenotypes of one organ more severely than another that is further along the developmental path.

From **Chapters 4 and 5**, UPI was associated with changes in postmortem organ weights, reduced vascular and metabolic functions, and aberrant renal functions in offspring from both maternal and paternal lines, regardless of birth weight. The presence of these physiological changes was seen as early as embryonic day 20 (e.g., reduced E20 nephron number in F2 males and females in the maternal line) to 12 months after birth (e.g., reduced glucose-stimulated first-phase insulin secretion in F3 males in the paternal line). Additionally, there were parental origin-specific effects on the transmission of IUGR phenotypes, as alterations

to the offspring postmortem organ weights were more significant in the paternal line, while vascular and metabolic dysfunctions were more severe in the maternal line. Regarding renal dysfunction, F2 offspring from the paternal line were presented with more symptoms than the maternal line. Future studies should compare the renal functions between paternal and maternal lines once the maternal F3 generation of this model is analysed. In addition, it would be ideal to explore the phenotypes in F2 and F3 offspring when F1 IUGR male and F1 IUGR female are mated. We would expect to see an exacerbated phenotype and possibly more sex differences. On top of this, within each parental line, there was a sex-specific effect on the appearance of IUGR phenotypes. For example, blood pressure has been shown to increase in IUGR males only in the maternal line, while there was minimal effect on blood pressure in both males and females from the paternal line. Postnatal day (PN35) nephron number was not different compared to sham in both F2 males and females from the maternal line, but was reduced in F2 females from the paternal line. Renal dysfunction was more severe in F2 males compared to females, or F3 females compared to males in the paternal line. These findings are in line with the sex-specific differences in incidence of chronic diseases in humans, verifying that the investigation of IUGR and the associated disease risks in humans should also be carried out within each sex group.

Results reported in **Chapter 3** agree with previous publications of changes to epigenetic mechanisms in tissues of growth restricted offspring, which might be the reason for the transmission patterns of IUGR phenotypes (**Chapter 2**). Our findings also suggest that different epigenetic mechanisms might interact with each other to regulate gene expression, increasing the complexity of unravelling and identifying the epigenetic mechanisms involved. A limitation of this study was the unavailability of F1 samples for DNA methylation analysis at E20 timepoint (an important point in nephron formation, at which *Dnmt3a* was altered, and

nephron number was also previously shown to be decreased in F2 offspring), as well as later postnatal time points. Additionally, the cellular heterogeneity presented in the kidney samples, including various specialised epithelial and endothelial cell types, might be a confounding factor. A potential approach to this issue would be to look at single-cell RNA sequencing in the kidneys in both males and females in subsequent generations to see 1) what are the sex-specific differences, 2) are there cell type-specific differences, and 3) if changes seen in F2 are also seen in F3, indicating a truly transgenerational phenotype. The mode of transmission can also be explored, such as through sperm for the paternal line. If such differences and changes are observed, we would then further investigate whether epigenetics mechanisms were involved by looking at DNA methylation, histone modifications, and long non-coding RNAs.

In conclusion, research presented in this Thesis further supports the importance early life insults during pregnancy impacting future offspring health (the Developmental Origins of Health and Disease theory). Increased cardiovascular dysfunction, renal dysfunction, and metabolic disease risks are often linked to a poor developmental environment. The investigation of alterations to epigenetic mechanisms in offspring that were exposed to *in utero* insults in the animal models would provide the foundation for future studies to investigate similar disease markers or mechanisms in humans.

References

1. Beaumann M, Delhaes F, Menétrey S, Joye S, Vial Y, Baud D, Magaly JG, Tolsa J-F, Peyter A-C. Intrauterine growth restriction is associated with sex-specific alterations in the nitric oxide/cyclic GMP relaxing pathway in the human umbilical vein. *Placenta*. 2020;93:83-93. doi: doi:10.1016/j.placenta.2020.02.014.
2. Tarnovski L, Brinar IV, Kirhmajer MV, Vrkić TZ, Laganović M. Sex differences in cardiovascular risk factors and renal function among young adults after intrauterine growth restriction [Report]. *Acta Clinica Croatica*. 2021;60:164+.
3. Roseboom T, de Rooij S, Painter R. The Dutch famine and its long-term consequences for adult health. *Early Human Development*. 2006;82(8):485-491. doi: <https://doi.org/10.1016/j.earlhumdev.2006.07.001>.

APPENDIX A

REVIEW ARTICLE:

THE ROLE OF ANGIOTENSIN II

AND RELAXIN

IN VASCULAR ADAPTATION

TO PREGNANCY

Statement of Authorship

Statement of Authorship

Title of Paper	The role of angiotensin II and relaxin in vascular adaptation to pregnancy		
Publication Status	<input checked="" type="checkbox"/> Published	<input type="checkbox"/> Accepted for Publication	
	<input type="checkbox"/> Submitted for Publication	<input type="checkbox"/> Unpublished and Unsubmitted work written in manuscript style	
Publication Details	Doan, T. N. A., Bianco-Miotto, T., Parry, L., & Winter, M. (2022). The role of angiotensin II and relaxin in vascular adaptation to pregnancy. <i>Reproduction</i> , 164(4), R87-R99. https://doi.org/10.1530/REP-21-0428 .		

Principal Author

Name of Principal Author (Candidate)	Ngoc Anh Thu Doan		
Contribution to the Paper	Literature search, data interpretation and manuscript drafting		
Overall percentage (%)	85		
Certification:	This paper reports on original research I conducted during the period of my Higher Degree by Research candidature and is not subject to any obligations or contractual agreements with a third party that would constrain its inclusion in this thesis. I am the primary author of this paper.		
Signature		Date	6.11.2023

Co-Author Contributions

By signing the Statement of Authorship, each author certifies that:

- i. the candidate's stated contribution to the publication is accurate (as detailed above);
- ii. permission is granted for the candidate to include the publication in the thesis; and
- iii. the sum of all co-author contributions is equal to 100% less the candidate's stated contribution.

Name of Co-Author	Tina Bianco-Miotto		
Contribution to the Paper	Conception and design of article, critical revision and contribution to intellectual content		
Signature		Date	6.11.2023

Name of Co-Author	Laura Parry		
Contribution to the Paper	Conception and design of article, critical revision and contribution to intellectual content		
Signature		Date	6/11/2023

Name of Co-Author	Marnie Winter		
Contribution to the Paper	Conception and design of article, critical revision and contribution to intellectual content		
Signature		Date	6.11.23

Title: The role of angiotensin II and relaxin in vascular adaptation to pregnancy

Short title: Vascular adaptation in pregnancy

In Brief statement: There is a pregnancy-induced vasodilation of blood vessels, which is known to have a protective effect on cardiovascular function and can be maintained postpartum. This review outlines the cardiovascular changes that occur in a healthy human and rodent pregnancy, as well as different pathways that are activated by angiotensin II and relaxin that result in blood vessel dilation.

Key words: pregnancy, cardiovascular system, vascular endothelial cells, vasodilation, vasoconstriction, angiotensin II, relaxin

Word count: 5292

Authors: Thu Ngoc Anh Doan^{1,2}, Tina Bianco-Miotto^{1, 2}, Laura Parry^{2,3}, and Marnie Winter⁴

¹School of Agriculture, Food and Wine, & Waite Research Institute, University of Adelaide, Adelaide, South Australia, Australia

²Robinson Research Institute, University of Adelaide, Adelaide, South Australia, Australia

³School of Biological Sciences, University of Adelaide, Adelaide, South Australia, Australia

⁴Future Industries Institute, University of South Australia, Adelaide, South Australia, Australia

Corresponding author: Marnie Winter

Corresponding author [ORCID iD](#): 0000-0002-7499-789X

Corresponding author postal address: University of South Australia, Mawson Lakes
Campus (MM2-01), Mawson Lakes, South Australia, 5095

Corresponding author e-mail: Marnie.Winter@unisa.edu.au

Other authors' emails: thu.doan@adelaide.edu.au, tina.bianco@adelaide.edu.au,
laura.parry@adelaide.edu.au

ABSTRACT

During pregnancy, systemic and uteroplacental blood flow increase to ensure an adequate blood supply that carries oxygen and nutrients from the mother to the fetus. This results in changes to the function of the maternal cardiovascular system. There is also a pregnancy-induced vasodilation of blood vessels, which is known to have a protective effect on cardiovascular health/function. Additionally, there is evidence that the effects of maternal vascular vasodilation are maintained post-partum, which may reduce the risk of developing high blood pressure in the next pregnancy and reduce cardiovascular risk later in life. At both non-pregnant and pregnant stages, vascular endothelial cells produce a number of vasodilators and vasoconstrictors, which transduce signals to the contractile vascular smooth muscle cells to control the dilation and constriction of blood vessels. These vascular cells are also targets of other vasoactive factors, including angiotensin II (Ang II) and relaxin. The binding of Ang II to its receptors activates different pathways to regulate the blood vessel vasoconstriction/vasodilation, and relaxin can interact with some of these pathways to induce vasodilation. Based on the available literature, this review outlines the cardiovascular

changes that occur in a healthy human pregnancy, supplemented by studies in rodents. A specific focus is placed on vasodilation of blood vessels during pregnancy; the role of endothelial cells and endothelium-derived vasodilators will also be discussed. Additionally, different pathways that are activated by Ang II and relaxin that result in blood vessel dilation will also be reviewed.

INTRODUCTION

Cardiac output is represented by heart beats per minute (heart rate) and the volume of blood pumped into the aorta from the left ventricle per minute (stroke volume) (Hunter and Robson, 1992). In a healthy human pregnancy, both local uterine blood flow and cardiac output increase. This ensures an adequate supply of oxygen and nutrients from the mother to the fetus (Hunter and Robson, 1992, Melchiorre *et al.*, 2012). The elevation of cardiac output usually starts from the 5th week of gestation, reaches maximum value at 20 to 32 weeks of gestation (heart rate nearly 45% higher than pre-pregnancy value), and returns to pre-pregnancy levels 2 weeks post-partum (Hunter and Robson, 1992, Meah *et al.*, 2016). Simultaneously, alterations in maternal vascular function occur to accommodate increased blood flow.

Vasodilation or relaxation of blood vessels, which occurs from early to mid-gestation, is known to be an adaptation to protect the maternal cardiovascular system throughout pregnancy, as it maintains a normal or decreased pressure when the volume of blood being pumped from the heart into these vessels increases (Guyton, 1981, Hunter and Robson, 1992). Specifically, despite an increase in plasma volume by 6 weeks of gestation, a decrease in both peripheral and renal vascular resistance results in decreased blood pressure and

increased renal flow (West *et al.*, 2016). This rise in plasma volume and decrease in vascular resistance is also likely accounted for in part by arterial underfilling with 85% of the volume residing in the venous circulation (Davison, 1984). These adaptations help reduce the risk of developing hypertensive complications such as preeclampsia (Conrad, 2011, Osol *et al.*, 2019), which predisposes women to a 3.5-fold, 2.1-fold, and 1.8-fold higher risk for developing hypertension, coronary heart disease, and stroke, later in life (Bellamy *et al.*, 2007, Carpenter, 2007, Lykke *et al.*, 2009, Yinon *et al.*, 2010, Naderi *et al.*, 2017, Thilaganathan and Kalafat, 2019). Findings in both human and animal studies have also suggested that blood vessel dilation is maintained post-partum, which may decrease the risk of developing hypertension in subsequent pregnancies and lower the risk of developing cardiovascular disease later in life (Gunderson *et al.*, 2008, van der Heijden *et al.*, 2009, Morris *et al.*, 2015, Morris *et al.*, 2020).

This literature review will cover vasculature changes, specifically blood vessel vasodilation during pregnancy and post-partum in a normal pregnancy in both human and rodents. In addition, it will also discuss the role of angiotensin II (Ang II) and relaxin in vascular adaptation during pregnancy, different pathways that are activated by the binding of Ang II to its receptors, and the potential interaction between relaxin and Ang II receptors. Changes to the above pathways when there is endothelial dysfunction, similar to that which may occur in preeclampsia, will also be reviewed.

MATERIALS AND METHODS

A literature search for primary peer-reviewed papers that investigate maternal blood vessel dilation during pregnancy and its mechanisms was conducted in PubMed and Web of Sciences using search terms “pregnancy vasodilation”, “vascular endothelial cells”, “vascular

smooth muscle cells”, “angiotensin II”, and “relaxin” up to June 2022. There were 193 papers retrieved based on the search terms. Papers that are not in English and were not available in full-text were excluded. The final number of papers retained was 136.

RESULTS AND DISCUSSION

Vasculature changes in a healthy human pregnancy

Changes in mean arterial pressure

Mean arterial pressure (MAP, mmHg) is an indicator of the average pressure in blood vessels during one cardiac cycle (Cnossen *et al.*, 2008). MAP is calculated using the formula, $(2 \text{ diastolic pressure} + \text{systolic pressure})/3$, in which diastolic pressure is the blood pressure measured when the heart relaxes, and systolic pressure is measured when the heart contracts (Cnossen *et al.*, 2008). Most studies of healthy women (non-smokers, have normal body mass index with no history of blood pressure-related disorders and/or usage of hypertensive medication) in their first pregnancy (primiparous women) reported a reduction in MAP (by a maximum of 2 - 3.4 mmHg of the non-pregnant level) in the first two trimesters of pregnancy and an increase to pre-pregnancy value (79 - 83 mmHg) from the 3rd trimester until term (Kametas *et al.*, 2001, Simmons *et al.*, 2002, Morris *et al.*, 2014, Melchiorre *et al.*, 2016). In the second or third pregnancy, MAP values within each trimester are lower compared to primiparous women (Bernstein *et al.*, 2005). Moreover, there was a negative correlation ($r = -0.31$) between the interval between pregnancies (11 – 67 months) and the degree of changes in MAP throughout a pregnancy, suggesting that a shorter interval between pregnancies is associated with a greater decrease in MAP (Bernstein *et al.*, 2005). However, MAP always reaches the highest value within the third trimester, compared to other trimesters, regardless of the number of previous pregnancies (Bernstein *et al.*, 2005). On the other hand, other

studies have reported a further decrease in blood pressure at post-partum in both primiparous women and women who had two or more pregnancies (Gunderson *et al.*, 2008, Morris *et al.*, 2015). Specifically, primiparous women had decreased MAP, by 4.8 mmHg, at 14 months post-partum (Morris *et al.*, 2015), or decreased mean adjusted diastolic and systolic blood pressure (by 1.50 mmHg and 2.06 mmHg, respectively) at up to 20 years post-partum, compared to pre-pregnancy values (Gunderson *et al.*, 2008). Similarly, at 20 years post-partum, women who had two or more pregnancies had a further decrease in diastolic and systolic blood pressure (1.29 mmHg and 1.89 mmHg, respectively), compared to non-pregnant women (Gunderson *et al.*, 2008). However, both studies mainly focused on Caucasian or women of colour, hence the results may not be generalised for all ethnic minorities (Gunderson *et al.*, 2008, Morris *et al.*, 2015). Additionally, these studies did not investigate changes in blood pressure measures during pregnancy.

Similar to changes observed in humans, rodent studies have also reported a decrease in MAP during pregnancy (Barron *et al.*, 2010, Mirabito Katrina *et al.*, 2014, Mirabito Colafella *et al.*, 2017). In pregnant mice, MAP gradually decreased from early gestation and reached the lowest value (-6 ± 2 mmHg) at gestational day 9 (Mirabito Katrina *et al.*, 2014, Mirabito Colafella *et al.*, 2017), which is an adaptation to the pregnancy-induced increase in heart rate (+60 bpm compared to pre-pregnancy value) (Mirabito Colafella *et al.*, 2017). Both heart rate and MAP then increased to pre-pregnancy values from day 19-20 of gestation (late gestation) (Mirabito Katrina *et al.*, 2014, Mirabito Colafella *et al.*, 2017), and this value of MAP was also confirmed at 2 weeks post-partum (88 ± 2 mmHg) (Mirabito Katrina *et al.*, 2014).

Changes in uterine arterial function

Besides changes in MAP, uterine artery function is also altered during pregnancy, as the cardiac output and uteroplacental circulation increase (Bernstein *et al.*, 2002, Osol and Moore, 2014). As expected, elevated uterine artery mean flow velocity, that is, the rate by which blood travelled through the blood vessels per unit of time, has been reported throughout pregnancy (Palmer *et al.*, 1992, Dickey and Hower, 1995, Bernstein *et al.*, 2002, Rigano *et al.*, 2010). In order to compensate for this, average uterine artery diameter increases from mid-gestation (2.6 mm) to late pregnancy (3.0 mm) (Palmer *et al.*, 1992, Rigano *et al.*, 2010). Uterine artery resistance index (Dickey and Hower, 1995) and uterine artery pulsatility index also decrease when examined in early pregnancy (Bernstein *et al.*, 2002, Ogueh *et al.*, 2011). However, it should be noted that pregnancy induced changes in the uterine circulation and its resistance is a result of far more than remodelling and vascular reactivity changes of the uterine artery itself. For instance, there was an increase by approximately 2-fold the diameter of arcuate arteries (smaller branches of uterine arteries) and radial arteries (smaller branches of arcuate arteries) in normal pregnancies, from 6.1 to 20.5 weeks of gestation (Allerkamp *et al.*, 2021).

In agreement with human studies, examination of rodent uterine arteries has also reported maternal blood vessel dilation as an adaptation to pregnancy (Cooke and Davidge, 2003, van der Heijden *et al.*, 2009, Barron *et al.*, 2010, Vodstreich *et al.*, 2012). In late pregnancy, rats (van der Heijden *et al.*, 2009, Barron *et al.*, 2010) and mice (Cooke and Davidge, 2003) have an increase in arterial vasodilation within the uterus compared to non-pregnant controls, with a 35% increase in diameter of radial arteries (Barron *et al.*, 2010), and a 20% increase in the methacholine-induced vasodilation response of the uterine artery when measured using wire

myography (Cooke and Davidge, 2003). The enlargement in uterine artery diameter has also been reported in pregnant animals at 1 week (Morris *et al.*, 2020) and 10 days (van der Heijden *et al.*, 2009) post-partum, which may help maintain a high uterine blood flow, and, hence, may be advantageous for subsequent pregnancies (van der Heijden *et al.*, 2009).

Changes in mesenteric function

Similar to the observations in uterine arteries, mesenteric arteries of late-pregnant mice (day 17-18) show increased sensitivity towards vasodilators (e.g. methacholine) (Cooke and Davidge, 2003) and a decreased sensitivity towards vasoconstrictors (e.g. Ang II) by half the non-pregnant control (Marshall *et al.*, 2016). Additionally, in mesenteric arteries of late-pregnant rats, there was a decrease in myogenic reactivity, represented by decreased contraction of smooth muscle cells in response to induced intraluminal flow and pressure (Meyer *et al.*, 1997). This reduction in myogenic reactivity was associated with a decrease in the shear stress that blood vessels experience during pregnancy (-4% in late-pregnant rats vs +54.7% in non-pregnant control) likely a protective mechanism of the maternal vasculature system (Meyer *et al.*, 1997). Interestingly, there is also evidence for a maintenance of pregnancy-induced vasodilation effect, as the mesenteric artery distensibility (i.e. the ability to dilate and constrict passively in response to changes in pressure) in pregnant rats was shown to increase considerably throughout pregnancy and was approximately 30% higher than in non-pregnant controls at 4 weeks post-partum (Morris *et al.*, 2020).

Changes in renal arterial function

As previously mentioned, it is generally accepted that renal vascular resistance decreases to accommodate for increased renal blood flow during pregnancy. Indeed, using the renal Para-aminohippurate (PAH) clearance method, most human studies reported a significant increase in maternal renal blood flow from as early as the 6th week up to week 36 of gestation, reflecting a reduction in renal vascular resistance (Sims and Krantz, 1958, Dunlop, 1981, Sturgiss *et al.*, 1996, Chapman *et al.*, 1998). Renal vascular resistance (calculated using MAP and renal blood flow) was shown to decrease concurrently (Chapman *et al.*, 1998).

Interestingly, increased renal blood flow was even found at up to 25 weeks post-partum, compared to non-pregnant controls (Sims and Krantz, 1958). In contrast, investigation of renal arterial resistive index (RI) using Doppler-based measurement reported either no change in RI throughout gestation (Dib *et al.*, 2003), or a significant increase in RI in gestational weeks' 16-36 (Kurjak *et al.*, 1992, Ogueh *et al.*, 2011). RI is calculated using systolic and diastolic velocities, therefore, might also be influenced by other central haemodynamic parameters rather than the renal vascular resistance itself. As a result, differences in the examination methods/measures, as well as examination intervals and number of samples, are potential explanations for the conflicting results. Similar to the results found in human studies, pregnant rats either had increased renal blood flow at mid- and late-gestation (Matthews and Taylor, 1960), or no change in renal blood flow at early- and late-gestation (Davison and Lindheimer, 1980), represented by increased PAH clearance. However, the former study was done in anaesthetised rats, while the latter was done in unanaesthetised rats. Meanwhile, pregnant rats at mid-gestation were reported to have a significant decrease in myogenic reactivity of small renal arteries compared to non-pregnant control, supporting the potential vasodilation effect of pregnancy on the renal vascular function (Gandley *et al.*, 2001, Novak *et al.*, 2001).

A summary of vasculature changes in healthy human and rodent pregnancy is shown in **Table**

1. Although this review discusses the function and biochemical aspects of isolated vessels from pregnant humans and animals, it should be noted that there are remarkable differences in blood vessel behaviour between and within different organs, hence, it is important for future studies to investigate and provide a better understanding of the pregnancy-specific vasodilation effects on the maternal vasculature system as a whole. Additionally, although rodent studies are the most common, other studies on maternal blood vessel vasodilation during gestation have also been performed in larger animal models such as rabbits, sheep and guinea pigs (White *et al.*, 2000, Brooks *et al.*, 2001, Thompson and Weiner, 2001, Morschauer *et al.*, 2014, Rosenfeld and Roy, 2014).

Table 1. Vasculature changes during healthy human and rodent pregnancy and in post-partum period, relative to pre-pregnancy and/or non-pregnant control (↓: decreased, ↑: increased, -: returned to non-pregnant/pre-pregnancy value, N/A: no information available/yet investigated). MAP: mean arterial pressure; UAD: uterine artery dilation; MAD: mesenteric artery dilation; SAD: small renal artery diameter; RVR: renal vascular resistance; RI: resistance index; L-NAME: N ω -nitro-L-arginine methyl ester. Renal blood flow (RBF) was measured using the Para-aminohippurate clearance method. RVR was calculated using MAP and RBF. An increase in RBF and/or SAD reflects a decrease in renal vascular resistance. Renal resistance index (RI) was calculated using systolic and diastolic velocities.

Observation	Control	Early pregnancy	Mid-pregnancy	Late pregnancy	Post-partum	References
MAP (human)	71-90 mmHg	69-90 mmHg (↓)	65-90 mmHg (↓)	67-94 mmHg (-)	72-93 mmHg (↓)	(Kametas et al., 2001, Simmons et al., 2002, Bernstein et al., 2005, Gunderson et al., 2008, Morris et al., 2014, Morris et al., 2015, Melchiorre et al., 2016)
MAP (rodent)	101-105 mmHg (rats)	93-97 mmHg (↓)	N/A	N/A	N/A	(Barron et al., 2010, Mirabito Katrina et al., 2014, Mirabito Colafella et al., 2017)
	90-103 mmHg (mice)	N/A	-4 to -8 mmHg (change in MAP, ↓)	+8 to +12 mmHg (change in MAP, -)	N/A	

UAD (human)	1.3-1.5 mm	N/A	2.6-3.0 mm (↑)	3.0-3.6 mm (↑)	N/A	(Palmer et al., 1992, Dickey and Hower, 1995, Bernstein et al., 2002, Rigano et al., 2010, Ogueh et al., 2011)
UAD (rodent)	150 μm (rats)	N/A	N/A	190 μm (↑)	150-190 μm (↑)	(Cooke and Davidge, 2003, van der Heijden et al., 2009, Barron et al., 2010, Morris et al., 2020)
	N/A	N/A	N/A	~150% non-pregnant control value (mice; ↑)	~150% non-pregnant control value (↑)	
MAD (human)	(Have not been investigated)					
MAD (rodent)	Lowest passive distensibility (rats)	N/A	N/A	Increased passive distensibility (↑)		(Meyer et al., 1997, Cooke and Davidge, 2003, Marshall et al., 2016, Morris et al., 2020)
	N/A	N/A	N/A	Increased methacholine-induced vasodilation, decreased L-NAME-induced constriction (Mice; ↑)	N/A	
RVR (human)	RI: 0.61-0.65	0.65-0.67 (↑)			0.62 (-)	

	RBF: ~400-600 mL/min	~700-1000 mL/min (↑)		~600-1000 mL/min (↑)	~400-700 mL/min (↑)	(Sims and Krantz, 1958, Dunlop, 1981, Sturgiss et al., 1996, Chapman et al., 1998, Dib et al., 2003, Ogueh et al., 2011)
	RVR: ~7000 sec.cm ⁻⁵	~3500-4500 sec.cm ⁻⁵ (↓)			N/A	
RVR (rodent)	RBF (rats): 5.86-6.82 mL/min	6.45-7.11 mL/L (-)	8.48 mL/L (↑)	5.44-7.44 mL/L (↑)	N/A	(Matthews and Taylor, 1960, Davison and Lindheimer, 1980, Gandley et al., 2001, Novak et al., 2001)
	Renal myogenic reactivity (rats): 1.1-5.5	N/A	1.3-3.7 (↓)	N/A	N/A	
	-3% increase in SAD (rats)	N/A	+8% increase in SAD (↓ vascular resistance)	N/A	N/A	

Roles of endothelial cells and endothelium-derived vasodilators

From the above, it is clear that there is a pregnancy-induced vasodilation effect on the maternal blood vessels, which can potentially be maintained post-partum. These physiological changes are mainly caused by activities of vascular endothelial cells and smooth muscle cells. Endothelial cells produce a number of vasodilators and vasoconstrictors, such as nitric oxide (NO) and endothelin 1, respectively, which transduce signals to the contractile vascular smooth muscle cells to control the constriction and dilation of blood vessels (Rensen *et al.*, 2007, Sandoo *et al.*, 2010, Gao *et al.*, 2016, Touyz *et al.*, 2018).

During pregnancy, there is an increase in the production of vasodilators by endothelial cells, as well as the sensitivity of endothelial cells themselves towards vasodilators. For instance, there is an increase in production of the vasodilators, NO and hydrogen sulphide (H₂S), and the vasodilator-producing enzymes, endothelial NO synthase (eNOS) and cystathionine beta-synthase (CBS) in uterine artery endothelial cell (hUAEC) cultures from pregnant women at late gestation (week 35-36), compared to non-pregnant women (Zhang *et al.*, 2017).

Moreover, treatment of hUAECs with 10 ng/mL vascular endothelial growth factor (VEGF), a vasodilator, resulted in an even higher protein expression of eNOS and CBS (Zhang *et al.*, 2017). As expected, when the endothelium-derived vasodilators, such as nitric oxide synthase (NOS) (Cooke and Davidge, 2003, Barron *et al.*, 2010) or prostaglandin H synthase (PGHS) (Cooke and Davidge, 2003) was inhibited (by Nomega-Nitro-L-arginine methyl ester hydrochloride (L-NAME) or meclofenamate, respectively) in pregnant rodents, the pregnancy-specific vasodilation effect, including the increase in blood vessel diameter and

sensitivity towards methacholine of uterine arteries, was diminished or abolished (Cooke and Davidge, 2003, Barron *et al.*, 2010).

Similarly, in eNOS deficient mice, the increase in uterine artery diameter until day 10 post-partum was eliminated (van der Heijden *et al.*, 2009). The pregnancy-induced change in renal artery myogenic reactivity during midterm was also attenuated by the inhibition of either NOS or endothelin type B receptor (Gandley *et al.*, 2001), or the removal of circulating relaxin (Novak *et al.*, 2001), a 6-kDa ovarian peptide hormone that induces NO production of endothelial cells and, hence, functions as a vasodilator during pregnancy (Conrad, 2011). Likewise, relaxin-deficient mice lost the pregnancy-specific increased sensitivity towards methacholine and decreased sensitivity towards Ang II in their mesenteric arteries (Leo *et al.*, 2014a, Marshall *et al.*, 2016).

There is evidence that there might also be an adaptation of the maternal vasculature system towards the aberrant vascular relaxation during pregnancy. Specifically, in the presence of L-NAME, myogenic tone (i.e. the capability to sustain vasoconstriction (Johansson, 1989)) of uterine arteries in late pregnant rats decreased from $39 \pm 3.2\%$ to $11 \pm 5.0\%$, whereas myogenic tone of uterine arteries in the non-pregnant control group increased from $5 \pm 2.6\%$ to $31 \pm 3.1\%$ (Barron *et al.*, 2010), suggesting a pregnancy-induced re-modelling of uterine arteries that resulted in a decrease in arterial stiffness (Patzak *et al.*, 2018) that was pregnancy specific in rats. Additionally, there was a greater uterine artery diameter in eNOS-deficient mice at 2 days post-partum compared to non-pregnant mice, proposing an alternative source of NO and/or an alternative relaxation pathway (van der Heijden *et al.*, 2009).

Biochemical pathways of maternal blood vessel vasodilation in pregnancy

As mentioned above, endothelial cells produce vasoactive factors that interact with the smooth muscle cells to control the vascular function during pregnancy. Interestingly, endothelial cells and smooth muscle cells are also targets of other vasoconstrictors and vasodilators. In order to gain a better understanding of the underlying mechanisms of vascular adaptation to pregnancy, numerous studies have focused on the renin-angiotensin system and the peptide hormone relaxin. This section will highlight different biochemical pathways that are influenced by the above factors, which can cause blood vessel vasoconstriction or vasodilation.

Renin-angiotensin system

The renin-angiotensin system is known to have a significant effect on regulating blood pressure, including during pregnancy. While renin, a protease, is produced from juxtaglomerular cells of the kidney; angiotensinogen, the angiotensin precursor, is a product of the liver (Timmermans *et al.*, 1993). The generation of biologically-active Ang II, a vasoconstrictor, requires the cleavage of angiotensinogen by renin, in order to generate angiotensin I (Ang I), which is converted to Ang II by the angiotensin-converting enzyme (ACE) (Timmermans *et al.*, 1993). There are numerous Ang II receptors that have been extensively studied over the last few decades, two of which are angiotensin type 1 (AT1) receptor and angiotensin type 2 (AT2) receptor (Bottari *et al.*, 1993). The two receptors, despite having a similar affinity towards Ang II, are distinguished by their different affinities towards antagonists that bind to them and later inhibit their binding to Ang II (Bottari *et al.*, 1993). Additionally, AT1 and AT2 receptors are expressed in both vascular endothelial cells

and vascular smooth muscle cells (Bottari *et al.*, 1993, Allen *et al.*, 2000, Henrion *et al.*, 2001).

Early in pregnancy there is an increase in the maternal plasma Ang II level to stimulate the sodium absorbing and holding capability of blood vessels (Lumbers and Pringle, 2013). This is suggested to be an adaptive mechanism that helps maintain homeostasis as the maternal cardiac output and blood volume increase during pregnancy (Irani and Xia, 2011, Lumbers and Pringle, 2013). Nonetheless, since the 1970s, researchers have reported a trend of weakened responsiveness of blood vessels in the midgestational period, represented by vascular resistance, towards the vasoconstriction effect of infused Ang II in normotensive, but not hypertensive, pregnant women (Gant *et al.*, 1973). One of the potential explanations for the above observation is the pregnancy-specific enhanced AT2 receptor and/or decreased AT1 receptor expression (Takeda-Matsubara *et al.*, 2004, Chen *et al.*, 2007, Ferreira *et al.*, 2009, Mirabito Katrina *et al.*, 2014, Cunningham *et al.*, 2016, Cunningham *et al.*, 2018). In general, AT1 and AT2 receptors have opposite effects in regulating blood pressure, in both the non-pregnant state and during pregnancy (Irani and Xia, 2008, Kawai *et al.*, 2017). The binding of Ang II, dependent on the ratio of AT1/AT2 receptors, causes either a vasoconstriction or a vasodilation outcome, when the receptor is either AT1 or AT2, respectively (Chen *et al.*, 2007). Lack of AT1 receptor expression in female transgenic Ang II-enhanced/AT1-knockout mice caused a significant decline in the systemic blood pressure (by 13% the wild-type mice) measured at mid-gestation (Chen *et al.*, 2007). Meanwhile, inhibition of the AT2 receptor by an added antagonist (PD123319) in wild-type mice caused an increase in blood pressure (Chen *et al.*, 2007). In AT2 receptor-knockout mice, mid-gestational MAP did not change from the pre-pregnancy value, whereas a significant reduction by 6 ± 2 mmHg was seen in wild-type mice (Mirabito *et al.*, 2014). At gestational

day 20, MAP of wild-type mice was similar to the pre-pregnancy value, while MAP of AT2 receptor knockout mice increased by 13 ± 7 mmHg (Mirabito *et al.*, 2014). Additionally, there was no change in the renal AT1 receptor mRNA expression in AT2 receptor knockout mice, compared to a reduced expression in wild-type mice (Mirabito Katrina *et al.*, 2014).

In rats, AT2 receptor mRNA expression measured in the maternal aorta, renal artery, and mesangial cells (main component of renal glomeruli in the renal cortex) at day 12-14 of pregnancy significantly increased compared to the non-pregnant control, whereas there were no changes in AT1 receptor mRNA expression (Ferreira *et al.*, 2009). The Ang II-induced increase in calcium concentration in mesangial cells of pregnant rats was more than two-fold lower compared to the non-pregnant control, suggesting a reduction in sensitivity of renal cells towards Ang II in the midgestational period (Ferreira *et al.*, 2009). On the contrary, Ang II-induced renal vascular resistance and renal mitochondrial oxidative stress at late gestation increased when the AT1 receptor function was enhanced by its agonist autoantibodies (AT1-AA), which are detectable in preeclamptic pregnancies (Cunningham *et al.*, 2016, Cunningham *et al.*, 2019). These phenotypes were reduced and/or inhibited by the AT1-AA inhibitor ('n7AAc') (Cunningham *et al.*, 2018, Cunningham *et al.*, 2019), suggesting the vasoconstriction-inducing effect of the AT1 receptor, which is usually decreased in a normal pregnancy but increased with preeclampsia. Further emphasising the importance of this system in pregnancy health and disease, in preeclampsia hypersensitivity of the AT1 receptor through its heterodimerisation leads to increased Ang II responsiveness (Abdalla *et al.*, 2001b, Quitterer and AbdAlla, 2021).

In regards to different biochemical pathways that are activated by the binding of Ang II to a receptor, different consequential signalling cascades can lead to either vasoconstriction or vasodilation. For instance, when bound by Ang II, AT1 receptor interacts with heterotrimeric G-proteins, which then transduces signals to protein tyrosine kinase (PTK) and Rho guanine nucleotide exchange factors (Rho GEFs) (Kawai *et al.*, 2017). Although PTK and Rho GEFs activate other molecules in different pathways, such as phosphoinositide-3-kinase (PIK3), phospholipase C (PLC), or Ras homolog family member A (RhoA) (Ushio-Fukai *et al.*, 1998, Seki *et al.*, 1999, Lutz *et al.*, 2005), the final endpoint, vasoconstriction, is similar (**Figure 1**). On the contrary, the binding of Ang II to the AT2 receptor inhibits the RhoA/Rho kinase pathway and causes vasodilation (Savoia *et al.*, 2005) (**Figure 2**). There are likely more molecules involved in these pathways that are yet to be discovered. Therefore, further research is required to determine which specific pathway(s) are altered as an adaptation to pregnancy.

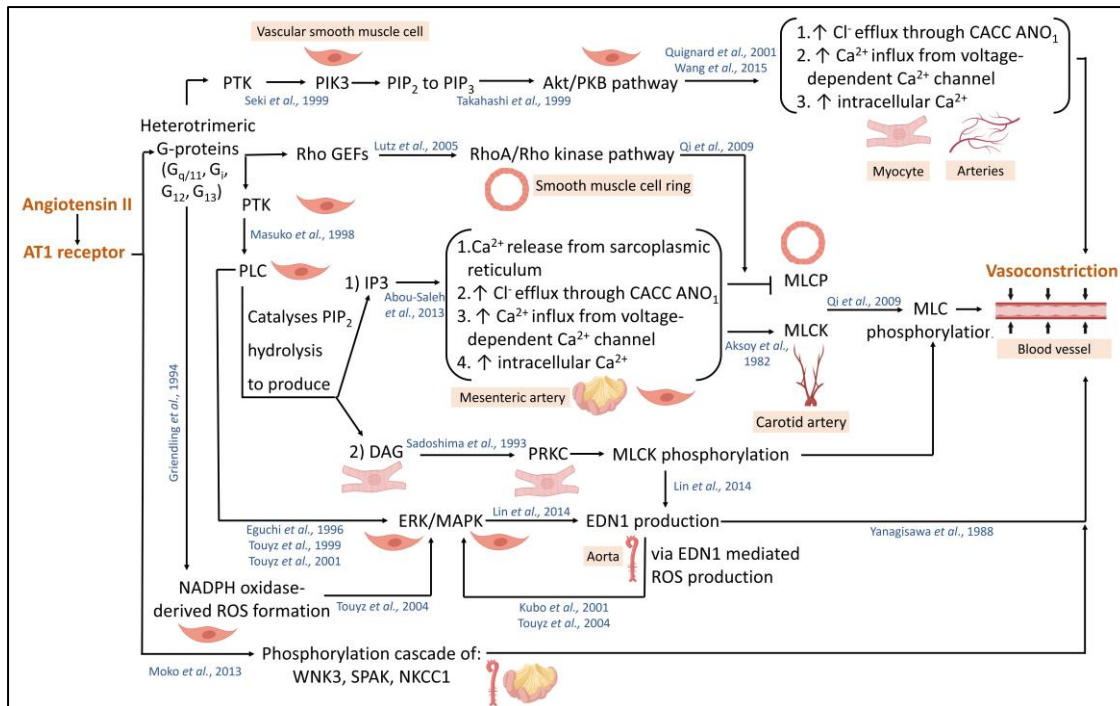


Figure 1. Different pathways activated as a result of the binding of Angiotensin II to the AT1 receptor which result in vasoconstriction. Organs and/or cell types in which the pathways were studied are shown. →, activates/binds, ⊥, inhibits. PRKC, protein kinase C, PTK, protein tyrosine kinase, PIK3, phosphoinositide-3-kinase, PIP₂, phosphatidylinositol 4,5-bisphosphate, PIP₃, phosphatidylinositol (3,4,5)-trisphosphate, PKB, protein kinase B, PLC, phospholipase C, Rho GEFs, Rho guanine nucleotide exchange factors, IP₃, inositol triphosphate, DAG, diacylglycerol, ROS, reactive oxygen species, CACC, calcium-activated chloride channel, MLCK, myosin light chain kinase, MLCP, myosin light chain phosphatase, ERK, extracellular-signal-regulated kinase, MAPK, mitogen-activated protein kinase, EDN1, endothelin 1, WNK3, with-no-lysine kinase 3, SPAK, STE20/SPS1-related proline/alanine-rich kinase, NKCC1, Na–K–Cl cotransporter isoform 1 (Aksoy *et al.*, 1982, Yanagisawa *et al.*, 1988, Sadoshima and Izumo, 1993, Archer *et al.*, 1994, Griendling *et al.*, 1994, Eguchi *et al.*, 1996, Ushio-Fukai *et al.*, 1998, Seki *et al.*, 1999, Takahashi *et al.*, 1999, Touyz *et al.*, 1999, Kubo *et al.*, 2001, Quignard *et al.*, 2001, Touyz *et al.*, 2001, Touyz *et al.*, 2004, Lutz *et*

et al., 2005, Qi *et al.*, 2009, Abou-Saleh *et al.*, 2013, Zeniya *et al.*, 2013, Lin *et al.*, 2014, Wang *et al.*, 2015). Created with BioRender.com.

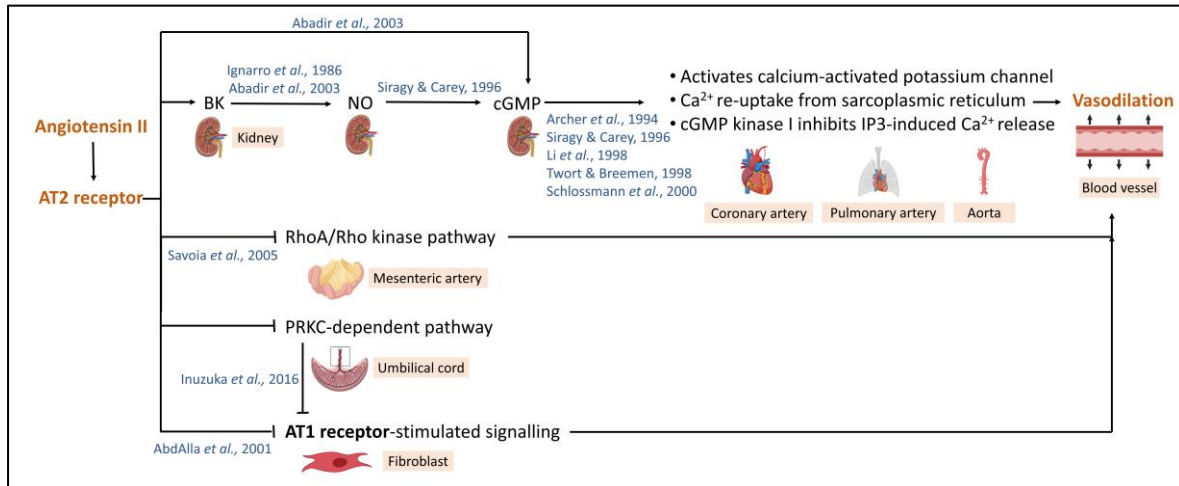


Figure 2. Different pathways activated as a result of the binding of Angiotensin II to the AT2 receptor which result in vasodilation. Organs and/or cell types in which the pathways were studied are shown. →, activates/binds, ⊥, inhibits. BK, bradykinin, NO, nitric oxide, cGMP, cyclic guanosine monophosphate, PRKC, protein kinase C, IP3, inositol triphosphate (Ignarro *et al.*, 1986, Twort and Breemen, 1988, Siragy and Carey, 1996, Li *et al.*, 1998, Schlossmann *et al.*, 2000, AbdAlla *et al.*, 2001a, Savoia *et al.*, 2005, Inuzuka *et al.*, 2016). Created with BioRender.com.

Relaxin

The Human 2 (H2) relaxin and its two orthologs in rodents, Mouse 1 (M1) relaxin and Rat 1 (R1) relaxin, are produced by the ovarian corpus luteum and the placenta (Sherwood, 2004, Marshall *et al.*, 2017c). The most studied role of relaxin is that on the mesenteric, renal and uterine blood vessels. However, it likely also plays a role in the placental vasculature. Despite

limited information regarding its functional role in the placenta, it has been shown to be important for survival of cytotrophoblast cells (Conrad, 2016, Marshall *et al.*, 2017b)

Relaxin binds several receptors, including the relaxin/insulin-like family peptide receptor 1 (RXFP1) (Jelinic *et al.*, 2014), which is mostly found on the surface of vascular endothelial and vascular smooth muscle cells (Jelinic *et al.*, 2014), except the human umbilical artery endothelial cells (Sarwar *et al.*, 2016). Relaxin is known to play an essential role in blood vessel vasodilation, including during pregnancy, and the evidence of this role comes from both animal (Ferreira *et al.*, 2009, McGuane *et al.*, 2011, Vodstcil *et al.*, 2012, Leo *et al.*, 2014b, Marshall *et al.*, 2016, Marshall *et al.*, 2017a, Mirabito Colafella *et al.*, 2017) and human (Quattrone *et al.*, 2004, McGuane *et al.*, 2011, Sarwar *et al.*, 2016) studies. Relaxin-knockout mice have an elevated heart rate throughout pregnancy, in association with higher MAP compared to wild-type mice at both mid-gestation (gestational day 9; 9.7 mmHg higher) and late-gestation (gestational day 19; 7.2 mmHg higher) (Mirabito Colafella *et al.*, 2017). Moreover, the pregnancy-induced decreased sensitivity of mesenteric arteries towards the vasoconstriction effect of Ang II was eliminated in relaxin-deficient pregnant mice (Marshall *et al.*, 2016). In contrast, when relaxin-deficient mice were treated with exogenous relaxin at day 12.5 to 17.5 of gestation, the Ang II-induced contraction of mesenteric arteries was reduced by more than half the contraction seen in untreated mice (Marshall *et al.*, 2017a).

As both Ang II and relaxin are involved in the regulation of the maternal vasculature system during pregnancy, there is a question of whether relaxin interacts with any of the molecules/pathways induced by the binding of Ang II to its receptors. Indeed, the addition of

exogenous relaxin (1000 ng/mL) into human umbilical vein endothelial cells (HUVECs) increased *NOS II* expression by 15 times compared to the untreated cells (Quattrone *et al.*, 2004). Consequently, the protein expression of NOS II and the NO production were increased by more than double the untreated control. In support of this finding, the direct addition of serelaxin, a recombinant form of relaxin, into either human umbilical artery smooth muscle cell (HUASMC) or human umbilical vein smooth muscle cell (HUASMC) monoculture induced cGMP accumulation within the smooth muscle cells (Sarwar *et al.*, 2016), which interferes with the release of Ca^{2+} from the sarcoplasmic reticulum into the smooth muscle cell intracellular space, hence affecting its contractile phenotype (Touyz *et al.*, 2018). This is known as one of the key steps involved in the Ang II-AT2-NO/cGMP pathway that can lead to vasodilation (Figure 2). The addition of serelaxin into either HUVECs or human coronary artery endothelial cells (HCAECs) that were co-cultured with HUASMCs and HUASMCs also induced cGMP accumulation within the smooth muscle cells (Sarwar *et al.*, 2016). Additionally, when the endothelial cells were treated with L-N^G-nitro arginine (NOARG), a NOS inhibitor, the relaxin-induced cGMP accumulation was significantly reduced. Besides NO and cGMP, relaxin was also shown to cause a vasodilation effect via the activation of bradykinin (BK) (Leo *et al.*, 2014b) and the PI₃K-Akt pathway (Dimmeler *et al.*, 1999, McGuane *et al.*, 2011, Lian *et al.*, 2018), which are also involved in the Ang II – AT1/AT2 receptor regulation of blood vessels (**Figures 1 and 2**). Taken together, relaxin interacts with various factors and pathways in endothelial and vascular smooth muscle cells leading to vasodilation.

These results therefore give rise to another question of whether relaxin interacts with the Ang II receptors. A study on rat renal myofibroblasts reported that relaxin treatment decreased renal fibrosis by increasing extracellular-signal-regulated kinase (ERK) phosphorylation and

NOS phosphorylation, by approximately double the untreated control, and decreasing expression of TGFB1, pSmad2, and alpha-smooth muscle actin to a similar level compared to the untreated control (Chow *et al.*, 2014). However, these effects were abolished when the AT2 receptor activity was blocked by PD123319 or when there was no cell surface AT2 receptor expression (Chow *et al.*, 2014). Bioluminescence resonance energy transfer saturation assays of human embryonic renal cells also confirmed the presence of RXFP1-AT2 receptor heterodimer when RXFP1 was bound by relaxin (Chow *et al.*, 2014). Likewise, evidence of the RXFP-AT1 heterodimer was found in rat renal myofibroblasts (Chow *et al.*, 2019) and human cardiac myofibroblasts (Chow *et al.*, 2019, Wang *et al.*, 2020), suggesting that Ang II receptors are important for the function of relaxin, and that relaxin can indirectly activate the AT1/AT2 receptors function via the formation of RXFP1-AT1/AT2 complex. However, it is not clear whether there is a Relaxin-Ang II receptor interaction in vascular endothelial and smooth muscle cells, and whether such event is responsible for the vasodilation of maternal blood vessels during pregnancy.

Besides relaxin and the renin-angiotensin system, there is a range of other factors, such as oestrogen and progesterone - the two sex hormones that also play important roles in remodelling of the maternal vascular system during pregnancy (Kodogo *et al.*, 2019). Moreover, these hormones also interact with the renin-angiotensin system and pathways that are activated by the binding of Ang II to its receptors. Indeed increased levels of progesterone and prostacyclin may lead to resistance of Ang II effects (Gant *et al.*, 1980, Irani and Xia, 2011). In-depth discussion on the role of these factors has been reviewed elsewhere (Lumbers and Pringle, 2013, Wetendorf and DeMayo, 2014, Kodogo *et al.*, 2019).

Ang II/relaxin in preeclampsia

The role of Ang II/relaxin, in the maternal vasculature system during pregnancy is important for the investigation of aberrant haemodynamic functions in pregnancy complications such as preeclampsia (Lumbers *et al.*, 2019). Briefly, in preeclampsia abnormal placental development leads to the increased release of factors into the maternal circulation (including renin and AT1-AAAs) and over activation of the AT1 receptor and vasoconstriction. Moreover, low levels of relaxin in the first trimester have been identified in women who later develop late onset preeclampsia (Post Uiterweer *et al.*, 2020). Better understanding of the relationship between Ang II pathways and relaxin in uncomplicated pregnancies is critical to understand the role of relaxin in complications such as preeclampsia.

FUTURE PERSPECTIVES

Interestingly, endothelial and smooth muscle cells are mechanosensitive with changes in blood flow and blood pressure during pregnancy altering the shear stress and stretch these cells experience, which can in turn alter their expression and function (Boo *et al.*, 2002, Rodríguez and González, 2014, Jufri *et al.*, 2015). Moreover, it is known that at least some of the relevant receptors within the relaxin-RXFP1-Ang II pathways are themselves mechanosensitive. For example, the AT1 receptor which can be mechanically activated through an Ang II independent mechanism and can lead to actin remodelling and changes in myogenic responsiveness (Hong *et al.*, 2016). Therefore, dynamic cellular culture under shear stress may hold further insights and should be considered when studying interactions within these pathways, *in vitro*. For example, with the use of organ-on-chip microfluidic models which better mimic specific aspects of the *in vivo* cellular physiological environment (Huh *et al.*, 2011, Ganesan *et al.*, 2017). Indeed, microfluidic models have been shown to recreate the

mechanical forces and shear stress similar to what the cells would experience within blood vessels (Ostrowski *et al.*, 2014, Gray and Stroka, 2017, van Engeland *et al.*, 2018). In addition, studies of animal models, in which functional responses of blood vessels can be measured using wire myography, pressure myography (Leo *et al.*, 2014a, Marshall *et al.*, 2016, Marshall *et al.*, 2017a, Marshall *et al.*, 2018) and arteriography (Morris *et al.*, 2020), can be used to investigate vasodilation in regards to altered Relaxin-Ang II receptor interaction at different time points during pregnancy and post-partum. This might allow future studies to look at similar changes in humans and provide prevention strategies or pathways for treatment.

CONCLUSION

In summary, it is important to understand the underlying mechanisms of maternal vasculature adaptation, such as relaxin-RXFP1-Ang II receptor interactions, in a healthy human pregnancy. This might help explain why there is potentially a protective effect on the vasculature system post-partum in women that have a healthy pregnancy. In addition, by understanding the biochemical pathways involved in maternal vasculature adaptation to pregnancy, this may help shed light on how these pathways may be disrupted in pregnancy complicated by gestational hypertension or preeclampsia.

ACKNOWLEDGMENTS

MW would like to acknowledge the financial support of the National Health and Medical Research Council (Development grant: APP1171821).

CONFLICT OF INTERESTS

The authors declare that there is no conflict of interest.

AUTHOR CONTRIBUTION STATEMENT

TBM, LP, MW conception and design of article; TNAD literature search, data interpretation and manuscript drafting; TBM, LP, MW critical revision and contribution to intellectual content.

DATA AVAILABILITY STATEMENT: Data availability is not applicable to this article as no new data were created or analysed in this study

REFERENCES

- ABDALLA, S., LOTHER, H., ABDEL-TAWAB, A. M. & QUITTERER, U. 2001a. The Angiotensin II AT2 receptor is an AT1 receptor antagonist. *Journal of Biological Chemistry*, 276, 39721-39726.
- ABDALLA, S., LOTHER, H., MASSIERY, A. & QUITTERER, U. 2001b. Increased AT1 receptor heterodimers in preeclampsia mediate enhanced angiotensin II responsiveness. *Nature medicine*, 7, 1003-1009.
- ABOU-SALEH, H., PATHAN, A. R., DAALIS, A., HUBRACK, S., ABOU-JASSOUM, H., AL-NAEIMI, H., RUSCH, N. J. & MACHACA, K. 2013. Inositol 1,4,5-trisphosphate (IP3) receptor up-regulation in hypertension is associated with sensitization of Ca²⁺ release and vascular smooth muscle contractility. *The Journal of biological chemistry*, 288, 32941-32951.

- AKSOY, M. O., MURPHY, R. A. & KAMM, K. E. 1982. Role of Ca²⁺ and myosin light chain phosphorylation in regulation of smooth muscle. *American Journal of Physiology-Cell Physiology*, 242, C109-C116.
- ALLEN, A. M., ZHUO, J. & MENDELSON, F. A. O. 2000. Localization and function of angiotensin AT1 receptors. *American Journal of Hypertension*, 13, S31-S38.
- ALLERKAMP, H. H., CLARK, A. R., LEE, T. C., MORGAN, T. K., BURTON, G. J. & JAMES, J. L. 2021. Something old, something new: digital quantification of uterine vascular remodelling and trophoblast plugging in historical collections provides new insight into adaptation of the utero-placental circulation. *Human Reproduction*, 36, 571-586.
- ARCHER, S. L., HUANG, J. M., HAMPL, V., NELSON, D. P., SHULTZ, P. J. & WEIR, E. K. 1994. Nitric oxide and cGMP cause vasorelaxation by activation of a charybdotoxin-sensitive K channel by cGMP-dependent protein kinase. *Proceedings of the National Academy of Sciences of the United States of America*, 91, 7583-7587.
- BARRON, C., MANDALA, M. & OSOL, G. 2010. Effects of pregnancy, hypertension and nitric oxide inhibition on rat uterine artery myogenic reactivity. *Journal of Vascular Research*, 47, 463-471.
- BELLAMY, L., CASAS, J.-P., HINGORANI, A. D. & WILLIAMS, D. J. 2007. Pre-eclampsia and risk of cardiovascular disease and cancer in later life: systematic review and meta-analysis. *British Medical Journal*, 335, 974.
- BERNSTEIN, I. M., THIBAUT, A., MONGEON, J. A. & BADGER, G. J. 2005. The influence of pregnancy on arterial compliance. *Obstetrics and gynecology*, 105, 621.
- BERNSTEIN, I. M., ZIEGLER, W. F., LEAVITT, T. & BADGER, G. J. 2002. Uterine artery hemodynamic adaptations through the menstrual cycle into early pregnancy. *Obstetrics & Gynecology*, 99, 620-624.

- BOO, Y. C., SORESCU, G., BOYD, N., SHIOJIMA, I., WALSH, K., DU, J. & JO, H. 2002. Shear stress stimulates phosphorylation of endothelial nitric-oxide synthase at Ser1179 by Akt-independent mechanisms: role of protein kinase A. *Journal of Biological Chemistry*, 277, 3388-3396.
- BOTTARI, S. P., DE GASPARO, M., STECKELINGS, U. M. & LEVENS, N. R. 1993. Angiotensin II receptor subtypes: characterization, signalling mechanisms, and possible physiological implications. *Frontiers in Neuroendocrinology*, 14, 123-171.
- BROOKS, V. L., CLOW, K. A., WELCH, L. S. & GIRAUD, G. D. 2001. Does nitric oxide contribute to the basal vasodilation of pregnancy in conscious rabbits? *American Journal of Physiology - Regulatory, Integrative and Comparative Physiology*, 281, 1624-1632.
- CARPENTER, M. W. 2007. Gestational diabetes, pregnancy hypertension, and late vascular disease. *Diabetes Care*, 30, S246-S250.
- CHAPMAN, A. B., ABRAHAM, W. T., ZAMUDIO, S., COFFIN, C., MEROUANI, A., YOUNG, D., JOHNSON, A., OSORIO, F., GOLDBERG, C., MOORE, L. G., DAHMS, T. & SCHRIER, R. W. 1998. Temporal relationships between hormonal and hemodynamic changes in early human pregnancy. *Kidney International*, 54, 2056-2063.
- CHEN, K., MERRILL, D. C. & ROSE, J. C. 2007. The importance of Angiotensin II subtype receptors for blood pressure control during mouse pregnancy. *Reproductive Sciences*, 14, 694-704.
- CHOW, B. S. M., KOCAN, M., BOSNYAK, S., SARWAR, M., WIGG, B., JONES, E. S., WIDDOP, R. E., SUMMERS, R. J., BATHGATE, R. A. D., HEWITSON, T. D. & SAMUEL, C. S. 2014. Relaxin requires the angiotensin II type 2 receptor to abrogate renal interstitial fibrosis. *Kidney International*, 86, 75-85.
- CHOW, B. S. M., KOCAN, M., SHEN, M., WANG, Y., HAN, L., CHEW, J. Y., WANG, C., BOSNYAK, S., MIRABITO-COLAFELLA, K. M., BARSHA, G., WIGG, B.,

JOHNSTONE, E. K. M., HOSSAIN, M. A., PFLEGER, K. D. G., DENTON, K. M., WIDDOP, R. E., SUMMERS, R. J., BATHGATE, R. A. D., HEWITSON, T. D. & SAMUEL, C. S. 2019. AT1R-AT2R-RXFP1 functional crosstalk in myofibroblasts: impact on the therapeutic targeting of renal and cardiac fibrosis. *Journal of the American Society of Nephrology*, 30, 2191-2207.

CNOSSEN, J. S., VOLLEBREGT, K. C., VRIEZE, N. D., RIET, G. T., MOL, B. W. J., FRANX, A., KHAN, K. S. & POST, J. A. M. V. D. 2008. Accuracy of mean arterial pressure and blood pressure measurements in predicting pre-eclampsia: systematic review and meta-analysis. *BMJ : British Medical Journal*, 336, 1117.

CONRAD, K. P. 2011. Maternal vasodilation in pregnancy: the emerging role of relaxin. *American journal of physiology. Regulatory, integrative and comparative physiology*, 301, R267-R275.

CONRAD, K. P. 2016. G-Protein-coupled receptors as potential drug candidates in preeclampsia: targeting the relaxin/insulin-like family peptide receptor 1 for treatment and prevention. *Human reproduction update*, 22, 647-664.

COOKE, C.-L. M. & DAVIDGE, S. T. 2003. Pregnancy-Induced alterations of vascular function in mouse mesenteric and uterine arteries. *Biology of Reproduction*, 68, 1072-1077.

CUNNINGHAM, M., CASTILLO, J., IBRAHIM, T., CORNELIUS, D. C., CAMPBELL, N., AMARAL, L., VAKA, V., USRY, N., WILLIAMS, J. & LAMARCA, B. 2018. AT1-AA (Angiotensin II type 1 receptor agonistic autoantibody) blockade prevents preeclamptic symptoms in placental ischemic rats. *Hypertension*, 71, 886-893.

CUNNINGHAM, M. W., VAKA, V. R., MCMASTER, K., IBRAHIM, T., CORNELIUS, D. C., AMARAL, L., CAMPBELL, N., WALLUKAT, G., MCDUFFY, S., USRY, N., DECHEND, R. & LAMARCA, B. 2019. Renal natural killer cell activation and

mitochondrial oxidative stress; new mechanisms in AT1-AA mediated hypertensive pregnancy. *Pregnancy Hypertension*, 15, 72-77.

CUNNINGHAM, M. W., WILLIAMS, J. M., AMARAL, L., USRY, N., WALLUKAT, G., DECHEND, R. & LAMARCA, B. 2016. Agonistic autoantibodies to the Angiotensin II type 1 receptor enhance Angiotensin II-induced renal vascular sensitivity and reduce renal function during pregnancy. *Hypertension*, 68, 1308-1313.

DAVISON, J. M. 1984. Renal haemodynamics and volume homeostasis in pregnancy. *Scandinavian journal of clinical and laboratory investigation*, 44, 15-27.

DAVISON, J. M. & LINDHEIMER, M. D. 1980. Changes in renal haemodynamics and kidney weight during pregnancy in the unanaesthetized rat. *The Journal of Physiology*, 301, 129-136.

DIB, F. R., DUARTE, G., SALA, M. M., FERRIANI, R. A. & BEREZOWSKI, A. T. 2003. Prospective evaluation of renal artery resistance and pulsatility indices in normal pregnant women. *Ultrasound in Obstetrics & Gynecology*, 22, 515-519.

DICKEY, R. P. & HOWER, J. F. 1995. Ultrasonographic features of uterine blood flow during the first 16 weeks of pregnancy. *Human reproduction (Oxford, England)*, 10, 2448.

DIMMELER, S., FLEMING, I., FISSLTHALER, B., HERMANN, C., BUSSE, R. & ZEIHNER, A. M. 1999. Activation of nitric oxide synthase in endothelial cells by Akt-dependent phosphorylation. *Nature*, 399, 601-605.

DUNLOP, W. 1981. Serial changes in renal haemodynamics during normal human pregnancy. *BJOG : an international journal of obstetrics and gynaecology*, 88, 1-9.

EGUCHI, S., MATSUMOTO, T., MOTLEY, E. D., UTSUNOMIYA, H. & INAGAMI, T. 1996. Identification of an essential signaling cascade for Mitogen-activated Protein Kinase Activation by Angiotensin II in cultured rat vascular smooth muscle cells: possible

requirement of Gq-mediated p21ras activation coupled to a Ca²⁺/calmodulin-sensitive tyrosine kinase. *Journal of Biological Chemistry*, 271, 14169-14175.

FERREIRA, V. M., GOMES, T. S., REIS, L. A., FERREIRA, A. T., RAZVICKAS, C. V., SCHOR, N. & BOIM, M. A. 2009. Receptor-induced dilatation in the systemic and intrarenal adaptation to pregnancy in rats. *PLoS ONE*, 4, e4845.

GANDLEY, R. E., CONRAD, K. P. & MCLAUGHLIN, M. K. 2001. Endothelin and nitric oxide mediate reduced myogenic reactivity of small renal arteries from pregnant rats. *American Journal of Physiology-Regulatory, Integrative and Comparative Physiology*, 280, R1-R7.

GANESAN, M. K., FINSTERWALDER, R., LEB, H., RESCH, U., NEUMÜLLER, K., DE MARTIN, R. & PETZELBAUER, P. 2017. Three-dimensional coculture model to analyze the cross talk between endothelial and smooth muscle cells. *Tissue engineering. Part C, Methods*, 23, 38-49.

GANT, N. F., DALEY, G. L., CHAND, S., WHALLEY, P. J. & MACDONALD, P. C. 1973. A study of angiotensin II pressor response throughout primigravid pregnancy. *The Journal of clinical investigation*, 52, 2682.

GANT, N. F., WORLEY, R. J., EVERETT, R. B. & MACDONALD, P. C. 1980. Control of vascular responsiveness during human pregnancy. *Kidney International*, 18, 253-258.

GAO, Y., CHEN, T. & RAJ, J. U. 2016. Endothelial and smooth muscle cell interactions in the pathobiology of pulmonary hypertension. *American Journal of Respiratory Cell and Molecular Biology*, 54, 451-460.

GRAY, K. M. & STROKA, K. M. 2017. Vascular endothelial cell mechanosensing: New insights gained from biomimetic microfluidic models. *Seminars in Cell & Developmental Biology*, 71, 106-117.

- GRIENDLING, K., MINIERI, C., OLLERENSHAW, J. D. & ALEXANDER, R. W. 1994. Angiotensin-II stimulates NADH and NADPH oxidase activity in cultured vascular smooth-muscle cells. *Circulation Research*, 74, 1141-1148.
- GUNDERSON, E. P., CHIANG, V., LEWIS, C. E., CATOV, J., QUESENBERRY, C. P., JR., SIDNEY, S., WEI, G. S. & NESS, R. 2008. Long-term blood pressure changes measured from before to after pregnancy relative to nonparous women. *Obstetrics and gynecology*, 112, 1294-1302.
- GUYTON, A. C. 1981. The relationship of cardiac output and arterial pressure control. *Circulation*, 64, 1079.
- HENRION, D., KUBIS, N. & LÉVY BERNARD, I. 2001. Physiological and pathophysiological functions of the AT2 subtype receptor of Angiotensin II. *Hypertension*, 38, 1150-1157.
- HONG, K., ZHAO, G., HONG, Z., SUN, Z., YANG, Y., CLIFFORD, P. S., DAVIS, M. J., MEININGER, G. A. & HILL, M. A. 2016. Mechanical activation of angiotensin II type 1 receptors causes actin remodelling and myogenic responsiveness in skeletal muscle arterioles. *The Journal of physiology*, 594, 7027-7047.
- HUH, D., HAMILTON, G. A. & INGBER, D. E. 2011. From 3D cell culture to organs-on-chips. *Trends in cell biology*, 21, 745-754.
- HUNTER, S. & ROBSON, S. C. 1992. Adaptation of the maternal heart in pregnancy. *British Heart Journal*, 68, 540-543.
- IGNARRO, L. J., HARBISON, R. G., WOOD, K. S. & KADOWITZ, P. J. 1986. Activation of purified soluble guanylate cyclase by endothelium-derived relaxing factor from intrapulmonary artery and vein: stimulation by acetylcholine, bradykinin and arachidonic acid. *Journal of Pharmacology and Experimental Therapeutics*, 237, 893-900.

INUZUKA, T., FUJIOKA, Y., TSUDA, M., FUJIOKA, M., SATOH, A. O., HORIUCHI, K., NISHIDE, S., NANBO, A., TANAKA, S. & OHBA, Y. 2016. Attenuation of ligand-induced activation of angiotensin II type 1 receptor signaling by the type 2 receptor via protein kinase C. *Scientific Reports*, 6, 21613.

IRANI, R. A. & XIA, Y. 2008. The functional role of the Renin-Angiotensin system in pregnancy and preeclampsia *Placenta*, 29, 763-771.

IRANI, R. A. & XIA, Y. 2011. Renin angiotensin signaling in normal pregnancy and preeclampsia. *Seminars in nephrology*, 31, 47-58.

JELINIC, M., LEO, C.-H., POST UITERWEER, E. D., SANDOW, S. L., GOOI, J. H., WLODEK, M. E., CONRAD, K. P., PARKINGTON, H., TARE, M. & PARRY, L. J. 2014. Localization of relaxin receptors in arteries and veins, and region-specific increases in compliance and bradykinin-mediated relaxation after *in vivo* serelaxin treatment. *The FASEB Journal*, 28, 275-287.

JOHANSSON, B. 1989. Myogenic tone and reactivity: definitions based on muscle physiology. *J Hypertens Suppl*, 7, S5-S9.

JUFRI, N. F., MOHAMEDALI, A., AVOLIO, A. & BAKER, M. S. 2015. Mechanical stretch: physiological and pathological implications for human vascular endothelial cells. *Vascular cell*, 7, 8.

KAMETAS, N. A., MCAULIFFE, F., COOK, B., NICOLAIDES, K. H. & CHAMBERS, J. 2001. Maternal left ventricular transverse and long-axis systolic function during pregnancy. *Ultrasound in Obstetrics & Gynecology*, 18, 467-474.

KAWAI, T., FORRESTER, S. J., O'BRIEN, S., BAGGETT, A., RIZZO, V. & EGUCHI, S. 2017. AT1 receptor signaling pathways in the cardiovascular system. *Pharmacological research*, 125, 4-13.

- KODOGO, V., AZIBANI, F. & SLIWA, K. 2019. Role of pregnancy hormones and hormonal interaction on the maternal cardiovascular system: a literature review. *Clinical Research in Cardiology*, 108, 831-846.
- KUBO, T., IBUSUKI, T., CHIBA, S., KAMBE, T. & FUKUMORI, R. 2001. Mitogen-activated protein kinase activity regulation role of angiotensin and endothelin systems in vascular smooth muscle cells. *European Journal of Pharmacology*, 411, 27-34.
- KURJAK, A., VIDOVIC, M. I., VELEMIR, D. & ZALUD, I. 1992. Renal arterial Resistance Index in pregnant and nonpregnant women: evaluation with color and pulse Doppler ultrasound. 20, 11-14.
- LEO, C. H., JELINIC, M., GOOI, J. H., TARE, M. & PARRY, L. J. 2014a. A vasoactive role for endogenous relaxin in mesenteric arteries of male mice. *PLOS ONE*, 9, e107382.
- LEO, C. H., JELINIC, M., PARKINGTON, H. C., TARE, M. & PARRY, L. J. 2014b. Acute intravenous injection of serelaxin (Recombinant Human Relaxin-2) causes rapid and sustained Bradykinin-mediated vasorelaxation. *Journal of the American Heart Association*, 3, e000493.
- LI, P.-L., JIN, M.-W. & CAMPBELL, W. B. 1998. Effect of selective inhibition of soluble guanylyl cyclase on the K_{Ca} channel activity in coronary artery smooth muscle. *Hypertension*, 31, 303-308.
- LIAN, X., BEER-HAMMER, S., KÖNIG, G. M., KOSTENIS, E., NÜRNBERG, B. & GOLLASCH, M. 2018. RXFP1 receptor activation by relaxin-2 induces vascular relaxation in mice via a $G\alpha_i2$ -protein/PI3K β / γ /nitric oxide-coupled pathway. *Frontiers in Physiology*, 9.
- LIN, Y.-J., KWOK, C.-F., JUAN, C.-C., HSU, Y.-P., SHIH, K.-C., CHEN, C.-C. & HO, L.-T. 2014. Angiotensin II enhances endothelin-1-induced vasoconstriction through upregulating endothelin type A receptor. *Biochemical and Biophysical Research Communications*, 451, 263-269.

- LUMBERS, E. R., DELFORCE, S. J., ARTHURS, A. L. & PRINGLE, K. G. 2019. Causes and consequences of the dysregulated maternal renin-angiotensin system in preeclampsia. *Frontiers in endocrinology (Lausanne)*, 10.
- LUMBERS, E. R. & PRINGLE, K. G. 2013. Roles of the circulating renin-angiotensin-aldosterone system in human pregnancy. *American Journal of Physiology-Regulatory, Integrative and Comparative Physiology*, 306, R91-R101.
- LUTZ, S., FREICHEL-BLOMQUIST, A., YANG, Y., RÜMENAPP, U., JAKOBS, K. H., SCHMIDT, M. & WIELAND, T. 2005. The guanine nucleotide exchange factor p63RhoGEF, a specific link between Gq/11-coupled receptor signaling and RhoA. *Journal of Biological Chemistry*, 280, 11134-11139.
- LYKKE, J. A., LANGHOFF-ROOS, J., SIBAI, B. M., FUNAI, E. F., TRICHE, E. W. & PAIDAS, M. J. 2009. Hypertensive pregnancy disorders and subsequent cardiovascular morbidity and type 2 diabetes mellitus in the mother. *Hypertension*, 53, 944.
- MARSHALL, S. A., LEO, C. H., GIRLING, J. E., TARE, M., BEARD, S., HANNAN, N. J. & PARRY, L. J. 2017a. Relaxin treatment reduces angiotensin II-induced vasoconstriction in pregnancy and protects against endothelial dysfunction. *Biology of Reproduction*, 96, 895-906.
- MARSHALL, S. A., LEO, C. H., SENADHEERA, S. N., GIRLING, J. E., TARE, M. & PARRY, L. J. 2016. Relaxin deficiency attenuates pregnancy-induced adaptation of the mesenteric artery to angiotensin II in mice. *American Journal of Physiology-Regulatory, Integrative and Comparative Physiology*, 310, R847-R857.
- MARSHALL, S. A., SENADHEERA, S. N., JELINIC, M., O'SULLIVAN, K., PARRY, L. J. & TARE, M. 2018. Relaxin deficiency leads to uterine artery dysfunction during pregnancy in mice. *Frontiers in Physiology*, 9.

- MARSHALL, S. A., SENADHEERA, S. N., PARRY, L. J. & GIRLING, J. E. 2017b. The role of relaxin in normal and abnormal uterine function during the menstrual cycle and early pregnancy. *Reproductive sciences (Thousand Oaks, Calif.)*, 24, 342-354.
- MARSHALL, S. A., SENADHEERA, S. N., PARRY, L. J. & GIRLING, J. E. 2017c. The role of relaxin in normal and abnormal uterine function during the menstrual cycle and early pregnancy. *Reproductive Sciences*, 24, 342-354.
- MATTHEWS, B. F. & TAYLOR, D. W. 1960. Effects of pregnancy on inulin and para-aminohippurate clearances in the anaesthetized rat. *The Journal of Physiology*, 151, 385-389.
- MCGUANE, J. T., DEBRAH, J. E., SAUTINA, L., JARAJAPU, Y. P. R., NOVAK, J., RUBIN, J. P., GRANT, M. B., SEGAL, M. & CONRAD, K. P. 2011. Relaxin induces rapid dilation of rodent small renal and human subcutaneous arteries via PI3 kinase and nitric oxide. *Endocrinology*, 152, 2786-2796.
- MEAH, V. L., COCKCROFT, J. R., BACKX, K., SHAVE, R. & STÖHR, E. J. 2016. Cardiac output and related haemodynamics during pregnancy: a series of meta-analyses. *Heart*, 102, 518-526.
- MELCHIORRE, K., SHARMA, R., KHALIL, A. & THILAGANATHAN, B. 2016. Maternal cardiovascular function in normal pregnancy. *Hypertension*, 67, 754-762.
- MELCHIORRE, K., SHARMA, R. & THILAGANATHAN, B. 2012. Cardiac structure and function in normal pregnancy. *Current opinion in obstetrics & gynecology*, 24, 413.
- MEYER, M. C., OSOL, G. & MCLAUGHLIN, M. 1997. Flow Decreases Myogenic Reactivity of Mesenteric Arteries From Pregnant Rats. *Journal of the Society for Gynecologic Investigation*, 4, 293-297.
- MIRABITO COLAFELLA, K. M., SAMUEL, CHRISHAN S. & DENTON, KATE M. 2017. Relaxin contributes to the regulation of arterial pressure in adult female mice. *Clinical Science*, 131, 2795-2805.

MIRABITO KATRINA, M., HILLIARD LUCINDA, M., WEI, Z., TIKELLIS, C., WIDDOP ROBERT, E., VINH, A. & DENTON KATE, M. 2014. Role of inflammation and the Angiotensin type 2 receptor in the regulation of arterial pressure during pregnancy in mice. *Hypertension*, 64, 626-631.

MORRIS, E. A., HALE, S. A., BADGER, G. J., MAGNESS, R. R. & BERNSTEIN, I. M. 2015. Pregnancy induces persistent changes in vascular compliance in primiparous women. *American Journal of Obstetrics & Gynecology*, 212, 633.e1-633.e6.

MORRIS, E. A., MANDALA, M., KO, N. L. & OSOL, G. 2020. Postpartum persistence of maternal uterine vascular gestational adaptation in rodents. *Reprod Sci*, 27, 611-620.

MORRIS, R., SUNESARA, I., RUSH, L., ANDERSON, B., BLAKE, P. G., DARBY, M., SAWARDECKER, S., NOVOTNY, S., BOFILL, J. A. & MARTIN, J. N. 2014. Maternal hemodynamics by thoracic impedance cardiography for normal pregnancy and the postpartum period. *Obstetrics and gynecology*, 123, 318.

MORSCHAUSER, T. J., RAMADOSS, J., KOCH, J. M., YI, F. X., LOPEZ, G. E., BIRD, I. M. & MAGNESS, R. R. 2014. Local effects of pregnancy on Connexin proteins that mediate Ca²⁺-associated uterine endothelial NO synthesis. *Hypertension (Dallas, Tex. 1979)*, 63, 589-594.

NADERI, S., TSAI, S. & KHANDELWAL, A. 2017. Hypertensive disorders of pregnancy. *Current Atherosclerosis Reports*, 19, 1-6.

NOVAK, J., DANIELSON, L. A., KERCHNER, L. J., SHERWOOD, O. D., RAMIREZ, R. J., MOALLI, P. A. & CONRAD, K. P. 2001. Relaxin is essential for renal vasodilation during pregnancy in conscious rats. *The Journal of clinical investigation*, 107, 1469-1475.

OGUEH, O., CLOUGH, A., HANCOCK, M. & JOHNSON, M. R. 2011. A longitudinal study of the control of renal and uterine hemodynamic changes of pregnancy. *Hypertension in Pregnancy*, 30, 243-259.

- OSOL, G., LING KO, N. & MANDALA, M. 2019. Plasticity of the maternal vasculature during pregnancy. *Annual Review of Physiology*, 81, 89-111.
- OSOL, G. & MOORE, L. G. 2014. Maternal uterine vascular remodeling during pregnancy. *Microcirculation*, 21, 38-47.
- OSTROWSKI, M. A., HUANG, N. F., WALKER, T. W., VERWIJLEN, T., POPLAWSKI, C., KHOO, A. S., COOKE, J. P., FULLER, G. G. & DUNN, A. R. 2014. Microvascular endothelial cells migrate upstream and align against the shear stress field created by impinging flow. *Biophysical journal*, 106, 366-374.
- PALMER, S. K., ZAMUDIO, S., COFFIN, C., PARKER, S., STAMM, E. & MOORE, L. G. 1992. Quantitative estimation of human uterine artery blood flow and pelvic blood flow redistribution in pregnancy. *Obstetrics and gynecology*, 80, 1000.
- PATZAK, A., BRAUN, D., SCHLEIFENBAUM, J. & KÜCHLER, G. 2018. Muscular arterial tone is a determinant of peripheral muscular artery stiffness. *Journal of Hypertension*, 36, e70.
- POST UITERWEER, E. D., KOSTER, M. P. H., JEYABALAN, A., KUC, S., SILJEE, J. E., STEWART, D. R., CONRAD, K. P. & FRANX, A. 2020. Circulating pregnancy hormone relaxin as a first trimester biomarker for preeclampsia. *Pregnancy hypertension*, 22, 47-53.
- QI, F., OGAWA, K., TOKINAGA, Y., UEMATSU, N., MINONISHI, T. & HATANO, Y. 2009. Volatile anesthetics inhibit Angiotensin II-induced vascular contraction by modulating myosin light chain phosphatase inhibiting protein, CPI-17 and regulatory subunit, MYPT1 phosphorylation. *Anesthesia & Analgesia*, 109, 412-417.
- QUATTRONE, S., CHIAPPINI, L., SCAPAGNINI, G., BIGAZZI, B. & BANI, D. 2004. Relaxin potentiates the expression of inducible nitric oxide synthase by endothelial cells from human umbilical vein in in vitro culture. *Molecular Human Reproduction*, 10, 325-330.

QUIGNARD, J.-F., MIRONNEAU, J., CARRICABURU, V., FOURNIER, B., BABICH, A., NÜRNBERG, B., MIRONNEAU, C. & MACREZ, N. 2001. Phosphoinositide 3-Kinase γ mediates Angiotensin II-induced stimulation of L-type calcium channels in vascular myocytes. *Journal of Biological Chemistry*, 276, 32545-32551.

QUITTERER, U. & ABDALLA, S. 2021. Pathological AT1R-B2R protein aggregation and preeclampsia. *Cells*, 10, 2609.

RENSEN, S. S. M., DOEVENDANS, P. A. F. M. & VAN EYS, G. J. J. M. 2007. Regulation and characteristics of vascular smooth muscle cell phenotypic diversity. *Netherlands heart journal : monthly journal of the Netherlands Society of Cardiology and the Netherlands Heart Foundation*, 15, 100-108.

RIGANO, S., FERRAZZI, E., BOITO, S., PENNATI, G., PADOAN, A. & GALAN, H. 2010. Blood flow volume of uterine arteries in human pregnancies determined using 3D and bi-dimensional imaging, angio-Doppler, and fluid-dynamic modeling. *Placenta*, 31, 37-43.

RODRÍGUEZ, I. & GONZÁLEZ, M. 2014. Physiological mechanisms of vascular response induced by shear stress and effect of exercise in systemic and placental circulation. *Frontiers in Pharmacology*, 5.

ROSENFELD, C. R. & ROY, T. 2014. Prolonged uterine artery nitric oxide synthase inhibition modestly alters basal uteroplacental vasodilation in the last third of ovine pregnancy. *American journal of physiology. Heart and circulatory physiology*, 307, H1196-H1203.

SADOSHIMA, J. & IZUMO, S. 1993. Signal transduction pathways of angiotensin II-induced c-fos gene expression in cardiac myocytes *in vitro*. Roles of phospholipid-derived second messengers. *Circulation Research*, 73, 424-438.

- SANDOO, A., VAN ZANTEN, J. J. C. S. V., METSIOS, G. S., CARROLL, D. & KITAS, G. D. 2010. The endothelium and its role in regulating vascular tone. *The open cardiovascular medicine journal*, 4, 302-312.
- SARWAR, M., SAMUEL, C. S., BATHGATE, R. A., STEWART, D. R. & SUMMERS, R. J. 2016. Enhanced serelaxin signalling in co-cultures of human primary endothelial and smooth muscle cells. *British journal of pharmacology*, 173, 484-496.
- SAVOIA, C., TABEL, F., YAO, G., SCHIFFRIN, E. L. & TOUYZ, R. M. 2005. Negative regulation of RhoA/Rho kinase by angiotensin II type 2 receptor in vascular smooth muscle cells: role in angiotensin II-induced vasodilation in stroke-prone spontaneously hypertensive rats. *Journal of Hypertension*, 23, 1037-1045.
- SCHLOSSMANN, J., AMMENDOLA, A., ASHMAN, K., ZONG, X. & ET AL. 2000. Regulation of intracellular calcium by a signalling complex of IRAG, IP3 receptor and cGMP kinase Ibeta. *Nature*, 404, 197-201.
- SEKI, T., YOKOSHIKI, H., SUNAGAWA, M., NAKAMURA, M. & SPERELAKIS, N. 1999. Angiotensin II stimulation of Ca²⁺-channel current in vascular smooth muscle cells is inhibited by lavendustin-A and LY-294002. *Pflügers Archiv*, 437, 317-323.
- SHERWOOD, O. D. 2004. Relaxin's physiological roles and other diverse actions. *Endocrine Reviews*, 25, 205-234.
- SIMMONS, L. A., GILLIN, A. G. & JEREMY, R. W. 2002. Structural and functional changes in left ventricle during normotensive and preeclamptic pregnancy. *American Journal of Physiology-Heart and Circulatory Physiology*, 283, H1627-H1633.
- SIMS, E. A. & KRANTZ, K. E. 1958. Serial studies of renal function during pregnancy and the puerperium in normal women. *The Journal of clinical investigation*, 37, 1764-1774.

SIRAGY, H. M. & CAREY, R. M. 1996. The subtype-2 (AT2) angiotensin receptor regulates renal cyclic guanosine 3', 5'-monophosphate and AT1 receptor-mediated prostaglandin E2 production in conscious rats. *The Journal of clinical investigation*, 97, 1978-1982.

STURGISS, S. N., WILKINSON, R. & DAVISON, J. M. 1996. Renal reserve during human pregnancy. *Am J Physiol*, 271, F16-20.

TAKAHASHI, T., TANIGUCHI, T., KONISHI, H., KIKKAWA, U., ISHIKAWA, Y. & YOKOYAMA, M. 1999. Activation of Akt/protein kinase B after stimulation with angiotensin II in vascular smooth muscle cells. *American Journal of Physiology-Heart and Circulatory Physiology*, 276, H1927-H1934.

TAKEDA-MATSUBARA, Y., IWAI, M., CUI, T.-X., SHIUCHI, T., LIU, H.-W., OKUMURA, M., ITO, M. & HORIUCHI, M. 2004. Roles of angiotensin type 1 and 2 receptors in pregnancy-associated blood pressure change. *American Journal of Hypertension*, 17, 684-689.

THILAGANATHAN, B. & KALAFAT, E. 2019. Cardiovascular system in preeclampsia and beyond. *Hypertension*, 73, 522-531.

THOMPSON, L. P. & WEINER, C. P. 2001. Pregnancy enhances G protein activation and nitric oxide release from uterine arteries. *American Journal of Physiology-Heart and Circulatory Physiology*, 280, H2069-H2075.

TIMMERMANS, P. B., WONG, P. C., CHIU, A. T., HERBLIN, W. F., BENFIELD, P., CARINI, D. J., LEE, R. J., WEXLER, R. R., SAYE, J. A. & SMITH, R. D. 1993. Angiotensin II receptors and angiotensin II receptor antagonists. *Pharmacological reviews*, 45, 205.

TOUYZ, R. M., ALVES-LOPES, R., RIOS, F. J., CAMARGO, L. L., ANAGNOSTOPOULOU, A., ARNER, A. & MONTEZANO, A. C. 2018. Vascular smooth muscle contraction in hypertension. *Cardiovascular Research*, 114, 529-539.

- TOUYZ, R. M., EL MABROUK, M., HE, G., WU, X. H. & SCHIFFRIN, E. L. 1999. Mitogen-activated protein/extracellular signal-regulated kinase inhibition attenuates angiotensin II-mediated signaling and contraction in spontaneously hypertensive rat vascular smooth muscle cells. *Circ Res*, 84, 505-15.
- TOUYZ, R. M., HE, G., EL MABROUK, M., DIEP, Q., MARDIGYAN, V. & SCHIFFRIN, E. L. 2001. Differential activation of extracellular signal-regulated protein kinase 1/2 and p38 mitogen activated-protein kinase by AT 1 receptors in vascular smooth muscle cells from Wistar-Kyoto rats and spontaneously hypertensive rats. *Journal of Hypertension*, 19, 553-559.
- TOUYZ, R. M., YAO, G., VIEL, E., AMIRI, F. & SCHIFFRIN, E. L. 2004. Angiotensin II and endothelin-1 regulate MAP kinases through different redox-dependent mechanisms in human vascular smooth muscle cells. *Journal of Hypertension*, 22, 1141-1149.
- TWORT, C. H. & BREEMEN, C. V. 1988. Cyclic guanosine monophosphate-enhanced sequestration of Ca^{2+} by sarcoplasmic reticulum in vascular smooth muscle. *Circulation Research*, 62, 961-964.
- USHIO-FUKAI, M., GRIENGLING, K. K., AKERS, M., LYONS, P. R. & ALEXANDER, R. W. 1998. Temporal dispersion of activation of phospholipase C- β 1 and - γ isoforms by Angiotensin II in vascular smooth muscle cells: role of α q/11, α 12, and β γ G protein subunits. *Journal of Biological Chemistry*, 273, 19772-19777.
- VAN DER HEIJDEN, O. W. H., ESSERS, Y. P. G., WIJNANDS, E., MEY, J. G. R., PEETERS, L. L. H. & VAN EYS, G. J. J. M. 2009. Postpartum reversal of the pregnancy-induced uterine artery remodeling in young, aging, and eNOS-deficient mice. *Reproductive Sciences*, 16, 642-649.
- VAN ENGELAND, N. C. A., POLLET, A. M. A. O., DEN TOONDER, J. M. J., BOUTEN, C. V. C., STASSEN, O. M. J. A. & SAHLGREN, C. M. 2018. A biomimetic microfluidic

model to study signalling between endothelial and vascular smooth muscle cells under hemodynamic conditions. *Lab on a chip*, 18, 1607-1620.

VODSTRCIL, L. A., TARE, M., NOVAK, J., DRAGOMIR, N., RAMIREZ, R. J., WLODEK, M. E., CONRAD, K. P. & PARRY, L. J. 2012. Relaxin mediates uterine artery compliance during pregnancy and increases uterine blood flow. *FASEB Journal*, 26, 4035-4044.

WANG, B., LI, C., HUAI, R. & QU, Z. 2015. Overexpression of ANO1/TMEM16A, an arterial Ca²⁺-activated Cl⁻ channel, contributes to spontaneous hypertension. *Journal of Molecular and Cellular Cardiology*, 82, 22-32.

WANG, C., PINAR, A. A., WIDDOP, R. E., HOSSAIN, M. A., BATHGATE, R. A. D., DENTON, K. M., KEMP-HARPER, B. K. & SAMUEL, C. S. 2020. The anti-fibrotic actions of relaxin are mediated through AT2R-associated protein phosphatases via RXFP1-AT2R functional crosstalk in human cardiac myofibroblasts. *The FASEB Journal*, 0, 1-17.

WEST, C. A., SASSER, J. M. & BAYLIS, C. 2016. The enigma of continual plasma volume expansion in pregnancy: Critical role of the renin-angiotensin-aldosterone system. *American Journal of Physiology - Renal Physiology*, 311, F1125-F1134.

WETENDORF, M. & DEMAYO, F. J. 2014. Progesterone receptor signaling in the initiation of pregnancy and preservation of a healthy uterus. *The International journal of developmental biology*, 58, 95-106.

WHITE, M. M., MCCULLOUGH, R. E., DYCKES, R., ROBERTSON, A. D. & MOORE, L. G. 2000. Chronic hypoxia, pregnancy, and endothelium-mediated relaxation in guinea pig uterine and thoracic arteries. *American Journal of Physiology-Heart and Circulatory Physiology*, 278, H2069-H2075.

YANAGISAWA, M., KURIHARA, H., KIMURA, S., TOMOBE, Y., KOBAYASHI, M., MITSUI, Y., YAZAKI, Y., GOTO, K. & MASAKI, T. 1988. A novel potent vasoconstrictor peptide produced by vascular endothelial cells. *Nature*, 332, 411-415.

YINON, Y., KINGDOM JOHN, C. P., ODUTAYO, A., MOINEDDIN, R., DREWLO, S., LAI, V., CHERNEY DAVID, Z. I. & HLADUNEWICH MICHELLE, A. 2010. Vascular dysfunction in women with a history of preeclampsia and intrauterine growth restriction. *Circulation*, 122, 1846-1853.

ZENIYA, M., SOHARA, E., KITA, S., IWAMOTO, T., SUSAKI, K., MORI, T., OI, K., CHIGA, M., TAKAHASHI, D., YANG, S.-S., LIN, S.-H., RAI, T., SASAKI, S. & UCHIDA, S. 2013. Dietary salt intake regulates WNK3-SPAK-NKCC1 phosphorylation cascade in mouse aorta through Angiotensin II. *Hypertension*, 62, 872-878.

ZHANG, H. H., CHEN, J. C., SHEIBANI, L., LECHUGA, T. J. & DONG-BAO, C. 2017. Pregnancy augments VEGF-stimulated *in vitro* angiogenesis and vasodilator (NO and H₂S) production in human uterine artery endothelial cells. *The Journal of Clinical Endocrinology and Metabolism*, 102, 2382-2393.

The role of angiotensin II and relaxin in vascular adaptation to pregnancy

Thu Ngoc Anh Doan^{1,2}, Tina Bianco-Miotto^{1,2}, Laura Parry^{2,3} and Marnie Winter⁴

¹School of Agriculture, Food and Wine, Waite Research Institute, University of Adelaide, Adelaide, South Australia, Australia, ²Robinson Research Institute, University of Adelaide, Adelaide, South Australia, Australia, ³School of Biological Sciences, University of Adelaide, Adelaide, South Australia, Australia and ⁴Future Industries Institute, University of South Australia, Adelaide, South Australia, Australia

Correspondence should be addressed to M Winter; Email: Marnie.Winter@unisa.edu.au

Abstract

In brief: There is a pregnancy-induced vasodilation of blood vessels, which is known to have a protective effect on cardiovascular function and can be maintained postpartum. This review outlines the cardiovascular changes that occur in a healthy human and rodent pregnancy, as well as different pathways that are activated by angiotensin II and relaxin that result in blood vessel dilation.

Abstract: During pregnancy, systemic and uteroplacental blood flow increase to ensure an adequate blood supply that carries oxygen and nutrients from the mother to the fetus. This results in changes to the function of the maternal cardiovascular system. There is also a pregnancy-induced vasodilation of blood vessels, which is known to have a protective effect on cardiovascular health/function. Additionally, there is evidence that the effects of maternal vascular vasodilation are maintained post-partum, which may reduce the risk of developing high blood pressure in the next pregnancy and reduce cardiovascular risk later in life. At both non-pregnant and pregnant stages, vascular endothelial cells produce a number of vasodilators and vasoconstrictors, which transduce signals to the contractile vascular smooth muscle cells to control the dilation and constriction of blood vessels. These vascular cells are also targets of other vasoactive factors, including angiotensin II (Ang II) and relaxin. The binding of Ang II to its receptors activates different pathways to regulate the blood vessel vasoconstriction/vasodilation, and relaxin can interact with some of these pathways to induce vasodilation. Based on the available literature, this review outlines the cardiovascular changes that occur in a healthy human pregnancy, supplemented by studies in rodents. A specific focus is placed on vasodilation of blood vessels during pregnancy; the role of endothelial cells and endothelium-derived vasodilators will also be discussed. Additionally, different pathways that are activated by Ang II and relaxin that result in blood vessel dilation will also be reviewed.

Reproduction (2022) **164** R87–R99

Introduction

Cardiac output is represented by heart beats per minute (heart rate) and the volume of blood pumped into the aorta from the left ventricle per minute (stroke volume) (Hunter & Robson 1992). In a healthy human pregnancy, both local uterine blood flow and cardiac output increase. This ensures an adequate supply of oxygen and nutrients from the mother to the fetus (Hunter & Robson 1992, Melchiorre *et al.* 2012). The elevation of cardiac output usually starts from the 5th week of gestation, reaches maximum value at 20–32 weeks' of gestation (heart rate nearly 45% higher than pre-pregnancy value), and returns to pre-pregnancy levels 2 weeks post-partum (Hunter & Robson 1992, Meah *et al.* 2016). Simultaneously, alterations in maternal vascular function occur to accommodate increased blood flow.

Vasodilation or relaxation of blood vessels, which occurs from early to mid-gestation, is known to be an adaptation to protect the maternal cardiovascular system throughout pregnancy, as it maintains a normal or decreased pressure when the volume of blood being pumped from the heart into these vessels increases (Guyton 1981, Hunter & Robson 1992). Specifically, despite an increase in plasma volume by 6 weeks of gestation, a decrease in both peripheral and renal vascular resistance results in decreased blood pressure and increased renal flow (West *et al.* 2016). This rise in plasma volume and decrease in vascular resistance is also likely accounted for in part by arterial underfilling with 85% of the volume residing in the venous circulation (Davison 1984). These adaptations help reduce the risk of developing hypertensive complications such as preeclampsia (Conrad 2011, Osol *et al.* 2019), which

predisposes women to a 3.5-fold, 2.1-fold, and 1.8-fold higher risk for developing hypertension, coronary heart disease, and stroke, later in life (Bellamy *et al.* 2007, Carpenter 2007, Lykke *et al.* 2009, Yinon *et al.* 2010, Naderi *et al.* 2017, Thilaganathan & Kalafat 2019). Findings in both human and animal studies have also suggested that blood vessel dilation is maintained post-partum, which may decrease the risk of developing hypertension in subsequent pregnancies and lower the risk of developing cardiovascular disease later in life (Gunderson *et al.* 2008, van der Heijden *et al.* 2009, Morris *et al.* 2015, 2020).

This literature review will cover vasculature changes, specifically blood vessel vasodilation during pregnancy and post-partum in a normal pregnancy in both human and rodents. In addition, it will also discuss the role of angiotensin II (Ang II) and relaxin in vascular adaptation during pregnancy, different pathways that are activated by the binding of Ang II to its receptors, and the potential interaction between relaxin and Ang II receptors. Changes to the pathways mentioned earlier when there is endothelial dysfunction, similar to that which may occur in preeclampsia, will also be reviewed.

Materials and methods

A literature search for primary peer-reviewed papers that investigate maternal blood vessel dilation during pregnancy and its mechanisms was conducted in PubMed and Web of Sciences using search terms 'pregnancy vasodilation', 'vascular endothelial cells', 'vascular smooth muscle cells', 'angiotensin II', and 'relaxin' up to June 2022. There were 193 papers retrieved based on the search terms. Papers that are not in English and were not available in full text were excluded. The final number of papers retained was 136.

Results and discussion

Vasculature changes in a healthy human pregnancy

Changes in mean arterial pressure

Mean arterial pressure (MAP, mmHg) is an indicator of the average pressure in blood vessels during one cardiac cycle (Cnossen *et al.* 2008). MAP is calculated using the formula $(2 \text{ diastolic pressure} + \text{systolic pressure})/3$, in which diastolic pressure is the blood pressure measured when the heart relaxes, and systolic pressure is measured when the heart contracts (Cnossen *et al.* 2008). Most studies of healthy women (non-smokers, have normal BMI with no history of blood pressure-related disorders and/or usage of hypertensive medication) in their first pregnancy (primiparous women) reported a reduction in MAP (by a maximum of 2–3.4 mmHg of the non-pregnant level) in the first two trimesters of pregnancy and an increase to pre-pregnancy value (79–83 mmHg) from the third trimester until term (Kametas *et al.* 2001, Simmons *et al.* 2002, Morris *et al.* 2014, Melchiorre *et al.*

2016). In the second or third pregnancy, MAP values within each trimester are lower compared to primiparous women (Bernstein *et al.* 2005). Moreover, there was a negative correlation ($r = -0.31$) between the interval between pregnancies (11–67 months) and the degree of changes in MAP throughout a pregnancy, suggesting that a shorter interval between pregnancies is associated with a greater decrease in MAP (Bernstein *et al.* 2005). However, MAP always reaches the highest value within the third trimester, compared to other trimesters, regardless of the number of previous pregnancies (Bernstein *et al.* 2005). On the other hand, other studies have reported a further decrease in blood pressure at post-partum in both primiparous women and women who had two or more pregnancies (Gunderson *et al.* 2008, Morris *et al.* 2015). Specifically, primiparous women had decreased MAP, by 4.8 mmHg, at 14 months post-partum (Morris *et al.* 2015), or decreased mean adjusted diastolic and systolic blood pressure (by 1.50 and 2.06 mmHg, respectively) at up to 20 years post-partum, compared to pre-pregnancy values (Gunderson *et al.* 2008). Similarly, at 20 years post-partum, women who had two or more pregnancies had a further decrease in diastolic and systolic blood pressure (1.29 mmHg and 1.89 mmHg, respectively), compared to non-pregnant women (Gunderson *et al.* 2008). However, both studies mainly focused on Caucasian or women of colour; hence, the results may not be generalised for all ethnic minorities (Gunderson *et al.* 2008, Morris *et al.* 2015). Additionally, these studies did not investigate changes in blood pressure measures during pregnancy.

Similar to changes observed in humans, rodent studies have also reported a decrease in MAP during pregnancy (Barron *et al.* 2010, Mirabito *et al.* 2014, Mirabito Colafella *et al.* 2017). In pregnant mice, MAP gradually decreased from early gestation and reached the lowest value (-6 ± 2 mmHg) at gestational day 9 (Mirabito *et al.* 2014, Mirabito Colafella *et al.* 2017), which is an adaptation to the pregnancy-induced increase in heart rate ($+60$ b.p.m. compared to pre-pregnancy value) (Mirabito Colafella *et al.* 2017). Both heart rate and MAP then increased to pre-pregnancy values from day 19–20 of gestation (late gestation) (Mirabito *et al.* 2014, Mirabito Colafella *et al.* 2017), and this value of MAP was also confirmed at 2 weeks post-partum (88 ± 2 mmHg) (Mirabito *et al.* 2014).

Changes in uterine arterial function

Besides changes in MAP, uterine artery function is also altered during pregnancy, as the cardiac output and uteroplacental circulation increase (Bernstein *et al.* 2002, Osol & Moore 2014). As expected, elevated uterine artery mean flow velocity, that is, the rate by which blood travelled through the blood vessels per unit of time, has been reported throughout pregnancy (Palmer *et al.* 1992, Dickey & Hower 1995, Bernstein *et al.* 2002,

Rigano *et al.* 2010). In order to compensate for this, the average uterine artery diameter increases from mid-gestation (2.6 mm) to late pregnancy (3.0 mm) (Palmer *et al.* 1992, Rigano *et al.* 2010). Uterine artery resistance index (Dickey & Hower 1995) and uterine artery pulsatility index also decrease when examined in early pregnancy (Bernstein *et al.* 2002, Ogueh *et al.* 2011). However, it should be noted that pregnancy-induced changes in the uterine circulation and its resistance is a result of far more than remodelling and vascular reactivity changes of the uterine artery itself. For instance, there was an increase by approximately 2-fold in the diameter of arcuate arteries (smaller branches of uterine arteries) and radial arteries (smaller branches of arcuate arteries) in normal pregnancies, from 6.1 to 20.5 weeks of gestation (Allerkamp *et al.* 2021).

In agreement with human studies, examination of rodent uterine arteries has also reported maternal blood vessel dilation as an adaptation to pregnancy (Cooke & Davidge 2003, van der Heijden *et al.* 2009, Barron *et al.* 2010, Vodstrcil *et al.* 2012). In late pregnancy, rats (van der Heijden *et al.* 2009, Barron *et al.* 2010) and mice (Cooke & Davidge 2003) have an increase in arterial vasodilation within the uterus compared to non-pregnant controls, with a 35% increase in diameter of radial arteries (Barron *et al.* 2010), and a 20% increase in the methacholine-induced vasodilation response of the uterine artery when measured using wire myography (Cooke & Davidge 2003). The enlargement in uterine artery diameter has also been reported in pregnant animals at 1 week (Morris *et al.* 2020) and 10 days (van der Heijden *et al.* 2009) post-partum, which may help maintain a high uterine blood flow and, hence, may be advantageous for subsequent pregnancies (van der Heijden *et al.* 2009).

Changes in mesenteric function

Similar to the observations in uterine arteries, mesenteric arteries of late-pregnant mice (day 17–18) show increased sensitivity towards vasodilators (e.g. methacholine) (Cooke & Davidge 2003) and a decreased sensitivity towards vasoconstrictors (e.g. Ang II) by half the non-pregnant control (Marshall *et al.* 2016). Additionally, in mesenteric arteries of late-pregnant rats, there was a decrease in myogenic reactivity, represented by the decreased contraction of smooth muscle cells in response to induced intraluminal flow and pressure (Meyer *et al.* 1997). This reduction in myogenic reactivity was associated with a decrease in the shear stress that blood vessels experience during pregnancy (−4% in late-pregnant rats vs +54.7% in non-pregnant control) likely a protective mechanism of the maternal vasculature system (Meyer *et al.* 1997). Interestingly, there is also evidence for maintenance of pregnancy-induced vasodilation effect, as the mesenteric artery distensibility (i.e. the ability to dilate and constrict

passively in response to changes in pressure) in pregnant rats was shown to increase considerably throughout pregnancy and was approximately 30% higher than in non-pregnant controls at 4 weeks post-partum (Morris *et al.* 2020).

Changes in renal arterial function

As previously mentioned, it is generally accepted that renal vascular resistance decreases to accommodate for increased renal blood flow during pregnancy. Indeed, using the renal para-aminohippurate (PAH) clearance method, most human studies reported a significant increase in maternal renal blood flow from as early as the 6th week up to week 36 of gestation, reflecting a reduction in renal vascular resistance (Sims & Krantz 1958, Dunlop 1981, Sturgiss *et al.* 1996, Chapman *et al.* 1998). Renal vascular resistance (calculated using MAP and renal blood flow) was shown to decrease concurrently (Chapman *et al.* 1998). Interestingly, increased renal blood flow was even found at up to 25 weeks post-partum, compared to non-pregnant controls (Sims & Krantz 1958). In contrast, the investigation of renal arterial resistive index (RI) using Doppler-based measurement reported either no change in RI throughout gestation (Dib *et al.* 2003) or a significant increase in RI in gestational weeks' 16–36 (Kurjak *et al.* 1992, Ogueh *et al.* 2011). RI is calculated using systolic and diastolic velocities and, therefore, might also be influenced by other central haemodynamic parameters rather than the renal vascular resistance itself. As a result, differences in the examination methods/measures, as well as examination intervals and number of samples, are potential explanations for the conflicting results. Similar to the results found in human studies, pregnant rats either had increased renal blood flow at mid-gestation and late gestation (Matthews & Taylor 1960) or no change in renal blood flow at early gestation and late gestation (Davison & Lindheimer 1980), represented by increased PAH clearance. However, the former study was done in anaesthetised rats, while the latter was done in unanaesthetised rats. Meanwhile, pregnant rats at mid-gestation were reported to have a significant decrease in myogenic reactivity of small renal arteries compared to non-pregnant control, supporting the potential vasodilation effect of pregnancy on the renal vascular function (Gandley *et al.* 2001, Novak *et al.* 2001).

A summary of vasculature changes in healthy human and rodent pregnancy is shown in Table 1. Although this review discusses the function and biochemical aspects of isolated vessels from pregnant humans and animals, it should be noted that there are remarkable differences in blood vessel behaviour between and within different organs; hence, it is important for future studies to investigate and provide a better understanding of the pregnancy-specific vasodilation effects on the maternal vasculature system as a whole. Additionally, although

Table 1 Vasculature changes during healthy human and rodent pregnancy and in post-partum period, relative to pre-pregnancy and/or non-pregnant control.

Observation/species	Control	Early pregnancy	Mid-pregnancy	Late pregnancy	Post-partum	References
MAP						
Human	71–90 mmHg	69–90 mmHg (↓)	65–90 mmHg (↓)	67–94 mmHg (–)	72–93 mmHg (↓)	Kametas <i>et al.</i> (2001), Simmons <i>et al.</i> (2002), Bemstein <i>et al.</i> (2005), Gunderson <i>et al.</i> (2008), Morris <i>et al.</i> (2014, 2015), Melchiorre <i>et al.</i> (2016)
Rodent						Barron <i>et al.</i> (2010), Mirabito <i>et al.</i> (2014), Mirabito Colafella <i>et al.</i> (2017)
Rats	101–105 mmHg	93–97 mmHg (↓)	N/A	N/A	N/A	
Mice	90–103 mmHg	N/A	–4 to –8 mmHg (change in MAP, ↓)	+8 to +12 mmHg (change in MAP, ↑)	N/A	Palmer <i>et al.</i> (1992), Dickey & Hower (1995), Bemstein <i>et al.</i> (2002), Rigano <i>et al.</i> (2010), Ogueh <i>et al.</i> (2011)
UAD						Cooke & Davidge (2003), van der Heijden <i>et al.</i> (2009), Barron <i>et al.</i> (2010), Morris <i>et al.</i> (2020)
Human	1.3–1.5 mm	N/A	2.6–3.0 mm (↑)	3.0–3.6 mm (↑)	N/A	
Rodent						
Rats	150 µm	N/A	N/A	190 µm (↑)	150–190 µm (↑)	Meyer <i>et al.</i> (1997), Cooke & Davidge (2003), Marshall <i>et al.</i> (2016), Morris <i>et al.</i> (2020)
Mice	N/A	N/A	N/A	–150% non-pregnant control value (↑)	–150% non-pregnant control value (↑)	
MAD ^a						
Rodent						
Rats	Lowest passive distensibility	N/A	N/A	Increased passive distensibility (↑)	Increased passive distensibility (↑)	
Mice	N/A	N/A	N/A	Increased methacholine-induced vasodilation, decreased L-NAME-induced constriction (↑)	N/A	
RVR						
Human						Sims and Krantz (1958), Dunlop (1981), Sturgiss <i>et al.</i> (1996), Chapman <i>et al.</i> (1998), Dib <i>et al.</i> (2003), Ogueh <i>et al.</i> (2011)
RI	0.61–0.65	0.65–0.67 (↑)	0.65–0.67 (↑)	0.65–0.67 (↑)	0.62 (–)	
RBF, mL/min	–400–600	–700–1000 (↑)	–600–1000 (↑)	–600–1000 (↑)	–400–700 (↑)	
RVR, sec.cm ⁻⁵	–7000	–3500–4500 (↓)	–3500–4500 (↓)	–3500–4500 (↓)	N/A	
Rodent (rats)						Mathews & Taylor (1960), Davison & Lindheimer (1980), Gandleley <i>et al.</i> (2001), Novak <i>et al.</i> (2001)
RBF, mL/L	5.86–6.82 mL/min	6.45–7.11 (–)	8.48 (↑)	5.44–7.44 (↑)	N/A	
RMR	1.1–5.5	N/A	1.3–3.7 (↓)	N/A	N/A	
SAD	–3% increase	N/A	+8% (↓ vascular resistance)	N/A	N/A	

Renal blood flow (RBF) was measured using the para-aminohippurate clearance method. RVR was calculated using MAP and RBF. An increase in RBF and/or SAD reflects a decrease in renal vascular resistance. Renal resistance index (RI) was calculated using systolic and diastolic velocities. ↓, decreased; ↑, increased; –: returned to non-pregnant/pre-pregnancy value. ^aNot investigated in humans. L-NAME, N-nitro-L-arginine methyl ester; MAD, mesenteric artery dilation; MAP, mean arterial pressure; N/A, no information available/yet investigated; RI, resistance index; RMR, renal myogenic reactivity; RVR, renal vascular resistance; SAD, small renal artery diameter; UAD, uterine artery dilation.

rodent studies are the most common, other studies on maternal blood vessel vasodilation during gestation have also been performed in larger animal models such as rabbits, sheep, and guinea pigs (White *et al.* 2000, Brooks *et al.* 2001, Thompson & Weiner 2001, Morschauer *et al.* 2014, Rosenfeld & Roy 2014).

Roles of endothelial cells and endothelium-derived vasodilators

From the above, it is clear that there is a pregnancy-induced vasodilation effect on the maternal blood vessels, which can potentially be maintained post-partum. These physiological changes are mainly caused by activities of vascular endothelial cells and smooth muscle cells. Endothelial cells produce a number of vasodilators and vasoconstrictors, such as nitric oxide (NO) and endothelin 1, respectively, which transduce signals to the contractile vascular smooth muscle cells to control the constriction and dilation of blood vessels (Rensen *et al.* 2007, Sandoo *et al.* 2010, Gao *et al.* 2016, Touyz *et al.* 2018).

During pregnancy, there is an increase in the production of vasodilators by endothelial cells, as well as the sensitivity of endothelial cells themselves towards vasodilators. For instance, there is an increase in production of the vasodilators, NO and hydrogen sulphide, and the vasodilator-producing enzymes, endothelial NO synthase (eNOS) and cystathionine beta-synthase (CBS) in uterine artery endothelial cell (hUAEC) cultures from pregnant women at late gestation (week 35–36), compared to non-pregnant women (Zhang *et al.* 2017). Moreover, treatment of hUAECs with 10 ng/mL vascular endothelial growth factor, a vasodilator, resulted in an even higher protein expression of eNOS and CBS (Zhang *et al.* 2017). As expected, when the endothelium-derived vasodilators, such as NO synthase (NOS) (Cooke & Davidge 2003, Barron *et al.* 2010) or prostaglandin H synthase (Cooke & Davidge 2003) was inhibited (by Nomega-Nitro-L-arginine methyl ester hydrochloride (L-NAME) or meclofenamate, respectively) in pregnant rodents, the pregnancy-specific vasodilation effect, including the increase in blood vessel diameter and sensitivity towards methacholine of uterine arteries, was diminished or abolished (Cooke & Davidge 2003, Barron *et al.* 2010).

Similarly, in eNOS-deficient mice, the increase in uterine artery diameter until day 10 post-partum was eliminated (van der Heijden *et al.* 2009). The pregnancy-induced change in renal artery myogenic reactivity during midterm was also attenuated by the inhibition of either NOS or endothelin type B receptor (Gandley *et al.* 2001), or the removal of circulating relaxin (Novak *et al.* 2001), a 6-kDa ovarian peptide hormone that induces NO production of endothelial cells and, hence, functions as a vasodilator during pregnancy (Conrad 2011). Likewise, relaxin-deficient mice lost the pregnancy-

specific increased sensitivity towards methacholine and decreased sensitivity towards Ang II in their mesenteric arteries (Leo *et al.* 2014a, Marshall *et al.* 2016).

There is evidence that there might also be an adaptation of the maternal vasculature system towards the aberrant vascular relaxation during pregnancy. Specifically, in the presence of L-NAME, myogenic tone (i.e. the capability to sustain vasoconstriction (Johansson 1989)) of uterine arteries in late pregnant rats decreased from $39 \pm 3.2\%$ to $11 \pm 5.0\%$, whereas myogenic tone of uterine arteries in the non-pregnant control group increased from $5 \pm 2.6\%$ to $31 \pm 3.1\%$ (Barron *et al.* 2010), suggesting a pregnancy-induced re-modelling of uterine arteries that resulted in a decrease in arterial stiffness (Patzak *et al.* 2018) that was pregnancy specific in rats. Additionally, there was a greater uterine artery diameter in eNOS-deficient mice at 2 days post-partum compared to non-pregnant mice, proposing an alternative source of NO and/or an alternative relaxation pathway (van der Heijden *et al.* 2009).

Biochemical pathways of maternal blood vessel vasodilation in pregnancy

As mentioned earlier, endothelial cells produce vasoactive factors that interact with the smooth muscle cells to control the vascular function during pregnancy. Interestingly, endothelial cells and smooth muscle cells are also targets of other vasoconstrictors and vasodilators. In order to gain a better understanding of the underlying mechanisms of vascular adaptation to pregnancy, numerous studies have focused on the renin–angiotensin system and the peptide hormone relaxin. This section will highlight different biochemical pathways that are influenced by the factors mentioned earlier, which can cause blood vessel vasoconstriction or vasodilation.

Renin–angiotensin system

The renin–angiotensin system is known to have a significant effect on regulating blood pressure, including during pregnancy. While renin, a protease, is produced from juxtaglomerular cells of the kidney; angiotensinogen, the angiotensin precursor, is a product of the liver (Timmermans *et al.* 1993). The generation of biologically active Ang II, a vasoconstrictor, requires the cleavage of angiotensinogen by renin, in order to generate angiotensin I, which is converted to Ang II by the angiotensin-converting enzyme (ACE) (Timmermans *et al.* 1993). There are numerous Ang II receptors that have been extensively studied over the last few decades, two of which are angiotensin type 1 (AT1) receptor and angiotensin type 2 (AT2) receptor (Bottari *et al.* 1993). The two receptors, despite having a similar affinity towards Ang II, are distinguished by their different affinities towards antagonists that bind to them

and later inhibit their binding to Ang II (Bottari *et al.* 1993). Additionally, AT1 and AT2 receptors are expressed in both vascular endothelial cells and vascular smooth muscle cells (Bottari *et al.* 1993, Allen *et al.* 2000, Henrion *et al.* 2001).

Early in pregnancy there is an increase in the maternal plasma Ang II level to stimulate the sodium absorbing and holding capability of blood vessels (Lumbers & Pringle 2014). This is suggested to be an adaptive mechanism that helps maintain homeostasis as the maternal cardiac output and blood volume increase during pregnancy (Irani & Xia 2011, Lumbers & Pringle 2014). Nonetheless, since the 1970s, researchers have reported a trend of weakened responsiveness of blood vessels in the midgestational period, represented by vascular resistance, towards the vasoconstriction effect of infused Ang II in normotensive, but not hypertensive, pregnant women (Gant *et al.* 1973). One of the potential explanations for the earlier observation is the pregnancy-specific enhanced AT2 receptor and/or decreased AT1 receptor expression (Takeda-Matsubara *et al.* 2004, Chen *et al.* 2007, Ferreira *et al.* 2009, Mirabito *et al.* 2014, Cunningham *et al.* 2016, 2018). In general, AT1 and AT2 receptors have opposite effects in regulating blood pressure, in both the non-pregnant state and during pregnancy (Irani & Xia 2008, Kawai *et al.* 2017). The binding of Ang II, dependent on the ratio of AT1/AT2 receptors, causes either a vasoconstriction or a vasodilation outcome, when the receptor is either AT1 or AT2, respectively (Chen *et al.* 2007). Lack of AT1 receptor expression in female transgenic Ang II-enhanced/AT1-knockout mice caused a significant decline in the systemic blood pressure (by 13% the WT mice) measured at mid-gestation (Chen *et al.* 2007). Meanwhile, inhibition of the AT2 receptor by an added antagonist (PD123319) in WT mice caused an increase in blood pressure (Chen *et al.* 2007). In AT2 receptor-knockout mice, mid-gestational MAP did not change from the pre-pregnancy value, whereas a significant reduction by 6 ± 2 mmHg was seen in WT mice (Mirabito *et al.* 2014). At gestational day 20, MAP of WT mice was similar to the pre-pregnancy value, while MAP of AT2 receptor-knockout mice increased by 13 ± 7 mmHg (Mirabito *et al.* 2014). Additionally, there was no change in the renal AT1 receptor mRNA expression in AT2 receptor-knockout mice, compared to a reduced expression in WT mice (Mirabito *et al.* 2014).

In rats, AT2 receptor mRNA expression measured in the maternal aorta, renal artery, and mesangial cells (main component of renal glomeruli in the renal cortex) at day 12–14 of pregnancy significantly increased compared to the non-pregnant control, whereas there were no changes in AT1 receptor mRNA expression (Ferreira *et al.* 2009). The Ang II-induced increase in calcium concentration in mesangial cells of pregnant rats was more than two-fold lower compared to the non-pregnant control, suggesting a reduction in sensitivity of

renal cells towards Ang II in the midgestational period (Ferreira *et al.* 2009). On the contrary, Ang II-induced renal vascular resistance and renal mitochondrial oxidative stress at late gestation increased when the AT1 receptor function was enhanced by its agonist autoantibodies (AT1-AA), which are detectable in preeclamptic pregnancies (Cunningham *et al.* 2016, 2019). These phenotypes were reduced and/or inhibited by the AT1-AA inhibitor ('n7AAc') (Cunningham *et al.* 2018, 2019), suggesting the vasoconstriction-inducing effect of the AT1 receptor, which is usually decreased in a normal pregnancy but increased with preeclampsia. Further emphasising the importance of this system in pregnancy health and disease, in preeclampsia hypersensitivity of the AT1 receptor through its heterodimerisation leads to increased Ang II responsiveness (Abdalla *et al.* 2001b, Quitterer & Abdalla 2021).

In regards to different biochemical pathways that are activated by the binding of Ang II to a receptor, different consequential signalling cascades can lead to either vasoconstriction or vasodilation. For instance, when bound by Ang II, AT1 receptor interacts with heterotrimeric G-proteins, which then transduces signals to protein tyrosine kinase (PTK) and Rho guanine nucleotide exchange factors (Rho GEFs) (Kawai *et al.* 2017). Although PTK and Rho GEFs activate other molecules in different pathways, such as phosphoinositide-3-kinase (PIK3), phospholipase C, or Ras homolog family member A (RhoA) (Ushio-Fukai *et al.* 1998, Seki *et al.* 1999, Lutz *et al.* 2005), the final endpoint, vasoconstriction, is similar (Fig. 1). On the contrary, the binding of Ang II to the AT2 receptor inhibits the RhoA/Rho kinase pathway and causes vasodilation (Savoia *et al.* 2005) (Fig. 2). There are likely more molecules involved in these pathways that are yet to be discovered. Therefore, further research is required to determine which specific pathway(s) are altered as an adaptation to pregnancy.

Relaxin

The Human 2 relaxin and its two orthologs in rodents, Mouse 1 relaxin and Rat 1 relaxin, are produced by the ovarian corpus luteum and the placenta (Sherwood 2004, Marshall *et al.* 2017c). The most studied role of relaxin is that on the mesenteric, renal, and uterine blood vessels. However, it likely also plays a role in the placental vasculature. Despite limited information regarding its functional role in the placenta, it has been shown to be important for the survival of cytotrophoblast cells (Conrad 2016, Marshall *et al.* 2017b).

Relaxin binds several receptors, including the relaxin/insulin-like family peptide receptor 1 (RXFP1) (Jelinic *et al.* 2014), which is mostly found on the surface of vascular endothelial and vascular smooth muscle cells (Jelinic *et al.* 2014), except the human umbilical artery endothelial cells (Sarwar *et al.* 2016). Relaxin is known

to play an essential role in blood vessel vasodilation, including during pregnancy, and the evidence of this role comes from both animal (Ferreira *et al.* 2009, McGuane *et al.* 2011, Vodstrcil *et al.* 2012, Leo *et al.* 2014b, Marshall *et al.* 2016, 2017a, Mirabito Colafella *et al.* 2017) and human (Quattrone *et al.* 2004, McGuane *et al.* 2011, Sarwar *et al.* 2016) studies. Relaxin-knockout mice have an elevated heart rate throughout pregnancy, in association with higher MAP compared to WT mice at both mid-gestation (gestational day 9; 9.7 mmHg higher) and late gestation (gestational day 19; 7.2 mmHg higher) (Mirabito Colafella *et al.* 2017). Moreover, the pregnancy-induced decreased sensitivity of mesenteric arteries towards the vasoconstriction effect of Ang II was eliminated in relaxin-deficient pregnant mice (Marshall *et al.* 2016). In contrast, when relaxin-deficient mice were treated with exogenous relaxin at days 12.5–17.5 of gestation, the Ang II-induced contraction of mesenteric arteries

was reduced by more than half the contraction seen in untreated mice (Marshall *et al.* 2017a).

As both Ang II and relaxin are involved in the regulation of the maternal vasculature system during pregnancy, there is a question of whether relaxin interacts with any of the molecules/pathways induced by the binding of Ang II to its receptors. Indeed, the addition of exogenous relaxin (1000 ng/mL) into human umbilical vein endothelial cells (HUVECs) increased NOS II expression by 15 times compared to the untreated cells (Quattrone *et al.* 2004). Consequently, the protein expression of NOS II and the NO production were increased by more than double the untreated control. In support of this finding, the direct addition of serelexin, a recombinant form of relaxin, into either human umbilical artery smooth muscle cell (HUASMC) or human umbilical vein smooth muscle cell (HUVSMC) monoculture induced cGMP accumulation within the smooth muscle cells (Sarwar *et al.* 2016), which interferes

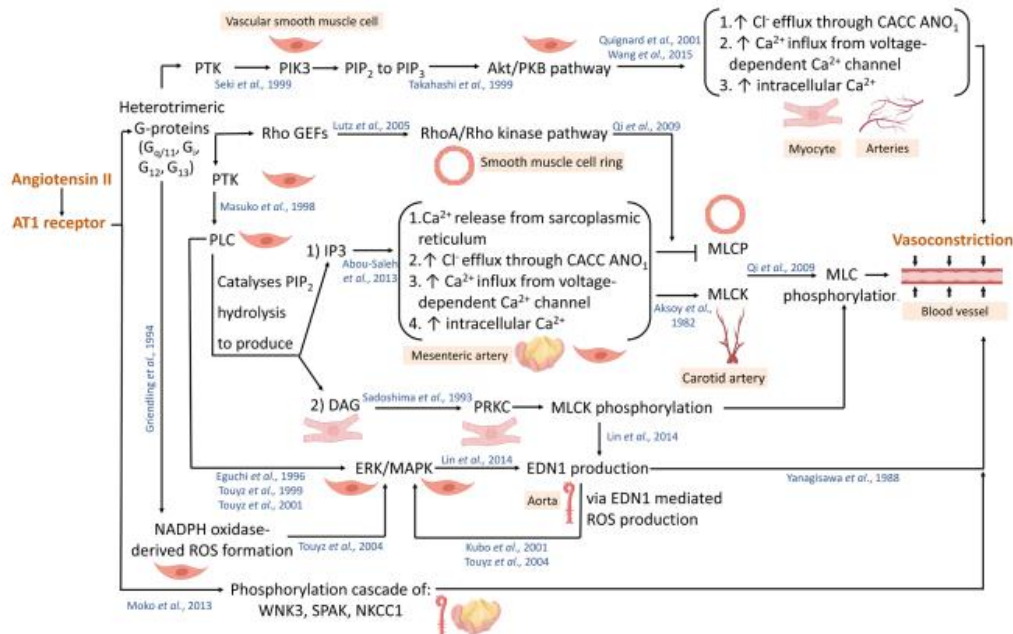


Figure 1 Different pathways activated as a result of the binding of Angiotensin II to the AT1 receptor which result in vasoconstriction. Organs and/or cell types in which the pathways were studied are shown. →, activates/binds; —, inhibits. PRKC, protein kinase C; PTK, protein tyrosine kinase; PIK3, phosphoinositide-3-kinase; PIP₂, phosphatidylinositol 4,5-bisphosphate; PIP₃, phosphatidylinositol (3,4,5)-trisphosphate; PKB, protein kinase B; PLC, phospholipase C; Rho GEFs, Rho guanine nucleotide exchange factors; IP₃, inositol triphosphate; DAG, diacylglycerol; ROS, reactive oxygen species; CACC, calcium-activated chloride channel; MLCK, myosin light chain kinase; MLCP, myosin light chain phosphatase; ERK, extracellular-signal-regulated kinase; MAPK, mitogen-activated protein kinase; EDN1, endothelin 1; WNK3, with-no-lysine kinase 3; SPAK, STE20/SPS1-related proline/alanine-rich kinase; NKCC1, Na⁺-K⁺-Cl⁻ cotransporter isoform 1 (Aksoy *et al.* 1982, Yanagisawa *et al.* 1988, Sadoshima & Izumo 1993, Archer *et al.* 1994, Griendling *et al.* 1994, Eguchi *et al.* 1996, Ushio-Fukai *et al.* 1998, Seki *et al.* 1999, Takahashi *et al.* 1999, Touyz *et al.* 1999, 2001, 2004, Kubo *et al.* 2001, Quignard *et al.* 2001, Lutz *et al.* 2005, Qi *et al.* 2009, Abou-Saleh *et al.* 2013, Zeniya *et al.* 2013, Lin *et al.* 2014, Wang *et al.* 2015). Created with BioRender.com.

<https://rep.bioscientifica.com>

Reproduction (2022) 164 R87–R99

Downloaded from Bioscientifica.com at 18/31/2023 02:08:05AM
via free access

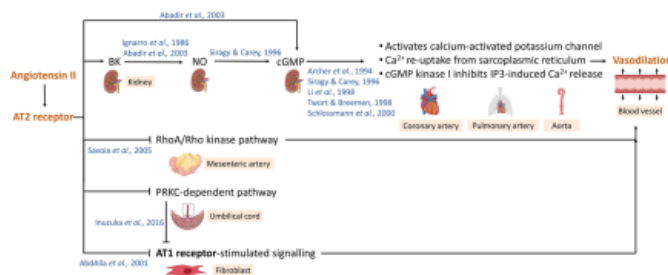


Figure 2 Different pathways activated as a result of the binding of Angiotensin II to the AT2 receptor which result in vasodilation. Organs and/or cell types in which the pathways were studied are shown. →, activates/binds; −, inhibits. BK, bradykinin; NO, nitric oxide; cGMP, cyclic GMP; PRKC, protein kinase C; IP3, inositol triphosphate (Ignarro *et al.* 1986, Twort & Breemen 1988, Siragy & Carey 1996, Li *et al.* 1998, Schlossmann *et al.* 2000, Abdalla *et al.* 2001a, Savoia *et al.* 2005, Inuzuka *et al.* 2016). Created with BioRender.com.

with the release of Ca^{2+} from the sarcoplasmic reticulum into the smooth muscle cell intracellular space, hence affecting its contractile phenotype (Touyz *et al.* 2018). This is known as one of the key steps involved in the Ang II-AT2-NO/cGMP pathway that can lead to vasodilation (Fig. 2). The addition of serelexin into either HUVECs or human coronary artery endothelial cells that were co-cultured with HUASMCs and HUVSMCs also induced cGMP accumulation within the smooth muscle cells (Sarwar *et al.* 2016). Additionally, when the endothelial cells were treated with L-NG-nitro arginine (NOARG), a NOS inhibitor, the relaxin-induced cGMP accumulation was significantly reduced. Besides NO and cGMP, relaxin was also shown to cause a vasodilation effect via the activation of bradykinin (Leo *et al.* 2014b) and the PI_3K -Akt pathway (Dimmeler *et al.* 1999, McGuane *et al.* 2011, Lian *et al.* 2018), which are also involved in the Ang II-AT1/AT2 receptor regulation of blood vessels (Figs 1 and 2). Taken together, relaxin interacts with various factors and pathways in endothelial and vascular smooth muscle cells leading to vasodilation.

These results, therefore, give rise to another question of whether relaxin interacts with the Ang II receptors. A study on rat renal myofibroblasts reported that relaxin treatment decreased renal fibrosis by increasing extracellular-signal-regulated kinase phosphorylation and NOS phosphorylation, by approximately double the untreated control, and decreasing expression of TGF β 1, pSmad2, and alpha-smooth muscle actin to a similar level compared to the untreated control (Chow *et al.* 2014). However, these effects were abolished when the AT2 receptor activity was blocked by PD123319 or when there was no cell surface AT2 receptor expression (Chow *et al.* 2014). Bioluminescence resonance energy transfer saturation assays of human embryonic renal cells also confirmed the presence of RXFP1-AT2 receptor heterodimer when RXFP1 was bound by relaxin (Chow *et al.* 2014). Likewise, evidence of the RXFP-AT1 heterodimer was found in rat renal myofibroblasts (Chow *et al.* 2019) and human cardiac myofibroblasts (Chow *et al.* 2019, Wang *et al.* 2020), suggesting that Ang II receptors are important for the function of relaxin and that relaxin can indirectly activate the AT1/AT2 receptors

function via the formation of RXFP1-AT1/AT2 complex. However, it is not clear whether there is a relaxin-Ang II receptor interaction in vascular endothelial and smooth muscle cells, and whether such event is responsible for the vasodilation of maternal blood vessels during pregnancy.

Besides relaxin and the renin-angiotensin system, there is a range of other factors, such as oestrogen and progesterone—the two sex hormones that also play important roles in remodelling of the maternal vascular system during pregnancy (Kodogo *et al.* 2019). Moreover, these hormones also interact with the renin-angiotensin system and pathways that are activated by the binding of Ang II to its receptors. Indeed increased levels of progesterone and prostacyclin may lead to resistance of Ang II effects (Gant *et al.* 1980, Irani & Xia 2011). An in-depth discussion on the role of these factors has been reviewed elsewhere (Lumbers & Pringle 2014, Wetendorf & Demayo 2014, Kodogo *et al.* 2019).

Ang II/relaxin in preeclampsia

The role of Ang II/relaxin in the maternal vasculature system during pregnancy is important for the investigation of aberrant haemodynamic functions in pregnancy complications such as preeclampsia (Lumbers *et al.* 2019). Briefly, in preeclampsia, abnormal placental development leads to the increased release of factors into the maternal circulation (including renin and AT1-AAAs) and over-activation of the AT1 receptor and vasoconstriction. Moreover, low levels of relaxin in the first trimester have been identified in women who later develop late-onset preeclampsia (Post Uiterweer *et al.* 2020). A better understanding of the relationship between Ang II pathways and relaxin in uncomplicated pregnancies is critical to understand the role of relaxin in complications such as preeclampsia.

Future perspectives

Interestingly, endothelial and smooth muscle cells are mechanosensitive to changes in blood flow and blood pressure during pregnancy altering the shear stress and

stretch these cells experience, which can in turn alter their expression and function (Boo *et al.* 2002, Rodríguez & González 2014, Jufri *et al.* 2015). Moreover, it is known that at least some of the relevant receptors within the relaxin–RXFP1–Ang II pathways are themselves mechanosensitive. For example, the AT1 receptor can be mechanically activated through an Ang II-independent mechanism and can lead to actin remodelling and changes in myogenic responsiveness (Hong *et al.* 2016). Therefore, dynamic cellular culture under shear stress may hold further insights and should be considered when studying interactions within these pathways, *in vitro*. For example, the use of organ-on-chip microfluidic models which better mimic specific aspects of the *in vivo* cellular physiological environment (Huh *et al.* 2011, Ganesan *et al.* 2017). Indeed, microfluidic models have been shown to recreate the mechanical forces and shear stress similar to what the cells would experience within blood vessels (Ostrowski *et al.* 2014, Gray & Stroka 2017, van Engeland *et al.* 2018). In addition, studies of animal models, in which functional responses of blood vessels can be measured using wire myography, pressure myography (Leo *et al.* 2014a, Marshall *et al.* 2016, 2017a, 2018) and arteriography (Morris *et al.* 2020), can be used to investigate vasodilation in regards to altered relaxin–Ang II receptor interaction at different time points during pregnancy and post-partum. This might allow future studies to look at similar changes in humans and provide prevention strategies or pathways for treatment.

Conclusion

In summary, it is important to understand the underlying mechanisms of maternal vasculature adaptation, such as relaxin–RXFP1–Ang II receptor interactions, in a healthy human pregnancy. This might help explain why there is potentially a protective effect on the vasculature system post-partum in women that have a healthy pregnancy. In addition, understanding the biochemical pathways involved in maternal vasculature adaptation to pregnancy may help shed light on how these pathways may be disrupted in pregnancy complicated by gestational hypertension or preeclampsia.

Declaration of interest

The authors declare that there is no conflict of interest that could be perceived as prejudicing the impartiality of the research reported.

Funding

M W would like to acknowledge the financial support of the National Health and Medical Research Council (Development grant: APP1171821).

<https://rep.bioscientifica.com>

Data availability statement

Data availability is not applicable to this article as no new data were created or analysed in this study.

Author contribution statement

T B M, L P, M W conception and design of article; T N A D literature search, data interpretation and manuscript drafting; T B M, L P, M W critical revision and contribution to intellectual content.

References

- Abdalla S, Lother H, Abdel-Tawab AM & Quitterer U 2001a The angiotensin II AT2 receptor is an AT1 receptor antagonist. *Journal of Biological Chemistry* **276** 39721–39726. (<https://doi.org/10.1074/jbc.M105253200>)
- Abdalla S, Lother H, Massiery A & Quitterer U 2001b Increased AT1 receptor heterodimers in preeclampsia mediate enhanced angiotensin II responsiveness. *Nature Medicine* **7** 1003–1009. (<https://doi.org/10.1038/nm0901-1003>)
- Abou-Saleh H, Pathan AR, Daalis A, Hubrack S, Abou-Jassoum H, Al-Naeimi H, Rusch NJ & Machaca K 2013 Inositol 1,4,5-trisphosphate (IP3) receptor up-regulation in hypertension is associated with sensitization of Ca²⁺ release and vascular smooth muscle contractility. *Journal of Biological Chemistry* **288** 32941–32951. (<https://doi.org/10.1074/jbc.M113.496802>)
- Aksoy MO, Murphy RA & Kamm KE 1982 Role of Ca²⁺ and myosin light chain phosphorylation in regulation of smooth muscle. *American Journal of Physiology* **242** C109–C116. (<https://doi.org/10.1152/ajpcell.1982.242.1.C109>)
- Allen AM, Zhuo J & Mendelsohn FAO 2000 Localization and function of angiotensin AT1 receptors. *American Journal of Hypertension* **13** 315–385. ([https://doi.org/10.1016/s0895-7061\(99\)00249-6](https://doi.org/10.1016/s0895-7061(99)00249-6))
- Allerkamp HH, Clark AR, Lee TC, Morgan TK, Burton GJ & James JL 2021 Something old, something new: digital quantification of uterine vascular remodelling and trophoblast plugging in historical collections provides new insight into adaptation of the utero-placental circulation. *Human Reproduction* **36** 571–586. (<https://doi.org/10.1093/humrep/deaa303>)
- Archer SL, Huang JM, Hampl V, Nelson DP, Shultz PJ & Weir EK 1994 Nitric oxide and cGMP cause vasorelaxation by activation of a charybdotoxin-sensitive K channel by cGMP-dependent protein kinase. *PNAS* **91** 7583–7587. (<https://doi.org/10.1073/pnas.91.16.7583>)
- Barron C, Mandala M & Osol G 2010 Effects of pregnancy, hypertension and nitric oxide inhibition on rat uterine artery myogenic reactivity. *Journal of Vascular Research* **47** 463–471. (<https://doi.org/10.1159/000313874>)
- Bellamy L, Casas JP, Hingorani AD & Williams DJ 2007 Pre-eclampsia and risk of cardiovascular disease and cancer in later life: systematic review and meta-analysis. *BMJ* **335** 974. (<https://doi.org/10.1136/bmj.39335.385301.BE>)
- Bernstein IM, Ziegler WF, Leavitt T & Badger GJ 2002 Uterine artery hemodynamic adaptations through the menstrual cycle into early pregnancy. *Obstetrics and Gynecology* **99** 620–624. ([https://doi.org/10.1016/s0029-7844\(01\)01787-2](https://doi.org/10.1016/s0029-7844(01)01787-2))
- Bernstein IM, Thibault A, Mongeon JA & Badger GJ 2005 The influence of pregnancy on arterial compliance. *Obstetrics and Gynecology* **105** 621–625. (<https://doi.org/10.1097/01.AOG.0000152346.45920.45>)
- Boo YC, Sorescu G, Boyd N, Shiojima I, Walsh K, Du J & Jo H 2002 Shear stress stimulates phosphorylation of endothelial nitric-oxide synthase at Ser1179 by Akt-independent mechanisms: role of protein kinase A. *Journal of Biological Chemistry* **277** 3388–3396. (<https://doi.org/10.1074/jbc.M108789200>)
- Bottari SP, De Gasparo M, Steckelings UM & Levens NR 1993 Angiotensin II receptor subtypes: characterization, signalling mechanisms, and possible physiological implications. *Frontiers in Neuroendocrinology* **14** 123–171. (<https://doi.org/10.1006/frne.1993.1005>)
- Brooks VL, Clow KA, Welch LS & Giraud GD 2001 Does nitric oxide contribute to the basal vasodilation of pregnancy in conscious

Reproduction (2022) **164** R87–R99

- rabbits? *American Journal of Physiology: Regulatory, Integrative and Comparative Physiology* **281** R1624–R1632. (<https://doi.org/10.1152/ajpregu.2001.281.5.R1624>)
- Carpenter MW 2007 Gestational diabetes, pregnancy hypertension, and late vascular disease. *Diabetes Care* **30** (Supplement 2) S246–S250. (<https://doi.org/10.2337/dc07-s224>)
- Chapman AB, Abraham WT, Zamudio S, Coffin C, Merouani A, Young D, Johnson A, Osorio F, Goldberg C, Moore LG *et al.* 1998 Temporal relationships between hormonal and hemodynamic changes in early human pregnancy. *Kidney International* **54** 2056–2063. (<https://doi.org/10.1046/j.1523-1755.1998.00217.x>)
- Chen K, Merrill DC & Rose JC 2007 The importance of angiotensin II subtype receptors for blood pressure control during mouse pregnancy. *Reproductive Sciences* **14** 694–704. (<https://doi.org/10.1177/1933719107309060>)
- Chow BSM, Kocan M, Bosnyak S, Sarwar M, Wigg B, Jones ES, Widdop RE, Summers RJ, Bathgate RAD, Hewitson TD *et al.* 2014 Relaxin requires the angiotensin II type 2 receptor to abrogate renal interstitial fibrosis. *Kidney International* **86** 75–85. (<https://doi.org/10.1038/ki.2013.518>)
- Chow BSM, Kocan M, Shen M, Wang Y, Han L, Chew JY, Wang C, Bosnyak S, Mirabito-Colafella KM, Barsha G *et al.* 2019 AT1R-AT2R-RFXFP1 functional crosstalk in myofibroblasts: impact on the therapeutic targeting of renal and cardiac fibrosis. *Journal of the American Society of Nephrology* **30** 2191–2207. (<https://doi.org/10.1681/ASN.2019060597>)
- Crossen JS, Vollebregt KC, de Vrieze N, ter Riet G, Mol BW, Franx A, Khan KS & van der Post JA 2008 Accuracy of mean arterial pressure and blood pressure measurements in predicting pre-eclampsia: systematic review and meta-analysis. *BMJ* **336** 1117–1120. (<https://doi.org/10.1136/bmj.39540.522049.BE>)
- Conrad KP 2011 Maternal vasodilation in pregnancy: the emerging role of relaxin. *American Journal of Physiology: Regulatory, Integrative and Comparative Physiology* **301** R267–R275. (<https://doi.org/10.1152/ajpregu.00156.2011>)
- Conrad KP 2016 G-protein-coupled receptors as potential drug candidates in preeclampsia: targeting the relaxin/insulin-like family peptide receptor 1 for treatment and prevention. *Human Reproduction Update* **22** 647–664. (<https://doi.org/10.1093/humupd/dmw021>)
- Cooke CL & Davidge ST 2003 Pregnancy-induced alterations of vascular function in mouse mesenteric and uterine arteries. *Biology of Reproduction* **68** 1072–1077. (<https://doi.org/10.1095/biolreprod.102.009886>)
- Cunningham MW, Williams JM, Amaral L, Usry N, Wallukat G, Dechend R & Lamacra B 2016 Agonistic autoantibodies to the angiotensin II type 1 receptor enhance angiotensin II-induced renal vascular sensitivity and reduce renal function during pregnancy. *Hypertension* **68** 1308–1313. (<https://doi.org/10.1161/HYPERTENSIONAHA.116.07971>)
- Cunningham MW, Castillo J, Ibrahim T, Cornelius DC, Campbell N, Amaral L, Vaka VR, Usry N, Williams JM & Lamacra B 2018 AT1-AA (angiotensin II type 1 receptor agonistic autoantibody) blockade prevents preeclamptic symptoms in placental ischemic rats. *Hypertension* **71** 886–893. (<https://doi.org/10.1161/HYPERTENSIONAHA.117.10681>)
- Cunningham MW, Vaka VR, McMaster K, Ibrahim T, Cornelius DC, Amaral L, Campbell N, Wallukat G, McDuffey S, Usry N *et al.* 2019 Renal natural killer cell activation and mitochondrial oxidative stress; new mechanisms in AT1-AA mediated hypertensive pregnancy. *Pregnancy Hypertension* **15** 72–77. (<https://doi.org/10.1016/j.preghy.2018.11.004>)
- Davison JM 1984 Renal haemodynamics and volume homeostasis in pregnancy. *Scandinavian Journal of Clinical and Laboratory Investigation: Supplementum* **169** 15–27. (<https://doi.org/10.3109/00365518409085373>)
- Davison JM & Lindheimer MD 1980 Changes in renal haemodynamics and kidney weight during pregnancy in the unanaesthetized rat. *Journal of Physiology* **301** 129–136. (<https://doi.org/10.1113/jphysiol.1980.sp013194>)
- Dib FR, Duarte G, Sala MM, Ferriani RA & Berezowski AT 2003 Prospective evaluation of renal artery resistance and pulsatility indices in normal pregnant women. *Ultrasound in Obstetrics and Gynecology* **22** 515–519. (<https://doi.org/10.1002/uog.240>)
- Dickey RP & Hower JF 1995 Ultrasonographic features of uterine blood flow during the first 16 weeks of pregnancy. *Human Reproduction* **10** 2448–2452. (<https://doi.org/10.1093/oxfordjournals.humrep.a136317>)
- Dimmeler S, Fleming I, Fisslthaler B, Hermann C, Busse R & Zeiher AM 1999 Activation of nitric oxide synthase in endothelial cells by Akt-dependent phosphorylation. *Nature* **399** 601–605. (<https://doi.org/10.1038/21224>)
- Dunlop W 1981 Serial changes in renal haemodynamics during normal human pregnancy. *British Journal of Obstetrics and Gynaecology* **88** 1–9. (<https://doi.org/10.1111/j.1471-0528.1981.tb00929.x>)
- Eguchi S, Matsumoto T, Motley ED, Utsunomiya H & Inagami T 1996 Identification of an essential signaling cascade for mitogen-activated protein kinase activation by angiotensin II in cultured rat vascular smooth muscle cells: possible requirement of Gq-mediated p21ras activation coupled to a Ca²⁺/calmodulin-sensitive tyrosine kinase. *Journal of Biological Chemistry* **271** 14169–14175. (<https://doi.org/10.1074/jbc.271.24.14169>)
- Ferreira VM, Gomes TS, Reis LA, Ferreira AT, Razvickas CV, Schor N & Boim MA 2009 Receptor-induced dilatation in the systemic and intrarenal adaptation to pregnancy in rats. *PLoS ONE* **4** e4845. (<https://doi.org/10.1371/journal.pone.0004845>)
- Gandley RE, Conrad KP & McLaughlin MK 2001 Endothelin and nitric oxide mediate reduced myogenic reactivity of small renal arteries from pregnant rats. *American Journal of Physiology: Regulatory, Integrative and Comparative Physiology* **280** R1–R7. (<https://doi.org/10.1152/ajpregu.2001.280.1.R1>)
- Ganesan MK, Finsterwalder R, Leb H, Resch U, Neumüller K, De Martin R & Petzelbauer P 2017 Three-dimensional coculture model to analyze the cross talk between endothelial and smooth muscle cells. *Tissue Engineering: Part C, Methods* **23** 38–49. (<https://doi.org/10.1089/ten.tec.2016.0299>)
- Gant NF, Daley GL, Chand S, Whalley PJ & Macdonald PC 1973 A study of angiotensin II pressor response throughout primigravid pregnancy. *Journal of Clinical Investigation* **52** 2682–2689. (<https://doi.org/10.1172/JCI107462>)
- Gant NF, Worley RJ, Everett RB & Macdonald PC 1980 Control of vascular responsiveness during human pregnancy. *Kidney International* **18** 253–258. (<https://doi.org/10.1038/ki.1980.133>)
- Gao Y, Chen T & Raj JU 2016 Endothelial and smooth muscle cell interactions in the pathobiology of pulmonary hypertension. *American Journal of Respiratory Cell and Molecular Biology* **54** 451–460. (<https://doi.org/10.1165/rcmb.2015-0323TR>)
- Gray KM & Stroka KM 2017 Vascular endothelial cell mechanosensing: new insights gained from biomimetic microfluidic models. *Seminars in Cell and Developmental Biology* **71** 106–117. (<https://doi.org/10.1016/j.semcdb.2017.06.002>)
- Griending KK, Minieri CA, Ollerenshaw JD & Alexander RW 1994 Angiotensin-II stimulates NADH and NADPH oxidase activity in cultured vascular smooth-muscle cells. *Circulation Research* **74** 1141–1148. (<https://doi.org/10.1161/01.res.74.6.1141>)
- Gunderson EP, Chiang V, Lewis CE, Catov J, Quesenberry Jr CP, Sidney S, Wei GS & Ness R 2008 Long-term blood pressure changes measured from before to after pregnancy relative to nonparous women. *Obstetrics and Gynecology* **112** 1294–1302. (<https://doi.org/10.1097/AOG.0b013e31818da09b>)
- Guyton AC 1981 The relationship of cardiac output and arterial pressure control. *Circulation* **64** 1079–1088. (<https://doi.org/10.1161/01.cir.64.6.1079>)
- Henrion D, Kubis N & Lévy Bernard I 2001 Physiological and pathophysiological functions of the AT2 subtype receptor of angiotensin II. *Hypertension* **38** 1150–1157. (<https://doi.org/10.1161/hy1101.096109>)
- Hong K, Zhao G, Hong Z, Sun Z, Yang Y, Clifford PS, Davis MJ, Meining GA & Hill MA 2016 Mechanical activation of angiotensin II type 1 receptors causes actin remodelling and myogenic responsiveness in skeletal muscle arterioles. *Journal of Physiology* **594** 7027–7047. (<https://doi.org/10.1113/jp272834>)
- Huh D, Hamilton GA & Ingber DE 2011 From 3D cell culture to organ-on-chips. *Trends in Cell Biology* **21** 745–754. (<https://doi.org/10.1016/j.tcb.2011.09.005>)
- Hunter S & Robson SC 1992 Adaptation of the maternal heart in pregnancy. *British Heart Journal* **68** 540–543. (<https://doi.org/10.1136/hrt.68.12.540>)
- Ignarro LJ, Harbison RG, Wood KS & Kadowitz PJ 1986 Activation of purified soluble guanylate cyclase by endothelium-derived relaxing factor from intrapulmonary artery and vein: stimulation by acetylcholine, bradykinin and arachidonic acid. *Journal of Pharmacology and Experimental Therapeutics* **237** 893–900.

- Inuzuka T, Fujioka Y, Tsuda M, Fujioka M, Satoh AO, Horiuchi K, Nishide S, Nanbo A, Tanaka S & Ohba Y 2016 Attenuation of ligand-induced activation of angiotensin II type 1 receptor signaling by the type 2 receptor via protein kinase C. *Scientific Reports* **6** 21613. (<https://doi.org/10.1038/srep21613>)
- Irani RA & Xia Y 2008 The functional role of the renin-angiotensin system in pregnancy and preeclampsia. *Placenta* **29** 763–771. (<https://doi.org/10.1016/j.placenta.2008.06.011>)
- Irani RA & Xia Y 2011 Renin angiotensin signaling in normal pregnancy and preeclampsia. *Seminars in Nephrology* **31** 47–58. (<https://doi.org/10.1016/j.semnephrol.2010.10.005>)
- Jelinic M, Leo CH, Post Uiterweer ED, Sandow SL, Gooi JH, Wlodek ME, Conrad KP, Parkington H, Tare M & Parry LJ 2014 Localization of relaxin receptors in arteries and veins, and region-specific increases in compliance and bradykinin-mediated relaxation after *in vivo* serelaxin treatment. *FASEB Journal* **28** 275–287. (<https://doi.org/10.1096/fj.13-233429>)
- Johansson B 1989 Myogenic tone and reactivity: definitions based on muscle physiology. *Journal of Hypertension: Supplement* **7** S5–S8; discussion S9.
- Jufri NF, Mohamedali A, Avolio A & Baker MS 2015 Mechanical stretch: physiological and pathological implications for human vascular endothelial cells. *Vascular Cell* **7** 8. (<https://doi.org/10.1186/s13221-015-0033-z>)
- Kametas NA, McAuliffe F, Cook B, Nicolaides KH & Chambers J 2001 Maternal left ventricular transverse and long-axis systolic function during pregnancy. *Ultrasound in Obstetrics and Gynecology* **18** 467–474. (<https://doi.org/10.1046/j.0960-7692.2001.00574.x>)
- Kawai T, Forrester SJ, O'Brien S, Baggett A, Rizzo V & Eguchi S 2017 AT1 receptor signaling pathways in the cardiovascular system. *Pharmacological Research* **125** 4–13. (<https://doi.org/10.1016/j.phrs.2017.05.008>)
- Kodogo V, Azibani F & Sliwa K 2019 Role of pregnancy hormones and hormonal interaction on the maternal cardiovascular system: a literature review. *Clinical Research in Cardiology* **108** 831–846. (<https://doi.org/10.1007/s00392-019-01441-x>)
- Kubo T, Ibusuki T, Chiba S, Kambe T & Fukumori R 2001 Mitogen-activated protein kinase activity regulation role of angiotensin and endothelin systems in vascular smooth muscle cells. *European Journal of Pharmacology* **411** 27–34. ([https://doi.org/10.1016/s0014-2999\(00\)00857-8](https://doi.org/10.1016/s0014-2999(00)00857-8))
- Kurjak A, Vidovic M, Velemir D & Zalud I 1992 Renal arterial Resistance Index in pregnant and nonpregnant women: evaluation with color and pulse Doppler ultrasound. *Journal of Perinatal Medicine* **20** 11–14. (<https://doi.org/10.1515/jpme.1992.20.1.11>)
- Leo CH, Jelinic M, Gooi JH, Tare M & Parry LJ 2014a A vasoactive role for endogenous relaxin in mesenteric arteries of male mice. *PLoS ONE* **9** e107382. (<https://doi.org/10.1371/journal.pone.0107382>)
- Leo CH, Jelinic M, Parkington HC, Tare M & Parry LJ 2014b Acute intravenous injection of serelaxin (recombinant human relaxin-2) causes rapid and sustained bradykinin-mediated vasorelaxation. *Journal of the American Heart Association* **3** e000493. (<https://doi.org/10.1161/JAHA.113.000493>)
- Li PL, Jin MW & Campbell WB 1998 Effect of selective inhibition of soluble guanylyl cyclase on the K_{Ca} channel activity in coronary artery smooth muscle. *Hypertension* **31** 303–308. (<https://doi.org/10.1161/01.hyp.31.1.303>)
- Lian X, Beer-Hammer S, König GM, Kostenis E, Nürnberg B & Gollasch M 2018 RXFP1 receptor activation by relaxin-2 induces vascular relaxation in mice via a $G\alpha 2$ -protein/PBK β /nitric oxide-coupled pathway. *Frontiers in Physiology* **9** 1234. (<https://doi.org/10.3389/fphys.2018.01234>)
- Lin YJ, Kwok CF, Juan CC, Hsu YP, Shih KC, Chen CC & Ho LT 2014 Angiotensin II enhances endothelin-1-induced vasoconstriction through upregulating endothelin type A receptor. *Biochemical and Biophysical Research Communications* **451** 263–269. (<https://doi.org/10.1016/j.bbrc.2014.07.119>)
- Lumbers ER & Pringle KG 2014 Roles of the circulating renin-angiotensin-aldosterone system in human pregnancy. *American Journal of Physiology: Regulatory, Integrative and Comparative Physiology* **306** R91–R101. (<https://doi.org/10.1152/ajpregu.00034.2013>)
- Lumbers ER, Delforce SJ, Arthurs AL & Pringle KG 2019 Causes and consequences of the dysregulated maternal renin-angiotensin system in preeclampsia. *Frontiers in Endocrinology* **10** 563. (<https://doi.org/10.3389/fendo.2019.00563>)
- Lutz S, Freichel-Blomquist A, Yang Y, Rumenapp U, Jakobs KH, Schmidt M & Wieland T 2005 The guanine nucleotide exchange factor p63RhoGEF, a specific link between Gq/11-coupled receptor signaling and RhoA. *Journal of Biological Chemistry* **280** 11134–11139. (<https://doi.org/10.1074/jbc.M411322200>)
- Lykke JA, Langhoff-Roos J, Sibai BM, Funai EF, Triche EW & Paidas MJ 2009 Hypertensive pregnancy disorders and subsequent cardiovascular morbidity and type 2 diabetes mellitus in the mother. *Hypertension* **53** 944–951. (<https://doi.org/10.1161/HYPERTENSIONAHA.109.130765>)
- Marshall SA, Leo CH, Senadheera SN, Girling JE, Tare M & Parry LJ 2016 Relaxin deficiency attenuates pregnancy-induced adaptation of the mesenteric artery to angiotensin II in mice. *American Journal of Physiology: Regulatory, Integrative and Comparative Physiology* **310** R847–R857. (<https://doi.org/10.1152/ajpregu.00506.2015>)
- Marshall SA, Leo CH, Girling JE, Tare M, Beard S, Hannan NJ & Parry LJ 2017a Relaxin treatment reduces angiotensin II-induced vasoconstriction in pregnancy and protects against endothelial dysfunction. *Biology of Reproduction* **96** 895–906. (<https://doi.org/10.1093/biolre/fox023>)
- Marshall SA, Senadheera SN, Parry LJ & Girling JE 2017b The role of relaxin in normal and abnormal uterine function during the menstrual cycle and early pregnancy. *Reproductive Sciences* **24** 342–354. (<https://doi.org/10.1177/1933719116657189>)
- Marshall SA, Senadheera SN, Parry LJ & Girling JE 2017c The role of relaxin in normal and abnormal uterine function during the menstrual cycle and early pregnancy. *Reproductive Sciences* **24** 342–354. (<https://doi.org/10.1177/1933719116657189>)
- Marshall SA, Senadheera SN, Jelinic M, O'Sullivan K, Parry LJ & Tare M 2018 Relaxin deficiency leads to uterine artery dysfunction during pregnancy in mice. *Frontiers in Physiology* **9** 255. (<https://doi.org/10.3389/fphys.2018.00255>)
- Matthews BF & Taylor DW 1960 Effects of pregnancy on inulin and para-aminohippurate clearances in the anaesthetized rat. *Journal of Physiology* **151** 385–389. (<https://doi.org/10.1113/jphysiol.1960.sp006445>)
- McGuane JT, Debrah JE, Sautina L, Jarajapu YP, Novak J, Rubin JP, Grant MB, Segal M & Conrad KP 2011 Relaxin induces rapid dilation of rodent small renal and human subcutaneous arteries via P13 kinase and nitric oxide. *Endocrinology* **152** 2786–2796. (<https://doi.org/10.1210/en.2010-1126>)
- Meah VL, Cockcroft JR, Backx K, Shave R & Stöhr EJ 2016 Cardiac output and related haemodynamics during pregnancy: a series of meta-analyses. *Heart* **102** 518–526. (<https://doi.org/10.1136/heartjnl-2015-308476>)
- Melchiorre K, Sharma R & Thilaganathan B 2012 Cardiac structure and function in normal pregnancy. *Current Opinion in Obstetrics and Gynecology* **24** 413–421. (<https://doi.org/10.1097/GCO.0b013e328359826f>)
- Melchiorre K, Sharma R, Khalil A & Thilaganathan B 2016 Maternal cardiovascular function in normal pregnancy: evidence of maladaptation to chronic volume overload. *Hypertension* **67** 754–762. (<https://doi.org/10.1161/HYPERTENSIONAHA.115.06667>)
- Meyer MC, Osol G & McLaughlin M 1997 Flow decreases myogenic reactivity of mesenteric arteries from pregnant rats. *Journal of the Society for Gynecologic Investigation* **4** 293–297.
- Mirabito KM, Hilliard LM, Wei Z, Tikellis C, Widdop RE, Vinh A & Denton KM 2014 Role of inflammation and the angiotensin type 2 receptor in the regulation of arterial pressure during pregnancy in mice. *Hypertension* **64** 626–631. (<https://doi.org/10.1161/HYPERTENSIONAHA.114.03189>)
- Mirabito Colafella KM, Samuel CS & Denton KM 2017 Relaxin contributes to the regulation of arterial pressure in adult female mice. *Clinical Science* **131** 2795–2805. (<https://doi.org/10.1042/CS20171225>)
- Morris R, Sunesara I, Rush L, Anderson B, Blake PG, Darby M, Sawardecker S, Novotny S, Bofil JA & Martin JN 2014 Maternal hemodynamics by thoracic impedance cardiography for normal pregnancy and the postpartum period. *Obstetrics and Gynecology* **123** 318–324. (<https://doi.org/10.1097/AOG.000000000000104>)
- Morris EA, Hale SA, Badger GJ, Magness RR & Bernstein IM 2015 Pregnancy induces persistent changes in vascular compliance in primiparous women. *American Journal of Obstetrics and Gynecology* **212** 633.e1–633.e6. (<https://doi.org/10.1016/j.ajog.2015.01.005>)

- Morris EA, Mandala M, Ko NL & Osol G 2020 Postpartum persistence of maternal uterine vascular gestational adaptation in rodents. *Reproductive Sciences* **27** 611–620. (<https://doi.org/10.1007/s43032-019-00062-z>)
- Morschauer TJ, Ramadoss J, Koch JM, Yi FX, Lopez GE, Bird IM & Magness RR 2014 Local effects of pregnancy on connexin proteins that mediate Ca²⁺-associated uterine endothelial NO synthesis. *Hypertension* **63** 589–594. (<https://doi.org/10.1161/HYPERTENSIONAHA.113.01171>)
- Naderi S, Tsai SA & Khandelwal A 2017 Hypertensive disorders of pregnancy. *Current Atherosclerosis Reports* **19** 15. (<https://doi.org/10.1007/s11883-017-0648-z>)
- Novak J, Danielson LA, Kerchner LJ, Sherwood OD, Ramirez RJ, Moalli PA & Conrad KP 2001 Relaxin is essential for renal vasodilation during pregnancy in conscious rats. *Journal of Clinical Investigation* **107** 1469–1475. (<https://doi.org/10.1172/JCI11975>)
- Ogueh O, Clough A, Hancock M & Johnson MR 2011 A longitudinal study of the control of renal and uterine hemodynamic changes of pregnancy. *Hypertension in Pregnancy* **30** 243–259. (<https://doi.org/10.3109/10641955.2010.484079>)
- Osol G & Moore LG 2014 Maternal uterine vascular remodeling during pregnancy. *Microcirculation* **21** 38–47. (<https://doi.org/10.1111/micc.12080>)
- Osol G, Ko NL & Mandala M 2019 Plasticity of the maternal vasculature during pregnancy. *Annual Review of Physiology* **81** 89–111. (<https://doi.org/10.1146/annurev-physiol-020518-114435>)
- Ostrowski MA, Huang NF, Walker TW, Verwijlen T, Poplawski C, Khoo AS, Cooke JP, Fuller GG & Dunn AR 2014 Microvascular endothelial cells migrate upstream and align against the shear stress field created by impinging flow. *Biophysical Journal* **106** 366–374. (<https://doi.org/10.1016/j.bpj.2013.11.4502>)
- Palmer SK, Zamudio S, Coffin C, Parker S, Stamm E & Moore LG 1992 Quantitative estimation of human uterine artery blood flow and pelvic blood flow redistribution in pregnancy. *Obstetrics and Gynecology* **80** 1000–1006.
- Patzak A, Braun D, Schleifenbaum J & Küchler G 2018 Muscular arterial tone is a determinant of peripheral muscular artery stiffness. *Journal of Hypertension* **36** e70. (<https://doi.org/10.1097/01.hjh.0000539158.19151.9b>)
- Post Uiterweer ED, Koster MPH, Jeyabalan A, Kuc S, Siljee JE, Stewart DR, Conrad KP & Franx A 2020 Circulating pregnancy hormone relaxin as a first trimester biomarker for preeclampsia. *Pregnancy Hypertension* **22** 47–53. (<https://doi.org/10.1016/j.preghy.2020.07.008>)
- Qi F, Ogawa K, Tokinaga Y, Uematsu N, Minonishi T & Hatano Y 2009 Volatile anesthetics inhibit angiotensin II-induced vascular contraction by modulating myosin light chain phosphatase inhibiting protein, CPI-17 and regulatory subunit, MYPT1 phosphorylation. *Anesthesia and Analgesia* **109** 412–417. (<https://doi.org/10.1213/ane.0b013e3181ac6d96>)
- Quattrone S, Chiappini L, Scapagnini G, Bigazzi B & Bani D 2004 Relaxin potentiates the expression of inducible nitric oxide synthase by endothelial cells from human umbilical vein in vitro culture. *Molecular Human Reproduction* **10** 325–330. (<https://doi.org/10.1093/molehr/gah040>)
- Quignard JF, Mironneau J, Carricaburu V, Fournier B, Babich A, Nürnberg B, Mironneau C & Macrez N 2001 Phosphoinositide 3-kinase γ mediates angiotensin II-induced stimulation of L-type calcium channels in vascular myocytes. *Journal of Biological Chemistry* **276** 32545–32551. (<https://doi.org/10.1074/jbc.M102582200>)
- Quitterer U & Abdalla S 2021 Pathological AT1R-B2R protein aggregation and preeclampsia. *Cells* **10** 2609. (<https://doi.org/10.3390/cells10102609>)
- Rensen SSM, Doevendans PAFM & Van Eys GJJM 2007 Regulation and characteristics of vascular smooth muscle cell phenotypic diversity. *Netherlands Heart Journal* **15** 100–108. (<https://doi.org/10.1007/BF03085963>)
- Rigano S, Ferrazzi E, Boito S, Pennati G, Padoan A & Galan H 2010 Blood flow volume of uterine arteries in human pregnancies determined using 3D and bi-dimensional imaging, angio-Doppler, and fluid-dynamic modeling. *Placenta* **31** 37–43. (<https://doi.org/10.1016/j.placenta.2009.10.010>)
- Rodríguez I & González M 2014 Physiological mechanisms of vascular response induced by shear stress and effect of exercise in systemic and placental circulation. *Frontiers in Pharmacology* **5** 209. (<https://doi.org/10.3389/fphar.2014.00209>)
- Rosenfeld CR & Roy T 2014 Prolonged uterine artery nitric oxide synthase inhibition modestly alters basal uteroplacental vasodilation in the last third of ovine pregnancy. *American Journal of Physiology: Heart and Circulatory Physiology* **307** H1196–H1203. (<https://doi.org/10.1152/ajpheart.00996.2013>)
- Sadoshima J & Izumo S 1993 Signal transduction pathways of angiotensin II-induced c-fos gene expression in cardiac myocytes in vitro. Roles of phospholipid-derived second messengers. *Circulation Research* **73** 424–438. (<https://doi.org/10.1161/01.res.73.3.424>)
- Sandoo A, Van Zanten JJCSV, Metsios GS, Carroll D & Kitas GD 2010 The endothelium and its role in regulating vascular tone. *Open Cardiovascular Medicine Journal* **4** 302–312. (<https://doi.org/10.2174/1874192401004010302>)
- Sarwar M, Samuel CS, Bathgate RA, Stewart DR & Summers RJ 2016 Enhanced serelaxin signalling in co-cultures of human primary endothelial and smooth muscle cells. *British Journal of Pharmacology* **173** 484–496. (<https://doi.org/10.1111/bph.13371>)
- Savoia C, Tabet F, Yao G, Schiffrin EL & Touyz RM 2005 Negative regulation of RhoA/Rho kinase by angiotensin II type 2 receptor in vascular smooth muscle cells: role in angiotensin II-induced vasodilation in stroke-prone spontaneously hypertensive rats. *Journal of Hypertension* **23** 1037–1045. (<https://doi.org/10.1097/01.hjh.0000166845.49850.39>)
- Schlossmann J, Ammendola A, Ashman K, Zong X, Huber A, Neubauer G, Wang GX, Allescher HD, Korth M, Wilm M et al. 2000 Regulation of intracellular calcium by a signalling complex of IRAG, IP3 receptor and cGMP kinase I β . *Nature* **404** 197–201. (<https://doi.org/10.1038/35004606>)
- Seki T, Yokoshiki H, Sunagawa M, Nakamura M & Sperelakis N 1999 Angiotensin II stimulation of Ca²⁺-channel current in vascular smooth muscle cells is inhibited by lavendustin-A and LY-294002. *Pflügers Archiv* **437** 317–323. (<https://doi.org/10.1007/s004240050785>)
- Sherwood OD 2004 Relaxin's physiological roles and other diverse actions. *Endocrine Reviews* **25** 205–234. (<https://doi.org/10.1210/er.2003-0013>)
- Simmons LA, Gillin AG & Jeremy RW 2002 Structural and functional changes in left ventricle during normotensive and preeclamptic pregnancy. *American Journal of Physiology: Heart and Circulatory Physiology* **283** H1627–H1633. (<https://doi.org/10.1152/ajpheart.00966.2001>)
- Sims EA & Krantz KE 1958 Serial studies of renal function during pregnancy and the puerperium in normal women. *Journal of Clinical Investigation* **37** 1764–1774. (<https://doi.org/10.1172/JCI103769>)
- Siragy HM & Carey RM 1996 The subtype-2 (AT₂) angiotensin receptor regulates renal cyclic guanosine 3',5'-monophosphate and AT₁ receptor-mediated prostaglandin E₂ production in conscious rats. *Journal of Clinical Investigation* **97** 1978–1982. (<https://doi.org/10.1172/JCI118630>)
- Sturgiss SN, Wilkinson R & Davison JM 1996 Renal reserve during human pregnancy. *American Journal of Physiology* **271** F16–F20. (<https://doi.org/10.1152/ajprenal.1996.271.1.F16>)
- Takahashi T, Taniguchi T, Konishi H, Kikkawa U, Ishikawa Y & Yokoyama M 1999 Activation of Akt/protein kinase B after stimulation with angiotensin II in vascular smooth muscle cells. *American Journal of Physiology* **276** H1927–H1934. (<https://doi.org/10.1152/ajpheart.1999.276.6.H1927>)
- Takeda-Matsubara Y, Iwai M, Cui TX, Shiuchi T, Liu HW, Okumura M, Ito M & Horiuchi M 2004 Roles of angiotensin type 1 and 2 receptors in pregnancy-associated blood pressure change. *American Journal of Hypertension* **17** 684–689. (<https://doi.org/10.1016/j.amjhyper.2004.03.680>)
- Thilaganathan B & Kalafat E 2019 Cardiovascular system in preeclampsia and beyond. *Hypertension* **73** 522–531. (<https://doi.org/10.1161/HYPERTENSIONAHA.118.11191>)
- Thompson LP & Weiner CP 2001 Pregnancy enhances G protein activation and nitric oxide release from uterine arteries. *American Journal of Physiology: Heart and Circulatory Physiology* **280** H2069–H2075. (<https://doi.org/10.1152/ajpheart.2001.280.5.H2069>)
- Timmermans PB, Wong PC, Chiu AT, Herblin WF, Benfield P, Carini DJ, Lee RJ, Wexler RR, Saye JA & Smith RD 1993 Angiotensin II receptors and angiotensin II receptor antagonists. *Pharmacological Reviews* **45** 205–251.
- Touyz RM, El Mabrouk M, He G, Wu XH & Schiffrin EL 1999 Mitogen-activated protein/extracellular signal-regulated kinase inhibition attenuates angiotensin II-mediated signaling and contraction in spontaneously hypertensive rat vascular smooth muscle cells. *Circulation Research* **84** 505–515. (<https://doi.org/10.1161/01.res.84.5.505>)

- Touyz RM, He G, El Mabrouk M, Diep Q, Mardigyan V & Schiffrin EL 2001 Differential activation of extracellular signal-regulated protein kinase 1/2 and p38 mitogen activated-protein kinase by AT 1 receptors in vascular smooth muscle cells from Wistar-Kyoto rats and spontaneously hypertensive rats. *Journal of Hypertension* **19** 553–559. (<https://doi.org/10.1097/00004872-200103001-00006>)
- Touyz RM, Yao G, Viel E, Amiri F & Schiffrin EL 2004 Angiotensin II and endothelin-1 regulate MAP kinases through different redox-dependent mechanisms in human vascular smooth muscle cells. *Journal of Hypertension* **22** 1141–1149. (<https://doi.org/10.1097/00004872-200406000-00015>)
- Touyz RM, Alves-Lopes R, Rios FJ, Camargo LL, Anagnostopoulou A, Arner A & Montezano AC 2018 Vascular smooth muscle contraction in hypertension. *Cardiovascular Research* **114** 529–539. (<https://doi.org/10.1093/cvr/cvy023>)
- Twort CH & Breemen CV 1988 Cyclic guanosine monophosphate-enhanced sequestration of Ca²⁺ by sarcoplasmic reticulum in vascular smooth muscle. *Circulation Research* **62** 961–964. (<https://doi.org/10.1161/01.res.62.5.961>)
- Ushio-Fukai M, Griendling KK, Akers M, Lyons PR & Alexander RW 1998 Temporal dispersion of activation of phospholipase C- β 1 and - γ isoforms by angiotensin II in vascular smooth muscle cells: role of α q11, α 12, and β γ G protein subunits. *Journal of Biological Chemistry* **273** 19772–19777. (<https://doi.org/10.1074/jbc.273.31.19772>)
- van der Heijden OWH, Essers YPG, Wijnands E, Mey JGR, Peeters LLH & Van Eys GJJM 2009 Postpartum reversal of the pregnancy-induced uterine artery remodeling in young, aging, and eNOS-deficient mice. *Reproductive Sciences* **16** 642–649. (<https://doi.org/10.1177/1933719109333660>)
- Van Engeland NCA, Pollet AMAO, Den Toonder MJM, Bouten CVC, Stassen OMJA & Sahlgren CM 2018 A biomimetic microfluidic model to study signalling between endothelial and vascular smooth muscle cells under hemodynamic conditions. *Lab on a Chip* **18** 1607–1620. (<https://doi.org/10.1039/c8lc00286j>)
- Vodstrcil LA, Tare M, Novak J, Dragomir N, Ramirez RJ, Wlodek ME, Conrad KP & Parry LJ 2012 Relaxin mediates uterine artery compliance during pregnancy and increases uterine blood flow. *FASEB Journal* **26** 4035–4044. (<https://doi.org/10.1096/fj.12-210567>)
- Wang B, Li C, Huai R & Qu Z 2015 Overexpression of ANO1/TMEM16A, an arterial Ca²⁺-activated Cl⁻ channel, contributes to spontaneous hypertension. *Journal of Molecular and Cellular Cardiology* **82** 22–32. (<https://doi.org/10.1016/j.yjmcc.2015.02.020>)
- Wang C, Pinar AA, Widdop RE, Hossain MA, Bathgate RAD, Denton KM, Kemp-Harper BK & Samuel CS 2020 The anti-fibrotic actions of relaxin are mediated through AT2R-associated protein phosphatases via RXFP1-AT2R functional crosstalk in human cardiac myofibroblasts. *FASEB Journal* **34** 8217–8233. (<https://doi.org/10.1096/fj.201902506R>)
- West CA, Sasser JM & Baylis C 2016 The enigma of continual plasma volume expansion in pregnancy: critical role of the renin-angiotensin-aldosterone system. *American Journal of Physiology: Renal Physiology* **311** F1125–F1134. (<https://doi.org/10.1152/ajprenal.00129.2016>)
- Wetendorf M & Demayo FJ 2014 Progesterone receptor signaling in the initiation of pregnancy and preservation of a healthy uterus. *International Journal of Developmental Biology* **58** 95–106. (<https://doi.org/10.1387/ijdb.140069mw>)
- White MM, Mccullough RE, Dyckes R, Robertson AD & Moore LG 2000 Chronic hypoxia, pregnancy, and endothelium-mediated relaxation in guinea pig uterine and thoracic arteries. *American Journal of Physiology: Heart and Circulatory Physiology* **278** H2069–H2075. (<https://doi.org/10.1152/ajpheart.2000.278.6.H2069>)
- Yanagisawa M, Kurihara H, Kimura S, Tomobe Y, Kobayashi M, Mitsui Y, Yazaki Y, Goto K & Masaki T 1988 A novel potent vasoconstrictor peptide produced by vascular endothelial cells. *Nature* **332** 411–415. (<https://doi.org/10.1038/332411a0>)
- Yinon Y, Kingdom JC, Odutayo A, Moineddin R, Drewlo S, Lai V, Cherney DZ & Hladunewich MA 2010 Vascular dysfunction in women with a history of preeclampsia and intrauterine growth restriction: insights into future vascular risk. *Circulation* **122** 1846–1853. (<https://doi.org/10.1161/CIRCULATIONAHA.110.948455>)
- Zeniya M, Sohara E, Kita S, Iwamoto T, Susa K, Mori T, Oi K, Chiga M, Takahashi D, Yang SS *et al.* 2013 Dietary salt intake regulates WNK3-SPAK-NKCC1 phosphorylation cascade in mouse aorta through angiotensin II. *Hypertension* **62** 872–878. (<https://doi.org/10.1161/HYPERTENSIONAHA.113.01543>)
- Zhang HH, Chen JC, Sheibani L, Lechuga TJ & Chen DB 2017 Pregnancy augments VEGF-stimulated *in vitro* angiogenesis and vasodilator (NO and H₂S) production in human uterine artery endothelial cells. *Journal of Clinical Endocrinology and Metabolism* **102** 2382–2393. (<https://doi.org/10.1210/je.2017-00437>)

Received 6 May 2022

First decision 9 June 2022

Revised manuscript received 14 August 2022

Accepted 26 August 2022

APPENDIX B

SUPPLEMENTARY DATA OF

CHAPTER 4 – TIME POINT

EFFECT FOR REPEATED

MEASUREMENTS, INCLUDING

BODY WEIGHT,

BLOOD PRESSURE,

GLUCOSE TOLERANCE TEST

AND INSULIN CHALLENGE

Supplementary data. Time point effect of repeated measurements during the examination of body weight, blood pressure and metabolic function (glucose tolerance test (GTT) and insulin challenge (IC)) of rat offspring. As body weight, blood pressure, and GTT/IC responses of each offspring were measured over time, both treatment (sham (control) or restricted (IUGR) and time point (body weight: birth to 12 months, systolic blood pressure: 2 months to 12 months, GTT: basal to 120 min, and IC: basal to 90 min) were considered as fixed effects in the linear mixed-effect model. Results are averaged over the levels of control_restricted. Estimated marginal means (emmeans) of the linear mixed-effect model were reported instead of the sample's observed/descriptive means. As emmeans were extracted from the assumption that all groups had the same variance (balanced population), standard deviations (SD) were not reported. Instead, standard errors (SE) of emmeans were reported. Degrees-of-freedom method used was Kenward-Roger. Confidence level used was 95%. Values within cells coloured in grey are non-significant.

Body weight:

F1 males							
contrast			estimate	SE	df	t.ratio	p.value
12mo	-	2mo	226.155	2.6349	376.93	85.83	<.0001
12mo	-	3mo	147.403	2.47782	375.84	59.489	<.0001
12mo	-	4mo	100.031	2.49484	375.28	40.095	<.0001
12mo	-	6mo	51.933	2.40375	375.77	21.605	<.0001
12mo	-	9mo	18.539	2.45072	375.86	7.565	<.0001
12mo	-	birth	442.954	2.79518	380.42	158.471	<.0001
12mo	-	PN14	424.945	2.49455	376.12	170.349	<.0001
12mo	-	PN35	364.229	2.49774	376.71	145.824	<.0001
12mo	-	PN7	435.862	2.55613	376.16	170.516	<.0001
2mo	-	3mo	-78.752	2.62968	376.94	-29.947	<.0001
2mo	-	4mo	-126.124	2.66741	377.85	-47.283	<.0001
2mo	-	6mo	-174.222	2.56824	377.12	-67.837	<.0001
2mo	-	9mo	-207.616	2.62008	378.39	-79.24	<.0001
2mo	-	birth	216.8	2.923	379.58	74.17	<.0001
2mo	-	PN14	198.79	2.64533	377.01	75.147	<.0001

2mo	-	PN35	138.074	2.65264	377.65	52.052	<.0001
2mo	-	PN7	209.707	2.70491	376.39	77.528	<.0001
3mo	-	4mo	-47.372	2.49832	374.88	-18.962	<.0001
3mo	-	6mo	-95.47	2.39985	374.57	-39.782	<.0001
3mo	-	9mo	-128.864	2.44328	374.41	-52.742	<.0001
3mo	-	birth	295.551	2.79513	380.62	105.738	<.0001
3mo	-	PN14	277.541	2.49434	375.33	111.268	<.0001
3mo	-	PN35	216.826	2.4937	375.4	86.949	<.0001
3mo	-	PN7	288.459	2.55534	375.48	112.885	<.0001
4mo	-	6mo	-48.098	2.42745	375.03	-19.814	<.0001
4mo	-	9mo	-81.492	2.47289	375.23	-32.954	<.0001
4mo	-	birth	342.923	2.82638	381.69	121.33	<.0001
4mo	-	PN14	324.913	2.52204	375.89	128.83	<.0001
4mo	-	PN35	264.198	2.52148	375.96	104.779	<.0001
4mo	-	PN7	335.831	2.58146	375.53	130.094	<.0001
6mo	-	9mo	-33.394	2.3695	374.35	-14.093	<.0001
6mo	-	birth	391.021	2.72216	379.5	143.644	<.0001
6mo	-	PN14	373.011	2.41328	374.52	154.566	<.0001
6mo	-	PN35	312.296	2.41278	374.6	129.434	<.0001
6mo	-	PN7	383.929	2.49057	375.63	154.153	<.0001
9mo	-	birth	424.415	2.76536	379.84	153.476	<.0001
9mo	-	PN14	406.405	2.46371	374.99	164.957	<.0001
9mo	-	PN35	345.69	2.46306	375.04	140.35	<.0001
9mo	-	PN7	417.323	2.53694	376.37	164.499	<.0001
birth	-	PN14	-18.01	2.80311	379.98	-6.425	<.0001
birth	-	PN35	-78.725	2.80019	379.72	-28.114	<.0001
birth	-	PN7	-7.092	2.8686	380.82	-2.472	0.287
PN14	-	PN35	-60.715	2.48952	373.72	-24.388	<.0001
PN14	-	PN7	10.917	2.57853	376.26	4.234	0.001
PN35	-	PN7	71.633	2.57795	376.34	27.787	<.0001

F2 males							
contrast			estimate	SE	df	t.ratio	p.value
12mo	-	16mo	-30.188	2.99824	469.95	-10.068	<.0001
12mo	-	2mo	261.704	2.3128	472.04	113.154	<.0001
12mo	-	4mo	123.881	2.35439	470.3	52.617	<.0001
12mo	-	6mo	73.689	2.31917	475.09	31.774	<.0001
12mo	-	9mo	27.923	2.45824	454.59	11.359	<.0001
12mo	-	birth	476.385	2.88864	497.68	164.917	<.0001
12mo	-	PN14	458.118	2.27477	478.08	201.391	<.0001
12mo	-	PN35	393.186	2.25269	476.3	174.541	<.0001
12mo	-	PN7	470.809	2.22703	478.96	211.406	<.0001
16mo	-	2mo	291.891	2.79662	478.7	104.373	<.0001
16mo	-	4mo	154.068	2.83375	478.1	54.369	<.0001
16mo	-	6mo	103.877	2.79893	480.14	37.113	<.0001

16mo	-	9mo	58.111	2.92917	472.09	19.839	<.0001
16mo	-	birth	506.573	3.30523	500.54	153.264	<.0001
16mo	-	PN14	488.305	2.76344	482.92	176.702	<.0001
16mo	-	PN35	423.374	2.74871	482.87	154.026	<.0001
16mo	-	PN7	500.996	2.72519	484.13	183.839	<.0001
2mo	-	4mo	-137.823	2.0409	460.87	-67.531	<.0001
2mo	-	6mo	-188.014	1.99481	459.86	-94.252	<.0001
2mo	-	9mo	-233.781	2.20768	469.11	-105.894	<.0001
2mo	-	birth	214.681	2.61699	487.02	82.034	<.0001
2mo	-	PN14	196.414	1.95085	471.9	100.681	<.0001
2mo	-	PN35	131.483	1.92832	470.7	68.185	<.0001
2mo	-	PN7	209.105	1.89722	471.87	110.216	<.0001
4mo	-	6mo	-50.191	2.04025	459.22	-24.601	<.0001
4mo	-	9mo	-95.958	2.25134	467.43	-42.623	<.0001
4mo	-	birth	352.504	2.65867	488.36	132.587	<.0001
4mo	-	PN14	334.237	2.00111	471.78	167.026	<.0001
4mo	-	PN35	269.306	1.97657	469.98	136.249	<.0001
4mo	-	PN7	346.928	1.95041	473.67	177.875	<.0001
6mo	-	9mo	-45.766	2.21144	471.88	-20.695	<.0001
6mo	-	birth	402.696	2.62504	490.38	153.406	<.0001
6mo	-	PN14	384.428	1.95655	475.26	196.483	<.0001
6mo	-	PN35	319.497	1.92881	472.12	165.644	<.0001
6mo	-	PN7	397.119	1.89682	473.89	209.36	<.0001
9mo	-	birth	448.462	2.79977	495.98	160.178	<.0001
9mo	-	PN14	430.195	2.16601	475.57	198.612	<.0001
9mo	-	PN35	365.263	2.14334	473.98	170.418	<.0001
9mo	-	PN7	442.886	2.11721	477.01	209.184	<.0001
birth	-	PN14	-18.267	2.58177	492.45	-7.076	<.0001
birth	-	PN35	-83.199	2.56203	490.81	-32.474	<.0001
birth	-	PN7	-5.576	2.5314	488.6	-2.203	0.4562
PN14	-	PN35	-64.931	1.85436	457.68	-35.016	<.0001
PN14	-	PN7	12.691	1.82438	459.4	6.956	<.0001
PN35	-	PN7	77.623	1.79773	458.24	43.178	<.0001

F2 females							
contrast			estimate	SE	df	t.ratio	p.value
12mo	-	2mo	97.3399	1.22883	535.98	79.214	<.0001
12mo	-	4mo	36.5762	1.232391	534.62	29.679	<.0001
12mo	-	6mo	18.8255	1.241361	536.98	15.165	<.0001
12mo	-	9mo	5.3867	1.351254	518.71	3.986	0.0025
12mo	-	birth	255.9637	1.537348	562.46	166.497	<.0001
12mo	-	PN14	237.6901	1.207301	544.69	196.877	<.0001
12mo	-	PN35	181.4631	1.214996	542.96	149.353	<.0001
12mo	-	PN7	250.0078	1.211374	546.28	206.384	<.0001
2mo	-	4mo	-60.7637	0.895701	514.62	-67.839	<.0001

2mo	-	6mo	-78.5145	0.904863	514.08	-86.769	<.0001
2mo	-	9mo	-91.9533	1.081512	530.52	-85.023	<.0001
2mo	-	birth	158.6237	1.256547	544.54	126.238	<.0001
2mo	-	PN14	140.3502	0.855109	524.84	164.131	<.0001
2mo	-	PN35	84.1232	0.867876	522.89	96.93	<.0001
2mo	-	PN7	152.6679	0.860024	526.81	177.516	<.0001
4mo	-	6mo	-17.7507	0.908053	512.47	-19.548	<.0001
4mo	-	9mo	-31.1895	1.086148	530.45	-28.716	<.0001
4mo	-	birth	219.3875	1.257093	541.47	174.52	<.0001
4mo	-	PN14	201.1139	0.86113	524.79	233.547	<.0001
4mo	-	PN35	144.8869	0.873642	525.43	165.842	<.0001
4mo	-	PN7	213.4316	0.866112	526.9	246.425	<.0001
6mo	-	9mo	-13.4388	1.095979	533.07	-12.262	<.0001
6mo	-	birth	237.1382	1.265431	543.52	187.397	<.0001
6mo	-	PN14	218.8647	0.8721	526.92	250.963	<.0001
6mo	-	PN35	162.6377	0.884637	527.1	183.847	<.0001
6mo	-	PN7	231.1824	0.877105	528.98	263.574	<.0001
9mo	-	birth	250.577	1.414779	559.3	177.114	<.0001
9mo	-	PN14	232.3035	1.055131	539.72	220.165	<.0001
9mo	-	PN35	176.0764	1.065618	538.82	165.234	<.0001
9mo	-	PN7	244.6212	1.059814	541.37	230.815	<.0001
birth	-	PN14	-18.2735	1.229058	548.2	-14.868	<.0001
birth	-	PN35	-74.5005	1.240285	549.32	-60.067	<.0001
birth	-	PN7	-5.9558	1.231452	547.46	-4.836	0.0001
PN14	-	PN35	-56.227	0.824539	517.06	-68.192	<.0001
PN14	-	PN7	12.3177	0.812358	512.36	15.163	<.0001
PN35	-	PN7	68.5447	0.82821	516.38	82.762	<.0001

F3 males							
contrast			estimate	SE	df	t.ratio	p.value
12mo	-	16mo	-19.035	2.47909	517.67	-7.678	<.0001
12mo	-	2mo	240.095	1.82583	516.47	131.5	<.0001
12mo	-	4mo	109.966	1.76712	515.82	62.229	<.0001
12mo	-	6mo	60.332	1.77028	514.91	34.08	<.0001
12mo	-	9mo	20.778	1.96107	499.81	10.595	<.0001
12mo	-	birth	464.944	2.61521	556.29	177.784	<.0001
12mo	-	PN14	445.611	1.73081	522.76	257.458	<.0001
12mo	-	PN35	382.481	1.73624	523.09	220.292	<.0001
12mo	-	PN7	458.506	1.74205	523.93	263.2	<.0001
16mo	-	2mo	259.13	2.37793	525.38	108.973	<.0001
16mo	-	4mo	129.001	2.33539	525.39	55.237	<.0001
16mo	-	6mo	79.367	2.33299	523.42	34.02	<.0001
16mo	-	9mo	39.813	2.49039	517.28	15.986	<.0001
16mo	-	birth	483.979	3.01634	548.69	160.452	<.0001
16mo	-	PN14	464.647	2.30265	527.63	201.788	<.0001
16mo	-	PN35	401.516	2.30677	527.72	174.06	<.0001

16mo	-	PN7	477.541	2.3125	528.34	206.504	<.0001
2mo	-	4mo	-130.13	1.58121	505.48	-82.298	<.0001
2mo	-	6mo	-179.763	1.58094	503.44	-113.707	<.0001
2mo	-	9mo	-219.318	1.84184	516.77	-119.075	<.0001
2mo	-	birth	224.848	2.46928	548.89	91.058	<.0001
2mo	-	PN14	205.516	1.53499	512.8	133.888	<.0001
2mo	-	PN35	142.386	1.543	514.23	92.278	<.0001
2mo	-	PN7	218.411	1.55213	517.72	140.717	<.0001
4mo	-	6mo	-49.633	1.51897	502.15	-32.676	<.0001
4mo	-	9mo	-89.188	1.78447	516.25	-49.98	<.0001
4mo	-	birth	354.978	2.41665	544.72	146.888	<.0001
4mo	-	PN14	335.646	1.47387	514.66	227.731	<.0001
4mo	-	PN35	272.516	1.48461	517.82	183.56	<.0001
4mo	-	PN7	348.541	1.49079	520.04	233.796	<.0001
6mo	-	9mo	-39.554	1.78633	514.79	-22.143	<.0001
6mo	-	birth	404.612	2.42533	548.05	166.828	<.0001
6mo	-	PN14	385.279	1.47591	512.95	261.046	<.0001
6mo	-	PN35	322.149	1.48503	515.63	216.931	<.0001
6mo	-	PN7	398.174	1.49336	518.57	266.629	<.0001
9mo	-	birth	444.166	2.62721	556.1	169.064	<.0001
9mo	-	PN14	424.834	1.74867	523.35	242.947	<.0001
9mo	-	PN35	361.703	1.75384	523.47	206.236	<.0001
9mo	-	PN7	437.729	1.76008	524.76	248.699	<.0001
birth	-	PN14	-19.332	2.39438	551.87	-8.074	<.0001
birth	-	PN35	-82.463	2.40804	554.74	-34.245	<.0001
birth	-	PN7	-6.437	2.40783	554.33	-2.674	0.1871
PN14	-	PN35	-63.13	1.4149	504.74	-44.618	<.0001
PN14	-	PN7	12.895	1.42099	504.6	9.075	<.0001
PN35	-	PN7	76.025	1.43116	506.82	53.121	<.0001

F3 females							
contrast			estimate	SE	df	t.ratio	p.value
12mo	-	2mo	93.6682	1.545866	372.97	60.593	<.0001
12mo	-	4mo	30.6111	1.731734	386	17.677	<.0001
12mo	-	6mo	14.4986	1.547464	371.49	9.369	<.0001
12mo	-	9mo	6.476	1.659294	360.19	3.903	0.004
12mo	-	birth	258.9442	1.94452	388.09	133.166	<.0001
12mo	-	PN14	239.8794	1.536034	376.97	156.168	<.0001
12mo	-	PN35	184.8261	1.524771	377.71	121.216	<.0001
12mo	-	PN7	252.4986	1.561514	379.77	161.701	<.0001
2mo	-	4mo	-63.0571	1.262562	369.93	-49.944	<.0001
2mo	-	6mo	-79.1696	1.034495	351.42	-76.53	<.0001
2mo	-	9mo	-87.1922	1.240691	364.51	-70.277	<.0001
2mo	-	birth	165.276	1.52139	373.49	108.635	<.0001
2mo	-	PN14	146.2112	1.013743	362.84	144.229	<.0001
2mo	-	PN35	91.1578	0.993692	362.12	91.737	<.0001

2mo	-	PN7	158.8304	1.047436	369.3	151.637	<.0001
4mo	-	6mo	-16.1125	1.267641	368.62	-12.711	<.0001
4mo	-	9mo	-24.1351	1.466853	385.83	-16.454	<.0001
4mo	-	birth	228.3331	1.648767	359.71	138.487	<.0001
4mo	-	PN14	209.2683	1.255657	379.28	166.66	<.0001
4mo	-	PN35	154.2149	1.235952	376.63	124.774	<.0001
4mo	-	PN7	221.8875	1.280835	380.77	173.237	<.0001
6mo	-	9mo	-8.0226	1.246318	363.74	-6.437	<.0001
6mo	-	birth	244.4456	1.528083	373.46	159.969	<.0001
6mo	-	PN14	225.3808	1.023655	363.82	220.173	<.0001
6mo	-	PN35	170.3274	1.002325	361.84	169.932	<.0001
6mo	-	PN7	238	1.058529	370.6	224.84	<.0001
9mo	-	birth	252.4682	1.712382	388.88	147.437	<.0001
9mo	-	PN14	233.4034	1.230835	371.14	189.63	<.0001
9mo	-	PN35	178.35	1.213763	371.25	146.94	<.0001
9mo	-	PN7	246.0226	1.260707	375.49	195.147	<.0001
birth	-	PN14	-19.0648	1.513129	378.37	-12.6	<.0001
birth	-	PN35	-74.1181	1.495588	376.23	-49.558	<.0001
birth	-	PN7	-6.4456	1.529406	378.44	-4.214	0.001
PN14	-	PN35	-55.0533	0.959288	352.64	-57.39	<.0001
PN14	-	PN7	12.6192	1.00676	354.27	12.534	<.0001
PN35	-	PN7	67.6726	0.992019	356.02	68.217	<.0001

Blood pressure:

F1 males							
contrast			estimate	SE	df	t.ratio	p.value
12mo	-	2mo	9.14374	2.33691	197.04	3.913	0.0017
12mo	-	3mo	0.35911	2.22127	195.12	0.162	1
12mo	-	4mo	-3.76419	2.26504	192.33	-1.662	0.5587
12mo	-	6mo	-3.23133	2.21134	192.92	-1.461	0.6893
12mo	-	9mo	1.42573	2.21169	193.32	0.645	0.9874
2mo	-	3mo	-8.78463	2.3455	194.93	-3.745	0.0032
2mo	-	4mo	-12.9079	2.41157	205.83	-5.353	<.0001
2mo	-	6mo	-12.3751	2.36651	200.27	-5.229	<.0001
2mo	-	9mo	-7.71801	2.36023	201.8	-3.27	0.0158
3mo	-	4mo	-4.1233	2.29628	196.1	-1.796	0.4709
3mo	-	6mo	-3.59044	2.24609	198.53	-1.599	0.6005
3mo	-	9mo	1.06662	2.23736	193.84	0.477	0.9969
4mo	-	6mo	0.53286	2.29099	197.41	0.233	0.9999
4mo	-	9mo	5.18992	2.29708	195.77	2.259	0.216
6mo	-	9mo	4.65705	2.23969	198.48	2.079	0.3024

F2 males							
contrast			estimate	SE	df	t.ratio	p.value
12mo	-	16mo	-1.25973	2.16736	207.69	-0.581	0.9922
12mo	-	2mo	9.80047	1.60393	211.83	6.11	<.0001
12mo	-	4mo	-1.81445	1.65962	208.99	-1.093	0.8837
12mo	-	6mo	-2.48075	1.63297	211.52	-1.519	0.6523
12mo	-	9mo	-2.67275	1.71441	191.68	-1.559	0.6265
16mo	-	2mo	11.0602	2.11539	224.28	5.228	<.0001
16mo	-	4mo	-0.55472	2.15611	219.98	-0.257	0.9998
16mo	-	6mo	-1.22102	2.1259	219.32	-0.574	0.9926
16mo	-	9mo	-1.41302	2.19964	209.98	-0.642	0.9876
2mo	-	4mo	-11.6149	1.54495	205.85	-7.518	<.0001
2mo	-	6mo	-12.2812	1.52264	205.24	-8.066	<.0001
2mo	-	9mo	-12.4732	1.63742	212.37	-7.618	<.0001
4mo	-	6mo	-0.6663	1.59232	215.34	-0.418	0.9983
4mo	-	9mo	-0.8583	1.69235	210.13	-0.507	0.9959
6mo	-	9mo	-0.192	1.67569	217.08	-0.115	1
F2 females							
contrast			estimate	SE	df	t.ratio	p.value
12mo	-	2mo	7.94294	1.90744	227.92	4.164	0.0004
12mo	-	4mo	-2.94526	1.91885	240.35	-1.535	0.5408
12mo	-	6mo	-2.068	1.91752	236.67	-1.078	0.8175
12mo	-	9mo	-1.18779	2.06799	206.55	-0.574	0.9787
2mo	-	4mo	-10.8882	1.52888	214.65	-7.122	<.0001
2mo	-	6mo	-10.0109	1.53179	215.49	-6.535	<.0001
2mo	-	9mo	-9.13073	1.75748	221.44	-5.195	<.0001
4mo	-	6mo	0.87727	1.52879	210.42	0.574	0.9788
4mo	-	9mo	1.75747	1.76702	233.77	0.995	0.8576
6mo	-	9mo	0.8802	1.7681	232.79	0.498	0.9875

F3 males							
contrast			estimate	SE	df	t.ratio	p.value
12mo	-	16mo	1.23885	2.88484	271.39	0.429	0.9981
12mo	-	2mo	28.02272	2.11427	266.43	13.254	<.0001
12mo	-	4mo	13.58028	2.09135	264.54	6.494	<.0001
12mo	-	6mo	6.20829	2.06637	263.51	3.004	0.0343
12mo	-	9mo	-0.60076	2.27392	242.1	-0.264	0.9998
16mo	-	2mo	26.78386	2.80055	283.79	9.564	<.0001
16mo	-	4mo	12.34143	2.77907	280.66	4.441	0.0002
16mo	-	6mo	4.96944	2.76248	282.06	1.799	0.4681
16mo	-	9mo	-1.83961	2.91983	272.46	-0.63	0.9887
2mo	-	4mo	-14.4424	1.93251	254.52	-7.473	<.0001
2mo	-	6mo	-21.8144	1.90516	250.61	-11.45	<.0001
2mo	-	9mo	-28.6235	2.16625	269.7	-13.213	<.0001
4mo	-	6mo	-7.37199	1.87756	248.19	-3.926	0.0015
4mo	-	9mo	-14.181	2.142	265.3	-6.62	<.0001

6mo	-	9mo	-6.80905	2.11353	262.44	-3.222	0.0178
F3 females							
contrast			estimate	SE	df	t.ratio	p.value
12mo	-	2mo	11.06249	2.06799	183.84	5.349	<.0001
12mo	-	4mo	3.73692	2.07199	183.8	1.804	0.3747
12mo	-	6mo	6.47939	2.14191	182.15	3.025	0.0235
12mo	-	9mo	2.16563	2.21315	167.86	0.979	0.8646
2mo	-	4mo	-7.32557	1.50023	156.94	-4.883	<.0001
2mo	-	6mo	-4.5831	1.60274	165.74	-2.86	0.038
2mo	-	9mo	-8.89686	1.70745	170.6	-5.211	<.0001
4mo	-	6mo	2.74247	1.60813	164.87	1.705	0.4335
4mo	-	9mo	-1.57129	1.71558	175.78	-0.916	0.8905
6mo	-	9mo	-4.31376	1.80122	170.67	-2.395	0.1217

GTT plasma glucose at 6 months of age:

F2 males							
contrast			estimate	SE	df	t.ratio	p.value
10min	-	120min	7.693571	0.756095	104	10.175	<.0001
10min	-	20min	-0.2567	0.756095	104	-0.34	1
10min	-	30min	0.209911	0.756095	104	0.278	1
10min	-	45min	2.252768	0.756095	104	2.979	0.0825
10min	-	5min	0.797589	0.756095	104	1.055	0.9792
10min	-	60min	3.600357	0.756095	104	4.762	0.0002
10min	-	90min	5.311071	0.756095	104	7.024	<.0001
10min	-	basal	9.221875	0.756095	104	12.197	<.0001
120min	-	20min	-7.95027	0.756095	104	-10.515	<.0001
120min	-	30min	-7.48366	0.756095	104	-9.898	<.0001
120min	-	45min	-5.4408	0.756095	104	-7.196	<.0001
120min	-	5min	-6.89598	0.756095	104	-9.121	<.0001
120min	-	60min	-4.09321	0.756095	104	-5.414	<.0001
120min	-	90min	-2.3825	0.756095	104	-3.151	0.0524
120min	-	basal	1.528304	0.756095	104	2.021	0.5324
20min	-	30min	0.466607	0.756095	104	0.617	0.9995
20min	-	45min	2.509464	0.756095	104	3.319	0.0326
20min	-	5min	1.054286	0.756095	104	1.394	0.8976
20min	-	60min	3.857054	0.756095	104	5.101	0.0001
20min	-	90min	5.567768	0.756095	104	7.364	<.0001
20min	-	basal	9.478571	0.756095	104	12.536	<.0001
30min	-	45min	2.042857	0.756095	104	2.702	0.1601
30min	-	5min	0.587679	0.756095	104	0.777	0.9973
30min	-	60min	3.390446	0.756095	104	4.484	0.0006
30min	-	90min	5.101161	0.756095	104	6.747	<.0001
30min	-	basal	9.011964	0.756095	104	11.919	<.0001
45min	-	5min	-1.45518	0.756095	104	-1.925	0.5985

45min	-	60min	1.347589	0.756095	104	1.782	0.6936
45min	-	90min	3.058304	0.756095	104	4.045	0.0031
45min	-	basal	6.969107	0.756095	104	9.217	<.0001
5min	-	60min	2.802768	0.756095	104	3.707	0.0098
5min	-	90min	4.513482	0.756095	104	5.969	<.0001
5min	-	basal	8.424286	0.756095	104	11.142	<.0001
60min	-	90min	1.710714	0.756095	104	2.263	0.3744
60min	-	basal	5.621518	0.756095	104	7.435	<.0001
90min	-	basal	3.910804	0.756095	104	5.172	<.0001

F2 females							
contrast			estimate	SE	df	t.ratio	p.value
10min	-	120min	7.512143	0.781577	123.49	9.612	<.0001
10min	-	20min	0.586018	0.781577	123.49	0.75	0.9979
10min	-	30min	2.081483	0.789426	123.22	2.637	0.1825
10min	-	45min	3.390518	0.781577	123.49	4.338	0.001
10min	-	5min	0.110143	0.781577	123.49	0.141	1
10min	-	60min	5.677381	0.792216	123.78	7.166	<.0001
10min	-	90min	7.311143	0.781577	123.49	9.354	<.0001
10min	-	basal	9.463775	0.789426	123.22	11.988	<.0001
120min	-	20min	-6.92613	0.758415	123.01	-9.132	<.0001
120min	-	30min	-5.43066	0.768915	123.28	-7.063	<.0001
120min	-	45min	-4.12163	0.758415	123.01	-5.435	<.0001
120min	-	5min	-7.402	0.758415	123.01	-9.76	<.0001
120min	-	60min	-1.83476	0.768766	123.19	-2.387	0.3007
120min	-	90min	-0.201	0.758415	123.01	-0.265	1
120min	-	basal	1.951632	0.768915	123.28	2.538	0.2244
20min	-	30min	1.495465	0.768915	123.28	1.945	0.5843
20min	-	45min	2.8045	0.758415	123.01	3.698	0.0096
20min	-	5min	-0.47588	0.758415	123.01	-0.627	0.9994
20min	-	60min	5.091363	0.768766	123.19	6.623	<.0001
20min	-	90min	6.725125	0.758415	123.01	8.867	<.0001
20min	-	basal	8.877757	0.768915	123.28	11.546	<.0001
30min	-	45min	1.309035	0.768915	123.28	1.702	0.7439
30min	-	5min	-1.97134	0.768915	123.28	-2.564	0.2129
30min	-	60min	3.595898	0.779425	123.53	4.614	0.0003
30min	-	90min	5.22966	0.768915	123.28	6.801	<.0001
30min	-	basal	7.382292	0.776916	123.01	9.502	<.0001
45min	-	5min	-3.28038	0.758415	123.01	-4.325	0.001
45min	-	60min	2.286863	0.768766	123.19	2.975	0.0817
45min	-	90min	3.920625	0.758415	123.01	5.169	<.0001
45min	-	basal	6.073257	0.768915	123.28	7.898	<.0001
5min	-	60min	5.567238	0.768766	123.19	7.242	<.0001
5min	-	90min	7.201	0.758415	123.01	9.495	<.0001
5min	-	basal	9.353632	0.768915	123.28	12.165	<.0001

60min	-	90min	1.633762	0.768766	123.19	2.125	0.4613
60min	-	basal	3.786394	0.779425	123.53	4.858	0.0001
90min	-	basal	2.152632	0.768915	123.28	2.8	0.1261

F3 males							
contrast			estimate	SE	df	t.ratio	p.value
10min	-	120min	8.473571	0.852539	79	9.939	<.0001
10min	-	20min	-0.54757	0.852539	79	-0.642	0.9993
10min	-	30min	1.288461	0.86897	79.24	1.483	0.8602
10min	-	45min	1.983	0.852539	79	2.326	0.3397
10min	-	5min	2.614286	0.852539	79	3.066	0.0691
10min	-	60min	4.491714	0.852539	79	5.269	<.0001
10min	-	90min	6.664	0.852539	79	7.817	<.0001
10min	-	basal	10.33771	0.852539	79	12.126	<.0001
120min	-	20min	-9.02114	0.852539	79	-10.582	<.0001
120min	-	30min	-7.18511	0.86897	79.24	-8.269	<.0001
120min	-	45min	-6.49057	0.852539	79	-7.613	<.0001
120min	-	5min	-5.85929	0.852539	79	-6.873	<.0001
120min	-	60min	-3.98186	0.852539	79	-4.671	0.0004
120min	-	90min	-1.80957	0.852539	79	-2.123	0.4659
120min	-	basal	1.864143	0.852539	79	2.187	0.4244
20min	-	30min	1.836032	0.86897	79.24	2.113	0.4723
20min	-	45min	2.530571	0.852539	79	2.968	0.0884
20min	-	5min	3.161857	0.852539	79	3.709	0.011
20min	-	60min	5.039286	0.852539	79	5.911	<.0001
20min	-	90min	7.211571	0.852539	79	8.459	<.0001
20min	-	basal	10.88529	0.852539	79	12.768	<.0001
30min	-	45min	0.694539	0.86897	79.24	0.799	0.9966
30min	-	5min	1.325825	0.86897	79.24	1.526	0.8401
30min	-	60min	3.203254	0.86897	79.24	3.686	0.0118
30min	-	90min	5.375539	0.86897	79.24	6.186	<.0001
30min	-	basal	9.049254	0.86897	79.24	10.414	<.0001
45min	-	5min	0.631286	0.852539	79	0.74	0.998
45min	-	60min	2.508714	0.852539	79	2.943	0.0942
45min	-	90min	4.681	0.852539	79	5.491	<.0001
45min	-	basal	8.354714	0.852539	79	9.8	<.0001
5min	-	60min	1.877429	0.852539	79	2.202	0.4145
5min	-	90min	4.049714	0.852539	79	4.75	0.0003
5min	-	basal	7.723429	0.852539	79	9.059	<.0001
60min	-	90min	2.172286	0.852539	79	2.548	0.2258
60min	-	basal	5.846	0.852539	79	6.857	<.0001
90min	-	basal	3.673714	0.852539	79	4.309	0.0015

F3 females							
contrast			estimate	SE	df	t.ratio	p.value
10min	-	120min	7.488333	0.708668	80	10.567	<.0001
10min	-	20min	-1.615	0.708668	80	-2.279	0.3671
10min	-	30min	0.460833	0.708668	80	0.65	0.9992
10min	-	45min	2.485833	0.708668	80	3.508	0.0202
10min	-	5min	2.065	0.708668	80	2.914	0.1008
10min	-	60min	4.538333	0.708668	80	6.404	<.0001
10min	-	90min	5.410833	0.708668	80	7.635	<.0001
10min	-	basal	10.21583	0.708668	80	14.416	<.0001
120min	-	20min	-9.10333	0.708668	80	-12.846	<.0001
120min	-	30min	-7.0275	0.708668	80	-9.916	<.0001
120min	-	45min	-5.0025	0.708668	80	-7.059	<.0001
120min	-	5min	-5.42333	0.708668	80	-7.653	<.0001
120min	-	60min	-2.95	0.708668	80	-4.163	0.0024
120min	-	90min	-2.0775	0.708668	80	-2.932	0.0966
120min	-	basal	2.7275	0.708668	80	3.849	0.007
20min	-	30min	2.075833	0.708668	80	2.929	0.0971
20min	-	45min	4.100833	0.708668	80	5.787	<.0001
20min	-	5min	3.68	0.708668	80	5.193	0.0001
20min	-	60min	6.153333	0.708668	80	8.683	<.0001
20min	-	90min	7.025833	0.708668	80	9.914	<.0001
20min	-	basal	11.83083	0.708668	80	16.694	<.0001
30min	-	45min	2.025	0.708668	80	2.857	0.1153
30min	-	5min	1.604167	0.708668	80	2.264	0.3763
30min	-	60min	4.0775	0.708668	80	5.754	<.0001
30min	-	90min	4.95	0.708668	80	6.985	<.0001
30min	-	basal	9.755	0.708668	80	13.765	<.0001
45min	-	5min	-0.42083	0.708668	80	-0.594	0.9996
45min	-	60min	2.0525	0.708668	80	2.896	0.1051
45min	-	90min	2.925	0.708668	80	4.127	0.0028
45min	-	basal	7.73	0.708668	80	10.908	<.0001
5min	-	60min	2.473333	0.708668	80	3.49	0.0213
5min	-	90min	3.345833	0.708668	80	4.721	0.0003
5min	-	basal	8.150833	0.708668	80	11.502	<.0001
60min	-	90min	0.8725	0.708668	80	1.231	0.9471
60min	-	basal	5.6775	0.708668	80	8.012	<.0001
90min	-	basal	4.805	0.708668	80	6.78	<.0001

GTT plasma insulin at 6 months of age

F2 males							
contrast			estimate	SE	df	t.ratio	p.value
10min	-	120min	0.274968	0.154034	103.07	1.785	0.6917
10min	-	20min	-0.41075	0.154034	103.07	-2.667	0.1731
10min	-	30min	-0.30682	0.154034	103.07	-1.992	0.5525
10min	-	45min	-0.09851	0.154034	103.07	-0.64	0.9993
10min	-	5min	0.12345	0.154034	103.07	0.801	0.9966
10min	-	60min	0.236129	0.154034	103.07	1.533	0.8373
10min	-	90min	0.284075	0.154034	103.07	1.844	0.6529
10min	-	basal	0.621575	0.154034	103.07	4.035	0.0032
120min	-	20min	-0.68571	0.151233	103	-4.534	0.0005
120min	-	30min	-0.58179	0.151233	103	-3.847	0.0062
120min	-	45min	-0.37348	0.151233	103	-2.47	0.2592
120min	-	5min	-0.15152	0.151233	103	-1.002	0.9849
120min	-	60min	-0.03884	0.151233	103	-0.257	1
120min	-	90min	0.009107	0.151233	103	0.06	1
120min	-	basal	0.346607	0.151233	103	2.292	0.3567
20min	-	30min	0.103929	0.151233	103	0.687	0.9989
20min	-	45min	0.312232	0.151233	103	2.065	0.503
20min	-	5min	0.534196	0.151233	103	3.532	0.0172
20min	-	60min	0.646875	0.151233	103	4.277	0.0014
20min	-	90min	0.694821	0.151233	103	4.594	0.0004
20min	-	basal	1.032321	0.151233	103	6.826	<.0001
30min	-	45min	0.208304	0.151233	103	1.377	0.9038
30min	-	5min	0.430268	0.151233	103	2.845	0.1151
30min	-	60min	0.542946	0.151233	103	3.59	0.0144
30min	-	90min	0.590893	0.151233	103	3.907	0.0051
30min	-	basal	0.928393	0.151233	103	6.139	<.0001
45min	-	5min	0.221964	0.151233	103	1.468	0.8677
45min	-	60min	0.334643	0.151233	103	2.213	0.4055
45min	-	90min	0.382589	0.151233	103	2.53	0.2303
45min	-	basal	0.720089	0.151233	103	4.761	0.0002
5min	-	60min	0.112679	0.151233	103	0.745	0.998
5min	-	90min	0.160625	0.151233	103	1.062	0.9782
5min	-	basal	0.498125	0.151233	103	3.294	0.0352
60min	-	90min	0.047946	0.151233	103	0.317	1
60min	-	basal	0.385446	0.151233	103	2.549	0.2217
90min	-	basal	0.3375	0.151233	103	2.232	0.3936

F2 females							
contrast			estimate	SE	df	t.ratio	p.value
10min	-	120min	0.117304	0.072159	114.3	1.626	0.7888
10min	-	20min	-0.36825	0.072159	114.3	-5.103	<.0001
10min	-	30min	-0.45172	0.072159	114.3	-6.26	<.0001

10min	-	45min	-0.14398	0.074717	114.62	-1.927	0.5967
10min	-	5min	0.118581	0.074379	114.17	1.594	0.806
10min	-	60min	-0.16909	0.072159	114.3	-2.343	0.3257
10min	-	90min	-0.01034	0.072159	114.3	-0.143	1
10min	-	basal	0.352222	0.073263	114.01	4.808	0.0002
120min	-	20min	-0.48556	0.07064	114.01	-6.874	<.0001
120min	-	30min	-0.56903	0.07064	114.01	-8.055	<.0001
120min	-	45min	-0.26128	0.073247	114.36	-3.567	0.015
120min	-	5min	0.001277	0.073292	114.46	0.017	1
120min	-	60min	-0.28639	0.07064	114.01	-4.054	0.0029
120min	-	90min	-0.12764	0.07064	114.01	-1.807	0.6776
120min	-	basal	0.234918	0.072159	114.3	3.256	0.0384
20min	-	30min	-0.08347	0.07064	114.01	-1.182	0.9588
20min	-	45min	0.224274	0.073247	114.36	3.062	0.0657
20min	-	5min	0.486832	0.073292	114.46	6.642	<.0001
20min	-	60min	0.199167	0.07064	114.01	2.819	0.1211
20min	-	90min	0.357917	0.07064	114.01	5.067	0.0001
20min	-	basal	0.720474	0.072159	114.3	9.985	<.0001
30min	-	45min	0.307746	0.073247	114.36	4.201	0.0017
30min	-	5min	0.570304	0.073292	114.46	7.781	<.0001
30min	-	60min	0.282639	0.07064	114.01	4.001	0.0035
30min	-	90min	0.441389	0.07064	114.01	6.248	<.0001
30min	-	basal	0.803946	0.072159	114.3	11.141	<.0001
45min	-	5min	0.262558	0.075576	114.44	3.474	0.02
45min	-	60min	-0.02511	0.073247	114.36	-0.343	1
45min	-	90min	0.133643	0.073247	114.36	1.825	0.6659
45min	-	basal	0.4962	0.074717	114.62	6.641	<.0001
5min	-	60min	-0.28767	0.073292	114.46	-3.925	0.0045
5min	-	90min	-0.12892	0.073292	114.46	-1.759	0.7086
5min	-	basal	0.233642	0.074379	114.17	3.141	0.053
60min	-	90min	0.15875	0.07064	114.01	2.247	0.383
60min	-	basal	0.521307	0.072159	114.3	7.224	<.0001
90min	-	basal	0.362557	0.072159	114.3	5.024	0.0001

F3 males							
contrast			estimate	SE	df	t.ratio	p.value
10min	-	120min	-0.21714	0.143025	80	-1.518	0.8437
10min	-	20min	-0.46514	0.143025	80	-3.252	0.042
10min	-	30min	-0.646	0.143025	80	-4.517	0.0007
10min	-	45min	-0.55914	0.143025	80	-3.909	0.0057
10min	-	5min	0.074857	0.143025	80	0.523	0.9998
10min	-	60min	-0.40171	0.143025	80	-2.809	0.1291
10min	-	90min	-0.194	0.143025	80	-1.356	0.9104
10min	-	basal	0.252857	0.143025	80	1.768	0.7026
120min	-	20min	-0.248	0.143025	80	-1.734	0.7239
120min	-	30min	-0.42886	0.143025	80	-2.998	0.0819

120min	-	45min	-0.342	0.143025	80	-2.391	0.3031
120min	-	5min	0.292	0.143025	80	2.042	0.5198
120min	-	60min	-0.18457	0.143025	80	-1.29	0.9313
120min	-	90min	0.023143	0.143025	80	0.162	1
120min	-	basal	0.47	0.143025	80	3.286	0.0383
20min	-	30min	-0.18086	0.143025	80	-1.265	0.9385
20min	-	45min	-0.094	0.143025	80	-0.657	0.9992
20min	-	5min	0.54	0.143025	80	3.776	0.0088
20min	-	60min	0.063429	0.143025	80	0.443	1
20min	-	90min	0.271143	0.143025	80	1.896	0.6186
20min	-	basal	0.718	0.143025	80	5.02	0.0001
30min	-	45min	0.086857	0.143025	80	0.607	0.9995
30min	-	5min	0.720857	0.143025	80	5.04	0.0001
30min	-	60min	0.244286	0.143025	80	1.708	0.7399
30min	-	90min	0.452	0.143025	80	3.16	0.0539
30min	-	basal	0.898857	0.143025	80	6.285	<.0001
45min	-	5min	0.634	0.143025	80	4.433	0.0009
45min	-	60min	0.157429	0.143025	80	1.101	0.9725
45min	-	90min	0.365143	0.143025	80	2.553	0.2234
45min	-	basal	0.812	0.143025	80	5.677	<.0001
5min	-	60min	-0.47657	0.143025	80	-3.332	0.0336
5min	-	90min	-0.26886	0.143025	80	-1.88	0.6293
5min	-	basal	0.178	0.143025	80	1.245	0.9438
60min	-	90min	0.207714	0.143025	80	1.452	0.8735
60min	-	basal	0.654571	0.143025	80	4.577	0.0006
90min	-	basal	0.446857	0.143025	80	3.124	0.0593

F3 females							
contrast			estimate	SE	df	t.ratio	p.value
10min	-	120min	0.020833	0.134194	80	0.155	1
10min	-	20min	-0.41167	0.134194	80	-3.068	0.0687
10min	-	30min	-0.40167	0.134194	80	-2.993	0.083
10min	-	45min	-0.31083	0.134194	80	-2.316	0.3451
10min	-	5min	0.213333	0.134194	80	1.59	0.8075
10min	-	60min	-0.05917	0.134194	80	-0.441	1
10min	-	90min	-0.04917	0.134194	80	-0.366	1
10min	-	basal	0.4425	0.134194	80	3.297	0.0371
120min	-	20min	-0.4325	0.134194	80	-3.223	0.0455
120min	-	30min	-0.4225	0.134194	80	-3.148	0.0556
120min	-	45min	-0.33167	0.134194	80	-2.472	0.2616
120min	-	5min	0.1925	0.134194	80	1.434	0.881
120min	-	60min	-0.08	0.134194	80	-0.596	0.9996
120min	-	90min	-0.07	0.134194	80	-0.522	0.9998
120min	-	basal	0.421667	0.134194	80	3.142	0.0565
20min	-	30min	0.01	0.134194	80	0.075	1
20min	-	45min	0.100833	0.134194	80	0.751	0.9978

20min	-	5min	0.625	0.134194	80	4.657	0.0004
20min	-	60min	0.3525	0.134194	80	2.627	0.1922
20min	-	90min	0.3625	0.134194	80	2.701	0.1641
20min	-	basal	0.854167	0.134194	80	6.365	<.0001
30min	-	45min	0.090833	0.134194	80	0.677	0.9989
30min	-	5min	0.615	0.134194	80	4.583	0.0005
30min	-	60min	0.3425	0.134194	80	2.552	0.2237
30min	-	90min	0.3525	0.134194	80	2.627	0.1922
30min	-	basal	0.844167	0.134194	80	6.291	<.0001
45min	-	5min	0.524167	0.134194	80	3.906	0.0058
45min	-	60min	0.251667	0.134194	80	1.875	0.6323
45min	-	90min	0.261667	0.134194	80	1.95	0.582
45min	-	basal	0.753333	0.134194	80	5.614	<.0001
5min	-	60min	-0.2725	0.134194	80	-2.031	0.5272
5min	-	90min	-0.2625	0.134194	80	-1.956	0.5778
5min	-	basal	0.229167	0.134194	80	1.708	0.74
60min	-	90min	0.01	0.134194	80	0.075	1
60min	-	basal	0.501667	0.134194	80	3.738	0.0099
90min	-	basal	0.491667	0.134194	80	3.664	0.0126

IC plasma glucose at 6 months of age

F2 males							
contrast			estimate	SE	df	t.ratio	p.value
20min	-	40min	0.576071	0.198393	51.01	2.904	0.0414
20min	-	60min	0.115893	0.198393	51.01	0.584	0.9768
20min	-	90min	-0.30865	0.202313	51.34	-1.526	0.551
20min	-	basal	-2.51696	0.198393	51.01	-12.687	<.0001
40min	-	60min	-0.46018	0.198393	51.01	-2.32	0.1554
40min	-	90min	-0.88472	0.202313	51.34	-4.373	0.0006
40min	-	basal	-3.09304	0.198393	51.01	-15.59	<.0001
60min	-	90min	-0.42454	0.202313	51.34	-2.098	0.2365
60min	-	basal	-2.63286	0.198393	51.01	-13.271	<.0001
90min	-	basal	-2.20831	0.202313	51.34	-10.915	<.0001
F2 females							
contrast			estimate	SE	df	t.ratio	p.value
20min	-	40min	0.12625	0.231051	56	0.546	0.9819
20min	-	60min	-0.3025	0.231051	56	-1.309	0.6867
20min	-	90min	-0.62125	0.231051	56	-2.689	0.0684
20min	-	basal	-3.25438	0.231051	56	-14.085	<.0001
40min	-	60min	-0.42875	0.231051	56	-1.856	0.353
40min	-	90min	-0.7475	0.231051	56	-3.235	0.0168
40min	-	basal	-3.38063	0.231051	56	-14.632	<.0001
60min	-	90min	-0.31875	0.231051	56	-1.38	0.6431
60min	-	basal	-2.95188	0.231051	56	-12.776	<.0001
90min	-	basal	-2.63313	0.231051	56	-11.396	<.0001

F3 males							
contrast			estimate	SE	df	t.ratio	p.value
20min	-	40min	0.8475	0.232455	40	3.646	0.0064
20min	-	60min	0.3025	0.232455	40	1.301	0.6919
20min	-	90min	-0.12833	0.232455	40	-0.552	0.9811
20min	-	basal	-3.35333	0.232455	40	-14.426	<.0001
40min	-	60min	-0.545	0.232455	40	-2.345	0.1523
40min	-	90min	-0.97583	0.232455	40	-4.198	0.0013
40min	-	basal	-4.20083	0.232455	40	-18.072	<.0001
60min	-	90min	-0.43083	0.232455	40	-1.853	0.3585
60min	-	basal	-3.65583	0.232455	40	-15.727	<.0001
90min	-	basal	-3.225	0.232455	40	-13.874	<.0001
F3 females							
contrast			estimate	SE	df	t.ratio	p.value
20min	-	40min	0.227	0.306542	32	0.741	0.9452
20min	-	60min	-0.232	0.306542	32	-0.757	0.941
20min	-	90min	-0.644	0.306542	32	-2.101	0.2445
20min	-	basal	-3.684	0.306542	32	-12.018	<.0001
40min	-	60min	-0.459	0.306542	32	-1.497	0.5716
40min	-	90min	-0.871	0.306542	32	-2.841	0.0557
40min	-	basal	-3.911	0.306542	32	-12.758	<.0001
60min	-	90min	-0.412	0.306542	32	-1.344	0.6665
60min	-	basal	-3.452	0.306542	32	-11.261	<.0001
90min	-	basal	-3.04	0.306542	32	-9.917	<.0001

GTT plasma glucose at 12 months of age

F2 males							
contrast			estimate	SE	df	t.ratio	p.value
10min	-	120min	6.549571	0.878976	108.1	7.451	<.0001
10min	-	20min	-1.71875	0.825492	108	-2.082	0.4909
10min	-	30min	-0.47313	0.825492	108	-0.573	0.9997
10min	-	45min	0.968125	0.825492	108	1.173	0.9605
10min	-	5min	3.205625	0.825492	108	3.883	0.0054
10min	-	60min	2.09875	0.825492	108	2.542	0.224
10min	-	90min	4.815879	0.841898	108.03	5.72	<.0001
10min	-	basal	11.11313	0.825492	108	13.462	<.0001
120min	-	20min	-8.26832	0.878976	108.1	-9.407	<.0001
120min	-	30min	-7.0227	0.878976	108.1	-7.99	<.0001
120min	-	45min	-5.58145	0.878976	108.1	-6.35	<.0001
120min	-	5min	-3.34395	0.878976	108.1	-3.804	0.007
120min	-	60min	-4.45082	0.878976	108.1	-5.064	0.0001
120min	-	90min	-1.73369	0.894996	108.14	-1.937	0.5899
120min	-	basal	4.563554	0.878976	108.1	5.192	<.0001
20min	-	30min	1.245625	0.825492	108	1.509	0.849
20min	-	45min	2.686875	0.825492	108	3.255	0.0389

20min	-	5min	4.924375	0.825492	108	5.965	<.0001
20min	-	60min	3.8175	0.825492	108	4.625	0.0003
20min	-	90min	6.534629	0.841898	108.03	7.762	<.0001
20min	-	basal	12.83188	0.825492	108	15.545	<.0001
30min	-	45min	1.44125	0.825492	108	1.746	0.7168
30min	-	5min	3.67875	0.825492	108	4.456	0.0007
30min	-	60min	2.571875	0.825492	108	3.116	0.0573
30min	-	90min	5.289004	0.841898	108.03	6.282	<.0001
30min	-	basal	11.58625	0.825492	108	14.036	<.0001
45min	-	5min	2.2375	0.825492	108	2.711	0.1565
45min	-	60min	1.130625	0.825492	108	1.37	0.9067
45min	-	90min	3.847754	0.841898	108.03	4.57	0.0004
45min	-	basal	10.145	0.825492	108	12.29	<.0001
5min	-	60min	-1.10688	0.825492	108	-1.341	0.9165
5min	-	90min	1.610254	0.841898	108.03	1.913	0.6066
5min	-	basal	7.9075	0.825492	108	9.579	<.0001
60min	-	90min	2.717129	0.841898	108.03	3.227	0.0421
60min	-	basal	9.014375	0.825492	108	10.92	<.0001
90min	-	basal	6.297246	0.841898	108.03	7.48	<.0001

F2 females							
contrast			estimate	SE	df	t.ratio	p.value
10min	-	120min	6.721689	0.898857	110.29	7.478	<.0001
10min	-	20min	-2.90313	0.881485	110	-3.293	0.0347
10min	-	30min	-1.88	0.881485	110	-2.133	0.4569
10min	-	45min	0.541875	0.881485	110	0.615	0.9995
10min	-	5min	1.793125	0.881485	110	2.034	0.5233
10min	-	60min	2.261828	0.902298	110.56	2.507	0.2403
10min	-	90min	5.09375	0.881485	110	5.779	<.0001
10min	-	basal	10.29563	0.881485	110	11.68	<.0001
120min	-	20min	-9.62481	0.898857	110.29	-10.708	<.0001
120min	-	30min	-8.60169	0.898857	110.29	-9.57	<.0001
120min	-	45min	-6.17981	0.898857	110.29	-6.875	<.0001
120min	-	5min	-4.92856	0.898857	110.29	-5.483	<.0001
120min	-	60min	-4.45986	0.919347	110.82	-4.851	0.0001
120min	-	90min	-1.62794	0.898857	110.29	-1.811	0.6748
120min	-	basal	3.573936	0.898857	110.29	3.976	0.0039
20min	-	30min	1.023125	0.881485	110	1.161	0.9629
20min	-	45min	3.445	0.881485	110	3.908	0.0049
20min	-	5min	4.69625	0.881485	110	5.328	<.0001
20min	-	60min	5.164953	0.902298	110.56	5.724	<.0001
20min	-	90min	7.996875	0.881485	110	9.072	<.0001
20min	-	basal	13.19875	0.881485	110	14.973	<.0001
30min	-	45min	2.421875	0.881485	110	2.747	0.1437
30min	-	5min	3.673125	0.881485	110	4.167	0.002
30min	-	60min	4.141828	0.902298	110.56	4.59	0.0004

30min	-	90min	6.97375	0.881485	110	7.911	<.0001
30min	-	basal	12.17563	0.881485	110	13.813	<.0001
45min	-	5min	1.25125	0.881485	110	1.419	0.888
45min	-	60min	1.719953	0.902298	110.56	1.906	0.611
45min	-	90min	4.551875	0.881485	110	5.164	<.0001
45min	-	basal	9.75375	0.881485	110	11.065	<.0001
5min	-	60min	0.468703	0.902298	110.56	0.519	0.9999
5min	-	90min	3.300625	0.881485	110	3.744	0.0085
5min	-	basal	8.5025	0.881485	110	9.646	<.0001
60min	-	90min	2.831922	0.902298	110.56	3.139	0.0536
60min	-	basal	8.033797	0.902298	110.56	8.904	<.0001
90min	-	basal	5.201875	0.881485	110	5.901	<.0001

F3 males							
contrast			estimate	SE	df	t.ratio	p.value
10min	-	120min	7.862209	0.571403	78.08	13.759	<.0001
10min	-	20min	-1.70529	0.571403	78.08	-2.984	0.0851
10min	-	30min	-1.21196	0.571403	78.08	-2.121	0.467
10min	-	45min	0.704204	0.587105	78.2	1.199	0.9543
10min	-	5min	2.028876	0.571403	78.08	3.551	0.0179
10min	-	60min	2.773876	0.571403	78.08	4.855	0.0002
10min	-	90min	5.771376	0.571403	78.08	10.1	<.0001
10min	-	basal	9.922209	0.571403	78.08	17.365	<.0001
120min	-	20min	-9.5675	0.556042	78	-17.206	<.0001
120min	-	30min	-9.07417	0.556042	78	-16.319	<.0001
120min	-	45min	-7.15801	0.571454	78.08	-12.526	<.0001
120min	-	5min	-5.83333	0.556042	78	-10.491	<.0001
120min	-	60min	-5.08833	0.556042	78	-9.151	<.0001
120min	-	90min	-2.09083	0.556042	78	-3.76	0.0094
120min	-	basal	2.06	0.556042	78	3.705	0.0112
20min	-	30min	0.493333	0.556042	78	0.887	0.9931
20min	-	45min	2.409495	0.571454	78.08	4.216	0.0021
20min	-	5min	3.734167	0.556042	78	6.716	<.0001
20min	-	60min	4.479167	0.556042	78	8.055	<.0001
20min	-	90min	7.476667	0.556042	78	13.446	<.0001
20min	-	basal	11.6275	0.556042	78	20.911	<.0001
30min	-	45min	1.916161	0.571454	78.08	3.353	0.0319
30min	-	5min	3.240833	0.556042	78	5.828	<.0001
30min	-	60min	3.985833	0.556042	78	7.168	<.0001
30min	-	90min	6.983333	0.556042	78	12.559	<.0001
30min	-	basal	11.13417	0.556042	78	20.024	<.0001
45min	-	5min	1.324672	0.571454	78.08	2.318	0.3444
45min	-	60min	2.069672	0.571454	78.08	3.622	0.0145
45min	-	90min	5.067172	0.571454	78.08	8.867	<.0001
45min	-	basal	9.218005	0.571454	78.08	16.131	<.0001
5min	-	60min	0.745	0.556042	78	1.34	0.9159

5min	-	90min	3.7425	0.556042	78	6.731	<.0001
5min	-	basal	7.893333	0.556042	78	14.196	<.0001
60min	-	90min	2.9975	0.556042	78	5.391	<.0001
60min	-	basal	7.148333	0.556042	78	12.856	<.0001
90min	-	basal	4.150833	0.556042	78	7.465	<.0001

F3 females							
contrast			estimate	SE	df	t.ratio	p.value
10min	-	120min	9.1125	0.775073	80	11.757	<.0001
10min	-	20min	-0.48083	0.775073	80	-0.62	0.9994
10min	-	30min	1.140833	0.775073	80	1.472	0.865
10min	-	45min	3.613333	0.775073	80	4.662	0.0004
10min	-	5min	2.1875	0.775073	80	2.822	0.1251
10min	-	60min	6.071667	0.775073	80	7.834	<.0001
10min	-	90min	8.3325	0.775073	80	10.751	<.0001
10min	-	basal	11.78333	0.775073	80	15.203	<.0001
120min	-	20min	-9.59333	0.775073	80	-12.377	<.0001
120min	-	30min	-7.97167	0.775073	80	-10.285	<.0001
120min	-	45min	-5.49917	0.775073	80	-7.095	<.0001
120min	-	5min	-6.925	0.775073	80	-8.935	<.0001
120min	-	60min	-3.04083	0.775073	80	-3.923	0.0055
120min	-	90min	-0.78	0.775073	80	-1.006	0.9842
120min	-	basal	2.670833	0.775073	80	3.446	0.0242
20min	-	30min	1.621667	0.775073	80	2.092	0.4859
20min	-	45min	4.094167	0.775073	80	5.282	<.0001
20min	-	5min	2.668333	0.775073	80	3.443	0.0245
20min	-	60min	6.5525	0.775073	80	8.454	<.0001
20min	-	90min	8.813333	0.775073	80	11.371	<.0001
20min	-	basal	12.26417	0.775073	80	15.823	<.0001
30min	-	45min	2.4725	0.775073	80	3.19	0.0498
30min	-	5min	1.046667	0.775073	80	1.35	0.9125
30min	-	60min	4.930833	0.775073	80	6.362	<.0001
30min	-	90min	7.191667	0.775073	80	9.279	<.0001
30min	-	basal	10.6425	0.775073	80	13.731	<.0001
45min	-	5min	-1.42583	0.775073	80	-1.84	0.6561
45min	-	60min	2.458333	0.775073	80	3.172	0.0523
45min	-	90min	4.719167	0.775073	80	6.089	<.0001
45min	-	basal	8.17	0.775073	80	10.541	<.0001
5min	-	60min	3.884167	0.775073	80	5.011	0.0001
5min	-	90min	6.145	0.775073	80	7.928	<.0001
5min	-	basal	9.595833	0.775073	80	12.381	<.0001
60min	-	90min	2.260833	0.775073	80	2.917	0.1
60min	-	basal	5.711667	0.775073	80	7.369	<.0001
90min	-	basal	3.450833	0.775073	80	4.452	0.0009

GTT plasma insulin at 12 months of age

F2 males							
contrast			estimate	SE	df	t.ratio	p.value
10min	-	120min	-0.46	0.13571	111.11	-3.389	0.0261
10min	-	20min	-0.745	0.13308	111	-5.598	<.0001
10min	-	30min	-0.5938	0.13308	111	-4.462	0.0006
10min	-	45min	-0.6188	0.13308	111	-4.649	0.0003
10min	-	5min	0.04188	0.13308	111	0.315	1
10min	-	60min	-0.4775	0.13308	111	-3.588	0.0141
10min	-	90min	-0.2925	0.13308	111	-2.198	0.4143
10min	-	basal	-0.1031	0.13308	111	-0.775	0.9973
120min	-	20min	-0.285	0.13571	111.11	-2.1	0.4786
120min	-	30min	-0.1338	0.13571	111.11	-0.986	0.9865
120min	-	45min	-0.1588	0.13571	111.11	-1.17	0.9611
120min	-	5min	0.50185	0.13571	111.11	3.698	0.0099
120min	-	60min	-0.0175	0.13571	111.11	-0.129	1
120min	-	90min	0.16748	0.13571	111.11	1.234	0.9471
120min	-	basal	0.35685	0.13571	111.11	2.629	0.1866
20min	-	30min	0.15125	0.13308	111	1.137	0.9673
20min	-	45min	0.12625	0.13308	111	0.949	0.9895
20min	-	5min	0.78688	0.13308	111	5.913	<.0001
20min	-	60min	0.2675	0.13308	111	2.01	0.5398
20min	-	90min	0.4525	0.13308	111	3.4	0.0253
20min	-	basal	0.64188	0.13308	111	4.823	0.0002
30min	-	45min	-0.025	0.13308	111	-0.188	1
30min	-	5min	0.63563	0.13308	111	4.776	0.0002
30min	-	60min	0.11625	0.13308	111	0.874	0.9939
30min	-	90min	0.30125	0.13308	111	2.264	0.3731
30min	-	basal	0.49063	0.13308	111	3.687	0.0103
45min	-	5min	0.66063	0.13308	111	4.964	0.0001
45min	-	60min	0.14125	0.13308	111	1.061	0.9784
45min	-	90min	0.32625	0.13308	111	2.452	0.2674
45min	-	basal	0.51563	0.13308	111	3.875	0.0055
5min	-	60min	-0.5194	0.13308	111	-3.903	0.005
5min	-	90min	-0.3344	0.13308	111	-2.513	0.2375
5min	-	basal	-0.145	0.13308	111	-1.09	0.9746
60min	-	90min	0.185	0.13308	111	1.39	0.8993
60min	-	basal	0.37438	0.13308	111	2.813	0.1233
90min	-	basal	0.18938	0.13308	111	1.423	0.8866

F2 females							
contrast			estimate	SE	df	t.ratio	p.value
10min	-	120min	-0.0455	0.06309	128.9	-0.721	0.9984
10min	-	20min	-0.3282	0.06111	128.32	-5.371	<.0001
10min	-	30min	-0.3076	0.06223	128.82	-4.942	0.0001
10min	-	45min	-0.197	0.06198	128.51	-3.178	0.0469
10min	-	5min	0.03732	0.06111	128.32	0.611	0.9995
10min	-	60min	-0.1374	0.06303	128.71	-2.18	0.425
10min	-	90min	-0.0203	0.06223	128.82	-0.327	1
10min	-	basal	0.23543	0.06111	128.32	3.853	0.0056
120min	-	20min	-0.2827	0.062	128.56	-4.56	0.0004
120min	-	30min	-0.2621	0.06281	128.23	-4.173	0.0018
120min	-	45min	-0.1515	0.06288	128.81	-2.409	0.288
120min	-	5min	0.08279	0.062	128.56	1.335	0.9187
120min	-	60min	-0.0919	0.06391	129.27	-1.438	0.8808
120min	-	90min	0.02515	0.06281	128.23	0.4	1
120min	-	basal	0.28091	0.062	128.56	4.531	0.0004
20min	-	30min	0.02061	0.06113	128.43	0.337	1
20min	-	45min	0.13121	0.06091	128.26	2.154	0.4418
20min	-	5min	0.3655	0.06003	128.02	6.089	<.0001
20min	-	60min	0.19078	0.06197	128.52	3.078	0.0618
20min	-	90min	0.30786	0.06113	128.43	5.036	0.0001
20min	-	basal	0.56361	0.06003	128.02	9.389	<.0001
30min	-	45min	0.1106	0.062	128.63	1.784	0.6927
30min	-	5min	0.34489	0.06113	128.43	5.642	<.0001
30min	-	60min	0.17017	0.06304	128.95	2.699	0.1584
30min	-	90min	0.28725	0.06197	128.02	4.635	0.0003
30min	-	basal	0.543	0.06113	128.43	8.882	<.0001
45min	-	5min	0.23429	0.06091	128.26	3.847	0.0057
45min	-	60min	0.05957	0.06264	128.28	0.951	0.9894
45min	-	90min	0.17665	0.062	128.63	2.849	0.1116
45min	-	basal	0.4324	0.06091	128.26	7.099	<.0001
5min	-	60min	-0.1747	0.06197	128.52	-2.819	0.1199
5min	-	90min	-0.0576	0.06113	128.43	-0.943	0.99
5min	-	basal	0.19811	0.06003	128.02	3.3	0.033
60min	-	90min	0.11708	0.06304	128.95	1.857	0.6441
60min	-	basal	0.37283	0.06197	128.52	6.016	<.0001
90min	-	basal	0.25575	0.06113	128.43	4.184	0.0017

F3 males							
contrast			estimate	SE	df	t.ratio	p.value
10min	-	120min	-0.6517	0.13703	80	-4.756	0.0003
10min	-	20min	-0.6458	0.13703	80	-4.713	0.0003
10min	-	30min	-0.825	0.13703	80	-6.021	<.0001
10min	-	45min	-0.55	0.13703	80	-4.014	0.0041
10min	-	5min	0.06917	0.13703	80	0.505	0.9999
10min	-	60min	-0.7025	0.13703	80	-5.127	0.0001
10min	-	90min	-0.5033	0.13703	80	-3.673	0.0122
10min	-	basal	0.15917	0.13703	80	1.162	0.9621
120min	-	20min	0.00583	0.13703	80	0.043	1
120min	-	30min	-0.1733	0.13703	80	-1.265	0.9384
120min	-	45min	0.10167	0.13703	80	0.742	0.998
120min	-	5min	0.72083	0.13703	80	5.26	<.0001
120min	-	60min	-0.0508	0.13703	80	-0.371	1
120min	-	90min	0.14833	0.13703	80	1.082	0.9752
120min	-	basal	0.81083	0.13703	80	5.917	<.0001
20min	-	30min	-0.1792	0.13703	80	-1.308	0.9263
20min	-	45min	0.09583	0.13703	80	0.699	0.9987
20min	-	5min	0.715	0.13703	80	5.218	<.0001
20min	-	60min	-0.0567	0.13703	80	-0.414	1
20min	-	90min	0.1425	0.13703	80	1.04	0.9806
20min	-	basal	0.805	0.13703	80	5.875	<.0001
30min	-	45min	0.275	0.13703	80	2.007	0.5433
30min	-	5min	0.89417	0.13703	80	6.525	<.0001
30min	-	60min	0.1225	0.13703	80	0.894	0.9927
30min	-	90min	0.32167	0.13703	80	2.347	0.3273
30min	-	basal	0.98417	0.13703	80	7.182	<.0001
45min	-	5min	0.61917	0.13703	80	4.518	0.0007
45min	-	60min	-0.1525	0.13703	80	-1.113	0.9706
45min	-	90min	0.04667	0.13703	80	0.341	1
45min	-	basal	0.70917	0.13703	80	5.175	0.0001
5min	-	60min	-0.7717	0.13703	80	-5.631	<.0001
5min	-	90min	-0.5725	0.13703	80	-4.178	0.0023
5min	-	basal	0.09	0.13703	80	0.657	0.9992
60min	-	90min	0.19917	0.13703	80	1.453	0.873
60min	-	basal	0.86167	0.13703	80	6.288	<.0001
90min	-	basal	0.6625	0.13703	80	4.835	0.0002

F3 females							
contrast			estimate	SE	df	t.ratio	p.value
10min	-	120min	0.37967	0.15667	72	2.423	0.2876
10min	-	20min	-0.3968	0.15667	72	-2.533	0.2342
10min	-	30min	-0.1233	0.15667	72	-0.787	0.9969
10min	-	45min	-0.097	0.15667	72	-0.619	0.9994
10min	-	5min	0.43	0.15667	72	2.745	0.151
10min	-	60min	0.18833	0.15667	72	1.202	0.9535
10min	-	90min	0.25633	0.15667	72	1.636	0.7817
10min	-	basal	0.64917	0.15667	72	4.143	0.0028
120min	-	20min	-0.7765	0.15667	72	-4.956	0.0002
120min	-	30min	-0.503	0.15667	72	-3.211	0.0484
120min	-	45min	-0.4767	0.15667	72	-3.042	0.0748
120min	-	5min	0.05033	0.15667	72	0.321	1
120min	-	60min	-0.1913	0.15667	72	-1.221	0.9491
120min	-	90min	-0.1233	0.15667	72	-0.787	0.9969
120min	-	basal	0.2695	0.15667	72	1.72	0.7323
20min	-	30min	0.2735	0.15667	72	1.746	0.7165
20min	-	45min	0.29983	0.15667	72	1.914	0.6067
20min	-	5min	0.82683	0.15667	72	5.277	<.0001
20min	-	60min	0.58517	0.15667	72	3.735	0.0106
20min	-	90min	0.65317	0.15667	72	4.169	0.0026
20min	-	basal	1.046	0.15667	72	6.676	<.0001
30min	-	45min	0.02633	0.15667	72	0.168	1
30min	-	5min	0.55333	0.15667	72	3.532	0.0196
30min	-	60min	0.31167	0.15667	72	1.989	0.5557
30min	-	90min	0.37967	0.15667	72	2.423	0.2876
30min	-	basal	0.7725	0.15667	72	4.931	0.0002
45min	-	5min	0.527	0.15667	72	3.364	0.0318
45min	-	60min	0.28533	0.15667	72	1.821	0.6682
45min	-	90min	0.35333	0.15667	72	2.255	0.3827
45min	-	basal	0.74617	0.15667	72	4.763	0.0003
5min	-	60min	-0.2417	0.15667	72	-1.543	0.8315
5min	-	90min	-0.1737	0.15667	72	-1.108	0.9711
5min	-	basal	0.21917	0.15667	72	1.399	0.8946
60min	-	90min	0.068	0.15667	72	0.434	1
60min	-	basal	0.46083	0.15667	72	2.941	0.0959
90min	-	basal	0.39283	0.15667	72	2.507	0.246

IC plasma glucose at 12 months of age

F2 males							
contrast			estimate	SE	df	t.ratio	p.value
20min	-	40min	1.088534	0.300307	53.38	3.625	0.0056
20min	-	60min	0.922284	0.300307	53.38	3.071	0.0266
20min	-	90min	0.815954	0.310135	53.23	2.631	0.079
20min	-	basal	-3.60522	0.300307	53.38	-12.005	<.0001
40min	-	60min	-0.16625	0.293674	53.02	-0.566	0.9794
40min	-	90min	-0.27258	0.306523	53.58	-0.889	0.8996
40min	-	basal	-4.69375	0.293674	53.02	-15.983	<.0001
60min	-	90min	-0.10633	0.306523	53.58	-0.347	0.9968
60min	-	basal	-4.5275	0.293674	53.02	-15.417	<.0001
90min	-	basal	-4.42117	0.306523	53.58	-14.424	<.0001
F2 females							
contrast			estimate	SE	df	t.ratio	p.value
20min	-	40min	0.511066	0.330784	55.73	1.545	0.5383
20min	-	60min	0.302316	0.330784	55.73	0.914	0.8904
20min	-	90min	-0.52643	0.330784	55.73	-1.591	0.509
20min	-	basal	-4.15081	0.330784	55.73	-12.548	<.0001
40min	-	60min	-0.20875	0.324358	55.03	-0.644	0.9671
40min	-	90min	-1.0375	0.324358	55.03	-3.199	0.0187
40min	-	basal	-4.66188	0.324358	55.03	-14.373	<.0001
60min	-	90min	-0.82875	0.324358	55.03	-2.555	0.0933
60min	-	basal	-4.45313	0.324358	55.03	-13.729	<.0001
90min	-	basal	-3.62438	0.324358	55.03	-11.174	<.0001

F3 males							
contrast			estimate	SE	df	t.ratio	p.value
20min	-	40min	1.703	0.352095	32	4.837	0.0003
20min	-	60min	1.721	0.352095	32	4.888	0.0003
20min	-	90min	1.364	0.352095	32	3.874	0.0042
20min	-	basal	-3.12	0.352095	32	-8.861	<.0001
40min	-	60min	0.018	0.352095	32	0.051	1
40min	-	90min	-0.339	0.352095	32	-0.963	0.8696
40min	-	basal	-4.823	0.352095	32	-13.698	<.0001
60min	-	90min	-0.357	0.352095	32	-1.014	0.8471
60min	-	basal	-4.841	0.352095	32	-13.749	<.0001
90min	-	basal	-4.484	0.352095	32	-12.735	<.0001
F3 females							
contrast			estimate	SE	df	t.ratio	p.value
20min	-	40min	0.621333	0.346499	36	1.793	0.3931
20min	-	60min	0.6075	0.346499	36	1.753	0.4157
20min	-	90min	-0.08067	0.346499	36	-0.233	0.9993

20min	-	basal	-3.64117	0.346499	36	-10.508	<.0001
40min	-	60min	-0.01383	0.346499	36	-0.04	1
40min	-	90min	-0.702	0.346499	36	-2.026	0.2746
40min	-	basal	-4.2625	0.346499	36	-12.302	<.0001
60min	-	90min	-0.68817	0.346499	36	-1.986	0.2931
60min	-	basal	-4.24867	0.346499	36	-12.262	<.0001
90min	-	basal	-3.5605	0.346499	36	-10.276	<.0001